Natural polymers for consolidation of the Oseberg artefacts

By

Jennifer Wakefield

This thesis is submitted to the University of Nottingham for degree of Doctor of Philosophy

January 2020

School of Biosciences

University of Nottingham

Sutton Bonington campus
Sutton Bonington
Leicestershire
LE12 5RD

Acknowledgements

I would like to take this opportunity to thank everyone who has helped me throughout my PhD. Professor Steve Harding helped and guided me throughout my PhD, even staying late to help. His dedication and love of the subject is an inspiration. Guy Channel trained me up on the AUC and advised me especially at the start of my PhD, and we always enjoyed the tea break conversations. Gleb Yakubov stayed late and went through how the mechanical testing analysis works. Gary Adams supported and guided me during my PhD. Rob Stockman gave advice for the chemistry section and had plenty of ideas I unfortunately did not have the time to follow up on. Thanks must also go to all the NCMH team for all their help, advice and friendship throughout my PhD; especially Vlad Dinu and Richard Gillis. I would like to acknowledge Pete Licence and Chris Moody for accepting me on to the centre of doctoral training programme, and the EPSRC for the funding that allowed me to do this work. Peri Williams I would like to thank for organising training and events for the CDT, and going out of her way to ask for feedback and really trying to improve the CDT programme.

I would also like to express my gratitude to the Saving Oseberg team for their support and advice whilst I was in Oslo, and for making me feel like part of the team. I would especially like to thank Susan Braovac for her recommendations based on her conservation experience, and Calin for teaching me how to use the EDS-SEM.

Finally, I would like to thank my friends and family. My mum, Marie-Christine Wakefield, my dad, Niall Wakefield, and my sister, Tamara Wakefield, have always supported me in whatever I wanted to do in life. They have encouraged and supported me throughout my PhD. My boyfriend Rory was always free even after a long day to listen to me talk about my work and help me talk things through when I was stuck. My friends Emma, Shona, Sarah, Craig, Sarah, Liam, Moe, Alisdair, Emerald and Vlad are the best friends I could ever have asked for and I always know they are there if I ever need them. I would also like to thank Shona, Rosie, Stephen, Rory and Kathleen for helping me proof-read my thesis.

My accomplishments are based on everyone who has been in my life and the invaluable support and advice they have given me.

Photo from the Oseberg excavation. University of Oslo Museum of Cultural Heritage

Natural polymers for consolidation of the Oseberg artefacts

Conservator Paul Johanessen at work on the Oseberg artefacts. University of Oslo Museum of Cultural Heritage

Abstract

Conservation is of vital importance for museums. The Viking Ship Museum has a particular problem in terms of conservation. It houses artefacts from the Oseberg Viking ship burial that are of great significance in terms of Viking history and are of national pride to Norway. These artefacts were buried in 834 AD, excavated in 1904, treated with alum and dried. The alum treatment, which started in 1905, led to them becoming acidic (pH 1-2), resulting in severe degradation of the artefacts. Current conservation methods have their limitations due to the alum previously used to conserve these artefacts, the removal of which could cause some of the most fragile artefacts to collapse entirely. However, some of the less fragile artefacts could cope with a water treatment. Even in that case, PEG, the most commonly used aqueous conservation treatment, may not be suitable due to the high concentration of acid and metal ions in some artefacts. Natural polymers pose some advantages to traditional methods in terms of sustainability and future use, so, for this reason, chitosan was initially investigated. Additionally, chitosan contains amine groups which may help to increase the pH and aid in metal chelation and in preventing hydrolysis reactions. The molecular weight of potential consolidants was determined with an analytical ultracentrifuge prior to wood treatment to determine the likelihood of wood penetration. This was followed by testing on artificially degraded wood and on archaeological wood. Chitosan gave good results in wood treatment tests, however, the use of acid for the dissolution of chitosan is a concern, hence, despite obtaining good results, an alternative aqueous treatment was sought. Chitosan acetate salt and

aminocellulose were researched using the same methodology. Chitosan acetate salt did not aid in consolidation. Aminocellulose produced good results for conservation, appearing suitable either alone or in combination with PEG and has potential advantages to PEG, although the long-term stability needs to be assessed.

For where an aqueous treatment could not be used this study investigated a silyl modified chitosan, already known to be soluble in organic solvents. The reaction was successfully carried out with the chitosan of desired molecular weight, which ensured penetration into the wood. The silyl modified chitosan was however, found to be very brittle and therefore not suitable for conservation. For comparison during this investigation known consolidants paraloid B72 and butvar B98 were also investigated. B72 appears suitable for immersion as a pre-consolidant, to be followed by washing out the acid and alum, or to be used in combination with calcium hydroxide nanoparticles. B98 appears preferable for injection. However, long term acid stability needs assessed: if stable, B98 may be suitable even without removal of alum; alternatively, it could be used in combination with calcium hydroxide.

This research demonstrates aminocellulose as a possible aqueous treatment and B72 or B98 as non-aqueous treatments. Stability of aminocellulose needs to be assessed and B72 and B98 require exploring in combination with calcium hydroxide. Mechanical testing and long-term stability require further investigation. These treatments may prove to be suitable consolidants for the Oseberg artefacts. In particular, aminocellulose could aid in the conservation of other artefacts with high acid and iron content, including newly discovered waterlogged artefacts.

Table of Contents

List of Figures

List of Tables

Abbreviations

AUC	Analytical ultracentrifugation
ASE	Anti shrink efficiency
η	Dynamic viscosity (Poise)
η_r	Relative viscosity
η_{red}, η_{inh}, $[\eta]$	Reduced, inherent, intrinsic viscosity (ml/g)
c	Concentration (g/ml)
Da	Daltons
f	Frictional coefficient (force/velocity) unit: dyn s cm^{-1}
f/f_0	Frictional ratio (ratio of friction coefficient of the macromolecule to that of a spherical particle of the same anhydrous volume)
k_H, k_K	Huggins, Kraemer constant
M_w, M_z	Weight average, z-average molecular weight/molar mass (Da, g/mol)
$M_w(r)$	Point weight average molecular weight at radial position r (Da, g/mol)
$M_{w,app}$	Apparent weight average molecular weight /molar mass (Da, g/mol)
ρ	Solution density (g/ml)
ρ_o	Solvent density (g/ml)
s	Sedimentation coefficient (Svedberg units S, where $1S=10^{-13}$ sec)
$s_{20,w}$	Sedimentation coefficient to standardised to the viscosity and density of water at a temperature 20^oC (S)
S	Svedberg (10^{-13} s)
s	Second (s)
ks	Gralen coefficient (ml/g)
ls-g*(s)	Least square Gaussian apparent fit of sedimentation coefficients
$\bar{v}$	Partial specific volume of the particle (ml/g)
ω	Rotor speed in radians per second ($\omega=2\pi\cdot rpm/60$)
r	Distance from centre of the rotor (cm)
v	Velocity (cm/sec)
N_A	Avogadro's number (6.02214×10^{23} mol^{-1})
D	Translation diffusion coefficient (cm^2/sec)
k_b	Boltzmann constant ($1.38064\ldots\times10^{-16}$ erg$\cdot K^{-1}$)
R	Gas constant ($8.31446\ldots\times10^7$ erg.$mole^{-1}.K^{-1}$)

T	Absolute temperature (K)
J(*r*)	Fringe displacement at radial position r
g	Gram
kg	Kilogram
h	Hour
eq	Equivalents
min	minutes
IR	Infrared spectroscopy
NMR	Nuclear magnetic resonance
mol	Mole
gfm	Gram formula mass
rt	Room temperature
aq	Aqueous
non-aq	Non-Aqueous
DCM	Di-chloromethane
DMSO	Dimethyl sulfoxide
THF	Tetrahydrofuran
Eq.	Equation
mL	Millilitre(s)
µL	Microlitre(s)
mm	Millimetre(s)
mg	Milligram(s)
MHz	Megahertz
NMR	Nuclear magnetic resonance
v/v	Volume per volume
w/v	Weight per volume
v/v	Weight per weight
TLC	Thin layer chromatography
sat.	Saturated
UV	Ultraviolet
M	Molar concentration
mmol	Millimoles
Stdv-	Standard deviation

P	Poise
Chit	Chitosan
Chit Ac	Chitosan acetate
AEA	6-deoxy-6-(2-aminoethyl) aminocellulose
HEA	6-deoxy-6-(2-hydroxyethyl) aminocellulose
PEG	Polyethyene gycol
IPA	isopropanol (isopropyl alcohol)
TBA	tert-butanol (tert-butyl alcohol)
Tg	Glass transition temperature
RH	Relative humidity
Vac	Vacuum
WPG	Weight percentage gain

Chapter 1. Previous conservation of the artefacts, existing consolidants and new possibilities

1.1 Importance of conservation for the future

From the Ancient Greeks and the Renaissance to present day, people have been collecting items from the past to show off, tell a story and to preserve them for the future. These days, this important aspect of society and learning has been passed on and entrusted to the museums of the world. Museums are therefore responsible for preserving artefacts for the future. Although there are private collectors, ordinary people are trusting museums to preserve the past for the future. Children are brought to museums to learn about the past and get inspired to learn more, whether they become scientists because of the amazing technologies of the past and the idea of improvement, are inspired to write or paint what they have seen of the past and present or are inspired to learn all they can about the past and become historians. The past can inspire and teach us things that have been forgotten. For example long lost medicines such as a cure recently re-discovered for antibacterial resistant bacteria (Boukraa and Sulaiman, 2009). Alternativelyit can teach us not to repeat the same mistakes and teach us of days gone by, of past civilisation, past triumphs, past defeats, past technologies and where we come from. It can inspire us to preserve all this for the future; if Ancient Egyptians can preserve the dead for thousands of years, surely we can preserve artefacts for future generations to see? (David, 2008).

These artefacts are not only important for their monetary value; they are important for learning about the past, through investigations as well as teaching children and inspiring future generations.

The Oseberg ship and its artefacts are one such example of artefacts that need to be preserved for the future. They are part of the history of Norway and a large part of Europe, as they represent the Vikings who occupied and traded with a large part of the world. This ship burial helps to illuminate the Viking-age burial practices and helps us to gain a better appreciation of their ideas of life and death. The artefacts are a looking glass into their world: What was buried, the choice and details of decoration and the extent of trade through the origin of the material or non-local design etc. These artefacts can be used to inspire and teach future generations and can be studied to learn more about these past cultures, and as science improves so does the potential for new discoveries. However, these potential new insights about the artefacts and the Viking culture they represent cannot be achieved if they are not preserved for the future.

1.2 Oseberg artefacts

1.2.1 Discovery

In 1903 a farmer, Knut Rom, in Oseberg in Vestfold, Norway thought he had found a ship whilst digging into a mound on his property. He contacted the University's Collection of National Antiquities in Oslo and two days later archaeologist, Professor Gustafson, started an investigation. It proved to be indeed a ship with decorated ornamentation. Professor Gustafson was convinced it was a Viking ship burial, however, with autumn quickly approaching he decided it would be prudent to wait until the following summer to start an excavation. The excavation took three months and received much public attention, so much so that fences had to be installed (See Figure 1-1) and Professor Gustafson complained that it was like working in an

exhibition (Braovac, 2015). Although the excavation itself did not take long, it took 21 years to restore the ship and finds. The ship was slowly dried out and great care was taken to reconstruct the ship with as much original timber as possible, hence 90% of the current ship on display is original timbers (Braovac, 2015).

Figure 1-1: Photo from the Oseberg excavation. University of Oslo Museum of Cultural Heritage.

The artefacts were treated differently; the majority were treated with alum. Prior to treatment, the objects (except ship fragments) needed to be moved to Oslo. To do this they were cleaned on site and then packed with moss and burlap. On arrival, the artefacts were kept underwater with a small amount of mercury chloride as a biocide in a zinc container (Braovac, 2015). This was to prevent them drying out and prevent cracking and shrinking before treatment.

1.2.2 Alum treatment

Figure 1-2: Photos from the conservation of the fourth sled conserved by Paul Jahannessen sometime before ca. 1912. Each sledge was treated and reconstructed from thousands of pieces (Braovac et al., 2018a).

The artefacts were threatened by slow and ongoing deterioration; hence a preservation treatment was required. Investigation into treatment with alum started in 1904 and full scale conservation started in 1905 (Braovac, 2015) (Figure 1-2 shows the reconstructure of a sled as an example of the work that took place). The alum method was developed in 1861 by C.F. Herbst, a Danish archaeologist, and was used until the 1950s. It was used worldwide but predominately in Scandinavia, especially Denmark and Sweden. Professor Gabriel Gustafson, the conservator at the time, visited

museums for 1 month looking for the best treatment method (Braovac, 2015). The National Museum of Denmark was using alum, and the results looked good. They had also started experimenting with glycerol but Professor Gabriel Gustafson deemed this was still too experimental (Braovac, 2015). This was fortunate, as glycerol was commonly used with alum after ca. 1910 with negative long-term effects (Braovac et al., 2018a). The glycerol is hydroscopic which combined with the alum, results in destruction of the artefacts often within a few decades (Braovac et al., 2018a). The conservation took place between 1095 and ca. 1912. A journal was kept which gives insight into the treatment; a summary is given by Braovac et al., (2018). For treatment, the nails were removed from the artefacts before the artefacts were placed in a copper tank of concentrated, dissolved alum (potassium aluminum sulfate dodecahydrate $KAl(SO_4)_2 \cdot 12H_2O$) and heated to approximately 90 ˚C. The length of the process was very dependent on the size of the object, varying between 2-36 h, but the average was 24 h. The idea behind the use of alum is that it forms crystals quickly upon cooling due to lower solubility at low temperatures, and this solid will replace the water filled voids in the wood, preventing shrinkage upon drying. It only penetrated 5 mm into the surface of the wood but gave good results in stabilising the wood before drying and preventing shrinking. However, the centre of the objects was not supported by the alum. After treatment the objects were cooled and washed with hot water then cold water. The nails were then replaced back into the artefacts. This removal of nails probably prevented further damage, as the metal ions at high temperatures could have sped up the degradation and movement of ions throughout the wood. After drying, the artefacts were coated with linseed oil through sequential application of turpentine with increasing concentrations of linseed oil, to allow increased penetration of the linseed

oil. The artefacts were then mounted with metal pins, screws, adhesives and putties. This method was used to treat thousands of fragments reconstructed into hundreds of items (see Figure 1-2 shows the reconstruction of one of the sleds). After restoration, the objects were then coated in several layers of resin. In the 1950s the objects were recoated with epoxy resin, confirmed by IR (Braovac and Dahl, 2015; Braovac et al., 2018a; Häggström and Sandström, 2013; Rosenqvist, 1959).

1.2.3 Consequence of Alum treatment

Analysis of the Oseberg ship compared to newly treated archaeological wood with alum and newly acid treated archaeological wood shows that although the degradation of Oseberg artefacts is much greater, similar patterns appear compared to acid and alum-treated degradation. This suggests that the major cause of degradation of the Oseberg artefacts is the acidic conditions caused by the alum treatment. If the acid treated samples were left for 100 years, it is predicted it would result in very similar degradation to that of the Oseberg artefacts (Braovac and Kutzke, 2012).

Archaeological wood that is not alum-treated can also experience some acid degradation. This is some sulfur in the wood from the burial environment. Shipwecks therefore have the greatest sulfur problems due to the sulphur content in the water and anaerobic bacteria that produce hydrogen sulfide (H_2S). When the artefacts are excavated and exposed to oxygen and aerobic bacteria the aerobic bacteria, convert this to sulfuric acid (H_2SO_4). Oxidation can also occur without bacteria, but this is very slow however iron can catylse the oxidation and accelerate the formation of sulfuric acid (Sandström et al., 2003). The hydrogen sulphide can also form pyrite (Fe_2S) in

combination with iron. Pyrite is then oxidised to sufuric acid and iron sulfate. Both pyrite oxidation and bacterial oxidation are implicated in the production of sulfuric acid in waterlogged woodern archaeological artefacts (Fellowes and Hagan, 2003). This would have been a factor when the Oserberg aretfacts were originally excavated, causing initial damage and the need for immediate conservation, however it would not have been as extreme as in the cases of shipwrecks excavated from the sea floor. In the case of the Oseberg artefacts the types of wood and levels of iron and sulfur would have played a role in the state of degradation after excavation. The most degraded artefacts then underwent alum treatment in order to be saved. The alum treatment however although allowing for preservation and reassembling of broken artefacts at the time is also the greatest cause of the sulfuric acid levels seen today.

Alum, potassium aluminum sulfate dodecahydrate ($KAl(SO_4)^2$ $12H_2O$) breaks down on heating to produce sulfuric acid (H_2S) which is the cause of acid in the Oseberg artefacts. In other artefacts high sulfuric acid has been produced by sulfate-reducing bacteria and has also been found to produce H_2S from sulfate, by using sulfate ions as electron acceptors for metabolising organic acids which results in H_2S formation (Fors and Sandström, 2006). Sea water with various sulfate salts penetrate the wood which can then be attacked by bacteria, and can be promoted in an anoxic environment. The Vasa ship is an example of wood which has a high pH due to sulfate salts from sea water and bacteria. High FeS content from sea water can also result in sulfate compounds which can in turn be used by bacteria and result in H_2S formation. The Vasa and the Mary Rose both face the same problem. The Mary Rose was one of Henry VIII's warships for the navy; she sank in 1545 after 35 years of service. The wreck was rediscovered in 1971 and the hull was salvaged in 1982 (Sandström et al., 2005).

Between 1994 and 2006 the ship was sprayed with PEG 200, followed by PEG 2000 till 2013, after which it was slowly air-dried (Preston et al., 2014). The Vasa was a royal warship that sank on her maiden voyage in 1628 and was raised in 1961 (Fors and Sandström, 2006).

Sulfate compounds can be oxidized once removed from the sea and this can be catalysed by iron ions. The middle lamella, which is lignin rich, is where a high concentration of organosulfur is found; H_2S reacts with lignin active sites in a nucleophilic reaction. Active sites include double bonds, ether and carbonyl groups (Fors and Sandström, 2006). This nucleophilic reaction could result in lignin degradation. Lignin is degraded by acid but to a limited extent compared to cellulose and hemicelluloses. Sulfuric acid breaks the β(1-4) glycosidic bond in cellulose and lignin, but there are more glycosidic bonds in cellulose than lignin (Fors and Sandström, 2006; Smidsrød et al., 1966).

Some polymers, such as hemicelluloses and lignin, are made up of a mixture of monomers with a variety of different links. Some links are more susceptible to acid attack than others which are more resistant. Hemicellulose is made up of xylosidic bonds, and mannosidic bonds which are easily hydrolysed by acid. Hemmicellulose also contains glycosidic bonds, which are hydrolysed by acid, but not as quickly as mannosidic bonds. Glucomannan is also depolymerised easily by acid. However, the link between uronic groups and xylose is very resistant. Lignin similarly has more and less susceptible points; α-ether structures are more susceptible to acid than β-ether structures. Similarly, phenolic structures are more reactive than non-phenolic structures. Ether bonds between carbohydrates and lignins are fairly resistant to acid.

Acid degradations lead to oxidation but acid is not the only cause of oxidation; metal ions can act as electron acceptors and can undergo Fenton type reactions. Oxidation can turn hydroxyl groups and ketone groups into carboxylic acids and cleave glycosidic linkages and aryl side chains (Braovac, 2015).

The problems seen with sulfuric acid in waterloged artefacts are very common, however, in the case of the Oseberg artefacts more sulfuric acid was actively although accidentally added. For waterlogged artefacts, the severity of the problem can be reduced by the addition of borax and boric acid; this acts as a fungicide but also neutralises sulfuric acid. Sodium hydrogen carbonate/ sodium carbonate (mole ratio 7:1) solutions/ poultice can also be used to increase the pH (Sandström et al., 2003). However, in the case of the Oseberg artefacts the wood is already dry and addition of moisture could agravate the situation. This makes this particular situation significantly less common and less researched.

The artefacts from the Oseberg ship burial are in very poor condition now. However, due to the resin and oil layers the damage is not obvious from the surface of the artefacts. Alum solution alone is already at pH 3.5-4 and alum decomposition occurs at high temperatures like those used to treat the artefacts. This decomposition leads to sulfuric acid formation, which attacks the cellulose and lignin of the wood causing extreme degradation. Analysis of the Oseberg ship artefacts compared to freshly alum-treated archaeological wood and acid treated wood shows that, although the degradation of Oseberg artefacts is much greater, similar patterns appear when compared to acid and alum-treated degradation. This suggests that the major cause of degradation of the Oseberg artefacts is the acidic conditions caused by the alum

treatment (Braovac and Kutzke, 2012). Alum breaks down on heating to produce sulfuric acid (H_2SO_4); sulfate-reducing bacteria have also been found to produce hydrogen sulfide (H_2S) from sulfate by using sulfate ions as electron acceptors for metabolising organic acids which results in H_2S formation (Fors and Sandström, 2006). Sulfuric acid breaks the β(1-4) glycosidic bond in cellulose and lignin; lignin is more resistant as there are fewer β(1-4) glycosidic bonds in lignin (Fors and Sandström, 2006; Smidsrød et al., 1966).

However, acid is not the only reason for damage. The alum only penetrated a few millimetres resulting in the centre drying differently than the outside of the piece of wood, meaning if the wooden artefact were thicker than a few millimetres the drying could have led to cracking. High humidity can cause alum to dissolve and then a decrease in humidity could cause it to re-crystallise; this could alter the distribution of alum throughout the wood.

The soaking and boiling of the wood could dislocate any small fragments that had already started to disintegrate. The process of boiling wood could possibly cause damage to the wood. In green wood it seems to affect the inner wood (heartwood) and outer wood (sapwood) of a tree differently. Boiling increases permeability and causes cell wall damage. In heartwood, permeability is overshadowed by cell wall damage, resulting in increased shrinkage on drying. In sap wood, permeability was significantly increased, allowing quicker drying and reduced shrinkage on drying (Chafe, 1993). These different effects of boiling wood could aggravate the situation; however, the aim of alum was to reduce the cracking by providing support.

Holes were drilled into large objects to improve penetration, but consequently, this damaged the artefacts by creating holes and also by increasing the acidic area. The alum and, in particular heating of the alum decreased the pH of the artefacts to between 1 and 2. The crystal formation prevents shrinking and cracking of the artefacts. However, the alum only penetrates a few millimetres which results in the centre drying differently to the outside of the object. This means if the object is thicker than a few millimetres the drying can lead to cracking. The humidity varied in the objects and this change in humidity could be a problem. High humidity could cause alum to dissolve and then a decrease could cause it to re-crystallise; this could alter the distribution of alum, which could make the cracking worse. Gustafson considered the alum with glycerol risky because it was new which was fortunate. Hygroscopic properties of glycerol aggravate the problems with alum, by causing the humidity to increase further destabilising the alum. The oil treatments were meant to reduce water vapour pressure, however, they resulted in creating a microenvironment, which prevented the damage of the artefacts being seen from the surface. Hence, why it took such a long time before that damage was noticed and the extent of it appreciated.

The presence of transition metal ions such as copper (Cu^{2+}), iron (Fe^{2+} and Fe^{3+}) and zinc (Zn^{2+}) also causes problems as they can participate in other non-enzymatic wood degrading reactions. There are various sources of these metals such as: original nails and decoration, pins and nails used in conservation, zinc and copper tanks used in the alum treatment and finally, but least problematic, is metals in the water from the burial process (Braovac, 2015). Although the water from burial contains some metal ions it is in negligible quantities compared to the nails and metals from treatment in tanks.

Iron ions have been found to catalyse acid led hydrolysis degradation reactions in the case of the Vasa and the Mary Rose resulting in greater degradation (Almkvist and Persson, 2008; Fors and Sandström, 2006; Haseneder et al., 2007; Hvilsted and Mortensen, 2010). Composite objects have also observed this degradation effect of iron as well as treatments such as PEG causing corrosion of the iron (Guilminot et al., 2002; Imazu et al., 2018; Selwyn et al., 1993). This makes composite objects difficult to treat. For wood with nails these are often removed for treatment of the wood and the original nails replaced after treatment which was carefully carried out for the Oseberg artefacts as well (Braovac et al., 2018a). In the case of the Oseberg, some artefacts do not have a great deal of iron in them; others have iron from the original nails as well as nails from restoration. However, no correlation has yet been found in Oseberg-tested wood between the iron concentration and the level of degradation (Braovac et al., 2018a). Nevertheless, great care should be taken in consolidation, where iron is present as treatment could change environmental conditions and potentially result in corrosion of the iron or iron catalysing hydrolysis in the future. This area requires more research to identify whether iron could be a problem in the case of the Oseberg artefacts.

Pyrolysis GC-MS has been used to assess the extent of degradation of the holocellulose (cellulose and hemicellulose) and lignin (Braovac et al., 2018a). In Oseberg wood not treated with alum, 15-68% is holocellulose and 32-85% is lignin which is comparable to freshly excavated waterlogged wood (14-61% holocellulose and 80-43% lignin). Sound wood has 58-78% holocellulose and 42-21% lignin, hence it is apparent that there are varying degrees of, but significant degradation in the waterlogged archaeological wood. It was discovered that the holocellulose is almost completely

depleted in the Oseberg alum-treated wood; 3-20% is holocellulose and 97-80% of what is left is lignin (Braovac et al., 2018a). The lignin has also been degraded but to a lesser extent than the holocellulose. However, the lignin shows clear evidence of oxidation (Figure 1-3). There is an increase in acid groups especially in the alum-rich regions (McQueen et al., 2017). It has been found that up to 80% of the lignin is oxidized in the Oseberg wood; in sound wood oxidized lignin makes up only 5-7% of total lignin (Braovac et al., 2018a). The combination of the absence of holocellulose and oxidation of lignin shows how degraded this wood is. Consolidation is required to replace strength lost from degradation of holocellulose. The fact that lignin and its state of oxidation forms the majority of the remaining wood is also important in terms of wood treatment and interaction of consolidations to the cell wall.

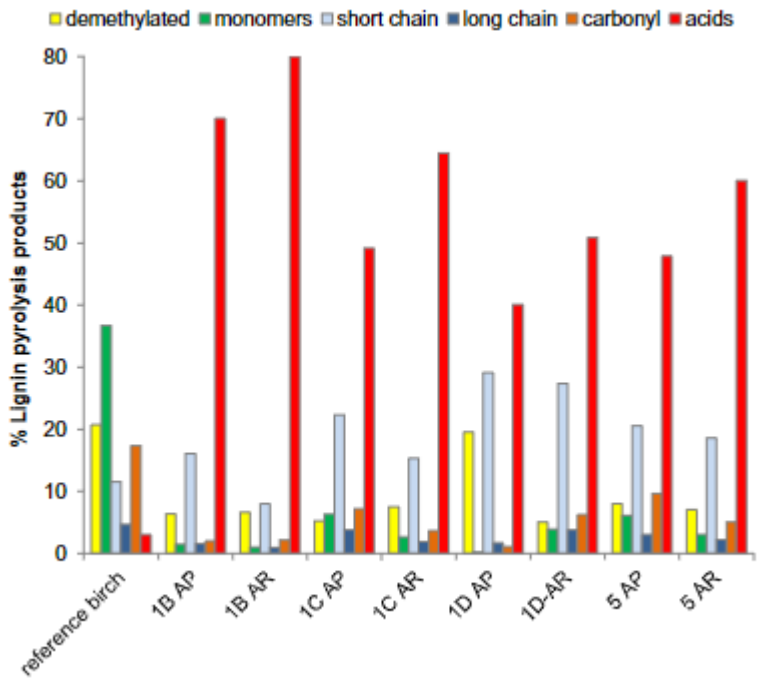

Figure 1-3: A plot from Lucejko 2017 work shows lignin degradation in Oseberg alum treated wood. AP stands for alum-poor regions of wood, AR stands for alum-rich wood (McQueen et al., 2017).

Analysis of the alum in the wood also resulted in surprises. The alum used appears to be a mix of potassium alum (as expected) and ammonium alum (Braovac et al., 2018a; McQueen et al., 2019). McQueen's research showed that the ammonium alum varies in concentration from 8 to 84 mol% in samples tested so far (McQueen et al., 2019). McQueen also found historical accounts of the similarity of the potassium and ammonium alum, and the difficulty of separation, which explains the random mixtures found. Alum purchased for conservation would have been a mixture of potassium and ammonium alum. Further investigations carried out by McQueen demonstrated that ammonium alum results in a solution with a pH of 3, compared to potassium alum with a pH of 1-2 (Braovac et al., 2018a; McQueen et al., 2019). However, the mixture of potassium alum and ammonium alum did not raise the pH compared to potassium alum alone (McQueen et al., 2019). The presence of both must be considered for conservation when anticipating potential reactions from changes in pH. Linseed oil presence should also be considered in conservation, as it has been found on a number of wood samples. Linseed oil treated artefacts appear to have undergone less degradation according to pyrolysis results (Łucejko et al., 2018). When carrying out conservation whether to actively try to remove the linseed oil prior to treatment or whether to leave it in place needs to be carefully considered. It will obviously be removed with non-aqueous treatment methods.

1.2.4 Summary of degradation effects

Waterlogged burial causes cellulose degradation through mild acidic hydrolysis and bacterial degradation. Alum treatment both prevented and caused cracking; it also caused the formation of sulfuric acid, which hydrolyses cellulose and to some extent lignin, and metal ions promoted hydrolysis. There would be concerns regarding future bacteria and fungi degradation, however this is limited by moisture and temperature controls. However, the addition of antimicrobial agents is still desirable as long as they do not cause any harm to the artefacts or conservators.

1.3 Past conservation problems

The realisation of the importance of preserving artefacts is not new and previous attempts have been both successful and unsuccessful. Unfortunately, the Oseberg ship finds were one of the cases where the conservation attempt was not entirely successful. Although cracking was prevented, it did not preserve the artefact in the long term and actually proved detrimental. It is one of many traditional treatments which are now causing problems for museums (Odegaard and Sadongei, 2005; Unger, 2012). However, it must be appreciated that attempts were made, and that without some of these, the artefacts would not be with us today.

1.4 Current Museum problems with conservation

Conservation is a major concern for all museums, although this concern is much greater when it comes to organic artefacts, which are more at risk than most artefacts.

Degradation can be more extreme but also happens at a faster rate hence, conservation must be carried out as soon as possible. Despite the urgency, great care must be taken to use the best possible conservation material for each individual object. It is vital that future consequences of the conservation technique are considered. This includes breakdown products, removal and future treatment. As the Oseberg artefacts have already been treated with alum, the interaction of future treatment materials with alum must also be investigated before any conservation materials are applied to the artefacts. This is a common problem encountered with artefacts that were treated in the Victorian times; conservators often did more harm than good and treatments are rarely removable (Fulcher, 2014; Koob, 1998). It is these sorts of situations that we hope will be avoided in the future by using reversible materials; that way if a mistake is made today it can be rectified in the future. Unfortunately, reversing a conservation treatment is often much harder with organic artefacts. In theory alum is removable, however, it would require boiling or at least some heating of the artefacts in copious amounts of water, and this will probably lead to further damage. Hence, it is essential that the new conservation material can cope with the presence of alum.

1.5 Criteria

1.5.1 Essential criteria

A consolidant for the Oseberg ship must be stable under acid conditions and on ageing, chelate metal ions and penetrate well into the wood.

1.5.2 Desired

A consolidant for the Oseberg ship should also be ideally non-toxic, inexpensive, UV protective, sustainable, reversible/re-treatable, antibacterial and antifungal.

1.6 Waterlogged wood degradation

1.6.1 Wood structure

The wood structure of waterlogged wood has some similarities to the Oseberg wood as it was originally waterlogged prior to the alum treatment. Waterlogged archaeological wood is also to be used as test pieces for treatment trials prior to testing alum-treated wood. The structure of wood cells' walls is shown below in Figure 1-4 and Figure 1-5.

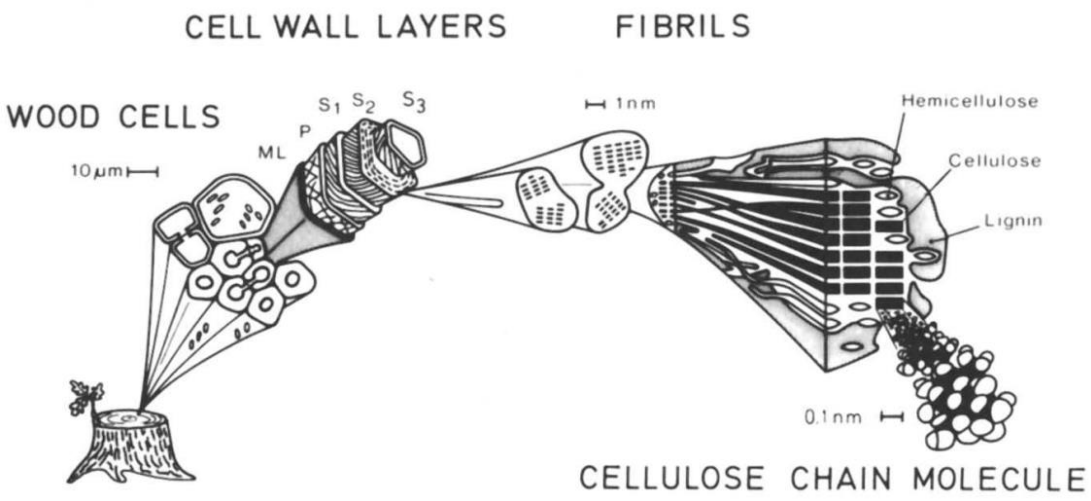

Figure 1-4: Illustration of the structure of wood cells (Hoffmann and Jones, 1989).

The fragility of waterlogged wood has been noticed for some time; Herbst from the National museum of Demark noticed in 1857 that wooden archaeological finds from

waterlogged sites must be kept wet and handled with care until they reach the museum (Björdal, 2012). It was in hopes of preserving the artefacts that the Oseberg artefacts were treated with alum. Different types of microbial attack and the damage they do to the cells is shown in Figure 1-6. Under waterlogged conditions bacterial

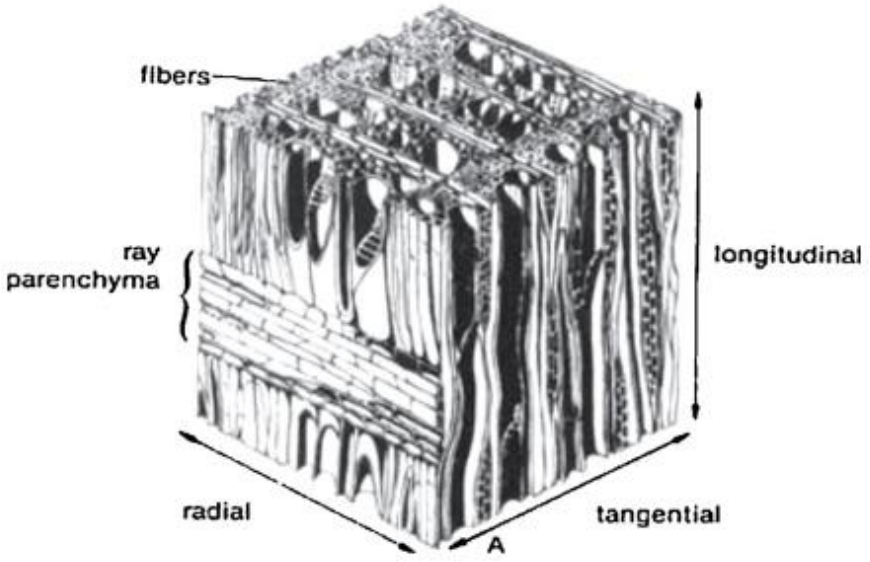

Figure 1-5: Image of the internal structure of wood (Nilsson and Rowell, 2012).

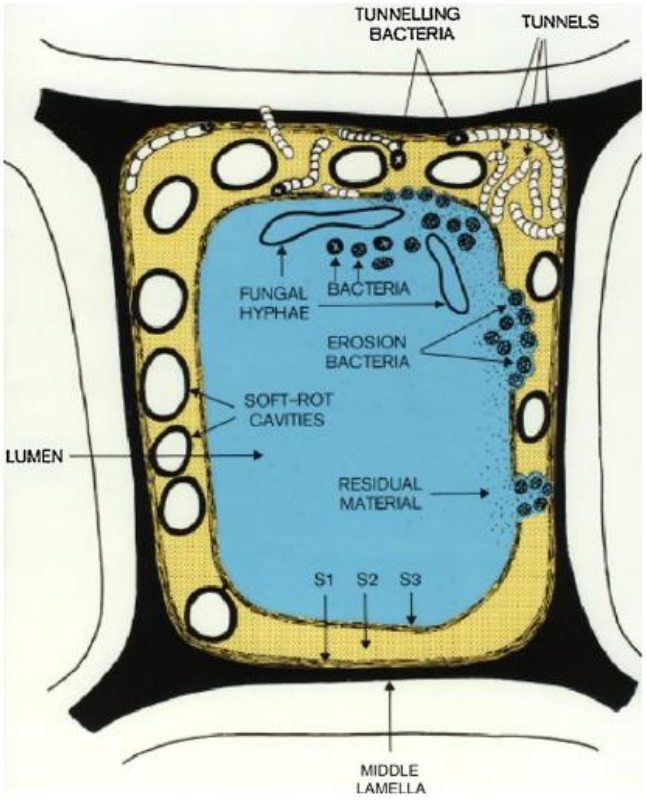

Figure 1-6: Illustration of the type of microbial degredation and the decay pattern they produce (Singh, 2012).

erosion, fungal soft rot and bacterial tunnelling are most common types of microorganism attacks (Singh, 2012). Bacterial erosion appears to be the most prevalent among the above. It has also been found that the extent of bacterial degradation is not linked to the age of the artefacts but rather to their depth, hence the oxygen levels. The type of wood also affects susceptibility to decay (Björdal, 2012). This is why the Oseberg ship is in better condition than the Oseberg artefacts. The Oseberg ship is made of oak whereas the Oseberg artefacts are made from a mixture of different types of wood including oak, ash, yew and pine, which are less susceptible to decay, and maple, alder, birch and possibly beech which are more prone to decay

(Braovac et al., 2018b). This meant that some of artefacts were very fragile on discovery and these were the ones treated with alum.

1.7 Current wood conservation methods

1.7.1 PEG

PEG (polyethylene glycol) has been used since the 1960s. It has been used on many wooden artefacts all over the world, from 1 cm artefacts, to ships such as the Vasa and the Mary Rose. Small artefacts are normally soaked for several weeks or months, whereas ships are sprayed over a matter of years. Low molecular weight PEG is soluble in water and organic solvents. PEG penetrates wood well and has been proven to prevent shrinkage. PEG has also been proven to produce acid on decomposition, determined by radiocarbon analysis of formic acid found in artefacts. The formic acid contained no C^{14} which means it came from petrochemicals, hence the PEG (Hvilsted and Mortensen, 2010). PEG decomposition has various causes, including elevated temperature, metal ions, biodegradation and UV radiation. PEG is relatively stable, which is clear from the fact that it has been used on multiple artefacts. For example, it was used on the Vasa 30 years ago and it is still in reasonably good condition, despite some degradation resulting in the formation of formic acid. Due to problems with past treatments it is now desirable for conservation treatments to be reversible. One of the benefits of the use of PEG is that it can be removed; however removal requires soaking the artefacts in water and this is only really be effective if the water is heated. The water and heat could, however, cause further damage to the artefacts on removal of PEG (Hocker et al., 2012). The problem with PEG is that it degrades to produce acid

and it is not sustainable as it comes from a non-renewable source (Walsh et al., 2014a), therefore a greener sourced material is desired. It is hoped that polysaccharides may be a greener source whilst being a good consolidate. Carboxymethyl cellulose has poorer penetration compared to PEG but is superior at preventing cracking (Hocker et al., 2012). Poor penetration is a concern, but further research is required. In the case of the Oseberg artefacts, the worry of cracking is negligible as the artefact is already dry. Therefore, the challenge now is to prevent the artefact falling apart and to prevent further degradation, although cracking is still an issue after re-immersion in water.

1.7.2 Kauramin (melamine and formaldehyde)

The melamine formaldehyde treatment method has been used since the 1960s and has since held many commercial names with slightly different mixtures: Arigal C and Lyofix are examples. Kauramin 800 is a proprietary mixture of oligomeric and monomeric forms of melamine and formaldehyde (Braovac et al., 2018a). The advantage of this treatment over PEG is that it forms on open structure after polymerisation when the solution reaches pH 6-7 (Braovac et al., 2018a; Cesar et al., 2017). Although PEG is theoretically reversible, in practice removal has been difficult, and as PEG fills the cells it could make retreatment difficult. Kauramine or the melamine and formaldehyde treatment is not reversible, which is seen as a severe disadvantage by some. Uger ruled out the melamine formaldehyde treatment for valuable cultural property because of lack of reversibility. However, the fact it has an open structure means retreatment may be easier. Reversibility is a heavily debated area among conservators these days, especially after finding previous detrimental treatments have been found to be very hard to remove (Appelbaum, 1987; Brajer,

2009). In some cases, with precondensates it has been found to cause considerable swelling of wood. The temperature of 50 ^{o}C is required for treatment and curing on drying is also a concern for archaeological artefacts. Melamine/formaldehyde treatments have however been found to be more water resistant and have very good resistance to light. They have also been found to protect against microorganism attack because of the formaldehyde. The wood can typically be identified by species afterwards, but C^{14} dating cannot be carried out. The resulting objects are often lightened by treatment and fast treatment can cause breaks and volume changes. However, the major advantage of melamine/formaldehyde treatments is re-treatability. One of the conservation problems with the use of Kauramine is in controlling the polymerisation rate. If polymerisation starts too soon it can be disastrous, as it cannot be removed (Cesar et al., 2017). FT-IR can now be used to monitor the polymerisation to better control this. In the case of the Oseberg artefacts, special care will need to be taken to wash out all the alum and especially the acid, as the treatment will polymerise faster at low pH. Experience is key to taking the wood out of solution at the right time; that and its lack of reversibility and lightening has slowed its general uptake by conservators. This might be a possibility, as it is thought re-treatability is more important than reversibility in terms of the Oseberg artefacts (Braovac et al., 2018a). However, more research is required.

1.7.3 Sucrose

Sucrose is a cheaper alternative to PEG and other consolidants. The procedure for treatment is very similar to that of the PEG method and is listed and described in the Nautical Archaeology at Texas A&M University conservation manual (Hamilton,

2010). Low concentrations of sucrose are initially used and then increased to saturation levels. In some cases, the temperature is increased to 50 ^{o}C. The wood is then dried under controlled humidity conditions which slowly reduced humidity from 70 to 50%. After treatment the wood must not be exposed to high humidity over 80% or the sugar can leach out. Hygroscopicity (the property of attracting and holding water molecules) of the sucrose can lead to absorption of water: this can cause leaching and cause the surface to become damp and sticky. Antibacterial and antifungal additives can be added to increase the effectiveness. Advantages of sucrose include being non-toxic, non-corrosive, non-volatile, inexpensive, water-soluble and reversible. Disadvantages are that the wood can become sticky, which can cause dirt to stick to the surface; it can also lighten the colour of the wood and can undergo hydrolysis (Parrent, 1985).

1.7.4 Rosin-Acetone

Rosin is used because it results in strong, light, dry wood, that can be easily repaired, glued and does not react with metal. The disadvantage is that it is a more expensive treatment and acetone is highly flammable. It is also a problem if it is used on artefacts that need to be reconstructed, as the wood loses flexibility and can splinter or break (Hamilton, 1999). This would be a factor for some of the Oseberg artefacts, which would have to be disassembled and re-assembled due to their size unless sprayed in which case acetone can be a bigger concern. 60% Rosin 100 and 60% rosin 459 were compared to a mixture of 30% colophony and 30% PEG 3400 and 11% Vinavil 8020S all disolved in acetone and the former two were found to be more effective for wood preservation (Giachi et al., 2011). Rosin 100 and 459 treated wood kept their shape better than Vinavil 8020S, and equilibrium moisture content was lower for rosin 100

and 459 than vinavil 8020S and PEG 3400 and colophony. The retention of rosin 100 and 459 was much higher than vinavil 8020S, and much more similar to PEG 3400 mixed with colophony.

1.7.5 Aquazol (poly(2-ethyl-2-oxazoline))

Aquazol is used in the conservation of artwork rather than artefacts. However, it is a water-soluble and organic soluble adhesive/consolidant and has been used for decorated wood conservation (Ebert et al., 2012). It is worth consideration and investigation for use in either conservation or simply to help decide what aspects are desirable and how to achieve them. Aquazol is a tertiary amide polymer; it is predominantly used for flaking paint. It is pH neutral, comes in various target molecular weights (50, 200 and 500 Da are used for conservation), it is thermal and light stable, has excellent shear properties, is non-toxic, has good tensile strength, and broad solubility, is resoluble, hence reversible, and has no noticeable effect on the colour of a piece. Artificial ageing shows good stability and it can be easily identified in the future through FTIR analysis which is useful for future investigations and conservation (Arslanoglu, 2003, 2004; Ebert et al., 2012).

Unfortunately aquazol cannot be used for the conservation of the Oseberg artefacts as it is not stable in acid conditions (Manchun et al., 2012). It is also not sustainable.

1.7.6 Alvar

Alvar, a polyvinyl acetal resin, was investigated around the same time as Butvar. Items recovered from a tomb by R. Young in the 1950s were treated with Alvar dissolved in

acetone. The wood was re-examined roughly 30 years later and some wood was found to be in very poor condition, as the Alvar was probably applied when wet and it barely penetrated below the surface, hence it did not actually strengthen the wood. Nevertheless, there were a few pieces with thick coatings of Alvar where its application does appear to have protected the decoration on the surface, and even after 30 years the Alvar was clear and colourless and removable (Spirydowicz et al., 2001a). However, as paint and inlaid surfaces are not the main concern for the Oseberg artefacts, the technique would not be appropriate due to the poor penetration.

1.7.7 Butvar 98 (Polyvinyl butyral resin)

Butvar replaced alvar due to good ageing characteristics (Johnson, 1994a). Butvar, is a thermosetting synthetic resins, such as epoxies and polyesters that were used in the 1960s and 1970s. However, these had numerous problems such as change in surface appearance, lack of reversibility and difficulty curing. Soluble thermoplastic resins such as polyvinyl butyral resin and various acrylic resins have been investigated and appear to be promising for wood conservation. Butvar has been successfully used to consolidate an 18th century wooden fire engine (Harrison, 2008). Butvar 98 was used for wood conservation by Pennsylvania Museum of Archaeology and Anthropology to conserve 37 pieces of furniture and more than 50 small wooden objects (Spirydowicz et al., 2001a). Butvar has a low a viscosity and has been shown to coat the cell walls and fill some lumina of cells, hence maintaining the micromorphological structure of wood. It has also been shown to increase the strength of wood (Spirydowicz et al., 2001a). The problem with butvar is that it is light sensitive. Accelerated ageing experiments showed butanal and water and a very small quantity

of organic acids were produced, which could be harmful in the long run (Harrison, 2008). Sensitivity to light, although a potential problem, is not a huge concern as the light levels, especially UV light, can be controlled. Conversely, the production of water could be a huge problem due to accelerating hydrolysis.

1.7.8 B72

Paraloid B72 is known to have many positive properties for conservation. It is a flexible polymer that dries clear and is less glossy than PVA and it has been found not to discolour even at high temperatures, hence theoretically on ageing (Hamilton, 1999). Paraloid B72 is made from two polymers - ethyl methacrylate and methyl acrylate (70:30) it has a Tg of 40^{o}C and a refractive index of 1.49 (Chapman and Mason, 2003). It is used for its stability in many areas of conservation. It has been used in stained glass conservation for loose paint (Chapman and Mason, 2003), fossil conservation (Larkin and Makridou, 1999; López-Polín, 2012a; Rutzky et al., 2005), ceramic conservation (Constâncio et al., 2010; Koob, 1986) stone conservation (Favaro et al., 2006) and bone conservation (Johnson, 1994b). B72 is mostly used in art conservation, but there has also been some research and use of it for wood conservation (Tuduce Trăistaru et al., 2011). The concern with B72 is the ester bonds in the structure which is acid sensitive. This is a concern for the alum-treated artefacts that are acidic.

1.7.9 Calcium or magnesium hydroxide nanoparticles

Calcium and magnesium hydroxide nanoparticles have been investigated for use on the Vasa ship. The use of nanoparticles has demonstrated that it can prevent further release of acid (Giorgi et al., 2005). However, on its own it would not be sufficient as it does not aid in consolidation. It could, however, be added as a supplement to a blend. This has been investigated by Andriulo et al. (2017), in which calcium hydroxide was combined with silanes (Andriulo et al., 2017).

1.7.10 Cellulose

Cellulose has been considered as a viable option as it is naturally found in wood. It is not hygroscopic like PEG and it is renewable. It is not very soluble in water, however modified cellulose such as methyl cellulose is soluble (Cipriani et al., 2010; Kučerová, 2012a). Nevertheless, there is great concern over the uses of cellulose for acidic wood conservation due to the obvious problem that cellulose had already been degraded by acid and hence will simply degrade again. This unfortunately outweighs the obvious advantages: it is naturally present in wood, it keeps the structure of wood and it is cheap to reinsert. The acid breaks down the β(1-4) glycosic bond, which means that the same problem will arise from the use of any other polysaccharide with that bond. However, the extent of degradation has been found to vary due to the presence of a carbohydroxy group (found in cellulose) or a uronic acid group (found in alginate). Polysaccharides with a carbohydroxy group break down at a faster rate than those with a uronic group. However, both do eventually breakdown (Smidsrød et al., 1966). Chitosan does not have a uronic group although NH_2 might act as another protective

group. However, there has been little published evidence giving a direct comparison of acidic breakdown speed of different macromolecules.

1.7.10.1 Cellulose derivatives

Cellulose derivatives have been investigated for the conservation of paper and wood (Feller and Wilt, 1990). There are mixed results regarding cellulose derivatives and their use in conservation. The investigation carried out by Bicchieri and Mucci (2009) showed that hydroxypropyl cellulose and polyvinyl alcohol were both very promising for paper conservation. It showed that hydroxypropyl cellulose did not produce acid over time and the reflectance factor is also not significantly effective. Hence, the brightness of the paper is not affected and the colour of the dyes were also not significantly affected (Bicchieri and Mucci, 2009). The polymer was found to depolymerise slightly overtime, but overall they concluded it would be suitable for paper conservation (Bicchieri and Mucci, 2009). However, research by Feller and Wilt (1990) found that ethers of cellulose, including hydroxypropyl cellulose, darkened over time meaning they are not suitable for conservation. They have excellent UV resistance but they also depolymerise over time and hence are not considered stable. A final reason for not using this treatment on Oseberg artefacts is that the ether celluloses degrade in acid at very similar rates to cellulose and hence are not acid stable and so they are not suitable for the conservation of Oseberg artefacts (Feller and Wilt, 1990).

1.7.11 Silanes and organosilanes (use of silicone oil)

Silicone oils has been investigated multiple times for conservation (Hamilton, 1999; Smith, 2003), but it has had very mixed recommendations (Kaye, 1995). Silicone oils and organosilanes have had very promising results with long term stability (Klosowski and Smith, 2003; Tejedor, 2010, 2012). Silicone oil is three times more expensive then PEG and not reversible (Mitchell, 2008; Smith, 2010). However, although not reversible, it is more stable than PEG and PEG is difficult to reverse in practice (Mitchell, 2008; Smith, 2010). Finally, silicone oils does not chelate metal ions, but some functionalised organosilanes may be able to (Oakley et al., 2004). Since metal ions are a major problem and considering the cost of the silanes, the additional cost of functionalising them and the lack of reversibility, silanes are not really the ideal treatment option. However, they should be considered after all other alternatives. Moreover, functionalising natural macromolecules is more promising. What ought to be considered, is silanes as cross-linkers between natural polymers. We know this is possible due to silanes cross-linking with cellulose and lignin in the wood, and we know it is stable. The use of a natural polymers as the main treatment might increase re-treatability.

1.7.12 Chitosan (Brief overview)

Chitosan is a natural polymer derived from chitin that is yet to be used for conservation but has been considered for use on the Mary Rose and for the Oseberg ship, both with some initial promising results. It is water-soluble, non-toxic, chelates metal ions, has antimicrobial properties and is sustainable. The fact that it is only soluble in water in

mildly acidic conditions could be a problem: however, it is possible to functionalise it to make it organic-soluble. This means two versions could be made: one which is organic soluble for the most deteriorated artefacts and a water-soluble version for the more robust artefacts and artefacts from other sites that are still waterlogged.

1.7.12.1 Mary Rose conservation problems, solutions and investigation of chitosan

The Mary Rose is a 16th century Royal Navy warship. She sank in battle with a French fleet in 1545 and was raised from the sea bed in 1982 (Walsh et al., 2014b, 2014a). Since then the ship has been treated with PEG but due to the problems with PEG an alternative treatment has been sought. For this reason, Walsh's group investigated modified polysaccharides due to their similarity to cellulose and lignin. The method used functionalized chitosan and guar with cucurbit[8]uril. Chitosan is naturally antibacterial; it has amine groups that are easily functionalised and it does not degrade into acidic products. Guar also does not degrade into acidic products and can be cross-linked with chitosan. However, guar does degrade in acid i.e. it is not acid stable, hence guar would not be suitable for the conservation of the Oseberg artefacts. Chitosan was functionalised with naphthol and catechol, helping to hinder biological activity and catechol also increases the chelation capability of chitosan for the Fe^{3+}. Moreover, through chelation more cross-linking occurs, which also means the material adapts to the content of Fe^{3+} in the wood, strengthening the system. The use of naphthol allows the crosslinking through cucurbit[8]uril, a macrocyclic molecule made up of 8 glycoluril (=$C_4H_2N_4O_2$=) monomers linked with methylene bridges (-CH_2-). Cucurbit[8]uril acts as a supramolecular host molecule which has high affinity for

positively charged molecules such a chitosan. Naphthol allows cucurbit[8]uril not to be affected by the quantity of Fe^{3+}, which could otherwise be affected by Fe^{3+} as the chelation also removed linking points. Guar was functionalised with viologen using methyl viologen (MV) attached through a boric acid(BA)-diol dynamic covalent interaction (Walsh et al., 2014b). This increased its antibacterial activity. Cucurbit[8]uril can be used to cross-link (MV-BA) guar with chitosan and the ternary complex formation is reversible, which is a desirable characteristic these days. Since many previously used conservation techniques have proven to be damaging to artefacts years later, it has become an important goal to find techniques that are reversible. This would enable the original substance to be removed and replaced if a better method of conservation is found. This technique appears promising as an all-in-one method. It is antibacterial, antifungal, reversible to some extent, removes Fe^{3+} though chelation and strengthens the wood by providing support (replacing the lost cellulose and lignin) and even adapts to the wood by strengthening the crosslinkage the more Fe^{3+} is in the wood. The reversibility of the tertiary structure through heat or water content shows real forward planning for future treatment. If a better method is found, the water content could be changed and therefore the viscosity changed by removing the tertiary structure, possibly allowing the material to flow out of the wood; however this area is still under investigation (Walsh et al., 2014b, 2014a). The fact that chitosan is a water-soluble treatment is an issue for the Oseberg artefacts, as there is real concern that water could result in further breakdown of the artefacts. The additional fact that guar is not stable under acid conditions means it cannot be used on the Oseberg artefacts. Penetration is also a concern, as the treatment was only tested on 5 mm x1 mm

sections, hence even evidence of good penetration may not truly reflect good penetration on larger pieces of wood.

1.7.12.2 Oseberg investigation of chitosan

Chitosan has previously been researched by Christensen in 2013 for use on the Oseberg artefacts, alongside other treatment options. Previous research on non-archaeological wood by other groups appears promising (to be described later). Hence, chitosan was investigated further. Two types of chitosan were used in this investigation: one high molecular weight chitosan from crabs purchased from Sigma-Aldrich and one low molecular weight from crab exoskeletons from Kitonor. For the experiments 2% chitosan was dissolved in 0.1 M CH_3COOH (acetic acid) overnight. It must be kept in mind that chitosan from Sigma and Kitonor are likely to have slightly different degrees of acetylation (DA) which could also affect results. Archaeological wood was cut and left soaking in a sealed beaker at room temperature for 2 weeks on average. After treatment, the wood was rinsed lightly with deionised water and frozen at -18 ^oC and freeze-dried at room temperature. During this research, it was found that chitosan would precipitate after less than a month in HCl, but even after 6 months would not precipitate in acetic acid, hence why it was chosen. It was also found that chitosan could dissolve up to 10% w/v_2 but it was very viscous until below 5% w/v_2 and unlikely to diffuse into the wood above 2% w/v_2. There was a concern that 1% w/v_2 would not be effective; consequently 2% was chosen for the experiments (Christensen, 2013). This is a concern when considering the use of chitosan on two levels (I) first that it is water-soluble and not organic-soluble and (II) second that low concentrations are required for penetration to be possible. However, chitosan could be

modified to be organic-soluble and this would lower the viscosity, therefore the concentration could also be increased. It is desirable however, that a water-soluble and an organic-soluble version is available to treat wood of varying levels of degradation.

During the experiments two wood samples became infected with fungi which shows chitosan is not sufficiently antifungal, however again this can be addressed through chitosan modifications or the addition of an antifungal (Christensen, 2013). The results of the treatment using an FEI Quanta 200 FEG-ESEM revealed that chitosan was not evenly distributed. Nevertheless, it did appear similar in nature to cellulose. However, it was theorised by Christensen that this observation may have more to do with the freeze-drying process than the polymers themselves. Another observation is that the chitosan did not appear to coat or penetrate intact cell walls, but instead simply diffused into degraded cell structures (See Fig.1-4). This property is both promising and worrying at the same time. Its lack of penetration could be problematic, however the fact that it does support degraded cells suggests its potential as a consolidant. The fact the support is only really required in degraded cells, and other cells are not affected, means it only provides support and does not change the rest of the wood. As

Christensen points out, it also means it might be possible to re-treat the wood if necessary in the future.

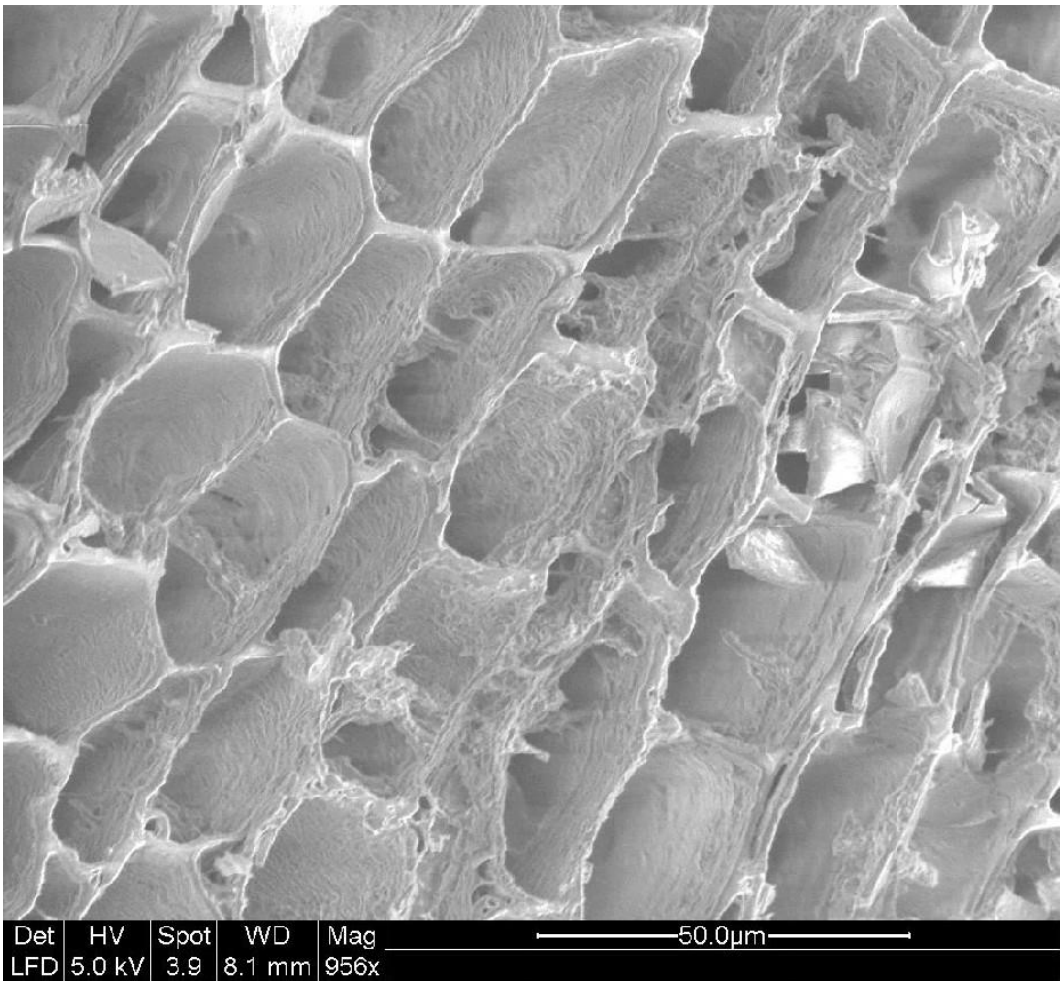

Figure 1-7: 4: An ESEM image of freeze-dried Viking Age wood (Christensen, 2013).

The archaeological wood used for observation of chitosan penetration was 2 x 0.75 x 0.75 cm in size (Christensen, 2013). This is a concern as some of the artefacts will be larger than this, hence even if full penetration of the wood is achieved it may not mean that full penetration would be achieved in an actual artefact. Alongside the use of two types of chitosan, chitosan was also depolymerised by KNO_2 to produce chitosan of lower molecular weight. In addition, the samples with this chitosan and depolymerised chitosan were also treated for 24 h at 60^{o}C.

Treated and untreated wood was investigated for glucosamine content to determine how much chitosan penetrated and remained in the wood. From Table 1 below, taken from Christensen 2013, it is clear that depolymerised chitosan is most effective at being absorbed by the wood (Christensen, 2013). Based on this study, further investigation into chitosan should focus on chitosan oligomers (depolymerised chitosan). It was also observed that chitosan did form a white layer but this could be washed off and, once washed, the untreated and treated samples did not appear different in appearance (Christensen et al., 2015a).

Table 1-1: The penetration of chitosan shown through glycosamine content in treated and untreated wood (Christensen, 2013)

Treatment	**Mean glucosamine content/µmol/g**	**Average chitosan weight/ kDaltons**
Untreated	10.5	None
Chitosan (Kitonor)	502	12.25
Depolymerised chitosan (Kitonor)	615	6.25
Chitosan (Sigma-Aldrich)	446	222.5
Chitosan (Kitonor), heated after impregnation	505	12.25
Depolymerised chitosan (Kitonor), heated	543	Not measured
Untreated but heated	10.5	None

The research by Christensen (2013), suggests that chitosan oligomers may help to overcome the problem of poor penetration and hence research into chitosan should continue. To improve properties, a co-polymer with chitosan and a second and maybe third polymer similar to Walsh's approach should be considered. However, all polymers must be organic soluble and acid stable.

1.8 Chitosan oligomers

1.8.1 Chitosan

1.8.1.1 Introduction

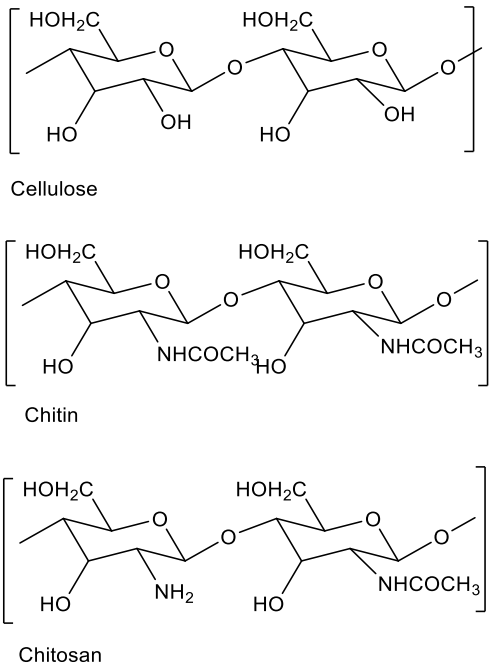

Figure 1-8: Structure of cellulose, chitin and chitosan.

Chitosan is the proposed place to start for finding a sustainable sourced polymer which may prove suitable for preserving wood, as it has a similar structure to cellulose (See Figure 1-8). Chitosan has been previously researched for this purpose and the research thus far has proved promising. However, the wood from the Mary Rose is distinctly different from the Oseberg ship; wet and only very mildly acidic rather than dry and incredibly acidic. Chitosan was used in a water-soluble form in the previous case, but for the Oseberg artefacts, chitosan would need to be dissolved in an organic solvent.

Chitosan has many desirable properties for this purpose, such as being antifungal, antibacterial, non-toxic and compatible for crosslinking. One of the most important is that it has a sustainable source; chitosan is produced from chitin which comes from the shells of crabs and shrimps collected from waste material from the canning process (Ravi Kumar, 2000). Chitosan is a partially N-deacetylated derivative of chitin; as a result the amount of N-deacetylation varies.

1.8.1.2 Sustainable source

Chitin can be sourced from crab and shrimp shells or fungal mycelia. It can be sustainably and easily sourced from the food industry waste material from the canning process of crabs and shrimps (Ravi Kumar, 2000; Rinaudo, 2006; Younes and Rinaudo, 2015). This sustainability, availability, inexpensive cost and similarity to cellulose means it could be used for years to come for wood preservation, if it can be functionalised to perfect its properties. Other treatment methods are either not suitable, ineffective, have too many side effects or are produced from petroleum which will become expensive in the near future and will eventually run out, preventing future use.

1.8.2 Properties and potential for wood conservation

1.8.2.1 Chemical properties

Chitosan is a cationic natural polymer with conformation type zone B (rigid rods) approaching zone C (semi-flexible rods) (Tombs and Harding, 1997). This is very important to keep in mind as it can affect whether it will be able to penetrate the wood. Ideally you do not want something too rigid or it may not penetrate, but if it is too

flexible it may result in folds, also preventing penetration into wood. The fact that chitosan is cationic could be useful, as this could make it easier to cross-link with other polymers which are more commonly anionic. Similarly, aminocellulose is also cationic with a similar structure to cellulose. It has also been found that cationic polymers are capable of chelating metal ions, and aminocellulose esters are stable at low pH (Jung and Berlin, 2005; Zarth et al., 2011). Due to this similarity they might also be worthy of future investigation.

1.8.2.2 Chelation

Chelation properties can be regarded as having chemical and biological properties, as chelation can have biological application and consequences. The chelation properties of chitosan have been known for some time and used in numerous industries: food, agriculture, water purification and medical (Onsosyen and Skaugrud, 1990; Ravi Kumar, 2000) (Dodson et al., 2012). Metal chelation can be a very desirable property; it can be used to remove heavy metals from water, or the body, preventing death from heavy metal poisoning. In agriculture it can control the release of essential metal ions for plant growth. It can also be useful in recovering precious metals (Onsosyen and Skaugrud, 1990; Ravi Kumar, 2000). This could become a very desirable trait with the realisation that rare metals are becoming less abundant and may cause issues in the future (Dodson et al., 2012). Sustainable chemistry is becoming more and more interested in not only reducing the use of these metals, but also in recovering them wherever possible and finding new ways to do this (Alonso et al., 2012). In finding new methods, attention has turned to bio-derived materials to provide a sustainable way of recovering metal for future use and hence improving the sustainable use of

metals (Dodson et al., 2015). Chitosan and chitosan derivatives are among the best bio-derived materials at absorbing metal ions and can absorb a variety of rare metals, including Au, Ir, Os, Pd, Pt and to a lesser extent Sr, but they can also absorb more common metals such as iron and copper (Burke et al., 2002; Dodson et al., 2015). Chitosan has been suggested as a support for metal catalysts to aid metal recovery, which includes Cu for click chemistry to be discussed later in the report as a way of functionalising polymers (Baig and Varma, 2013; Chtchigrovsky et al., 2009; Dodson et al., 2015).

The chelation properties of chitosan are due to the NH_3^+ group on chitosan which is a ligand for metal binding and to electrostatic attraction (Park et al., 1983; Vold et al., 2003). Chitosan binding of Cu^{2+} appears to be very dependent on pH and only occurs over pH 5 which is problematic as the pH of the Oseberg artefacts is pH 1-2. It might be possible to bring the pH up to 3-4. However, over pH 6 or 7 may not be prudent as other forms of degradation may occur which could do yet further damage. Chitosan should not be completely forgotten because of this, as it might be possible to modify it to improve it and it might still be useful for other artefacts that do not have such an extremely low pH. Hence, it is still worth further consideration. This lack of chelation ability below pH 5 is due to the charge on the NH_3^+ group and electrostatic repulsion (Park et al., 1983). If chitosan–metal cation complex formation occurs, for example with Cu^{2+}, there is a H^+ ion by-product, hence the pH may be due to decrease further on chelation. However, this also means at low pH chelation is difficult due to the presence of numerous H^+ ions driving the reaction away from metal complex formation (Vold et al., 2003).

Importantly for the conservation of the Oseberg artefacts, chitosan has been found to bind iron as well as copper, and chitosan derivatives have been found to be effective at low pH (Varma et al., 2004). This ability for derivatives to chelate at low pH is key to its success. Chitosan ETDA/DTPA complexes have been found to be effective at a much lower pH than pure chitosan and it was found that Cu^{2+} was absorbed at pH 1. Absorption of various metal ions was investigated in sulfuric acid (the same acid that is found in the artefacts) and an order of absorption was determined $Ga^{3+}=In^{3+}=Fe^{3+}=Cu^{2+}=Mo^{4+}>Ni^{2+}>\ V^{4+}>Zn^{2+}$, $Co^{2+}>Al^{3+}>>Mn^{2+}$ (Varma et al., 2004).

The good absorption of both Fe^{3+} and Cu^{2+} at low pH is very promising for the use of a chitosan derivative on the Oseberg artefacts. However, as an organic-soluble treatment is desired and the size of the molecule is a concern, EDTA chitosan itself may not be used, but the aim is to find an organic soluble derivative with the same properties. EDTA chitosan should still be investigated for the more robust artefacts which may withstand water treatment and could be considered for the Vasa ship. Another potential way of improving chelation of metal ions in acidic conditions is the addition of sulfonic groups to chitosan (Guibal, 2004) .

Another positive chelation property of chitosan, is that partial cross-linking of chitosan with a compound like glutaraldehyde increases the chelation ability (Varma et al., 2004). This is desirable for conservation, as to act as an effective consolidator chitosan could ideally be cross-linked *in situ* to stiffen the material, binding it to the wood and preventing leaking/leaching.

N-carboxymethyl chitosan has good absorption properties due to the incorporation of the glycine residue and it also reduces conformation rigidity which may be beneficial for wood penetration. Similarly, aspirate and serine derivatives had improved absorption (Varma et al., 2004).

Overall it appears that with functionalisation and crosslinking the chelation properties of chitosan can be improved further, especially at low pH, hence making it suitable for wood conservation, especially when considering some of its other properties as well.

1.8.2.3 Biological properties

Previous research on chitosan oligomers is promising in the context of biology despite the research not being geared towards conservation. It provides vital clues as to the potential desirable differences between chitosan and chitosan oligomers. The oligomers, unlike polymerised chitosan, are easily absorbed through the intestines into the blood. This, along with the known lower viscosity and the increased penetration found with smaller chitosan, suggests perhaps that the oligomers may be able to penetrate the wood when the chitosan itself could not. In addition these oligomers, as well as whole chitosan, have been found to have a variety of characteristics, including inhibitor effects with viruses, antitumor effects through enhancing the immune system and, most relevant to this study, have also proved to have antimicrobial effects. However, the MIC (minimum inhibitor concentration) does not appear to significantly change between the whole chitosan and oligomers (Kim and Rajapakse, 2005; No et al., 2002). Nevertheless, there does appear to be a general increased effect, with an increasing degree of deacetylation (Kim and Rajapakse, 2005). The fact that oligomers

do not have a significant decrease in antimicrobial activity is very promising and the chitosan oligomers could be functionalised to improve the activity further. The exact mechanism for the antibacterial property is not clear; nevertheless, the most accepted mechanism dictates that the cause of the antibacterial property is due to either prevention of material entering into the cell, or leakage of cell constituents caused by alterations to the permeability of the microbial cell membrane. A change of cell morphology from spherical to irregular has been observed, which indicates a separation of the cell membrane from the cell wall. Another suggested mechanism is by chelation of essential metals preventing its growth (Kim and Rajapakse, 2005).

It has been found that the positively charged nature of the chitosan allows it to bind to the bacterial cell wall. This is achieved through the positively charged amino groups interacting with the negatively charged carboxylic acid group of macromolecules on the bacterial cell surface (Kim and Rajapakse, 2005). Hence, it will be desirable to leave the amino group intact as much as possible in the hope that it will attach to the broken-down cell walls in the wood. This property could also allow cross-linking with another polymer to be added. Previous research also gives an idea of the desired size; it has been found that chitosan oligomers smaller than 2.2 kDa did not suppress growth but they did at 5.5 kDa and low molecular weight chitosan from 5-27 kDa were found to be effective (Kim and Rajapakse, 2005).

Another indication to improve the properties of chitosan derivatives comes from another study where asparagine residues were added via N-conjugation. The idea was that a potent positively charged group may improve the binding to the bacteria and hence its effects. This was found to be correct. Hence, if positive groups are added to

the chitosan, the antibacterial properties will be increased. The antifungal effects appear to follow the same path: the positive groups bind to negatively charged groups on the fungi surface and interfere with the growth and physiological function of the fungi (Kim and Rajapakse, 2005). The Oseberg artefacts have never had any fungal problems in the past and are not likely to have fungal problems in their current conditions in a museum. They are highly acidic and museum conditions maintain low moisture and a low temperature to reduce chances of fungal growth. However, increasing the pH, which is desired, and adding a polysaccharide i.e. food, could lead to fungal growth, although the museum environment should still prevent this. However, storage conditions are not always as good as exhibit conditions and many need significant improvement. The treatment itself is the most likely time for bacterial and fungal growth. Treatment may require between 2-16 weeks for small to medium artefacts in aqueous conditions, which can lead to microbial growth if there are no anti-bacterial or fungal agents in the treatment. It is also worth taking into account that there could be unforeseen circumstances, such as a poor economy or war, which could hinder the museum's capabilities for safeguarding artefacts. It has also been suggested that shifting climate zones, hence increasing temperatures, could also affect the temperature inside museums, and in colder regions could increase fungal growth in museums (Huijbregts et al., 2012). There are many organic artefacts that due to poor conditions in the past, have at some point since their excavation had some degree of fungal degradation and it is still a problem for museums in general today (Blanchette et al., 1994; Cappitelli and Sorlini, 2005; Ciferri, 2002; Dardes and Rothe, 1998; David, 2001; Ljaljević-Grbić et al., 2013; Meier, 2001; Pangallo et al., 2007; Sterflinger, 2010; Sterflinger and Piñar, 2013). Plastics from slightly more modern

times are now starting to reach museums and although many have suggested many forms of degradation due to light and chemical deterioration, biological deterioration has not really been thought to be an issue, but it has been found that there are some microorganisms which are capable of degrading synthetic polymers. This is an issue for plastic artefacts now reaching museums, but also for other artefacts which have been conserved with synthetic polymers; these are not immune to decay from microorganisms, as it was first thought, and there is now more research into this area (Cappitelli and Sorlini, 2008; Cappitelli et al., 2004). This is another reason why a natural polymer should not be disregarded, as synthetic polymers can also be degraded by microorganisms. Therefore, with all this in mind, an antifungal additive, provided it does not harm the artefacts, could still be a very sensible precaution to preserve the artefacts in the future.

Chitosan has also been found to act as an antioxidant and this effect appears to be due to the amino and hydroxyl groups which react with unstable free radicals to form a more stable macromolecule radical. However, this effect appears to be positively influenced by chitosan's ability to chelate Fe^{2+} through the lone pair on the amino group, which allows proton donation through the hydroxyl and amino groups (Kim and Rajapakse, 2005). This antioxidant effect appears to be increased with an increasing degree of acetylation and decreasing molecular weight. This information supports the use of oligomers rather than larger chains of chitosan and this chelation ability is very important for conservation.

1.8.3 Previous use for conservation

Chitosan has previously been tried for conservation purposes. However, penetration seems to be a problem, although depolymerised chitosan did appear to have improved penetration ability (Christensen, 2013). Similar problems were found by Walsh's team (2015) with their chitosan derivatives for conservation of the Mary Rose (previously described see page 16). Despite the penetration problems previously encountered, chitosan should not be disregarded as a conservation material but rather the method of application and the size of chitosan should be reconsidered. A mixture of spraying and injection may permit superior penetration as the degradation inside the wood is greater than the outside. Therefore, starting from the inside may increase overall penetration. Chitosan of especially short chains may leach out of the wood but polymerisation *in situ* and potentially cross-linking with another polymer, may prevent leaching and will increase the consolidation effect.

Chitosan oligomers might be the answer to poor penetration. Oligomers are short chains of polymers and as such are more likely to penetrate into the wood.

1.8.4 Previous use of chitosan to treat non-archaeological wood

There have been a few articles in the past decade which have focused on the use of chitosan for wood preservation outside archaeology (Eikenes et al., 2005; Kjøniksen et al., 1997; Larnøy et al., 2005, 2006a, 2006b). These articles collectively found that acetic acid is more effective than HCl for dissolving chitosan to increase penetration and there was increasing uptake with decreasing viscosity. Penetration is species

dependent, based on how the chitosan is taken up through the wood. Chitosan is taken up through fibrilles in the cell wall in soft wood which are very narrow and hence only monomers and oligomers can penetrate through the wood. In hardwood however, chitosan travels through vessels allowing for better penetration. The direction in which chitosan best penetrates through the wood is also dependent on the type of wood (Larnøy et al., 2005). It was also found that heat treatment increased hydrophobicity and elasticity of wood but also leads to discolouration (Larnøy et al., 2006b).

1.8.5 Reason for proposed use

Chitosan oligomers have many desirable properties for a conservative consolidant. They have low molecular weight, low viscosity, rigid rod/coiled rod shape, are non-toxic, natural and sustainable, they chelate metal ions and have antibacterial and antifungal properties. These attributes are highly desirable for a consolidant. However, chitosan oligomers are hydrophilic (water-soluble) which could be useful for preserving some artefacts, but the artefacts with the Oseberg Ship have been dried and some are so badly preserved that it would not be prudent to add water, as it could result in further hydrolysis and dislodgement of material. The fact that it is a natural polymer with a sustainable source and has many desirable properties makes it a perfect polymer to try to improve it for a conservation purpose which may allow for a water-soluble version and an organic-soluble version to be produced. The use of water or organic solvent could then be determined by the condition of the wood. Hence, the final outcome would not only be applicable to the Oseberg artefacts, but to a wide variety of artefacts and possibly for other industries, for example in the construction industry where wood needs to be kept in good condition for long periods of time, and also in

older buildings where old wood must be preserved. For example, treating an old windowsill and repainting could be cheaper but also means that original features can be kept. What must now be considered is how best to functionalise it to improve its properties and which if any, second polymer would be appropriate to cross polymerise it with, to add other properties which may be lacking in chitosan.

1.8.6 Functionalisation/modified

Functionalisation of natural polymers is one approach for dealing with the issues related to conservation such as avoidance of water (to avoid hydrolysis but also in relation to fragility of the artefacts), problems with metal ions and problems with bacteria growth. Functionalisation of natural products, however, retains some benefits of natural polymers in relation to the sustainability of producing the compound used for conservation and also its properties. This should result in it more closely resembling the compounds naturally found in wood, but it must be kept in mind that functionalisation will drastically change the properties of the natural polymer.

It is hard to predict all the changes in properties that the functionalisation will affect, hence the best way to address this is to re-characterise the polymer to determine the properties of the polymers and how they are different from the original compound. At this point, for conservation reasons, is it also vital to investigate how it interacts with lignin.

Possible modifications to make chitosan organic soluble are covered in Chapter 4

Chapter 2. Characterisation of chitosan and depolymerised chitosan for conservation

2.1 Introduction

2.1.1 Analytical ultracentrifugation

Analytical ultracentrifugation (AUC) is an established tool for characterising proteins and polysaccharides through determination of molecular weight, size and shape and by investigating interactions between macromolecules with "ligands" (other macromolecules or smaller moleculae) (Harding, 2012). It was invented in 1925 by Theodor Svedberg, who later won a Nobel Prize for his work on proteins in 1926, based on this technique (Harding, 2012; Svedberg, 1926). This technique is instrumental in work on macromolecules, both natural and synthetic, especially for biological purposes as it can characterise the molecules in their natural state using biologically relevant solutions (Cole et al., 2008). Analytical ultracentrifuge techniques of sedimentation velocity and sedimentation equilibrium are absolute, matric free techniques which do not require standards, making the results more reliable as there is not interference from a matrix (Harding et al., 2015). Analytical ultracentrifugation is broadly applicable, in that it can be applied to a variety of molecules in a variety of solutes and over a wide range of concentration. There are a variety of somewhat later techniques such as mass spectroscopy (MS) and gel permeation chromatography (GPC) which are complementary and provide a second means of analysis from a different method to analytical ultracentrifugation (Berkowitz and Philo, 2015). Gel permeation chromatography (GPC) relies on comparing results to a similar polymer of a known molecular weight (a standard); this works very well when a polymer has very similar properties to the standard but when these properties deviate, the error can be larger (Morris et al., 2009a). Therefore, AUC is still largely

used due to its power and versatility, theoretical simplicity and direct relevance to the solution (buffers can be used to mimic biological fluids, many macromolecules are pH dependent, measurement in the same conditions allows reasonable conclusions to be drawn) without the need for a separation matrix (Schuck, 2000).

It is also more suitable for looking at interactions, particularly ones that are concentration or solvent dependent, or involve very large molecular weights or polydispered systems. The real advantage is that because AUC is not a comparision method like GPC which compares the polymer to a standard, it can also analyse polymers in biologically relevant solutions, for example in buffers with the same pH as blood. It can also be used to identify and quantify macromolecular interactions and self-association in proteins and more recently aminocelluloses (Heinze et al., 2011; Nikolajski et al., 2014; Schuck, 2003). Finally, and most importantly, further information can be obtained by using it alongside other more modern methods, such as size exclusion chromatography and multi-angle light scattering, which is especially true for analysis of polysaccharides (Harding, 2005a). It can also act alongside other techniques for conformation purposes (Harding et al., 2015).

2.1.1.1 Relevance to project

The relevance to conservation of wood is twofold: firstly the determination of the size, conformation and flexibility of a candidate polymer consolidant will determine if it can penetrate into the wood. The distribution will also give an estimate of what proportion of a batch of polymer will be able to penetrate into the wood. Natural polymers have a range of molecular weight and this can be quite broad; knowing how

big this range is (its polydispersity) and where its range lies is key, along with the size and shape of the molecule for determining if a batch of natural polymer is likely or not to penetrate into the wood. There is rarely an abundance of archaeological wood to test on and the advantage of this work is that if it is found that a polymer has a substantial distribution at high molecular weight (>10000 Da) which will never penetrate the wood, it does not have to be tested on the precious rare wood. The molecular weight likely to penetrate the wood structure is dependent on shape. Polyethylene glycol (PEG) 200-4000 Da is used for conservation, depending on the state of degradation, but PEG is a long linear polymer, and polymers based on a glucose-like backbone will be shorter and have stiff chains which might increase the molecular weight which will penetrate well into the wood. AUC analysis, prior to wood treatment, could reduce wasting archaeological wood on tests that are incredibly unlikely to ever work. The second relevance to conservation of wood is that interaction with lignin, cellulose, or a secondary consolidant (a candidate lignin substituent or other polysaccharide 'like' guar gum or other yet to be investigated (McHale et al., 2016a; Walsh et al., 2014c, 2017) can be explored at the molecular level in the analytical ultracentrifuge so as to probe potentially favourable interactions within the wood.

2.1.1.2 Theory

The solution being investigated is inserted into the solution channel of a dual sector AUC cell and a reference solvent is placed in the other sector. Comparison to solvent helps to account for a baseline reading. The cell has transparent windows which allows light to be passed through the cell and the sedimenting profiles to be registered optically (Rayleigh interference or, if there is a chromophore, uv/vis absorbance) by

photomultipliers (absorbance) or a charge-coupled device (CCD) array (interference) (Harding, 1994). The high rotational speeds cause a gravitational field which causes the mass to redistribute accordingly. This results in the separation of molecules with larger molecules sedimenting first; additionally, compact molecules, such as spherical-shaped molecules, will sediment faster than random coil or rod-shaped molecules as there will be less friction between them. An analytical centrifuge can run up to 50,000 rev/min (Harding, 2012). There are two principal forms of AUC technique. The first of these, s*edimentation velocity* (SV) works at relatively high rotor speeds, hence creating a high centrifugal field in which back diffusion effects are relatively small. From the sedimentation rate or sedimentation coefficient distribution, hydrodynamic information can be provided about the size distribution, shape and interactions of macromolecules. The second principal form of AUC technique is s*edimentation equilibrium* (SE) which is established at lower centrifugal fields where there is an equilibrium between sedimentation and back diffusion which is formed. This provides molecular weight/ molar mass information directly (as there are no friction and shape effects) and also information about mass-action effects (association constants) and thermodynamic non-ideality effects. The partial specific volume of the polymer(s) defined by Tanford (1961) are required as well as the density and viscosity of the solvent (Cole et al., 2008; Tanford, 1961), as sedimentation properties depend also on the density difference between solute and solvent.

2.1.1.2.1 Sedimentation velocity analysis

Sedimentation velocity can be utilised to determine the sedimentation coefficient using the Svedberg equation (Eq. 2-1), the concentration dependant coefficient of the

sedimentation coefficient k_s (Gralén parameter) (Eq. 2-2) and the translation diffusion coefficient (D) from Stokes-Einstein equation (Eq. 2-3) and distribution/purity/interactions (Cole et al., 2008; Gillis, 2014).

$$s = \frac{v}{\omega^2 r} = \frac{M(1-\bar{v}\rho)}{N_A f} \quad \textbf{2.1}$$

M= molecular weight (Da) or molar mass (g/mol)
$\bar{v}$= partial specific volume of the particle (ml/g)
ρ_o= density of the solvent (g/ml)
ω= rotor speed in radians per second ($\omega=2\pi \cdot rpm/60$)
r=distance from centre of the rotor (cm)
v=velocity (cm/sec)
s=sediment coefficient (Svedberg units S, where $1S=10^{-13}$ sec)
f =frictional coefficient (dvn.sec/cm)
NA=Avogadro's number (6.02214×10^{23} mol^{-1})

The sedimentation coefficient $s_{20,w}$, like viscosity is dependent on concentration because of the effect of non-ideality which increases with increasing concentration (and approaches zero as $c \rightarrow 0$). To negate this effect, sedimentation coefficient analysis can be carried out at very low concentrations or s vs. c can be plotted based on Eq. 2.2 and extrapolating to zero concentration. Non-ideality can also be reduced by using a suitable buffer. The ions in the buffer will limit the interaction between molecules and therefore non-ideality.

$$\frac{1}{s_{20,w}} = \frac{k_s}{s^o_{20,w}} c + \frac{1}{s^o_{20,w}} \quad \textbf{2-2}$$

Plotting $1/s_{20,W}$ vs. c can be used to calculate k_s as the slope is equal to $k_s/s^o_{20,w}$ and the intercept is $1/s^o_{20,w}$ (Eq. 2.2)

k_s= concentration dependent parameter of the sedimentation coefficient (known as the Gralén parameter) (Harding et al., 2015; Morris et al., 2014).

$s_{20,w}$ = sedimentation coefficient normalized to standard conditions (viscosity and density of water at 20 ºC (S).

c=concentration (g/mol)

$$D = \frac{k_B T}{N_A f} \quad \textbf{2-3}$$

D=translation diffusion coefficient (cm^2/sec)

k_b=Boltzmann constant ($erg \cdot K^{-1}$)

$R = k_b N_A$ =gas constant ($erg.mole^{-1}.K^{-1}$)

The frictional coefficient can be eliminated by combining Svedberg equation (2-1) and Stokes-Einstein equation (Eq.2-3) to produce Eq.2-4 (Brown et al., 2011).

$$s = \frac{M(1-\bar{v}\rho)D}{RT} \quad \textbf{2-4}$$

Calculation of the sedimentation coefficient for one particular molecular species i.e. a tight group of molecular weights (monodispersed systems), requires only the rate of movement of the boundary and the value of rpm rotor speed. For a polydispersed system, where there is a range of different molecular weights, the shape of the boundary also becomes important: a boundary which not only will move due to sedimentation but will spread with time because of diffusion. The Lamm equation (Eq. 2-5), which describes change of concentration distribution along the cell (radius of the cell) with time, can be used; however, this needs to be solved with an algorithm that fits the data, looking for the optimum solution to the equation (Gillis, 2014; Harding et al., 2015). The plot showing differential distribution of sedimentation coefficients

g(s) vs. *s* which is obtained from this, shows change in concentration distribution with radius *r* over time *t*, for a polydisperse solution.

$$\frac{dc}{dt} = D\left[\left(\frac{d^2c}{dr^2} + \frac{1}{r}\left(\frac{dc}{dr}\right)\right)\right] - s\omega^2\left[r\frac{dc}{dr} + 2c\right] \quad \textbf{2-5}$$

Once the sedimentation coefficient is known (or the weight average sedimentation coefficient for a polydisperse distribution) it is usually adjusted to standard solvent condition (viscosity and density of water at 20.0 ^{o}C) to yield $s_{20,w}$ (Eq.2-6) (Gillis, 2014).

$$s_{20,w} = \frac{(1-\bar{v}\rho)_{20,w}}{(1-\bar{v}\rho)_{T,B}}\frac{\eta_{T,B}}{\eta_{20,w}}s_{T,B} \quad \textbf{2-6}$$

2.1.1.2.2 Analysis package (SEDFIT for SV)

The SEDFIT program was originally written by Schuck in 2000 and later updated by Damm and Schuck (2004). The latest version is 15.01b created in 2015. The program uses the host computer's processor(s) to find solutions to the Lamm equation (Eq. 2-5 above) (Gillis, 2014). SEDFIT solves the Lamm equation (Eq. 2-5) in terms of apparent distribution of sedimentation coefficients *ls-g*(s)* vs. *s*. Here, *ls* stands for "least squares analysis" and * for apparent due to presence of effects of non-ideality and diffusion. The plot *ls-g**(*s*) vs. *s* is often abbreviated as *g(s)* vs. *s* (see Harding et al, 2015). SEDFIT works by superimposing a fit: the model has a step system and tries to fit the stepped model as closely as possible to the real data. First, noise must be removed; this includes time invariant (TI) and radial invariant (RA) noise. Removing

TI noise removes any patterns which do not change during the course of the run and RI removes jitter from fringe displacement, an artefact of Fourier Transformation.

The *g*(*s*) vs. *s* plot is affected by diffusive broadening. In large macromolecules such as polysaccharides, the diffusion effect is small. SEDFIT can account for the diffusion with continuous distribution (continuous distribution of sedimentation coefficients) *c*(*s*) vs. *s* (Gillis, 2014).

In the *c(s*) vs. s method within SEDFIT, the diffusion is taken into account by finding the average frictional ratio (f/f_o), the drag of a molecule compared to a perfect sphere of the same mass determined with Eq. 2-9 which in turn is used to determine the diffusion coefficient via Eq. 2-7 and Eq. 2-8 rearranged to Eq.2-9. This leads to peak sharpening.

$$\frac{f}{f_0} = \frac{M(1-\bar{\nu}\rho_0)N_A}{N_A 6\pi\eta_0}\left(\frac{4\pi N_A}{3\bar{\nu}M}\right)^{\frac{1}{3}}\frac{1}{s} \quad \textbf{2-7}$$

$$\frac{f}{f_0} = \frac{k_B T}{6\pi\eta_0}\left(\frac{4\pi N_A}{3\bar{\nu}M}\right)^{\frac{1}{3}}\frac{1}{D} \quad \textbf{2-8}$$

$$D = \frac{k_B T}{6\pi\eta_0}\left(\frac{4\pi N_A}{3\bar{\nu}M}\right)^{\frac{1}{3}}\frac{1}{\left(\frac{f}{f_0}\right)} \quad \textbf{2-9}$$

Least squares method is used for data fitting: it is a method used for regression analysis to obtain solutions for overdetermined systems. An overdetermined system is one which has more equations than unknowns. Regression analysis is used in statistical modelling to estimate relationships between variables.

η_0= solvent viscosity

The *c*(*s*) method assumes all the molecular weights have the same frictional coefficient. For proteins this approximation is reasonable; for polysaccharides there is a broad range of frictional coefficients. Although not as accurate for polysaccharides, the c(s) method can still identify the presence of different components (Heinze et al., 2011).

This *c*(*s*) vs. distribution can also be transformed with SEDFIT to *c*(*M*) vs. *M,* giving the distribution in terms of molecular weight. It is good for an approximate estimate of molecular weight distribution but is much better suited for proteins than polysaccharides. For polysaccharides, it is better to use the Extended Fujita method (Harding et al., 2011a) as it makes no assumption about frictional coefficients.

2.1.1.2.3 Sedimentation equilibrium analysis

Sedimentation equilibrium is achieved at a lower centrifugal speed compared with sedimentation velocity: at lower speeds the backflow force, due to diffusion, becomes comparable to the centrifugal force and a steady state equilibrium is achieved between centrifugal force and diffusion in the opposite direction (see Figure 2-1, Eq. 2-10) (see Cole et al., 2008; Harding, 2012). Normally a speed of at least 10000 rev/min lower than for sedimentation velocity is used (Harding, 2005b).

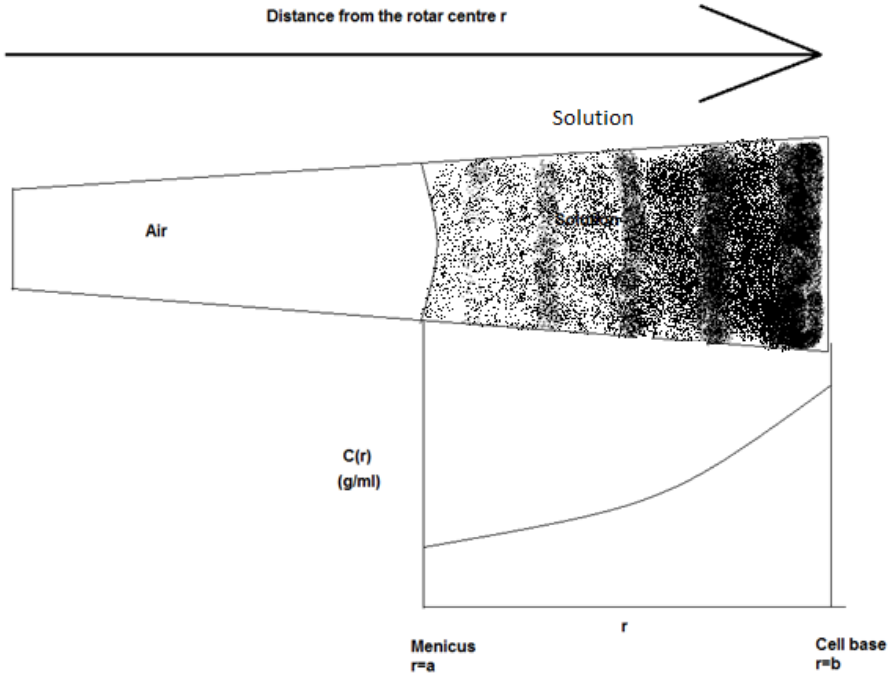

Figure 2-1: A plan view of AUC cell showing centrifugal force and equilibrium distribution of solution. Not to scale.

Sedimentation force

Diffusion force

At equilibrium, sedimentation and diffusion forces are equal and opposite.

$$\omega^2 r M(1-\bar{\nu}\rho) = \frac{RT}{c(r)}\frac{dc(r)}{dr} \quad \textbf{2-10}$$

From sedimentation From diffusion

Eq. 2-10 can be used to calculate weight average molecular mass (Harding et al., 2015; Svedberg, 1926).

Sedimentation equilibrium analysis is not based on the movement of molecules, hence although the time to reach equilibrium is affected by shape, the analysis is not. The analysis is based on the analysis of the concentration gradient curve of the equilibrium state pattern; the fact this is not dependent on shape makes it an absolute method (Gillis, 2014; Harding, 2005b). Rotor speed is important; if the speed is too high, large molecules will sediment to the base and molecular weight will be underestimated; if the speed is too low, the molecules will diffuse back to the meniscus and it will not be possible to analyse the curve.

The weight obtained by sedimentation equilibrium is the weight average molecular weights (M_w). For polysaccharides using Rayleigh interference, the M_n and M_z, the number average and *z*-average molecular weights obtained are not as reliable as the M_w. Schlieren optics are more suited for M_z evaluation (Harding, 2005b) but this optical system is not available on modern instrumentation.

At equilibrium, a concentration curve is formed which is stable. This can be analysed for simple monodispersed macromolecular solutions and data can be fitted to Eq. 2-11 (Gillis, 2014).

$$\frac{d\ln(c)}{dr^2} = \frac{\omega^2 r M(1-\bar{v}\rho)}{2RT} \qquad \textbf{2-11}$$

However, for the vast majority of polysaccharide systems, polydispersity can be high. Equation 2-11 is only valid for short regions of the concentration distribution. For evaluating the weight average molecular weight for the whole distribution, the MSTAR method is used, which was recently implemented into the software package known as SEDFIT-MSTAR (Creeth and Harding, 1982; Schuck et al., 2014a).

2.1.1.2.4 SEDFIT MSTAR analysis

The MSTAR algorithm was developed in 1982 by Creeth and Harding to determine the weight average molecular weight M_w for the whole solute distribution in a sample. It uses Eq. 2-12 to calculate *M*(r)* which is extrapolated to the cell base giving M_w.

$$M_r^* = \frac{(c(r)-c(a))}{kc(a)(r^2-a^2)+2k\int_a^r[c(r)-c(a)dr]} \quad \textbf{2-12}$$

k = a constant (conversion factor for sigma (σ) to molar mass = $(1-\bar{\nu}\rho_0)\omega^2/2RT$) depending on the partial specific volume, solvent density and rotor speed)

r = radial displacement (cm)

c(r) = concentration at radial position r (expressed in either g/ml or fringe displacement units if Rayleigh interference optics are used).

a = radial displacement at meniscus

b = radial displacement at the cell base or bottom

j(*r*) fringe displacement relative to meniscus

J(a) concentration (in fringe displacement units) at the meniscus

J(r) fringe displacement (=*j*(*r*) + *J*(*a*))

$$M^*(b) = M_{w,app} \quad \textbf{2-13}$$

where $M^*(b)$ is the value of M^* extrapolated to the cell base or bottom; $M_{w,app}$ is the apparent weight average molecular weight over the whole distribution (Eq. 2-13). The "app" signifies apparent molecular weight (i.e. not corrected for non-ideality). The algorithm has been inserted into SEDFIT for analysis creating SEDFIT-MSTAR (Schuck et al., 2014b). $M^*(r)$ is progressively closer to the $M_{w,app}$ towards the cell base, $r=b$, and by the time the base is reached (this usually requires a small extrapolation) $M^*(b) = M_{w,app}$ (see Figure 2-2). However, optical distortion at the cell base means extrapolation to the base has to be carried out to find $M_{w,app}$ (Harding, 2005b). To correct for non-ideality, $M_{w,app}$ needs to be plotted against concentration and extrapolated to zero concentration or analysis needs to be carried out at low concentrations so that such effects are negligible.

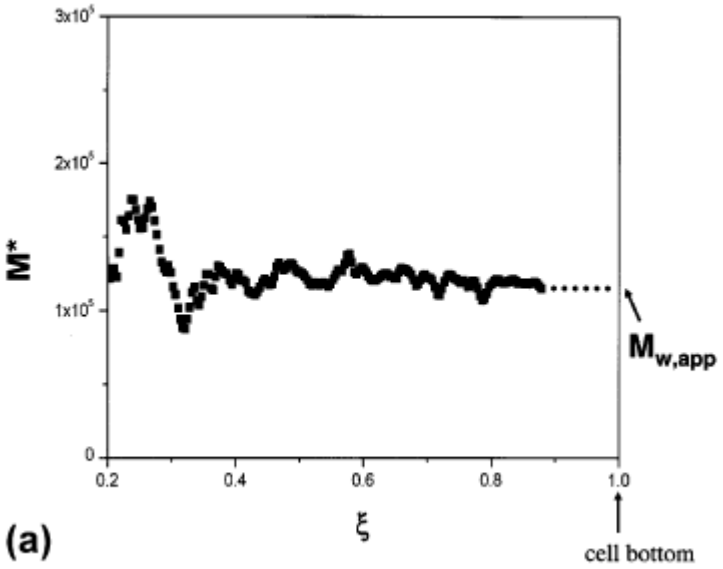

Figure 2-2: An example of an analytical ultracentrifugation sedimentation equilibrium MSTAR extrapolation to the cell base or bottom for a chitosan for determination of molar mass is a normalized radial position squared parameter. $\xi = (r^2-a^2)/(b^2-a^2)$ (Harding et al. 2005b.)

2.1.1.2.5 The plots given by SEDFIT-MSTAR

The SEDFIT-MSTAR algorithm yields:

(i) A distribution plot of molecular weights -*c(M)* vs. *M*. It is a low-resolution method based on least-squares fit (see Schuck et al. 2014). *c(M)* vs. *M* plot although good for proteins, is only very approximate for polysaccharides, but is still a useful supplement to more detailed analysis of a distribution such as MultiSig and the Extended Fujita Method (see below).

(ii) log concentration ln $c(r)$ vs. r^2. This plot includes the raw data and the smooth fit. A straight line shows a monodispersed ideal system. An upward curve (positive sloping concave up curve) is indicative of a polydispersed system. A downward curve (positive sloping concave down curve) indicates non-ideality.

(iii) M^* vs. r plot to yield $M_{w,app}$ as described above. At low concentration where non-ideality is usually small $M_{w,app} \sim M_w$. If non-ideality is present, a plot of $1/M_{w,app}$ against loading concentration c and extrapolation to zero concentration can yield M_w.

(iv) $M_{w,app}(c)$ vs. radius (terms of total signal across the entire cell). This plot is based on the previous $\ln(c(r))$ vs. r^2 plot converted using Eq. 2.11 at individual radial positions r in the ultracentrifuge cell.

2.1.1.2.6 Hinge point analysis in SEDFIT- MSTAR

This is the value of $M_{w,aap}(r)$ at the hinge point (Eq. 2-14). The hinge point is the radial position where the concentration $c(r)$ =the cell loading concentration c. At the hinge point, $M_{w,app}(r=r_{hinge}) = M_{w,app}$, the (apparent) weight average molecular weight over the whole distribution (Schuck et al, 2014).

$$M_{w,app}(r_{hinge}) = M_{w,app} \quad \textbf{2-14}$$

Having two different methods for analysis for $M_{w,app}$ from the same sedimentation equilibrium data, provides confidence in the results.

2.1.1.2.7 MultiSig analysis

MultiSig is another method for analysing sedimentation equilibrium (SE) data and the purpose of this method is to identify discrete components in a solution (Gillis et al., 2013a). This allows for the identification of self-association, impurity and aggregates. Each individual molecular weight within a batch of polymers, if run on its own would theoretically have its own curve with the Eq. 2-15, with $f(M)$ being a function of molecular weight which is given in Eq. 2-17 and $c_1(r)$, the concentration along the radius and $c(a)$ is the concentration at the meniscus.

$$c_1(r) = c_1(a)e^{f(M)} \quad \textbf{2-15}$$

The MultiSig software package (Gillis et al., 2013a) assumes that the polydisperse distribution can be approximated by 17 discrete components. Therefore, this c_1, c_2, c_3

$$c(r) = \sum_{i=1}^{i=17} c(a)e^{f(M)} \quad \textbf{2-16}$$

$$f(M) = \frac{M(1-\bar{\nu}\rho)\omega^2(r^2-a^2)}{2RT} \quad \textbf{2-17}$$

etc. to $c_{17,}$ resulting in Eq. 2-16 representing the whole distribution (Gillis, 2014; Gillis et al., 2013a).

MultiSig works in terms of σ as a representation of molecular weight Eq. 2.18

$$\sigma = M(1 - \bar{v}\rho_0)\omega^2/RT \quad \textbf{2-18}$$

The results from MultiSig give the M_w, M_z and M_n based on the equations 19-21. MultiSig analysis also gives the distribution of molecular weights reflected in 17 components. For a monodispersed macromolecule such as a protein, MultiSig analysis will give a single component unless it has aggregated. For polydispersed macromolecules such as polysaccharides, the distribution will be almost continuous, but the approximation of 17 components can work to approximate the maximum and minimum molecular weights and show where the majority of the distribution lies.

$$\sigma_w = \frac{1}{\sum_{i=1}^{i=n}(c_i\sigma_i/\sum c_i} \quad \textbf{2-19}$$

$$\sigma_n = \frac{1}{\sum_{i=1}^{i=n}(c_i/\sigma_i/\sum c_i} \quad \textbf{2-20}$$

$$\sigma_z = \frac{1}{\sum_{i=1}^{i=n}(c_i/\sigma_i^2/\sum c_i\sigma_i} \quad \textbf{2-21}$$

MultiSig-RADIUS can be used to analyse data along the radius of the cell. MultiSig-RADIUS gives M_w, M_n and M_z along the radius instead of the average. This is similar to the MSTAR $M_{w,app}$ vs. total signal but produces smoother data due to reduced noise (Gillis et al., 2013a). This plot can be useful in looking for self-association and for

monomeric molecular weight of a self-associating polymer, such as aminocellulose (Nikolajski et al., 2014).

2.1.1.2.8 Combining SV and SE results: The Extended Fujita Method

It is possible to combine SV and SE data to get an accurate distribution of molecular weights via the Extended Fujita method. The original Fujita method was the work of H.Fujita in 1962. He transformed the *g(s)* vs. *s* plot to an *f(M)* vs. *M* plot for randomly coiled polymers using Eq. 2-22:

$$f(M) = g(s).(\frac{ds}{dM}) \quad \textbf{2-22}$$

$$s = \kappa_s M^{0.5} \quad \textbf{2-23}$$

This uses the exponent 0.5 for random coil polymers and equation 2-23:

The Extended Fujita Method (Harding et al., 2011) extends this method for different shapes of polymers by using *b* as the exponent. *b*= 0.4-0.5 for a random coil, ~0.15-0.2 for a rod and 0.67 for a sphere. This allows for *f*(*M*) vs. *M* analysis of a wider range of macromolecules. It substitutes a general coefficient *b* for 0.5 in the above equation resulting in Eq. 2-24 and 2-25.

$$s = \kappa_s M^b \quad \textbf{2-24}$$

$$\left(\frac{ds}{dM}\right) = b.\kappa_s^{1/b}.s^{(b-1)/b}) \quad \textbf{2-25}$$

b is related to the Mark Houwink-Kuhn Sakurada (MHKS) a coefficient according to Tsvetkov relation (Morris et al., 2014):

$$b = \frac{2-a}{3} \quad \textbf{2-26}$$

$$\log s = \log \kappa_s + b log M \quad \textbf{2-27}$$

Using equation 2-26 or the logarithmic form (Eq. 2-27) it is possible to determine κ_s and b through knowing the sedimentation coefficient (from SV) and the weight average molecular weight M_w (from SE) for different molecular weights of the same polymer.

2.1.1.2.9 Partial specific volume ($\bar{v}$)

$\bar{v}$ correction can be done through a re-arrangement (Eq. 2-29 to 2-32) of Eq. 2-10 given again as Eq. 2-28.

$$\omega^2 r M(1-\bar{v}\rho) = \frac{RT}{c(r)}.\frac{dc(r)}{dr} \quad 2\text{-}28$$

$$\text{M}= (\frac{RT}{c(r)}.\frac{dc(r)}{dr})/\omega^2 r(1-\bar{v}\rho) \quad 2\text{-}29$$

$$\text{M}= \frac{1}{(1-\bar{v}\rho)}.\frac{\frac{RT}{c(r)}.\frac{dc(r)}{dr}}{\omega^2 r} \quad 2\text{-}30$$

$$\text{M}=(M_o/\frac{1}{(1-\bar{v1}\rho)}).\frac{1}{(1-\bar{v2}\rho)} \quad 2\text{-}32$$

To correct molecular weight from an approximate working $\bar{v}$ to correct $\bar{v}$ Eq. 2-32.

v1 original $\bar{v}$ used, v2 correct $\bar{v}$.

M_o old M calculated with v1.

2.2 Results

2.2.1 Chitosan

2.2.1.1 Chitosan SV

SV results show the distribution of chitosan in the form of ls *g(s)* vs. *s* (Figure 2-3a). The distribution is also clearly consistent at different concentrations showing reliability. The plots in Figure 2-3b show little concentration dependence. This means in the supporting electrolyte system, non-ideality is not significant. Therefore, the mean was taken as the "ideal" value s^o=1.28±0.05 S. It is also clear from Figure 2-3 that the sample is mono-dispersed and shows that the main distribution is between 0.5-2S. Sedimentation coefficient data can give a rough idea of molecular weight. However, as it is affected by shape as well as molecular weight, to get an accurate distribution of molecular weights that information must be combined with that of SE which gives the average molecular weight. Their average molecular weight will be determined from SE analysis alone, however an f(M) plot to be accurate can only be determined if SV and SE are carried out for five different molecular weights. The analysis of a second molecular weight was carried out but not a range of molecular weights. The time restriction on this project means this must be left to future work. The molecular weights were measured but they are too close together for this analysis to be accurate. A broader scope to determine f(M) through more molecular weight analysis or size exclusion chromatography- multiple angle light scattering (SEC-MALS) must be left for future work.

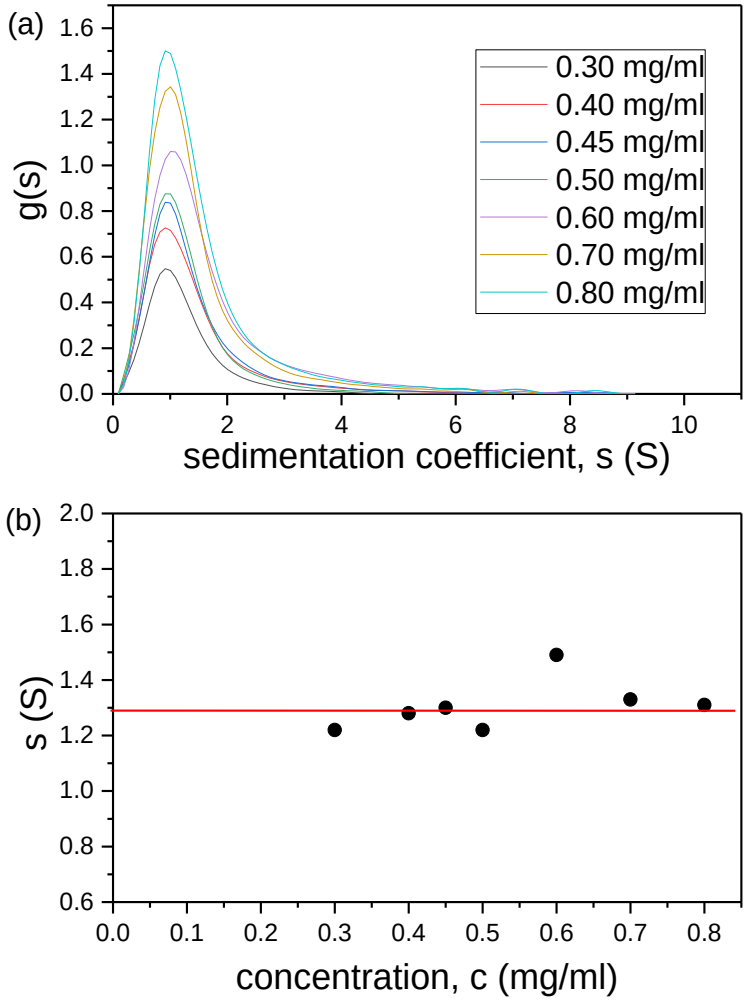

Figure 2-3: Analytical ultracentrifugation sedimentation velocity of sedimentation coefficient (a) Sedimentation coefficient distribution plots $g(s)$ vs. s (S) for Kitonor chitosan at different loading concentrations. (b) plot of s vs. c showing little evidence for significant non-ideality or self-association. The "ideal" value, s^o = (1.28 ± 0.05) S. s is taken as the mean, excluding the outlier (>2 standard deviations away from the mean).

2.2.1.2 Chitosan SE -20 mm cells, 48000 rpm

The longer 20 mm path length allows lower concentrations to be analysed; lower concentrations also lower effects on non-ideality. A high rotor speed was still used (48000 rpm) to give a satisfactory concentration distribution. Therefore, the results for SE should be more accurate. At that high speed, only 3 cells could be run at one time due to rotor specifications for high speeds. The advantage of the 12 mm cells is that

all 7 cells /7 concentrations could be run at the same time. However, these 20 mm cells allow low concentration to be investigated, limiting non-ideaility.

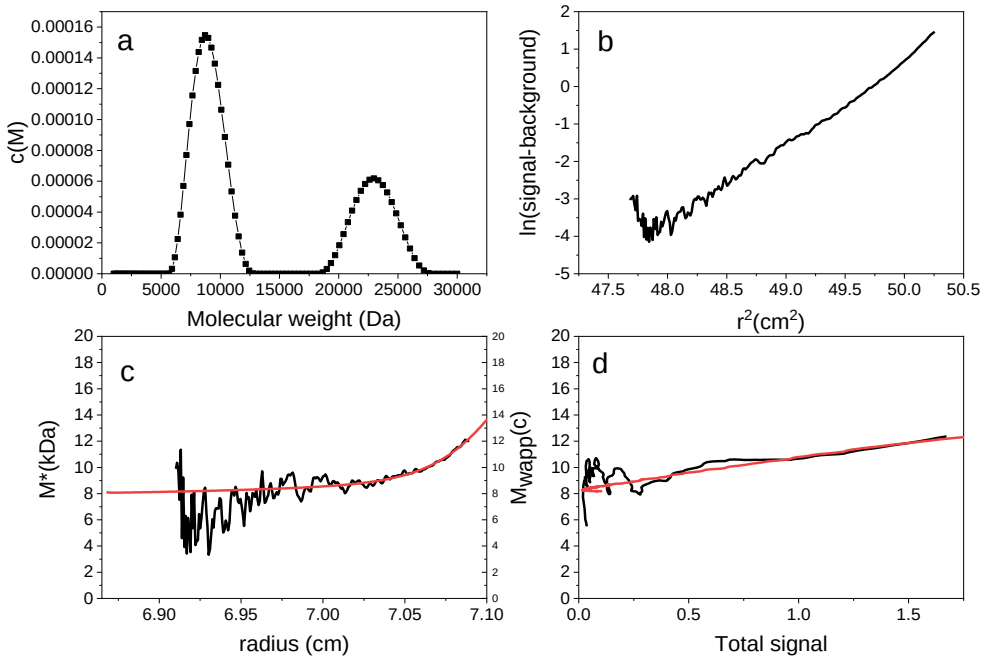

Figure 2-4: MSTAR results for 0.3 mg/ml chitosan (SE run at 48000 rpm). a) shows c(M) vs. M showing two species peaking ~ 8 kDa the other ~ 23 kDa. b) ln(c) vs. r^2 shows a straight line, i.e. no polydispersity and no non-ideality or alternatively equal polydispersity and non-ideaility cancelling each out. c) shows the M* extrapolation giving $M_{w,app}$ = 13.8 kDa. d) shows $M_{w,app}$(c) vs. total signal.

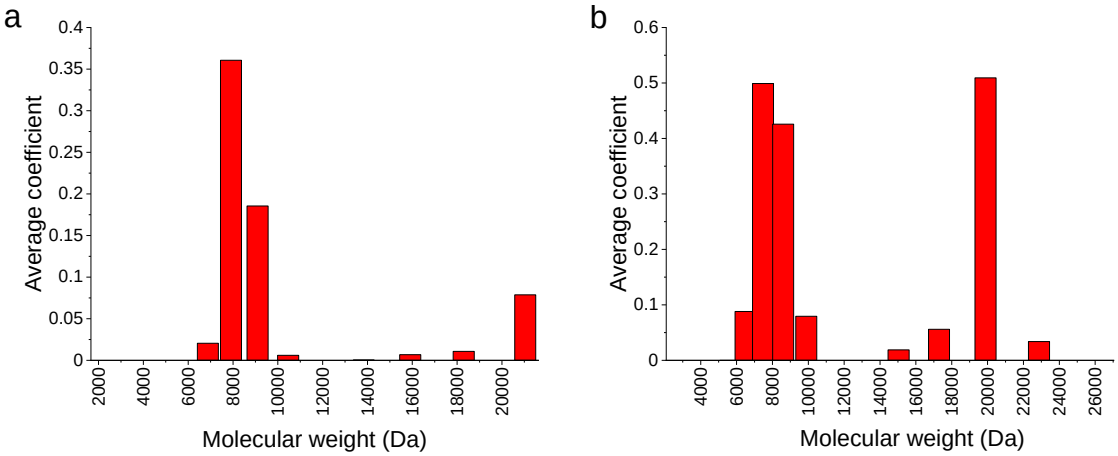

Figure 2-5: MultiSig results for 0.3 mg/ml chitosan. Plot a) is the first analysis and b) the second analysis. The presence of two discrete components ~ 8000 Da (major) and 22000 Da (minor component) is clear.

Figure 2-4 is the lowest concentration of this set, and therefore, should have the lowest non-ideality. Looking at the ln $c(r)$ (ln(signal-background) vs. r^2 plot shows upward curvature, indicating the presence of some degree of polydispersity (for these molecular sizes at such low concentrations, non-ideality effects are likely to be small) (Schuck et al., 2014b). The approximate c(M) vs. M profiles from SEDFIT-MSTAR seem to be reinforced by the MultiSig plot (Figure 2-5). The maximum and minimum where the majority of material lies can be estimated, with the minimum being ~6000 and the maximum ~25000 g.mol^{-1} with the largest proportion around (8000-9000) g.mol^{-1}. The M* extrapolation appears reliable, despite the upward turn near the cell base due to polydispersity.

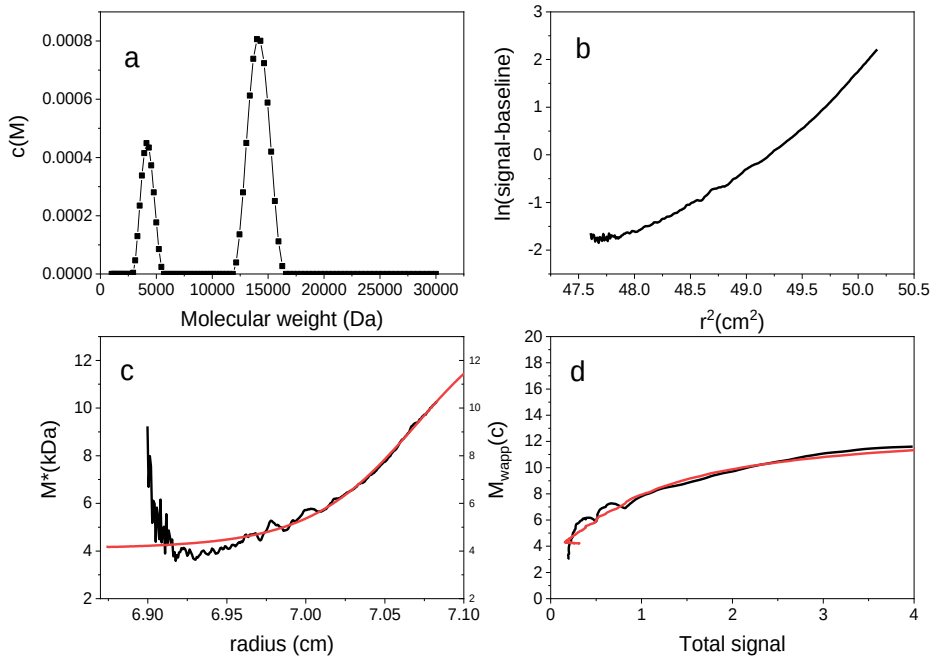

Figure 2-6: MSTAR results for 0.5 mg/ml chitosan (SE run at 48000 rpm). a) shows $c(M)$ vs. M showing two species peaking ~ 4 kDa the other ~ 14 kDa. b) ln(c) vs. r^2 shows an upward curve, i.e. polydispersity. c) shows the M* extrapolation giving $M_{w,app}$ = 11.7 kDa. d) shows $M_{w,app}(c)$ vs. total signal.

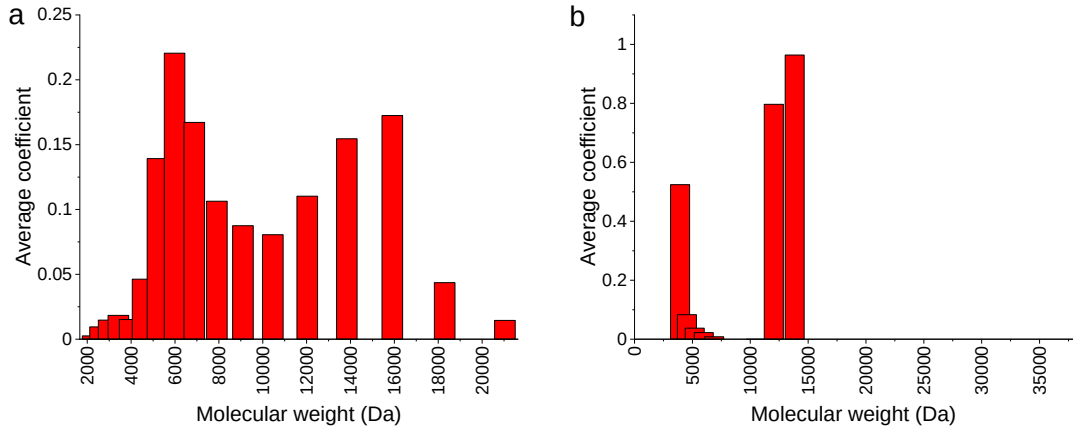

Figure 2-7: MultiSig results for 0.5 mg/ml chitosan. a) is the first analysis and b) the second analysis. The presence of two main components ~ 6000 and 14000 Da is clear but it is also clearly very polydisperse.

Though lowest concentrations are the most reliable, repeated analysis also increases reliability and low concentrations with low fringes can make analysis difficult and less reliable, so a few concentrations have been investigated for insurance. Polydispersity is more obvious from this lnc(r) vs. r^2 but non-ideality still does not appear to be present. Polydispersity is also clearly a problem from the c(M) vs. M and MultiSig average coefficient vs. M as analysis seems completely different. There is also steeper extrapolation for M*; this could be because the high speed resulted in greater sedimentation. Some higher molecular weights may have compacted at the base resulting in steep extrapolation but this can result in steeper extrapolation than needed to compensate for the molecular weights, resulting in a higher molecular weight than is present.

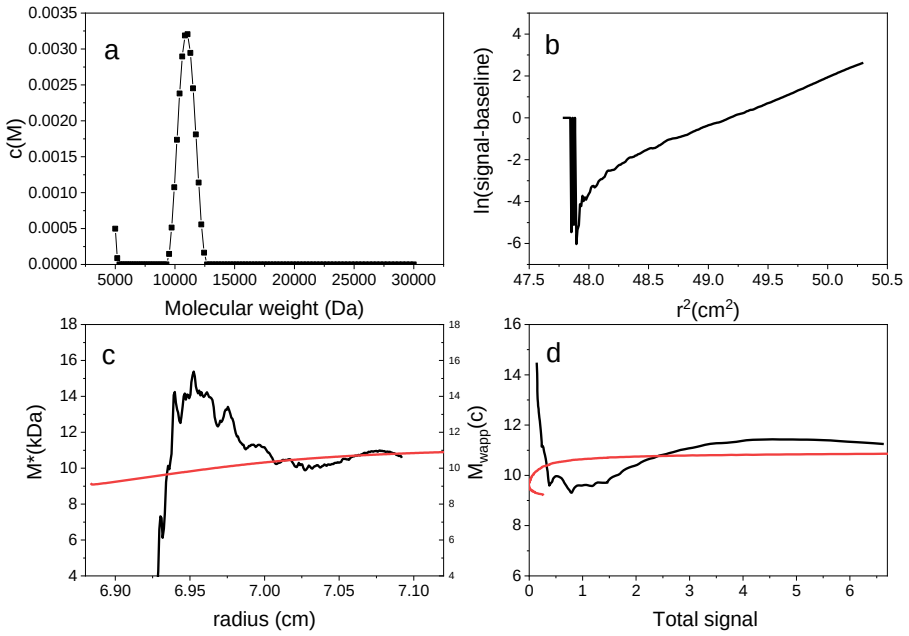

Figure 2-8: MSTAR results for 0.7 mg/ml chitosan (SE run at 48000 rpm). a) shows $c(M)$ vs. M showing one species peaking ~ 11 kDa the other peak is an artefact from the analysis. b) $\ln(c)$ vs. r^2 has a downward curve, this is indicative of non-ideality. c) shows the M* extrapolation giving $M_{w,app}$ = 10.9 kDa. d) shows $M_{w,app}(c)$ vs. total signal.

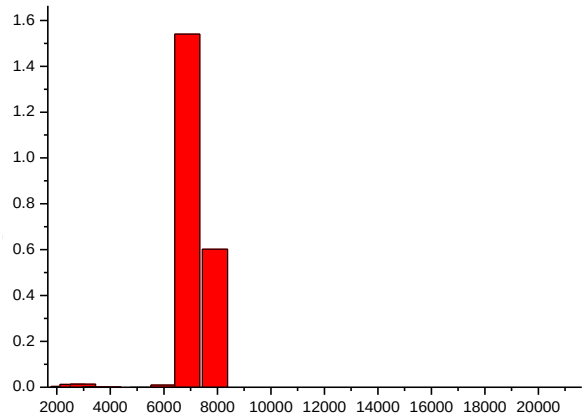

Figure 2-9: MULTISIG results for 0.7 mg/ml chitosan. The presence of one discrete component ~ 7000 Da is clear.

Figure 2-8 (0.7 mg/ml) lnc(r) vs. r^2 plot shows evidence of both non-ideality and polydispersity from both upward and downward curves respectively. Therefore, the results are still useful but must be considered in terms of concentration. That is i.e. for M_w to be established $M_{w,app}$ must be plotted against concentration to get a reliable M_w and should not be estimated from these results alone. Again, the polydispersity means the c(M) vs. M plot and MultiSig results should be questioned as it is highly unlikely there is such as small range of molecular weights.

Table 2-1: Results for SE Chitosan MSTAR analysis 48000 rpm. Buffer used was 0.2 M acetate.

concentration (mg/ml)	**$M_{w,app}$ (from M^*) kDa**	**Standard deviation (kDa)**	**Mz (kDa)**	**Poly dispersity index M_z/M_w**	**r_{hinge} cm**	**M_{wapp} (from M_w (r_{hinge}) kDa)**
0.3	13.8	6.9	17.2	1.25	7.045	10.6
0.5	11.7	4.4	13.3	1.14	7.046	10.3
0.7	10.9	0.9	11.0	1.01	7.062	11.4

The results for $M^*_{w,app}$, hinge $M_{w,app}$ and MultiSig $M_{w,app}$ for 0.5 and 0.7 mg/ml are all consistent (seeTable 2-1). However, non-ideality is clearly present at 0.7mg/ml, meaning results must be plotted against concentration. There were concerns over the speed that the SE was run at, as the sigma of the fringes vs. the radius was high i.e. steep curve, indicating that the speed might be too high for accurate analysis. MultiSig analysis (Figure 2-5 and Figure 2-7) was repeated twice for the lower two concentrations as seen in Fig A and B. These analyses are not the same due to variability in analysis. This highlights the problem with some of the MultiSig analysis. However, it does suggest a minimum molecular weight of 2000 Da and a maximum molecular weight of 25000 Da (Figure 2-5, 7 and 9). It would be good to repeat the

Table 2-2: Summary of SE chitosan MultiSig analysis, run at 48000 rpm. Buffer:0.2M acetate.

Concentration (mg/ml)	**MultiSig M_w (kDa)**	**MultiSig M_z (kDa)**	**Polydispersity M_z/M_w**	**MultiSig M_w (kDa)**	**MultiSig M_z (kDa)**	**Polydispersity M_z/M_w**
0.3	10.0	12.0	1.19	12.2	13.5	1.2
0.5	9.5	11.5	1.21	10.6	12.1	1.2
0.7	10.6	10.8	1.01			

MultiSig analysis for 35000 rpm, but this analysis is very time consuming and is very likely to yield similar results.

2.2.1.3 Chitosan SE -12 mm cells, 40000 rpm

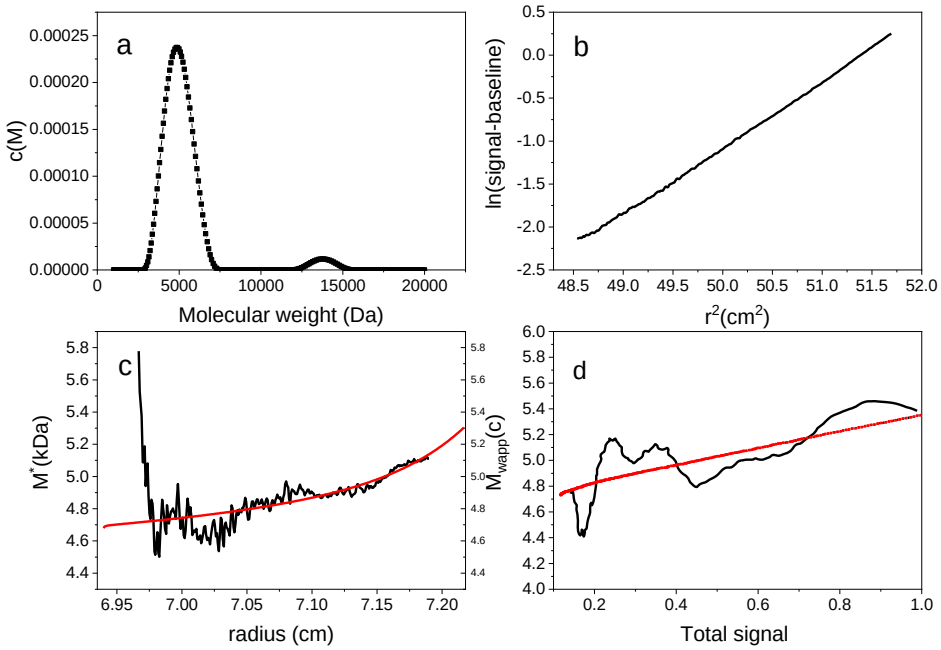

Figure 2-10: MSTAR results for 0.4 mg/ml chitosan (SE run at 40000 rpm). a) shows $c(M)$ vs. M showing one species peaking ~ 6 kDa; the other peak is an artefact from the analysis. b) ln(c) vs. r^2 has an upward curve, i.e. the system is polydispersed. c) shows the M^* extrapolation giving $M_{w,app}$ = 19.6 kDa. d) shows $M_{w,app}(c)$ vs. total signal.

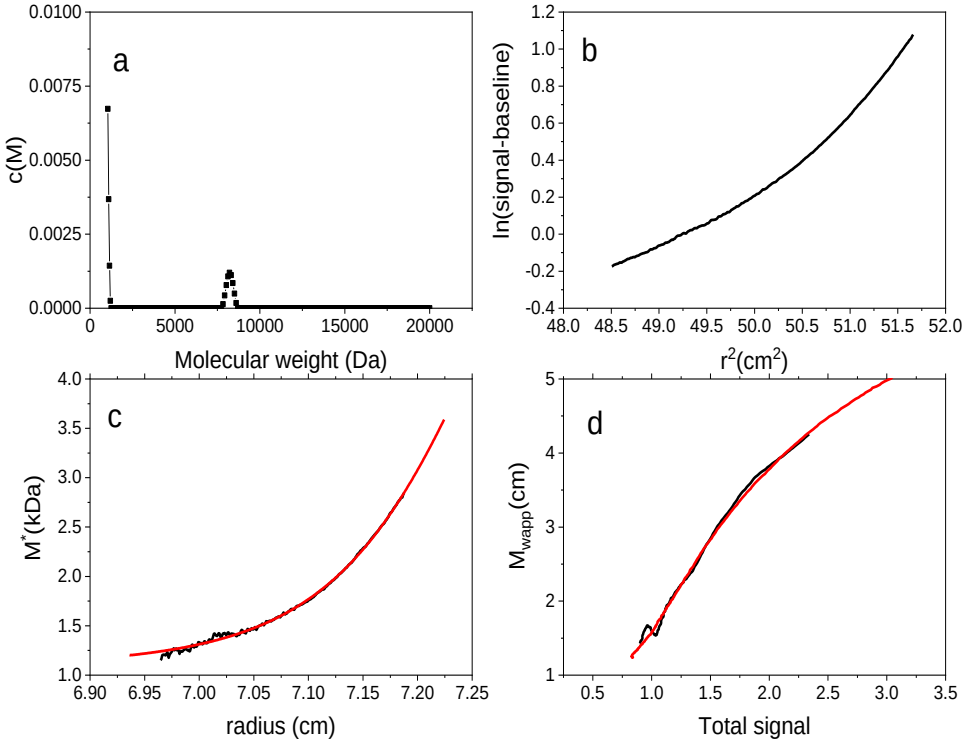

Figure 2-11: MSTAR results for 0.5 mg/ml chitosan (SE run at 40000 rpm). a) shows c(M) vs. M showing one species peaking ~ 6 kDa; the other peak is an artefact from the analysis. b) ln(c) vs. r2 has an upward curve, i.e. the system is polydispersed. c) shows the M* extrapolation giving $M_{w,app}$ = 19.4 kDa. d) shows $M_{w,app}(c)$ vs. total signal.

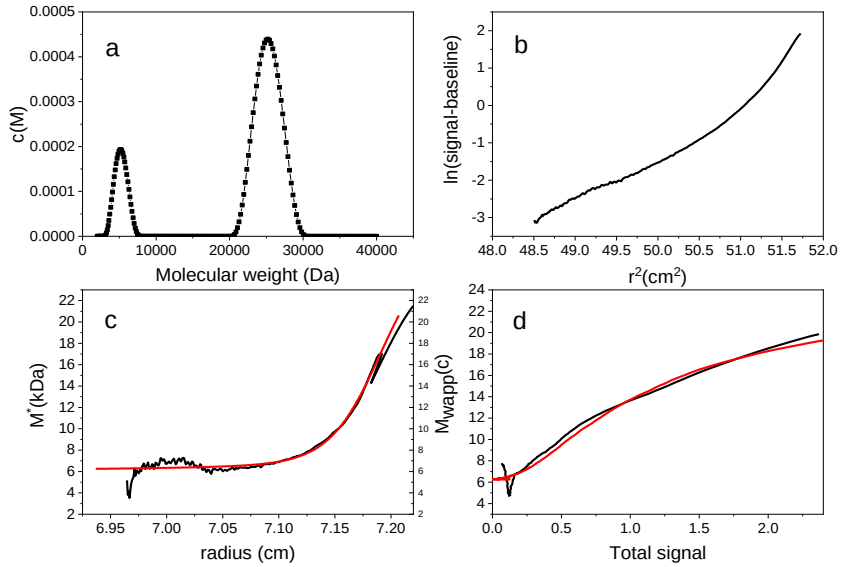

Figure 2-12: MSTAR results for 0.6 mg/ml chitosan (SE was run at 40000 rpm). a) shows c(M) vs. M showing two species peaking ~ 5 and 25 kDa. b) ln(c) vs. r2 has a downward and upward curve, i.e. the system is non-ideal and polydisperse. c) shows the M* extrapolation giving $M_{w,app}$=20.9 kDa. d) shows $M_{w,app}(c)$ vs total signal.

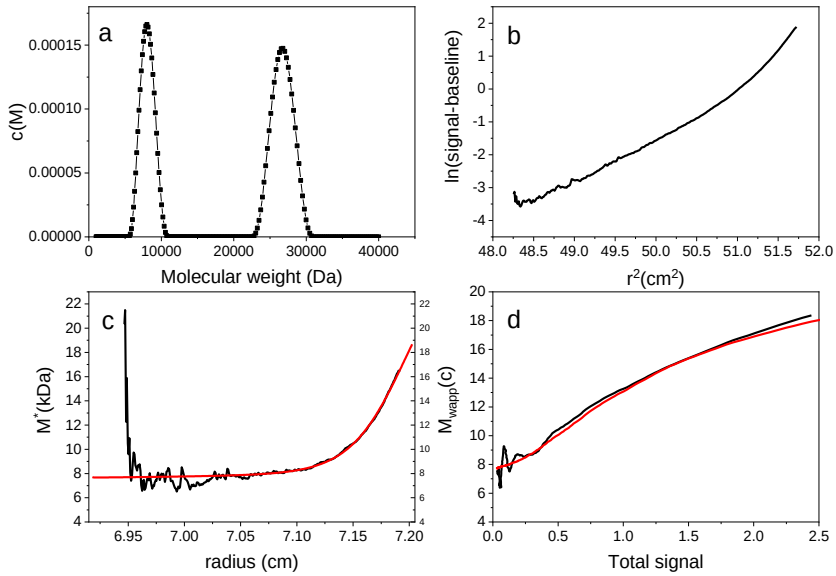

Figure 2-13: MSTAR results for 0.7 mg/ml chitosan (SE was run at 40000 rpm). a) shows $c(M)$ vs. M showing two species peaking ~ 8 and 27 kDa. b) ln(c) vs. r^2 has a downward and upward curve, i.e. the system is non-ideal and polydisperse. c) shows the M* extrapolation giving $M_{w,app}$ =18.9 kDa. d) shows $M_{w,app}(c)$ vs total signal.

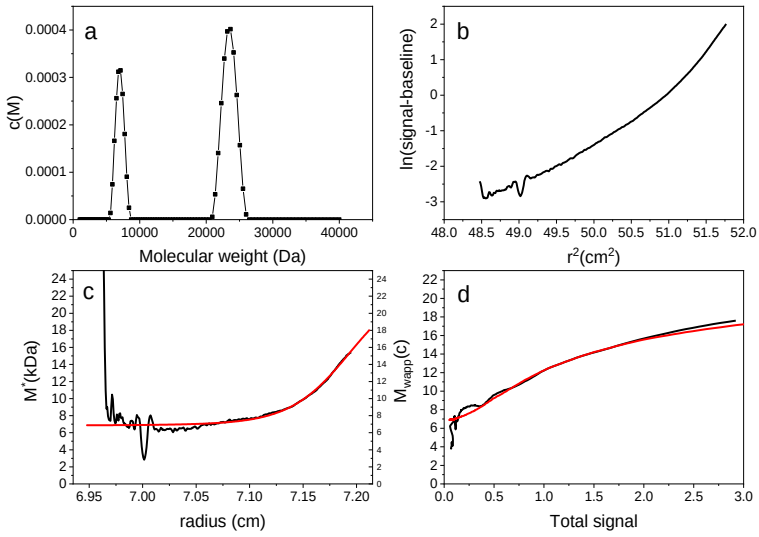

Figure 2-14: MSTAR results for 0.8 mg/ml chitosan (SE was run at 40000 rpm). a) shows c(M) vs. M showing two species peaking ~ 7 and 24 kDa. b) ln(c) vs. r^2 has an upward curve, i.e. the system is polydispersed. c) shows the M* extrapolation giving $M_{w,app}$ = 18.2 kDa. d) shows $M_{w,app}$(c) vs. total signal.

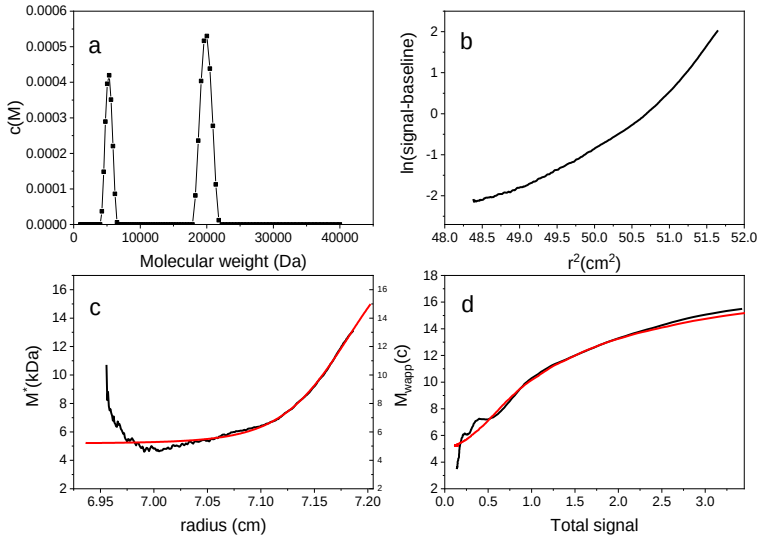

Figure 2-15: MSTAR results for 1.0 mg/ml chitosan (SE was run at 40000 rpm). a) shows c(M) vs. M showing two species peaking ~ 5 and 20 kDa. b) ln(c) vs. r^2 has an upward curve, i.e. the polydispersed. c) shows the M* extrapolation giving $M_{w,app}$ = 15.1 kDa. d) shows $M_{w,app}$(c) vs. total.

Table 2-3: SE chitosan MSTAR analysis results for 40000 rpm. Buffer:0.2 M acetate Parameters $\bar{v}$ =0.57 ml/g, solvent density 1.00111 g/ml, solvent viscosity 0.01118 Poise.

Concentration (mg/ml)	$M_{w,app}$ **(from** M^***) kDa**	Mz **(kDa)**	**Poly dispersity index** M_z/M_w	r_{hinge} **cm**	$M_{w,app}$ **from** $M_w(r_{hinge})$ **kDa**
0.4	19.6	26.6	1.36	7.145	11.9
0.5	19.4	26.4	1.36	7.148	12.4
0.6	20.9	25.1	1.20	7.152	14.9
0.7	18.9	23.5	1.24	7.153	13.2
0.8	18.2	21.5	1.18	7.154	14.3
1.0	15.1	18.3	1.21	7.139	12.3

The Figures 2-10 to 2-15 show the fit, MSTAR extrapolation, distribution and molecular weight along the cell. In this case the linear fit is given rather than the actual fit. Future work will involve reanalysing the data to show the fit that was used for the MSTAR analysis. However, from the data on the ln(c) vs. r^2 it is clear from all concentrations there is polydispersity and from 0.6 mg/ml there is clearly also some non-ideality present. The steep extrapolation of the M* indicates that there may have been larger molecular weights towards the base of the cell or that the speed was too high for the average molecular weight of this polymer. Therefore, this was re-run at 35000 rpm with 20 mm cells which allow for lower concentrations to still give accurate results. Looking at the data below, 0.4 and 0.5 mg/ml might have been too low to analyse in this case and the results might not be as accurate. It is already reported in the literature that 0.5 mg/ml is the minimum concentration for 12 mm cells (Harding et al., 2016). The chitosan was not heated or stored in a desiccator so it may have absorbed some water, hence when weighed out the concentration could be a little less than assumed. Looking at the very steep extrapolation for 0.4 and 0.5 mg/ml and given the hinge point analysis gives a very different result for 0.5 mg/ml; both of these should be discounted from future analysis and the chitosan reanalysed with 20 mm cells and at a lower speed.

2.2.1.4 Chitosan SE- 20 mm cells, 35000 rpm

Table 2-4: SE chitosan MSTAR analysis results for 35000 rpm. Buffer:0.2 M acetate. Parameters $\bar{v}$=0.57 ml/g, solvent density 1.00172 g/ml, solvent viscosity 0.011263 Poise

concentration (mg/ml)	***M*$_{w,app}$ (from *M**) kDa**	**Standard deviation (kDa)**	***Mz* (kDa)**	**Poly dispersity index *M*$_z$/*M*$_w$**	**r$_{hinge}$ cm**	***M*$_{wapp}$ from M$_w$(r$_{hinge}$) kDa**
0.3	25.5	14.4	33.7	1.32	7.076	15.7
0.4	17.0	11.3	34.5	2.03	7.049	12.9
0.5	18.8	10.1	24.2	1.29	7.061	14.8
0.6	18.5	8.8	22.6	1.22	7.065	14.8
0.6 (repeated analysis)	17.0	8.6	21.3	1.25	7.059	14.1
0.7	12.5	3.5	13.5	1.08	7.032	12.1
0.8	15.4	4.9	16.9	1.10	7.068	15.0
1.0	13.8	1.1	13.8	1.00	7.060	14.2
1.0 (repeated analysis)	13.6	0.8	13.7	1.01	7.038	13.6

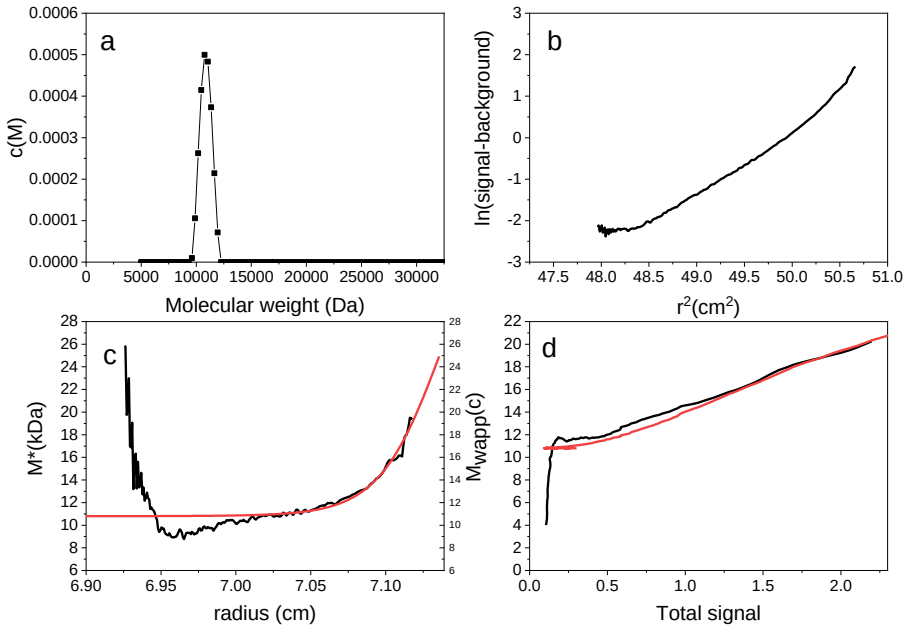

Figure 2-16: MSTAR results for 0.3 mg/ml chitosan (SE was run at 35000 rpm). a) shows c(*M*) vs. *M* showing one species peaking ~ 12 kDa; the second peak is an artefact of analysis due to the polydispersity and non-ideality of the sample making c(M) analysis inaccurate. b) ln(*c*) vs. r^2 has an upward and downward curve, i.e. is polydispersed and non ideal. c) shows the *M** extrapolation giving $M_{w,app}$ = 25.5 kDa. d) shows $M_{w,app}(c)$ vs. total signal

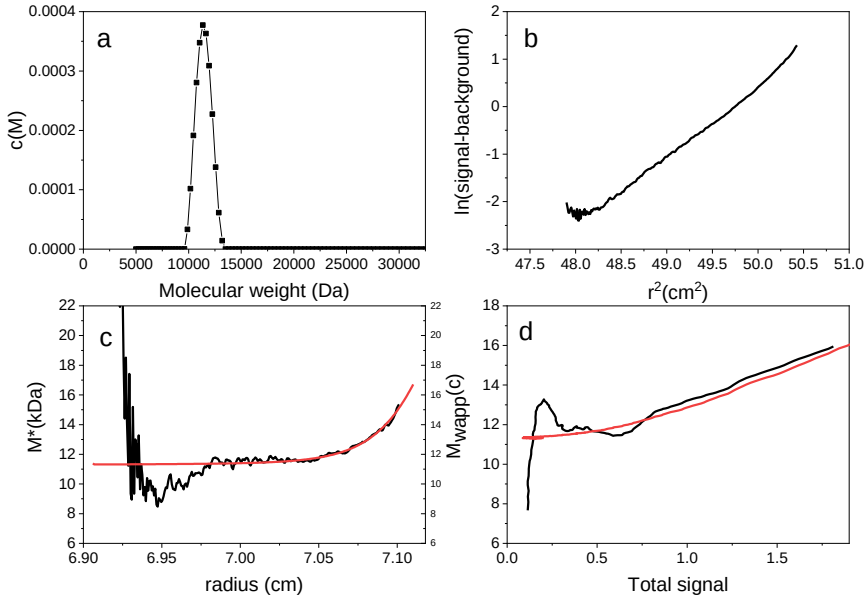

Figure 2-17: MSTAR results for 0.4 mg/ml chitosan (SE was run at 35000 rpm). a) shows c(*M*) vs. *M* showing one species peaking ~ 12 kDa; the second peak is an artefact of analysis due to the polydispersity and non-ideality of the sample making c(M) analysis inaccurate. b) ln(*c*) vs. r^2 has an upward and downward curve, i.e. is polydisperse and non ideal. c) shows the *M** extrapolation giving $M_{w,app}$ = 17 kDa. d) shows $M_{w,app}(c)$ vs. total signal

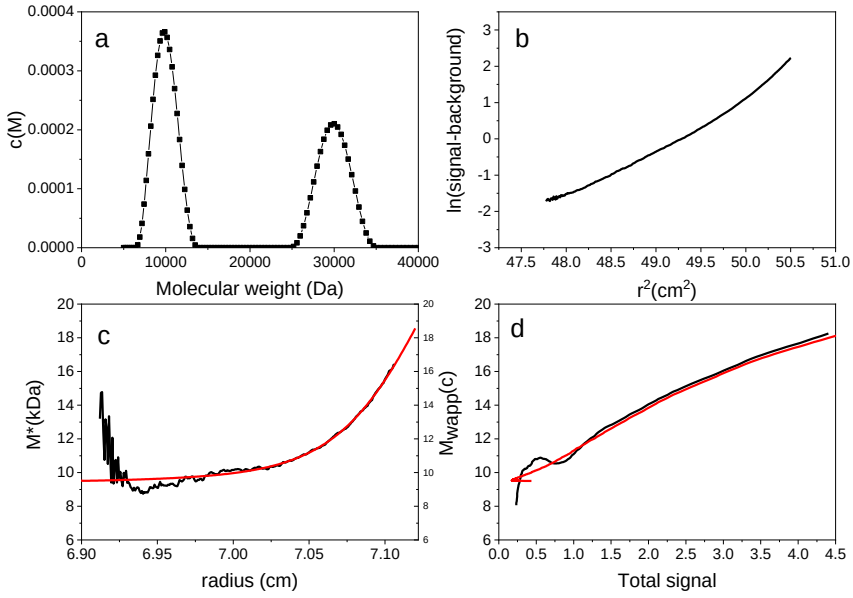

Figure 2-18: MSTAR results for 0.5 mg/ml chitosan (SE was run at 35000 rpm). a) shows *c*(*M*) vs. *M* showing two species peaking ~ 10 and 30 kDa. b) ln(*c*) vs. r^2 has an upward and downward curve, i.e. is polydispersed and non ideal. c) shows the *M** extrapolation giving $M_{w,app}$ = 18.8 kDa. d) shows $M_{w,app}(c)$ vs. total signal.

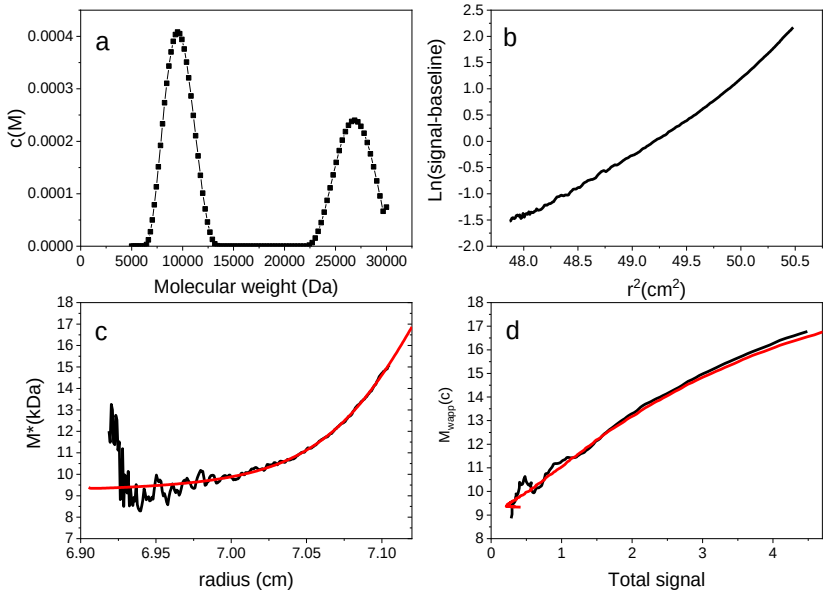

Figure 2-19: MSTAR results for 0.6 mg/ml chitosan (SE was run at 35000 rpm). a) shows $c(M)$ vs. M showing two species peaking ~ 10 and 27 kDa. b) ln(c) vs. r^2 has an upward curve, i.e. is polydispersed. c) shows the M^* extrapolation giving $M_{w,app}$ = 17 kDa. d) shows $M_{w,app}$ (c) vs. total signal. (Analysis was repeated as the analysis was not saved the first time hence the difference between published resultsand results shown here, first analysis gave a $M_{w,app}$ = 18.5 kDa and hinge $M_{w,app}$ = 14.8 kDa).

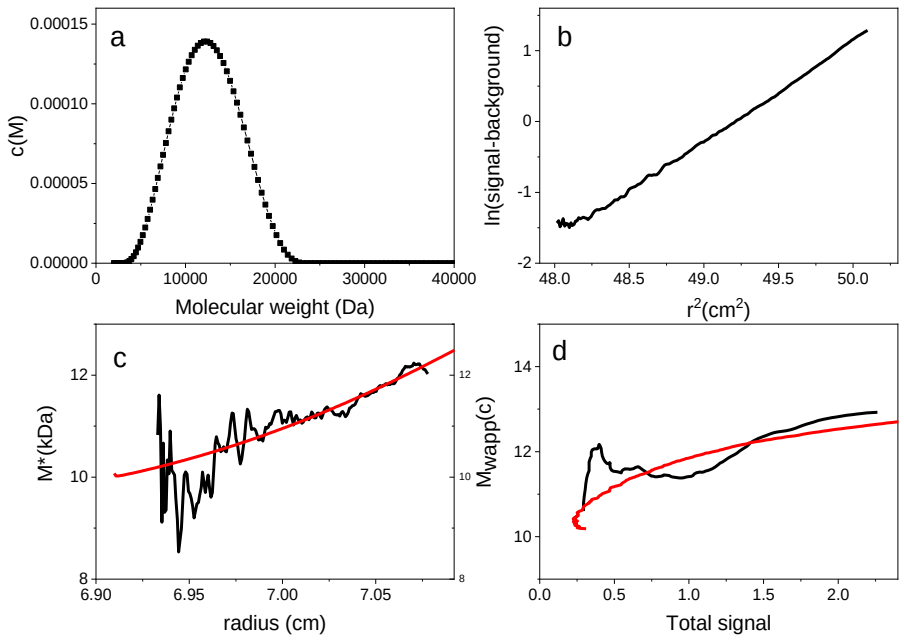

Figure 2-20: MSTAR results for 0.7 mg/ml chitosan (SE was run at 35000 rpm). a) shows c(M) vs. M showing one species peaking ~ 12.5 kDa. b ln(c) vs. r^2 is a straight line this is likely due to a combination of a polydisperse, non-ideal solution counteracting each other rather than an ideal monodispersed system suggested by a real straight line. c) shows the M^* extrapolation giving $M_{w,app}$ = 12.5 kDa. d) shows $M_{w,app}$(c) vs. total signal showing.

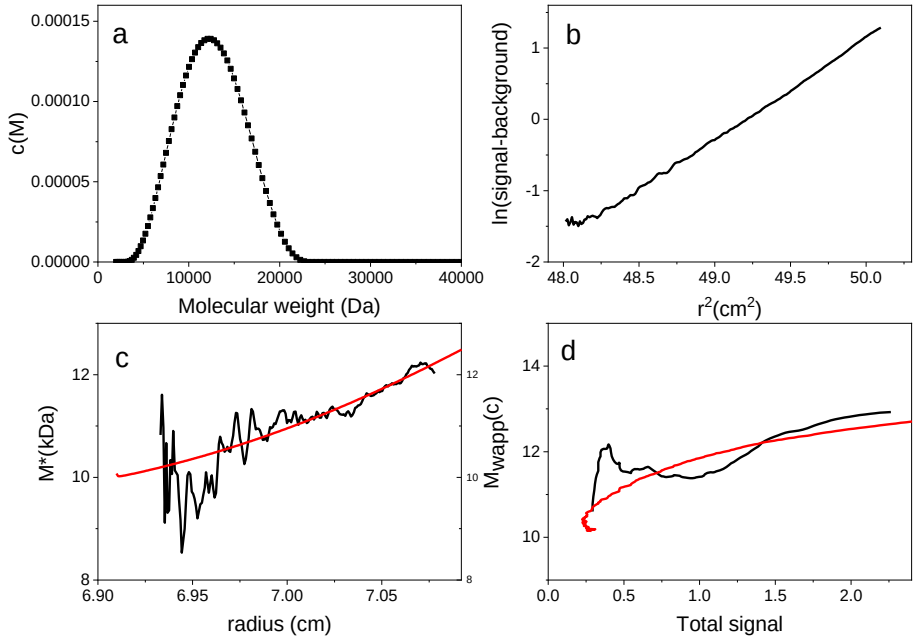

Figure 2-21: MSTAR results for 0.8 mg/ml chitosan (SE was run at 35000 rpm). a) shows $c(M)$ vs. M showing one species peaking ~ 12.5 kDa. b) ln(c) vs. r^2 is a straight line, this is likely due to a combination of a polydispersed, non ideal solution counteracting each other rather than an ideal monodispersed system suggested by a real straight line. c) shows the M^* extrapolation giving $M_{w,app}$ = 15.4 kDa. d) shows $M_{w,app}(c)$ vs. total signal.

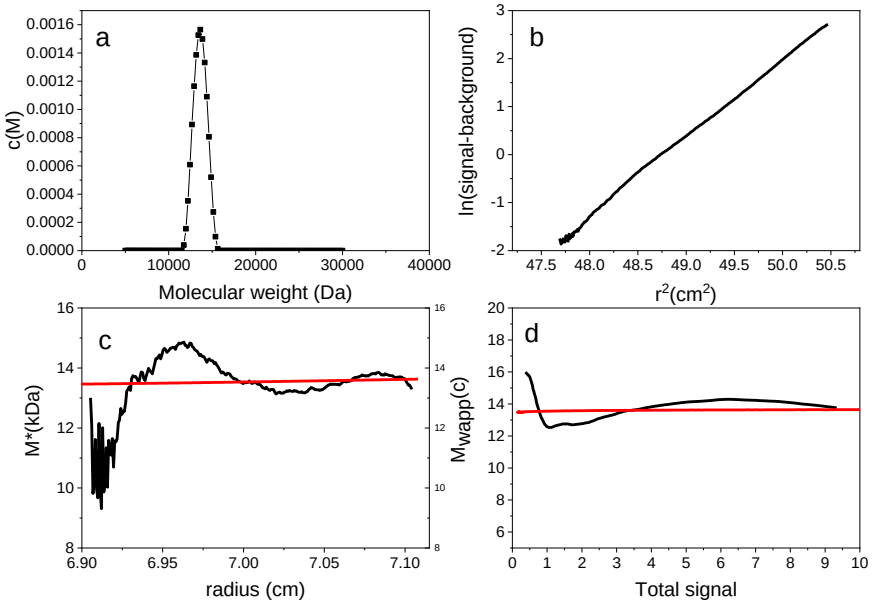

Figure 2-22: MSTAR results for 1 mg/ml chitosan (SE was run at 35000 rpm). a) shows $c(M)$ vs. M showing one species peaking ~ 14 kDa. b) ln(c) vs. r^2 has an upward curve suggesting a non ideal solution. c) shows the M^* extrapolation giving $M_{w,app}$ = 13.6 kDa. d) shows $M_{w,app}$ (c) vs. total signal. (Analysis was repeated as the analysis was not saved the first time hence the difference between published results and results shown here, first analysis gave a $M_{w,app}$ = 13.8 kDa and hinge $M_{w,app}$ = 14.2 kDa).

Table 2-4 and Figures 2-16 to 2-22 show the lowest concentration (0.3 mg/ml) M* extrapolation is a lot higher than for the other concentrations. It is not consistent with hinge point analysis and there is quite a steep extrapolation for M* analysis seen in Figure 2-16. All this suggests that 0.3 mg/ml might be too low a concentration for reliable results. The M* and hinge point analysis for the rest of the concentration are more constant and are even closer after 0.7 mg/ml. They are close to M_z and the extrapolations for M^* (Figure 21-22) are flatter, meaning the exploration to the baseline is more reliable. ln(c) vs. r2 for 0.3 mg/ml -0.6 mg/ml all show a bit of a downward curve hence some polydispersity. 0.7-1.0 mg/ml appears to be a straight line but it is very likely that the polydispersity and non-ideality are cancelling each other out, resulting in a straight line. It is also clear from the Mw,app vs. total signal that 0.7-1.0 mg/ml is not a good fit for the data. The lower concentrations show little non-ideality; however, the M* and hinge point Mw,app are not consistent below 0.7 mg/ml. Due to the steep extrapolation of the M* analysis, the hinge point analysis is more likely to be correct. The hinge point Mw was also similar for 35,000 and 40,000 rpm: see Figure 2-23 and Table 2-5 for a summary of hinge point at different speeds. There appears to be little evidence of concentration dependence, hence the average was taken of the 35,000 rpm (Figure 2-24); this gives an ideal value Mw = (14.2±1.2) kDa from the first analysis (published), Mw= (14.0±1.3) kDa from the second analysis which corresponds to the MSTAR results provided above (Figure 2-25). The averages of all three speeds were extrapolated to zero concentration to give a Mw=12.6 kDa (Figure 2-26). However, the lowest speed with a long path length cell is more likely to produce the most accurate results. A second analysis of cell 4 and 7 only gave slightly different results.

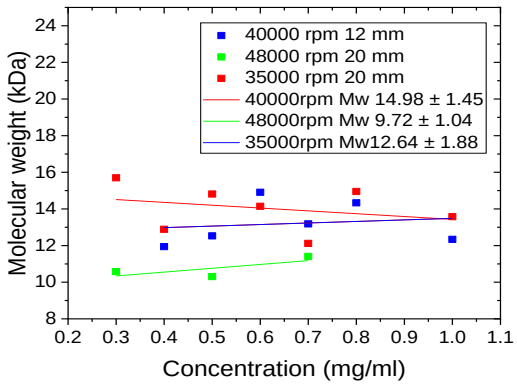

Figure 2-23: P Molecular weight vs. concentration, for all SE runs (MSTAR hinge point analysis), second analysis results for 35000 rpm. Blue 40000 rpm, green 48000 rpm, red 35000 rpm.

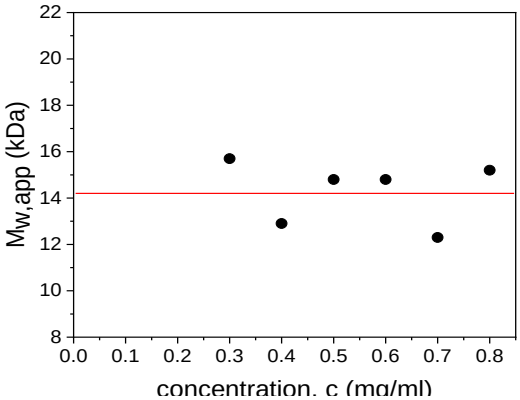

Figure 2-24: Plot of apparent weight average molecular weight $M_{w,app}$ vs. loading concentration, c for untreated Kitonor chitosan. SEDFIT-MSTAR used with the hinge-point method to extract $M_{w,app}$ values. Rotor speed = 35000 rpm. The ideal value M_w = (14.2±1.2) kDa from first analysis.

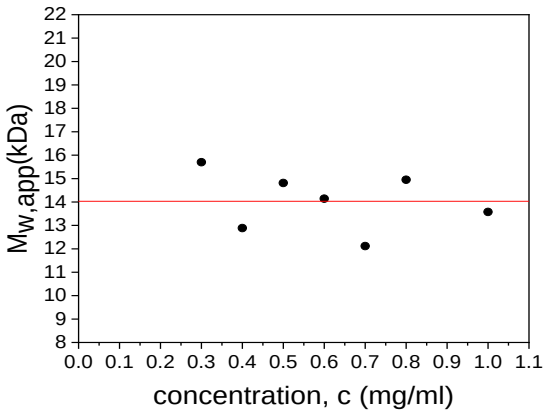

Figure 2-25: Plot of apparent weight average molecular weight $M_{w,app}$ vs. loading concentration, c for untreated Kitonor chitosan. SEDFIT-MSTAR used with the hinge-point method to extract $M_{w,app}$ values. Rotor speed = 35000 rpm. The ideal value M_w = (14.03±1.25) kDa from second analysis.

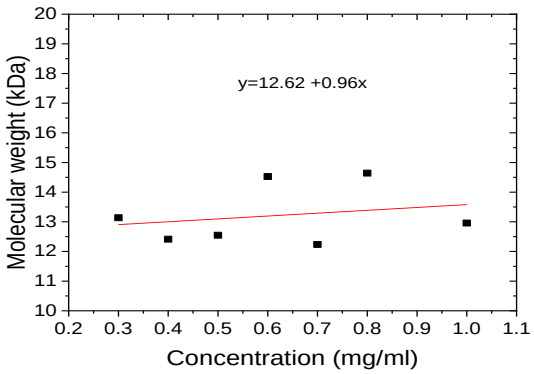

Figure 2-26: Plot of average molecular weight from hinge for all concentration all speeds vs. concentration for hinge point analysis, extrapolation shows the $M_{w,app}$ to be 12.6 kDa.

To try to better establish the distribution of molecular weights and confirm the M* results, MultiSig analysis was also performed on three concentrations (Figure 2-27). This shows species between 5-38 kDa with the majority lying between 10-20 kDa.

This would concur with the low s value observed from the sedimentation velocity experiment.

Table 2-5: Summary of SE results for chitosan analysed at different speeds. a) hinge M_w 35000 rpm; b) 40000 rpm; c) 48000 rpm. Evaluations were not always possible at the higher speeds. No sedimentation velocity was performed at 1 mg/ml, no sedimentation equilibrium at 0.45 mg/ml (8 hole rotor hence 7 concentrations limit).

c (g/ml)	***s* (S)**	**[a]$M_{w,app}$ (kDa)**	**[b]$M_{w,app}$ (kDa)**	**[c]$M_{w,app}$ (kDa)**
0.3	1.3	15.7	-	10.6
0.4	1.3	12.9	11.9	-
0.45	1.3	-	-	-
0.5	1.2	14.8	12.5	10.3
0.6	1.5	14.8	14.9	-
0.7	1.3	12.3	13.2	11.4
0.8	1.3	15.2	14.3	-
1.0	-	14.0	12.3	-

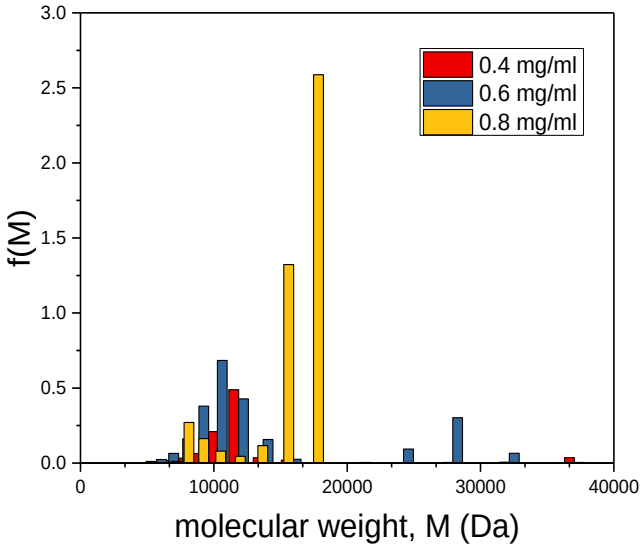

Figure 2-27: MultiSig analysis of the molecular weight distribution f(*M*) vs. *M* of Kitonor chitosan run at 35000 rpm at three concentrations. M_w = (14.1±1.2) kDa, M_z = (16.4 ± 1.2) kDa with a polydispersity index M_z/M_w ~ 1.2. The error is the standard deviation for the three concentrations.

2.2.2 Degraded chitosan

No SV analysis was carried out as there is too much back diffusion and molecules stayed along the meniscus making analysis impossible. This is the batch used for chemical modification. Table 2-6 shows MSTAR M_w, M_z and hinge point molecular weights are all similar. Figure 2-28 to Figure 2-34 show fits are very good and the extrapolation is steep but very smooth. The consistencies of analysis suggest that the results are reliable: a summary table is provided (Table 2-6).

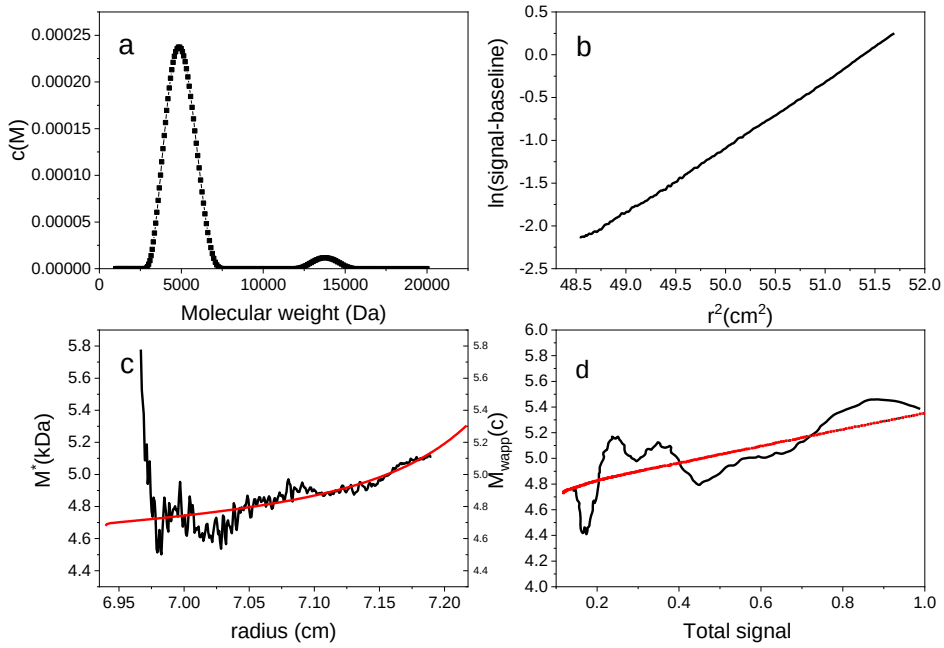

Figure 2-28: MSTAR results for 0.3 mg/ml degraded chitosan. a). shows $c(M)$ vs. M showing two species peaking ~ 5000 kDa the other ~ 13500 kDa. b) $\ln(c)$ vs. r^2 shows a straight line, i.e., no polydispersity and no non-ideality. c) shows the M^* extrapolation giving $M_{w,app}$ = 5.2 kDa. d). $M_{w,app}(c)$ vs. total signal showing a poor fit with the data which could be due to the low concentration.

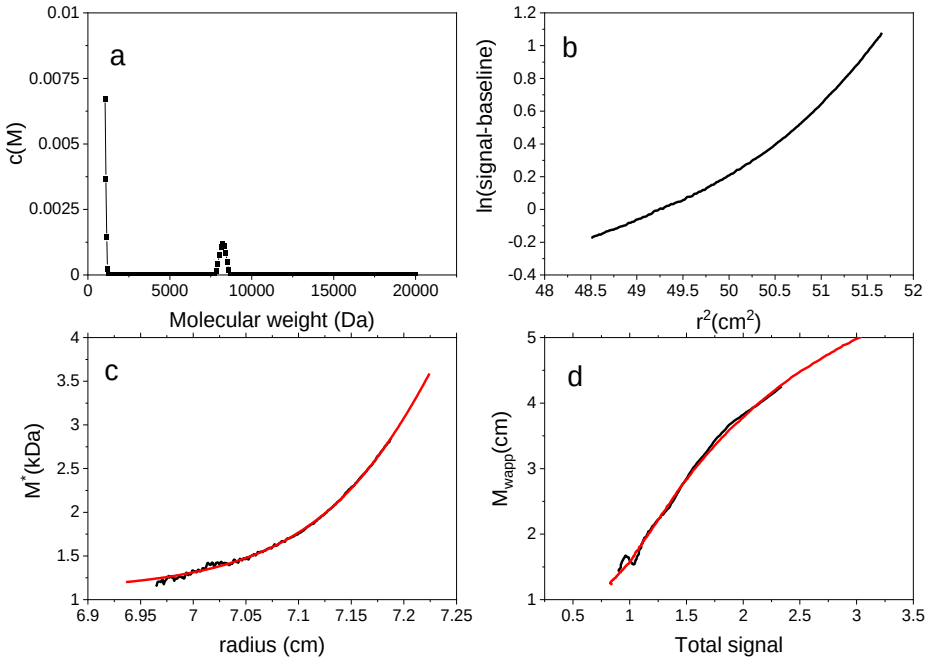

Figure 2-29: MSTAR results for 0.4 mg/ml degraded chitosan. a) shows $c(M)$ vs. M showing one species peaking ~ 8000 Da the line at the start is an artefact of the analysis. b) ln(c) vs. r^2 shows an upward curve i.e., the polymer is polydispersity. c) shows the M^* extrapolation giving $M_{w,app}$ = 3.6 kDa. d) $M_{w,app}(c)$ vs. total signal

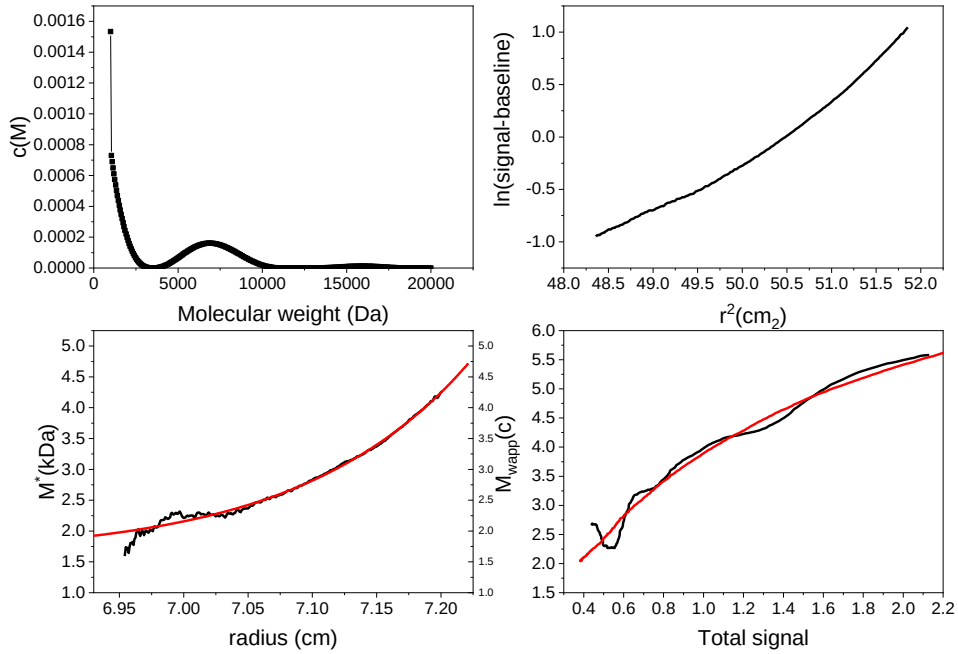

Figure 2-30: MSTAR results for 0.5 mg/ml degraded chitosan. a) shows c(M) vs. M showing one species peaking ~ 7000 Da the line at the start is an artefact of the analysis b) ln(c) vs. r^2 shows an upward curve, i.e., the polymer is polydispersity. c) shows the M* extrapolation giving $M_{w,app}$ = 4.8 kDa. d) $M_{w,app}(c)$ vs. total signal.

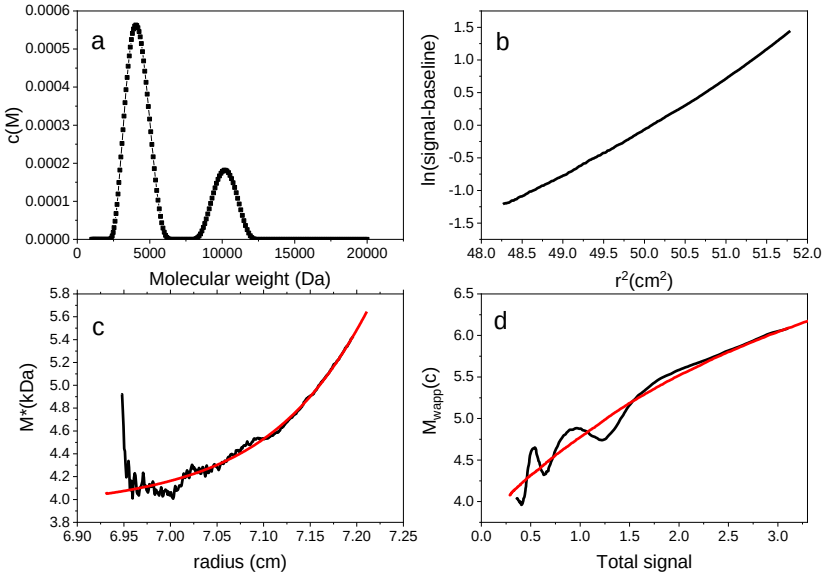

Figure 2-31: MSTAR results for 0.6 mg/ml degraded chitosan. a) shows $c(M)$ vs. M showing two species peaking ~ 4000 the other ~ 10000 Da b) ln(c) vs. r^2 shows an upward curve with some downward curve, i.e., the polymer is polydispersity and has non-ideality c) shows the M* extrapolation giving $M_{w,app}$ = 5.7 kDa. d) $M_{w,app}(c)$ vs. total signal.

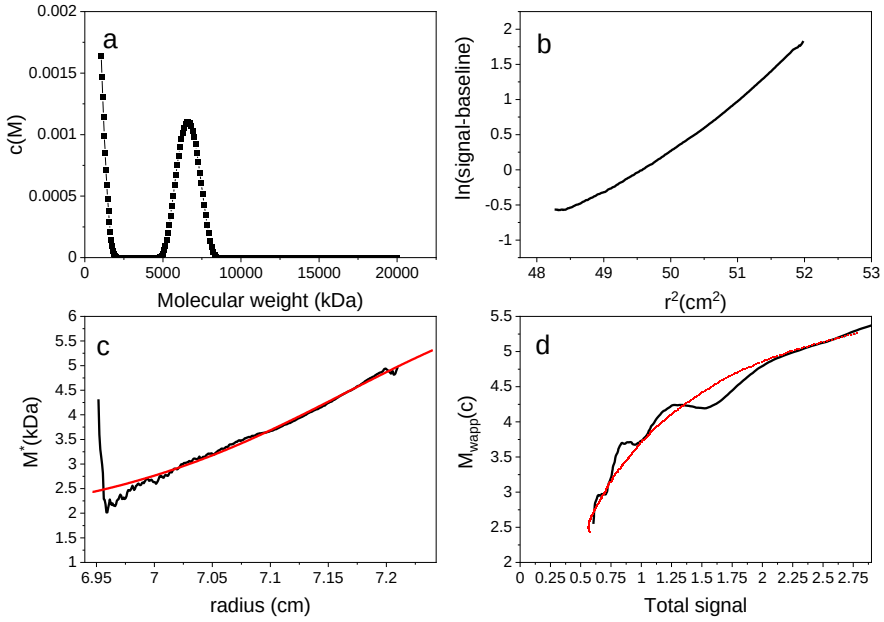

Figure 2-32: MSTAR results for 0.7 mg/ml degraded chitosan. a) shows c(M) vs. M showing one species peaking ~ 6500 Da the other peak is an artefact of the analysis b) ln(c) vs. r^2 shows an upward curve, i.e., the polymer is polydispersity c) shows the M* extrapolation giving $M_{w,app}$ = 5.3 kDa. d) $M_{w,app}(c)$ vs. total signal.

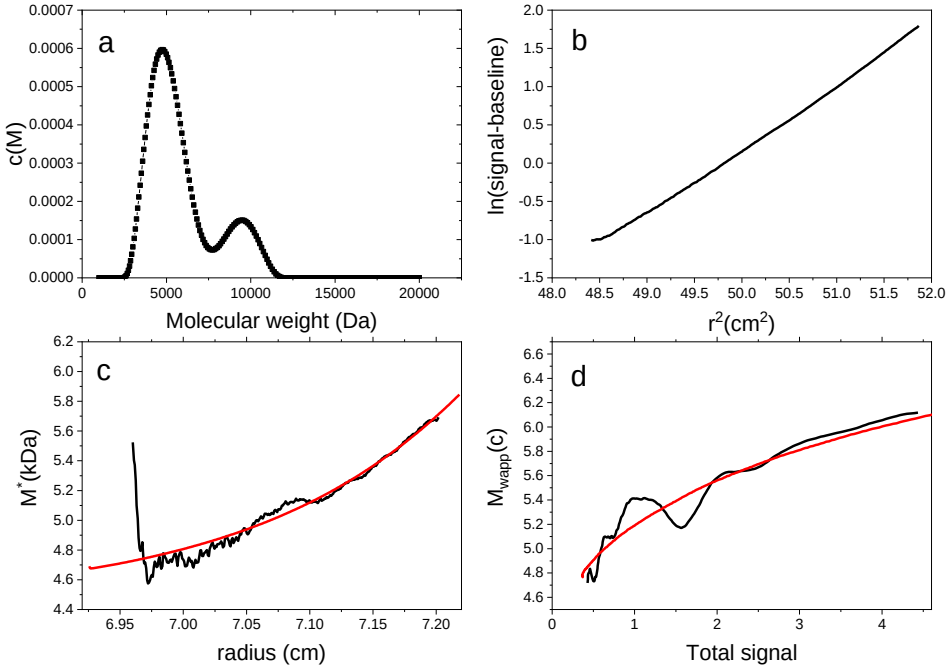

Figure 2-33: MSTAR results for 0.8 mg/ml degraded chitosan. a) shows c(M) vs. M showing two species peaking ~ 5000 the other ~ 90000 Da b) ln(c) vs. r^2 shows a relatively straight line; this is probably a downward curve counteracted by an upward curve, i.e., the system is polydisperse and non-ideal c) shows the M* extrapolation giving $M_{w,app}$ = 5.9 kDa. d) $M_{w,app}(c)$ vs. total signal.

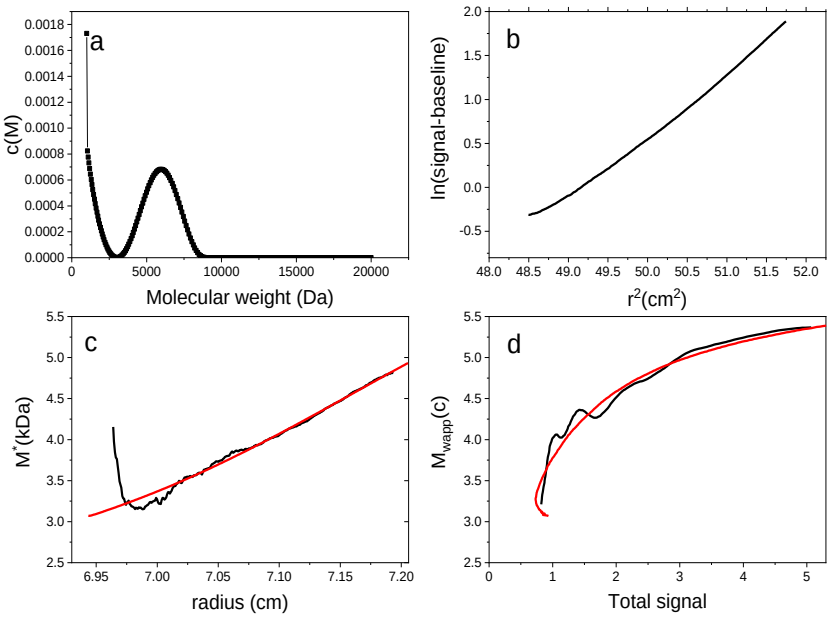

Figure 2-34: MSTAR results for 1.0 mg/ml degraded chitosan. a) shows $c(M)$ vs. M showing one species peaking ~ 6500 Da the other peak is an artefact of the analysis b) ln(c) vs. r^2 shows a relatively straight line; this is probably an upward curve counteracted by a downward curve i.e., the system is polydisperse and non-ideal c) shows the M* extrapolation giving $M_{w,app}$ = 4.9 kDa. d) $M_{w,app}(c)$ vs. total signal

Table 2-6: SE depolymerised chitosan MSTAR analysis results for experiment run at 40000 rpm. Buffer:0.2 M acetate. Parameters $\bar{v}$=0.57 ml/g, solvent density 1.00111 g/ml, solvent viscosity 0.01118 Poise.

Concentration (mg/ml)	***M*$_{w,app}$ (from *M**) kDa**	**Standard deviation (kDa)**	***Mz* (kDa)**	**Poly dispersity index *M*$_z$/*M*$_w$**	**r$_{hinge}$ cm**	***M*$_{w,app}$ from *M*$_w$(r$_{hinge}$) kDa**
0.3	5.2	1.7	5.7	1.10	7.115	4.9
0.4	3.6	3.4	6.9	1.92	7.124	3.3
0.5	4.8	3.5	7.3	1.52	7.121	4.2
0.6	5.7	2.7	7.0	1.23	7.115	5.1
0.7	5.3	2.4	6.4	1.21	7.141	5.2
0.8	5.9	2.4	6.5	1.10	7.118	5.6
1.0	4.9	2.1	5.8	1.18	7.111	4.8

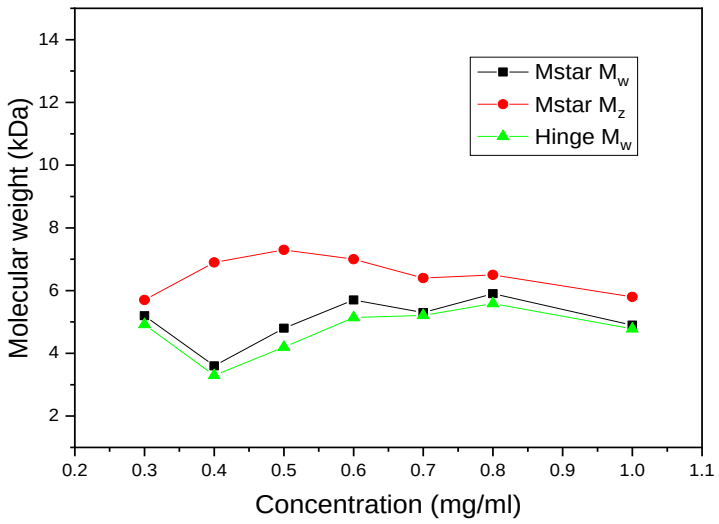

Figure 2-35: MSTAR $M_{w,app}$ vs. concentration. black M_w, red M_z and green for M_n showing the differences the M_w, M_z and M_n.

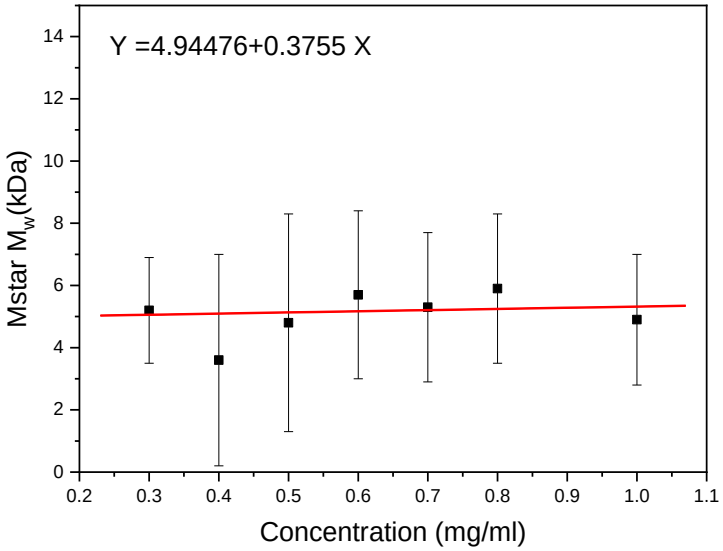

Figure 2-36: MSTAR results for $M_{w,app}$ vs. c. Line of best fit gives M_w=4.9 kDa.

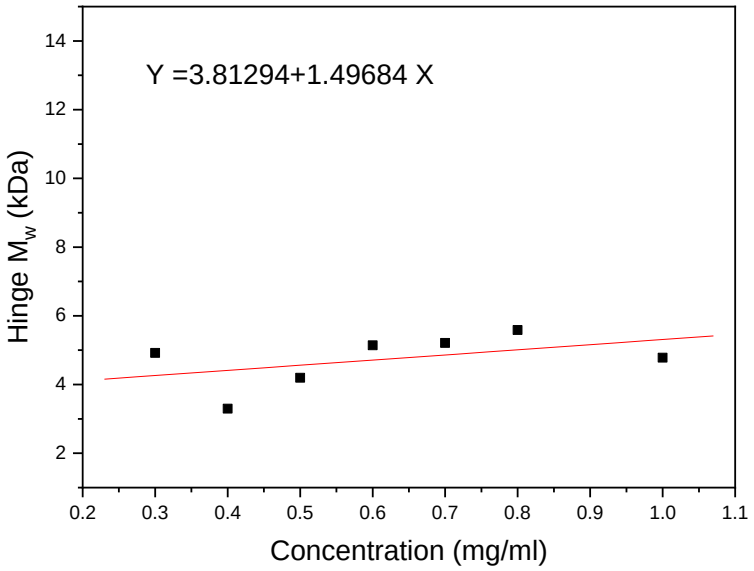

Figure 2-37: Plot of MSTAR Hinge $M_{w,app}$ vs. c Line of best fit gives M_w=3.8 kDa.

The *M** extrapolation and the hinge point extrapolation to zero are very similar (Figure 2-35 to Figure 2-38). However, the concentration dependence is negligible. Hence, the average M_w of the M* and hinge point analysis was taken which gives M_w= (4.9±0.7) kDa (see Figure 2-38).

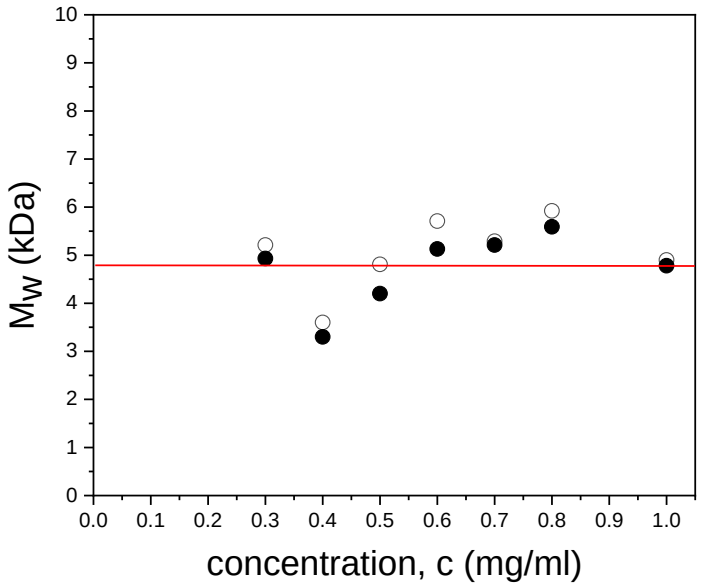

Figure 2-38: Plot of $M_{w,app}$ from SEDFIT-MSTAR vs. loading concentration, c for depolymerised chitosan (treated for 60 min) run at 40000 rpm. Non-ideality is negligible over the concentration range studied with $M_w \sim M_{w,app}$ = (4.9 ± 0.7) kDa. Filled circles: from hinge point and open circles from MSTAR.

To better establish distribution, as SV was not possible as the molecular weight was too small, MultiSig analysis of sedimentation equilibrium runs were carried out. SV was not possible as the polymer would not sediment sufficiently for analysis to be possible even at 50000 rpm.

MultiSig was run to try to establish distribution for the equilibrium experiment. This showed a distribution of between 0 to roughly 12 kDa (Figure 2-39).

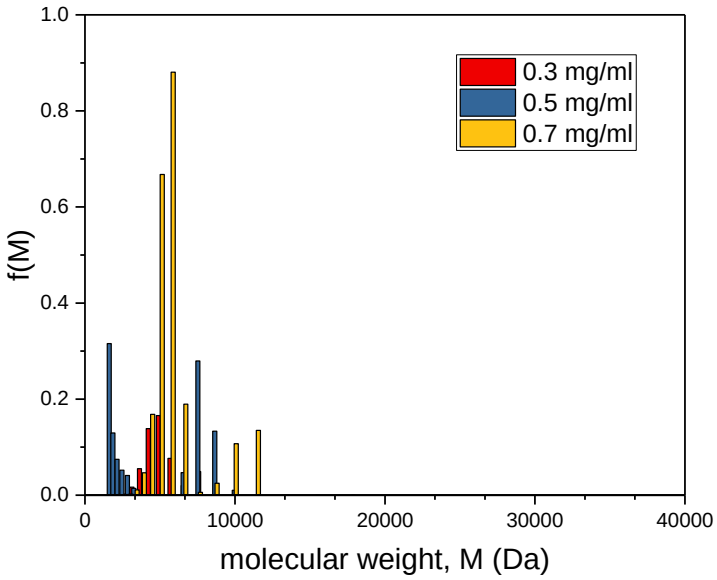

Figure 2-39: MultiSig analysis of the molecular weight distribution f(*M*) vs. *M* of depolymerised (treatment for 60 min) Kitonor chitosan run at 35000 rpm at three concentrations. M_w = (5.2 ±0.7) kDa, M_z = (6.1 ± 0.5) kDa, and M_z/M_w ~ 1.2. A clear shift to low molecular weights compared to the original chitosan.

2.2.2.1 Depolymerisation of chitosan over time

Table 2-7: SE results depolymerised chitosan MSTAR analysis run at 40000 rpm. time of reaction, concentration and MSTAR results Buffer:0.2 M acetate

Time h	**concentration (mg/ml)**	***M*$_{w,app}$ (from *M**) kDa**	***Mz* (kDa)**	**Poly dispersity index M_w/M_z**	**r_{hinge} cm**	***M*$_{w,app}$ from *M*$_w$ (r_{hinge}) kDa**
0.5	0.5	6.2	9.2	1.48	7.115	5.7
	0.6	7.5	8.6	1.15	7.115	7.1
	0.7	7.9	8.6	1.09	7.121	7.6
1	0.5	6.5	7.3	1.12	7.092	5.9
	0.6	6.4	7.8	1.22	7.120	5.9
	0.7	5.6	6.9	1.23	7.117	5.4
1.5h	0.5	Not analysable				
	0.6	4.8	5.9	1.23	7.145	4.6
	0.7	4.9	6.1	1.24	7.105	4.4

Investigation of depolymerisation for different reaction times was carried out. The summary Table 2-7 shows that the MSTAR ($M^* = M_{w,app}$) and hinge point $M_{w,app}$ values are very similar proving reliability of analysis. Averaging each concentration and plotting this against the time of reaction shows the rate of depolymerisation (Figure 2-40) and extrapolating the line back to zero gives the theoretical starting molecular weight (8 kDa). This suggests that despite the apparent linear rate of depolymerisation, there must have been a rapid depolymerisation at the start of the reaction followed by a slower rate of depolymerisation. This is to be expected as longer chains have more glycosidic bonds which could potentially be broken, hence, increased chance of being degraded first.

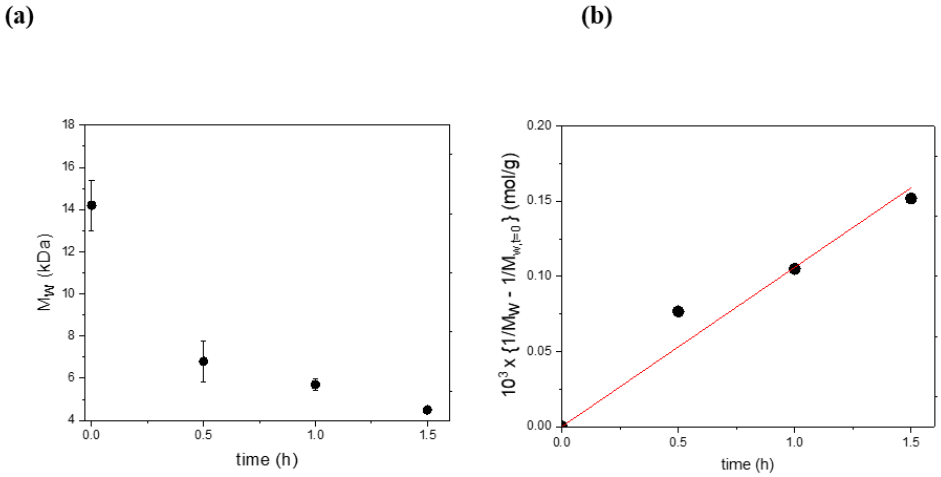

Figure 2-40: Results showing degradation of Kitonor chitosan as a function of treatment time with hydrogen peroxide and UV radiation. a) Reduction of weight average molecular weight. The error bars represent the average over different concentrations. b) Corresponding plot of $\{1/M_w - 1/M_{w,t=0}\}$ vs. time (Tanford, 1961). Decay constant k = (0.046 ±0.004) h^{-1}.

It is proven that chitosan of larger molecular weight is more susceptible to depolymerisation, this is from degradation experiments that show larger molecular weight chitosan initially degraded faster and then level off as the molecular weight is reduced (Mao et al., 2004). This was also observed this these experiments, an intial

large reduction in molecular weight from 0 to 0.5 h and then the rate is reduced and becomes steadier.

2.2.2.2 Depolymerisation of large batches of chitosan

Table 2-8: Molecular weight results for SE analysis of large batches (22 g) of depolymerised chitosan. SE of 3 concentrations of each batch.

Cell /batch	**Conc (mg/ml)**	**M_w (kDa)**	**Stdv (kDa)**	**M_z (kDa)**	**PDI (M_z/M_w)**	**Hinge radius (cm)**	**Hinge M_w (kDa)**
2/LB1	0.5	4.6		8.1	1.8		3.916
3/LB1	0.6	5.8		7.3	1.3		5.392
4/LB1	0.7	5.6		7.3	1.3		5.028
1/LB2	0.5	6.8	4.5	9.8	1.4		5.46
2/LB2	0.6	5.7	3.6	7.9	1.4	7.127	5.166
3/LB2	0.7	6	2.7	7.2	1.2	7.113	5.525
4/LB3	0.5	5.9	4.8	9.7	1.6	7.123	5.248
5/LB3	0.6	7	3.6	8.8	1.3	7.129	6.392
6/LB3	0.7	6.4	4.4	9.4	1.5	7.128	5.568
7/LB3	0.5	6.3	4.3	9.3	1.5	7.126	5.767
1/LB4	0.5	5.4	3.7	7.9	1.5	7.1	4.234
2/LB4	0.6	5.7	2.7	7	1.2	7.086	4.925
3/LB4	0.7	5.2	2.7	6.6	1.3	7.091	4.557
4/LB5	0.5	5.3	2.9	6.9	1.3	7.097	4.548
5/LB5	0.6	5.3	2.5	6.4	1.2	7.1	4.669
6/LB5	0.7	5.1	2.3	6.1	1.2	7.079	4.614
7/LB5	0.8	4.8	2	5.6	1.2	7.087	4.539

Chitosan was also depolymerised in 5 x 22 g batches. SE was run for each of these at 40000 rpm, 20 ^oC for 3-4 concentrations for each batch (Table 2-8). The average of these was then calculated from the three concentrations with a standard deviation as well (Table 2-11). The low concentration allowed for the average to be taken; three concentrations could not have been sufficient to eliminate non-ideality but these low concentrations should have minimised it. Three to four concentrations were chosen for

each as this allowed two batches to be run at once. After confirming the similarity between the batches, these were combined. The combined batches were reanalysed with seven concentrations to eliminate non-ideality and determine the molecular weight of the total material going forward for large-scale chemical modification (Table 2-10, Figure 2-41 and Figure 2-42). SV was run at 50000 rpm at 20 ^{o}C; however, the data was not analysable as the chitosan's molecular weight was too small to sediment.

Table 2-9: Average molecular weight results for SE analysis of large batches (22 g) of depolymerised chitosan. Average molecular weights of each batch along with over all average and standard deviation.

Batch	**Average M_w**	**M_z (kDa)**	**PDI (M_z/M_w)**	**Hinge M_w (kDa)**
LB1	5.33	7.57	1.42	4.78
LB2	5.33	8.30	1.56	5.31
LB3	6.43	9.30	1.45	5.74
LB4	5.43	7.17	1.32	4.57
LB5	5.13	6.25	1.22	4.59
Average	5.53	7.72	1.39	5.00
Sdv	0.52	1.15	2.23	0.51

Table 2-10: SE results of combined large batches (22 g) of depolymerised chitosan for seven concentrations.

Cell /batch	**Conc(mg/ml)**	**Signal loading**	**M_w (kDa)**	**Stdv (kDa)**	**M_z (kDa)**	**PDI (M_z/M_w)**	**Hinge radius cm**	**Hinge M_w (kDa)**
1	0.3	1.708	6.3	4.2	9.1	1.44	7.069	5.586
2	0.4	2.113	6.4	3.4	8.2	1.28	7.068	6.023
3	0.5	3.322	6.1	3	7.5	1.23	7.076	6.064
4	0.6	2.95	6.5	2.4	7.4	1.14	7.067	6.292
5	0.7	2.643	6.8	0.6	6.9	1.01	7.061	6.742
6	0.8	3.925	6.3	1.5	6.7	1.06	7.062	6.243
7	1	4.637	6.2	0.3	6.2	1.00	7.062	6.188

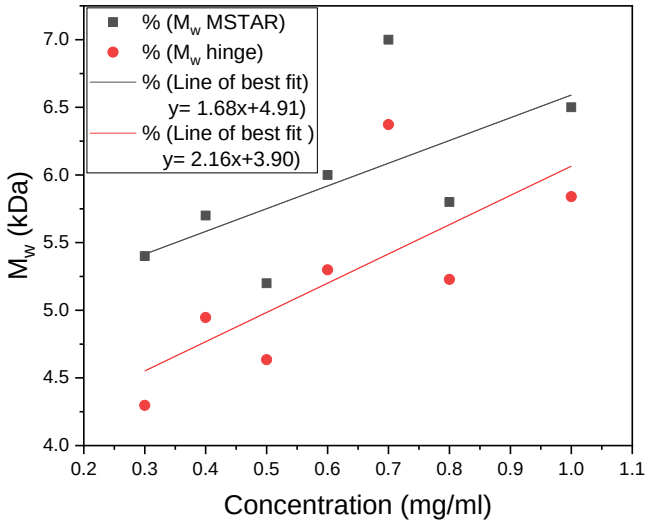

Figure 2-41: Plot of molecular weight vs. concentration for combined large batches. Line of best fit to account for non-ideality shows once non-ideality is taken into account MSTAR gives a M_w of 4.91 kDa and hinge point gives a M_w of 3.90 kDa.

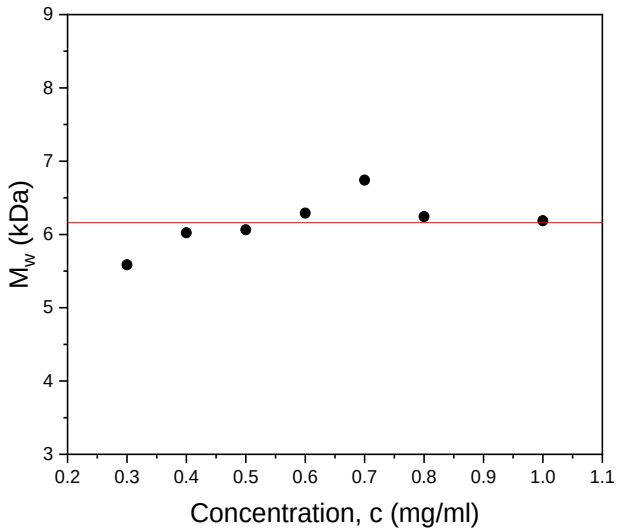

Figure 2-42: Plot of hinge point $M_{w,app}$ from SEDFIT-MSTAR vs. loading concentration, c for depolymerised chitosan run at 40000 rpm. Non-ideality is negligible over the concentration range studied with $M_w \sim M_{w,app}$ = (6.2 ± 0.3) kDa.

2.3 Discussion

Analysis was carried out using MSTAR *M** analysis, MSTAR hinge point and MultiSig. This allows for verification of results though three methods of analysis. MSTAR gives an overall weight average molecular weight (M_w) although it takes no account of distribution. MultiSig however, does give a distribution but will also give M_w. These values can then be compared for verification of correct analysis. Both methods are based on algorithms fit methods which means there can be a high level of human error in choosing fitting parameters, including: range to fit, start and end of cell base. These can be floated to decrease human error but this then relies on the computer finding the right point. Using multiple methods of analysis helps to verify results. MultiSig runs 20 iterations and takes the average for analysis. However, it can be found to have slightly different results when analysed a second time based on a different judgement of analysis parameters and because of the type of analysis (see section on MultiSig and Gilles et al. 2014). It is important to make sure the analysis range covers the full range of molecular weights and take into account that the lowest concentration is theoretically the most accurate.

Sedimentation equilibrium experiments at low concentrations such as (0.3-0.5) mg/ml have little effect from non-ideality. However, higher concentrations are affected by non-ideality and therefore, molecular weights obtained must be plotted against concentration and extrapolated back to zero to negate non-ideality effects (see section on SE).

AUC, SE and SV analysis can give an estimate of the polymer's molecular weight and distribution; this is vital to estimate the likelihood of penetrating into wood. It can help give an educated guess of consolidant potential, along with literature findings.

2.3.1 SE results

The sedimentation equilibrium analysis for the chitosan prior to depolymerisation showed some differences between speeds; this could be due to loss of optical registration towards the cell base of some of the higher molecular weight parts of the polydisperse distribution. As a result of this, a 35000 rpm run was used to calculate the ideal M_w. There appeared to be little non-ideality so the average was taken. The hinge point analysis was used as there was some steep extrapolation towards the cell base indicating the MSTAR analysis might be less reliable than the hinge point analysis. The ideal molecular weight was therefore found to be (14.2±1.2) kDa. To estimate a distribution of molecular weights f(M) vs. M, MultiSig analysis (Gillis et al., 2013b) was run on three concentrations. This determines the polydispersed distribution according to a 17-component system. MultiSig analysis revealed a distribution ranging between 5-37 kDa with components peaking between 10-17 kDa with an overall weight average of M_w~ (14.1±1.2) kDa in exact agreement with SEDFIT-MSTAR. The analysis also yields an M_z = (16.4 ± 1.2) kDa giving a polydispersity M_z/M_w ~ 1.2.

2.3.2 SV

The SV results show the distribution of chitosan *f*(*M*) vs. *M* from combining SV and SE data, gives a more accurate molecular weight distribution but it does rely on knowing two parameters: k and a. These can be taken from literature but as there can be variation, it would be better to measure these, which can be done by running SV and SE on a variety of molecular weights and plotting the data or running two molecular weights and solving simultaneous equations. This is the intention for future work. If it is assumed the average molecular weight is somewhere around the peak of that distribution, then there is clearly a quantity of chitosan that has a molecular weight greater than 12 kDa. The chitosan previously researched by Christensen in 2013 for use on the Oseberg is the same batch of chitosan used in this investigation which did penetrate the wood and 502 μmol/g of glucosamine was found in the wood. This is more than the higher molecular weight sigma chitosan 446 μmol/g of glucosamine but less than the degraded kitonor chitosan 615 μmol/g of glucosamine which suggests molecular weight plays a large factor. However, this could also be due to viscosity preventing penetration. Moreover, it could be that not all the chitosan can get into the wood which is why a degraded version with a higher proportion of lower molecular weights has an increased uptake. For comparison, when using PEG, the gold standard treatment method (different molecular weights used depending on degree of degradation of wood being treated (200-4000) Da), 4000 Da is the largest molecular weight commonly used for wood conservation. There have been a few investigations into penetration and uptake of varying molecular weights of PEG into wood. One paper suggests molecular weights as large as 58000 Da penetrate wood, another says 22000 Da can penetrate wood, but has reduced uptake compared to lower concentrations and

it also has a lower anti-shrinking efficacy which means it is not as good as a consolidant. The same paper also suggests that it could be the components up to 16000 Da which are responsible for the bulking (Jeremic et al., 2007). Tarkow et al. (1966) states only 3000 Da PEG could diffuse transversely along the wood in green wood (Tarkow et al., 1966). PEG of 3350 Da has also previously been reported by Grattan to not enter cell walls (Pearson, 2014). Archaeological wood is more degraded then fresh wood and therefore, uptake of PEG is greater and penetration is improved; however from experience, conservators tend to use PEG of no more than 4000 Da. Chitosan, however, has a different structure and higher molecular weights may not be as large in size compared to PEG and conformation and flexibility also play a role in penetration. Considering this previous research and the structure of chitosan, it is reasonable to say that the lower end of this distribution, >12 kDa, probably has better penetration and uptake. Half of the current distribution is over ~12 kDa, therefore it would be best to reduce the molecular weight so the entire range is lower than 12 kDa. Ideally, the majority should lie between 3-6 kDa which is slightly higher than ideal for PEG but this reflects the difference in structure. Chitosan of an average molecular weight of 6.5 kDa had better uptake of chitosan compared to 12.5 kDa; lowering this slightly might yet improve the uptake.

2.3.3 Depolymerisation of chitosan

Depolymerisation of chitosan with hydrogen peroxide is often performed with conventional heating; it successfully depolymerises it without any changes to the backbone (Tian et al., 2003). Conventional heating results in a lot of wasted energy. Two alternatives are possible: microwaves and UV light both require less energy and

hence, are more suitable in terms of sustainability (Hernández-Ledesma and Herrero, 2013; Li et al., 2012; Wang et al., 2005). There are chemical methods other than hydrogen peroxide but the advantage of hydrogen peroxide is the waste is water. See equations 2-33-2-39 which summerise these reactions:

$$R - NH_2 + H^+ = R - NH_3^+ \quad \textbf{2-33}$$

$$H_2O_2 = H^- + HOO^- \quad \textbf{2-34}$$

$$HOO^- \rightarrow O^{\cdot} + OH^- \quad \textbf{2-35}$$

$$H_2O_2 + HOO^- \rightarrow H^{\cdot} + O^{\cdot} + H_2O \quad \textbf{2-36}$$

$$H_2O_2 = 2xHO^{\cdot} \quad \textbf{2-37}$$

$$(GlcN)_m - (GlcN)_n + HO^{\cdot} \longrightarrow (GlcN^{\cdot})_m + (GlcN)_n + H_2O \quad \textbf{2-38}$$

$$(GlcN^{\cdot})_m - (GlcN)_n + H_2O \longrightarrow (GlcN)_m + (GlcN)_n \quad \textbf{2-39}$$

Water is a benign waste product and causes no environmental risk. Other reactions have involved more chemicals or catalysts but hydrogen peroxide, acetic acid and UV light as a catalyst are more environmentally friendly when it comes to disposal. It is also clear from the results that it produced the desired molecular weight (see below).

Mstar-40000 rpm (12 mm cells)

The $M_{app,w}$ was taken as the average M_w from both the hinge point and M* analysis, as both gave very similar results and there was not a steep extrapolation for the M* as

for the higher molecular weight chitosan. The non-ideality also appeared to be negligible. The $M_{app,w}$ was therefore found to be (4.9±0.7) kDa, a clear reduction in molecular weight from the native material by ~60%. 4.9kDa is deemed an appropriate molecular weight since PEG 4000 is used in conservation due to chitosan's different structure, it is likely that a larger average molecular weight will still penetrate the wood. 12 kDa chitosan is known to penetrate the wood therefore ~4.9 kDa would probably be small enough to penetrate the wood. The aim is to have a chitosan that is of low enough molecular weight i.e. less than 10 kDa, but averages around 5 kDa to penetrate the wood, but large enough to consolidate the wood i.e. greater than 2 kDa. MultiSig analysis showed a reduction in the highest molecular weight and the majority of the molecular weight from a range of (5-37) kDa peaking (10-17) kDa, to (0-12) kDa peaking around 5 kDa. This should guarantee the chitosan can penetrate the wood cells.

The degradation of chitosan was investigated further to determine the effect of the time of the reaction on molecular weight using the same surface area to volume ratio as in the previous reaction. Results show depolymerisation can be adapted to get the desired molecular weight. Chitosan's molecular weight is reduced though depolymerisation with hydrogen peroxide and UV light. 30, 60 and 90 min reaction times show that depolymerisation must start quickly but then the molecular weight steadily decreased. This shows that the reaction time can be adjusted depending on desired molecular weight.

We can estimate a depolymerisation decay constant k from the relation of Tanford (Eq. 33.12 in (Tanford, 1961) which provides a good approximation to the initial stages of the decay process (Eq. 2-40) – (see also Holme et al., 2008; Morris et al., 2009b):

$$\{1/x_w - 1/x_{w,\,t=0}\} = (k/2).\,t \qquad \textbf{2-40}$$

$$\{1/M_w - 1/M_{w,\,t=0}\} = (k/2m_o).\,t \qquad \textbf{2-41}$$

Since the weighted average degree of polymerisation x_w is just (M_w/m_o) with m_o the molecular weight of the repeat unit, Eq. 2-41 is with m_o for chitosan = 216 Da. From the slope of Fig. 6(b) this leads to an estimate for rate constant (k) ~ (0.046±0.004) h^{-1}.

Chitosan of various molecular weights can be used to determine more parameters such as *k* and *b* values required for *f*(*M*)vs. *M* plot to show distribution of molecular weight. However, a wide enough range of molecular weights was not investigated. This would be useful to follow up in the future.

Scaling up to 100 g was carried out by degrading five batches using the same surface area to volume ratio, hence, 22 g was used instead of batches of 20 g. The batches were found to have an average MSTAR M_w of 5.53 with a standard deviation of 0.52 and a hinge point of M_w of 5.00 kDa with a standard deviation of 0.51 and a polydispersity of 1.36 with a standard deviation of 0.10. This shows that depolymerisation is consistent. After combining all the batches and the mean was calculated, as non-

ideality was negligible, the molecular weight was found to be (6.2 ± 0.3) kDa from hinge point analysis.

High molecular weight polymers in general have lower solubility, therefore, lowering the molecular weight should also ease solubility and hence the viscosity, particularly in an organic solvent after chemical modification (see Chapter 4). Solubility, viscosity and molecular weight are all important factors in the penetration and uptake of a material into wood.

Producing kilograms of ~5 kDa chitosan would be possible using inflow UV chemistry or bath microwave processing. The main concern for this project is to find a method for conservation. Scaling up any process will only be considered once a suitable method is found but it is important to known that it is theoretically possible.

2.4 Future work

This work was followed up by aqueous treatment of artificially degraded wood and archaeological wood with chitosan and a second polysaccharide with an amine group like chitosan (aminocellulose) (Chapter 3). This work was followed by a small-scale chemical modification to find the most suitable modification followed by scale up (Chapter 4). This led on to non-aqueous wood treatment under various conditions: solvent, concentration, length of treatment, soaking vs. injecting and spraying and finally methods of drying: air drying vs. freeze drying (Chapter 7). Success of treatment will be determined through colour change, dimensional change, scanning electron microscopy (SEM), infrared (IR) microscopy, penetration tests, if possible a

humidity chamber (artificial ageing) and by comparison to the gold standard (PEG in water and *tert*-butanol) (see Chapter 6 and Chapter 7). This rigorous investigation shows reliability if these are good treatment options (Chapter 5, Chapter 6 and Chapter 7). This should be followed by investigation into the interaction of these polymers with lignin and breakdown products if possible.

2.5 Conclusion

SV and SE analysis of chitosan shows a single broad distribution ranging from 2.5-25 kDa with an average molecular weight of (14.2 ± 1.2) kDa. Christensen et al. (2015) showed that at least some of this distribution can penetrate fully into the wood. However, degraded chitosan ~6.25 Da (determined by GPC) shows higher uptake. This suggests some of the distribution of chitosan is too large to be taken up. The SE and SV resulting distribution plots support the idea that some of the distributional molecular weights might have been too high to penetrate the wood. About half the distribution appears to be higher than ~12 kDa. Degrading the chitosan successfully brought the average molecular weight down to ~4.9 kDa (~60% reduction in molecular weight) and hence also the fraction over 10 kDa. The low molecular weight will also help reduce the viscosity and will help with solubility in an organic solvent. The longer the polymer and larger the molecular weight, the harder it is to get it soluble in any solution. Water soluble and organic soluble options are required to tailor the treatment to objects to ensure the best results in terms of conservation and sustainability.

2.6 Experimental

2.6.1 Material

Chemicals

- Chitosan brand Kitonor ~12.5 kDa from previous analysis (Christensen et al., 2015b), obtained 2015 by the group in Olso.
- Acetic acid –Sigma Aldrich cas 64-19-7 code 895092 lot SZBE3396V
- Sodium acetate trihydrate –Sigma Aldrich cas 13-90-4 code 236500 lot SZBC2360V(only for SV and SE-48000rpm)
- Sodium acetate trihydrate – Alfa Aesar code A16230 lot 10195752
- 30% Hydrogen peroxide Sigma Aldrich cas 7722-84-1 lot SZBG1050V
- Sodium hydroxide AnalaR NORMAPUR cas 1310-73-2 product 28244.295 batch 16A080020
- Reverse osmosis Milli-Q water

Equipment

- UV light- low intensity 254 nm mercury lamp
- AUC- Beckman Instruments (Palo Alto, USA) Optima XLI Analytical Ultra-
- Centrifuge
- XL-I or XL-G epoxy AUC cells 12 mm
- XL-I titanium 20 mm AUC cells

- Anton Paar DMA 5000 density meter
- Anton Paar AMVn roll and ball viscometer
- Volumetric flasks were used to make up all concentrations except for cleaning solutions.

2.6.2 Method of depolymerisation

2.6.2.1 Degradation of chitosan (original batch)

This largely followed the procedure of Wang et al., (2005). First reaction was carried out using the method below.

Chitosan (4.0001 g) was dissolved in 2% acetic acid (100 ml) in a 1L beaker (diameter 10 cm, radius 5 cm, surface area 78.54 cm^2) and stirred for 1h to ensure the chitosan was fully dissolved. A UV lamp was on for 30 min then the chitosan was placed under UV light, 4% hydrogen peroxide (100 ml) added and stirred for 1h at room temperature (25 ^oC). Surface area to volume ratio was 0.39. The pH was then increased to above 8 using 2 M sodium hydroxide; this causes the chitosan to precipitate out of solution. This solution was then centrifuged, and the solid product washed with deionised water (3x50 ml) centrifuging this each time at 10,000 rpm for 10 min. The solid product was frozen in a -80 ^oC freezer overnight and freeze-dried. Yield was 2.878 g or 71.95%.

2.6.2.2 Degradation of chitosan small batch

This was the same as in the methodology described above but with chitosan (3.000 g), 2% acetic acid (75 ml), 4% hydrogen peroxide (75 ml). UV light for 1 h, RT=25 ^oC. 600 ml beak -4.25 cm radius, surface area 56.75 cm^2, surface area to volume ratio 0.38 cm^2. Yield 2.061 g or 68.7%.

Repeated but for 30 min under UV light with hydrogen peroxide. Yield 2.312 g or 77.07%

Repeated but for 1.5 h under UV light with hydrogen peroxide. Yield 1.966 g or 65.53%.

2.6.2.3 Degradation of chitosan large batches

Chitosan (22.000 g) was dissolved in 2% acetic acid (550 ml) in a rectangular dish with 2 magnetic stirrers (surface area 456 cm^2) and stirred for 1h to ensure the chitosan was fully dissolved. A UV lamp was on for 30 min then the chitosan was placed under UV light, 4% hydrogen peroxide (550 ml) added and stirred for 1 h. Surface area to volume ratio was 0.41. The pH was then increased to above 8 using 2 M sodium hydroxide and tested with pH paper; this causes the chitosan to precipitate out of solution. This solution was then centrifuged and the solid product was then washed with 3x50ml deionised water centrifuging this each time at 10,000 rpm for 5 min. The solid product was frozen in a -80 ^oC freezer overnight and freeze-dried. Yield large batches (LB): (LB 1) 15.498 g 70.44%; (LB2) 15.719 g 71.45%; (LB3) 17.036 g 77.44 %, (LB4) 15.288 g 69.49%; (LB5) 17.120 g 77.81%.

2.6.3 AUC analysis

1.1.1.1 Cell assembly

The cells were assembled as shown by an eloquent diagram produced by Cole and Hensen (See Figure 2-43) (Cole and Hansen, 1999). The sapphire window and centre piece seal together and keep the analyte solution and buffer in the sectors. The double sector means the solute solution can be compared to the reference (buffered used to make the solute solution) meaning any sedimentation in the solvent can be accounted

for. The cells were carefully assembled, then double checked to make sure they were clean and without any damage before assembly and being filled. The sectors were wider away from the centre of the rotor. The cells once filled were very carefully aligned sometimes with the aid of a magnifying glass to ensure perfect alignment and a small piece of foam was placed above the screws to ensure that once aligned the cells would not move as perfect alignment is vital (Channell et al., 2018). For short path length cells (12 mm) epoxy cells were used; for long path length cells (20 mm) titanium cells were used. SV used short path length cells with 395 µl buffer injected into one sector and 405 µl solute solution injected into the other sector. 4 hole or 8 hole rotor was used depending on the experiment and type of cells. For SE 100 µl was injected into both sectors for sample and reference in 12 mm cells or 145 µl for sample and reference in 20 mm titanium cells. The minimum concentration for SE is (0.2-0.3) mg/ml with long path length cells and the minimum concentration for 12 mm path length cells is ~0.5 mg/ml. In polysaccharides, non-ideality can still be significant due to high affinity for solvent and high exclusion volumes (Schuck et al., 2014b). Therefore, several concentrations are required and these molecular weights were plotted with extrapolation to zero concentration. Analysis was carried out with SEDFIT, SEDFIT MSTAR and MultiSig. The graphs were then created using Microcal ORIGIN.

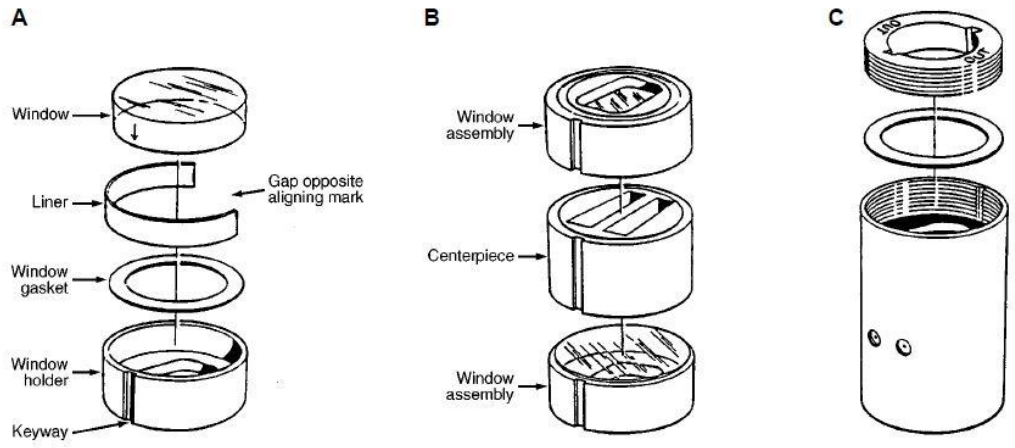

Figure 2-43: Cell assembly in three steps: A, B and C. Images taken from Cole and Hansen (1999).

1.1.1.2 Cleaning cells

Cells must be perfectly clean prior to use as any dust or contamination would affect results and give a false impression of the sample or if contamination is identified lead to having to re-run the sample. The cells were checked before each experiment to confirm they were clean and re-cleaned if they had collected any dust. The cells were cleaned either via *in situ* cleaning for low concentration samples or by disassembling to clean the cell. The cleaning solutions are the same for *in situ* cleaning as for general cleaning. The centre piece and sapphire windows were cleaned with the solvents below in the following order: 1 ml experiment buffer; 1 ml 2% detergent (nutricon); 1 ml 5% acetic acid; 3x 1 ml deionised water; 2x 2ml ethanol.

The cells used had two drilled holes in at the top. This allows the cells to be easily filled and allows for *in situ* cleaning. Rather than disassembling the cell two tubes were placed in each sector, one drawing air or fluid out of the cell using a vacuum and one drawing air or fluid into the cell. The *in situ* cleaning involves using a vacuum pump

to bubble cleaning solutions through the cell and then drying the cell by pulling air into the cell.

For general cleaning: the cell is emptied, disassembled and then the centre piece and sapphire windows are cleaned. During the detergent phase the sapphire windows are rubbed on tissue to ensure any surface contamination is removed and the centre pieces cleaned with a small brush. The cell components are then dried.

2.6.3.1 AUC SV and SE run

The buffer used for chitosan analysis was 0.2 M acetate buffer. Ionic strength is required to shield charges on separate polymer molecules and allow for accurate analysis by reduced non-ideality. SE concentrations were 0.3, 0.4, 0.5, 0.6, 0.7, 0.8 and 1.0 mg/ml; SV concentration varied, details of which can be found in Appendix 1-3. The density of the buffer was measured using a density meter and viscosity was measured using a roll and ball viscometer. Partial specific volume ($\bar{v}$) of chitosan is 0.57 (ml/g) (Morris et al., 2009a).

2.6.3.2 SV Methodology for Chitosan

SV run of chitosan was run at 5000 rpm. AUC XL-I cells were used with 395 µl of sample and 405 µl reference. 8 cell rotar was used. Seven concentration: 0.3, 0.4, 0.45, 0.5, 0.6, 0.7 and 0.8 mg/ml of chitosan in 0.2 M acetate buffer with the same 0.2 M acetate buffer as the reference was used in analysis.

AUC was run at 3000 rpm, the fringes were then optimised, subsequently the AUC was run at 50000 rpm using interference. Analysis was carried out using SEDFIT.

Acetate buffer theroretical pH 4.3 was made by mixing 64.68 ml of 0.2 M sodium acetate (2.7222 g in 100 ml reverse osmosis (RO) water) with 185.32 ml of 0.2 M acetic acid (2.862 ml in 250 ml RO water).

Chitosan (1.0004 g) was dissolved in 0.2 M acetate buffer (100 ml) to produce a 1 mg/ml stock solution.

pH 4.34
Density 1.00171 g/cm^3 (average of 5 measurements)
Viscosity 0.00959 (P) (average 5 measurements-roll and ball viscometer)

2.6.3.3 SE methodology

2.6.3.3.1 Standard procedure

1 ml/ml stock solution used to make up different concentrations in 0.2 M acetate buffer.

AUC was run at 3000 rpm fringes optimised, run at 48000 rpm fringes re-optimised before starting method. Interference was run at 48000 rpm for 3 days, test to equilibrium in SEDFIT was used to check the sample had equilibrated. The first five scans (except where movement was observed in which case first scan or two were

used) and last 5 scans were used for analysis using Mstar, Mstar hinge point and MultiSig. This allows for verification of results though three methods of analysis.

Below is the buffers with viscosity and density and related experiment.

2.6.3.3.2 Buffer 1 for chitosan 48000 rpm- 20 mm cells

Table 2-11: Buffer for analysis of chitosan (run at 48,000rpm)

Buffer	**Theorectical pH**	**Measured pH**	**Sodium acetate**	**Acetic acid**	**Density (g/cm^3)**	**Dyn Viscosity (P)**
Buffer 1 for Chitosan 48000 rpm	4.3	4.19	64.68 ml of 0.2 M sodium acetate (2.7220 in 100ml reverse osmosis (RO) water)	185.32 ml of 0.2 M acetic acid (2.862ml in 250ml RO water)	1.001617 (average of 5 measurements)	Viscosity 0.009501 (average 5 measurements at 20^{o}C with a 50^{o} angle)

Chitosan (0.1004 g) was dissolved in 0.2 M acetate buffer (100 ml) to produce a 1 mg/ml stock solution. Concentrations: 0.3, 0.5, 0.7 mg/ml chitosan in 0.2 M acetate buffer.

2.6.3.3.3 Buffer 2 Acetate buffer –SE chitosan and degraded chitosan

Table 2-12: Buffer for analysis of chitosan (run at 40,000rpm) and degraded chitosan batch 1

Buffer	**Theoretical pH**	**Measured pH**	**Sodium acetate**	**Acetic acid**	**Water**	**Density (g/cm^3)**	**Dyn Viscosity (P)**
Buffer 2	4.3	4.43	1.760 g	2.122 ml	250 ml	1.00111 (average of 5 measurements)	0.01118 (average 5 measurements at 20 ^{o}C with a 50^{o} angle)

2.6.3.3.4 Chitosan

Chitosan (0.2500 g) was dissolved in 0.2 M acetate buffer (25 ml) to produce a 1 mg/ml stock solution. Concentrations analysed were 0.4, 0.5, 0.6, 0.7, 0.8 and 1.0 mg/ml chitosan in 0.2 M acetate buffer.

2.6.3.3.5 Degraded Chitosan (Batch 1)

Degraded chitosan (0.0250 g) (Batch 1) was dissolved in 0.2 M acetate buffer (25 ml) to produce a 1 mg/ml stock solution. Concentrations analysed were: 0.3, 0.4, 0.5, 0.6, 0.7, 0.8 and 1.0 mg/ml degraded chitosan in 0.2 M acetate buffer.

2.6.3.3.6 Buffer 3 Acetate buffer –SE chitosan and degraded chitosan

Table 2-13: Buffer for analysis of chitosan (run at 35,000 rpm) and degraded chitosan batch 2 (1 h) and 3 (1.5 h)

Buffer	**Theoretical pH**	**Measured pH**	**Sodium acetate**	**Acetic acid**	**Water**	**Density (g/cm^3)**	**Dyn Viscosity (P)**
Buffer 3	4.3	4.13	3.5208 g	4.244 ml	500 ml	1.00172 (average of 5 measurements)	0.011263 (average of 5 measurements at 20 ^oC with a 50^o angle)

2.6.3.3.7 Chitosan 35000 rpm-20 mm cells

Chitosan (0.10001 g) was dissolved in 0.2 M acetate buffer (100 ml) to produce a 1 mg/ml stock solution. Concentrations analysed were: 0.3, 0.4, 0.5, 0.6, 0.7, 0.8 and 1.0 mg/ml degraded chitosan in 0.2 M acetate buffer.

2.6.3.3.8 Degraded chitosan batch 2 (1 h) 40000 rpm-12 mm cells

Degraded chitosan (0.1003 g) (Batch 2) was dissolved in 0.2 M acetate buffer (100 ml) to produce a 1mg/ml stock solution. Concentrations analysed were 0.5, 0.6, 0.7 mg/ml.

2.6.3.3.9 Degraded chitosan batch 3 (1.5 h) 40000 rpm-12 mm cells

Degraded chitosan (Batch 3) (0.1000 g) was dissolved in 0.2 M acetate buffer (100 ml) to produce a 1 mg/ml stock solution. Concentrations analysed were 0.5, 0.6, 0.7 mg/ml.

2.6.3.3.10 Buffer 4 Degraded chitosan large batch 1 40000 rpm-12 mm cells

Table 2-14: Buffer for analysis of degraded chitosan batch 3

Buffer	**Theoretical pH**	**Measured pH**	**Sodium acetate**	**Acetic acid**	**Water**	**Density (g/cm^3)**	**Dyn Viscosity (P)**
Buffer 4	4.3	4.16	1.7618 g	2.122 ml	250 ml	1.00173 (average of 5 measurements)	0.011275 (average of 5 measurements at 20oC with a 50o angle)

Degraded chitosan (0.1005 g) (Batch 1-oven dried) was dissolved in 0.2 M acetate buffer (100 ml) to produce a 1 mg/ml stock solution.

Degraded chitosan (0.0500 g) (From batch 1 which was potential contaminated and not fully dry) was dissolved in 0.2 M acetate buffer (50 ml) to produce a 1 mg/ml stock solution.

Results of both were the same. There were concerns the sample was not fully dry after freeze drying so it was placed in the oven. This resulted in a yellower-looking sample but measurements showed it to be the same as the sample not oven dried.

Concentrations analysed were 0.5, 0.6, 0.7 mg/ml.

2.6.3.3.11 Buffer 5 Degraded chitosan batch (0.5 h) 40,000 rpm-12 mm cells

Table 2-15: Buffer for analysis of degraded chitosan 0.5 h

Buffer	**Theoretical pH**	**Measured pH**	**Sodium acetate**	**Acetic acid**	**Water**	**Density**	**Dyn Viscosity (P)**
Buffer 5	4.3	4.16	1.7613 g	2.122 ml	250 ml	1.00172 (average of 5 measurements)	0.011264 (average of 5 measurements at 20°C with a 50° angle)

Degraded chitosan (1.0003 g) was dissolved in 0.2 M acetate buffer (100 ml) to produce a 1 mg/ml stock solution. Concentrations analysed were 0.5, 0.6, 0.7 mg/ml.

2.6.3.3.12 Buffer 6 Acetate buffer –SE chitosan and degraded chitosan

Table 2-16: Buffer for analysis of large batches of degraded chitosan

Buffer	**Theoretical pH**	**Measured pH**	**Sodium acetate**	**Acetic acid**	**Water**	**Density (g/cm^3)**	**Dyn Viscosity (P)**
Buffer 6	4.3	4.16	3.5210 g	4.244 ml	500 ml	1.00172 (average of 5 measurements)	0.011252 (average of 5 measurements at 20°C with a 50° angle)

2.6.3.3.13 Large batch 2 degraded chitosan, 40000 rpm-12 mm cells

Degraded chitosan (0.1000 g) (Batch 3) was dissolved in 0.2 M acetate buffer (100 ml) to produce a 1 mg/ml stock solution. Concentrations analysed were 0.5, 0.6, 0.7 mg/ml.

2.6.3.3.14 Large batch 3 degraded chitosan, 40000 rpm-12 mm cells

Degraded chitosan (Batch 3) (0.1002 g) was dissolved in 0.2 M acetate buffer (100 ml) to produce a 1 mg/ml stock solution. Concentrations analysed were 0.5, 0.6, 0.7 mg/ml.

2.6.3.3.15 Large batch 4 degraded chitosan, 40000 rpm-12 mm cells

Degraded chitosan (0.1001g) (Batch 3) was dissolved in 0.2 M acetate buffer (100 ml) to produce a 1 mg/ml stock solution. Concentrations analysed were 0.5, 0.6, 0.7 mg/ml.

2.6.3.3.16 Large batch 5 degraded chitosan, 40000 rpm-12 mm cells

Degraded chitosan (0.1003g) (Batch 3) was dissolved in 0.2 M acetate buffer (100 ml) to produce a 1 mg/ml stock solution. Concentrations analysed were 0.5, 0.6, 0.7 mg/ml.

2.6.3.3.17 Buffer 7 Acetate buffer –Large batch combined

Buffer	**Theoretical pH**	**Measured pH**	**Sodium acetate**	**Acetic acid**	**Water**	**Density (g/cm^3)**	**Dyn Viscosity (P)**
Buffer 7	4.3	4.16	1.7604 g	2.122 ml	250 ml	1.00173 (average of 5 measurements)	0.010574 (average of 5 measurements at 20oC with a 50o angle)

2.6.3.3.18 Large batch combined degraded chitosan, 40000 rpm-20 mm cells

Degraded chitosan (0.1004 g) (Large batchs 1,2,3,4 and 5 combined) was dissolved in 0.2 M acetate buffer (100 ml) to produce a 1 mg/ml stock solution. Concentrations analysed were 0.3, 0.4, 0.5, 0.6, 0.7, 0.8, 1.0 mg/ml.

Chapter 3. Characterisation of aminocellulose for conservation

3.1 Introduction

Aminocellulose has a very similar chemical structure to cellulose; structurally it has side chain modifications at C6 to include amine groups (see Figure 3-1).

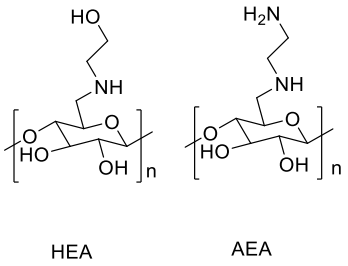

Figure 3-1: Structure of 2 aminocelluloses; HEA on the left and AEA on the right.

Aminocellulose is therefore similar in structure to chitosan. Aminocellulose poses an advantage over chitosan as it is soluble at a neutral pH. This avoids acetic acid being required, hence, if it proves to have similar consolidation abilities to chitosan, it could be even more advantageous. Aminocelluloses have a variety of potential applications in the biomedical field where there has recently been an increase in research into the use of natural polymers. This is because natural polymers are more likely to be biocompatible (Christensen et al., 2012; Cipriani et al., 2010; Croisier and Jérôme, 2013; Heinze et al., 2016; Kumbar et al., 2014; McHale et al., 2016a; Petersen and Gatenholm, 2011; Reis et al., 2008; Ulery et al., 2011; Walsh et al., 2017). Aminocelluloses have previously been investigated as a coating for glass biomedical equipment, such as implants with a biocompatiable/biofunctional film, and for retarting microbial activity. These investigations have produced positive results (Jung and Berlin, 2005; Jung et al., 2007; Roemhild et al., 2013). The potential advantage of aminocellulose use for coating medical devices lies in the fact that blood can form protein layers, which when in contact with foreign objects can lead to thrombotic

events; adding a biocompatible coating to medical devices that prevents protein build-up mayt help prevent adverse effects (Bulwan et al., 2012; Mannhalter, 1993). Another potential role is in the use of catheter-like devices, where the aminocellulose can prevent biofilm formation and thus, potentially prevent infection (Francesko et al., 2016). This relies on layers of aminocellulose and hyaluronic acid, hence, the self-association could affect this and could effect how easily this coating can be removed from devices as well. Another potential is for wound dressing; amino-functionalised cellulose carbamates have been investigated for this with promising results (Ganske et al., 2016). Self-association affecting the thickness of layers of amino-functionalised cellulose carbamates and how readily it can re-dissolve after the cotton has been coated and dried out, could be very important to this application.

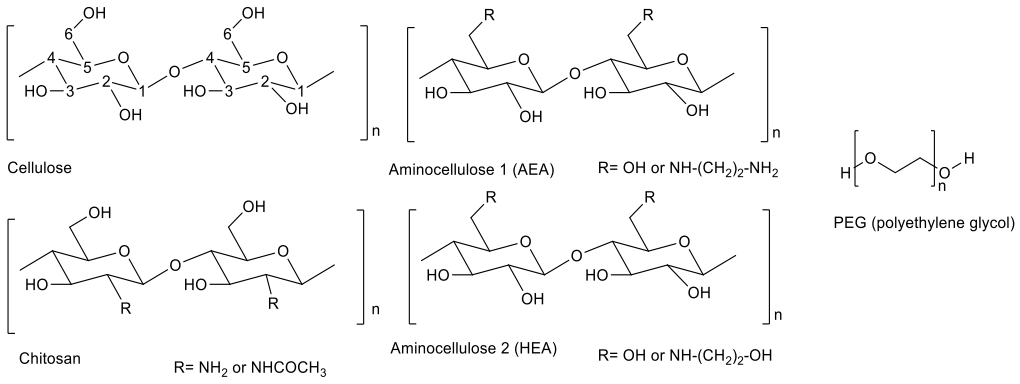

Figure 3-2: The structures of cellulose, aminocellulose (6-deoxy-6-(2-aminoethyl)aminocellulose), chitin (precursor of chitosan), chitosan and PEG (polyethylene glycol –the gold standard for conservation)

Biocompatibility, similarly to coated cotton, may also be useful for wood conservation if the molecular weight is low enough to penetrate the cells. Aminocellulose may strengthen the wood by providing a coating around each cell, therefore strengthening

the wood as a whole. The amino groups allow for solubility in water; allowing treatment with a water-based solution and may also prevent bacterial and fungal growth during treatment, and may chelate metal ions in composite artefacts, which contain iron and wood. Finally, the amino groups may provide a small alkaline reserve to help with the prevention of future acid build up and degradation. This is very important in terms of the Oseberg artefacts, which are currently highly acidic. Established consolidants have some disadvantages as discussed in Chapter 1 and aminocellulose may prove a good alternative.

6-deoxy-6-(2-aminoethyl) aminocellulose (AEA) is a water-soluble polymer with a range of low molecular weights (structure shown in Figure 3-2). An earlier study on an AEA (AEA-1) was found to have a monomeric molecular weight of 3250 Da; this then self-associates reversibly to form a polymer with a weight average molecular weight (M_w) of ~ 13000 Da (Nikolajski et al., 2014). AEA are produced by a nucleophilic displacement (SN_2) reaction of a tosyl group with ethenediamine (Heinze et al., 2016). This AEA aminocellulose had a DS of 0.83 and tosyl DS 0.2 has been found to reversibly self-associate, whereas for other aminocellulose, the self-association has been found to only be partially reversible (Heinze et al., 2011; Nikolajski et al., 2014). This investigation analyses a similar aminocellulose to AEA, previously analysed by Nikiolajski, only differing in the degree of substitution with a DS (amine, at C6) of 0.59, DS (Cl, at carbon atom C_l) of 0.24 and DS tosyl of 0 together with a 6-deoxy-6-(2-hydroxyethyl) aminocellulose (HEA-1) with a DS (ethanolamine) of 0.73, DS (Cl) of 0.15, DS (Tosyl) of 0.10 for comparison of the molecular weight and the self-association properties when a change is made from a

terminal NH_2 to an OH. The structure of AEA and HEA are shown in Figure 3-2 along with cellulose, chitosan and PEG for comparison.

AUC as described in Chapter 2 is a powerful matrix-free technique for examining hydrodynamic differences between polymers. Sedimentation velocity can determine the heterogeneity of a sample and identify self-association through comparison of the effect on concentration of the sedimentation coefficients on a heterogeneous sample. Sedimentation equilibrium can determine the average molecular weight of a sample and can also be used to confirm self-association and determine the monomeric molecular weight (Heinze et al., 2011; Nikolajski et al., 2014).

3.2 Results

3.2.1 Aminocellulose 1 (AEA)

MSTAR and MultiSig analysis have been carried out for a batch of aminocellulose (6-deoxy-6-(2-aminoethyl) aminocellulose) (AEA) donated by Prof. Heinze (University of Jena) produced by R. Hampe. The partial specific volume ($\bar{v}$) was also determined for use in the calculations via density measurements at various concentrations (see Figure 3-3).

3.2.1.1 Partial specific volume

$$\bar{v} = \frac{\left(\frac{1}{\rho_0}\right)}{1-\left(\frac{d\rho}{dc}\right)} \quad \textbf{(3-1)}$$

Equation 3-1 shows the calculation for the partial specific volume ($\bar{v}$) (Eikenberry, 1982). By plotting density vs. concentration is it is possible to determine the slope of the line (dρ/dc). Hence, it is possible to calculate the partial specific volume from the density of buffer and density at various concentrations. The partial specific volume is needed for analysis of sedimentation velocity and sedimentation equilibrium results. The partial specific volume for HEA is 0.614 ml/g.

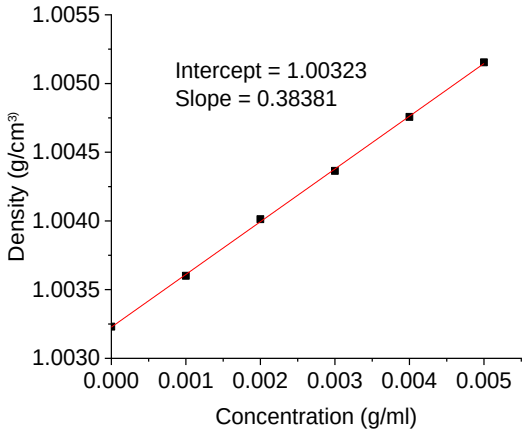

Figure 3-3: Density (g/cm^3) vs. concentration (g/ml) of AEA to aid in determination of $\bar{v}$.

3.2.1.2 SV

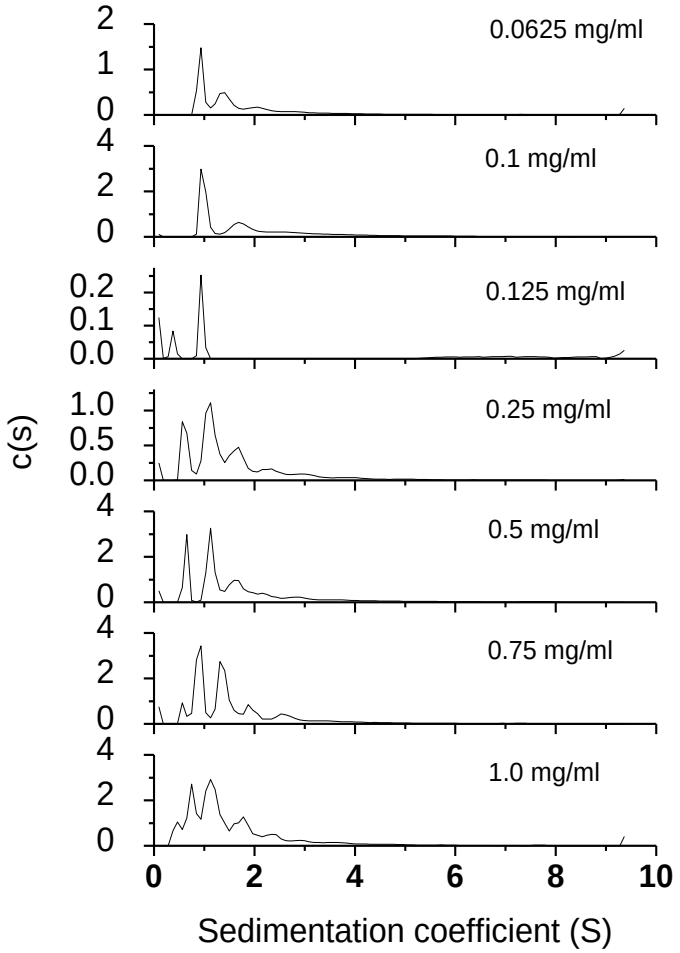

Figure 3-4: Sedimentation coefficient distribution plots of *c*(s) vs. *s* for AEA, different concentrations showing evidence of self-association. Frictional coefficient set to 3. 0.1 mg/ml sample leaked a little (correct $\bar{v}$ 0.614 ml/g was used here).

Self-association is not clear from Figure 3-4 although there is some broadening of the peaks. However, there is no clear evidence of self-association. The low molecular weights could be making the analysis problematic. Sedimentation equilibrium is expected to clarify the presence/absence of self-association.

3.2.1.3 SE-with approximate partial specific volume

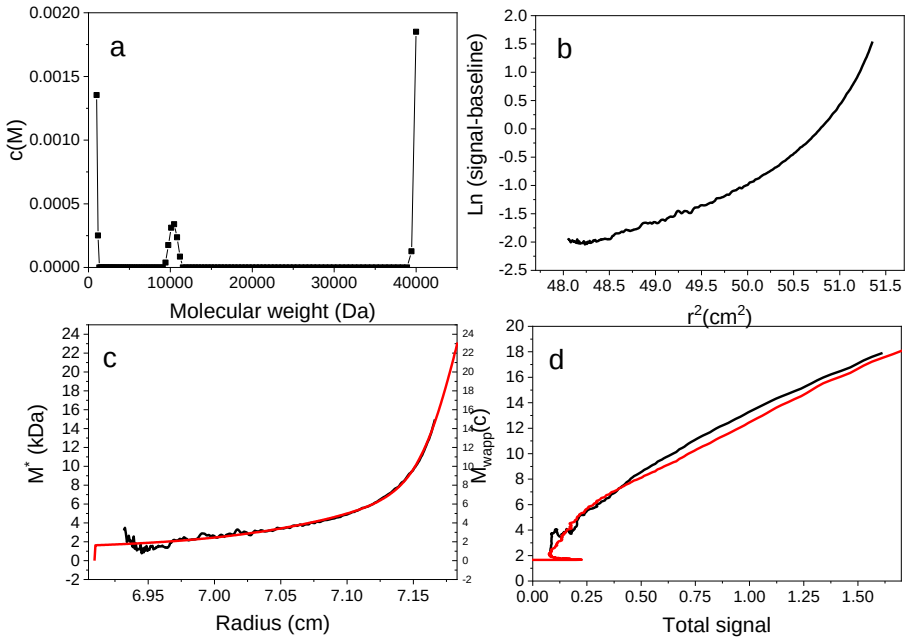

Figure 3-5: MSTAR analysis results of 0.3 mg/ml aminocellulose (SE was run at 40000 rpm). a.) Shows the molecular weight distribution c(M) vs. M showing one species peaking ~ 11 kDa. The front peak is an artefact of analysis and the final one is because of species greater than 40 kDa. b.) Log concentration ln(c) vs. r^2, where r is the radial distance from the centre rotation which has an upward curve suggesting polydispersity. c.) M* vs. r plot in black with the fit based on M* extrapolation giving $M_{w,app}$ = 23.9 kDa. d.) Gives the local or point apparent molecular weight at radial position r plotted vs. local concentration c(r) for different radial positions; the red line is the fit and the black the raw data of $M_{w,app}(c)$ vs. concentration (in total signal).

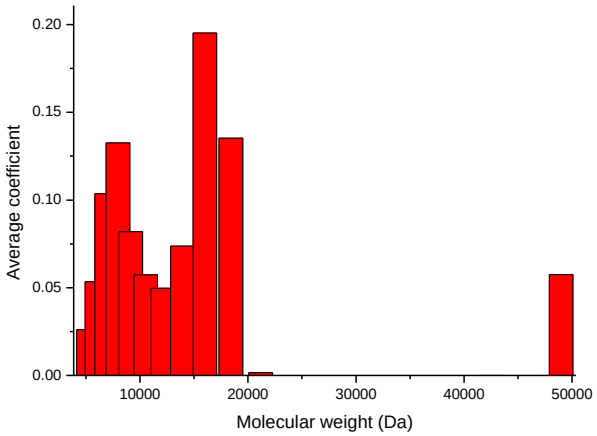

Figure 3-6: MultiSig distribution results of 0.3 mg/ml aminocellulose. The presence of three discrete components ~ 8000 and 15000 and 50000 Da is clear.

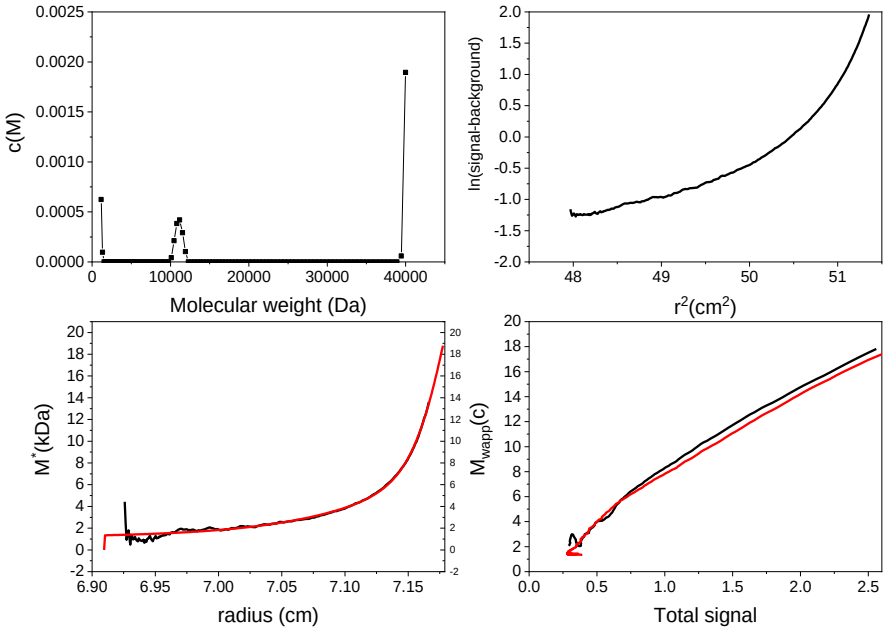

Figure 3-7: MSTAR analysis results of 0.4 mg/ml aminocellulose (SE 40000 rpm) a.) c(*M*) vs. *M* showing one species peaking ~ 12 kDa; the front peak is an artefact of analysis and the final one is because of species greater than 40 kDa. b.) Log concentration ln(*c*) vs. r^2, which has an upward curve suggesting polydispersity. c.) *M** vs. r plot in black with the fit based on M* extrapolation giving $M_{w,app}$ = 19.7 kDa. d.) of $M_{w,app}(c)$ vs. concentration (in total signal) the red line is the fit and the black the raw data showing a decent fit.

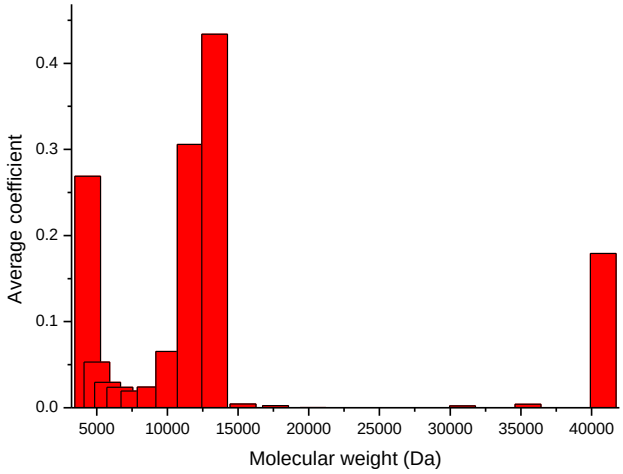

Figure 3-8: MultiSig distribution results of 0.4 mg/ml aminocellulose. The presence of three discrete components ~ 3000, 13000 (major) and 40000 Da is clear.

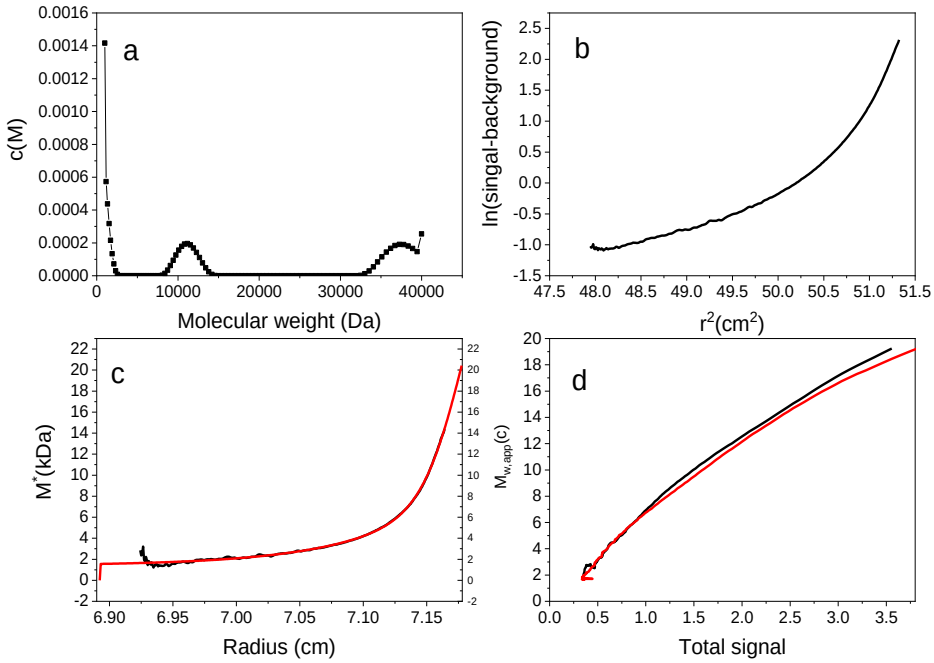

Figure 3-9: MSTAR results of 0.5 mg/ml aminocellulose (SE 40000 rpm) a.) c(*M*) vs. *M* showing one species peaking ~ 12 kDa and 37 kDa; the front peak is an artefact of analysis and the final one is because of species greater than 40 kDa. b.) Log concentration ln(*c*) vs. r^2, which has an upward curve suggesting polydispersity. c.) *M** vs. *r* plot in black with the fit based on *M** extrapolation giving $M_{w,app}$ =21.2 kDa. d.) of $M_{w,app}(c)$ vs. concentration (in total signal) the red line is the fit and the black the raw data showing a decent fit.

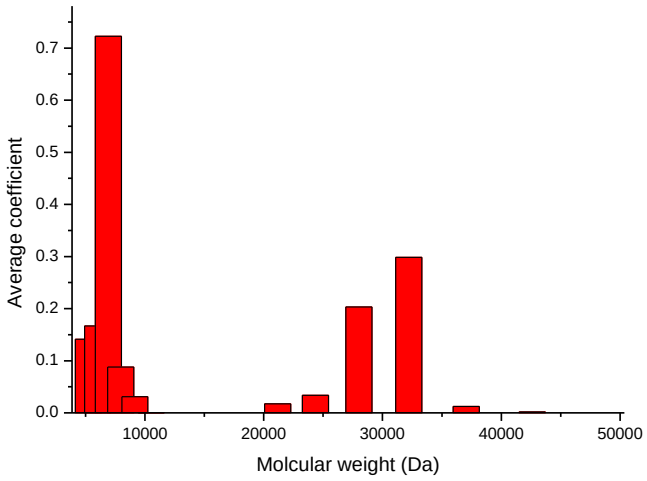

Figure 3-10: MultiSig distribution results of 0.5 mg/ml aminocellulose. The presence of two discrete components ~ 10000 Da (major) and 30000 Da (minor component) is clear.

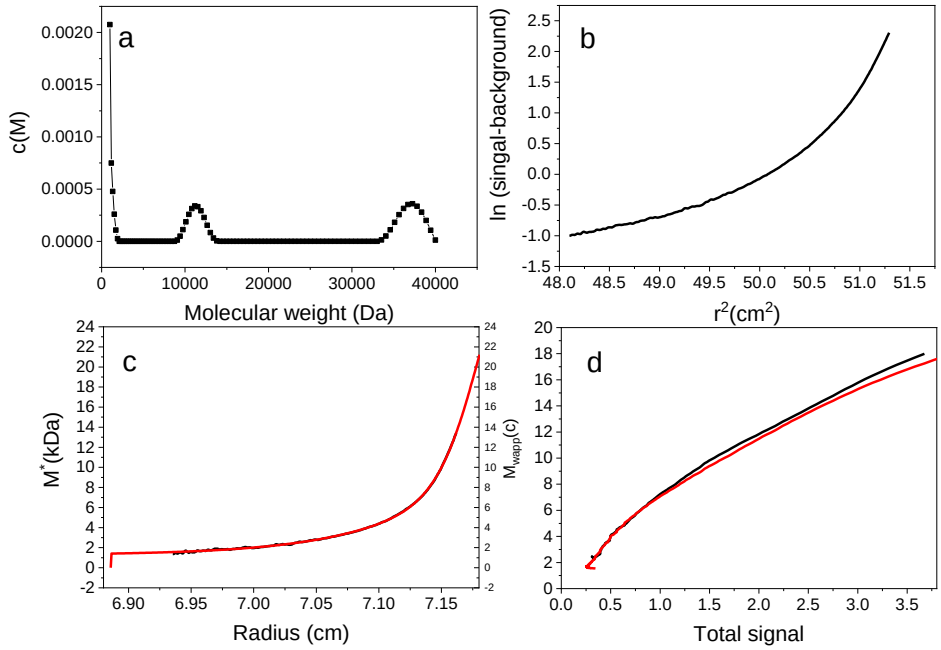

Figure 3-11: MSTAR results of 0.6 mg/ml aminocellulose (SE 40000 rpm) a.) $c(M)$ vs. M showing one species peaking ~ 10 and 36 kDa; the front peak is an artefact of analysis b.) Log concentration $\ln(c)$ vs. r^2, which has an upward curve suggesting polydispersity. c.) M^* vs. r plot in black with the fit based on M^* extrapolation giving $M_{w,app}$ = 22.7 kDa. d.) $M_{w,app}(c)$ vs. concentration (in total signal) the red line is the fit and the black the raw data showing a decent fit.

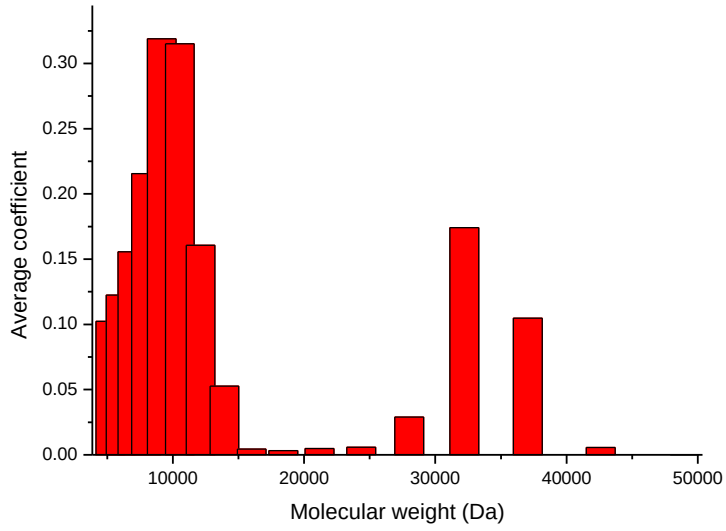

Figure 3-12: MultiSig distribution results of 0.6 mg/ml aminocellulose. The presence of two discrete components ~ 10000 Da (major) and 33000 Da (minor component) is clear.

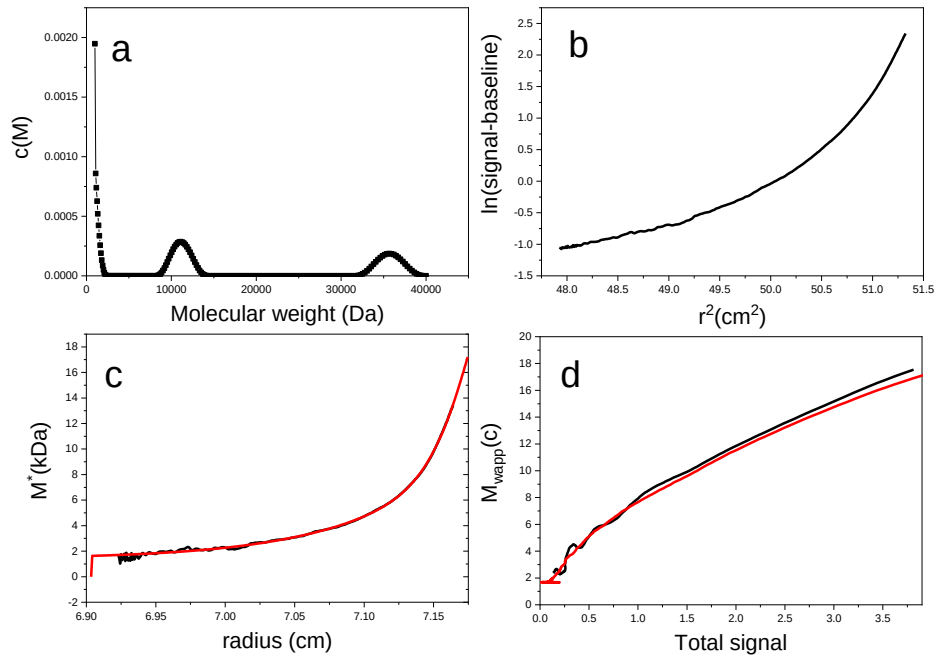

Figure 3-13: MSTAR results of 0.7 mg/ml aminocellulose (SE 40000 rpm) a.) $c(M)$ vs. M showing one species peaking ~ 11 and 36 kDa; the front peak is an artefact of analysis b.) Log concentration ln(c) vs. r^2, which has an upward curve suggesting polydispersity. c.) M^* vs. r plot in black with the fit based on M^* extrapolation giving $M_{w,app}$ = 17.8 kDa. d.) of $M_{w,app}(c)$ vs. concentration (in total signal) the red line is the fit and the black the raw data showing a decent fit.

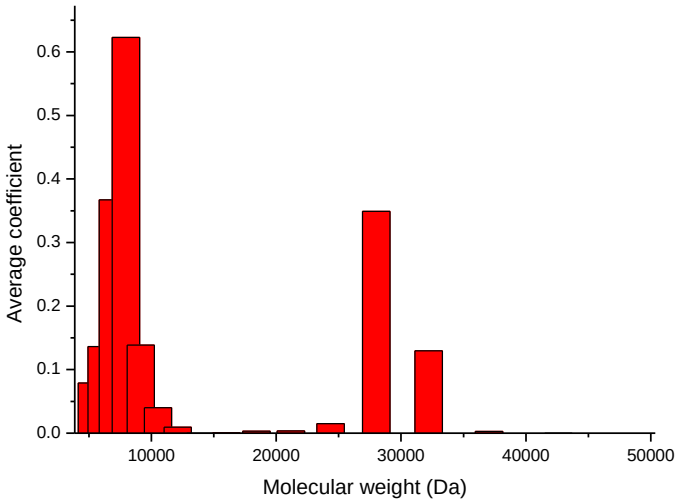

Figure 3-14: MultiSig distribution results of 0.7 mg/ml aminocellulose. The presence of two discrete components ~ 6000 Da (major) and 27000 Da (minor component) is clear.

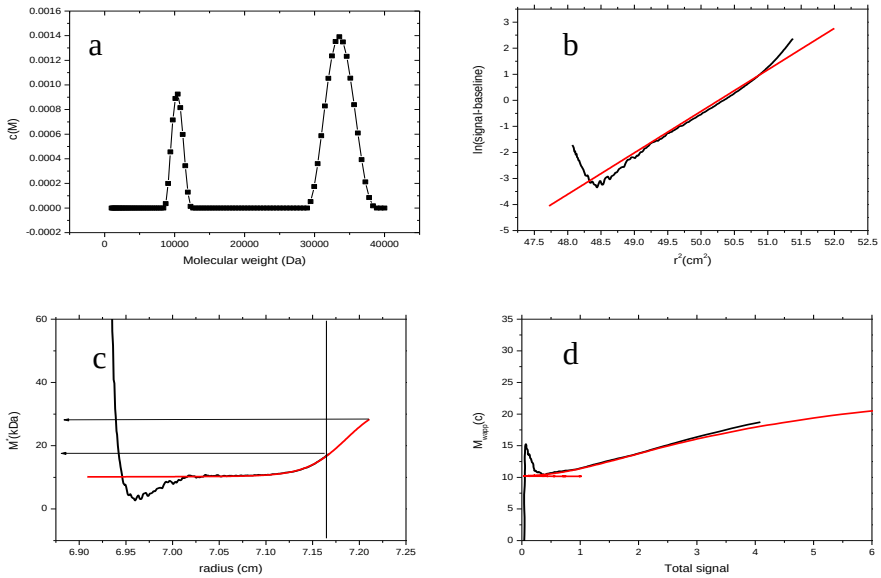

Figure 3-15: MSTAR results of 0.8 mg/ml aminocellulose (SE 40000 rpm) a.) $c(M)$ vs. M showing one species peaking ~ 10 and 33 kDa; the front peak is an artefact of analysis b.) Log concentration ln(c) vs. r^2, which has an upward curve suggesting polydispersity. c.) M^* vs. r plot in black with the fit based on M^* extrapolation giving $M_{w,app}$ = 28.7 kDa. d.) $M_{w,app}(c)$ vs. concentration (in total signal) the red line is the fit and the black the raw data showing a decent fit.

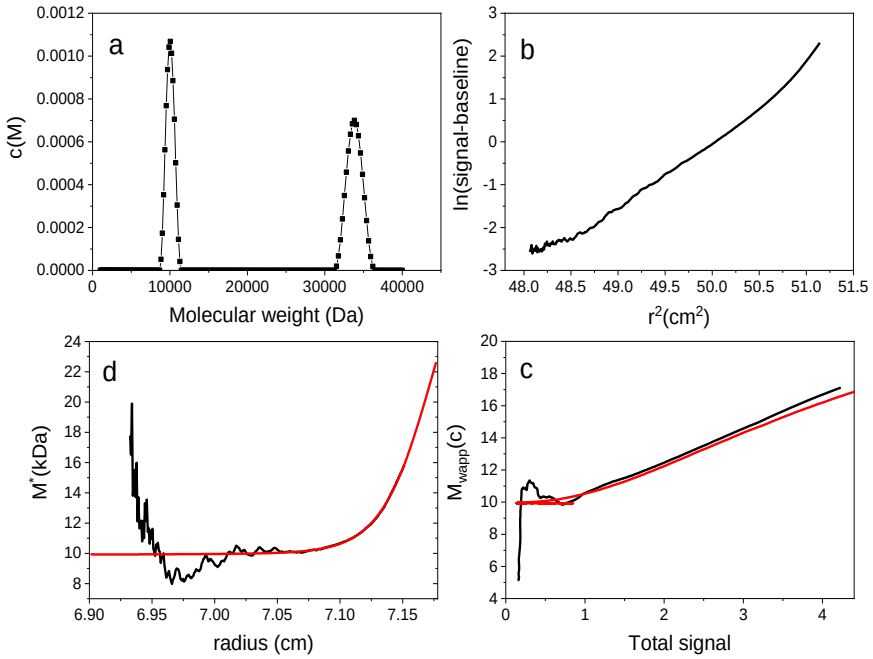

Figure 3-16: MSTAR results for 1.0 mg/ml aminocellulose (SE 40000 rpm) a.) $c(M)$ vs. M showing one species peaking ~ 10 and 34 kDa; the front peak is an artefact of analysis b.) Log concentration ln(c) vs. r^2, which has an upward curve suggesting polydispersity. c.) M^* vs. r plot in black with the fit based on M^* extrapolation giving $M_{w,app}$ = 23.1 kDa. d.) $M_{w,app}(c)$ vs. concentration (in total signal) the red line is the fit and the black the raw data showing a decent fit.

The 0.3–0.7 mg/ml ln(c) vs. r^2 plots (Figure 3-5, 7, 9, 11 and 13 plot b) show polydispersity from the upward curve, and non-ideality starts to become visible after 0.8 mg/ml (Figure 3-15and 16 plot b) where an upward and downward curve are both visible.

The $c(M)$ vs. M, shows the estimated distribution. However, SE does not give an accurate distribution and MSTAR is not really designed for this type of analysis. MultiSig analysis (Figure 3-6, 8 ,10 and 12) is better for this; however, it is designed for mono dispersed polymers and can only cope with clear species such as monomers, dimers, trimers etc. It is therefore better suited to protein analysis and is not suitable for polydispersed polysaccharides; therefore, all distributions shown here should be considered with caution, but both MSTAR and MultiSig together can give a rough estimation. Figure 3-5, 7, 9, 11, 13, 15 and 16 also include MSTAR extrapolation; M^* vs. radius (plot c) shows how the extrapolation to the base was carried out; this can be used to see if the final average molecular weight can be determined accurately. MSTAR has been plotted against concentration to determine M_w: Figure 16a; however, as observed in Figure 3-5, 7, 9, 11, 13, 15 and 16 plot c, the MSTAR extrapolation has a steep slope towards the base line. This indicates that there may have been larger molecules towards the base that the fit is struggling to account for. Therefore, the extrapolation could be overestimating the molecular weight. In this situation, it may be best to look to the hinge point analysis in the SEDFIT MSTAR programme for a more accurate molecular weight. The The MSTAR $M_{w,app}$ has also been plotted against concentration (Figure 3-17a). The hinge point $M_{w,app}$ has also been plotted against concentration (Figure 3-17b) giving a M_w of 11.4 kDa. Figure 3-17b excludes 0.8 mg/ml as it is more than twice the stdev out and hence, is an outlier. MultiSig analysis

shows that with concentration considered (Figure 3-17c), the M_w is 14.13 kDa excluding 0.6 mg/ml as an outlier, again more than twice the stdev. MultiSig concurs that hinge point analysis appears more accurate than MSTAR analysis, in this case due to the high molecular weight at the base of the cell interfering with the analysis. 40000 rpm was used for the analysis, despite some species being of higher molecular weight, as the intention of this study was to look for self-association and if present, determine the monomeric molecular weight. If the average molecular weight of the whole distribution needs to be evaluated for any reason, the sedimentation equilibrium data collection should be done again at a lower speed. The aim of this investigation was to determine the presence or absence of self-association and the corresponding monomeric molecular weight should self-association be present. The monomeric molecular weight is important to establish if the polymer has any chance of penetrating through to the centre of the wood.

SE-partial specific volume correction is given below; Table 3-1 gives the molecular weights with the original rough partial specific volume of 0.63 ml/g used; this was corrected when measured to 0.614 ml/g and corrected results given in Table 3-2.

Table 3-1: SE results of aminocellulose MSTAR and MultiSig analysis 40000 rpm. Buffer I=0.1M PBS Parameters ($\bar{v}$) =0.63 ml/g, solvent density 1.00334 g/ml, solvent viscosity 0.00931 Poise

concentration (mg/ml)	$M_{w,app}$ (from M*) kDa	Standard deviation (kDa)	Mz (kDa)	Poly dispersity index M_z/M_w	r_{hinge} (cm)	$M_{w,app}$ (from M_w (r_{hinge}) kDa	$M_{w,app}$ (from MultiSig) kDa
0.3	23.9	16.2	34.9	1.46	7.124	12.3	16.2
0.4	19.7	16.4	33.4	1.70	7.119	10.5	13.3
0.5	21.2	15.4	32.5	1.53	7.119	11.8	15
0.6	22.7	15	32.6	1.44	7.121	12.3	39.2
0.7	17.8	14	28.8	1.62	7.114	10.7	13.6
0.8	28.7	9.6	31.9	1.11	7.145	18.4	16.5
0.9	23.1	11.9	29.2	1.26	7.114	13.9	13.9

3.2.1.4 v-bar correction for SE

Table 3-2: SE results of aminocellulose MSTAR and MultiSig analysis 40000 rpm. Buffer I=0.1M PBS Parameters ($\bar{v}$) =0.614 (ml/g), solvent density 1.00334 g/ml, solvent viscosity 0.00931 Poise

concentration (mg/ml)	***M*$_{w,app}$ (from *M**) kDa**	**Standard deviation (kDa)**	***Mz* kDa**	**Poly dispersity index M_z/M_w**	**r_{hinge} (cm)**	**M_{wapp} (from M_w (r_{hinge}) kDa**	**$M_{w,app}$ (from MultiSig) kDa**
0.3	22.9	15.5	33.4	1.46	7.124	11.8	15.52
0.4	18.9	15.7	32	1.69	7.119	10.1	12.74
0.5	20.3	14.8	31.1	1.53	7.119	11.3	14.37
0.6	21.8	14.4	31.2	1.43	7.121	11.8	37.56
0.7	17.1	13.4	27.6	1.61	7.114	10.3	13.03
0.8	27.5	9.2	30.6	1.11	7.145	17.6	15.81
0.9	22.1	11.4	28	1.27	7.114	13.3	13.32

Table 3-2 gives the MSTAR, hinge point and MultiSig molecular weight calculated from the correct partial specific volume. The same data is presented in Figure 3-17 with a line of the average of the molecular weights plotted along with the data points. Values more then two standard deviations from the set were not included in the average. The average hinge point M_w and MultiSig M_w are similar however the MSTAR average is higher this will be because of the self association resulting in much larger molecular weights towards the cell base.

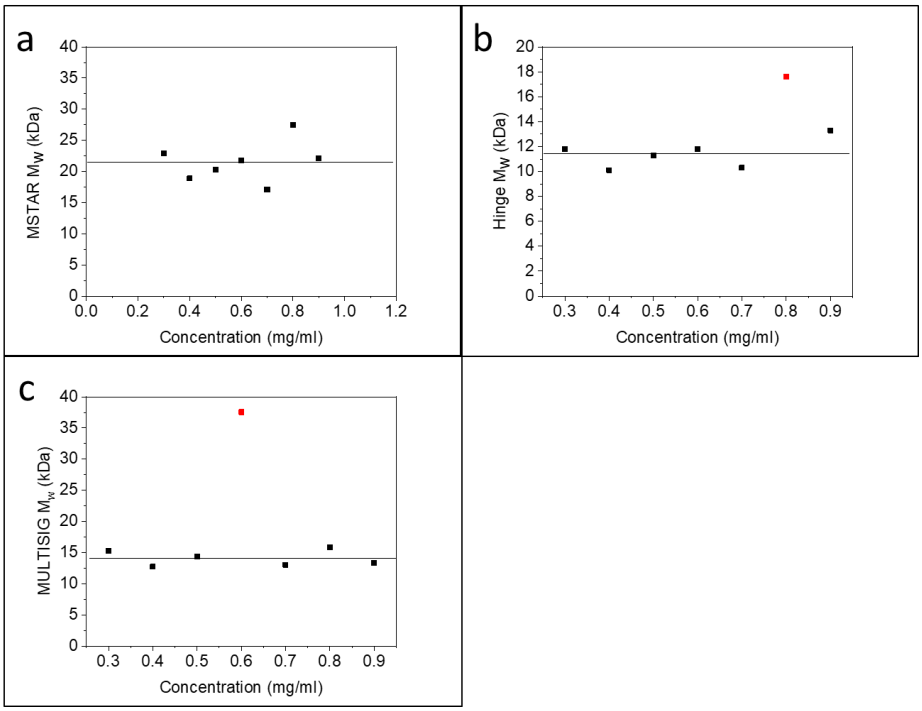

Figure 3-17: AEA SE results run at 40000 rpm analysed with a $\bar{v}$ of 0.614 ml/g, fom three types of analysis of SE results showing molecular weight (kDa) vs concentration (mg/ml). a) MSTAR analysis (0.8 and 1.0 mg/ml excluded due to non-ideality MSTAR M_w (21.5±3.3) kDa (from average (0.3-0.9) mg/ml), b) hinge analysis (0.8 mg/ml excluded as an outlier) Hinge M_w (11.4± 1.2) kDa. (c) MultiSig M_w (14.13±1.31) kDa (average (0.3-1.0) mg/ml excluding 0.6 mg/ml as an outlier).

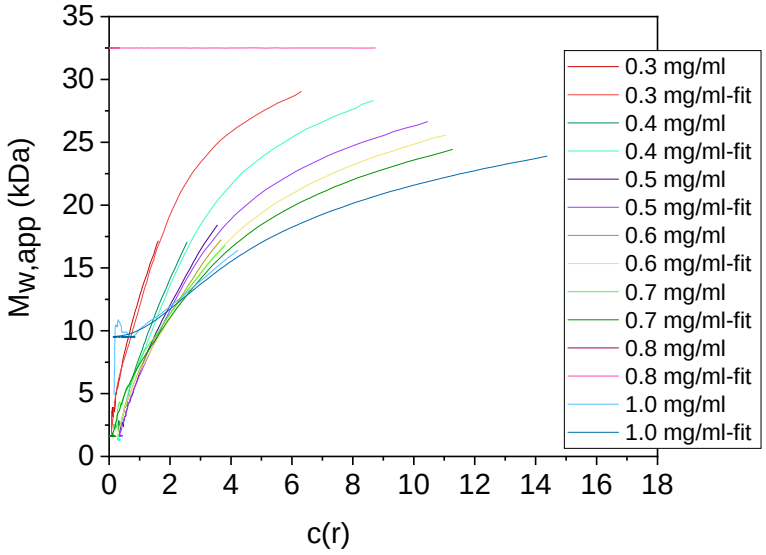

Figure 3-18: MSTAR analysis results $M_{wapp}(c)$ vs. concentration along the cells (c(r)). Loading concentrations 0.3-1.0 mg/ml corrected for $\bar{v}$ 0.614 ml/g and carried out with b-spine analysis. Plateauing between ~23-28 k(Da).

$M_{w,app}(c)$ vs. total signal shows the molecular weight vs. concentration along the cell length (Figure 3-18). This, when plotted against different loading concentrations, can show self-association, through the pattern of curves and if these overlap, this is evidence of a fully reversible self-association. Figures 18 and 19 show close alignment for 0.4-0.6 mg/ml at low concentration which suggests self-association. 0.3 mg/ml is too low a concentration to analyse for 12 mm cells and 0.7 may be too high and affected by non-ideality. The separation of the lines as the concentration increases, also reflects non-ideality. This therefore shows similar results to MultiSig analysis in Figure 3-21. However, the correlation is clearer from the MultiSig results.

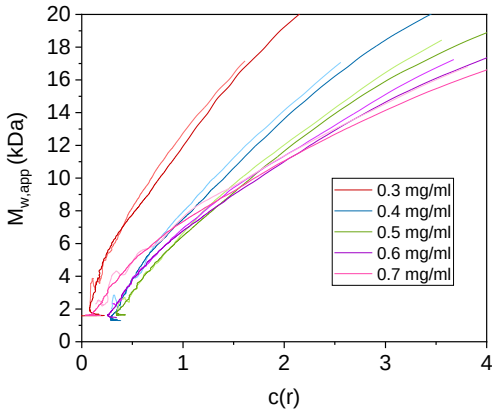

Figure 3-19: MSTAR analysis results of $M_{wapp}(c)$ vs. concentration along the cells (c(r)). Loading concentrations 0.3-0.7 mg/ml corrected for $\bar{v}$ 0.614 ml/g and carried out with b-spine analysis. All initial molecular weight appears to start at ~1.75 kDa.

Similarly to MSTAR, MultiSig M*z,app* vs. concentration along the cell can be plotted with different loading concentrations which can be used to look for self-association (Figure 3-19 a and b plotted using M_z). In this case there is a perfect overlap for different loading concentrations 0.4, 0.5 and 0.6 mg/ml up to ~12000 Da. This is suggestive of a fully reversible self-association for the binding of the first associations after which the association looks to only be partially reversible. This could also be from the effect of non-ideality becoming more apparent at higher concentrations.

Figure 3-20, plots of M_n, M_w, and M_z, also show self-association if the three forms of molecular weight converge to the same molecular weight at zero concentration, which these do, concurring with the results of Figure 3-21, proving self –association. A few points in both Figure 3-21 have been greyed out and not included in the b-spline fit, as they appear to be outliers.

The monomeric molecular weight can be determined from these MultiSig methods and both concur that the monomeric molecular weight is ~4500 Da.

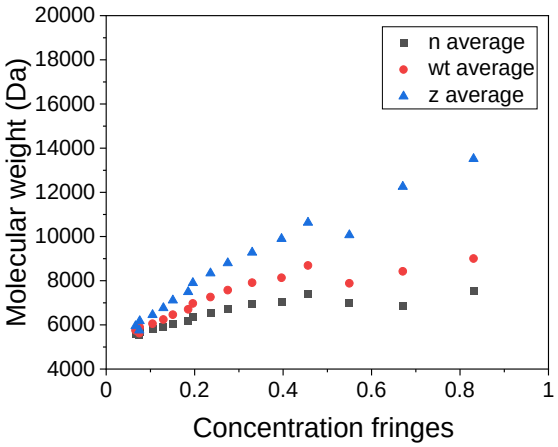

Figure 3-20: MultiSig analysis results shows the molecular weight increase with concentration along the cell showing M_n, M_w and M_z. All can be extrapolated back to ~ 5000 Da.

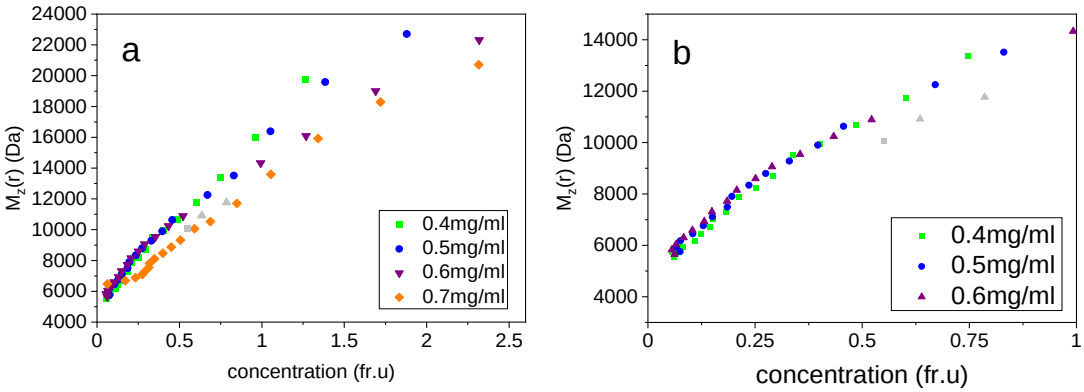

Figure 3-21: Determination of self-association and monomeric molecular weight a) Shows the molecular weight increase with concentration along the cell in fringe units for 4 loading concentrations 0.4-0.7 mg/ml. b) is simply an expansion on this without 0.7 mg/ml which is thought to show more non-ideality. These can be extrapolated back to ~ 5000 Da. Points in grey were outliers that have not been included in the final fit.

3.2.2 Aminocellulose 2 (HEA)

3.2.2.1 Partial specific volume

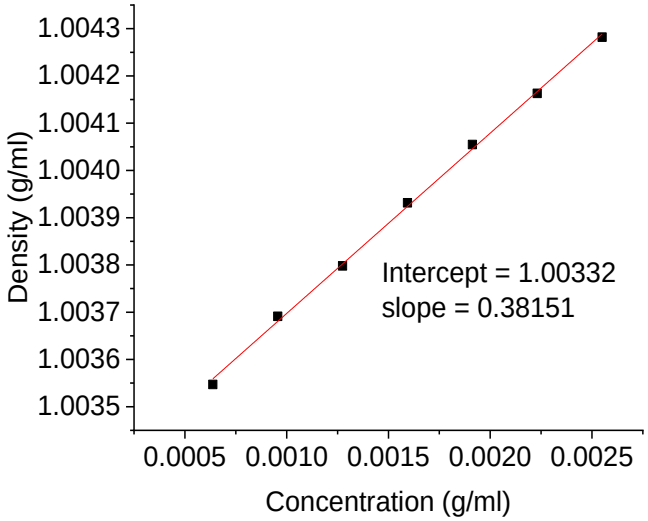

Figure 3-22: Density (g/cm^3) vs. concentration (g/ml) for HEA solutions determine partial specefic volume.

The partial specific volume for HEA was determined in the same manner as AEA through density measurements (see Figure 3-22). Concentrations were from weight: volume ratios however the moisture content was accounted for. The moisture content was checked by oven drying a sample. This sample was then not used in case the heat had affected the polymer, but knowledge of moisture content was accounted for in calculating concentrations for determining partial specific volume.

The $\bar{v}$ for HEA is 0.619 ml/g. This is in line with what is expected as neutral polysaccharides are known to be between 0.5–0.7 ml/g; previously other aminocelluoses have been found to have a partial specific volume between 0.59–0.67 ml/g (Harding, 2005c; Heinze, 2019).

3.2.2.2 SV

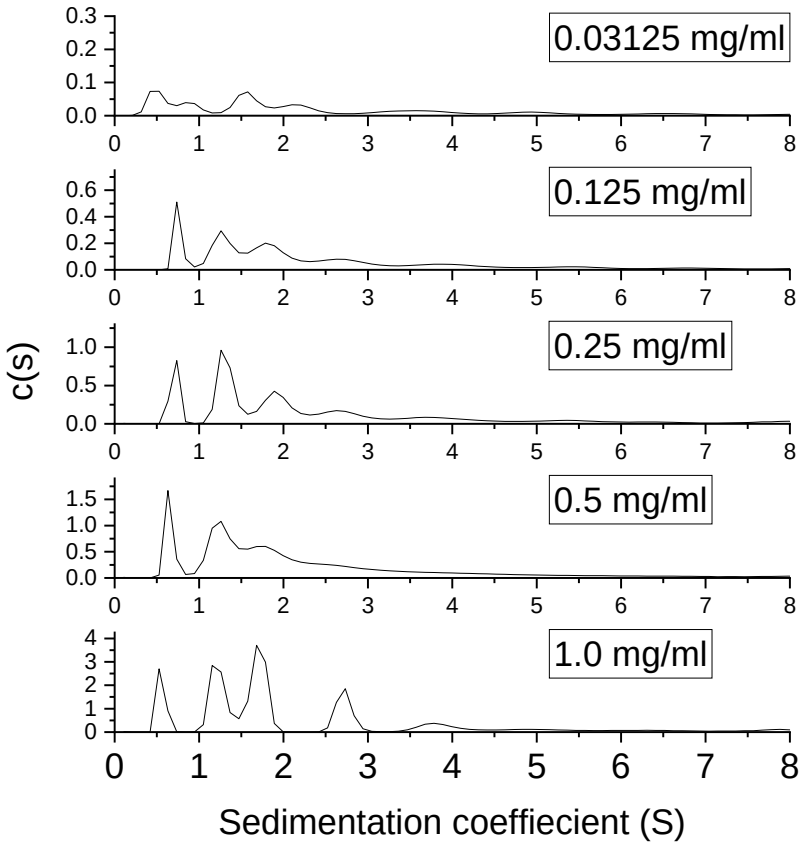

Figure 3-23: Sedimentation coefficient distribution plots of *c*(*s*) vs. *s* for HEA different concentrations showing evidence of self-association.for $\bar{v}$ of 0.619 ml/g.

Figure 3-23 shows that there is some self-association although the trend is not large. At higher concentrations, there are higher proportions of species with higher sedimentation coefficients. This was then confirmed with sedimentation equilibrium experiments.

3.2.2.3 SE

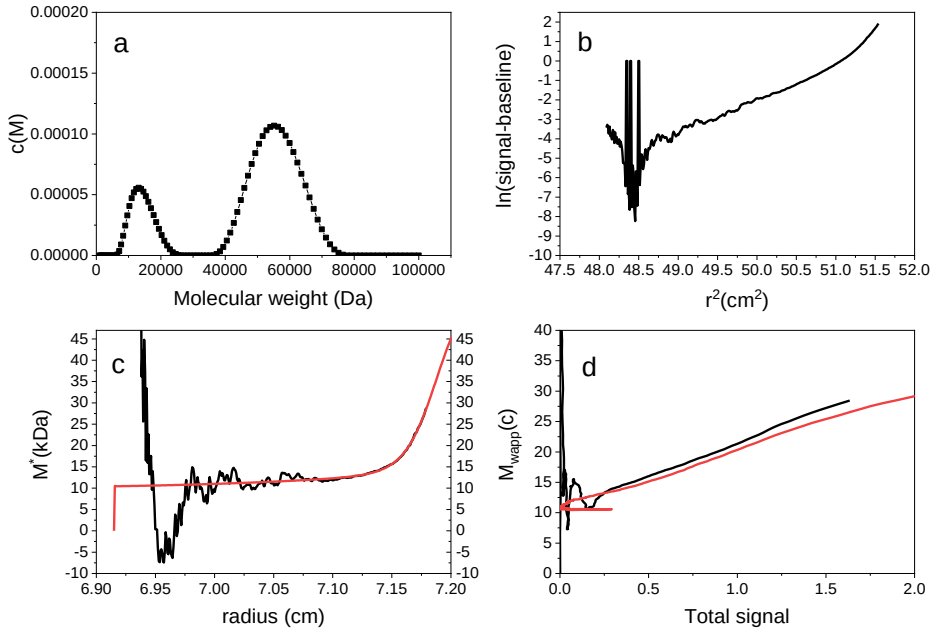

Figure 3-24: MSTAR results of 0.4 mg/ml aminocellulose (SE 40000 rpm) similar to . a.) c(M) vs. M showing one species peaking ~ 15 kDa and another ~ 55 kDa. b.) Log concentration ln(c) vs. r2, which has an upward curve suggesting polydispersity. c.) M* vs. r plot in black with the fit based on M* extrapolation giving Mw,app = 42.8 kDa. d.) Mw,app(c) vs. concentration (in total signal), the red line is the fit and the black the raw data showing a decent fit. The $\bar{v}$ used was 0.63 ml/g.

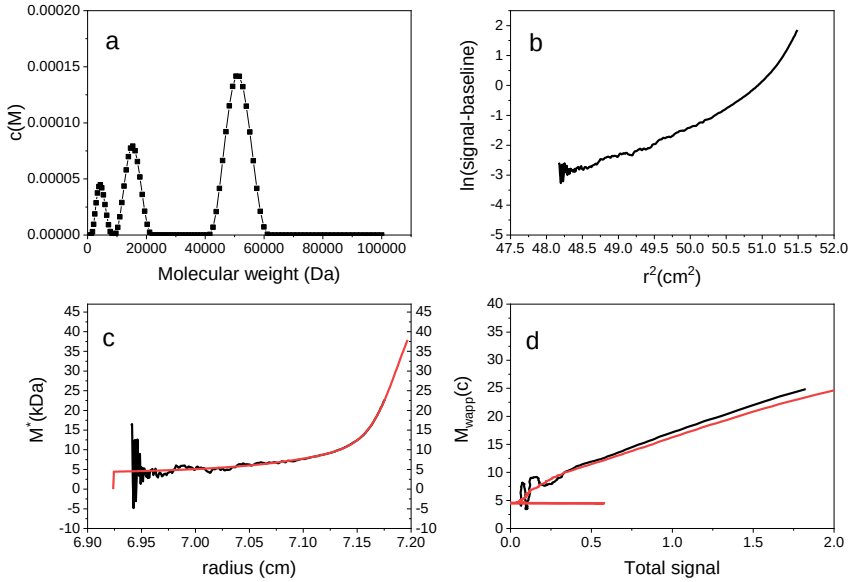

Figure 3-25: MSTAR results of 0.5 mg/ml aminocellulose (SE 40000 rpm) similar to . a.) c(M) vs. M showing three species peaking ~ 5, 15 and 50. b.) Log concentration ln(c) vs. r^2, which has an upward curve suggesting polydispersity. c.) M^* vs. r plot in black with the fit based on M^* extrapolation giving $M_{w,app}$ = 39.1 kDa. d.) $M_{w,app}(c)$ vs. concentration (in total signal) the red line is the fit and the black the raw data showing a decent fit. The $\bar{v}$ used was 0.63 ml/g.

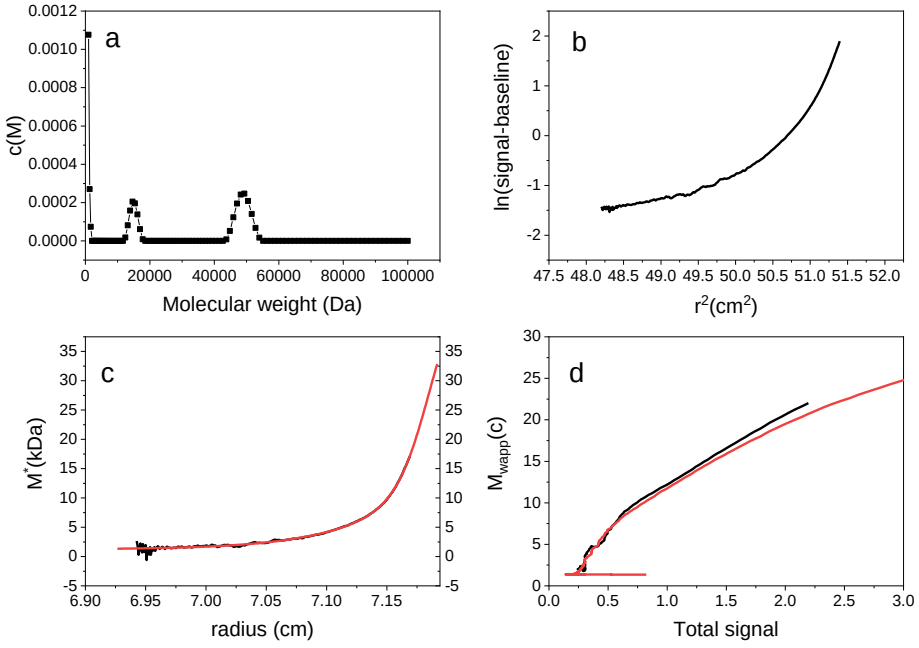

Figure 3-26: MSTAR results of 0.6 mg/ml aminocellulose (SE 40000 rpm) similar to . a.) $c(M)$ vs. M showing two species peaking ~ 15 and 50, the front peak is probably an artefact from analysis. b.) Log concentration ln(c) vs. r^2, which has a upward curve suggesting polydispersity. c.) M* vs. r plot in black with the fit based on M* extrapolation giving Mw,app = 33.9 kDa. d.) Mw,app(c) vs. concentration (in total signal) the red line is the fit and the black the raw data showing a decent fit. The $\bar{v}$ used was 0.63 ml/g.

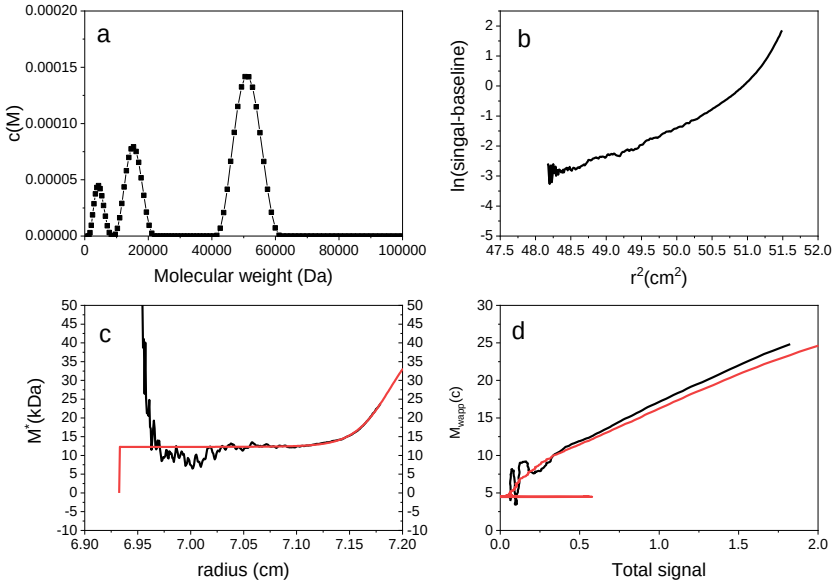

Figure 3-27: 0.7 mg/ml aminocellulose (SE 40000 rpm) MSTAR results similar to . a.) $c(M)$ vs. M showing two species peaking ~ 12 and 45 kDa. b.) Log concentration ln(c) vs. r^2, which has an upward curve suggesting polydispersity. c.) M^* vs. r plot in black with the fit based on M^* extrapolation giving $M_{w,app}$ = 35.0 kDa. d.) Mw,app(c) vs. concentration (in total signal) the red line is the fit and the black the raw data showing a decent fit. The $\bar{v}$ used was 0.63 ml/g.

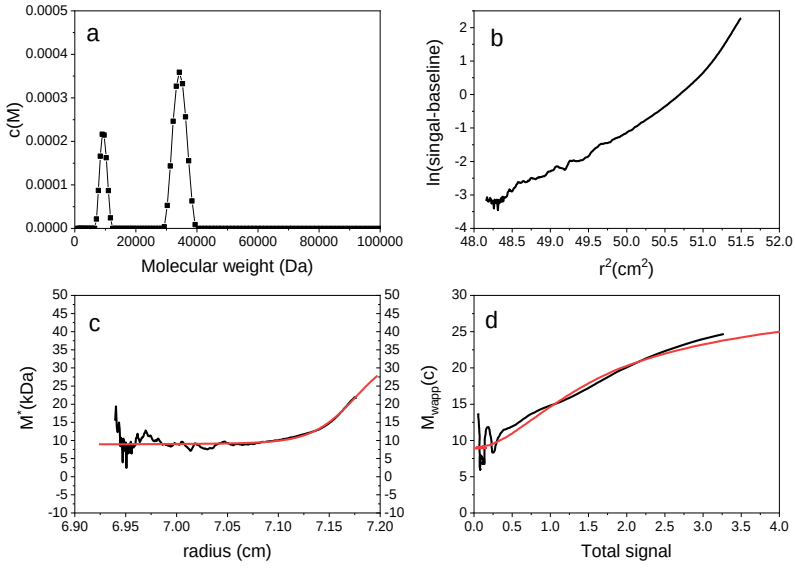

Figure 3-28: 0.9 mg/ml aminocellulose (SE 40000 rpm) MSTAR results similar to . a.) $c(M)$ vs. M showing two species peaking ~ 10 and 35 kDa. b.) Log concentration ln(c) vs. r^2, which has an upward curve suggesting polydispersity. c.) M^* vs. r plot in black with the fit based on M^* extrapolation giving $M_{w,app}$ = 28.2 kDa. d.) $M_{w,app}(c)$ vs. concentration (in total signal) the red line is the fit and the black the raw data showing a decent fit.The $\bar{v}$ used was 0.63 ml/g.

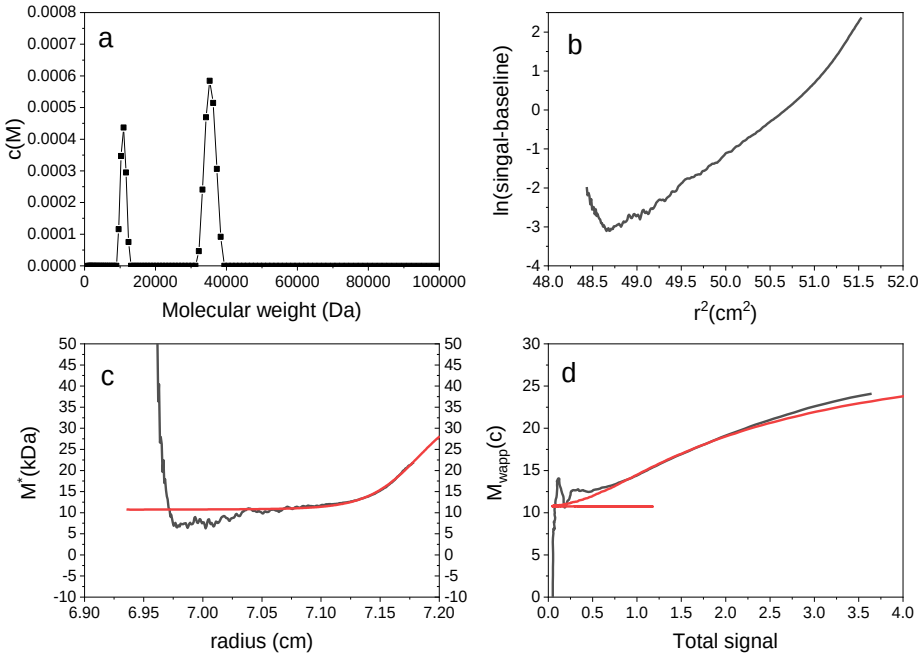

Figure 3-29: 1.0 mg/ml aminocellulose (SE 40000 rpm) MSTAR results similar to . a.) c(M) vs. M showing two species peaking ~ 12 and 35 kDa. b.) Log concentration ln(*c*) vs. r^2, which has an upward curve suggesting polydispersity. c.) M* vs. r plot in black with the fit based on M* extrapolation giving Mw,app = 28.7 kDa. d.) Mw,app(c) vs. concentration (in total signal) the red line is the fit and the black the raw data showing a decent fit. The $\bar{v}$ used was 0.63 ml/g.

The polydispersity and non-ideality in the system can be seen from Figure 3-24 to 29. Plot b shows ln(*c*) vs. r^2; in each of these there is an upward curve suggesting polydispersity which is expected from the SV analysis. Non-ideality is also apparent from a partial downward curve straightening the line for 1 mg/ml compared to 0.6 mg/ml in Figure 3-29 vs. Figure 3-26 respectively.

Although SE does not give an accurate description of molecular distribution, it can give a very rough idea. Figure 3-24 to 29 suggest two species around 15 kDa and another species between 35-50 kDa. Accuracy can be increased by combining SV and SE data together, but molecular weight and sedimentation coefficients must be known for several different molecular weights. SEC-MALLs can be used to obtain this data. However, this was not carried out in this project and would constitute potential future work to form an f(M) vs. (M) plot (Harding et al., 2011b).

MultiSig analysis can also give an idea of distribution, therefore this analysis was carried out, with Figure 3-30 showing the distribution obtained. Data was corrected for the correct $\bar{v}$ of 0.619. This shows similar results to MSTAR suggesting at least two species: one between 10-20 kDa and another 40-60 kDa. Although more species were seen in the SV experiment, it is not surprising that the species with higher sedimentation coefficients were not observed during this SE experiment due to the high speed used; hence, high molecular weight species would have sedimented early on and therefore were not observed.

MSTAR extrapolation *M** vs. radius (plot c) shows a very steep extrapolation to the cell base in Figure 3-24 to Figure 3-26; hence, for 0.4-0.6 mg/ml. In figures 3-26 to 3-28 from 0.7-1.0 mg/ml the extrapolation still has an upward curve but it is not as steep. This suggests the analysis for the 0.7-1.0 mg/ml of HEA might be more reliable than for lower concentrations. This also appears to fit closer with the hinge point analysis molecular weights and MultiSig analysis. The molecular weights were converted to the appropriate partial specific volume, determined via density measurements from Table 3-3 to Table 3-4, lowering the molecular weights slightly. The hinge point molecular weights and MultiSig molecular weights seem to concur (see Figure 3-30). The average hinge-point molecular weight is (19.9 ± 2) kDa and the MultiSig M_w is (22.46 ± 3.74) kDa (see Figure 3-31).

Table 3-3: Sedimentation equilibrium results for HEA. The $\bar{v}$ used was 0.63 ml/g.

concentration (mg/ml)	$M_{w,app}$ **(from** M***) kDa**	**Standard deviation (kDa)**	M_z **kDa**	**Poly dispersity index** M_w/M_z	r_{hinge} **(cm)**	$M_{w,app}$ **(from** M_w **(**r_{hinge}**) kDa)**	$M_{w,app}$ **(from MultiSig) kDa**
0.4	42.8	14.6	47.8	1.12	7.15	23.726	30.43
0.5	39.1	18.4	47.7	1.22	7.144	19.551	19.72
0.6	33.9	19.2	44.8	1.32	7.138	17.405	22.28
0.7	35	13.7	40.4	1.15	7.149	21.381	21.6
0.9	28.2	10.9	32.5	1.15	7.143	20.242	20.81
1	28.7	11	32.9	1.15	7.147	20.935	23.97

Table 3-4: Sedimentation equilibrium results for HE. The correct $\bar{v}$ of 0.619 ml/g. used for this table

c (g/ml)	**[a]**$M_{w,app}$ **(kDa)**	**[b]**$M_{w,app}$ **(kDa)**	**[c]**$M_{w,app}$ **(kDa)**
0.4	41.6	23.0	29.54 ± 0.08
0.5	38.0	19.0	19.15 ± 0.08
0.6	32.9	16.9	21.63 ± 0.01
0.7	34.0	20.8	20.97 ± 0.01
0.9	27.4	19.7	20.20 ± 0.05
1.0	27.9	20.3	23.28 ± 0.03

HEA a: MSTAR; b: hinge; c: MultiSig

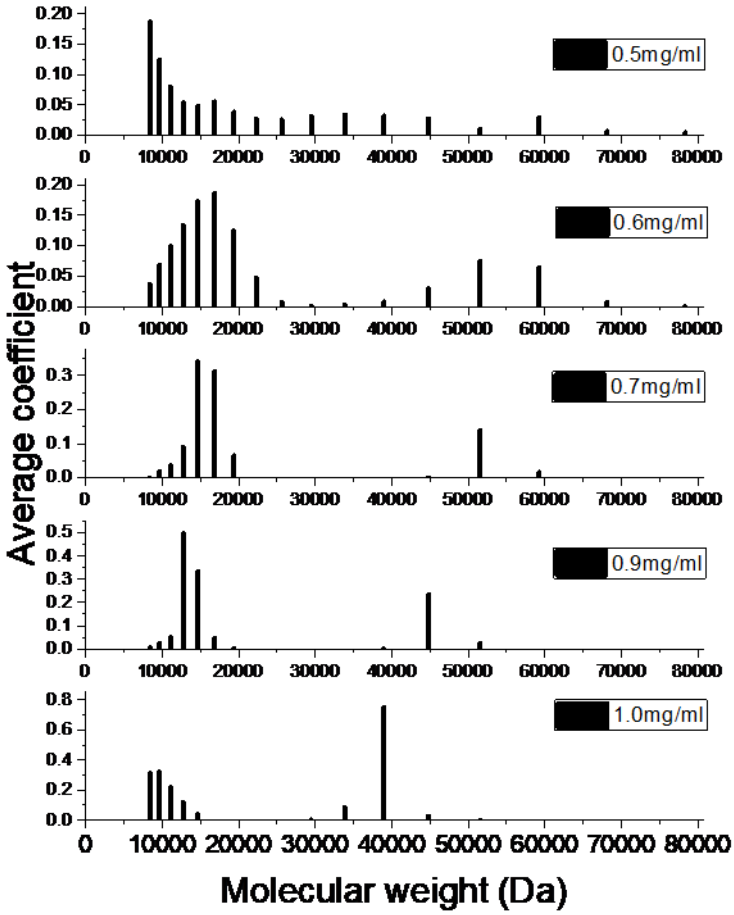

Figure 3-30: MultiSig distribution of molecular weights of HEA with $\bar{v}$ 0.619 ml/g presented through plots of average coefficient vs molecular weight (Da) with was fiited to 17 component system with 20 iterations this plot is the average of the 20 iterations for each loading concentration (0.5, 0.6, 0.7, 0.9 and 10) mg/ml.

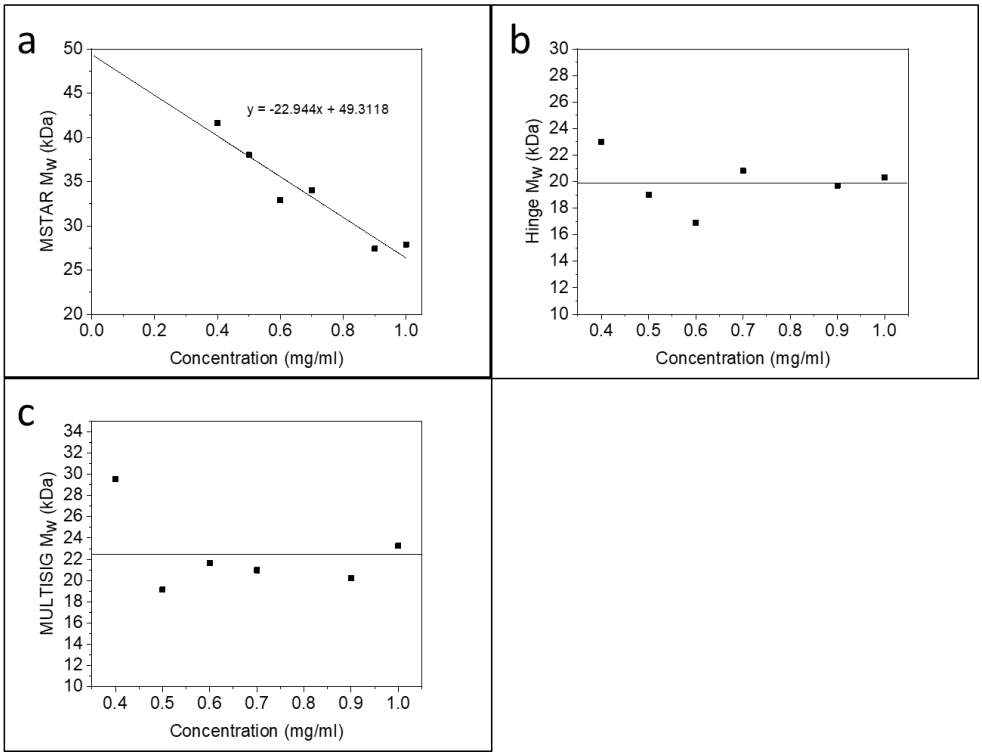

Figure 3-31: HEA results fom three types of analysis of SE results showing molecular weight (kDa) vs concentration (mg/ml) a) MSTAR M_w vs. concentration with a line of best fit resulting in M_w=(49.3±2.6) kDa. b) M_w vs. concentration (c) results from hinge point analysis Hinge M_w= (19.9 ± 2.0) kDa (from average 0.4 -1 mg/ml). c) MultiSig analysis M_w vs. concentration (c) MultiSig Mw= (22.46 ± 3.74) kDa (average excluding 0.4 mg/ml as an outlier, concentration may be too low). The molecular weight here are corrected for $\bar{v}$ 0.619 ml/g.

$M_{w,app}$ (r) vs. concentration for three loading concentrations (Figure 3-32) do not overlap which means the self-association is not fully reversible. Similar MultiSig analysis M_z(r) vs. concentration for the same 3 concentrations (Figure 3-33) show partial reversibility; the lines follow the same curve but do not overlap. However, this could also be due to lack of precision of the technique meaning it might be fully reversible. The monomeric molecular weight appears to be 5.5 kDa from both Figure 3-33 and Figure 3-34. The molecular weight appears to taper off between 37-40 kDa (Figure 3-33). Higher molecular weight species are expected from SV but due to the

high speed used, the higher molecular weight species would sediment too quickly to be observed.

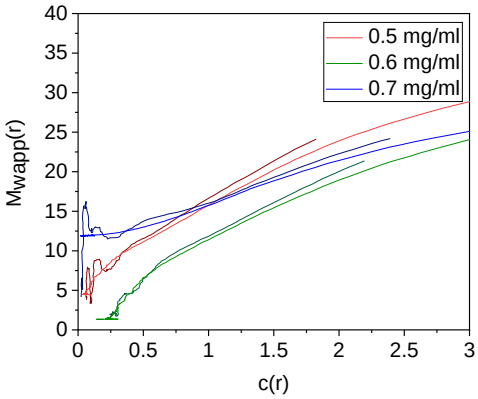

Figure 3-32: MSTAR M_{wapp} (r) vs. concentration along radius for 3 concentrations for HEA.

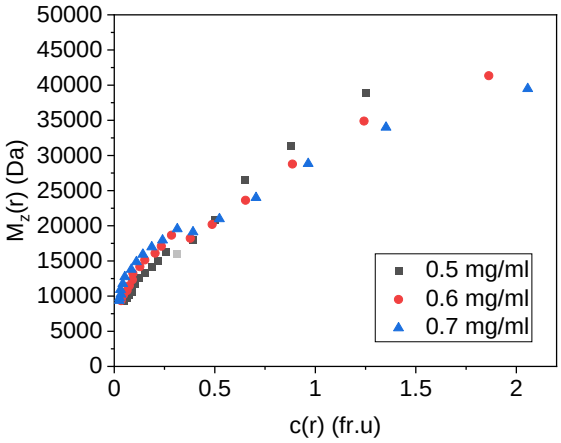

Figure 3-33: MultiSig shows the molecular weight increase with concentration along the cell of HEA. Shows weight average at different concentrations. The molecular weight here are corrected for $\bar{v}$ 0.619 ml/g. Outliers are in grey.

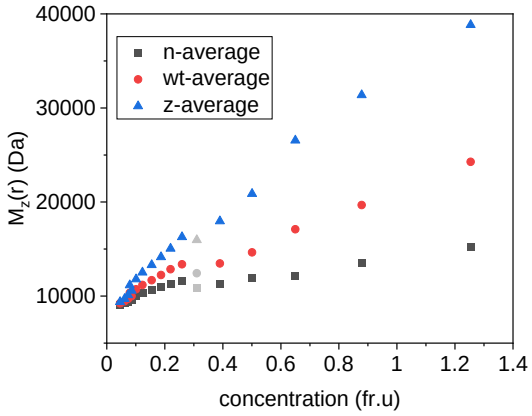

Figure 3-34: MultiSig shows the molecular weight increase with concentration along the cell of Aminocellulose 2. A shows the *n*, *wt*, and *z* average. The molecular weight here are corrected for $\bar{v}$ 0.619 ml/g. Outliers are in grey. b-spline fit used.

3.3 Discussion

3.3.1 Aminocellulose 1 (AEA)

3.3.1.1 SV

From the sedimentation velocity experiment of AEA, it is clear the aminocellulose is heterogeneous and contains multiple components as previously established by Nikolajski *et al.* (2014) in their analysis of another batch of AEA (see Figure 3-35). However, it is not clear if there is self-association involved: low concentrations were used to limit non-ideality but higher concentrations may have made the self-association more pronounced. Nikolajski *et al.* (2014) found the largest effect appeared to be between 1-2 mg/ml. Future work would include investigating higher concentrations. The results up to 1 mg/ml show lower sedimentation coefficients than were observed by Nikolajski et al. (2014), suggesting this batch of aminocellulose does not associate into as large species. This could be due to the lower amine content in the polymer. The smaller sedimentation coefficients are more promising in terms of wood consolidation, as smaller molecular weights are more likely to be absorbed into the wood.

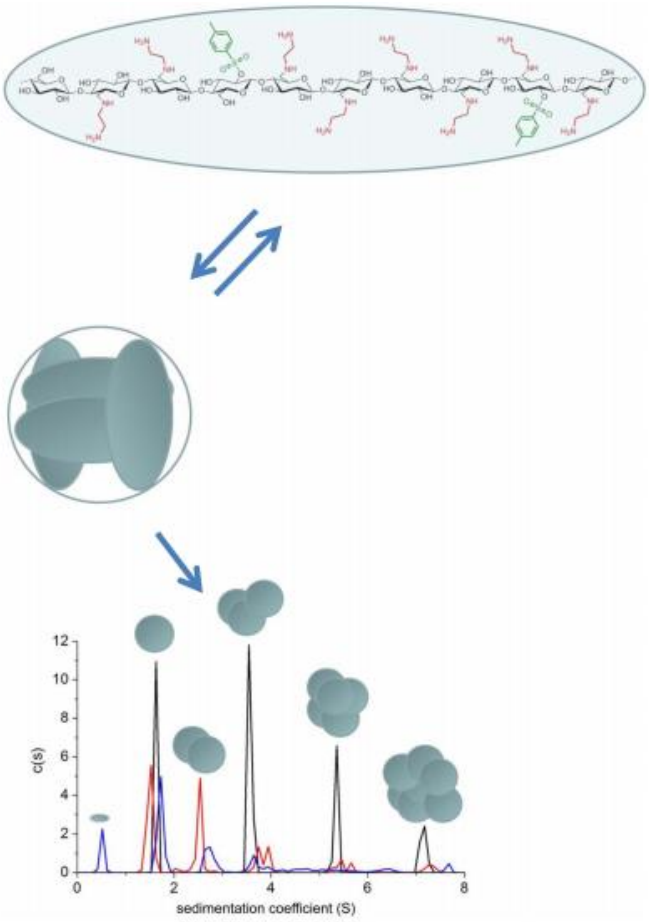

Figure 3-35: SV analysis of another batch of AEA from Nikolajski et al (2014). The blue line was of 0.75 mg/ml, red 1.0 mg/ml and black 2 mg/ml.

3.3.1.2 SE

The sedimentation equilibrium results clarified the presence of self-association through both the MSTAR and particularly the MultiSig analysis, which confirms there is self-association occurring and that this self-association is reversible. This means that there is a monomeric polymer which then combines into larger polymers at higher concentrations. To determine what the monomeric polymer molecular weight was and whether it was likely to enter the wood, an SE run was carried out and the molecular

weight was plotted against fringe concentration along the length of the cell for different loading concentration. If the molecular weight at the lowest concentration is the same for each loading concentration and if the increase of molecular weight along concentration increases at the same rate, this means that there is self-association. Extrapolating this line to zero gives the monomeric polymer molecular weight. MultiSig analysis (Figure 3-21b) showed the monomeric molecular weight as being around 4.5 kDa. This is a higher M_w than the batch of aminocellulose previously analysed by Nikolajski *et al.* (2014), but it seems like a reasonable molecular weight for wood conservation. A different batch of cellulose may have been used for the starting material which would explain the different monomeric molecular weight. This batch of AEA has a lower amine, DS 0.59, than the AEA analysed by Nikolajski *et al.* (2014), which had an amine DS of 0.83; this lower DS appears to have affected the way the molecule self-associates. The monomer, instead of forming a reversible tetramer like Nikolajski *et al.* (2014) found, appears to form a reversible dimer of 10 kDa, after which it self-associates further into a complex, but the system is no longer reversible. Clearly, lowering the amine content has reduced its ability to form large complexes, as the cationic nature is reduced.

Considering the monomeric molecular weight, the self-association and the fact aminocellulose is water soluble, this may be a more logical choice for a water-soluble option than chitosan and it has many benefits similar to chitosan. The advantage is that aminocelulose's self-association may form inside the wood, giving additional strength without the need for a cross linking agent. The fact that it does this whilst in solution, rather than on drying, may also limit the risk of the artefact shrinking and cracking as the polymer cross links and shrinks in size. The polymer may shrink a little but is still

in solution with more polymer being drawn in before drying, hence, this should strengthen the wood and reduce the risk of cracking. However, this hypothesis needs to be tested in practice. Colleagues have said that the self-associated polymer can be separated using sonication. In this case the solution can be sonicated prior to use, to increase the amount of monomeric polymers available to go into the wood. This is in the hopes that the cross linking will take place in the wood; obviously, if the self-association takes place before the polymer goes into the wood, it may prevent the polymer penetrating the wood. This needs to be investigated further; DLS may be able to help investigate this. Wood treatment on fragile wood may also help investigate whether the self-assocation within the wood is destructive, causing cracking, or if it helps consolidation.

3.3.2 Aminocellulose 2 (HEA)

A second aminocellulose, the hydroxyl derivative (6-deoxy-6-(2-hydroxyethyl) aminocellulose (HEA), was also investigated to give more options for wood treatment. This aminocellulose can be dried out, making it easier to obtain the desired concentration for wood treatment. AEA was sent as a 2% solution and it was suggested by the PhD student who produced it (Robert Hampe) that it aggregates on drying, making it difficult to work with unless it is kept in solution. AUC analysis was used to determine what difference the change from a terminal primary amine to a hydroxyl group would make in terms of the self-association. A different molecular weight was anticipated, as this modification was from the cellulose and not from the AEA previously analysed. The sedimentation coefficient shows multiple components like AEA; however, some species are of higher sedimentation coefficients. This

aminocellulose is likely to be of a higher molecular weight. This was confirmed with sedimentation equilibrium which found the hinge point molecular weight to be (19.9 ± 2) kDa, compared to (11.4 ± 1.2) kDa for AEA. High speed centrifugation was chosen both times to focus on self-association of the low molecular weight species. This means that higher molecular weights would have sedimented quickly. Therefore, the average molecular weight from the analysis at such high speeds might be deceptive. This is because higher molecular weights may not be accounted for, as they would have sedimented before the centrifuge reached 35000rpm or 40000rpm. Nevertheless, the sedimentation velocity experiments also suggest HEA contains higher molecular weights, so we can assume this is indeed the case, although the average molecular weight actually be a little higher may in both cases. The aggregation of HEA into larger molecular weights could be very important in coating wood cells in artefacts or medical devices, to ensure the coating is not too thick or too thin.

HEA, like AEA, was also found to self-associate from the MultiSig analysis; however, unlike in AEA, it appears to not have a perfect overlap of data, which could be due to only partial reversibility or from lack of precision of the AUC technique. Although accurate, AUC can lack precision when compared to other techniques such as mass spectroscopy; however if the result is instead due to partial reversibility this could have implications for HEA's use. Reversibility maybe prove important in re-dissolving material, for example in using aminocellulose in healing wounds.

The monomeric molecular weight of HEA also appears slightly higher at 5.5 kDa, compared to 5 kDa for AEA. This could have implications in terms of the wood treatment: the higher the molecular weight, the harder it is to penetrate the wood cells

due to the increase in its size and also often due to an increase in viscosity. All the loading concentrations show the molecular weights of AEA plateauing between 20-23 kDa whereas HEA is seen plateauing between 37-40 kDa. The higher molecular weights seen in HEA potentially block pores in the wood, preventing lower molecular weights from entering, hence, this could be problematic for wood conservation. However, the exact molecular weight of aminocellulose that could get penetrate the wood is not known as this has not previously been investigated. The larger the molecule, the greater its capacity to consolidate the wood but the lower the chance that it will be successful in fully penetrating the wood.

Therefore, both aminocelluloses should be tested on the artificially degraded wood to investigate whether one is not suitable to continue with. It would help evaluate if a lower molecular weight aminocellulose needs to be investigated. Alternatively, if these molecular weights are appropriate, which has greater consolidation capabilities.

3.4 Conclusion

Both aminocelluloses, AEA and HEA, show heterogeneity in the sample and both show self-association, this is evident in the sedimentation and confirmed with sedimentation equilibrium. A change from an NH_2 to an OH results in a lack of reversibility of self-association, as proven with sedimentation equilibrium through MultiSig radius analysis. This could have relevance in many applications, where its film properties and self-association properties are the reason why aminocellulose is chosen. This shows particular attention will have to be paid to the side chain as this can have a big affect on the properties. For wood conservation, higher monomeric

molecular weight and self-association may strengthen the wood; however, the lack of reversibility could be an issue if for any reason the aminocellulose needs to be removed, as it might affect solubility. For medical devices, the lack of reversibility may be desirable as it might mean coatings on devices last longer and these may also be thicker as the interaction does not reverse. For bandages, the higher molecular weight could be problematic, as it has been found with chitosan that the anti-bacterial properties are linked to molecular weight. The fact that the self-association is not reversible could affect this and lower the anti-bacterial efficiency. More work needs to be carried out to establish the effect that side chains have on anti-bacterial properties and ability to re-dissolve.

For wood conservation, if the polymer self-associates inside the wood, it could help strengthen the wood without the addition of a cross linker. Limiting the components of treatment can limit the risks. From SE, AEA has a monomeric molecular weight of ~4.5 kDa. This is very similar to the degraded chitosan which means it will be easier to compare results. HEA is of a slightly higher monomeric molecular weight ~5.5 kDa which could aid in greater consolidation; however, it self-associates to large molecular weights and this may prevent absorption into the wood (this is investigated in Chapter 6). Both chitosan and aminocellulose are promising in terms of molecular weight. Both are investigated in Chapter 6 for aqueous treatment of wood. However, the requirement of acetic acid in chitosan treatment is a disadvantage.

3.5 Experimental

In polysaccharides, non-ideality can still be significant even at low concentrations due to high affinity for solvent and high exclusion volumes (Schuck et al., 2014b). This is why several concentrations are required and plotting these molecular weights with extrapolation to zero concentration. The allows an accurate true molecular weight to be determined.

3.5.1 Material

Chemicals

- Aminocellulose (6-deoxy-6-(2-aminoethyl) aminocellulose) donated by Prof Heinze and produced by R. Hampe
- Di-sodium hydrogen orthophosphate dodecahydrate, Fisher scientific, lot: 1676088, CAS: 10039-32-4
- Sodium chloride, Fisher scientific, lot: 1410622, CAS:7647-14-5
- Potassium dihydrogen orthophosphate, Fisher scientific, lot: 1332230, CAS:7778-77-0
- Reverse osmosis water

Equipment

- AUC- Beckman Instruments (Palo Alto, USA) Optima XLI Analytical Ultra-Centrifuge
- AUC cells -12 mm epoxy optical path length cell
- Anton Paar DMA 5000 density meter
- Anton Paar AMVn roll and ball viscometer
- Volumetric flasks were used to make up all concentrations except for cleaning solutions.

3.5.2 Partial specific volume ($\overline{v}$) analysis

Density was measured for 5 concentration and the solvent using an Anton Parr density meter, and determined following the procedure of Kratky et al (1973) see equation 3-1. The equation gives the partial specific volume ($\overline{v}$) according to density of a specific concentration (Kratky et al., 1973). To determine the $\overline{v}$ at zero concentration. The $\overline{v}$ from each concentration must be extrapolated to zero, or the density extrapolated to zero, and the slope used to calculate the $\overline{v}$ (see equation 3-2).

$$\overline{\mathrm{v}}(\mathrm{c}) = \frac{1}{d_2}\left(1 - \frac{d-d_2}{c}\right) \quad \textbf{(3-1)}$$

d- density of solution
d_2-density of solvent
c-concentration
$\overline{\mathrm{v}}$ –-partial specific volume

$$\overline{\mathrm{v}} = \frac{\left(\frac{1}{\rho_0}\right)}{1-\left(\frac{d_p}{d_c}\right)} \quad \text{-} \quad \textbf{(3-2)}$$

ρ- density of solution
ρ_0-density of solvent
c-concentration
$\overline{\mathrm{v}}$ –partial specific volume

3.5.3 AUC Methodology

Sedimentation coefficient distributions and molecular weight determination of aminocellulose were determined using sedimentation velocity and sedimentation equilibrium respectively, in a Beckman XL-I analytical ultracentrifuge (AUC) equipped with Rayleigh interference optics, as previously described (Heinze *et al*, 2011; Nikolajski *et al*, 2014).The same general procedure as described in Chapter 2 for chitosan.

3.5.3.1 SV Methodology

3.5.3.1.1 AEA

The buffer used in SV analysis was I=0.1M Phosphate buffered saline (PBS) buffer pH 7 (2.298 g $Na_2HPO_4.12H_2O$, 0.781 g KH_2PO_4 and 1.462 g NaCl in 250ml RO water) make to double the desired concentration. Ionic strength is required to shield charges on separate polymer molecules and allow for accurate analysis by reducing non-ideality. The buffer was diluted by half for the reference (pH measured at 6.95 at 24 ^oC) and used to make up a stock solution (10 mg/ml) from 2% 6-deoxy-6(2-aminoethyl) aminocellulose (20 mg/ml). This was diluted further to make a 1 mg/ml stock solution using the reference solution.

Density of solvent 1.00334 g/cm^3 (average of 5 measurements)
Viscosity of solvent 0.00931 Poise (average 5 measurements-roll and ball viscometer)

This 1 mg/ml stock was used to make 7 concentrations by serial dilution 0.0625, 0.125, 0.25, 0.5 and 1 mg/ml solution and diluted to 0.75 and 0.1 mg/ml. The cells used for

AUC analysis were 12 mm optical path double sector cells (XL-I cells) with an epoxy centrepiece and sapphire windows in an aluminium housing: solution and solvent (buffer) reference channels were filled to 395 and 405 μL respectively. The cells were then placed in an 8 hole rotor. A rotor speed of 50000 rpm was employed. AUC was initially run at 3000 rpm and fringes optimised then run at 50000 rpm.

Analysis was carried out using SEDFIT (Dam and Schuck, 2004) which gave a least squares apparent distribution of sedimentation coefficient *g(s)* vs. sedimentation coefficient, *s (S)* and a diffusion corrected variant known as *c(s)* vs. *s* and the corresponding weight average sedimentation coefficient. All sedimentation coefficients were normalised to standard conditions (density and viscosity of water at 20.0 ^{o}C) – see Tanford, (1961). Graphs were then created using Microcal ORIGIN.

3.5.3.1.2 HEA

The same procedure was used as for AEA. A buffer solution of PBS pH 7 was made. The density and viscosity were measured as 1.00295 g/cm^3 and 0.01045 Poise respectively. A 1 mg/ml stock solution was made of HEA in the PBS buffer. This was then serially diluted from 1-0.015625 mg/ml. AUC SV experiment was run at 3000 rpm; fringes optimised and run at 45000 rpm. Analysis was carried out using SEDFIT (Dam and Schuck, 2004).

3.5.3.2 SE methodology

3.5.3.2.1 Standard procedure

A 12 mm path length cell was used, with shorter (100 µL) columns and a lower rotor speed, namely 40000 rpm at a temperature of 20.0 ^{o}C. High speeds were used to assess monomer-oligomer equilibrium as was carried out by Nikolajski *et al.* (2014). Scans with Rayleigh interference were taken every hour until equilibrium was reached. Loading concentrations from 0.30 to 1.0 mg/ml AEA in I=0.1M PBS and 0.4-1.0 mg/ml HEA in I=0.1M phosphate buffered saline (PBS) were employed to monitor for any associative or non-ideal effects, and these were negligible. Analysis was carried out using SEDFIT-MSTAR (Schuck *et al*, 2014) which provides the (apparent) weight average molecular weight $M_{w,app}$ (obtained from both M* analysis of Creeth & Harding, 1982, and the hinge point method – see (Schuck et al., 2014a). A second analysis was carried out using MultiSig (Gillis et al., 2013b) – which assumed thermodynamic ideality - using a 17 component system with 20 iterations for each concentration, allowing determination of molecular weight distributions and $M_w(r)$ vs. $c(r)$, and also the number $M_n(r)$ vs. r and z-average $M_z(r)$ vs. r as well, again for the different cell loading concentrations. Graphs were then created using Microcal ORIGIN.

All SEDFIT MSTAR and MultiSig analysis was carried out with a $\bar{v}$ value of 0.63 (ml/g) as an approximation, after a correction for the respective aminocellulose (0.614 (ml/g) for AEA and 0.619 (ml/g) for HEA).

3.5.3.2.2 AEA

The buffer used in analysis was phosphate buffered saline (PBS) buffer pH 7; the same batch as used for SV of AEA was used. Diluted by half for the reference and used to make up a 10 mg/ml stock solution from 2% (20 mg/ml). This was diluted further to make a 1 mg/ml stock solution using the reference solution.

Density of solvent 1.00334 g/cm^3 (average of 5 measurements)
Viscosity of solvent 0.00931 Poise (average 5 measurements – using a roll and ball viscometer)

Concentrations of 0.3, 0.4, 0.5, 0.6, 0.7, 0.8 and 1 mg/ml aminocellulose for SE were made up from the same 1 mg/ml stock solution of 6-deoxy-6(2-aminoethyl) aminocellulose as for the SV run. SE analysis was run at 40000 rpm in 12 mm cells.

3.5.3.2.3 HEA

The same procedure was used as for AEA.

A buffer solution of PBS pH 7 was made. The density and viscosity were measured as 1.00295 g/cm^3 and 0.01045 Poise respectively. A 1 mg/ml stock solution was made of HEA in the PBS buffer. This was then diluted to 0.4, 0.5, 0.6, 0.7, 0.9 and 1.0 mg/ml. SE analysis was run at 40000 rpm in 12 mm cells.

Chapter 4. Chemical modification of chitosan

4.1 Modification of Natural polymers for conservation

Functionalisation of natural polymers is one approach for addressing the issues related to conservation, such as: avoidance of water (to avoid hydrolysis but also to do with the fragility of the artefacts), problems with metal ions and fungal growth. Functionalisation of natural products, however, retains some of the benefits of natural polymers related to sustainable production and also their properties. This should result in polymers that resemble natural cellulose in the wood, but it is important to note that functionalisation would drastically change the properties of the natural polymer.

It is hard to predict all of the changes in properties that the functionalisation will affect. The best way to address this is to re-characterise the functionalised polymers to determine their properties and how they are different from the original polymer.

Chitosan has many properties that make it a suitable polymer for conservation. It is renewable, similar to cellulose from wood, can have a small molecular weight, is likely to hydrogen bond to lignin in the wood and chelates metal ions. The only problem is, it is only soluble in aqueous acetic acid and water would dissolve out alum. Therefore, it must be made organic soluble. Most research has been into water solubility of chitosan for drug delivery purposes, but there has been some research into organic solubility, mostly in-terms of protecting groups to aid other reactions, with the ultimate goal of water solubility. N-phthaloyl chitosan is most commonly discussed in literature (Ifuku et al., 2011a; Kurita et al., 2007). It allows the chitosan to be soluble in DMAc and to some extent DMSO, DMF, and pyridine, which widens the reactions that could

be done, particularly ones requiring a dry environment (Kim, 2013). O-trityl chitosan is another alternative which allows solubility in DMAc, DMF, DMSO, pyridine DCM and, to some extent, chloroform (Kim, 2013). This allows for further research into chitosan derivatives but unfortunately, none of these solvents would be suitable for wood conservation. Therefore, it is necessary to investigate other modifications, namely reductive amination, click chemistry and silylation.

4.2 Functionalisation/modified

Functionalisation of natural polymers is one approach to overcome the issues related to conservation such as avoidance of water (to avoid hydrolysis but also to do with the fragility of the artefacts), problems with metal ions and problems with bacteria growth. Functionalisation of natural products, however, retains some benefits of natural polymers in relation to sustainability of producing the compound used for conservation and also its properties. This should result in it more closely resembling the compounds naturally found in wood, but it must be kept in mind that functionalisation will drastically change the properties of the natural polymer.

It is hard to predict all the changes in properties that functionalisation will affect. The best way to address this is to re-characterise the polymer to determine the properties and how they are different from the original compound. At this point, for conservation reasons, is it also vital to investigate how it interacts with lignin.

4.2.1 Reductive amination

Reductive amination of chitosan has been carried out previously (Jatunov et al., 2012; Kurita and Isogai, 2010; Nikmawahda et al., 2015). These experiments cover a variety of aldehydes and have very similar methodologies, but the method of purification varies. This appears to be a high yielding reaction which allows for a large variety of substrates. The addition of benzene aldehydes has previously been explored. A benzene ring is highly hydrophobic, hence, its addition to chitosan may increase the hydrophobicity and allow for organic solubility. Phenols are water soluble and may improve the water solubility through the hydroxyl group and disruption of hydrogen bonding.

4.2.2 Click Chemistry

"Click chemistry" could be another suitable way to apply this functionalisation. Click chemistry was a term coined by Sharpless in 2001. It refers to a number of reactions that follow a set of conditions. It must be high yielding with a variety of starting materials, take place in no solvent or a benign solvent, it must be easy to perform, insensitive to oxygen or water, it must broadly applicable, use easily obtained reactants, have simple product isolation and have no or benign by-products. (Ball, 2007; Barner-Kowollik et al., 2011; Kolb and Sharpless, 2003)

This method was originally designed for drug discovery; however, it has had a large influence on polymer chemistry over the years. This could be a perfect starting point for functionalisation of polymers for artefact conservation as it has already been used

in polymer chemistry. It follows ideas of sustainable chemistry which can be beneficial in many ways for conservators. The use of benign or no solvents is appealing, as is the accessibility of reactants and the lack of toxic or unwanted by-products. Along with this, other reasons to use click chemistry is the ease of reactions and the fact that it is a set of well-known reactions. They are simple and well understood, thus avoiding numerous steps of very complicated and difficult reactions which are important for this purpose as further research is required following synthesis. The molecule will need to be fully characterised and tested on various pieces of wood with analysis of its effects. All of this takes time, hence, a simple reaction which achieves the desired result is required.Critically it must also be possible to produce on a scale that allows sufficient quantities to be made at an acceptable cost.

There is a 'toolbox' of chemical reactions available for click chemistry, which allows for the adaptation of a number of molecules which can be considered. Chitosan has a couple of functional groups, the NH_2 and the OH groups, that are obvious opportunities for click chemistry. Similarly, other polymers have the same type of functional groups that could be targeted for click chemistry. Hence, some reactions in the toolbox that make use of these functional groups are discussed below.

4.2.2.1 Reactions leading to click chemistry

Azides have proven useful for click chemistry. These azide click chemistry reactions follow cycloaddition of azides and alkynes to give triazoles via the Huisgen 1,3-dipolar cycloaddition. The advantage of azides is their stability; they are stable not only in

water and oxygen, but also the majority of organic synthesis conditions (Rostovtsev et al., 2002).

Huisgen 1,3-dipolar cycloaddition has previously been conducted on chitosan with methoxy poly (ethylene glycol) (MPEG-2000). An azide group was added to the chitosan at the NH_2; this was then reacted with the triple bond of an alkyne, attached to an alkane chain or an aromatic group. This can be carried out in a one pot synthesis. Many reactions have been tried, resulting in different degrees of substitution (Kulbokaite et al., 2009). Similarly, Ifuku *et al.* (2011) added azides to chitosan, replacing the OH on carbon 6 and reacted this with an alkyne to add a benzene ring, an alcohol group and an acid group. (Ifuku et al., 2011b).

If chitosan is to be used for the preservation of the Oseberg artefacts, it needs to be made organic soluble. One of the above methods could be used to add an alkyl chain, fatty acids or an aromatic group to make it organic soluble. This has already been done with PEG and chitosan, showing it is possible. However, 100% substitution would not be desirable, as the NH group may also come in useful for cross polymerisation or adding chelating agents. Finding the minimum substitution required to make the chitosan derivative organic soluble would be ideal.

Part of the reasoning behind the structure (use of click chemistry) is the possibility of a di- or tri- dentate ligand, made possible from the lone pairs on the OH on the chitosan, and N of the triazole. This could be incredibly useful for artefacts with a metal component or a large quantity of metal ions. Figure 4-1 shows how closely these lone pairs are arranged in space and therefore, their increased likelihood of being effective.

This triazole arrangement should improve their chelating ability, hence, it may remove the need to add a second added chelator whilst making it organic soluble.

There are a few options in which the alkyne can be used. It can be attached to an aromatic ring, 4-7 carbons branching alkyl chain such as tert butyl or fatty acid with a 6-7 carbon chain. These chains should allow the molecule to become soluble in organic solvents. However, establishing which is best in terms of solubility, chelation and penetration of wood would need to be determined by thorough testing. The recommendation is to produce a few variants with varying degrees of substitution, as the molecule should not need to be fully substituted to work.

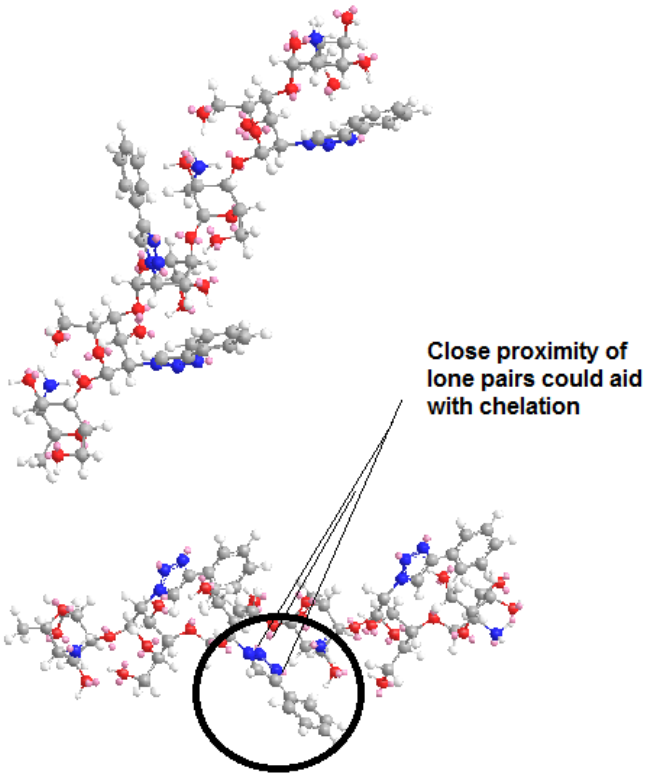

Figure 4-1: The structure of part of a proposed chitosan derivative with a phenyl group is shown above. Grey-carbon, white-hydrogen, red-oxygen, blue-nitrogen and pink for lone pairs. The lone pairs on the hydroxy group and on the nitrogen of the trizole are close enough together to chelate metal ions. The fact that this might even prove to be a tri dentate means it might prove powderful enough to chelate the metal ions in the wood. Chitosan is a chelator but by itself is not strong enough.

The problem with the above methods is that adding an azide to the chitosan is not the safest approach. Azides can be very reactive and explosive and having multiple azides on the same chitosan chain could be potentially dangerous. The starting materials are also not the safest to use. Therefore, this investigation takes a different approach: adding the alkyne on to chitosan and then clicking the desired group on through the azide attached to these compounds. This procedure is already known to be possible to produce relatively safely.

A method that uses a derivative of chitosan where the alkyne has been added to the chitosan has been published by Sarwar *et al*. (2015). This is a similar approach to those previously published; however, the OH is substituted instead of the NH_2, leaving the amide available for the addition of chelating agents and for cross linking later (See Figure 4-2). Sarwar's group researched these derivatives of chitosan in an attempt to produce derivatives with increased antimicrobial activity. They decided to attack the OH instead of the easier NH_2 in order to maintain the desirable properties related to pH dependence, amine dependant bioadhesion and antimicrobial effects. This reaction involved a greater number of steps, which is not desirable in terms of sustainability. However, it avoids the use of sodium azide, which is acutely toxic and commonly is used in similar reactions (Sarwar et al., 2015). The team produced a variety of derivatives of particular interest as a possible chitosan derivative for conservation and two others which may also be of interest. The compounds below (Figure 4-3) are the ones which may be useful to add to chitosan.

The paper by Sarwar *et al* (2015) is also promising, as it states these compounds were soluble in organic solvents. In addition, antibacterial, antifungal and cell viability

investigations were carried out and it was found that all the derivatives showed improved antibacterial activity when compared to chitosan. Compound 2 (R=phenyl) (See Fig. 8 and 9) showed gram positive activity between 62.5-125 vs 125-500 MIC μg/ml for pure chitosan. Similarly, 125 vs 250-500 gram negative bacteria and 375-1500 vs 3000 MIC μg/ml for antifungal activity (Sarwar et al., 2015). It suggests that this activity was due to the addition of the triazole ring.

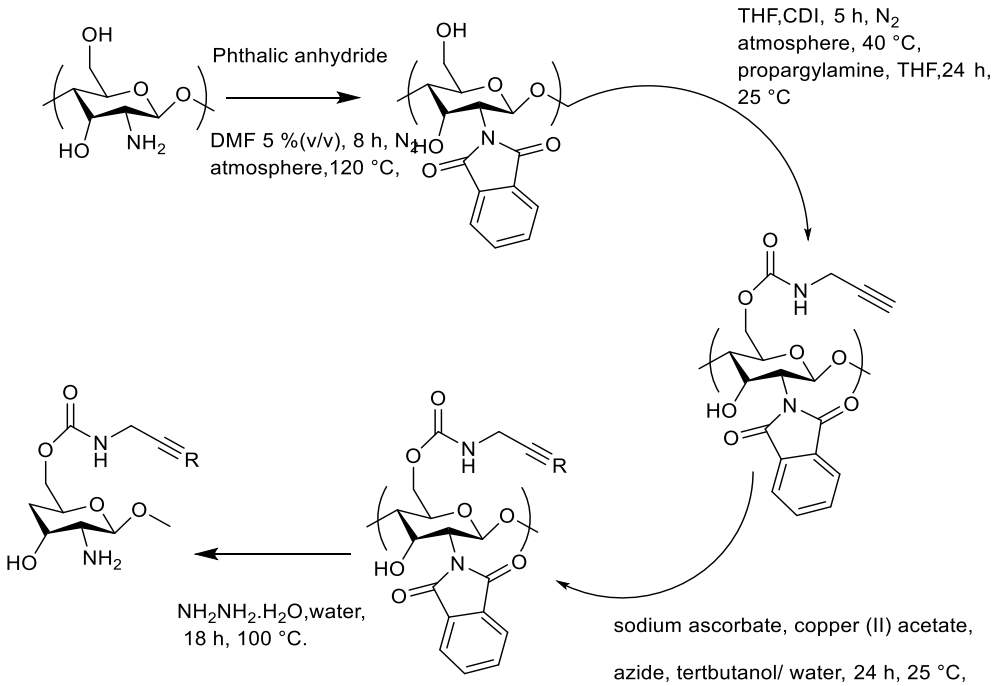

Figure 4-2: Synthesis of chitosan azide functional derivatives (Sarwar et al, 2015).

All derivatives were found to be non-toxic based on cell viability tests carried out on Chinese hamster lung fibroblast cell line V79 and human heptic cell line WRL68 (Sarwar et al., 2015).

This evidence of triazole addition on antibacterial and antifungal effects of chitosan, along with the suspected chelating ability, supports the use of click chemistry for chitosan functionisation. However, there are still two possible methods and a few potential R groups which could be considered.

From the information above, it is clear that there are a few options available for chitosan derivatives. Sarwar's method is safer than Kulbokaite's or Ifuku's methods. However, amide groups are not particularly acid stable, hence, Sarwar's method would not be suitable.

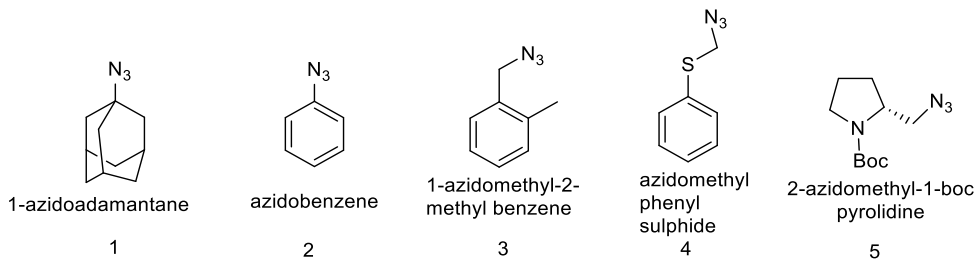

Figure 4-3: Azides investigated by Sarwar et al. (2015).

4.2.2.2 Click chemistry Approach investigated

An alternative would be to add the alkyne at the amine and then carry out the click chemistry. The difficulty in using this click chemistry cycloaddition of azides and alkynes approach is adding the alkyne onto the chitosan.

There are two options; first a halide alkylation reaction where the nitrogen on the chitosan attacks the carbon next to the halide. This releases the halide adding the chain with the alkyne group.

The second option is a reductive amination with an aldehyde is at the opposite end of the desired alkyne chain. The nitrogen attaches to the carbon connected to the oxygen via a reaction with a reagent. This can also be used to directly add a group to improve solubility; but the addition of the triazole ring may also improve chelation properties. The required aldehyde cannot be purchased and hence, must be produced prior to use.

4.2.2.2.1 Halide alkylation reaction

Halide alkylation reactions cannot be carried out in water as the halide will be replaced with a hydroxide group. This may cause a problem due to the insolubility of chitosan which may prevent the reaction from taking place. However, some reactions involve suspensions, hence, this may work regardless of solubility. The advantage of this method is that the starting material can be purchased. However, if unsuccessful, the reductive amination procedure could be an alternative route.

Previous halide alkylations with amines and propargyl bromide have been carried out on various substrates (Jeong et al., 2016; Lu et al., 2013; Mizoguchi et al., 2015). Therefore, this method may prove successful. These reactions are carried out in ACN with potassium carbonate sometimes with Et_3N at room temperature for 16-22 h with yields of 50-90%. This method would allow the alkyne to be added in one step, which could avoid unnecessary use of extra chemicals. However, this method may not work due to lack of solubility of chitosan.

4.2.2.2.2 Reductive amination

The aldehyde from alcohol alkyne chains has previously been reported (Phillips et al., 2015), although not possible to purchase, it can be produced. The concern is that it might not be very stable and therefore, may have to be used as soon as possible after preparation.

A Swern reaction was successfully used by Phillips *et al.* (2015) to oxidise 4-pentyn-1-ol and this could be used to produce the desired aldehyde. This method has a 90% yield and although one of the reagents (oxalyl chloride) is toxic, oxalyl chloride and its by-product, DMS, can easily be quenched with water and bleach respectively (Phillips et al., 2015). This reaction also does not require any additional heat. Although the work up is not ideal, the solvent can be recycled. Due to previous success, it is promising for producing the aldehyde which can then be used for the reductive amination. If this next step is successful, alternatives to the standard Swern reaction could be investigated further such as the odourless dodecyl methyl sulfide method developed by Oshugi *et al*. (2003). This not only eliminates DMS, which has a strong odour, but also DCM can be replaced by toluene or even acetone (Ohsugi et al., 2003). Due to time restrictions, this will only be investigated if the reductive aminations prove successful and only in future projects.

4.2.2.3 Cycloaddition of azides and alkynes (click chemistry)

The cycloaddition of azides and alkynes to produce triazoles via the Huisgen 1,3-dipolar cycloaddition, appears to be a good method based on the examples given previously. However, a range of different solvents and Cu(II) compounds have been

used for similar reactions. Sarwar et al. reacted 1 eq. alkyne (on chitosan), 0.71 eq. sodium ascorbate, 0.5 eq. copper acetate and 1eq. azide in 1/1 *tert*-butanol/H_2O at room temperature for 12 h (Sarwar et al., 2015). *Tert*-butanol/H_2O mix is commonly used along with sodium acetate; however, copper(II) sulfate is often used instead of copper(II) acetate (Baig and Varma, 2013; Barral et al., 2007; Rostovtsev et al., 2002). There are, however, a variety of solvents for click reactions and whether to use Cu(I) or use Cu(II) to produce Cu(1) is debated (Ellanki et al., 2012; Hein et al., 2008). However, reactions with chitosan derivatives have varied considerably in solvents. Kulbokaite et al. (2009) used 1 eq. azide (chitosan derivative), 0.05 M HCl, 0.033 eq. copper sulfate in water, 0.066 eq. sodium ascorbate in water, 0.4 eq. alkyne in DCM stirred at 40 ^oC for 24 h (Kulbokaite et al., 2009). Whereas Ifuku et al. (2012) used azide (chitosan derivative) in DMSO, copper sulfate pentahydrate in water, sodium ascorbate in water, triethyl amine and alkyne stirred at 70 ^OC for 48 h. This large variety of reaction methods makes it difficult to know which method or modified method is best to use. *Tert*-butanol/water is generally the preferred solvent, but the use of other solvents is likely to be due to solubility issues of modified chitosans. Since this project does not aim to produce any of the above methods it is hard to predict solubility. The best option therefore, is to use the most common method or the most sustainable; in this case Sarwar *et al's* (2015) method. *Tert*-butanol/water mix is commonly used and this reaction does not require heating and only takes 12 h instead of 24 or 48 h (Sarwar et al., 2015). The only concern is solubility of the modified chitosan. However, Sarwar *et al* (2015) states that the reactants were suspended in the solvent, thus, solubility might not be a problem. It is worth trying and then adapting

the methodology or attempting other methods to improve the solubility and hence, contact between reactants.

4.2.3 Silylation

More recent research by a group in Iceland has focused on silylations. Again this widens the reactions possible for chitosan (Rúnarsson et al., 2008a). Interestingly, this wider list of solvents now includes some more suitable solvents for conservation purposes: toluene, THF, hexane, ethyl acetate and isopropanol. The most widely known use of silylation is for GC-MS for acidic groups which could not easily pass through the column as they can stick to the solid phase; silyl ethers are generally more polar and more volatile than the precursor allowing for easier analysis. They are also used as protective groups for alcohol and amines. They can be removed, sometimes with acid, but often a fluoride ion is required as the Si-F bond is 30 kcal/mol stronger than the Si-O (Kim, 2013). This is also the basis for the sulfur(VI) fluoride exchange SuFEx click reactions (Dong et al., 2014a). Below is the order of acid and base stability of silyl ethers.

Order of acid stability (Kim, 2013)

TMS (1)<(TES (64)< TBDMS (20,000)<TIPS(70000) <TBDPS (5,000,000)

Order of base stability

TMS (1)<(TES (10-100)< TBDMS~TBDPS (20,000)<TIPS(100,000)

This means that for conservation of the wood, which is in an acidic environment, something like TBDMS or TIPS are more likely to be stable and capable of preserving the wood for a longer period of time (Madera-Santana et al., 2018). Therefore, based on this, TBDMS was investigated as there is already a paper showing chitosan can be made organic soluble with this addition. Assuming this shows some success, other reagents such as chloro dimethylthexyl silane will be investigated. This longer branched alkyl may improve solubility in organic solvents further. TIPS will also be investigated for improved acid stability and the propyl instead of methyl side groups may also improve solubility. Solubility is difficult to predict and the experimental work must be investigated to determine which is more promising. It must also be noted that the wood is in a dry condition, not in solution, hence, despite the fact it is acidic, the degradation reactions should be much slower. Silyl ether protection of cellulose has been found to improve thermal stability (Kim, 2013). This suggests it might improve long term stability.

Runarsson *et al.* 2008 have already managed to make chitosan of low molecular weight organic soluble through *tert*-butyldimethylsilyl addition (Rúnarsson et al., 2008a). This was achieved in DMF for chloride salt of chitosan oligomers MW 951kDa with imidazole and TBDMSCl (*tert*-butyldimethylsilyl chloride) and mesylate salt of chitosan polymer MW 8.1 kDa in DMSO with imidazole and TBDMCl. The salt formation prevents the addition of the silyl group at the nitrogen as well as aiding solubility. Other work has shown this salt can be made without the huge excess of acid, using equimolar amount in formamide or DMSO. Good solubility (completely soluble at 10% [w/v]) of final product, the oligomer, for the DS of 2.2 was achieved in NMP, DMF, DMSO, diethyl ether, triethylamine, pyridine, THF, acetone, 1-butanol, 2-

propanol, ethyl acetate, ethanol, DCM, chloroform (Rúnarsson et al., 2008a). A DS of 1.29 showed reduced solubility in diethyl ether, acetone and ethanol. The chitosan polymer with a DS of 1.94 reduced solubility in all solvents but was still completely soluble at 2.5% in pyridine, 1-butanol, 2-propanol and ethyl acetate. NMR showed successful formation of mesylated salt and also 3,6-di-O-TBDMS-chitosan and showed the TBDMS was added at both the 3 and 6 position and was also used to determine the DS (Rúnarsson et al., 2008a). The reactions were optimised by the same group (Song et al., 2010) resulting in a 90% yield for the mesylate and a 96% yield for the 3,6-di-O-TBDMS-chitosan polymer and lower excess of imidazole and TBDMCl. The excess was reduced to 2.5-fold excess of TBDMSCl. The polymer becomes superhydrophobic and this hydrophobicity may help to prevent swelling and subsequent shrinkage of the wood.

Tert-bultyldimethylsilyl cellulose also showed improved solubility in THF, $CHCl_3$, toluene and hexane (Heinze et al., 2007). This reaction was carried out in DMA with LiCl. However, only C6 and to some extent C2 were substituted, the C3 was not substituted in this case. This exact reaction could not be repeated with chitosan or aminocellulose as the nitrogen must be protected to prevent addition of TBDMS at the nitrogen.

4.2.4 Summary

The Oseberg artefacts are in a very fragile condition and in urgent need of a suitable consolidant. Current conservation methods are not suitable due to the fact they are either not organic soluble, do not chelate metal ions and/or are not stable in acid

conditions. Chitosan oligomers, if modified, could make a suitable consolidant material, due to its antibacterial and chelation properties and the fact it is sustainable, non-toxic and has plenty of opportunities for modification and cross linking. Click chemistry would add a triazole ring, to which an aliphatic chain, fatty acid chain or aromatic ring could be added. These chains will help make the chitosan organic soluble and the triazole ring could help with chelation and antifungal properties. In the same way that adding the side chains makes the chitosan organic soluble, other groups can be added to improve chelation and antimicrobial properties. Reductive amination modified chitosan can also be cross linked with itself, or another polymer, to improve consolidation properties. Aliginate, lignin and pectin are all good candidates and more research is required to determine which combinations should be used together and which cross linker would be best to use. Silylation would add a silyl group and has already been proven to aid solubility of chitosan in organic solvents.

4.3 Results/Discussion

The results and discussion first examine the solid-state NMR and then the liquid NMR results to assess whether the desired product was made. The solubility of products is then given and discussed. Silylation improved solubility, and so, this was scaled up. The molecular weight for TBDMS chitosan which was the chosen modification, was then calculated from AUC analysis of intermediate product and from the degree of substitution based on the NMR, to evaluate whether it is a possibility for wood conservation. Chapter 7 then investigates the TBDMS chitosan for wood conservation.

4.3.1 Solid state NMR

The results of chemical modification suggest whether an approach is successful and what modification could be made to improve the material further, or if a different method must be sought.

Carbon-13 cross-polarization/magic angle spinning nuclear magnetic resonance (^{13}C-CP/MAS NMR) was carried out on the original chitosan to confirm it was chitosan and to allow for comparison to modified chitosan (One effect of magic angle spinning solid state NMR is: small doublets of all peaks with a coupling of 12 kHz. This is due to the magic angle spinning method, which narrows broad peaks, increasing resolution.

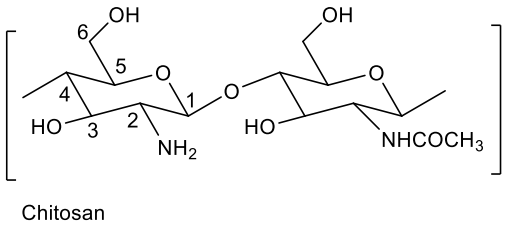

Figure 4-4: Structural diagram of chitosan with carbons labelled.

Figure 4-5, see Figure 4-4 for numbering of the carbons and hence corresponding protons). NMR showed the expected groups in the corrected area, including groups from the acetyl fraction. NMR can show groups present in a polymer but multiple overlapping groups can cause low resolution. Solid state NMR also has low resolution, but does avoid the solvent effects that liquid NMR has. Magic angle spinning improves resolution peaks, although the peaks are still broad when compared to liquid NMR. This NMR spectrum has been confirmed through comparison with multiple literature spectrums (Khan et al., 2014; Saito et al., 1987; Vieira et al., 2013).

One effect of magic angle spinning solid state NMR is: small doublets of all peaks with a coupling of 12 kHz. This is due to the magic angle spinning method, which narrows broad peaks, increasing resolution.

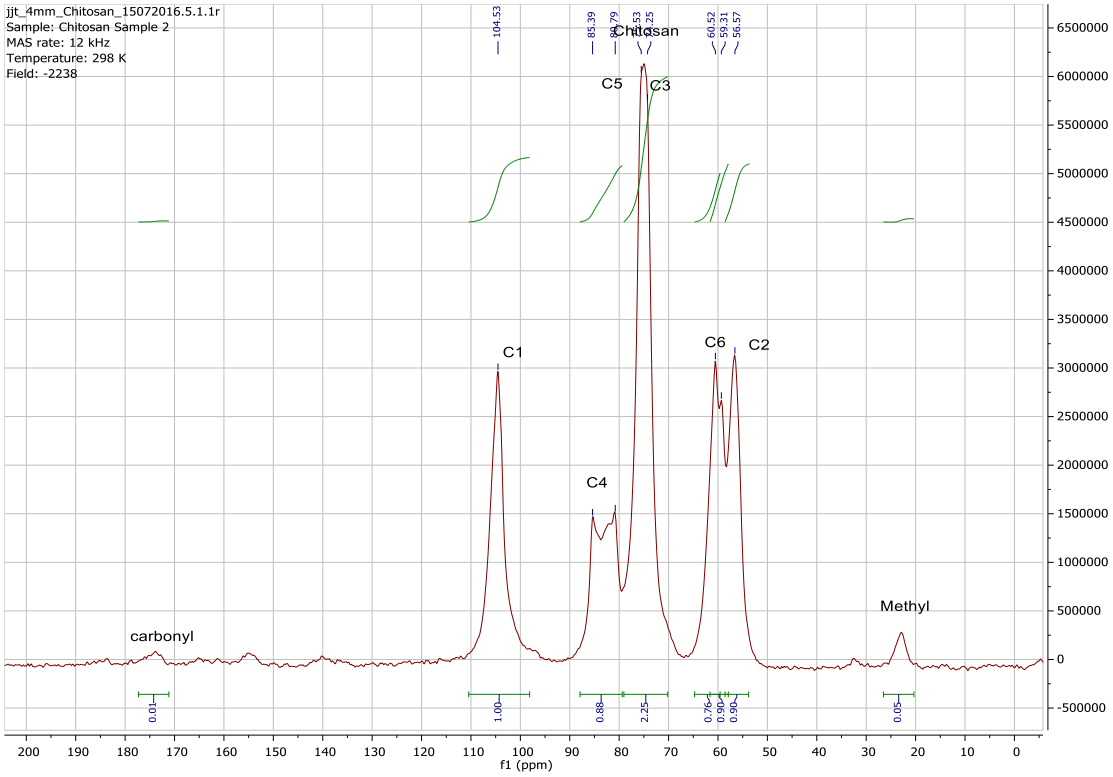

Figure 4-5: Solid state carbon 13 NMR of original Kitnor chitosan.

The scheme of each reaction is given, prior to the NMR results in the following order: reductive amination (Figure 4-6), click chemistry (Figure 4-12) and mesylate salt formation (Figure 4-35 and Figure 4-36) followed by silylation (Figure 4-40). Along with the NMRs, the structure is given with numbered carbons and hence corresponding hydrogens.

Reductive amination

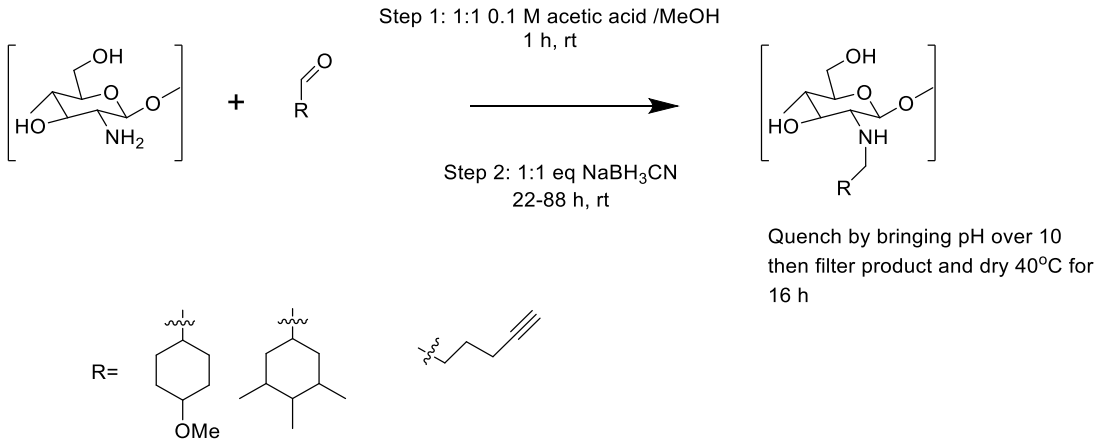

Figure 4-6: Reaction scheme for reductive amination of chitosan.

Reductive amination appears to have been successful in all instances (NMR Figure 4-7 and Figure 4-9 and corresponding structure Figure 4-8 and 4-10 respectively). Solid state NMR was used for analysis due to the insolubility of the products.

^{13}C NMR of chitosan with 4-methoxybenzaldehyde shows peaks at 113, 130 and 158 ppm (see Figure 4-7); these reflect C7, C8 & 9 and C10 as labelled in Figure 4-8. The broadened backbone peak is due to the methoxy group. This clearly shows the successful addition of the aromatic group and the backbone of chitosan is also clearly visible in this NMR.

NMR of chitosan with 3,4,5-trimethylbenaldehyde shows additional peaks at 19, 104, 129, 136, 208 and 216 ppm (Figure 4-9). This reflects the methyl's, C7, C8, C9 and 10 labelled in Figure 4-10, which clearly shows the addition of this aromatic group.

However, the reaction was left for too long resulting in the deterioration of the backbone which was visible by a significant change from the original chitosan peaks.

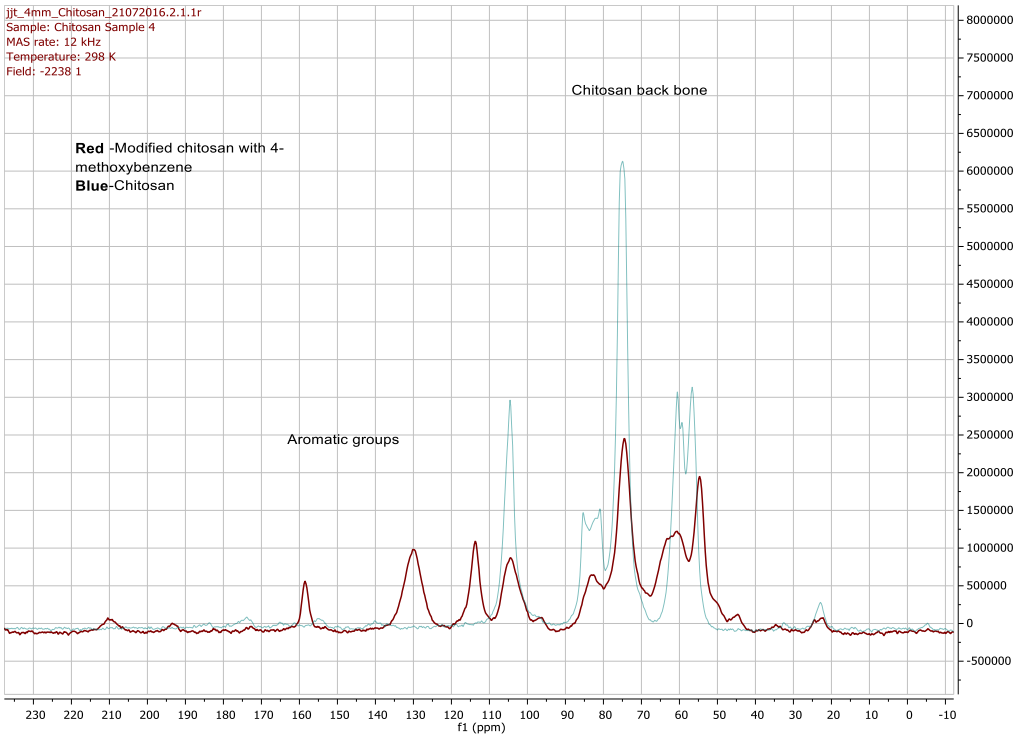

Figure 4-7: Solid state NMR 4-methoxybenzaldehyde.

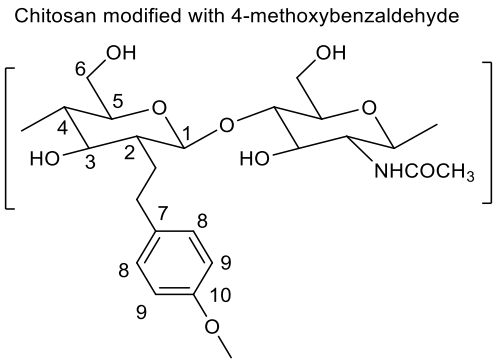

Figure 4-8: Structure of modified chitosan 4-methoxybenzaldehyde.

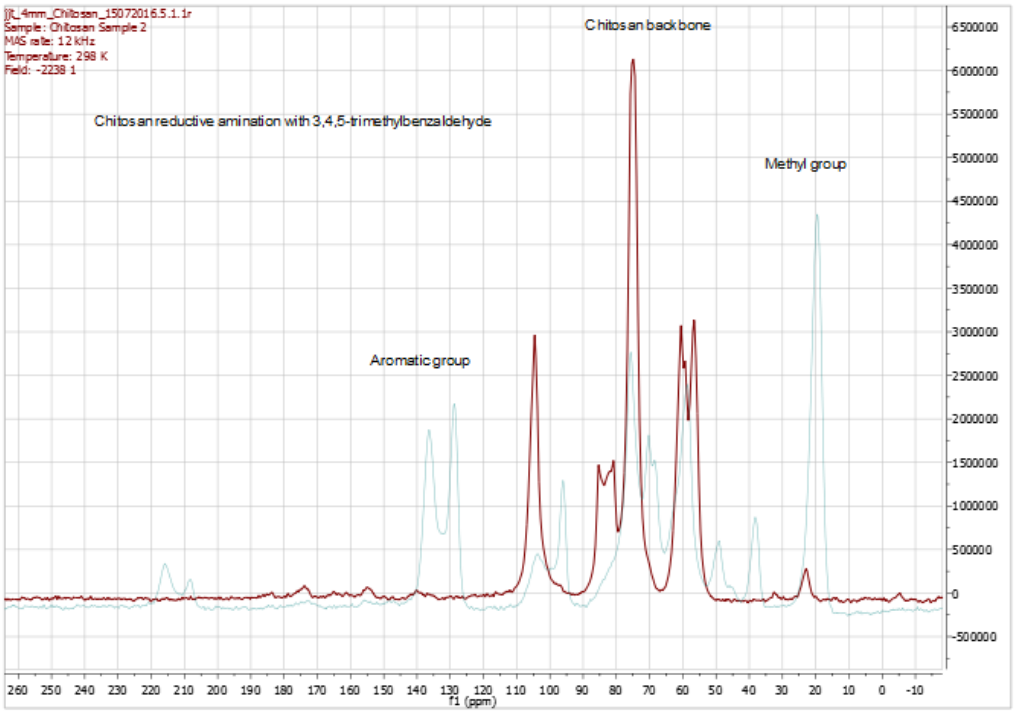

Figure 4-9: Solid state NMR of 3,4,5-trimethylbenzene chitosan in blue and chitosan in red.

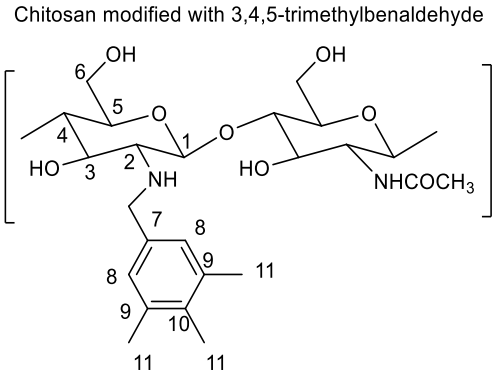

Figure 4-10: Structure of 3,4,5-trimethylbenzene with numbered carbons.

By comparing the results to the NMR data published by Hayashi et al. (2005) (Figure 4-11) of chitosan and glucosamine, it appears as if some of the polymer, but not all, may have been fully depolymerised to glucosamine, resulting in a mixture of

glucosamine and chitosan affecting the NMR spectrum of the backbone. There are also two additional aldehyde (C=O) peaks from the formation of an aldehyde at carbon 6 and carbon 4.

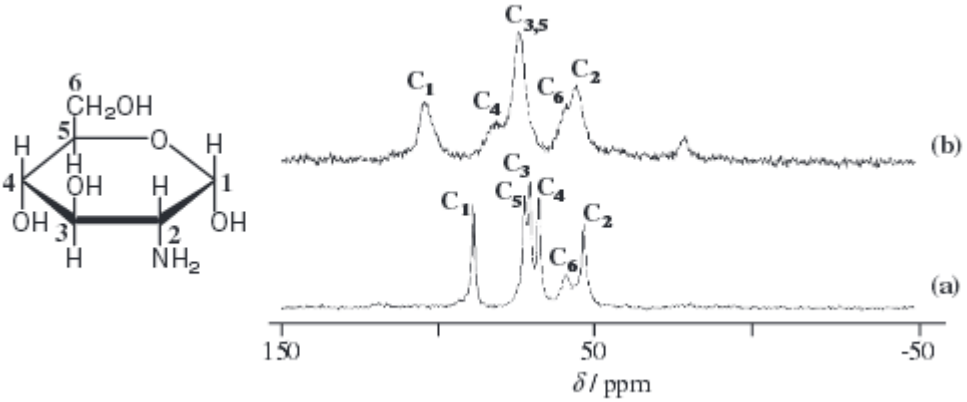

Figure 4-11: a) structure of glucosamine, b) chitosan solid state NMR (Hayashi et al. 2005).

4.3.1.1 Click chemistry

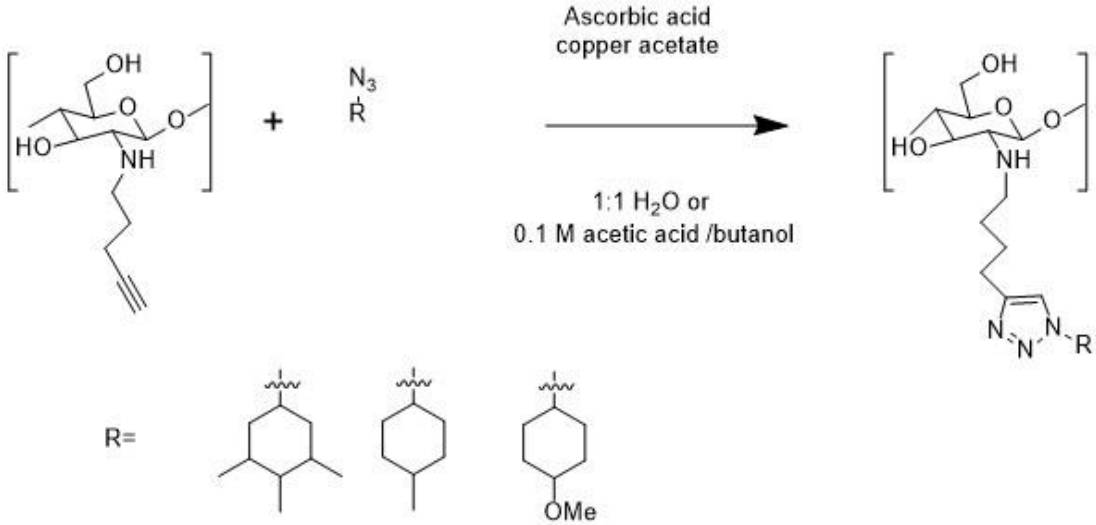

Figure 4-12: Reaction scheme for click chemistry reaction to add triazole group.

The NMR results showed 1-azido-4-methoxybenzene, 3,5-azido-4-dimethylbenzene, 1-azido-4-methylbezene and 4-pentynal were all successfully created based on methodology found in the literature. (see Table 4-1, a summary of Figure 4-14, Figure

4-15 and Figure 4-16. Figure 4-13 shows the structure of 1-azido-4methylbenzene with numbered carbons). This therefore proved the reaction was successful. Table 4-2 is a summary of Figure 4-18, Figure 4-19 and Figure 4-20. Figure 4-17 shows the structure with numbered carbons links up to Table 4-2; this proves the 1-azido-4-methoxybenzene was successfully made. Table 4-3 summarises Figure 4-22, Figure 4-23 and Figure 4-24. Figure 4-21 has the carbons numbered for 1-azido-3,5-methylbenzene. Finally, Table 4-4 summarises; Figure 4-27 and Figure 4-28. This aproved 4-pentynal was made. Figure 4-25 shows the numbering of the carbons.

1-azido-4methylbenzene

Table 4-1: Summary of ^{1}H (300 MHz) and ^{13}C (300 MHz) NMR spectroscopic data of 1-azido-4-methylbenzene in $CDCl_3$

Position	δ ^{13}C (ppm)	δ ^{13}C (ppm) 1-azido-methoxybenzene [a,b]	Type	δ ^{1}H/ppm (Mult J/Hz)	δ ^{1}H (ppm) 1-azido-methoxybenzene [a,b]
1	137.2	137.1	C		
2	134.6	134.5	C		
3	130.3	130.2	CH_2	7.18	7.14
4	118.8	118.7	CH_2	6.96	6.91
5	20.8	20.7	CH_3	2.37	2.32

[a] (Kitamura et al., 2014) +
[b] In $CDCl_3$

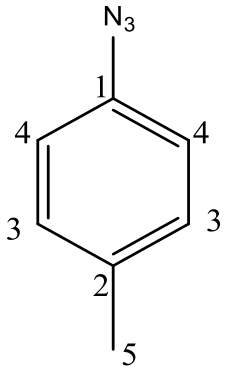

Figure 4-13:Carbon NMR assignment of 1-azido-4-methylbenzene

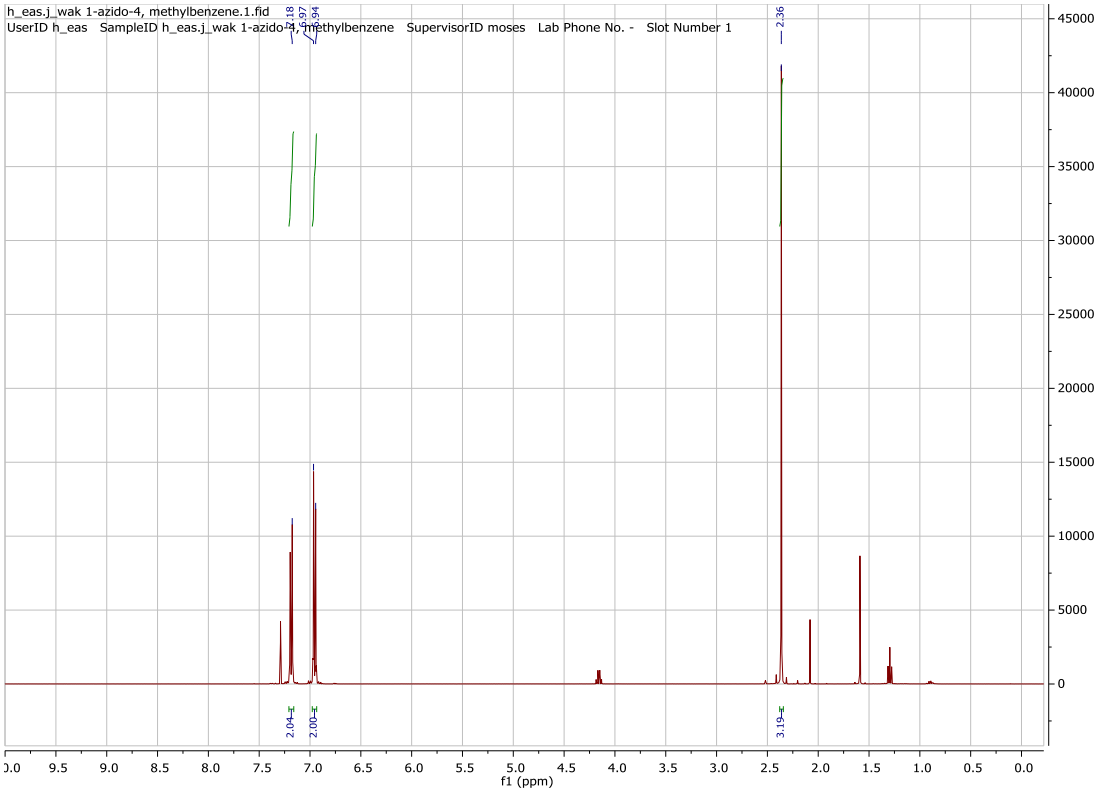

Figure 4-14:H^1 NMR of 1-azido-4-methylbenzene in $CDCl_3$

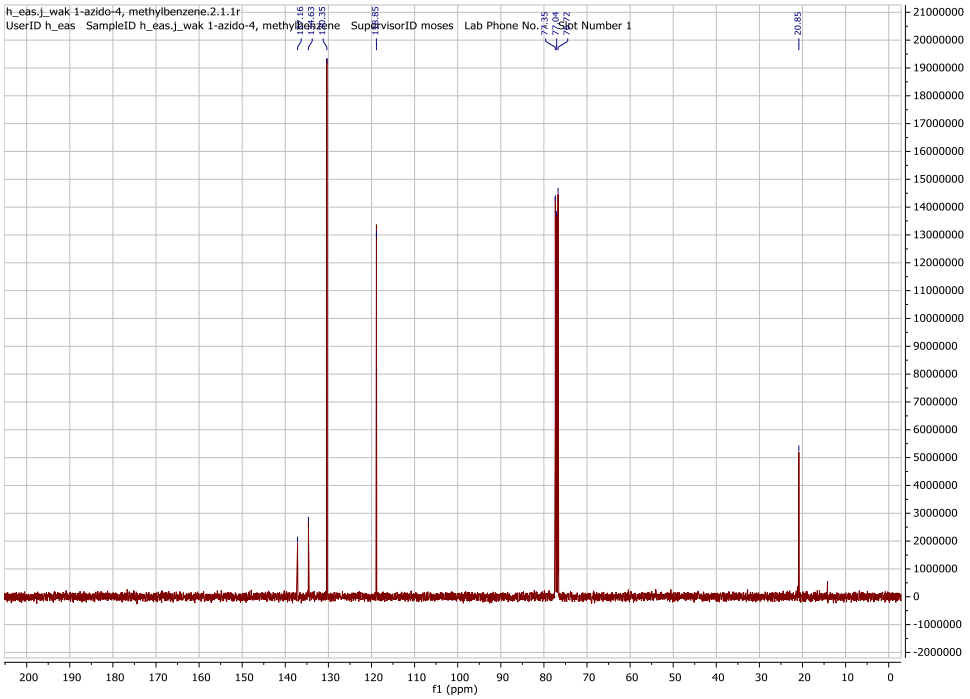

Figure 4-15: C^{13} NMR of 1-azido-4-methylbenzene in $CDCl_3$

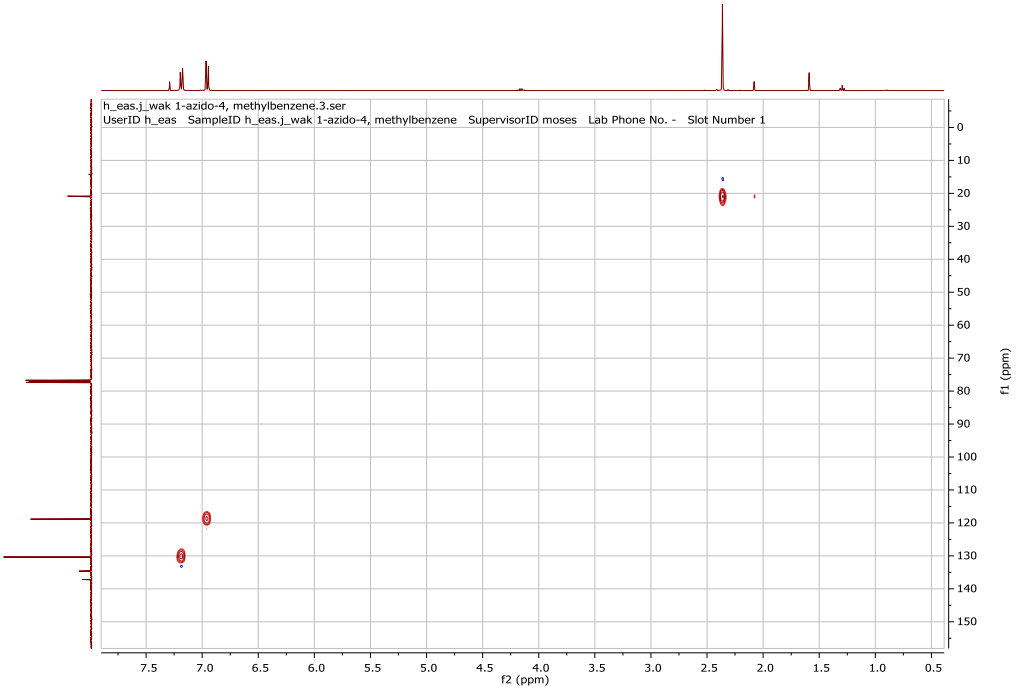

Figure 4-16: HSQC NMR of 1-azido-4-methylbenzene in $CDCl_3$

1-azido-4methoxybenzene

NMR data for aromatic azide compound 2

Table 4-2: Summary of ^{1}H (300 MHz) and ^{13}C (300 MHz) NMR spectroscopic data of 1-azido-4-methoxybenzene in $CDCl_3$.

Position	δ ^{13}C (ppm)	δ ^{13}C (ppm) 1-azido-methoxybenzene [a,b]	Type	δ ^{1}H/ppm (Mult J/Hz)	δ ^{1}H (ppm) 1-azido-methoxybenzene [a,b]
1	157.1		2xCH	6.95 (t, 8.99)	
2	132.5		2xCH	6.91 (t, 9.06)	
3	120.1		C		
4	115.3		C		
5	55,7		CH_3	s	

[a] Zhang et al., 2007, [b] In DMSO

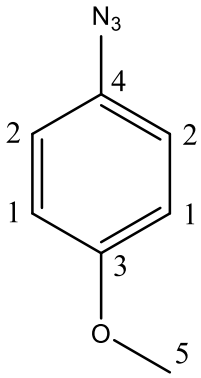

Figure 4-17: Carbon NMR assignment of 1-azido-4-methoxybenzene.

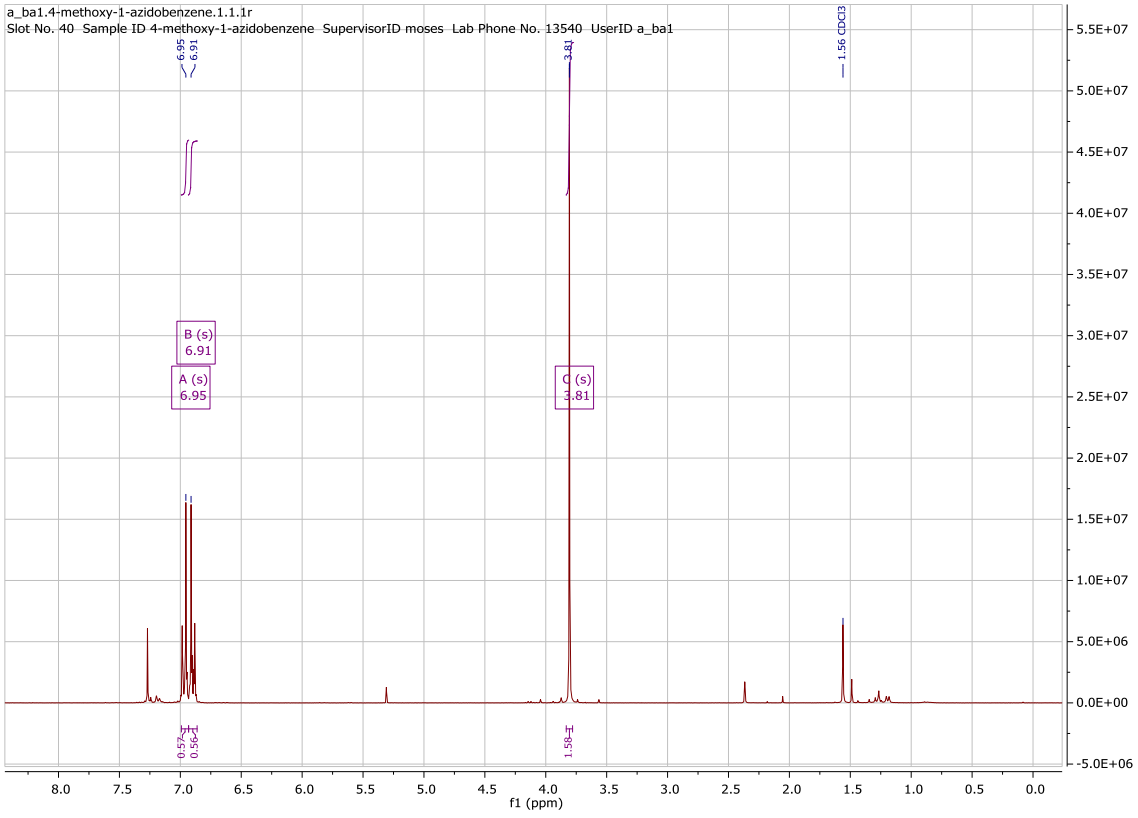

Figure 4-18: H^1 NMR of 1-azido-4-methoxybenzene in $CDCl_3$.

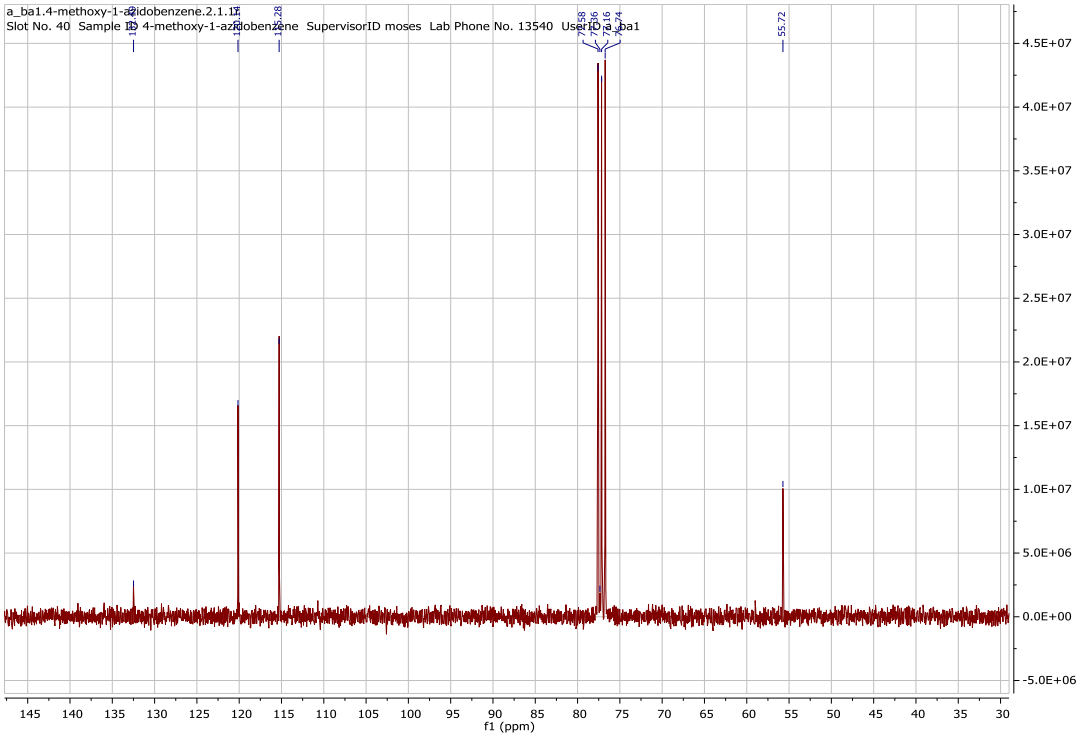

Figure 4-19: C^{13} NMR of 1-azido-4-methoxybenzene in $CDCl_3$.

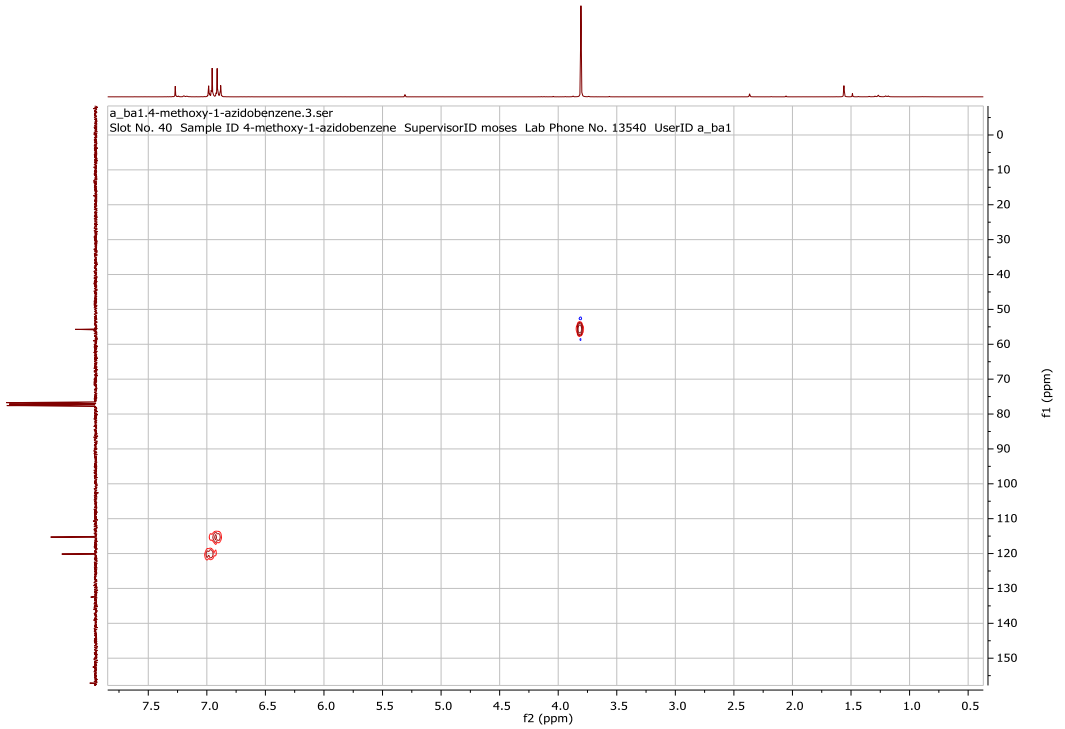

Figure 4-20: HSQC of 1-azido-4-methoxybenzene in $CDCl_3$.

1-azido-3,5-methylbenzene

NMR data for aromatic azide compound 3

Table 4-3: Summary of ^{1}H (300 MHz) and ^{13}C (300 MHz) NMR spectroscopic data of 1-azido-4-methoxybenzene in $CDCl_3$.

Position	δ ^{13}C (ppm)	δ ^{13}C (ppm) 1-azido-3,5-dimethybenzene [a,b]	Type	δ ^{1}H/ppm (Mult J/Hz)	δ ^{1}H (ppm) 1-azido-methoxybenzene [a,b]
1	139.6		CH	6.78 (s)	
2	126.7		2xCH	6.66(s)	
3	116.7		2xC		
5	21.2		2xCH_3	2.30 (s)	

[a] Zhang et al., 2007
[b] In DMSO

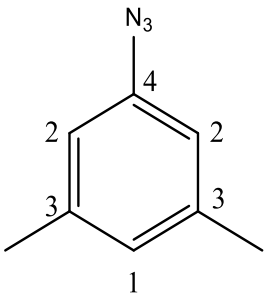

Figure 4-21: Carbon NMR assigment of 1-azido-3,5-dimethylbenzene.

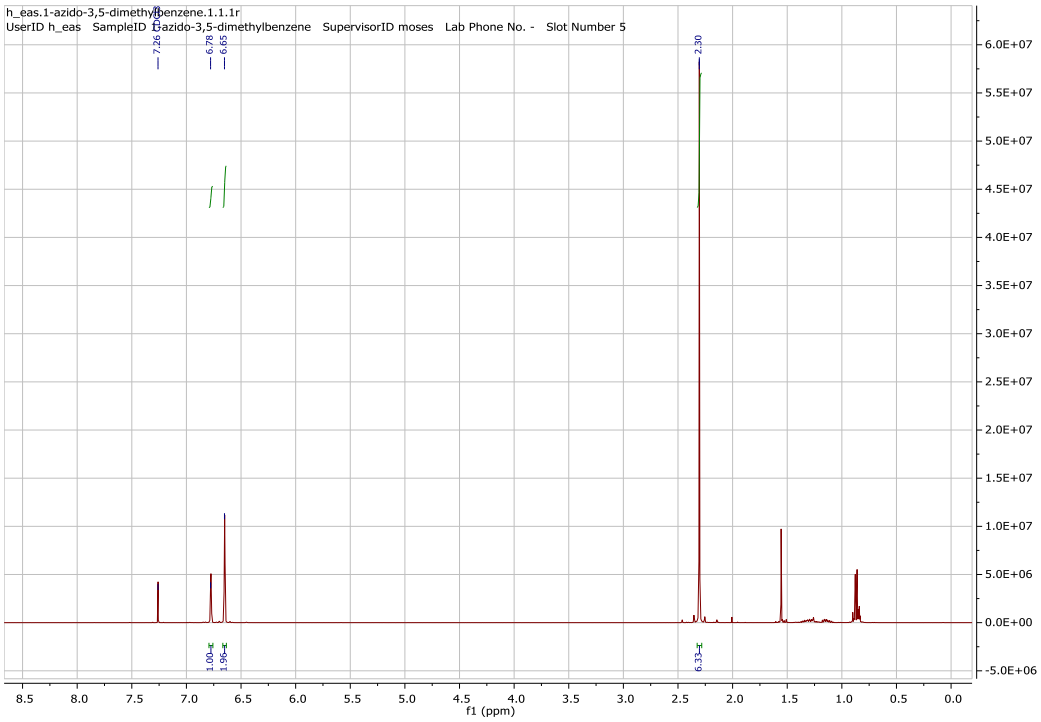

Figure 4-22: H^1 NMR of 1-azido-3,5-dimethylbenzene in $CDCl_3$.

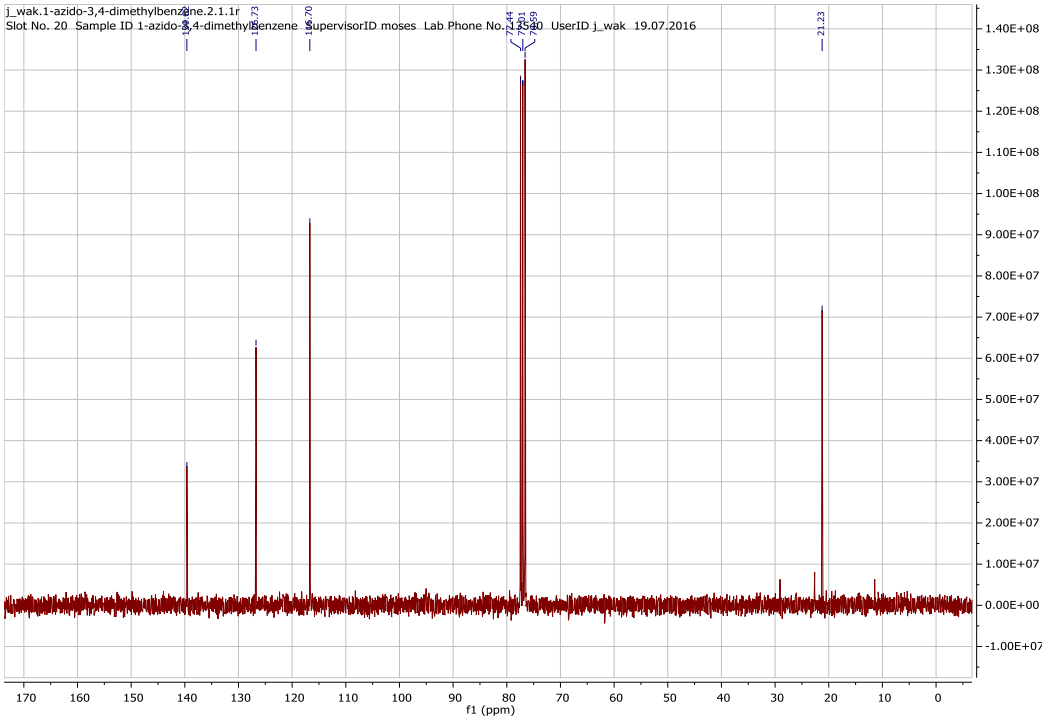

Figure 4-23: C^{13} NMR of 1-azido-3,5-dimethylbenzene in $CDCl_3$.

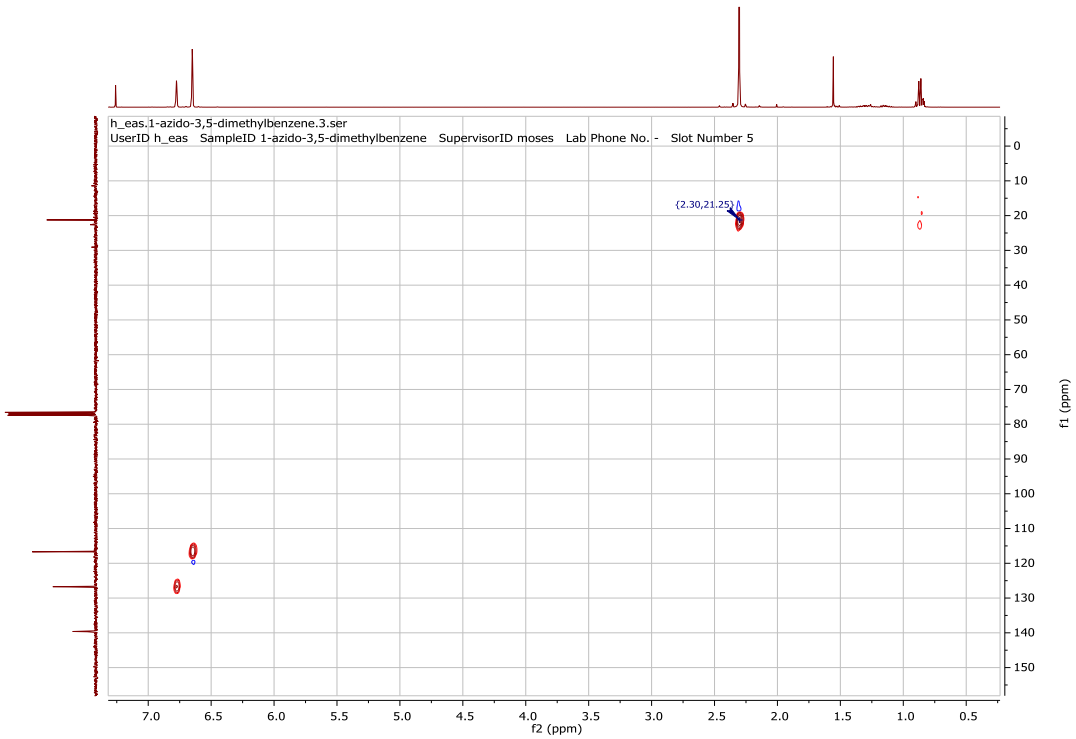

Figure 4-24: HSQC NMR of 1-azido-3,5-dimethylbenzene in $CDCl_3$.

4-pentynal

NMR data for product of swern reaction on 4-pentyn-1-ol

Table 4-4: Summary of ^{1}H (300 MHz) and ^{13}C (300MHz) NMR spectroscopic data of 4-pentynal in $CDCl_3$.

Position	δ ^{13}C (ppm)	δ ^{13}C (ppm) 1-azido-3,5-dimethybenzene [a,b]	Type	δ ^{1}H/ppm (Mult J/Hz)	δ ^{1}H (ppm) 1-azido-methoxybenzene [a,b]
1	200.1	199.9	CH	9.82	9.80
2	82.4	82.2	C		
3	69.4	69.1	CH	2.00	1.99
4	42.4	46.2	CH_2	2.71	2.70
5	11.7	11.3	CH_2	2.52	2.51

[a] (Phillips et al., 2015)
[b] In DMSO

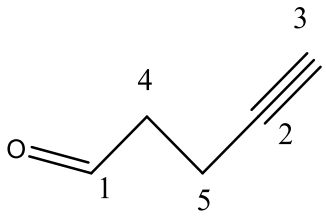

Figure 4-25: Carbon NMR assignment of 4-pentynal.

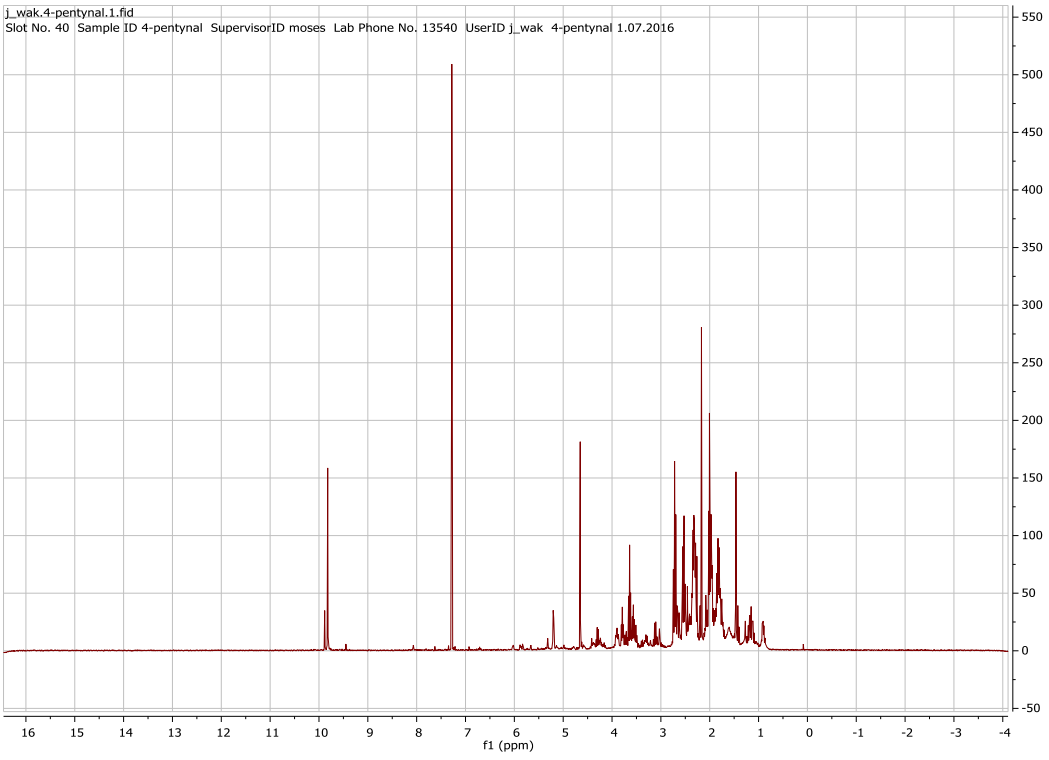

Figure 4-26: H^1 NMR results of first reaction to form 4-pentynal with wet solventsin of $CDCl_3$.

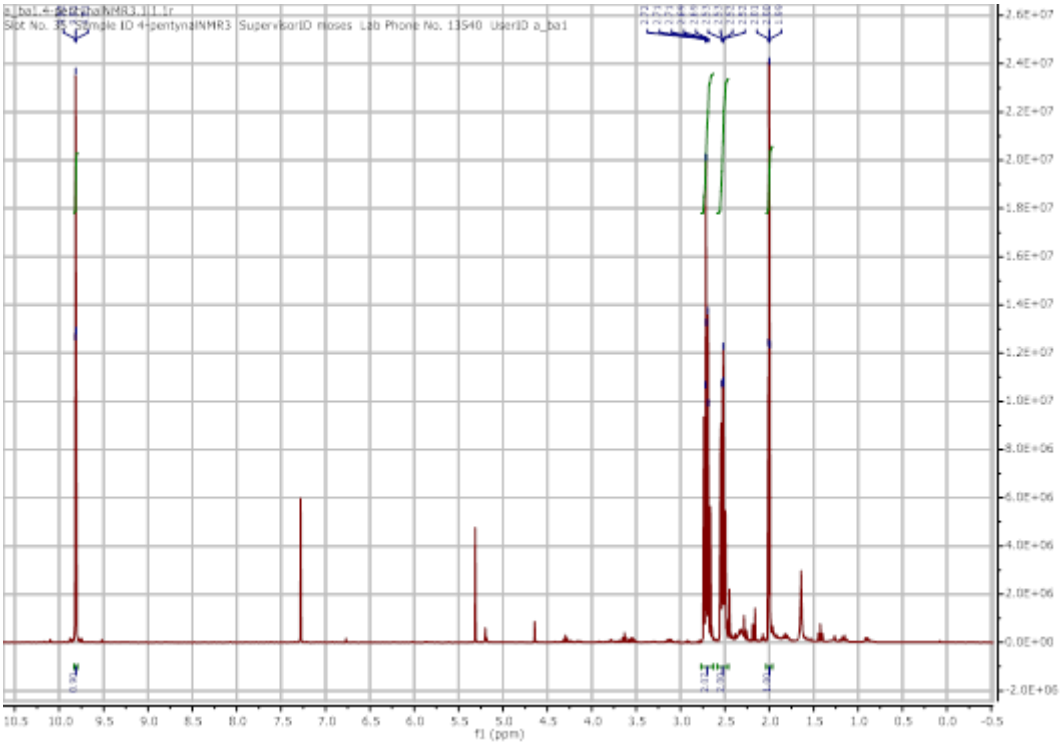

Figure 4-27: H^1 NMR of 4-pentynal in $CDCl_3$.

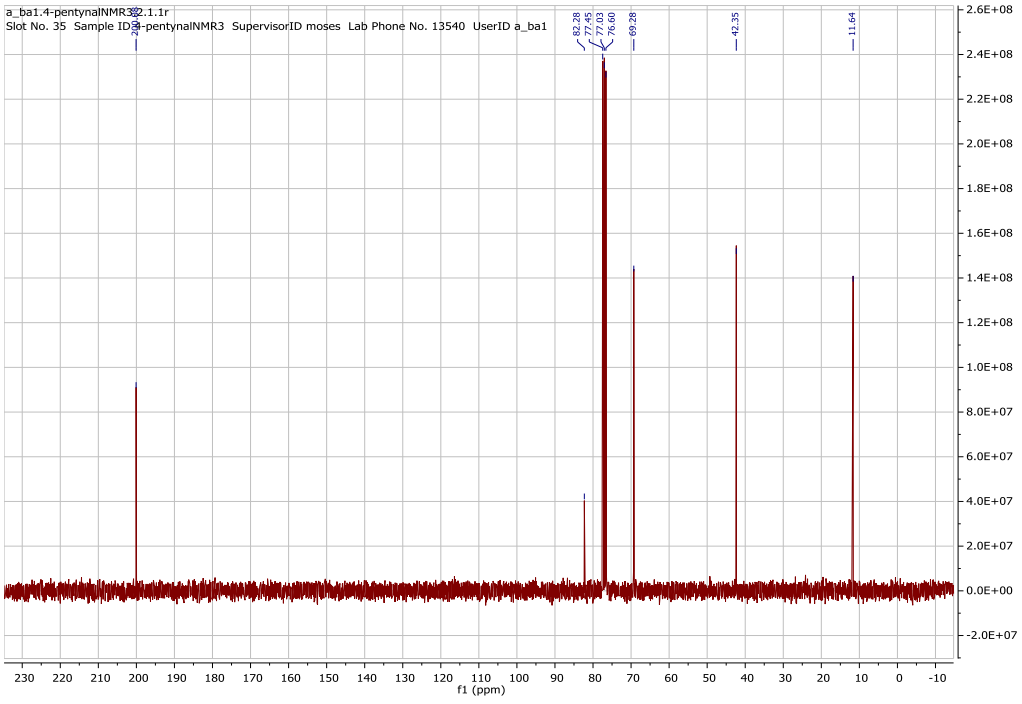

Figure 4-28: C^{13} NMR of 4-pentynal in $CDCl_3$.

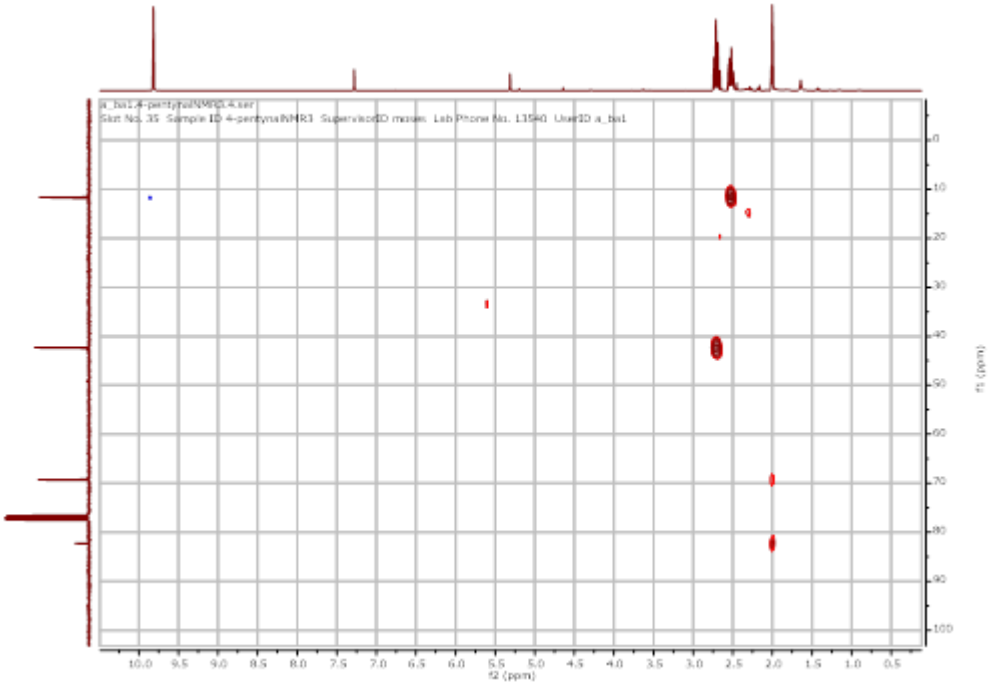

Figure 4-29: HSQC NMR of 4-pentynal in $CDCl_3$.

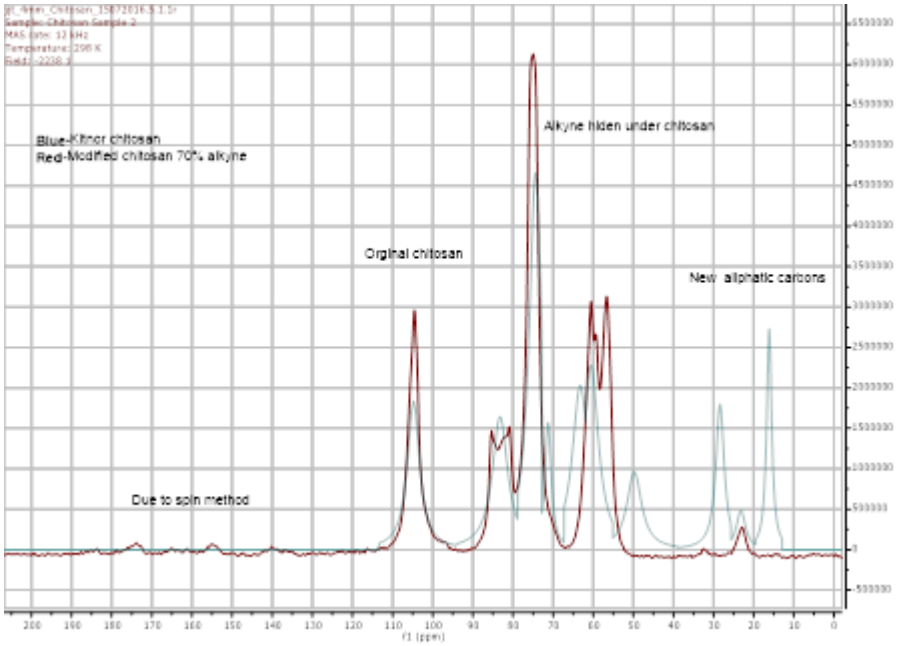

Figure 4-30: Solid state NMR of 70 % 4-pentynal chitosan in blue and chitosan in red.

The swern reaction to form 4-pentynal was evidently successful (see Figure 4-26 to Figure 4-30 summarised in Table 4-4 and carbons numbered in Figure 4-25). The reductive amination with 4-pentynal also appears successful, as a new aliphatic chain is seen in the NMR (Figure 4-30). The carbon triple bond, on the other hand, cannot be seen. Consequently, these often produce very small peaks and may be hidden under the chitosan backbone peaks. However, the presence of the alkyne could explain the broadening of the peaks seen at C4 and the side peak prior to the C3 and C5 peak. The addition of the aliphatic chain also explains the shift in the C2 from 56.6 to 63.3 ppm. NMR of pent-4-ynal gives δ 199.9, 82.2, 69.1, 46.2, 11.3 ppm in chloroform; these values will therefore be subject to small solvent effects. Chemdraw's NMR predict function gives the values of the alkyne at 84.7 and 71.3 ppm and carbon 2 as 61.1 ppm. These peaks are consistent with the changes observed in the chitosan peaks. Reductive amination resulted in a white powder, which upon drying, turned pink; this could signify that a reaction occurred such as cross-linking and this could explain why the click chemistry was unsuccessful. However, the NMR does suggest the change in the chitosan back-bone is likely to be from the alkyne. Therefore cross linking is less likely, or does not include all alkyne groups. There was concern regarding the lack of solubility of modified chitosan which could have prevented the reaction from working.

Three types of NMR have been previously used to the determine degree of decetylation; liquid NMR, C^{13} solid state NMR and N^{14} solid state NMR were all in agreement (Heux et al., 2000). This shows C^{13} solid-state NMR can be used to determine the degree of substitution. Reductive amination was carried out with equivalent quantities of 4-pentynal to monomer of chitosan to theoretically produce 100% substitution NMR. Results show roughly 70% substitution, observed from

regular solid-state NMR and confirmed via quantitative NMR. This more accurate method to determine substitution, was not carried out on all samples due to the time and equipment involved. The reaction was then carried out with 50% of the 4-pentynal, which resulted in roughly 30% substitution. Results of this are shown below in Figure 4-31, Figure 4-32 and Figure 4-33.

The equation (4-1)

$$S(t) = \frac{I_o}{1-\frac{T_{IPS}}{T_{IP}}} . (\exp\left(-\frac{T_P}{T_{IP}}\right) - exp\frac{T_S}{T_{IS}} \qquad 4\text{-}1$$

provides the intensity (I) in arbitrary units. Using this, results in a range of intensities for chitosan, for CH_2 from the alkyne, minimum and maximum combined gives (70 ± 4)% substitution with a large error due to poor fit (Figure 4-32) and for (30 ± 1)% alkyne substitution with a good fit (Figure 4-33).

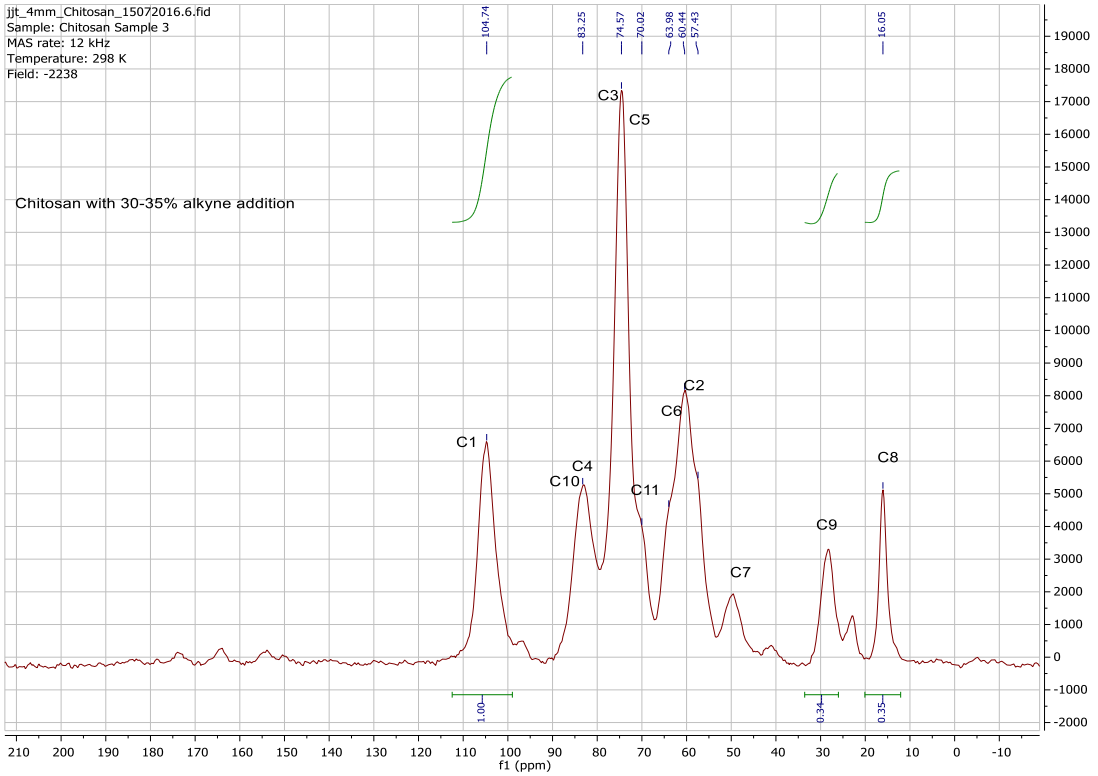

Figure 4-31: Solid state NMR of 30% 4-pentynal chitosan.

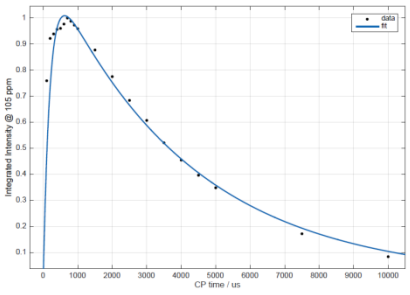

Figure 4-32: Quantitative fit for solid state NMR of 70% chitosan alkyne.

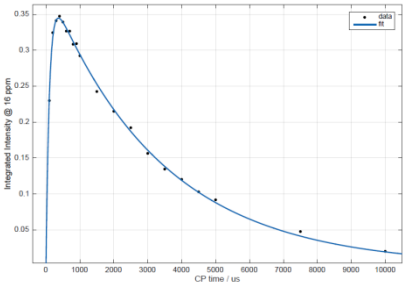

Figure 4-33: Quantitative fit for solid state NMR of 30% chitosan alkyne.

The Huisgen 1,3-dipolar cycloaddition reaction with 70% 4-pentynal substituted chitosan was tried in two different solvents. The modified chitosan was insoluble in water/butanol and the swelling in acetic acid/*tert*-butanol takes time. The modified

chitosan was not left to soak in the solvent before the reaction was started in either case. Therefore, the chitosan was not dissolved and this lack of solubility could have prevented the reaction taking place properly. One small peak in the NMR, (seen in Figure 4-34), can be observed in the aromatic range. This suggesting that the reaction worked. However, the chitosan backbone was completely changed/barely visible which suggests severe degradation of the chitosan. The reaction was in fairly mild conditions: at room temperature and in mildly acidic conditions with sodium ascorbate and copper acetate, which are not particularly strong reactants. The reason for the break-down when a similar reaction by Sarwar *et al*. (2015) was successful is unclear.

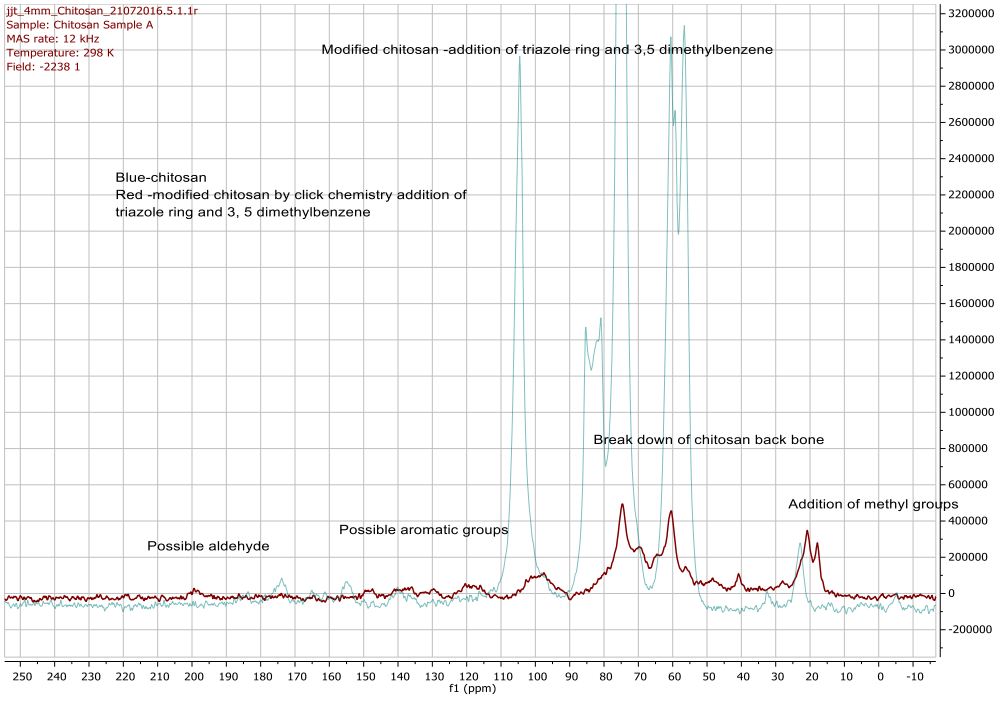

Figure 4-34: Solid state NMR chitosan blue and click product in red.

The NMR from the first click chemistry reaction is so poor that very few interpretations can be made and none should be relied upon. The methyl groups and groups at 60 and 74 ppm suggest that some of the original chitosan groups are present along with the aromatic group with attached methyls. However, the original backbone

structure has been lost, which could be from ring opening and severe degradation. The methyl groups suggest addition of the aromatic group. However, the methylene should still be visible. This is most likely a mixture of breakdown products, along with poor resolution resulting from the mixture, but could also be due to the size of the particles analysed. Since the reaction did not result in large lumps, the product was not ground down prior to NMR, which may have resulted in poor resolution. It is most likely a mixture of break-down products, otherwise some clear peaks may have been larger compared to the base line. If this reaction is to be repeated, another solvent such as DMSO or DCM and HCl should be used (Ellanki et al., 2012; Hein et al., 2008; Ifuku et al., 2011). However, with limited success and limited time for this project, it was decided not to make any more attempts but instead move on to another method; silylation.

4.3.2 Liquid NMR

The NMR results include the codes used during the experiments (Table 4-5). My initials- JW followed by 01 representing mesylate, 02 for TBDMS silylation, C chitosan and DC depolymerised chitosan. All of this is explained in the table, the work for this set was carried out at Friedrich Schiller University Jena, Germany. The large batches had similar notations but with an N at the start to signify the work was carried out at Nottingham University.

Table 4-5: The codes of reactions with products and starting materials with resulting degree of substitution.

Code	Stage/product	Starting polymer	Comments	DS
JW01DC	Mesylate	Depolymerised chitosan ~5 kDa		0.9 mesylate
JW01C	Mesylate	Chitosan~14 kDa		
JW02C	TBDMS chitosan	Chitosan ~14 kDa		2.75 TBDMS
JW02DC	TBDMS chitosan	Depolymerised chitosan ~5 kDa		0.91 TBDMS
JW02DCb	TBDMS chitosan	Depolymerised chitosan ~5 kDa	Toluene added to reaction to increase DS	1.73 TBDMS
JW02TC	TBDMS cellulose	Tosyl cellulose		1.22-1.36 TBDMS solvent dependant
JW03TC	TBDMS aminocellulose	Tosyl cellulose/TBDMS cellulose		0.72 TBDMS, 0.08 tosyl
JW03DC	TDS chitosan	Depolymerised chitosan ~5 kDa		0.69 TDS

4.3.2.1 Silylation

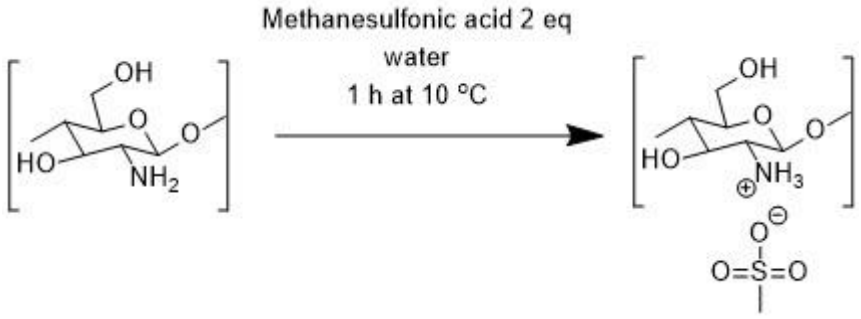

Figure 4-35: Reaction scheme for formation of the mesylate of chitosan.

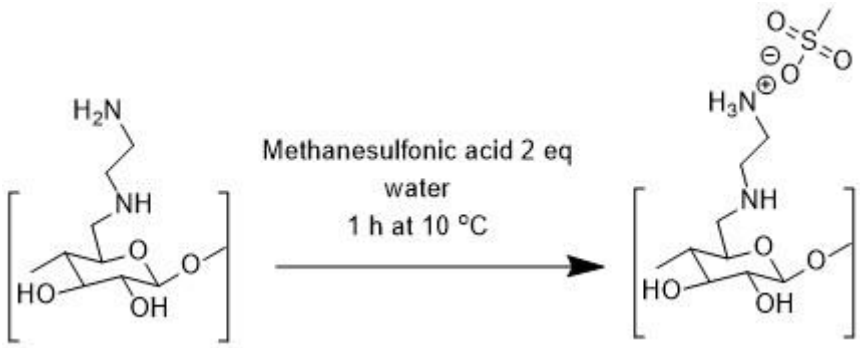

Figure 4-36: Reaction to form the mesylate of aminocellulose.

4.3.2.1.1 Mesylate

Limited quantities of degraded chitosan were made for initial trials of TBDMS modification of chitosan. For this reason, the first reaction was carried out with the polymer. This allowed for a comparison of the effect of chain length and a trial run. Chitosan mesylate (14 kDa) NMR is given in Figure 4-37 and resulted in 100% mesylate salt formation at the amine. A DS 0.98 was found from the NMR which is not possible as it is known have a DS of 0.1 acetyl at the nitrogen. This NMR shows 0.09 acetyl substitution which concurs with previously published work by Christensen. Christensen et al., (2015a) reporting the deceylation as 0.9 for the same batch of chitosan, we obtained the same batch of chitosan used by Christensen for reseach. This means the DS of the mesylate must be 0.9. Although NMR can be used to determine the degree of substitution, it is not 100% accurate. However, it does show that the mesylate was successfully produced for the chitosan polymer (14 kDa) (Figure 4-37, Figure 4-38).

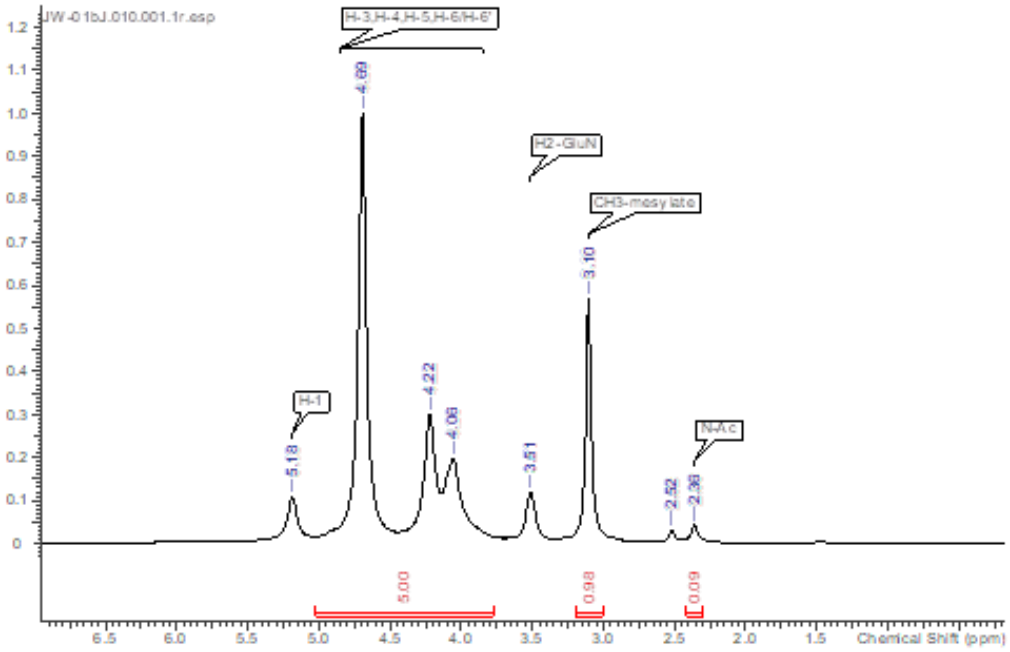

Figure 4-37: ^{1}H NMR of JW01C (mesylate of 14 kDa chitosan) carried out in D_2O at 400 Hz.

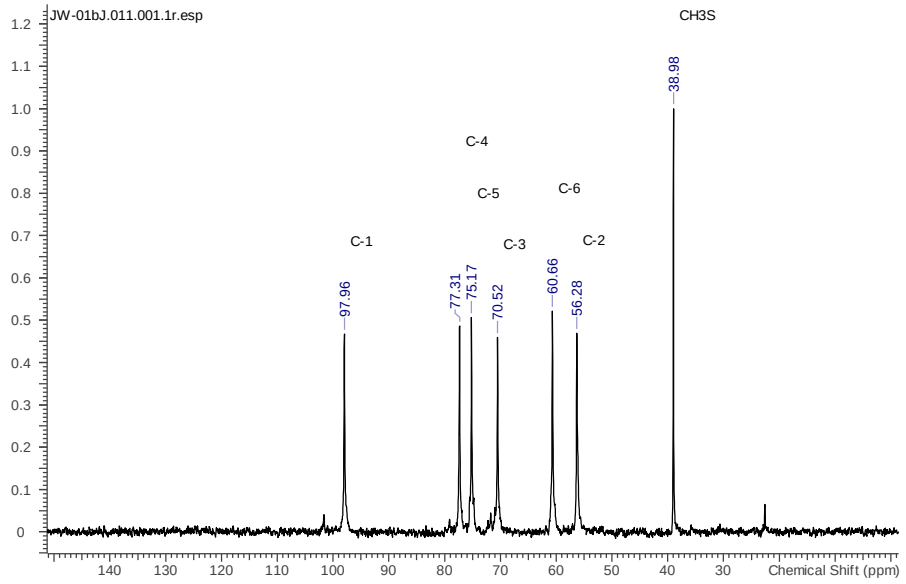

Figure 4-38:C^{13} NMR JW01C chitosan (14 kDa) mesylate in D_2O.

Figure 4-37 shows peaks at 4.87 ppm which is H1, 3.75-3.90 ppm is H3, H4, H5, H6 and H6', 3.21 is H2 and 2.80 ppm is H7 the methyl group of the mesylate (See numbering in Figure 4-39). This proves the chitosan mesylate has been produced. The

mesylate has a DS of 0.94 and N-acetate DS of 0.21. DS works out as more than 1, which is not possible and the DS of the acetate fraction has previously been determined as 0.1. 100% of the amine appears to have been mesylated.

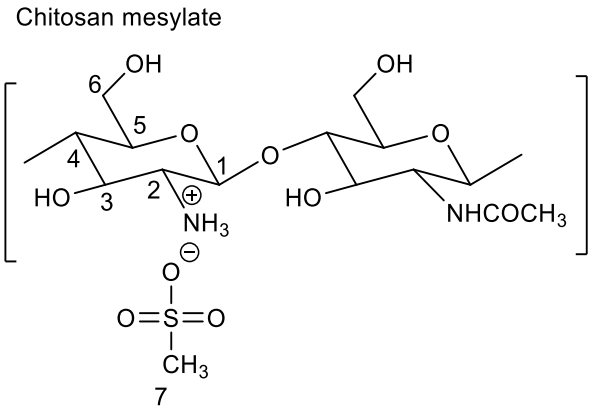

Figure 4-39: Mesylate chemical structure with carbons numbered.

4.3.2.1.2 Silylation –addition of TBDMS group

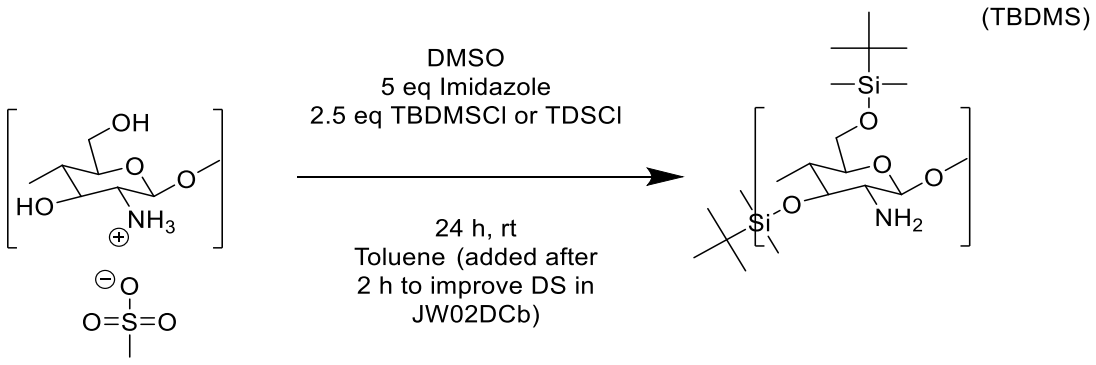

Figure 4-40: Reaction scheme for silylation of chitosan mesylate

Starting polymer chitosan 14 kDa. NMR (Figure 4-42 and Figure 4-43) shows the TBDMS group was successfully added. Figure 4-41 gives the structure of the TBDMS with the carbons numbered.

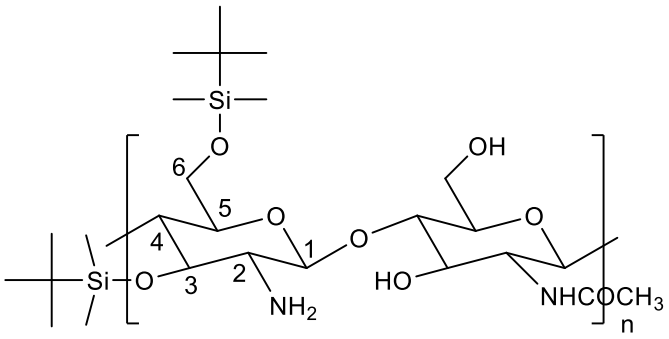

Figure 4-41: Structure of TBDMS chitosan with carbons numbered. DS 2.75

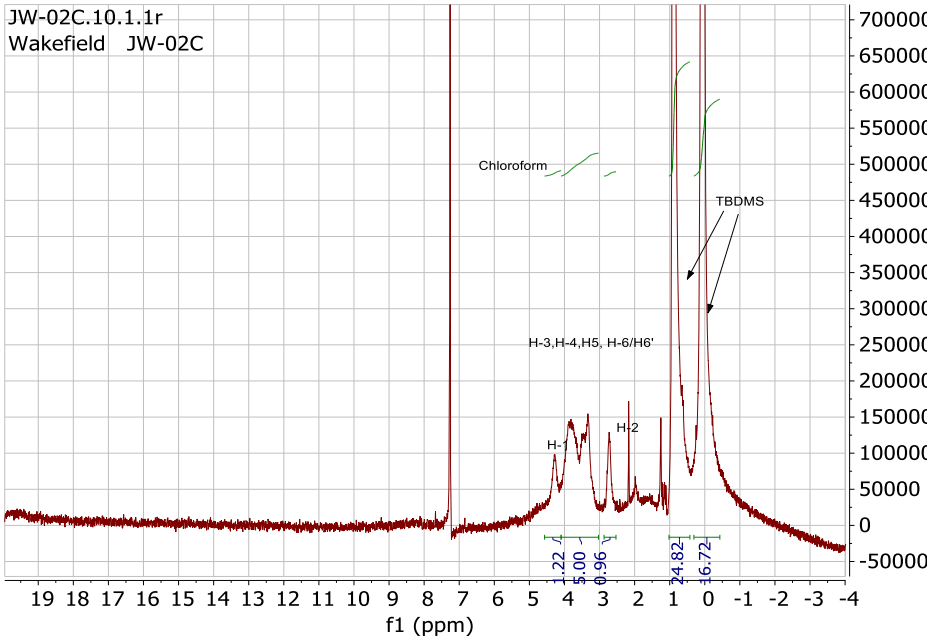

Figure 4-42:[1]H NMR in $CDCl_3$ at 400 Hz JW02C TBDMS chitosan (14 kDa) DS= 2.75.

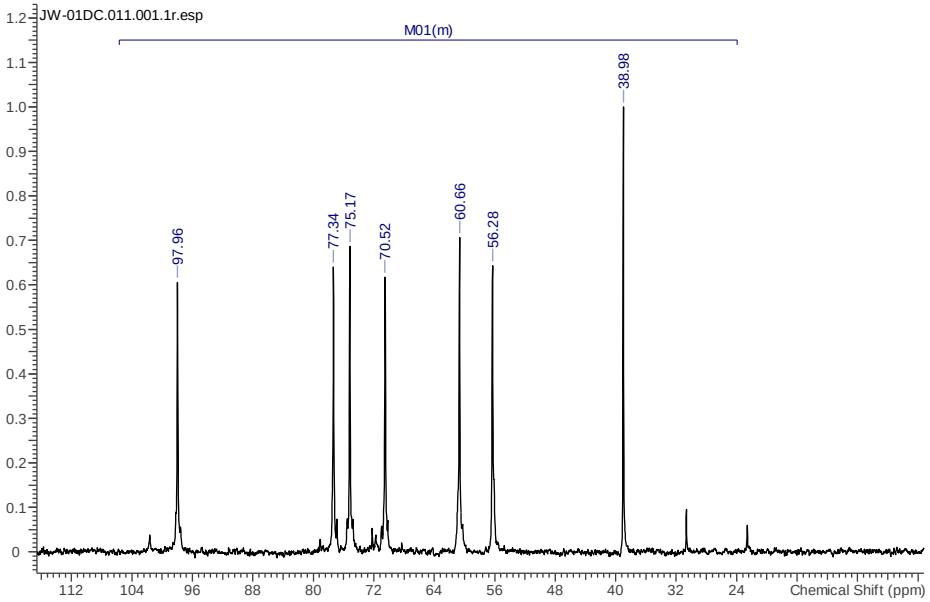

Figure 4-43:C^{13} NMR in D_2O of JW02DC (chitosan (14 kDa) mesylate).

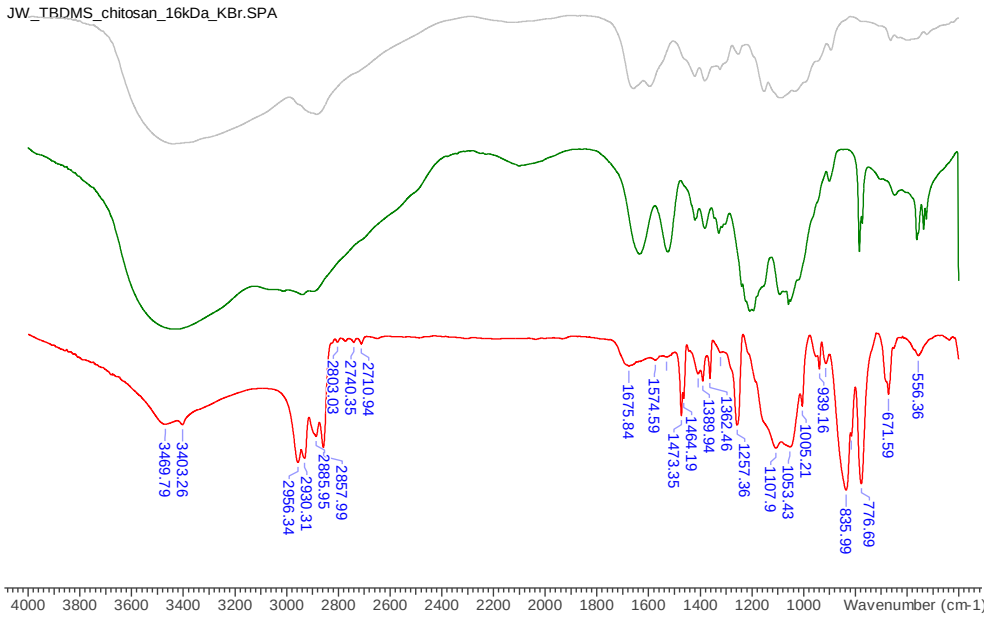

Figure 4-44: IR Grey-chitosan 14 kDa, green chitosan mesylate 14 kDa, blue TBDMS chitosan 14 kDa.

IR of chitosan modification (Figure 4-44) to TBDMS chitosan shows the intermediate and final product were successfully produced. TBDMS peaks 2956, 2930, 2886, 2857, 835 and 776 prove TBDMS has successfully been added.

4.3.2.1.3 Depolymerised chitosan (5 kDa) addition of TBDMS groups

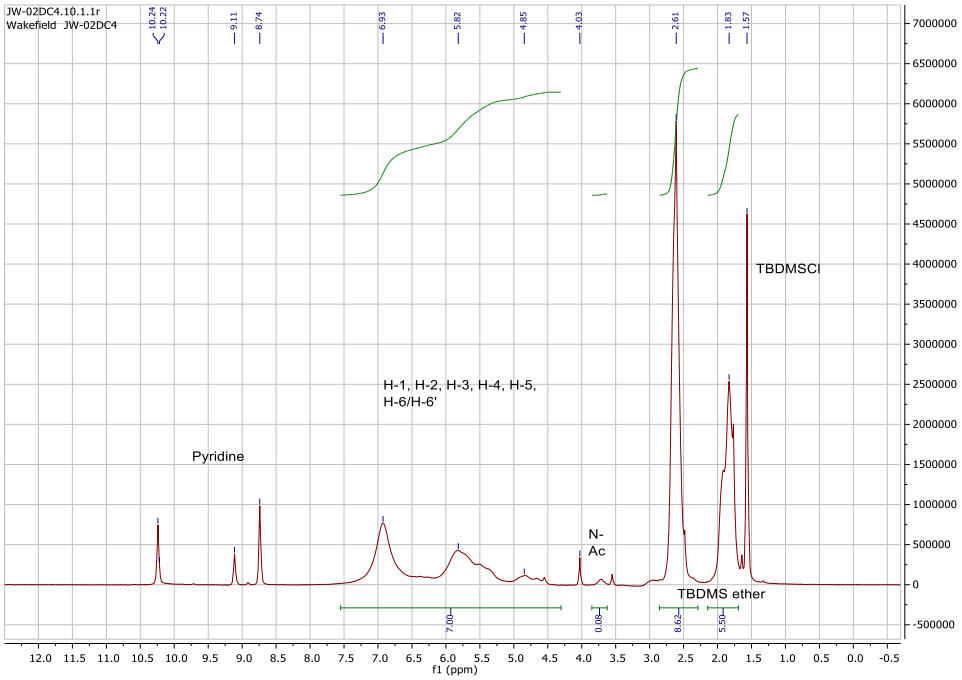

Figure 4-45: ^{1}H NMR of TBSMS chitosan (~5 kDa) JW02DC, solvent pyridine. Silyl DS 0.91.

Figure 4-45 is the NMR of the TBDMS product produced from the depolymerised chitosan (~5 kDa) which shows it was successfully produced but had a low degree of substitution (DS 0.91). It is thought this low degree of substitution was caused by a lack of solubility of the product which precipitated out of solution as a gel, preventing a higher degree of substitution being obtained. Thus, the next reaction (Figure 4-48) was carried out in the same manner but after 2 h toluene was added to help dissolve the product to allow the reaction to continue. This aided in solubility by increasing the DS to 1.73 which is discussed next. The improved DS is probably due to improved

solubility of the product in the solvent, allowing the reaction to continue which resulted a higher DS of the final product (See Figure 4-47 showing precipitation of the product and Figure 4-46 -showing precipitation start to redissolve). Later, repeat reactions showed a DS of up to 2.3.

Figure 4-46: The set-up of the experiment showing product is fully soluble after the addition of toluene.

Figure 4-47: Silylation of chitosan with TBDMS before addition of toluene.

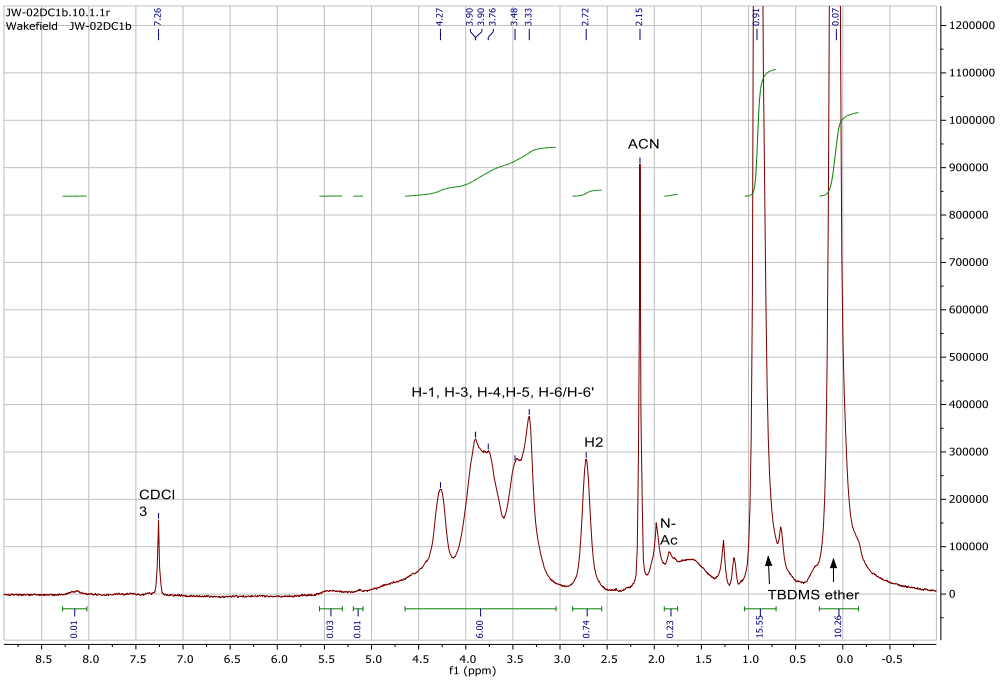

Figure 4-48: ^{1}H NMR of TBDMS chitosan (~5 kDa) with toluene in the reaction, JW02DCb, in $CDCl_3$. Silyl DS 1.73.

Figure 4-49 NMR of dimethyl thexylsilane chitosan (TDS chitosan) shows it is possible to change the substituting group to TDS instead of TBDMS. The degree of substitution was lower, at 0.69. Solubility as shown in the next section was reduced.

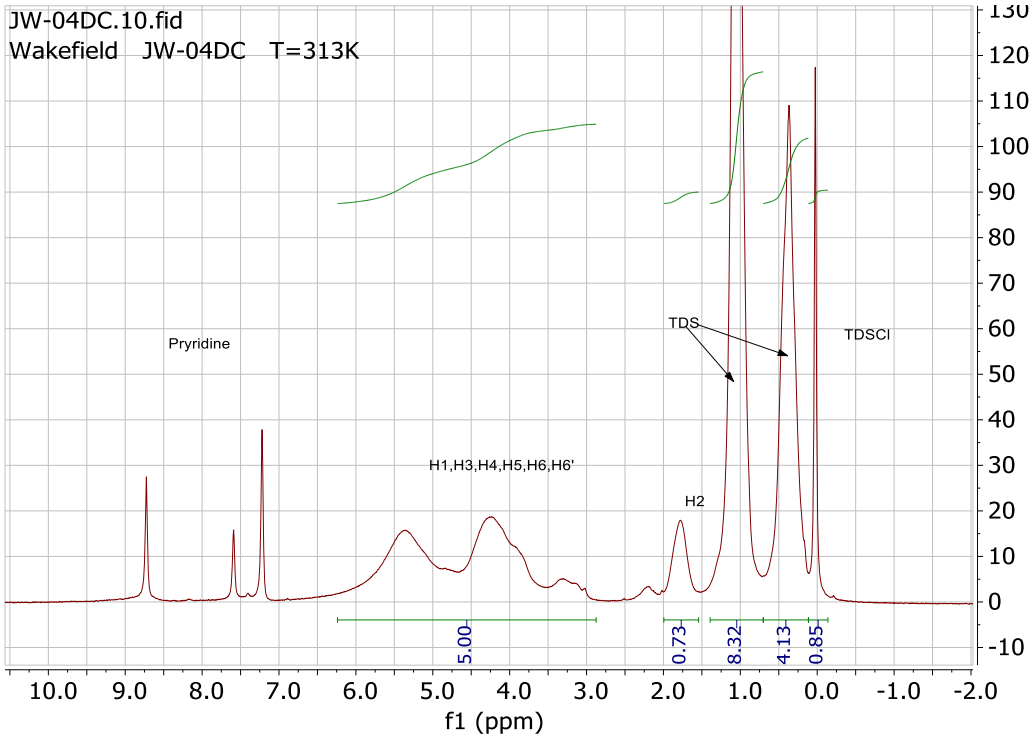

Figure 4-49: H^1 NMR JW04DC TDS depolymerised chitosan in pyridine. Silyl DS 0.69

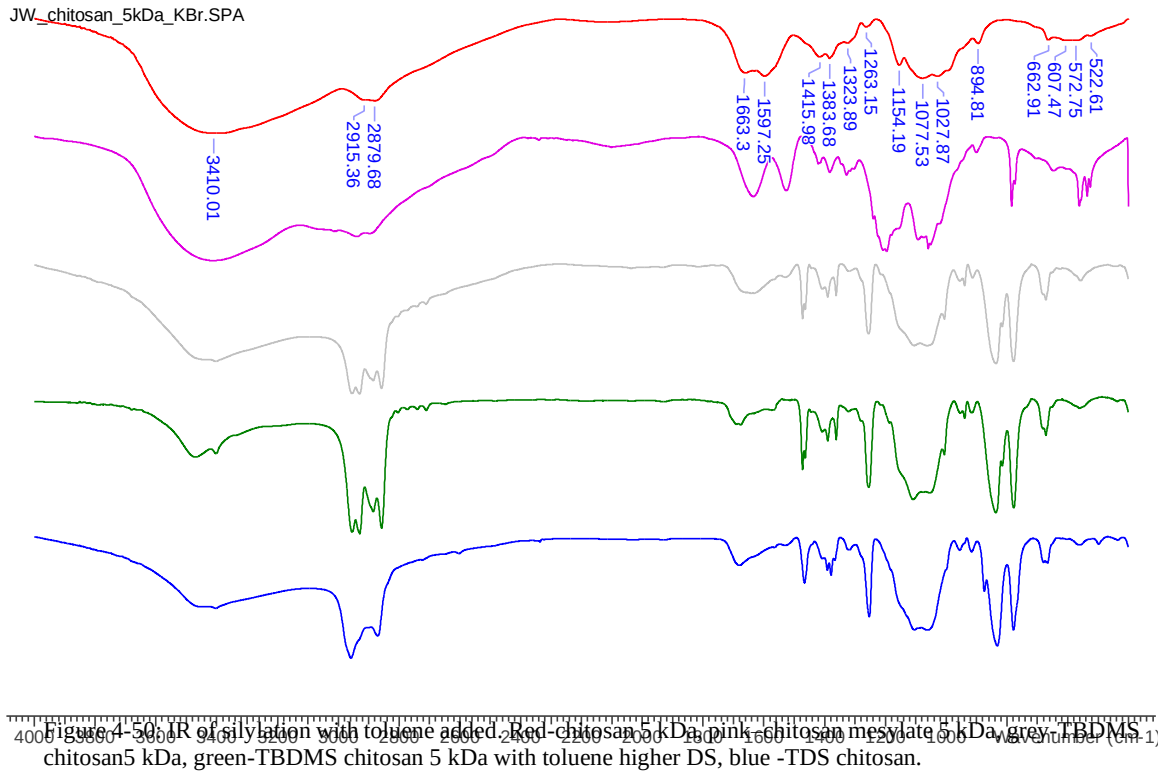

Figure 4-50: IR of silylation with toluene added. Red- chitosan 5 kDa, pink- chitosan mesylate 5 kDa, grey- TBDMS chitosan5 kDa, green-TBDMS chitosan 5 kDa with toluene higher DS, blue -TDS chitosan.

The IR analysis of silylation intermediate and its products show that the silylation was successful and that that the toluene increased in the silyl content (Figure 4-50).

TBDMS of tosyl cellulose substitution was successful as shown from NMRs carried out in DMSO and then triflouric acid shifting the water's peak from below the cellulose peaks. This shows the initial DS of 1.22 (Figure 4-51) was low due to the OH peaks under the cellulose peaks; the actually DS appears to be 1.36 (Figure 4-52). The tosyl substitution was reduced from 0.76 to 0.08, suggesting the DS of the aminogroup is 0.68 (Figure 4-53).

The substitution of TBDMS to aminocellulose AEA was not possible. Therefore, tosyl cellulose was used as the starting material instead and then, after the addition of TBDMS chitosan, the tosyl group was replaced with the amine group. See Figure 4-54 for the structure of the final product.

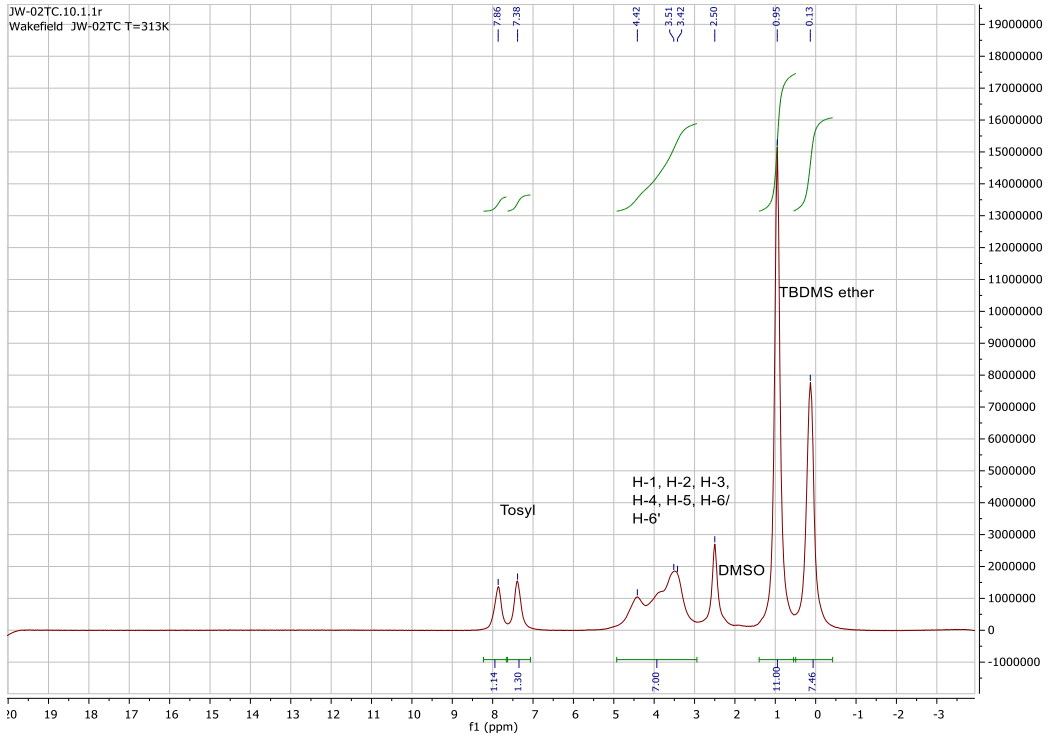

Figure 4-51: JW02TC, solvent DMSO. silyl DS 1.22, tosyl DS 0.65.

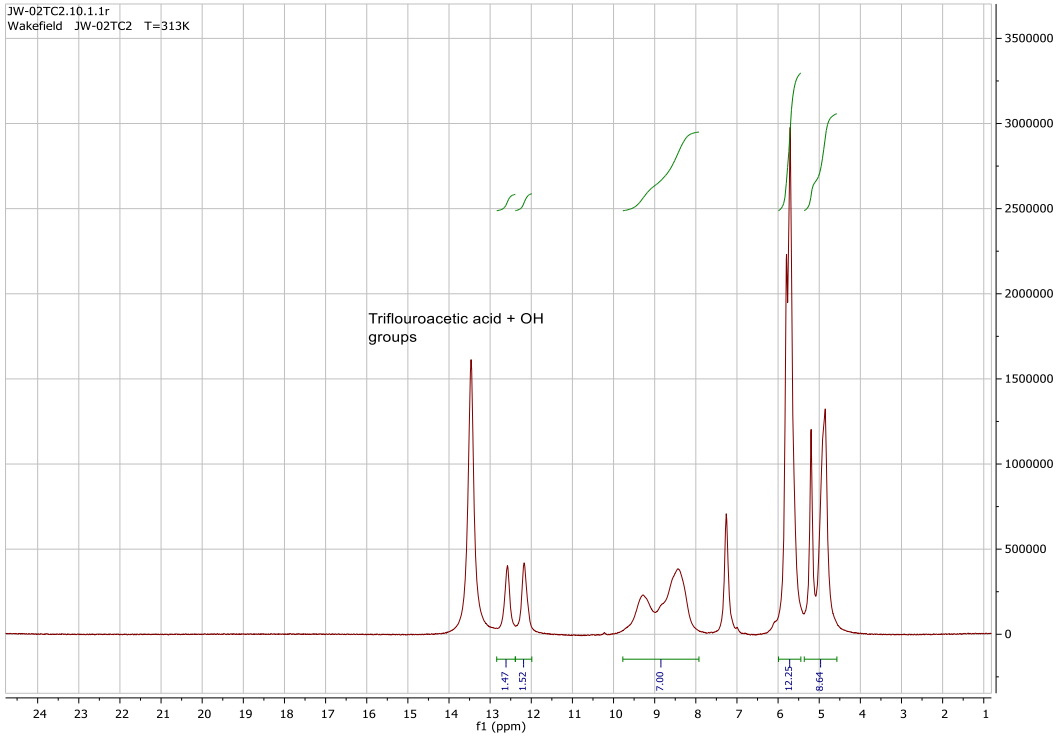

Figure 4-52: ^{1}H NMR of JW02TC, solvent DMSO +triflouric acid to shift water peak. Silyl DS 1.36, tosyl DS 0.76.

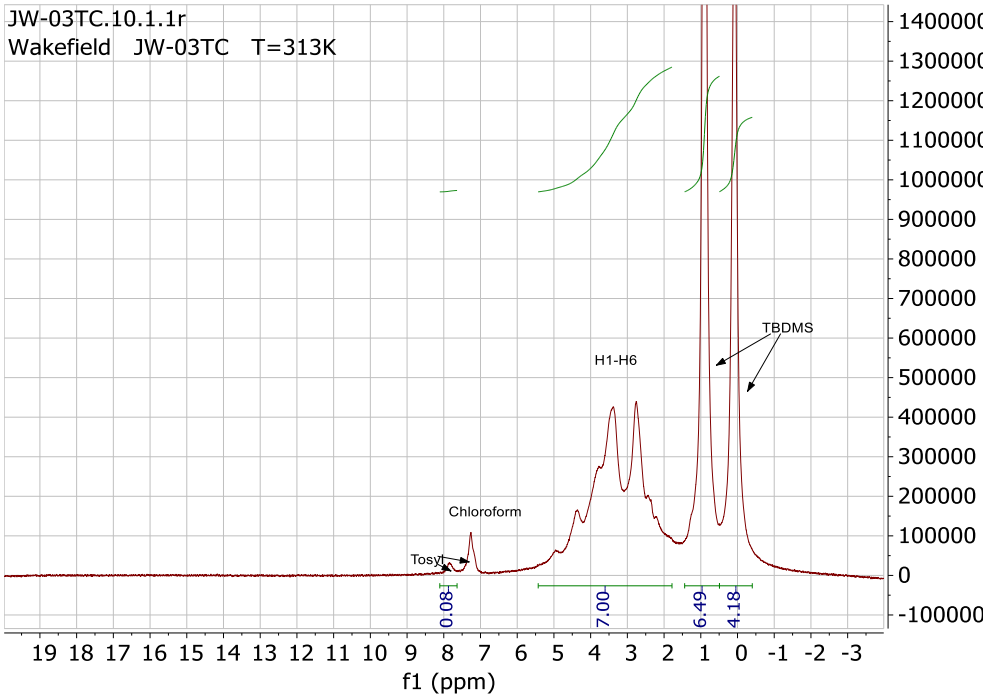

Figure 4-53: H^1 NMR 400 Hz. JW03TC in $CDCl_3$. TBDMS aminocellulose. DS 0.72 TBDMS, DS tosyl 0.08. Broad peaks make it hard to identify the amine addition through the CH_2 groups.

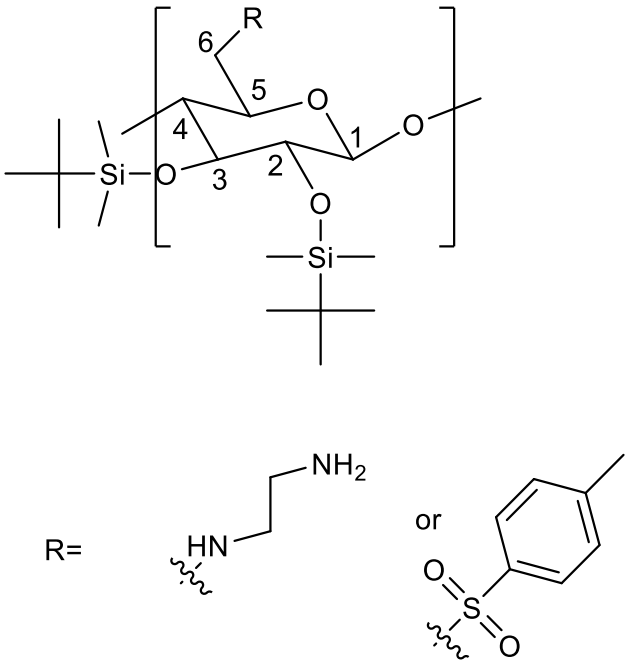

Figure 4-54: Structure of TBDMS aminocellulose

4.3.3 Solubility results

4.3.3.1 Reductive amination and click chemistry

A quick shake test was carried out with various solvents and these were checked again after being left overnight in case poor solubility had taken place. Table 4-6 and Table 4-7 show the solvents tested for each modified chitosan and their results. This shows that solubility in acetic acid decreased in all cases, indicating the addition of a hydrophobic group. However, none of these modifications showed improvement in solubility in any of the solvents except Dimethyl sulfoxide (DMSO) and Dimethylacetamide (DMA). These solvents are not desirable; DMA due to its toxicity and DMSO due to its very slow evaporation rates. Slow evaporation rates although generally a positive in terms of sustainability, makes it difficult to remove from the artefacts. DMSO is also hydroscopic, which suggests water may be drawn into the ship, increasing the rate of degradation.

Table 4-6: Solubility of modified chitosan x-not soluble, y-soluble, ±-forms a gel

Polymer/solvent	**Water**	**MeOH**	**Acetic acid**	**Acetone**	**Ethyl acetate**	**Diethyl ether**	**isopropanol**
Chitosan/4-merhoxy benzene	x	x	±	x	x		
Chitosan/3,4,5-trimethylbenzene	x	x	±	x	x		
Chitosan/4-pentyne	x	x	±	x	x	x	x
Chitosan/4-pentyne	x	x	±		x		x
Click reaction product 70%	x	x	x	x	x	x	x
Click reaction product 30%	x	x	x	x	x	x	x

and Table 4-7). However, for the reductive amination of chitosan we expected better solubility. The lack of solubility could be due to the aromatic groups being added rather than a long aliphatic chain, or it could be due to the size of the polymer and these groups are not sufficient, considering the size of the polymer, to make a significant difference. Similar work has been carried out with pentynal with similar results: the polymer became swollen with chloroform, pyridine, DCA (dichloroacetic acid) and was insoluble in DMSO and DMAc (N,N-dimethylacetamide). This suggests that pentynal is too small a chain to produce the hydrophobic properties required to make chitosan soluble in organic solvents (Kurita et al., 2002). Kurita *et al.* (2002) paper started with chitin and then produced chitosan using sodium hydroxide and there was no analysis of molecular weight; hence, it is likely that the chitosan used here was fairly large. This could also have prevented solubility. N-phthaloylation of chitosan improved the solubility of chitosan; however, again in DMF, DMAc, DMSO and pyridine which are not desirable solvents (Nishimura et al. 1991).

Table 4-7: Summary of solubility of reductive amination and click chemistry, x-not soluble, y-soluble, ±-forms a gel

Polymer/solvent	**Pentane**	**Toluene**	**Petroleum spirt**	**DMSO**	**DMA**
Chitosan/4-merhoxy benzene	x		x		±
Chitosan/3,4,5-trimethylbenzene		x	x	±	±
Chitosan/4-pentyne	x	x	x	±	±
Chitosan/4-pentyne	x		x	±	±
Click reaction product 70%	x	x	x	x	x
Click reaction product 30%	x	x	x	±	x

4.3.3.2 Silylation

A summary is given in Table 4-8 and photographic results shown in Figure 4-55, to Figure 4-60.

Table 4-8: Summary of solubilityof silyl modified chitosan

Solvent	**10%**					
Code (JW:	02C	02DC	02DCb (with toluene)	02TC	03TC	04DC
DMSO		P+++	P++		S	PH
Chloroform	G+++	P+++	+++	+++	+++	+++
isopropanol		H++	+++	H++	S	PH++
t-butanol		H++	+++	H++	S	P H++
Ethyl acetate	S	S	+++	+++	S	-
toluene	P	P+++	G	P	++	P –GH++
THF	P	P+++	+++	+++	+++	+++
hexane	-	-	S	-	-	-
Pyridine	P+++	+++				
*+++ soluble at 10%, S –swells, G-Gel, H-soluble with heating, P-Partial soluble gel, ++ soluble 5%, + soluble 2.5%						

Solubility tests have shown that chitosan (~12 kDa) could not be made completely organic soluble as the molecular weight was too high. However, degraded chitosan (~4.5 kDa) silylated with TBDMSCl, can be made organic soluble with the addition of toluene after a couple of hours to re-dissolve the product that forms. The product comes out of solution, as the reaction occurs, which reduces the effectiveness of the reaction. The addition of toluene allows the product to re-dissolve, allowing the reaction to continue (Figure 4-46). Therefore, the final product, with the addition of toluene to the reaction, had a higher DS than without toluene. This higher DS results in improved solubility. Where there was only partial solubility in isopropanol and t-butanol and only swelling in ethyl acetate, there is now complete solubility in all three solvents.

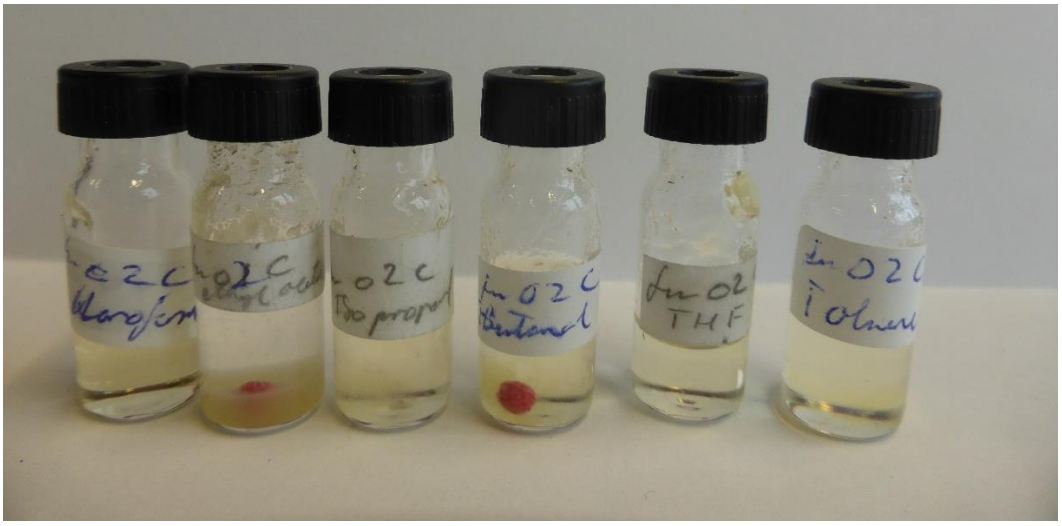

Figure 4-55: Solubility test results for JW02C – TBDMS chitosan (~12 kDa). Solvents left to right chloroform, ethyl acetate, isopropanol, t-butanol, THF and toluene.

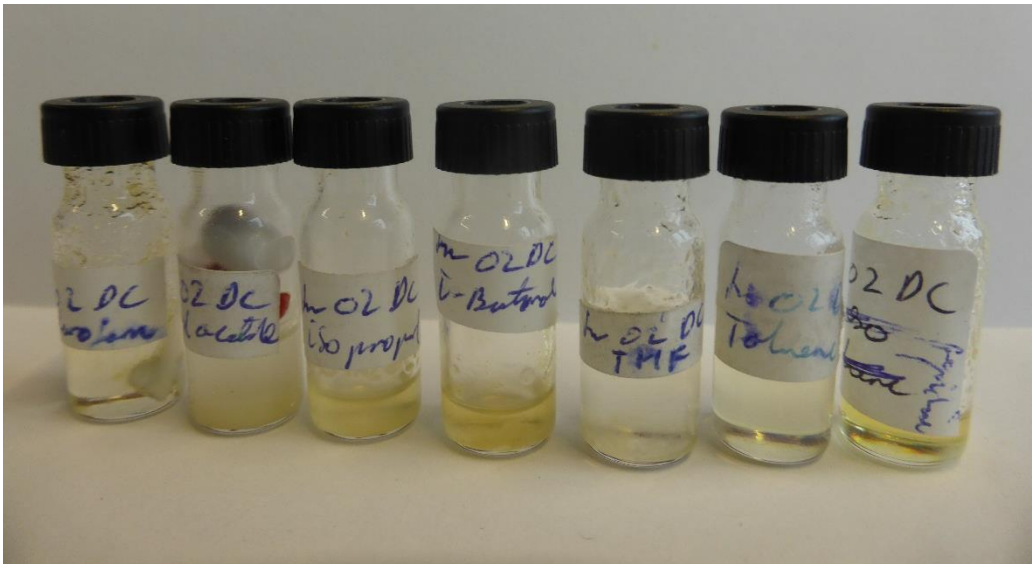

Figure 4-56: Solubility test results for JW02DC- TBDMS chitosan (~4.5 kDa). Solvents left to right chloroform, ethyl acetate, isopropanol, t-butanol, THF, toluene and pyridine

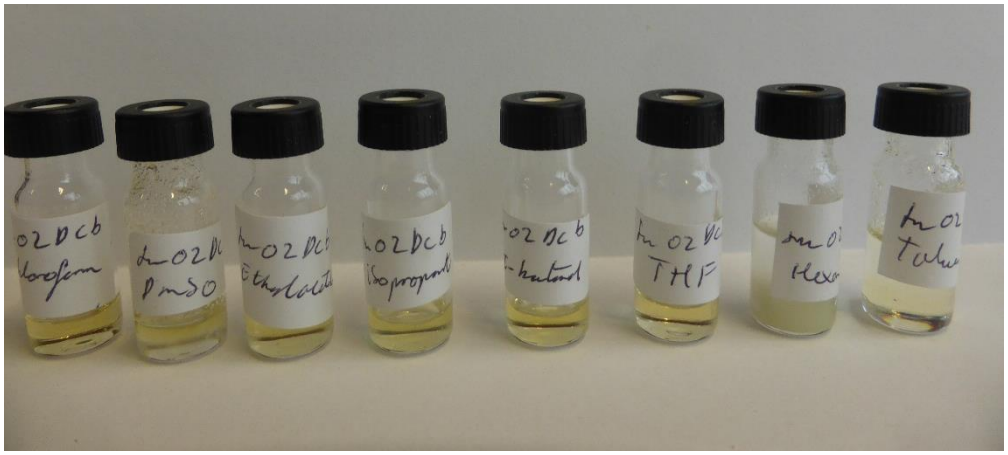

Figure 4-57: Solubility test results for JW02DCb- TBDMS chitosan (4.5 kDa) toluene in reaction. Solvents left to right chloroform, DMSO, ethyl acetate, isopropanol, t-butanol, THF, hexane and toluene.

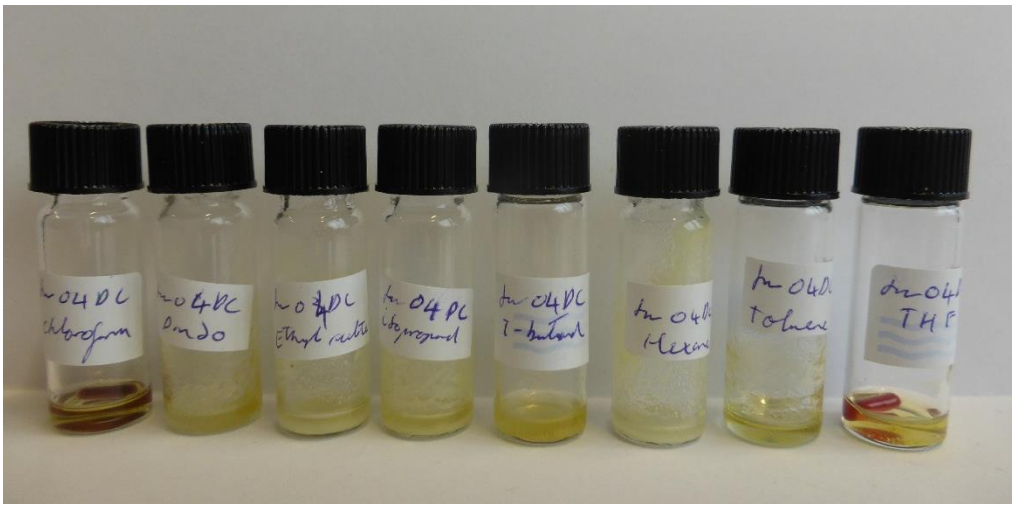

Figure 4-58: Solubility test results for JW04DC- TDS chitosan (~4.5 kDa). Solvents left to right chloroform, DMSO, ethyl acetate, isopropanol, t-butanol, hexane, toluene and THF.

Figure 4-59: Solubility test results for JW02TC -TBDMS-tosyl chitosan. Solvents left to right chloroform, DMSO, ethyl acetate, t-butanol, isopropanol, THF, hexane and toluene.

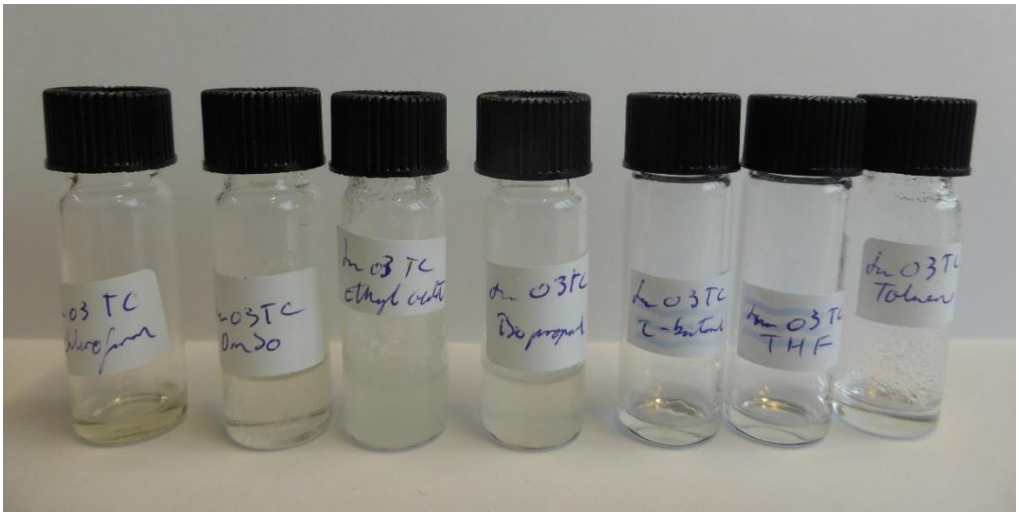

Figure 4-60: Solubility test results for JW03TC -TBDMS amino cellulose. Solvents left to right chloroform, DMSO, ethyl acetate, isopropanol, t-butanol, THF and toluene.

There is also good solubility in THF and reasonable solubility in toluene. However, these are not ideal in terms of sustainability and European regulation. Registration, Evaluation, Authorisation and Restriction of Chemicals (REACH) has now introduced restrictions of the use on toluene (Byrne et al., 2016). In terms of conservation, toluene does not cause as much swelling in wood, which is good, but the due to health effects resulting in increased regulation, it may be an ill-advised choice. THF is not as good

for sustainability but can often be replaced with Me-THF. Solubility in Me-THF should also be investigated in the future. However, isopropanol, t-butanol and ethyl acetate are all better in terms of health impact and flammability, which are key concerns in conservation and are recommended solvents to use in terms of sustainability (Alder et al., 2016; Welton, 2015). Ethyl acetate, isopropanol or t-butanol were always the goal for this project; other solvents were investigated in case the research proves of use to other fields of research in the future.

Degraded chitosan silylated with TDSCl showed similar solubility but with improved solubility in THF and t-butanol. However, this reaction could be repeated with the addition of toluene, similarly the reaction with TBDMS a precipate formed but it did take more time.

Aminocellulose did not share the same success. Mesylated aminocellulose was not sufficiently soluble in DMSO for the silyation step. Therefore, tosyl cellulose was silylated with the aim of replacing the tosyl group with the amine. The tosyl cellulose was incredibly soluble in organic solvents. This could prove very useful in cellulose modifications. However, when it came to the addition of the amine, the solubility decreased which could be due to the amine group or it could be due to the high pH during the reaction which removes some silyl groups. Future work will undertake the silyl addition of the aminocellulose mesylate at a higher temperature. However, lack of solubility could be a problem, and so this was not continued.

TIPSCl (Triisopropylsilyl chloride) could also be researched in the future as TIPS is more acid stable than the TBDMS bonds (Kim, 2013). However, it could be that the

propyl group is not bulky enough for organic solubility. If the solubility is as good as TBDMS chitosan, then maybe this could be used instead for the artefacts.

TBDMS chitosan, which gave the most promising results, was chosen to be scaled up to ~80g to allow for NMR, elemental analysis, solubility tests, followed by molecular weight analysis and was finally followed by wood treatment.

There are several treatment methods to be considered including: soaking vs spraying vs brushing and air-drying vs freeze-drying and the three solvents. Previous conservation investigations using ethyl acetate has shown that ethyl acetate from solvent baths can be recycled (McHale et al., 2016a). Recycling ethyl acetate for silylated chitosan treatment may be possible; this should be investigated to confirm this. Similarly, isopropanol and t-butanol could probably be recycled in the same manner. The advantage of using spraying or brushing is that a reduced solvent volume would be required. However, more solvent may be lost through evaporation than when using an immersion bath, in which the bath solvents could be recycled. Freeze-drying would only be possible with t-butanol and this method would allow the t-butanol to be collected and recycled. Collection of solvent would not be possible in cases of air-drying. Therefore, freeze-drying may pose an advantage. These methods will be compared both in terms of sustainability and conservation at a future stage in this research.

Tert-butanol has previously been used in conservation. It was used with PEG between the 1970s and 1990s but stopped being used in favour of water . However, prior to discontinuation, it was found to have good results. For example, it was used on the

wooden artefacts from the Sinan shipwreck in 1982. The artefacts were immersed in ethanol followed by t-butanol and then PEG 4000 in t-butanol in increasing concentration 10%→20%→30%→40% and then freeze-dried. The ink written on the artefacts was clearly legible after treatment and good results were obtained regardless of tree type or degree of decomposition (Kyushik et al., 2012). However, some thought that the diffusion of PEG into the wood was not as evenly distributed as it was in water and this was one reason some switched to aqueous solutions (Kyushik et al., 2012). An Investigation comparing several methods found that PEG in either t-butanol or water gave better results than glycol methacrylate, TEOS (tetra-ethyl ortho-silicate) and acetone-Rosin methods (Grattan, 1982). However, it was found that t-butanol baths became very dark and the wood became lighter, suggesting dissolution of wood material (Grattan, 1982). The treatments also use heat for high molecular weight PEG which could also potentially damage the wood. The silylated chitosan, however, was fully soluble in t-butanol at room temperature and did not require heating. This would also make it safer to use in terms of health.

4.3.4 TBDMS scale up

The addition of the TBDMS silyl groups successfully aided the dissolution of the chitosan in ethyl acetate and isopropanol. The next step was to see if this could be scaled up and to make at least 60 g of product in total to allow enough material for treatment of artificially degraded wood (laboratory degraded wood), archaeological wood and alum-treated wood if the first two experiments were successful.

The scale up was carried out in the chemistry department at the University of Nottingham. Initially, the reactions were repeated on a small scale to check for consistent results. If successful, the experiments could then be scaled up from 2g to 5g to 10 g and then finally to 20 g to obtain roughly 60 g final product. The NMR of the first successful reaction that was carried out in Jena is given above (Figure 4-48). This included the addition of toluene in the reaction to improve the DS. The reactions carried out in Nottingham followed the same procedure and gave the same NMR results but with slightly different degrees of substitution. Therefore, the DS is included in Table 4-9 but it has been decided not to show all of the NMR spectrums. The final NMR spectra that combined large batches is included below in Figure 4-65a.

Solubility also differed from the original batches. It was also found with a higher DS that although TBDMS chitosan was originally soluble in ethyl acetate it precipitated out with time (see Figure 4-61)

Table 4-9: DS of each batch of TBDMS chitosan.

Batch	**DS**
1	Not pure
2	Not pure
3	2.2
4	2.3
5	2.4
6	2.2
7	2.3
8	2.3
9	2.9
9 after a second wash	2.2

The molecular weight of the final product, the combined batches, is also important to know in order to estimate if the polymer can penetrate the wood fully and to determine if it breaks down during the modification process. AUC used in Chapter 2 is an accurate method for determining molecular weight of a polymer.

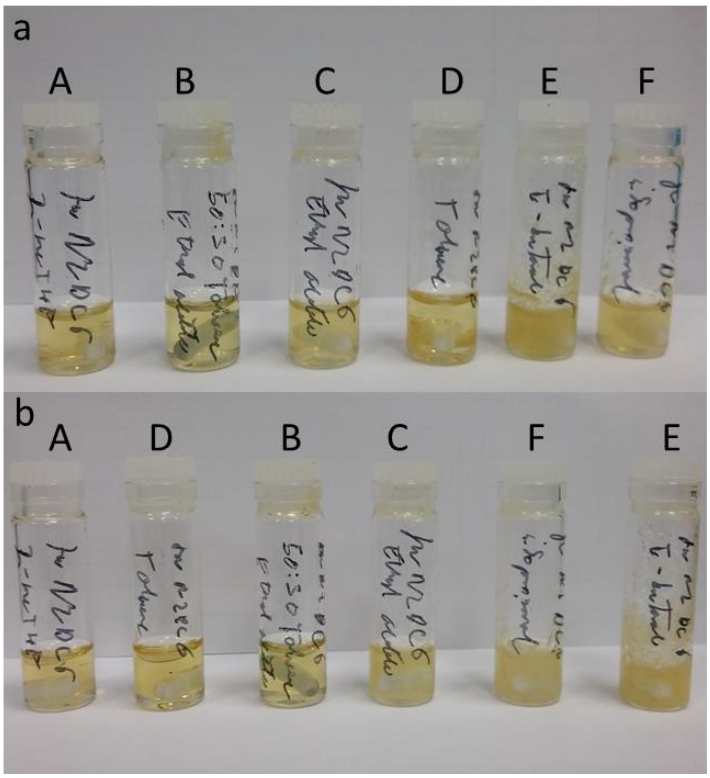

Figure 4-61: Solubility of TBDMS chitosan batch 6 (N2DC6) A) 2-meTHF, B) 50:50 toluene/ethyl acetate, C) ethyl acetate, D) toluene, E) t-butanol, F) isopropanol. a) shortly after the addition of solvents after stirring b) after 3 days

4.3.5 Characterisation of TBDMS chitosan batches NMR, IR.

4.3.5.1 Molecular weight of intermediate

Depolymerisation was previously shown to reduce the molecular weight of kitnor chitosan from M_w of (14.2 ± 1.2) kDa to (4.9 ± 0.7) kDa (Wakefield et al., 2018). This was scaled up in 5 batches of 22 g and was found to produce consistent results; M_w = (5.35±0.70) kDa (Wakefield et al., 2018). These 5 batches were combined before chemically modifying the polymer. From Figure 4-62, it can be seen that the molecular weight of the combined batch is M_w=. (6.2±0.3) kDa. This is an acceptable molecular weight to be used as a starting point to develop conservation material.

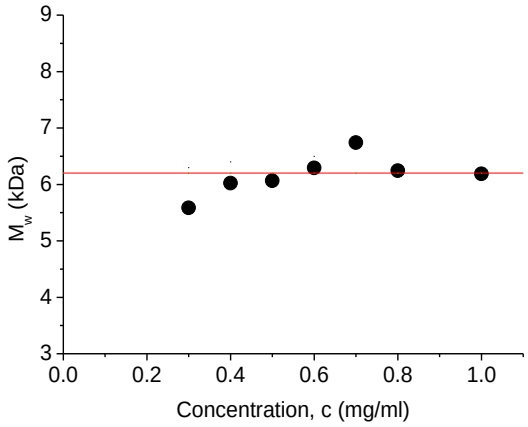

Figure 4-62: Plot of the hinge point $M_{w,app}$ from SEDFIT-MSTAR vs loading concentration, *c* for depolymerised chitosan run at 40000 rpm in acetate buffer. Non-ideality is negligible within the concentration range studied with $M_w \sim M_{w,app}$ = (6.2 ± 0.3) kDa.

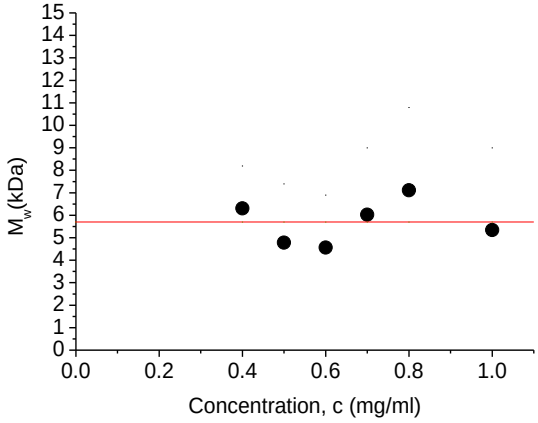

Figure 4-63: Plot of the hinge point $M_{w,app}$ from SEDFIT-MSTAR vs loading concentration, *c* for chitosan mesylate run at 40,000 rpm. Non-ideality is negligible within the concentration range studied with $M_w \sim M_{w,app}$ = (5.7 ± 1.0) kDa.

Song *et al.* (2010) produced a modified chitosan which is soluble in a range of organic solvents. The first step in the modification is to the make the salt form of the chitosan; this involved adding concentrated acid. This usually results in the degradation of the polymer backbone. In this case, the chitosan was suspended in water and the acid was

then added. The molecular weight of this polymer was determined via analytical ultracentrifuge sedimentation equilibrium to establish if it degraded the chitosan and if so, to what extent. SE showed that the molecular weight of chitosan mesylate was (5.7±1.0) kDa (Figure 4-63) using hinge point determination of molecular weight. The MSTAR extrapolation (Figure 4-64) was very steep towards the cell base, suggesting the extrapolation would not be accurate. The theoretical molecular weight, with the addition of the acetate, would be 9.4 kDa based on the molecular weight of chitosan. Thus, a 40% reduction polymer length occurred during the salt formation.

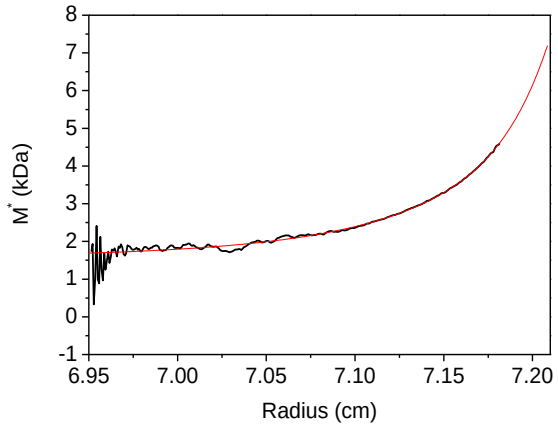

Figure 4-64: Plot of M* from SEDFIT-MSTAR vs radius along the cell for chitosan mesylate run at 35,000 rpm. The steep extrapolation to the cell base suggests that the hinge point analysis is more reliable in this case.

4.3.5.2 Theoretical molecular weight determination

The acid treatment step is a concern in terms of changing the molecular weight, but the silylation is not anticipated to degrade the backbone.

The molecular weight of the modified chitosan can therefore be predicted from the degree of substitution from the NMR DS=2.3 (Figure 4-65). This is combined with the

molecular weight of the precursors to determine polymer length (chitosan point average molecular weight =6.2 kDa (Figure 4-62) average n=37.5, chitosan mesylate point average molecular weight 5.7 kDa (Figure 4-63) average n=22.6) this gives a theoretical molecular weight of 9.7 kDa for the TBDMS chitosan.

The molecular weight of the final product could not be analysed via AUC as the buoyancy of the polymer meant that the polymer did not sediment in some solvents and other solvents were not compatible with the AUC cells.

The degree of substitution is the ratio of NMR integral of H2, H3, H4, H5, H6 and H6' divided by either set of hydrogens from the butyl groups of TBDMS chitosan, taking into account the number of protons. DS for TBDMS = ([$(CH_3)_3$]/[H-2-H-6'])x (6/9) (Rúnarsson et al., 2008a). This gave a DS of 2.3.

$$DP = Mw\ of\ chitosan\ mesylate / monomer\ Mw\ chitosan\ mesylate \quad \textbf{6-1}$$

$$Mw\ TBDMS\ chitosan\ DS2.3 = DP\ x \text{ monomer } Mw\ TBDMS\ chitosan\ DS2.3 \quad \textbf{6-2}$$

This gives a molecular weight of TBDMS chitosan (DS 2.3) of 9.7 kDa.

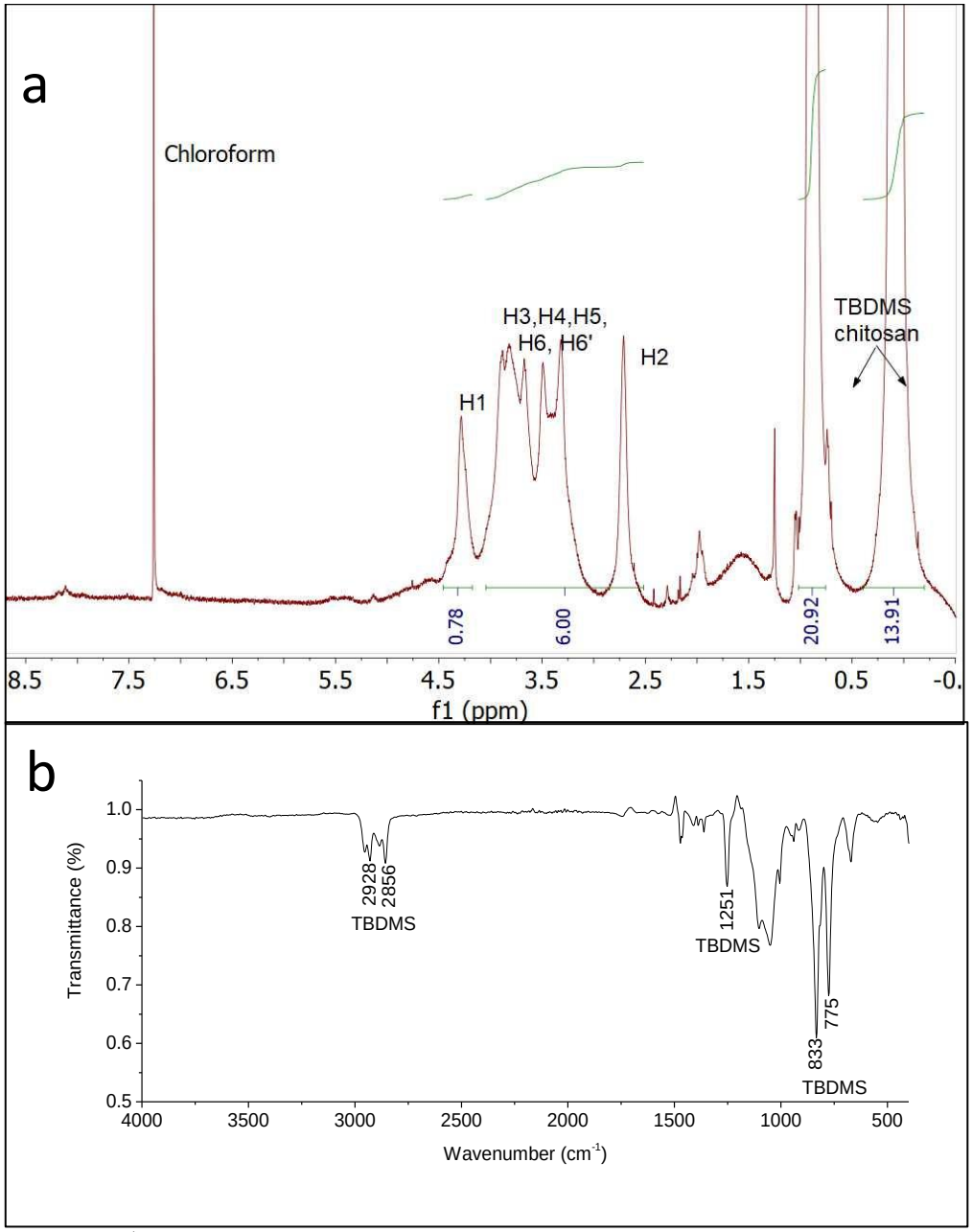

Figure 4-65: a) ^{1}H NMR of Di-TBDMS chitosan in $CDCl_3$; integrals shows a DS 2.3. b) IR spectrum of Di-TBDMS chitosan.

1.1.1 Potential of Di-TBDMS chitosan for wood conservation

The solubility of TBDMS chitosan in different solvents was assessed and TBDMS chitosan was found to start to precipitate in some solvents over time.

Solubility in a mixture of toluene and ethyl acetate (Figure 4-66) would allow for archaeological wood application of TBDMS chitosan. Toluene has previously been used for wood conservation and has been found to cause less swelling in wood than polar solvents (Mantanis et al., 1994). However, the solution would be very viscous, preventing the material entering the cell wall. Ethyl acetate has started to be investigated for wood conservation (McHale et al., 2016b); in terms of sustainability and wood swelling it is preferable to many other solvents. Adjusting the exact DS of TBDMS may allow ethyl acetate to be used alone.

Figure 4-66: Solubility and viscosity of TBDMS chitosan in toluene and ethyl acetate vs toluene alone.

Chitosan nitrogen group is key to its chelation properties and its ability to neutralise acid. The nitrogen group has been maintained with this modification. Ester groups have also been avoided, as they are sensitive to acid. Calcium hydroxide nanoparticles could possibility be combined with this treatment to increase the pH of the wood (Andriulo et al., 2018) . This would help prevent future degradation of the wood and TBDMS chitosan over time. Further research is required to determine if the modified chitosan retains some chelation properties. For waterlogged wood EDMA, EDTA and DTPA are chelating agents used to remove metal ions. This is done by binding to the metal ions and then washing them out (Sandström et al., 2003). This helps limits the quantity of iron ions in the wood. Thus, limits catalysis of hydrolysis and the breakdown of cellulose. In dry wood, options are limited; poultice can be used to help

draw out some of the iron ions. TBDMS chitosan is anticipated to help chelate iron ions which would prevent ions migrating through the wood and maybe limit its involvement in catalysis.

4.4 Conclusion

4.4.1 Conclusions of reductive amination and click chemistry

Chitosan has plenty of desirable properties for conservation: it is non-toxic, anti-fungal, inexpensive, sustainable and chelates metal ions. However, the chelation ability is not strong. Pure chitosan is too large to penetrate wood effectively and chitosan is not organic soluble (which is necessary to prevent alum leaching, which is in turn essential as alum maintains the structure). The chitosan was found to have a molecular weight of ~1400 kDa, which will very likely be too large to penetrate the wood and too large to be easily made organic soluble. The addition of aromatic groups and alkyne groups via reductive amination also proved successful. However, the addition of these groups was not sufficient to make the polymer organic soluble. A long alkyl chain, or shorter chitosan oligomers, may be required as starting material to make the polymer organic soluble. The addition of a triazole ring and an aromatic group to improve chelation, anti-fungal properties and solubility in organic solvents was not successful. This could have been due to the solubility of the alkyne chitosan in the reaction, or the cross linking prior to the start of the reaction. Chitosan was depolymerised in Chapter 2 using hydrogen peroxide and UV light in the presence of acetic acid to reduce the molecular weight to ~5 kDa. This lower molecular weight was used for the addition of tert-butyldimethyl silyl via a method by Rúnarsson et al.,

(2008). Another option to make chitosan organic solutble may be sulphur fluoride exchange (SuFEx) reactions which is another form of click chemistry (Dong et al., 2014).

4.4.2 Conclusion of silylation

The Oseberg artefacts, previously treated in 1905, now desperately need re-treatment if they are to survive for future generations to see. The previous alum treatment means some objects could not cope with a water-based treatment due to complete loss of cellulose resulting in very weak wood and, due to the fact alum is greatly supporting the wood in some pieces, therefore its removal could cause more damage. This means water soluble and organic soluble treatment options are required. PEG is not an ideal option due to iron corrosion, acid degradation, acidic breakdown product and sustainability. In terms of organic soluble options, current treatment options are limited and none are sustainable. They have conservation concerns linked to colour changes, UV stability and acid stability. Recent conservation investigations into chitosan have led into this being the focus of this investigation. AUC analysis (Chapter 2) has found that the chitosan previously investigated by Christensen et al. (2015b) had an average weight molecular weight of ~14 kDa. The distribution lies between 3-22 kDa. The higher end of this distribution a cause of concern regarding wood penetration; the molecular weight was reduced using UV light and hydrogen peroxide in aqueous acetic acid to ~5 kDa (Chapter 2). This molecular weight seems more feasible for solubility and for penetration into the wood. Chemical modification to make it water soluble through reductive amination was not successful. However, aminocellulose is water soluble and has a similar structure, molecular weight (monomeric molecular weight

~5 kDa) and has the advantage of self-association which could give the wood extra strength without the need for a cross linker. This could be used alone or in conjunction with a second polymer such as PEG, PEI or a second natural polymer. Degraded chitosan was successfully made organic soluble with the addition of TBDMS. However, the addition of toluene was needed to increase the DS to a level at which solubility was acceptable. Solubility in these three solvents is of particular interest for conservation, isopropanol, ethyl acetate and *tert*-butanol. Aminocellulose was also investigated for organic solubility but, as yet, has not been successful. Therefore, future work will focus on aminocellulose as a water-soluble treatment option and chitosan as the organic treatment. Having these two options is important to avoid the use of solvents where it is not necessary. It also allows alum to be retained in the most fragile artefacts where its removal is likely to cause more harm than good. The work, so far, shows real promise of finding a suitable consolidant for these very precious artefacts.

The solubility of TBDMS chitosan in toluene and ethyl acetate would allow for chitosan to be used as a non-aqueous treatment method for alum-treated wood. Aqueous treatments, though favourable in terms of sustainability, flammability and toxicity, would cause disintegration of the most fragile artefacts in the Oseberg collection and are therefore not an option for the most fragile subset of artefacts. Non-polar solvents are less likely to cause swelling of the artefacts and would protect the intricate carvings on the artefacts. The low molecular weight of the TBDMS chitosan produced is small enough to fully penetrate the wood cells.

4.5 Methods

4.5.1 Chemicals and Equipment

- Chitosan -Kitonor ANT 03.02.2015
- Aminocellulose AEA and HEA supplied by Thomas Heinze Jena University

To calaculate the equilivalents of reactants for reactions, the monomeric molar mass was used for the polymers chitosan and aminocellulose.

For degradation of chitosan

- Chitosan Kitonor ANT received 03.02.2015
- Acetic acid –Sigma Aldrich CAS 64-19-7 lot SZBC2360V
- 30% hydrogen peroxide –Sigma Aldrich
- Sodium hydroxide-Fisher
- Water-reverse osmosis water
- UV lamp – low intensity mercury UV lamp

For chemicals modification

- Thexyldimethylchlorosilane (TDSCl)-ABCR lot 1219662 CAS 67373-56-2
- 3,4-dihydroxylbenzaldehyde Sigma Aldrich lot mkbj6390v
- Methanesulfonic acid Acros organics lot A019837101 CAS 75-75-2
- t-butyldimethyl chlorosilane (TBDMSCl) ABCR lot 1009164 CAS
- 6-Desoxy-6-(-2-amino ethyl) aminocellulose –Robert Hampe DS=0.59 2% in water
- Toluene Extra dry Acrosseal Acros organics lot 1142900- seal old.
- NMR choloroform-d^1 lot B12472 Deutero Gmbh
- Acetic acid -Analak Normapar
- Ethylene diamine –Fluka lot BCBJ5732V
- Potasium carbonate -GRP Rectapor VWR prolab, product: 62724291, batch: 130180018
- Propargyl bromide solution-80% wt in toluene stabilized Acros organics code 131480500, Lot: A0343181, Cas:106-96-7
- Triethylamine-Fisher Code: T/3200/08, lot: 1668199, cas:121-44-8

- 4-methylbenzylamine -Acros organics-lot: A0212123, CAS:104-84-7
- Terrt-butylnitrite-fluka lot BCBG7028V, CAS: 540-80-7
- p-toluidine-Alfa Aesar lot: 10125711 CAS:106-49-0
- Solvents –Sigma Aldrich

Equipment

Jenna NMR

- 250 MHz, Avance I, BBO, BACS, 60x
- 400MHz, Avance III, BBFO, BACS, 60x

Nottingham NMR

- NMR Brüker 250, 400Hz and 600Hz

4.5.2 Degradation of chitosan (Described in Chapter 2)

The degradation of chitosan was based on work by (Wang et al., 2005).

X g chitosan was dissolved in y ml 2% acetic acid and stirred for 1 h to produce a 4% chitosan in total. y ml 4% hydrogen peroxide then added and stirred for 1 h under UV light at rt=25 °C. Total 2% chitosan, 1% acetic acid and 2% hydrogen peroxide. Surface area to volume ratio was kept to ~ 0.38. Yield 65-78%.

4.5.3 Reductive amination

4.5.3.1 Reductive amination of chitosan using sodium cyanoborohydride

This method was based on literature methodology (Jatunov *et al*., 2012; Kurita and Isogai, 2010; Nikmawahda *et al*., 2015). Figure 4-67 shows the reaction and a detailed reaction with the mechanism can be found in appendix 1.

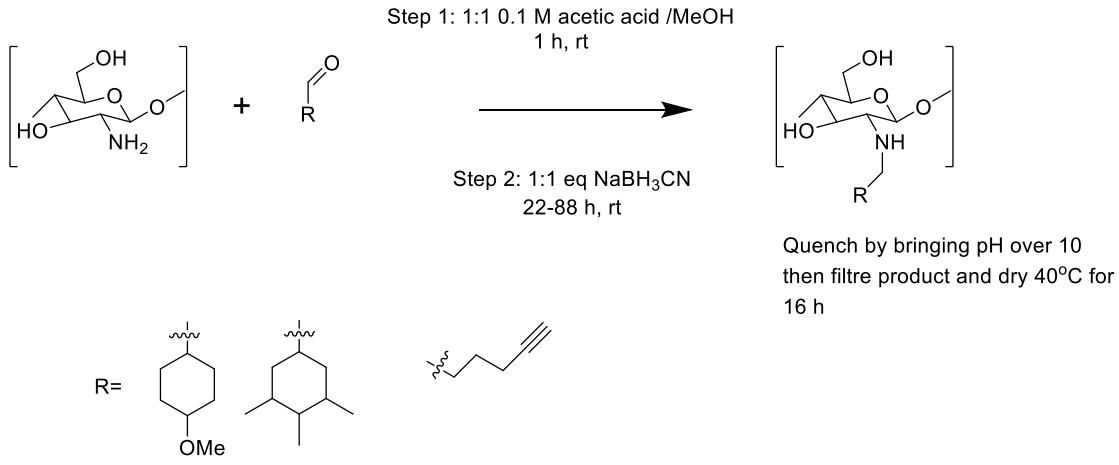

Figure 4-67: Reaction scheme for reductive amination of chitosan

4.5.3.2 Reductive amination General Procedure

4.5.3.2.1 Generalised Procedure

1eq of polymer was disolved in water (25 ml) (adjusted to pH5 or 0.1 M acetic acid); then methanol (25 ml) added. 1eq of benzaldehyde was added and stirred for 1 h at rt (22 ^{o}C); this formed the imine. 1eq cyanoborohydride was then added to reduce this and the reaction was stirred for 24 h. The pH was then adjusted to 10 using 1 M NaOH.

The precipitate was then washed using a magnetic stirrer in H_2O (50 ml), acetone (30 ml), H_2O (50 ml) and acetone (30 ml). The product was dried in a 40 ^oC vacuum oven. The filtrate and all glassware were treated with bleach to remove any trace of HCN. Solid state NMR was required. The product was insoluble in water and organic solvents.

4.5.3.2.2 Reductive amination of depolymerised chitosan with dihydroxybenzaldehyde (JW03DC)

Degraded chitosan (0.500 g) was dissolved in 0.1 M acetic acid (25 ml); then methanol (25 ml) was added. Next dihydroxybenzaldehyde (0.418 g, mmol) was added and stirred for 1 h at rt (22 ^oC); this forms the imine. The cyanoborohydride (0.189 g, mmol) was then added to reduce this and the reaction was stirred for 24h. The pH was then adjusted to 10 using 1 M NaOH. The precipitate was then washed, using a magnetic stirrer in H_2O (50 ml), acetone (30 ml), H_2O (50 ml) and acetone (30 ml). The product was dried in a 40 ^oC vacuum oven. The product collected was 0.651 g. The filtrate and all glassware were treated with bleach to remove any trace of HCN.

4.5.3.2.3 Reductive amination of aminocellulose with benzaldehyde (JW03A).

2% Aminocellulose (25 ml) was diluted in methanol (25 ml). The pH was then adjusted to 5 (the ideal pH for imine formation) using 2 M acetic acid. Dihydroxybenzaldehyde (0.370 g) was added and this was stirred for 1 h at rt (22 ^oC); this forms the imine. The cyanoborohydride (0.169 g) is then added to reduce this and the reaction is stirred for 24 h. The pH was then adjusted to 10 using 1M NaOH. The precipitate was then washed with stirred using a magnetic stirrer in H_2O (50 ml), acetone (30 ml), H_2O (20

ml) and acetone (40 ml). The product was dried in a 40 ^{o}C vacuum oven. The product weighed 0.661 g. The filtrate and all glassware were treated with bleach to remove any trace of HCN.

4.5.3.2.4 Reductive amination of chitosan with 4-methoxybezaldehyde

Chitosan (500 mg, 3.10 mmol) was dissolved in 0.1 M acetic acid (25 ml) in a round bottom flask, methanol (25 ml) and 4-methoxybezaldehyde (0.33 ml, 2.71 mmol) were added then stirred for 1 h with a magnetic stirrer at room temperature with a septum stopper on the round bottom flask. Afterwards, sodium cyanoborohydride (172 mg, 2.74 mmol) was added and a syringe needle added to the septum to release any gas that had formed but prevent entry of dust. This was left for 22 h at room temperature. Then pH was brought from 8 to 10 using 1 M NaOH added dropwise. The solution was then filtered and washed with deionised water with a few drops of 1 M NaOH to prevent the chitosan dissolving. The precipitate was then dried at 60 ^{o}C in a pre-weighed vial. The filtrate was quenched with a few ml of NaOCl (bleach) in deionised water and disposed of. The product weighed 0.7124 g.

Without the exact degree of substitution, it is impossible to determine a yield.

4.5.3.2.5 Reductive amination of chitosan with 2,4,6 trimethyl benzaldehyde

Chitosan (500 mg, 3.10 mmol) was dissolved in 0.1M acetic acid (25 ml) in around bottom flask, methanol (25 ml) and 2,4,6 trimethylbenzaldehyde (Mesitaldehyde) (0.4 ml, 2.71 mmol) were added and then stirred for 30 min with a magnetic stirrer at room temperature with a septum stopper on the round bottom flask. After sodium

cyanoborohydride (172 mg, 2.74 mmol) was added and a syringe needle was added to the septum to release any gas formed but prevent the entry of dust. This was left for 88 h at room temperature. The pH was brought from 8 to 10 using 1M NaOH added dropwise and the pH measured using universal pH paper and the solution was filtered and washed with deionised water with a few drops of 1 M NaOH to prevent the chitosan from dissolving. The precipitate was then dried at 60 ^{o}C in a pre-weighed vial. The filtrate was quenched with a few ml of NaOCl (bleach) in deionised water and disposed of. The product weighed 0.50884 g.

4.5.3.2.6 Reductive amination of chitosan with 4-pentynal (produced via the swern reaction from 4-pentyn-1-ol; see swern reaction below)

Carried out once using the same method as above, but scaled up to chitosan (1000 mg, 6.21 mmol) and 4-pentynal (0.5 ml) stirred for 85 h. This is because after 24 h no precipitate was observed. Precipitation had formed quickly with previous reactions. After 85 h some precipitate was visible and once quenched with NaOH more was formed. The product weighed 1.16031 g.

This was repeated with chitosan (1000 mg), but only half of the 4-pentynal (0.25 ml), with the intention of producing chitosan with 40-50 substitution. No precipitate was observed; precipitate had quickly formed with previous reactions. After 88 h, some precipitate was visible and more once quenched with NaOH. The product weighed 0.97564 g.

4.5.4 Halide alkylation

4.5.4.1 Halide alkylation of chitosan using propargyl bromide

This method was based on methodology by Gordon *et al*. (2000). Figure 4-68 shows the reaction and a detailed reaction can be found in appendix 1.

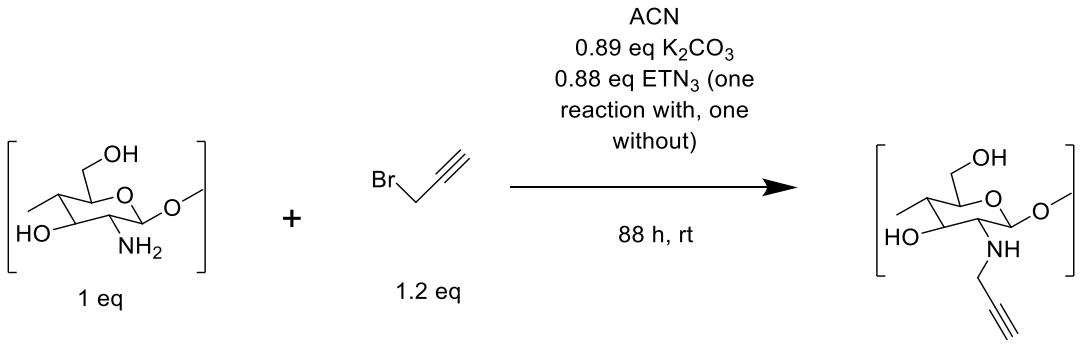

Figure 4-68: Reaction scheme for halide alkylation of chitosan with propargyl bromide. Reaction was proven unsuccessful by NMR.

4.5.4.1.1 Halide alkylation of chitosan using propargyl bromide

To chitosan (500 mg, 3.10 mmol), ACN (20 ml) and K_2CO_3 (380 mg, 2.75 mmol) was added followed by the addition of triethylamine (0.38 ml, 2.73 mmol), then propargyl bromide (0.4 ml, 3.71 mmol) and was stirred with a magnetic stirrer for 88 h at room temperature. The filtered precipitate was washed with 50 ml ACN and then 50 ml deionised H_2O. H_2O also quenches the filtrate. The precipitate is collected in a pre-weighted vial and dried at 60 ^oC. The product weighed 0.3982 g. The filtrate is mixed with ethyl acetate (50 ml) and the aqueous and organic phases were separated for separate disposal.

The same experiment as above was repeated without the triethylamine.

4.5.5 Oxidation (Swern reaction)

The oxidation of 4-pentyn-1-ol to pentynal method followed the methodology by Phillips *et al*. (2015).

Figure 4-69 shows the reaction.

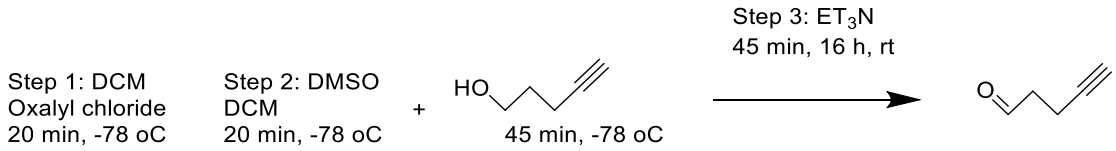

Figure 4-69: Reaction scheme for oxidation (swern reaction) of 4-pentyn-1-ol

4.5.5.1.1 Oxidation of 4-pentyn-1-ol to pentynal

Oxalyl chloride (2 ml, 23.6 mmol) and 46 ml DCM were added, then DMSO (3.1 ml) and DCM (8.8 ml) were added slowly over 20 min then stirred for 20 min under argon at -78 ^{o}C. 4-Pentyn-1-ol (1.8 ml, 19.3 mmol) was added over 10 min and was stirred for 45 min. After Et_3N (13.5 ml, 96.9 mmol) was added over 5 min then left for 45 min. Then it was slowly brought up to room temp then left overnight for 16 h. H_2O (50 ml) was added to quench the remaining oxalyl chloride. The layers were separated and the aqueous layer acidified to a pH of 3 with 1M HCl (~40 ml) added slowly and then extracted with DCM. The organic layers combined and was washed with 1% HCl (50 ml) with NaCl. The organic layer was then washed with sat $NaHCO_3$ (50 ml), followed by H_2O (3x15 ml) and then sat NaCl (50 ml). The organic layer was dried

over $MgSO_4$ and then dried on the rotary evaporator. Product (0.2016 g) NMR showed plenty of contamination from side products. It is thought this was due to the solvents not having been dried first. For this reason, the experiment was repeated but with glassware and solvents dried. It would have been difficult to purify the product, thefore reaction was repeated.

The Oxalyl chloride (2.5 ml, 29.5 mmol) was dissolved in freshly distilled DCM (60 ml), held under argon at -78 ^oC. DMSO (3.9 ml) and (11 ml DCM freshly distilled) were added over 15 min and the reaction was stirred for 30 min. 4-pentyn-1-ol (2.1 ml, 22.6 mmol) was mixed with DCM (5 ml) then added over 10 min and stirred for 50 min. Dried Et_3N (17 ml, 122.0 mmol) was then added over 5 min and stirred for 1 h. The reaction was then brought to room temperature and stirred for 16 h. Deionised H_2O (50 ml) was then added to quench any remaining oxalyl chloride. Layers then separated and aqueous layer acidified with 1M HCl to pH 2. The aqueous layer was then extracted with DCM (2x25 ml). The organic layers were then combined and washed with sat NaCl (50 ml) in 1% HCl. The organic layer was then washed with sat $NaHCO_3$ then with deionised H_2O (3x15 ml) and then sat NaCl (50 ml). The organic layer was then dried over $MgSO_4$ and concentrated on a rotary evaporator. Product 1.2051 g. The NMR showed some DCM was left. The solution for NMR was poured back in and condensed again on rotary evaporator and then the high vac for 1.5 h yield over 100% hence must be some remaining DCM or chloroform placed on the high vac for another 40 min. Some product lost which resulted in 65% yield. The NMR showed some DCM still remained but at the risk of losing more product it was decided to carry on the next reaction as it was.

4.5.6 Azide formation from amines

This method followed the method by Barral *et al*. (2007). Figure 4-70 shows the reaction and a detailed reaction can be found in appendix 1.

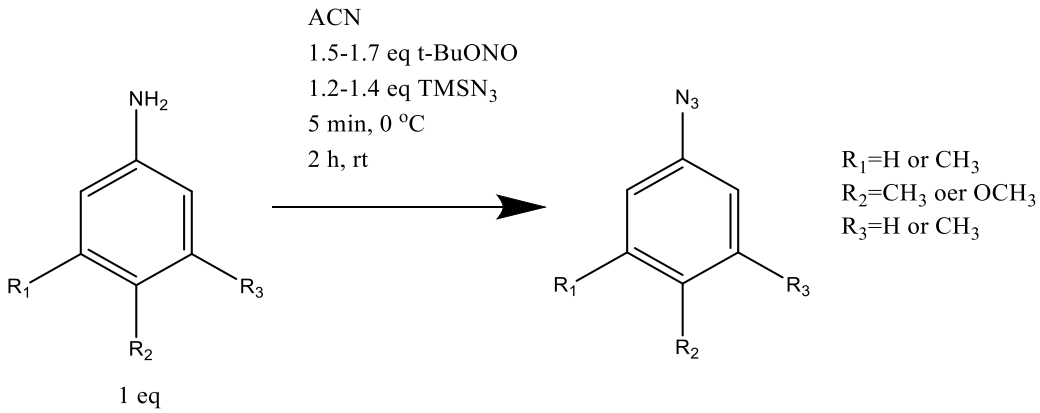

Figure 4-70: Reaction scheme for azide formation from amines.

4.5.6.1.1 1-azido-4methoxybenzene from 4-methoxybenzylamine

4-Methoxybenzylamine (200 mg, 1.46 mmol) was added to ACN (2 ml) which was cooled to 0 ^{O}C; then t-BuONO (290 µl, 2.43 mmol) and $TMSN_3$ (260 µl, 1.98 mmol) were added. The reaction was then warmed to rt and stirred for 2 h. TLC still showed some starting material but, due to time constraints, the reaction was worked up anyway. The mixture was concentrated and the products were separated on a silica column. The column was run with petroleum spirit then mixed with ethyl acetaste to produce 5, 7.5, 10, 15 and 20% ethyl acetate (in future heptane should be tried instead). The fractions were then checked using TLC to look for the product. The fractions were then combined and the solvent removed on the rotary evaporator. The product weighed 0.1333 g (0.894 mmol) with a yield of 61.23%.

4.5.6.1.2 1-azido-4methylbenzene from 4-methylbenzylamine

4-Methybenzylamine (228 mg, 2.13 mmol) was added to ACN (2 ml) which was then cooled to 0 ^{O}C, then t-BuONO (381 µl, 3.19 mmol) and $TMSN_3$ (336 µl, 2.55 mmol) added. The reaction was then warmed to room temp and stirred for 2 h. The mixture was then concentrated and products separated on a silica column. The column was run with petroleum spirit. The fractions were then checked using TLC to look for the product. The fractions were then combined, and the solvent removed on a rotary evaporator. The product weighed 0.221 g (1.66 mmol) with a yield 77.93%.

4.5.6.1.3 1-azido-3,5-dimethylbenzene from 3,5- dimethylbenzylamine

3,5- Dimethylbenzylamine (210 µl, 1.68 mmol) was added to ACN (2 ml) then cooled to 0 ^{O}C then t-BuONO (301 µl, 2.52 mmol) and $TMSN_3$ (265 µl, 2.02 mmol) added. The reaction was then warmed to room temperature and stirred for 1.5 h. The mixture was concentrated and products separated on a silica column. The column was run with petroleum spirit. The fractions were then checked using TLC to look for the product. The fractions were then combined and the solvent removed on the rotary evaporator. The product weighed 0.246 g (1.67 mmol) with a yield of 99.40%.

4.5.7 Click reaction (in this case cycloaddition of azides and alkynes to give triazoles via the Huisgen 1,3-dipolar cycloaddition)

The method was based on methodology by Sarwar *et al*. (2015). Figure 4-71 shows the reaction.

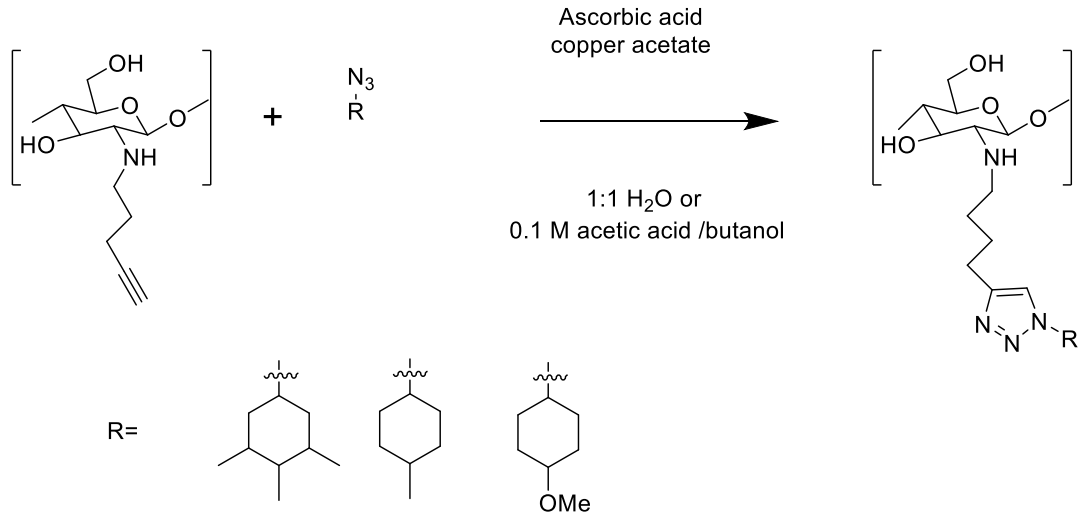

Figure 4-71: Reaction scheme for click chemistry reaction.

4.5.7.1.1 Addition of 1-azido-3-5-dimethylbenzene

Chitosan (200 mg, 0.957 mmol, 1 eq) was stirrer with sodium ascorbate (235 mg, 0.680 mmol,0.711 eq), copper acetate hydrate (96 mg, 0.478 mmol, 0.5 eq) and H_2O (10 ml), added to this was 1-azido-3-5-dimethylbenzene (142 mg, 0.957 mmol, 1 eq) with *tert*-butanol (5 ml). This was then stirred for 19 h, after which the product was collected by filtration and was washed with EDTA (0.1M Diaminoethanetetra acetic acid disodium salt solution) (4x10 ml), followed by methanol (2x20 ml). The product was then air dried for 3 h followed by vacuum drying for 2 h. The product weighed 0.4255 g.

4.5.7.1.2 Addition of 1-azido-3-5-dimethylbenzene

Chitosan (100 mg, 0.478 mmol) was stirrer with sodium ascorbate (67 mg, 0.338 mmol), copper acetate hydrate (48 mg, 0.240 mmol) and H_2O (5 ml) added to this was 1-azido-3-5-dimethylbenzene with *tert*-butanol (5 ml). This was then stirred for 19 h after which the product was collected by filtration and was washed with EDTA (0.1 M Diaminoethanetetra acetic acid disodium salt solution) (4x10 ml), followed by methanol (2x20 ml). The product weighed 0.426 g, yield N/A

0.1 M acetic acid was used instead of water for the second reaction, as there was a concern about the lack of solubility of the modified chitosan which may lead to reduced contact surface area and hence reduced substitution.

4.5.8 Silylation

4.5.8.1 Mesylate salt of chitosan/ aminocellulose

The silylation follows the methodology of Rúnarsson et al. (2008) and Song et al. (2010). The first step is mesylate salt formation; the reaction scheme is given in Figure 4-72. These reactions (JW01C JW01DC) differ from the of Rúnarsson et al. (2008) and Song et al. (2010) methodology as chitosan was suspened in water prior to the addition methanesulfonic acid. Experiment JW0A follows the same methodology but with aminocellulose 1 (AEA) see Figure 4-73.

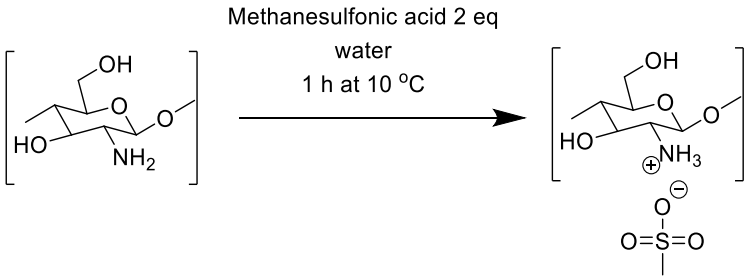

Figure 4-72: Reaction to form mesylate of chitosan

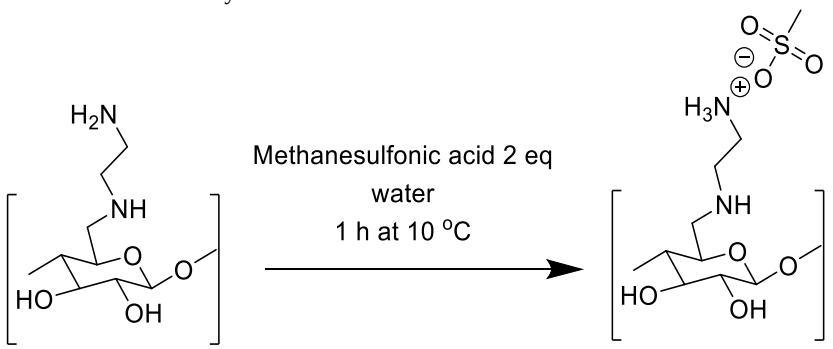

Figure 4-73: Reaction to form mesylate of aminocellulose

4.5.8.2 Protocol to form mesylate

Polymer 1eq (see Figure 4-72 and Figure 4-73) was stirred with a magnetic stirrer in 10 ml deionised water in a 10 °C water bath, forming a heterogenous mixture. Methanesulfonic acid 2 eq was then added dropwise: this formed a gel. The solution was then stirred for 1h at 10 °C with the viscosity slowly reducing. This solution was then very slowly poured into 70 ml ethanol and stirred with a magnetic stirrer. This was then filtered through a sinter funnel (centrifuge was needed in one case to collect all the product) and washed with 2x 30 ml ethanol, isopropanol or acetone (depending which it precipitated best in tested in a test tube) then 1x 30 ml acetone. The precipitate was then air-dried for 1 h and re-dissolved in 10 ml water and re-precipitated in 70 ml acetone. It was washed with acetone (30 ml). The product was air-dried for 1 h and then placed in a vacuum oven overnight.

4.5.8.2.1 Mesylate salt of chitosan

To chitosan ~16000 Da (161 g/mol (monomeric molar mass), 1.000 g, 6.21 mmol) deionised water (10 ml) was added and stirred with a magnetic stirrer in a 10 ^{o}C water bath, forming a heterogenous mixture. Methanesulfonic acid (96.11 g/mole, 1.48 ml, 12.41 mmol, 2 equimolar) was then added dropwise; this formed a gel. The solution was then stirred for 1 h at 10 ^{o}C with the viscosity slowly reducing. This solution was then very slowly poured into ethanol (50 ml) and stirred with a magnetic stirrer. Ethanol (20 ml) was used to help transfer remaining precipitant from beaker and rb flask. This was then filtered through a sinter funnel and washed with ethanol (2x 30 ml) then acetone (1x 30 ml). The precipitate was then air-dried for 1 h and re-dissolved in 10ml water and re-precipitated in acetone (50 ml) transferred with acetone (20 ml). This precipitant was placed in a beaker and washed with acetone (30 ml). This was then filtered and placed in a pre-weighed vial then air-dried for 1h and then placed in a vacumm oven overnight. Resulting in (gfm 242 g/mol 1.265 g, 5.23 mmol) 84.2% yield. Some product lost on transfer.

4.5.8.2.2 Mesylate salt of chitosan degraded polymer batch 1

Chitosan ~5000 Da (161 g/mole, 0.500 g, 3.1 mmol) was stirred with deionised water (5 ml) with a magnetic stirrer at 10 ^{o}C water bath, forming a heterogenous mixture. Methanesulfonic acid (96.11 g/mole, 0.74 ml, 6.2 mmol, 4 equimolar equivalents) was then added dropwise. The solution was then stirred for 1h at 10 ^{o}C with the viscosity slowly reducing. This solution was then very slowly poured into ethanol (30 ml) and residue from rb flask transferred with isopropanol (40 ml) stirred with a magnetic

stirrer (repeated experiments should be with isopropanol). This was then filtered through a sinter funnel and washed with isopropanol (2x 30 ml) then acetone (1x 30ml). The precipitate was then air-dried for 1 h and re-dissolved in water (3.0 ml) and re-precipitated in acetone (30 ml) transferred with acetone (20 ml). This was filtered and the precipitant placed in a beaker and washed with acetone (30 ml). This was then filtered placed in a pre-weighed vial then air-dried for 1 h and then placed in a vacuum oven overnight, resulting in 0.585 g, 2.42 mmol 78% yield. Some product lost on transfer and isopropanol would be a better precipitant.

JW01DC Yield **,** NMR H^1 N-Ac 2.06, mesylate 2.80, chitosan 3.21, 3.75, 3.90 and 4,87 ppm.

4.5.8.2.3 Mesylate salt of chitosan degraded polymer batch 2

Chitosan ~5000 Da (165.2 g/mole including 0.1 DA, 1.000 g, 6.05 mmol) was stirred with deionised water (5 ml) with a magnetic stirrer at 10 ^{o}C water bath, forming a heterogenous mixture. Methanesulfonic acid (96.11 g/mole, 0.80 ml, 6.2 mmol, 2 equimolar equivalents) was then added dropwise. The solution was then stirred for 1 h at 10 ^{o}C with the viscosity slowly reducing. (The solution was not completely clear so Methanesulfonic acid (96.11 g/mole, 0.80 ml, 6.2 mmol, 2 equimolar equivalents) was then added dropwise.) The product was precipitated in isopropanol (60 ml). This was then filtered through a sinter funnel but some went though the filter so a centrifuge was used the collect the product and washed with isopropanol (2x 30 ml) then acetone (1x 30 ml). The precipitate was then air-dried for 30 min and re-dissolved in water (5.0 ml) and re-precipitated in acetone (40 ml). The precipitate was washed with acetone

(30ml). The product was air-dried overnight then placed in a 40 vacuum oven weighted periodically until the weight remained constant, resulting in 1.155 g.

4.5.8.2.4 Mesylate salt of aminocellulose

Aminocellulose (50 ml 2%, 165.2 g/mole including 0.59DS, 1.000 g, mmol) was stirred with a magnetic stirrer in 100 ml rb flask, 0.1M Methanesulfonic acid was added drop wise till pH 7; this was left for 1h, pH adjusted to 7 again with pH paper. This was then reduced on the rotary evaporator to roughly 10 ml then more acid was added to make it 1.25 excess. Total Methanesulfonic acid (96.11 g/mole, 0.80 ml, 6.2 mmol, 2 equimolar equivalents) was then added dropwise. The solution was then stirred for 1 h at 10 ^{o}C with the viscosity slowly reducing. (The solution was not completely clear so Methanesulfonic acid (96.11 g/mole, ml, mmol, 1.25 equimolar equivalents). The product was precipitated in 60 ml acetone. The precipitate was redisolved in water (15 ml) and re-precipitate in acetone (60 ml) then washed with acetone (40 ml). The producted was then re-dissolved in water (20 ml). Followed by precipitatation in acetonitrile (120 ml), washed with isopropanol (30 ml) then washed acetone (2x 30 ml). Dried in 40 ^{o}C oven weighted periodically until the weight remained constant. Resulting in 0.649 g of product.

JW01A – Not analysable due to poor solubility

4.5.8.3 3.5ii Silylation of chitosan / tosyl cellulose

The silylation follows the methodology of Rúnarsson et al. (2008) and Song et al. (2010). The reaction scheme for reaction with chitosan mesylate is given in Figure 4-74. The reaction scheme with tosyl cellulose is given in Figure 4-75

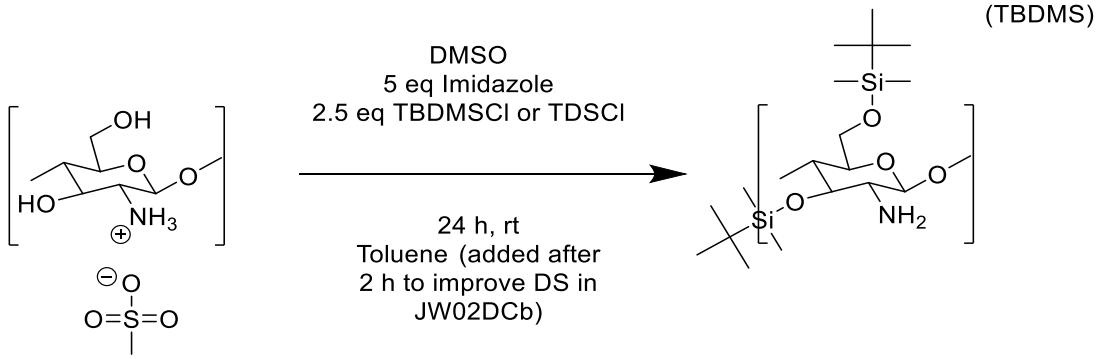

Figure 4-74:Silylation of chitosan mesylate

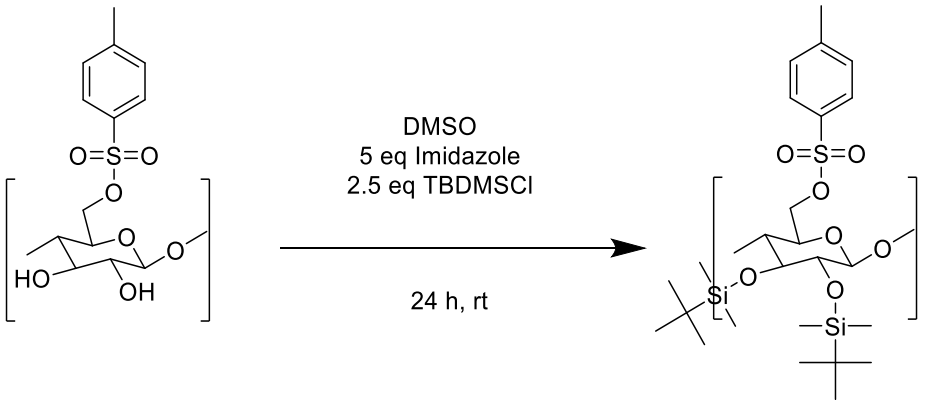

Figure 4-75: Reaction scheme for silylation of tosyl cellulose

4.5.8.4 Protocol for silylation

Chitosan mesylate or tosyl cellulose (1 eq OH groups) was dissolved in dry DMSO (6.5 ml). Stirred for 1 h under nitrogen with gentle heating with a heat gun until dissolved. Imidazole (5 eq) and TBDMCl (2.5 eq), were dissolved in dry DMSO (5 ml) under nitrogen (an extra 1ml DMSO was used to dissolve and transfer TBDMCl

which struggled to dissolve). This was then added dropwise to the chitosan mesylate or tosyl cellulose at room temperature still under nitrogen. A thick solid gel was formed in 10 min; the reaction was then left for another 22 h. (toluene was added after 2 h in JW02DCb). The precipitate was then filtered and the product was washed in deionised water (3x40 ml). The first 40 ml was washed in a beaker using a mechanical mixer (blitzer) to break up the solid gel. The product was filtered then finally washed in 40ml acetonitrile and in a beaker and then filtered then washed with another 10ml. This resulted in a very fine white powder. This was dried in the fume hood for 1h and then overnight in a 60 ^{o}C vacuum oven.

4.5.8.4.1 Silylation of chitosan polymer (16000 Da)

Chitosan mesylate (gfm 242 g/mol, 500 mg, 2.07 mmol, 4.14 mmol OH,) was dissolved in dry DMSO (6.5 ml) and stirred for 1 h under nitrogen with gentle heating with a heat gun till dissolved. Imidazole (gfm 68.077 g/mol, 1.432 g, 21.4 mmol 5x excess) and TBDMCl (gfm 150.72 g/mol, 1.584 g, 10.51 mmol, 2.5 x excess), was dissolved in dry DMSO (5 ml) under nitrogen. (RB flask could have been better prepared and may not have been completely dry or oxygen free, solution went from colourless to cloudy extra DMSO (1 ml) was used to dissolve and transfer TBDMCl which struggled to dissolve). This was then added dropwise to the chitosan mesylate at room temperature still under nitrogen. A thick solid gel was formed in 10 min; the reaction was then left for another 22 h. The precipitate was then filtered and the product washed in deionised water (3x40 ml). The first 40 ml was washed in a beaker using a mechanical mixer (blitzer) to break up the solid gel. This was then filtered, and the next two washes were in a beaker wither a magnetic stirrer. This filtered product was

finally washed in acetonitrile (40 ml) and in a beaker and then filtered as washed with another 10ml. This resulted in a very fine white powder. This was dried in the fumehood for 1 h and then overnight in a 60 ^{o}C vacuum oven. This resulted in 0.559 g, gfm 389.44 g/mol, 69.3% yield.

4.5.8.4.2 Silylation of chitosan degraded polymer (5000 Da)

Chitosan mesylate (gfm 242 g/mol, 400 mg, 1.65 mmol, 3.31 mmol OH,) was dissolved dry in DMSO (5.5 ml) and stirred for 1 h under nitrogen with gentle heating with a heat gun till dissolved. Imidazole (gfm 68.077 g/mol, 1.146 g, 16.8 mmol 5x excess) and TBDMCl (gfm 150.72 g/mol, 1.27 g, 8.42 mmol, 2.5 x excess), was dissolved in dry DMSO (4.5 ml) under nitrogen. This was then added dropwise to the chitosan mesylate at room temperature still under nitrogen. A thick solid gel was formed in 10 min; the reaction was then left for another 26 h. The precipitate was then filtred and the product washed in deionised water (3x40 ml). The first 40 ml was washed in a beaker using a mechanical mixer (blitzer) to break up the solid gel. This was then filtered, and the next two washes were in a beaker with a magnetic stirrer. This filtered product was finally washed in 40 ml acetonitrile and then filtered and washed with another 10ml. This resulted in a very fine white powder. This was dried in the fumehood for 1 h and then overnight in a 40 ^{o}C vacuum oven. This resulted in 0.357 g, gfm 389.44, 27.69% yield, check again **JW02DC** H^1 (Pyridine) silyl 1.57, 2.61, chitosan backbone 4.03 - 6.93 ppm. DS 0.91

4.5.8.4.3 Silylation of chitosan degraded polymer (5000 Da) with TBDMSCl (with toluene)

Chitosan mesylate (gfm 251.6 g/mol, 500 mg, 1.99 mmol, 3.97 mmol OH) was dissolved in dry DMSO (5.5 ml) and stirred under nitrogen with gentle heating with a heat gun untill dissolved. Imidazole (gfm 68.077 g/mol, 1.353 g, 19.87 mmol 5x excess) and TBDMCl (gfm 150.72 g/mol, 1.511 g, 10.03 mmol, 2.5 x excess), was dissolved in dry DMSO (5 ml) under nitrogen (extra 0.5 ml DMSO was used to dissolve and transfer TBDMCl which struggled to dissolve). This was then added dropwise to the chitosan mesylate at room temperature still under nitrogen. A thick solid gel was formed in 10 min; the reaction was then left for another 2 h after which toluene (5 ml) was added and the reaction left for a further 22 h. H_2O (60 ml) was then added and an emulsion formed. To this, NaCl (2 g) was added to try and aid extraction (probably made extraction more difficult). The product was extracted with ethyl acetate (3x 50 ml), the ethyl acetate was washed H_2O (2x 50 ml). The ethyl acetate fraction was then washed with brine (3x50 ml). Ethyl acetate was dried over $MgSO_4$. The $MgSO_4$ was filtered off and the ethyl acetate concentrated on the rotary evaporator till ~10 ml left. Half precipitated in acetone and half in acetonitrile (acetonitrile is better for this). This was combined, filtered and washed with acetonitrile (2x20 ml). This was dried in the fumehood overnight then dried in a 40 ^oC vacuum oven. The yield produced was 0.402 g **JW02DCb** H^1 (Chloroform) silyl 0.07, 0.91, chitosan backbone 2.72 – 4.27 ppm. DS 1.73

4.5.8.4.4 Silylation with 5000 Da Chitosan with TDSCl

Chitosan mesylate (gfm 242 g/mol, 400 mg, 1.65 mmol, 3.31 mmol OH) was dissolved in dry DMSO (5.5 ml). It was stirred for 1 h under nitrogen with gentle heating using a heat gun until dissolved. Imidazole (gfm 68.077 g/mol, 1.146 g, 16.8 mmol 5x excess) and TBDMCl (gfm 150.72 g/mol, 1.27 g, 8.42 mmol, 2.5 x excess), were dissolved in dry DMSO (4.5 ml) under nitrogen. This was then added dropwise to the chitosan mesylate at room temperature still under nitrogen. A thick solid gel was formed after 9 h, then H_2O (50 ml) was added. The precipitate was then filtered, and the product was washed in deionised water (3x50 ml). The first 40ml was washed in a beaker using a mechanical mixer (blitzer) to break up the solid gel. This was then filtered and the next two washes were in a beaker with a magnetic stirrer. This filtered product was finally washed in acetonitrile (30 ml) in a beaker and transferred to filter with another 10ml. This resulted in a very fine white powder. Unfortunately, this sample was accidentally dropped and some of it was lost. The remainder was dried in the fumehood overnight and dried in a 40 ^{o}C vacuum oven. This resulted in 0.322 g yield.

4.5.8.5 Silylation of aminocellulose

Mesylated aminocellulose was not soluble in DMSO only slight swelling after heating and 1 day, hence silylation not possible.

4.5.8.5.1 Addition of amine group to silyl tosyl cellulose –To form silyl aminocellulose

Experiment JW03TC

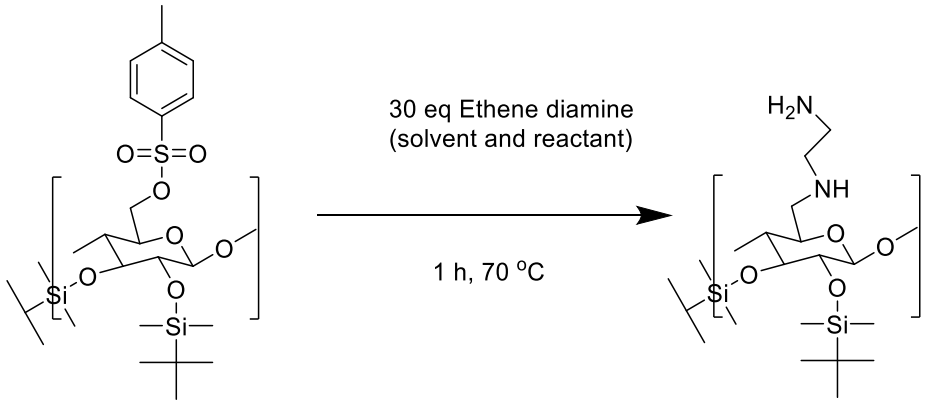

Figure 4-76: Reaction scheme for amine replacement of tosyl group on silyl tosyl cellulose

4.5.8.6 Protocol

1 eq of silyl tosyl cellulose was added to ethylene diamine (25 eq) used as solvent and reactant (recoverable and recyclable) heated to 70 °C for 5 h. The product precipitated in H_2O filtered, the precipitate washed with 30 ml H_2O then washed with 1x30 ml H_20 with 1 ml 1 M NaOH added to remove tosyl ion stirred 30 min. The product then washed 1x30 ml H_2O. Product dried overnight in fume hood the dried in 60 °C vacuum oven.

4.5.8.6.1 Silylation of tosyl cellulose

Tosyl cellulose (1 g DS 0.63, 3.86 mmol 9.1482 mmol OH) was dissolved in DMSO (12.9 ml) under nitrogen. Imidazole (3.114 g, 45.741 mmol), TBDMSCl (3.447 g, 22.871 mmol) was dissolved in DMSO (9.9 ml) under nitrogen. This was added

dropwise to the tosyl cellulose and the reaction was left for 24 h at rt. A precipitant formed, which was filtered, then water (100 ml) was passed though the filter to wash/harden the product. More precipitant was formed; this was thought to be more product so this precipitate was collected. Some product was lost though the sint (water should have been added to the rb flask). The precipitate was then washed with H_2O (2x 50 ml) for 10 min, H_2O (1x 50 ml) for 30 min. (partially soluble in ACN) re-precipitated in H_2O, filtered, washed with isopropanol-formed a putty. Evaporated overnight precipitated in H_2O, filtered dried 60 ^oC vacuum oven. The resulted product a yield of 0.813 g. **JW02TC** Yield , H^1 silyl 0.13, 0.95 chitosan backbone 2.50-4.42, tosyl 7.38, 7.86 DS silyl 1.22, DS tosyl 0.65.

4.5.8.6.2 Replacement of tosyl group with amine group

Ethylene diamine (2.1 ml) was added to silyl tosyl cellulose (0.500 g,1.256 mmol). This was heated to 70 ^oC for 5 h. Ethylene diamine was used as solvent and reactant. It has been found that this means the ethylene diamine can be recovered and recycled. The product was then precipitated in H_2O-75ml (transferred with additional 20 ml) to filter the product. The precipitate was washed with H_2O (30 ml) then washed with H_20 (1x30 ml) with 1M NaOH (1 ml) added to remove tosyl ion: this was stirred for 30 min and washed in H_2O (1x30 ml). Finally, it was washed with acetonitrile (20 ml). The yield produced was 0.205 g

4.5.9 Solubility tests

Product (20 mg) dissolution was attempted in solvent (20 µl) stirred in vial with a magnetic stirrer. Where dissolution was difficult a heat gun was used to see if gentle heating would result in dissolution. -photographs taken to aid description.

4.5.10 Scale up of TBDMS chitosan

4.5.10.1 Reactions chitosan mesylate

4.5.10.1.1 Materials

- Chitosan (5000 Da) is depolymerised chitosan from chitosan with a formula weight of 16000 Da. The depolymerised procedure is explained in Chapter 2.
- Methanesulfonic acid, CAS 75-75-2, Alfa Aesar, A13565 lot 10198453. Fw 96.11

4.5.10.1.2 Chitosan mesylate (Nottingham batch 1 -N1DC1)

Chitosan (5000 Da) (5 g, F.W. 165.2, 30.267 mmol) was suspended in water (40 ml) in a 10 ^{o}C ice bath. Methanesulfonic acid (2 ml) was then added: this forms the salt of chitosan which is water soluble. The solution turns clear and to be sure the salt has fully formed the reaction is left for 1 h. After this the product is precipitated in isopropanol (200 ml, another 50 for transfer). (Song *et al*., 2010 used ethanol but isopropanol appears to be a better precipitant). The product is filtered and washed while stirring in a beaker with isopropanol (1x 100 ml 30 min, 1x 50 ml 15 min) the

product was filtered between washes and then washed with acetone (50 ml). The product is then filtered once again and left to air dry for 1 h after which the product is re-dissolved in 15 ml H_2O. The product is then re-precipitated in acetone (50 ml) and washed with acetone (25 ml). A white powder is formed. This was air-dried overnight and then dried using a vacuum and heating mantel set to 40 ^oC (a 40 ^oC vacuum oven can be used if available). The resulting product weighed 6.8518 g.

Table 4: Mesylate batch 1-4 differences. Components in order of above reaction

Batch	**chitosan g, mmol, eq**	**water**	**methansulfonic acid**	**isopropanol**	**isopropanol washes**	**acetone washes**	**water**	**Acetone**	**Acetone washes**
1	5.0,30.27,1.0	73.3	2.0	108.0	1x43.2, 1x21.6	1x22.3	27.5	22.3	1x22.3
2	10.0, 60.5,1	68.8	2.0	75.6	1x28.1	1x17.9	32.1	22.3	2x11.2
3	20.0,121.1,1	59.6	2.0	54.0	2x13.5	2x13.9	27.5	33.4	2x13.9
4	20.0, 121.1,1	59.6	2.0	54.0	2x13.5	2x13.9	27.5	27.9	2x13.9

4.5.10.2 Reactions TBDMS chitosan

4.5.10.2.1 Materials

- Chitosan mesylate from above reactions
- TBDMSCl
- Imidazole
- DMSO-anhydrous
- Toluene -freshly distilled, distillation towers
- Magnesium sulfate
- Sodium sulfate

4.5.10.2.2 TBDMS Chitosan (Nottingham batch 7 -N2DC7)- example

Chitosan mesylate (gfm 251.6 g/mol, 12.0008 g, mmol, mmol OH) was dissolved in dry DMSO (130 ml) in an oven dried flask under a flow of N_2. Imidazole (gfm 68.077 g/mol, 32.4765 g, mmol 5x excess) and TBDMCl (gfm 150.72 g/mol, 35.9638 g, mmol), was dissolved in dry DMSO (110 ml) under nitrogen, extra DMSO (20 ml) was used for transfer. This was then added dropwise to the chitosan mesylate at room temperature still under nitrogen (5-10 ml was lost during transfer). After 2 h dry toluene (130 ml) was added and the reaction was left stirring under argon for another 22 h. H_2O (50 ml) was then added and an emulsion formed. This was extracted with ethyl acetate (3 x 75 ml) then a further ethyl acetate (1 x 50 ml). The ethyl acetate fraction was then washed with brine (3x50 ml). Ethyl acetate was dried over $MgSO_4$. The $MgSO_4$ was filtered off and the ethyl acetate concentrated on the rotary evaporator until ~30 ml left. The product was precipitated in acetonitrile 300 ml washed 4x75 ml. This was dried in the fumehood overnight then dried in a 40 ^oC vacuum oven. The resulting yield was ~13.2723 g.

Table 5: Differences in TBDMS chitosan production between batches. Note argon ran out during the night in batch 6. DS of bath 9 went down to 2.2 after being washed again.

Batch	**Chitosan mesylate (g, mmol OHeq)**	**DMSO eq.**	**Imidazole eq.**	**TBDMSCl eq.**	**DMSO eq.**	**Toluene eq.**	**Water eq.**	**Ethyl acetate eq.**	**Brine washes ml**	**Isopropanol eq.**	**Isopropanol washes eq.**	**DS**
1	2.000,7.95, 15.90, 1 eq OH	17. 72	4.90	1.34	4.87	8.31	69.84	9435.00	3x50	116.96	2x58	Not pure
2	2.000,7.95, 15.90, 1 eq OH	17.72	5.00	2.50	17.72	11.88	139.68	18870.00	3x50	194.93	3x97	Not pure
3	2.000,7.95, 15.90, 1 eq OH	17.72	5.00	2.50	19.49	11.88	139.68	12580.00	3x50	194.93	3x38	2.2
4	5.000,19.87, 39.74,1eq OH	21.26	5.00	2.50	17.72	13.07	69.84	5032.00	3x50	77.97	3x29	2.3
5	10.000,19.87, 39.74,1eq OH	19.48	4.99	2.50	23.03	17.81	69.82	2515.25	3x50	97.44	2x39	2.4
6	9.995, 39.72, 79.45, 1eq OH	23.04	5.00	2.50	23.04	15.45	34.94	2454.33	3x50	78.01	4x24	2.2
7	12.001, 47.69, 95.40, 1eq OH	19.19	5.00	2.50	19.19	12.87	29.10	2882.72	3x50	97.46	4x24	2.3
8	11.999, 47.69, 95.38, 1eq OH	14.77	5.00	2.50	20.67	11.88	58.20	2621.01	3x50	97.47	4x24	2.3
9	17.952, 71.34, 142.70, 1eq OH	14.80	5.00	2.52	14.80	11.91	38.90	9435.00	3x50	65.15	4x24	2.9

4.5.11 Determination of molecular weight of chitosan mesylate

The weight of chitosan mesylate was determined via sedimentation equilibrium using a Beckman XL-I analytical ultracentrifuge (AUC). 12 mm optical path double sector cells used used and filled with 100 μL of sample ands reference. A concentration series of 0.4-1.0 mg/ml chitosan mesylate in 0.10 M phosphate-bufered solution supplemented with NaCl to an ionic strength of 0.10 were analysed at 40,000 rpm using rayleigh interference optics. Measurements were taken every hour and analysed using SEDFIT-MSTAR to determine the (apparent) weight-average molar mass $M_{w,app}$. A value for the partial specifc volume ($\bar{\upsilon}$) of 0.57 mL/g was used (Morris et al. 2009). The density of the buffer was measured using an Anton Paar DMA 5000 density meter (Density 1.00295 g/cm^3) and viscosity was measured using an Anton Paar AMVn roll and ball viscometer (Viscosity 0.01045 Poise)

Chapter 5. Wood analysis techniques

5.1 Introduction - Analysis of effectiveness of treatments

The Oseberg artefacts are in desperate need of re-conservation to prevent further damage and to keep the artefacts for the future. Despite this being true, it is also important to find the right consolidant. Consolidants can be difficult to remove even when using reversible consolidants and due to the fragile nature of some artefacts, many may not withstand such steps. Hence, re-conservation can also be expensive and dangerous for the artefacts. Therefore, considerable care must be taken to fully assess possible consolidants before allocating one to be used and to determine if a new consolidant is better than an existing consolidant.

One commonly used parameter to compare consolidation ability is to look for weight percentage gain (WPG) (Muhcu et al., 2017; Tuduce Trăistaru et al., 2011). However, this does not help determine distribution of the consolidant within the wood; hence this must be combined with other methods such as scanning electron microscopy (SEM), Infrared spectroscopy (IR) and x-ray tomography (Kučerová, 2012b; Timar et al., 2014; Tuduce Trăistaru et al., 2011). Any colour change also requires consideration as ideally, treated artefacts would retain the same appearance as before treatment. This Chapter will outline the techniques used to assess the investigation of wood treatment discussed in Chapter 6 and Chapter 7.

5.2 Percentage weight gain, volume changes

Weight percentage gain (WPG) is commonly used in wood conservation to determine the weight increase as a percentage of the original weight: see equation 5-1 to determine how much consolidant was taken up into the wood (Broda et al., 2018; Can and Sivrikaya, 2016; Muhcu et al., 2017; Tuduce Trăistaru et al., 2011).

$$WPG = \frac{M_2 - M_1}{M_1} x100 \quad \textbf{5-1}$$

M_1= mass before, M_2= mass after treatment

Can and Sivrikaya (2016) used oven-dried weights for the calculations. Muchu et al. (2017) used weights of wood that were conditioned, pre- and post- treatment, at a set humidity, to account for weight differences due to humidity. All the wood was weighed on the same day and the humidity recorded for this investigation. After treatment, the wood was again kept in the same room and the weight was again recorded along with the humidity. The humidity was within 2% of the original humidity and hence, should have had little effect on weight changes.

Another method that is used is retention of impregnation products γ (Giachi et al., 2010) calculated from Eq. 5-2.

$$\gamma = 100\%.\frac{m_{AT} - m_{AMT}}{m_{ANT}} \quad \textbf{5-2}$$

m_{AT} is the oven-dried mass of treated samples, m_{ANT} is the estimated oven-dried weight before treatment using maximum water content calculated from Eq. 5.3 (Giachi et al., 2010).

$$m_{ANT} = \frac{m_{WNT}}{1-MWC} \quad \textbf{5-3}$$

M_{WNT} = wet mass of untreated samples.

Volume change is another important aspect, as ideally the appearance of the artefacts must remain unchanged (Eq. 5-4). Shrinkage is expected although undesirable when treating waterlogged wood but swelling is expected when treating dry wood (Broda et al., 2018; Muhcu et al., 2017).

$$Percentage\ volume\ change = \frac{V_0-V_1}{V_0} \text{ x } 100 \quad \textbf{5-4}$$

V_0 is the initial volume and V_1 is the volume after treatment.

Anti-shrink efficiency (ASE) is regularly used in conservation to test the effectiveness of a treatment on waterlogged wood calculated from Eq. 5-5 (Babiński, 2015; Broda et al., 2018; Lionetto and Frigione, 2012; Majka et al., 2018).

$$ASE = \frac{S_u-S_t}{S_u} x100 \quad \textbf{5-5}$$

S_u is the average shrinkage of untreated wood (air-dried wood) and S_t is the shrinkage of the treated sample. Anti-shrink efficiency (ASE) is better for tracking the improvement effect of the consolidant than shrinkage alone. Grattan et al. (1980)

suggested at least a 75% ASE would be required to be used in conservation (Broda et al., 2018; Grattan et al., 1980), but it is deemed insufficient today. Today more than 90% would be required and ideally more than 95% ASE. Along with ASE, it is important to know the state of wood degradation, as less degraded wood will show less shrinkage and less consolidation effect. The way wood degradation is generally reported is through moisture content. This is calculated from Eq. 5-6 (W = weight). The dry weight is the oven dry weight and the wet weight taken after surface water has been removed with tissue before drying the wood.

$$Moisture\ content = \frac{W_{Wet} - W_{Dry}}{W_{Dry}} \quad \textbf{5-6}$$

5.3 Spectrophotometer-colour changes

A spectrophotometer was used to measure colour before and after treatment to assess colour change. A spectrophotometer has three components: (1) a light source, (2) a monochromator and (3) a photodetector. The monochromator is used to select the individual wavelengths. The total colour change (ΔE) is based on three chromatic coordinates of the CIELAB colour system: a* green-red axis, b* blue-yellow axis and L* the black-white axis describes the lightness. It is calculated from $\Delta E^*_{2,1} = [(\Delta L^*)_2 + (\Delta a^*)_2 + (\Delta b^*)_2]^{1/2}$. CIE stands for Commission Internationale de l'Eclairage, which translates as International Commission on Illumination. This system has been used since 1931 (Johnston-Feller, 2002). CEILAB can also easily be converted to the Analysis of Variance (ANOVA) system, another well-known system for colour change. Colour change using CEILAB has been used in conservation to look at light degradation, artificial ageing and effect of treatment (Agresti et al., 2013; Calienno et

al., 2015; Malik et al., 2018; Matsuo et al., 2011; Munteanu et al., 2016; Pelosi, 2011). Colour change is a non-destructive way of monitoring degradation which is a major benefit. Colour change can also be used in the selection of new conservation treatments, as it is desirable to keep the appearance of the wood. It helps to monitor the degradation of the consolidant. (See Chapter 6 and Chapter 7 for colour change and treatment comparison).

5.4 Scanning electron microscopy (SEM)

5.4.1 Background

Scanning electron microscopy works in a similar way to light microscopy but instead of a light beam, an electron beam is used. First, the sample is coated with another material, for example, carbon, gold, platinum or chromium, which makes the sample conductive (Bell, 2012). As the electron beam interacts with the sample surface it produces secondary electrons, backscatter electrons and X-rays. These can be used to produce separate images to form one complete SEM image (Ponting, 2004).

Secondary electrons are low-energy electrons which originate from the electron beam colliding with the surface atoms of a sample. These electrons can only penetrate 10nm through the surface; hence, only secondary electrons on an outward trajectory will be detected. This means that secondary electrons can give very precise detail of the topology. Surface areas, which are forward pointing towards the detector, are therefore the brightest; hence, the use of secondary electrons helps with accurate topology (Bell,

2012). Backscattered electrons are electrons that have been deflected from the nucleus of an atom (Bell, 2012). Elemental analyses usually use the backscatter electrons.

5.4.2 Archaeological science

SEM is widely used in biology and archaeology and now is also being used in conservation. SEM has revealed a great deal for archaeology.

5.4.3 Wood degradation

SEM has also been used to determine the state of deterioration of wooden artefacts. The damage caused by tunnelling and erosion bacteria has been identified through SEM (Björdal et al., 1999; Powell et al., 2001). Powell et al. (2001) investigated the decay of modern wood that had been buried. Powell et al's investigation also considered the extent of degradation at different locations on an archaeological site, as *in-situ* preservation is practiced at that site. The SEM showed which parts of the wood had most erosion and the type of wood which were most affected, in order to determine which parts of the site were more prone to decay (Powell et al., 2001).

SEM investigations have also included types of deterioration relevant to the Oseberg artefacts. Comparing the sulphuric acid (H_2SO_4) pH2 effect on wood to the effect of water, sulphuric acid indicates 1.5 times more degradation of the middle lamella and cell walls (Hamed et al., 2012). Another investigation by Wang (2018) investigating biofuels and green chemicals considered an acid pre-treatment for wood before enzymatic saccharification to release a high yield of sugars. Acid pre-treatment affected different woods a little differently but Fourier-transform infrared

spectroscopy (FTIR) showed polysaccharide degradation in all samples and SEM showed pitting as a result of acid treatment (Wang et al., 2018).

The Oseberg artefacts were treated with alum; this treatment involved production of sulfuric acid. Braovac and Kutzke (2012) showed that the Oseberg wooden artefacts that have been treated with alum had a similar IR spectra to acid degraded wood, suggesting acid might be the major contributing factor in the degradation of the wood (Braovac and Kutzke, 2012). Braovac (2017-2018) worked on artificially degrading wood with the aim to have standardised pieces of wood upon which to test consolidants. The problem with archaeological wood is that its condition varies greatly, so when testing consolidants, this can cause problems. It can be hard to tell if one consolidant is better than the other or if another factor such as the state of degradation was a larger factor.

Fungal growth has also been observed though SEM (Macchioni et al., 2012). SEM is a versatile tool that is used to examine the types of wood degradation that have occurred, such as bacterial, fungal and acidic degradation. Knowing the state of preservation is important when deciding the choice of treatment for conservation. SEM can also be used to determine the penetration of a consolidant and discover whether it coats or fills the cells.

5.4.4 Consolidants

SEM was used to investigate antifungal properties of consolidants such as Paraloid and Regalrez. From the SEM, it is clear both consolidants decrease fungal growth of both white and brown rot in different tree types, although the antifungal property is more effective in poplar trees than spruces (Clausi et al., 2011). Clausi et al.'s (2011) research showed fungal colonies on the wood decreased even further by combining the consolidants. Fungal growth has not been a concern with the Oseberg artefacts: they are well stored and the acidity in the wood probably limits fungal growth. Other research has focused on the consolidants themselves and how they interact with wood. This method of wood treatment with Paraloid has also been investigated using different solvent systems i.e. ethanol/acetone treatment vs. toluene. Here, SEM was also used to determine how paraloid fills the wood (Chapter 7). From the SEM, it is clear that Paraloid fills the cell lumen but not the vessels (Tuduce Trăistaru et al., 2011). Giachi et al. (2011) investigated colophony, Rosin 100, Rosin 459, PEG 3400 and Vinavil 8020S, comparing acetone soluble consolidants using SEM and comparing treated wood to untreated wood, observing that consolidants filled the interior of the cells. However, at least in the case of colophony, although the interior of the cells were filled, the vessel lumina were still empty (Giachi et al., 2011). SEM is key to determining if a consolidant has penetrated all the way through the wood. It can also aid in determining how consolidants interact with the wood. This is important for establishing how effective they might be and how best to re-treat the wooden artefact should it become necessary. Therefore, this is one of the key methods for establishing the suitability of materials as consolidants.

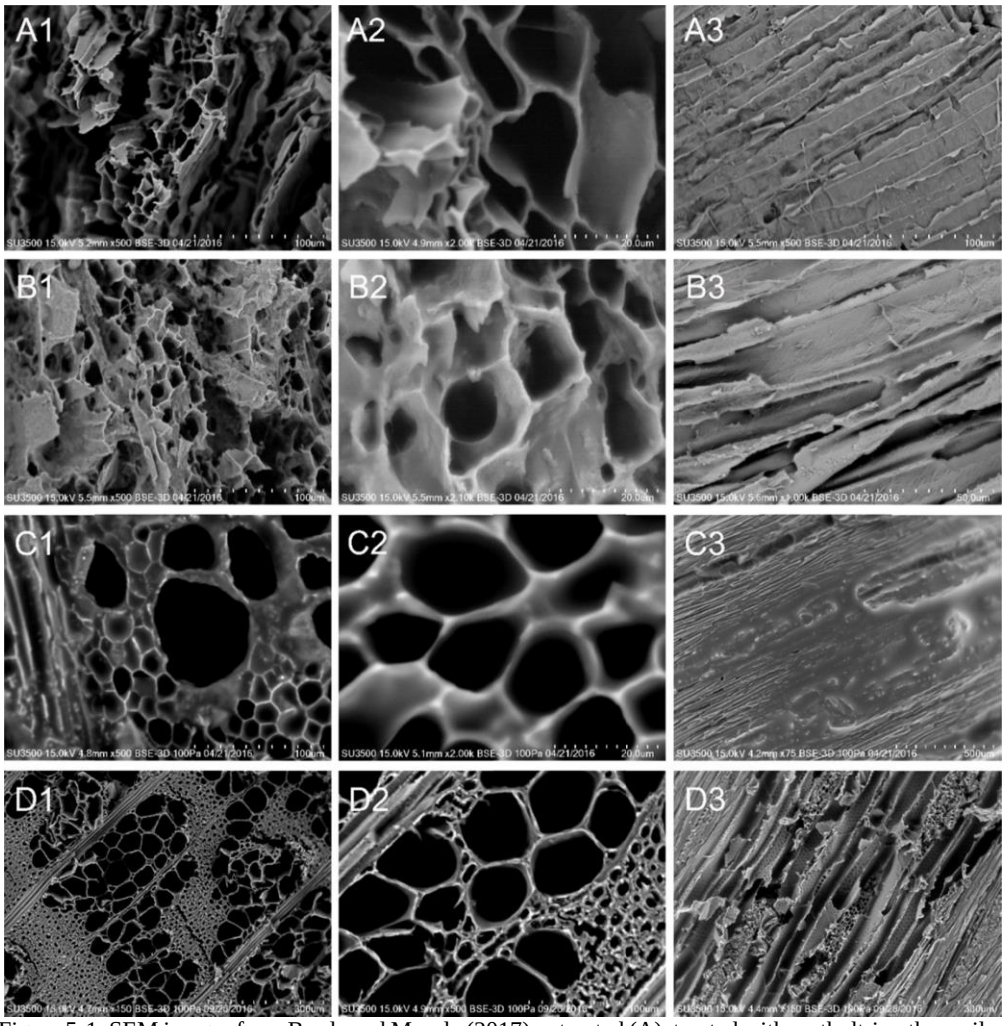

Figure 5-1: SEM images from Broda and Mazela (2017) untreated (A), treated with methyltrimethoxysilane (MTMOS) (B), treated with PEG (C), contemporary elm wood (D).

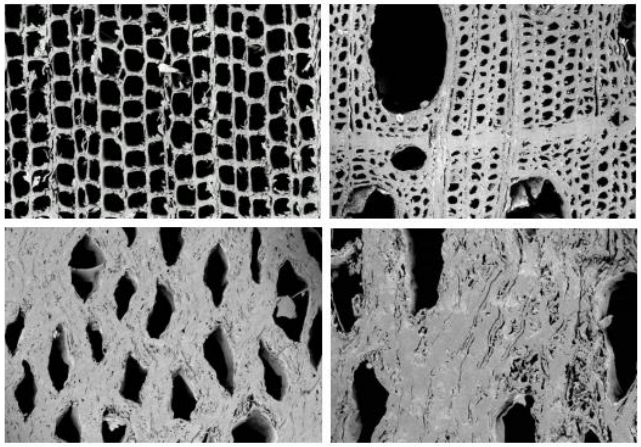

Figure 5-2: Example SEM image of air-dried waterlogged wood (Schindelholz et al., 2005).

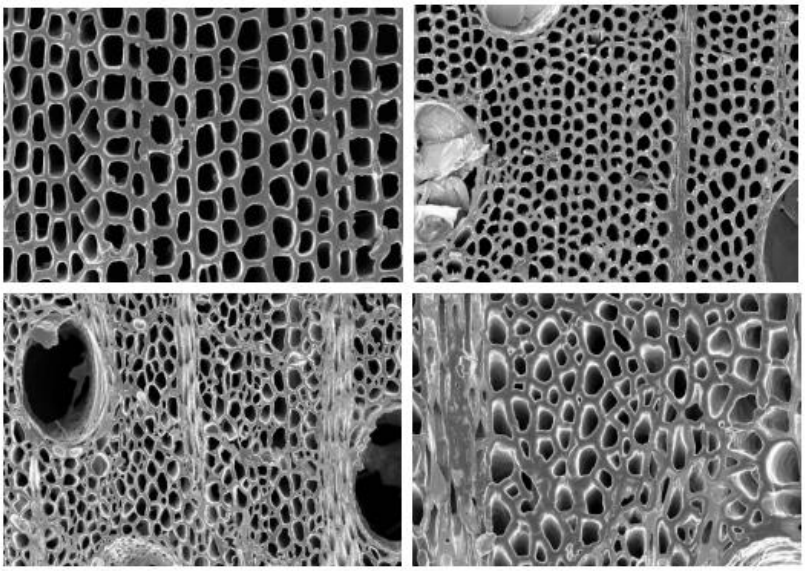

Figure 5-3: Example SEM image of freeze-dried waterlogged wood (Schindelholz et al. 2005).

The methodology of treatment has also been investigated through SEM (Figure 5-1) including length of treatment and application method, in the case of non-aqueous treatment. Drying and treatment or retreatment of wood can cause damage to wood and the method of drying has been found to have a significant effect, which can be seen through the SEM's images shown in Figure 5-2, Figure 5-3 and Figure 5-4. These images clearly show that freeze-drying causes the least damage to the cells (Schindelholz et al., 2005). This investigation also aims to include comparing air-drying vs. freeze-drying and aqueous treatment vs. non-aqueous treatment.

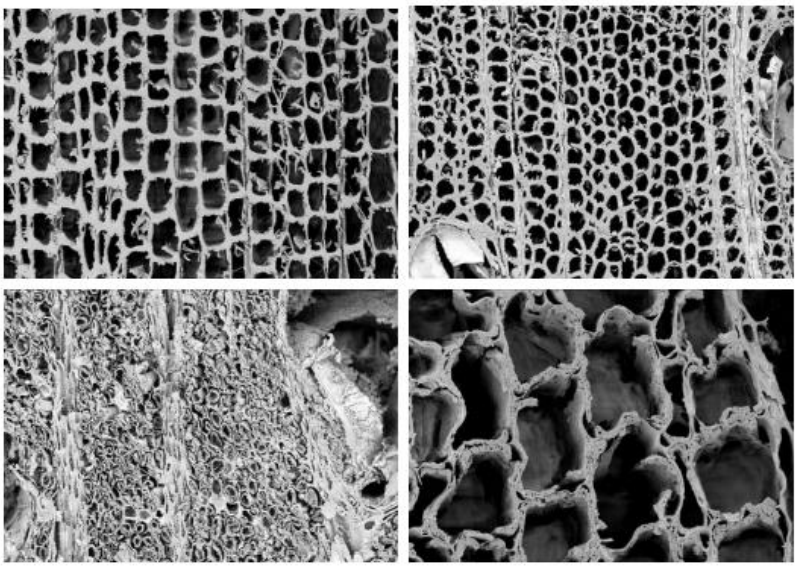

Figure 5-4: Example SEM image of suppercritically-dried waterlogged wood (Schindelholz et al., 2005).

5.4.5 Oseberg artefacts

SEM has also been used to investigate the Oseberg artefacts. McQueen et al. (2017) were able to show the alum inside the wood using SEM. It also showed more damage to the cells in alum-rich areas of the wood determined via chemical analysis (see Figure 5-5) and the crystals of alum provide more key support in alum-rich wood as the cells are so degraded. This is important as it also suggests that alum-poor wood can probably be treated with water in general, but more attention has to be paid to alum-rich wood and in many cases, these might require alum to be left in and an organic treatment method to be chosen. However, treatment will be on a case-by-case basis based on the level of degradation.

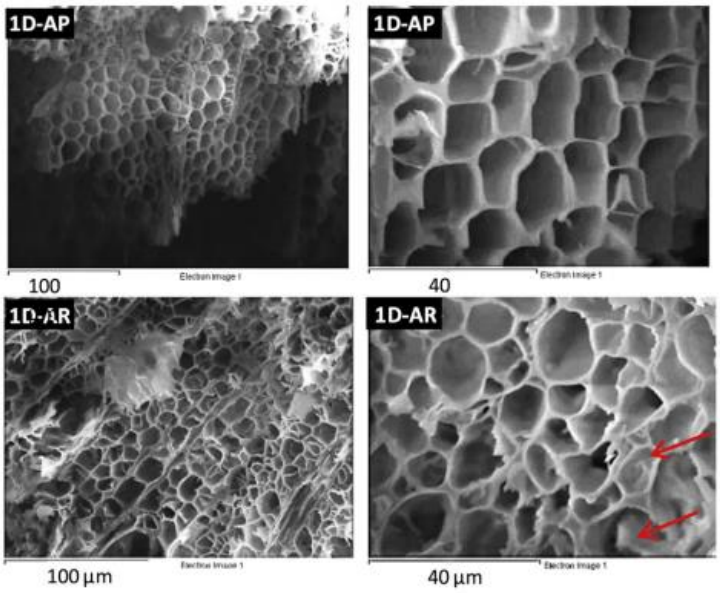

Figure 5-5: SEM image of Oseberg wood with alum-poor area (AP) and alum-rich area (AR) (McQueen et al., 2017)

Recent re-treatment trials support the concept of needing at least two treatment options: one aqueous and one non-aqueous. Oseberg wood pieces selected for re-treatment trials were categorised by Braovac and Sahlstedt in the Saving Oseberg group into three groups based on the visual state of degradation and previous experience of aqueous treatment: low risk — based on no cracks or fragmentation signs; medium risk — inner voids and/or cracks and/or fragmentation/powdering signs; and finally high risk — powdering, spontaneously or when handled. Wood fragments from each category were first desalinated in water and then treated with PEG; the wood from the more degraded wood category fell apart in the water (Braovac and Sahlstedt, 2019). This again highlights the need for at least one non-aqueous treatment method.

Christensen et al. (2012) used environmental scanning electron microscope (ESEM) to investigate cellulose treatment of Viking wood. The SEM image shows the cellulose

fibres that formed (Figure 5-6), which can be compared to the control and chitosan-treated wood (Figure 5-7). Figure 5-7 shows that unlike cellulose, chitosan appears to stick to the edge of the cell wall. This could aid in giving additional strength and make re-treatment easier, as the centre of the cell can still be filled if necessary.

ESEM is also going to be used in this investigation to determine if the chitosan derivative and aminocellulose penetrate the wood and how they behave inside the wood. More details of ESEM are given below.

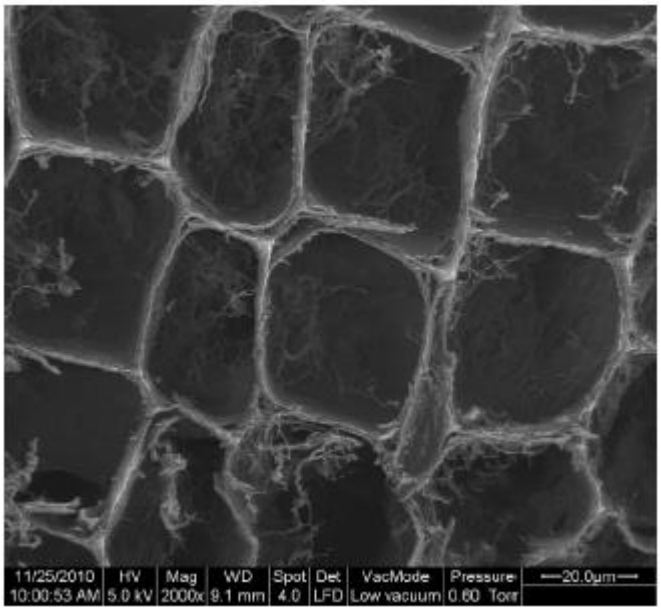

Figure 5-6: SEM image of cellulose treated wood (Christensen et al., 2012).

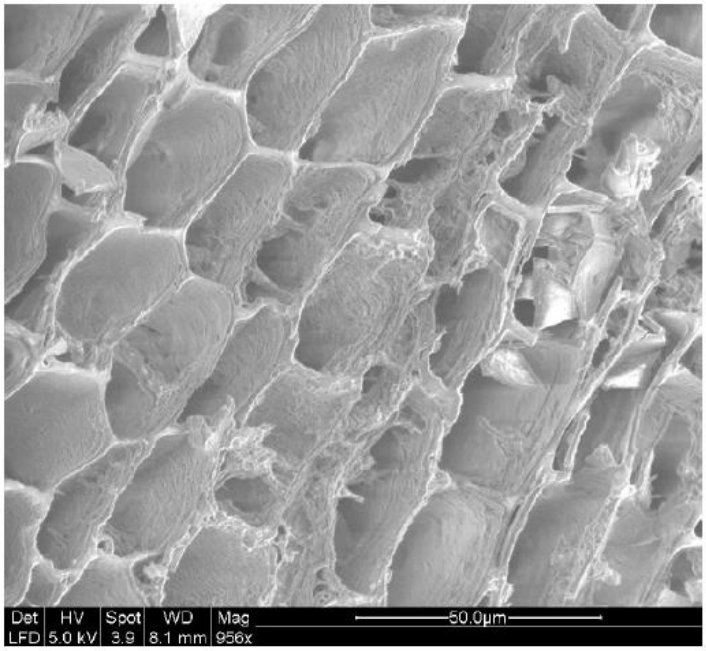

Figure 5-7: SEM image of waterlogged wood treated with chitosan in aq. acetic acid and freeze-dried (Christensen et al., 2015).

5.4.6 Environmental scanning electron microscopy

1.1.1.1 Introduction

Environmental scanning electron microscopy (ESEM) has additional advantages for conservation over traditional SEM. Traditional SEM requires samples to be dry, solid and electrically conductive, often achieved by coating with carbon. ESEM does not require pre-coating the sample and allows soft and moist materials to be viewed. It is best to view archaeological materials in their natural state as the process of drying could cause further degradation. This is especially true for waterlogged wood but also true for museum artefacts. Most museums are temperature and moisture controlled, or at least monitored and the relative humidity is normally kept at 40-60% (Atkinson,

2014). Drying a sample containing water past 40-60% relative humidity can cause further cracking of the wood. Therefore, ESEM has an advantage over traditional SEM as the samples do not need to be dried and coated. However, the images have lower resolution, contrast and sharpness (Hamed at al., 2012). ESEM can also cause beam damage to the wood at higher magnifications (Turkulin et al., 2007).

ESEM is more complicated to optimise; voltage, pressure, scanning rate, humidity, distance and magnification can all be adapted to try and get the best possible image. Magnification of SEM goes up to 50,000x whereas ESEM produces about 8000x times magnification. Turkulin et al. (2007) gives guidelines on optimising the image.

1.1.1.2 Modes of operation and parameters

There are four different modes of operation for ESEM with different ranges of pressure: high vacuum 10–6 mbar/Torr, low vacuum 0.8 Torr, low vacuum short distance 1.8 Torr and wet mode between 1–10 Torr. The high vacuum operational mode requires the wood to be dry and coated with a conductive material as with SEM. Low vacuum or wet vacuum modes are the ones more suitable for archaeological wood. At low vacuum, water pressures below 2 but above 1.5 Torr have been found to impair the signal and therefore the quality of the image. The best contrast in images for wood has generally been found with vapour pressures of 0.5 Torr (Turkulin et al., 2007). Another parameter which can be altered is the voltage which is generally in the range of 5–10 kV. Better resolution is generally found with higher voltages; however, with wood, higher voltages can also result in beam damage. For porous material like wood, a working distance of >10 mm is beneficial. However, at a longer working

distance scattering can occur. This can be countered by voltage but not in the case of wood as higher voltages can cause wood damage. 10 kV is appropriate for a 15 mm working distance and for 5–10 Kx magnification, the voltage can be increased by 1.5 kV and the vapour pressure of 1–1.5 Torr can be used (Turkulin et al., 2007). Turkulin et al. (2007) used 5 kV, 1500x mag, 9.1 mm WD and 0.5 Torr and spot size 3.0. Christensen (2013) used 5 kV, 958 magnification, spot size 3.9 and 8.1mm working distance (WD) for analysis of chitosan-treated wood and 5 kV, 1200x, spot size 4, 5.8 mmWD for cellulose-treated wood, 5 kV, 1000x Mag, 9.1 mm WD and 0.6 Torr pressure for wood treated with cellulose and PEG (Christensen, 2013). McHale used 8 kV, 982x mag, 8.4 mm WD, spot size 4.5 with 130 Pa pressure (McHale et al., 2016a). These parameters will be used as a starting point and then optimised with the aim of getting the best image for the pieces of wood being analysed.

Low vacuum short distance mode is very similar to low vacuum mode, but allows for slightly higher pressures and a smaller working distance to be used; this means higher magnification can be obtained (Turkulin et al., 2007).

WET mode allows for 100% humidity to be used. This means samples can stay wet for the analysis, therefore not changing the environment the sample is in. However, for wood this mode has not yielded the best images (Turkulin et al., 2007).

5.5 Infrared

Fourier-transform infrared spectroscopy (FTIR) can be used to identify treatments that were previously used on an artefact. An example is the case of a coffin that was

analysed and found to have been treated with B72. It was also observed that there was gypsum and animal glue on the coffin, probably from the original painting of the coffin (Afifi et al., 2019). IR works because different types of bonds stretching absorb at different wavelengths and this can help identify functional groups in molecules. In terms of conservation, this can be used to investigate the presence of a molecule in wood by looking for a distinct functional group which is not present in the wood. FTIR can also be used to investigate the level of degradation of the wood (Fors and Richards, 2010; Jones, 2010). FTIR has also been explored as a method of determining if consolidants have penetrated into wood (McHale et al., 2017). It also has been previously used to investigate the penetration and dispersion of a number of consolidants including B72 and beeswax (Timar et al., 2011).

5.6 Tape test

Tape tests have not been used before in wood conservation but they have been used in stone and plaster conservation (Drdácký and Slížková, 2013; Drdácký et al., 2012). The test has not been standardised for wood but the Saving Oseberg team is planning to work on that.

The “scotch test”, “peeling test” or “tape test” has been used for more than 40 years in conservation to investigate consolidation of stone. Drdácký et al. (2012) discuss the problems with standardising the tape test. A standardised method is available for steel using the automated system, CoilScooter, to analyse the quality of steel plates. American Society for Testing and Materials (ASTM) D 3359-08 is a standardised method developed for metal. ASTM D4214-07 is used for evaluating the

degree of chalking of exterior paint films. Similar methods are being developed for stone conservation and have successfully been used to show a difference between unweathered marble, weathered marble and treated weathered marble (Drdácký et al., 2012). However, there are still several problems. In particular, the variability in adhesion strength is a problem with the tape. Consolidation tests for a given experiment should use the same tape brand, to minimize error. Even so, standardisation is a problem, and therefore, if the same experiment were to be repeated in another laboratory, different results are likely to be obtained. If another roll of tape was used, the results could be completely different due to the quality of adhesion/amount of adhesive on sections of tape. The angle of peeling of the tape is also a consideration, as well as the speed of removal of the tape. The smoothness of the surface has also been identified as a concern for wood, as well as stone and mortar (Drdácký et al., 2012). Repeating the peeling test in the same place, slowly results in reduced material being removed (Drdácký et al., 2012). However, that is due to the immediate surface being removed, such as the loose particles, not increased consolidation. Drdácký et al. (2012) developed two methods. The first is to use double-sided tape mounted on square paper: the paper is cut to a specific size and placed in a plastic bag and weighed. This is then transported to where the sample is being taken, the cover sheet of the adhesive is removed and replaced in the bag and the adhesive is then applied to the surface using a finger or eraser. After 90 seconds of application, the tape is removed at 10 mm/s at a 90 degree angle. This is then inserted into the bag to be weighed later. The second method uses one-sided tape cut immediately prior to use. This is weighed and applied to the surface and re-weighed with a 0.0001 balance. This was repeated 10 times in the same place. This is normally repeated in at least three other places. Linear regression

is then used to evaluate the removal of material from the same place. The same group further developed this method for mortar as well and took moisture into account (Drdácký and Slížková, 2013). This method also appears to work on plaster, but the surface must be brushed first to remove loose material (Aguilar et al., 2018; Drdácký and Slížková, 2015). Again, concerns of roughness affecting results and sampling tape came forth. Others also use the tape test as a simple method to use in the field (Blaeuer et al., 2013).

Many of the problems discussed above are also a problem for wood. This method can still be used despite the above concerns. However, it must have a control and be compared to a known treatment to improve ability to compare results. To try to minimise the error, the same roll of tape was used for all experiments. Some initial trials were carried out with tapes of different strength to find one appropriate for the very weak wood. The same person, myself, carried out all tape tests, which limits operator error. The tape was smoothed over three times with as close to the same pressure as possible (this was not measured). Tape sizes of 1 cm^2 were used, with results reported in grams of material removed per cm^2. The brand of the tape is given in the methodology; however, it may not be possible to obtain in future and the tape may not be homogenous within the same tape and even less likely to be homogenous between different rolls of tape. Three treated samples were investigated for each consolidant which were then compared to the three controls treated solely with water. The tape test was carried out on all six sides of the wood to reduce error and account for variability in samples. However, it is not possible to directly compare results but simply to establish whether a treatment was better than a control and is better or worse than a known treatment. In this way, you can compare how treatments in different

experiments compare to a known treatment, such as PEG, but you cannot compare different experiments directly to each other.

5.7 Tomography - synchrotron radiation computer tomography (SR-CT)

Computerised tomography (CT) uses rotating X-ray sources and a detector to obtain a 3D image based on radio density. MicroCT scans have been used to investigate wood, due to their higher resolution down to 1 micron. Synchrotron radiation produces monochromatic X-ray beams with a range of energy. This allows for higher quality CT images with increased contrast, compared to standard X-ray CT (Bugani et al., 2008). This method has been used to investigate PEG of various molecular weights, PPG (polypropylene glycol), colophony and poly-isoeugenol distribution in archaeological wood (Bugani et al., 2008, 2009). This method has been used here to examine newly developed consolidants and compare them to existing consolidants. Alum-treated wood has also been investigated using SR-CT to investigate alum distribution and will be used in the future to examine how consolidants are distributed in wood previously treated with alum (McQueen et al., 2017).

5.8 Mechanical testing

5.8.1 3-point bend test

Young's modulus (E) or modulus of elasticity (MOE) is a measurement of the stiffness of a material. It is calculated from the stress divided by the strain of the material see

Eq. 5-7 (Hearn, 1997). This information can be obtained from the three-point bend test (Figure 5-8). Young's modulus (E) or modulus of elasticity (MOE) is defined by the Eq. 5-7, 5.8 and 5.9 (Bradley, 1984; Bronitsky, 1986; Hearn, 1997; Hollenberg et al., 1971; Mirzaei et al., 2017; Roberts et al., 2013) which can be re-arranged to give Eq. 5-10 to 5-14. It is a common way to test mechanical properties of wood. The logathemics form of Eq. 5-14 gives 4-15 which follows that of a straight line (Eq. 5-16). This means that by plotting force again deformation it is possible to calculate E through a series of re-arranged Eq. 5-17 to 5-23.

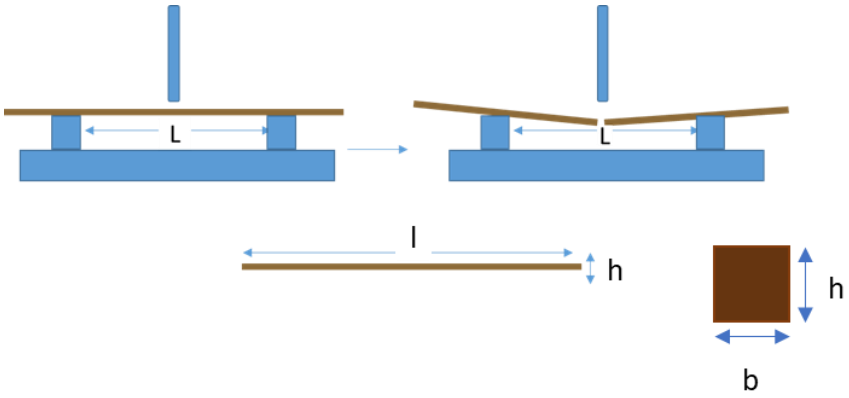

Figure 5-8: Diagram of 3-point bend test analysis set up and point of measurements.

$$\sigma = E.\varepsilon \qquad \textbf{5-7}$$

$\sigma = maximum\ stress\ at\ failure$

$\varepsilon = Strain$

E=Young's modulus = MOE for rectangular cross section

$$\sigma = \frac{3F.L}{2.bh^2} \qquad \textbf{5-8}$$

$$\varepsilon = \frac{2h\delta}{L^2} \qquad \textbf{5-9}$$

F= force

δ= deformation

$$E = \frac{\sigma}{\varepsilon} = \frac{(\frac{3F.L}{2bh^2})}{(\frac{2h\delta}{L^2})} = ((\frac{F}{\delta}).3L^3)/4w^4 \quad \textbf{5-10}$$

$$E4w^4 = ((\frac{F}{\delta}).3L^3) \quad \textbf{5-11}$$

$$(\frac{F}{\delta}).3L^3 = 4w^4E \quad \textbf{5-12}$$

$$(\frac{F}{\delta}) = \frac{4w^4\,E}{3L^3} \quad \textbf{5-13}$$

$$F = \frac{4w^4\,E\delta}{3L^3} \quad \textbf{5-14}$$

$$\log F = \log \delta + \log \frac{4w^4\,E}{3L^3} \quad \textbf{5-15}$$

$$y = mx + c \quad \textbf{5-16}$$

By plotting log F by log δ it is possible to determine the intercept = $log\,\frac{4w^4\,E}{3L^3}$

$$c = \log \frac{4w^4\,E}{3L^3} \quad \textbf{5-17}$$

$$10^c = 10^{\log \frac{4w^4\,E}{3L^3}} \quad \textbf{5-18}$$

$10^c = \frac{4w^4\,E}{3L^3}$ for square cross section **5-19**

$10^c = \frac{4bh^3\,E}{3L^3}$ for rectangular cross section **5-20**

$$4bh^3\,E = 10^c.3L^3 \quad \textbf{5-21}$$

$$E = \frac{10^c.3L^3}{4bh^3} \quad \textbf{5-22}$$

$$\frac{F}{\delta} = linear\ slope = 10^c \quad \textbf{5-23}$$

The 3-point bend test has been used before in conservation to analyse effects of consolidants. Sucrose, sucralose and trehalose were investigated by treating artificially degraded tongue depressors and using a 3-point bend test. The cross-head was lowered at a rate of 5mm/minute and the force was recorded at a rate of 20 times per second (Tahira et al., 2017). They found the magnitude of the MOE to be in the following order: degraded untreated wood <fresh wood<60% sucrose< 60% sucralose< 60% trehalose. For stress at failure, the order was the same, suggesting that both methods can be used to evaluate strength.

From the three-point bend test, it is also possible to determine the modulus of rupture (MOR) from equation (4-24) (Hein and Brancheriau, 2018).

$$MOR = \frac{3xFxL}{2xexh^2} \qquad \textbf{5-24}$$

F = load force at the fracture point (N)
L = Length of support (m)
h = thickness (m)
e = width (m)

Plotting MOR vs. MOE can help to distinguish the effects of archaeological wood treatment. It has previously been used to investigate PEG and keratin wood treatment (Endo et al., 2010).

The 3-point bend test would be a good way to assess mechanical properties of treated archaeological wood; however, 2 cm long pieces are too small for this analysis. Hence,

another method is sought for assessing mechanical properties of treated archaeological wood.

5.8.2 Fruit penetrometer

The pin test has been used in conservation to assess the level of degradation; however, it is a qualitative assessment. Degradation level via the pin test can be carried out with the addition of a pilodyn, which standardises the pressure at which the pin goes into the wood (Gregory et al., 2007). In an attempt to obtain a quantitative assessment, Petrou and Pournou (2018) used a fruit penetrometer to determine hardness of wood and to investigate the extent of degradation of waterlogged archaeological wood. The fruit penetrometer was adapted with a pin to allow this assessment of wood. The force required to penetrate a set distance into the wood can give an idea of degradation. This data was compared to moisture content and basic density which also gives an idea of the extent of degradation. The data from both methods concurred suggesting suitability of the method (Petrou and Pournou, 2018). Consolidation treatment should strengthen wood and hence, increase mechanical properties. Therefore, this method could theoretically be used not only to assess state of degradation but also to determine the degree to which the consolidants strengthen the wood.

5.9 Combining assessment methods

A combination of these methods should be able to indicate whether or not a consolidation treatment is effective and worth testing on artefacts. The weight increase along with SEM, IR and X-ray tomography can be used to assess whether the

consolidant penetrates the wood. Swelling and ASE can assess whether the treatment would lead to deformation of the wood. The colour change measured with the spectrophotometer would also help to determine any appearance change of the wood. Finally, the fruit penetrometer along with the tape test could help to assess the effect of treatment on the strength and cohesion of the wood following treatment. The three-point bend test can be used to assess how the treatment affects strength and/or flexibility of sound wood samples. Together, this produces a complete picture of the effect of a consolidant in order to decide whether it is suitable to use on artefacts.

Chapter 6. Aqueous wood conservation

6.1 Introduction

6.1.1 Ethical concerns of conservation

Conservation of artefacts may appear to be a modern concern. However, preservation of older items has been going on for a long time, from restoration of mummies in ancient Egypt (Aufderheide, 2009), to Romans repairing Samian pottery with metal rivets (Watkinson, 2018) and Kintsugi (the Japanese technology of gold joinery repair of pottery) which dates back to the 17th century (Hammill, 2016).

As early as the 19th century, there were state funded projects, for example, to conserve ancient mosaics preserved in France. International conferences started in Rome in 1930, hosted by the International Museum Office of the League of Nations (later ICOM) (Victoria and Albert Museum, 2011). Following this conference, one was held in Athens in 1931 which led to the Charter of Athens (1931), when ethical codes were first set to create common ground. Today there are multiple organisations across the world setting these codes or guidelines, such as, the United Kingdom Institute for Conservation (generally known as UKIC, now ICON); European Confederation of Conservator-Restorers' Organisation (ECCO) and the American Institute for Conservation of Historic and Artistic Works (AIC). There are differences in emphasis in these codes, but the principles are the same.

Guidelines can be found on the websites of these organisations. The following is a summary of guidelines: the legality of the artefacts being treated with the statement that anything known to be illegal should be reported; the standard of care should not

be affected by the monetary or aesthetic value of the artefacts. An object made of gold, or a beautiful painting, may not have more archaeological importance than an everyday wooden tool, which can be rare to find. Therefore, all objects should be given the best possible care. However, not all artefacts will receive the same treatment as it depends on the storage conditions, current state of degradation, type of material and finance available for treatment. The guidelines also cover the competence of the conservator, documentation, level of intervention restoration vs. conservation, health and safety, keeping up to date, integrity of the object and integrity of the conservator to choose the best treatment without thought of remuneration (Hamilton, 1975).

6.1.2 Restoration vs conservation vs preservation

Prior to the 1970s, restoration rather than conservation was more common: the emphasis was based on aesthetics of the archaeological artefacts final result. This would include greater intervention and could even include repair and replacement of parts. Now this approach is often seen as unacceptable without first assessing whether it is absolutely necessary (Watkinson, 2018). Hamilton (1975) also states conservation is a priority over restoration and "artifact conservation should not detract from the natural appearance of the object nor alter any of its scientific attributes. The conservator should strive to process specimens so that they retain as much diagnostic data as possible and yet remain chemically stable… In addition, all treatments should, if feasible, be reversible whenever possible."

When it comes to artefacts, it is no longer thought that everything should be restored to the original condition (Watkinson, 2018). Wear and tear can tell archaeologists how

an object was used and is therefore valuable information. Post-depositional changes can also be important. They give important information regarding decay and previous restoration and futhermore show how we looked after and cared for objects in the past. There is debate whether all previous repairs should be removed or whether modifications are now part of an object's history and therefore should also be preserved. However, this is artefact dependent and also depends on the story the museum is trying to tell. Obviously, treatment that is causing damage to the artefact should evidently be removed. When it comes to the Oseberg artefacts, there is still debate whether the alum should be removed, as it is not 100% clear if the alum is currently causing damage.

6.1.3 Reversibility

Reversibility of conservation techniques is another topic that is heavily debated. Previously, it was not thought of at all; then there was a phase when every consolidant had to be reversible to even be considered. Now, reversibility is still seen as useful, but its importance is context dependent. So long as the artefacts can be re-treated, a non-reversible treatment can still be considered if there is a greater benefit (Christensen et al., 2012; Collis, 2015; Smith, 2003; Turk et al., 2019). The reason for the debate is that, in the past, there have been many old conservation attempts that are now causing problems (as discussed in Chapter 1). The Oseberg artefacts are one such example. Although alum can be dissolved in water to be removed, this step can still cause a lot of damage, in some cases where alum is the main component holding the wood structure together. The alum treatment is itself now known to cause damage. Whether alum salts themselves are contributing to active decay is still uncertain. It is

preferable to remove it if it is managable to do so. However, it is not an easy task. S. Braovac working at the Viking Ship Museum in Oslo has recently undertaken some investigations into this (not yet published) and found that some pieces of wood are stable enough to be soaked in water, which removes alum and acidity. These pieces can then be re-treated with PEG, the current gold standard for conservation of waterlogged wood. The problem is that some pieces are now in such poor condition that the removal of alum would cause irreparable damage.

The fact old treatments cannot always be removed has made conservators think twice before applying a treatment, because the same might be said for the current treatments in 50 years' time. Great care must be taken; reversible consolidants may be removed if they turn out to do damage. The other option is to ensure the possibility of retreatment in the future by not filling all the cells in wood with consolidant. If the treatment deteriorates over time, the artefact can be re-treated even if the original treatment cannot be removed. Funding and facilities for research are necessary to try and determine the suitability of a new treatment and how it might age; however, time and funding is not always possible. PEG, for example, breaks down forming formic acid that can degrade cellulose and PEG very slowly but this is accelerated in the presence of an iron catalyst (Almkvist and Persson, 2008). The most important thing is to preserve the artefact straight away if it is at immediate risk. If a non-reversible treatment is the only thing that will preserve it well, then a decision might have to be made to use it and deal with the consequences later. In principle if there is any option at all that an object can be at least re-treated in future, even if the treatment is not reversible, this is acceptable. However, ideally a reversible treatment can be used if it

will work that way. If the technique is later found to cause damage it can be removed, or if a better technique is discovered in the future, that can be used (Hamilton, 1975).

6.1.4 Future research

Future archaeological research also needs to be considered as some conservation techniques will hamper future research efforts, such as carbon dating. For carbon dating to be possible all modern consolidant must be removed. Research has shown it might be possible to remove B72 and shellac, but not nitrocellulose or vinyl acetate-derived polymers (such as PVA) (Brock et al., 2018).

Chemical intervention can interfere with dating and isotope analysis and possibly also DNA analysis through contamination (Brock et al., 2018; López-Polín, 2012b). Ideally, prior to conservation, any planned archaeological scientific work should be undertaken if possible and small samples should be taken for future analysis as long as doing so does not cause visible or significant damage. New analytical techniques are continuously being developed.

The Oseberg artefacts are at risk from deterioration and there are small signs of ongoing damage visible. In this case, previous conservation attempts will already interfere with potential future archaeological analyses.

6.1.5 Sustainability

Sustainability of the wood for the future is the point of conservation. However, sustainability of the treatment itself has only just started to be discussed, for example

by McHale *et al.* (2017). Sustainability is defined as meeting the needs of the present generation without destroying resources the future generation will need (Keeble, 1988). Fossil fuels will eventually run out and there is much debate as to when this will occur; estimates vary with some saying that oil resources will only last for another 35 years (Shafiee and Topal, 2009). Fossil fuels are used in almost everything we do today from cars, clothes, food packaging, and medicine to conservation. Every industry will slowly have to change and adapt. When fossil fuels are finite, it is inevitable that they will become more expensive and when limited, they will be reserved for the most important things such as medicine. Every industry will have to make a change sooner or later and that includes conservation.

Improvements in sustainability are required in all fields including conservation. This can be carried out by limiting solvent and waste and discovering new sustainable treatment materials. Limiting solvent, consolidant and recycling as much as possible will also make it cheaper to undertake conservation and therefore make funds stretch further.

6.1.6 Testing samples

Testing material is not something that is categorically discussed, but it is known to be an issue. The most accurate test material would comprise of actual objects to be treated; sometimes there are less archaeologically important pieces from the same site found together with the artefacts of interest. These are obviously the most similar wood samples to the ones to be treated which can be used as test pieces. However, discarded archaeological material is often in very limited supply, as it not often kept. It is also

possible to use test material obtained from another archaeological site, but this too is in limited supply. The other problem with using discarded archaeological wood is the variation in condition. Even with the same fragment, there can be great variation from the surface to the middle of the wood. When trying to assess conservation methods, this variation can really hamper efforts. Therefore, fresh wood artificially degraded in the laboratory can be a useful alternative for testing treating treatments, fresh wood is readily available, and the degradation applied to it is likely to be more consistent. Kennedy and Pennington (2014) degraded some tongue depressors for their research on sugar-based consolidants. This appeared to work well and showed the extent of consolidation by the sugars. Another advantage of this is they can be used for mechanical testing leading to destruction of the test piece. However, the downside of using tongue-depressors is that they are very thin so will not show how effectively a consolidant will penetrate into the wood. The best compromise is to start with artificially degraded wood to test the effect of consolidants in uniformly degraded wood, then test archaeological wood to get a closer analogue to the actual artefacts to be conserved and finally test material from the original collection to be conserved. However, this is obviously dependent on research time, available funding and facilities. For the Oseberg collection, this is possible, hence this chapter will cover testing material using artificially degraded wood and archaeological wood. Future work will be to apply a selection of consolidants on alum-treated archaeological wood prepared in the laboratory and finally on test fragments from the Oseberg collection, if the treatments are successful.

6.1.7 Wood treatment and importance of documentation

Documentation is vital to conservation research. Past documentation by previous conservators helps us understand what previously happened to artefacts, and therefore, how best to re-conserve them. We are fortunate to have some notes from Professor Gabriel Gustafson. He visited various museums in Denmark, Germany and Switzerland to find the best treatment for the Oseberg artefacts (Rosenquist, 1969). After deciding on the alum method, he undertook experiments to try and find the best concentrations for woods in different conditions (Rosenquist, 1969). We have some of these notes and it gives us a better idea how pieces were treated, and we can see what worked and what did not, with time. From the notes and condition of the wood, it is clear that combining glycerol and alum is worse than alum alone (Häggström and Sandström, 2013). Documentation of wood before and after treatment allows us to determine which treatment is preferable according to colour, weight and fragility (Babiński, 2007; Spirydowicz et al., 2001b). Documentation is also useful to revisit twenty years in the future to understand potential degradation and how that problem correlates to the exact conservation method. Chapter 4 covers what was documented in this project and why.

6.1.8 Artificial ageing of wood

In the paper industry, it has been found that accelerated ageing (thermal ageing) is generally a good match to natural ageing (Zervos, 2010). The exact mechanism of degradation and ageing has been heavily debated, particularly the extent to which oxidation plays a role (Whitmore and Bogaard, 1994; Zervos, 2010; Zou et al., 1994).

Hydrolysis is the main cause of paper degradation; the glycosidic bonds between the glucose moieties tend to be the first to break. This acid hydrolysis can be accelerated by the presence of acid. Acid can come from alum used in the pulping process, iron-gall ink (9^{th}-20^{th} century), a product of ageing from the breakdown of hemicellulose, atmospheric pollution, neighbouring packaging material (hence why acid free paper is used for packaging artefacts as most paper and cardboard is acidic) and finally acidic metabolites from microorganisms (Zervos, 2010). In the case of the wooden Oseberg artefacts, the acid predominately comes from the alum used for its conservation in 1905. UV exposure is also known to promote oxidation through the formation of free radicals. The presence of lignin is known to have antioxidant properties and it helps in protecting paper from free radical damage, it has been found to protect cellulose from UV degradation (Barclay et al., 1997; Zervos, 2010). The effect of light is not a major concern for museums as this can be limited with the use of special light bulbs and films over the windows to block UV exposure (Cassar, 2013; Stainforth, 2006). Research into sustainable films has successfully harnessed this potential and created modified cellulose films with lignin attached to the cellulose backbone. It has been found that films with 2% lignin showed 100% protection of UV-B (280-320nm) and more than 90% of UV-A (320-400nm) (Sadeghifar et al., 2017). Atmospheric pollution has been found to accelerate degradation, which needs to be considered for museums; however, options are often limited to restrict damage (Blades et al., 2000; Buda and Sandu, 2015; Grzywacz, 2006; Hatchfield, 2002). Pollution can clearly have an effect on degradation but when investigating artificial ageing, this is not worth including into the mix and it simply adds more variables except for specific investigations into the effect of pollution. The effect of pollution is not part of our investigations; air in the

museum is not currently filtered, but fragile artefacts are in closed glass display cases (newly changed in 2014) limiting the pollution exposure. Air flow throughout the museum is currently being investigated, as managing air flow can be important in limiting the build-up of pollutants.

For artificial ageing of paper, sealed vessels appear to best resemble natural ageing. Sealed ageing more closely resembles natural ageing because volatiles from degradation are kept close to the paper and absorbed by the paper (Zervos, 2010). This is worth noting for accelerated ageing investigations. However in terms of developing a starting material to investigate treatments, 80% RH and 90 ^{o}C would take too long to reach the state that the wood is in today if starting from fresh wood. However, this could be used later to try to predict which consolidant might be best to preserve the artefacts for the future. Although the degradation process is very similar to paper in terms of the cellulose, wood has a lot more lignin, which would have affected the degradation, and more chemical processes would have been involved. The artefacts today have already lost the majority of their cellulose and so lignin is mostly what remains.

In the case of the Oseberg artefacts, the sulfuric acid caused hydrolytic degradation of cellulose (Braovac and Kutzke, 2012). Investigations are still underway to determine whether alum salts (in the solid state) are actively involved in ongoing degradation. It could be that the extreme increase in degradation in Oseberg wood is caused by the sulfuric acid, as a result of the alum treatment and is subsequently catalysed by the iron in the wood. It is still not entirely clear if the alum acts as a catalyst as well, or only the iron. Iron from iron rods used in conservation of the artefacts have been

corroded by the acid in the wood and have resulted in the formation of iron sulfates. The iron ions are a concern as these have migrated though the wood and reacted with the alum, forming various complexes. However, iron sulfates do not appear to have formed on linseed coated wood with original nails. Either the original nails were less prone to corrosion or the linseed oil has had a protective effect (McQueen et al., 2018). This shows the variability of artefacts in the collection and iron needs to be considered but the variation in corrosion of iron is also a factor that must be considered in conservation treatments. At this point iron has not been found to have a strong link to the state of degradation in the wood and does not appear to pose a current risk (Braovac et al., 2018a). However, a change in environment with the addition of a new consolidate should change this situation and this needs to be taken into account. Chelating polymers may help mitigate potential future problems.

To investigate new treatments, it is desirable to limit the number of variables; hence, although alum causes significant damage to wood, this will not initially be investigated. The damage from alum is also only noticeable through chemical analysis, or years later. Alum treatment was used for about one hundred years over much of northern Europe before the problems of alum became apparent. For this research, heavily degraded wood was needed within a few months. To achieve this, chemical degradation was required.

Kennedy and Pennington (2014) investigated treatment of waterlogged wood with sugars but had a similar problem of wanting repeatable testing material so they chemically degraded tongue depressors with 1% sodium hydroxide for 1 week then washed with distilled water till pH7 was achieved in roughly 3 days (Kennedy and

Pennington, 2014). After these were air-dried and compared to waterlogged samples, the air-dried and base-treated samples warped whereas those waterlogged did not, showing degradation had occurred.

This investigation is interested in the penetration of the molecules as well as the consolidation effects, hence the tongue depressors are not appropriate as they are too thin. The types of wood the Oseberg artefacts are made of are largely diffuse porous wood varieties such as pine, maple, birch and ash (Amberger, 2019). S. Brovac prepared the artificially degraded wood for this project using 20 cm birch staves as birch is one of the types of wood in the collection. The wood immersed in 1% sodium hydroxide for 1 week is unlikely to sufficiently degrade the wood, hence, longer treatment or multiple treatments were required than used by Kennedy and Pennington (2014). The ultimate aim is to treat the Oseberg wood and this has been affected by acid degradation; hence, to optimise degradation and simulate the acid degradation, both acid and alkali degradation were used.

6.2 Methodology

6.2.1 Artificially degrading wood

Birch staves were artificially degraded by S. Braovac for this project and for others in the Saving Oseberg group. This wood is referered to as artificially degraded wood or laboratory degraded wood throughout this thesis. S. Braovac included preparation of this wood in an annual report in a section on deliverables for the Museum (Braovac, 2018). The staves were purchased from a Norwegian food store, where they are readily

available for a local cuisine. The wood genus was confirmed as birch, *Betula*, *spp*. from light microscopy. They were 18x1x1 cm weighing 9-11 g each. 50 Staves were degraded in two batches. The first batch was used for this project, both aqueous and non-aqueous (Chapter 6 and Chapter 7). The density of the undegraded wood batch 1 was (0.689 ± 0.070) g/cm^3, determined from the dimensions and mass at ambient conditions (30-50% RH). The wood was waterlogged at 90 ºC. The wood was then immersed in a solution of 5% sulfuric acid (vol/vol) to degrade the holocellulose, followed by rinsing. Subsequent the wood was treatment with 5% sodium hydroxide (w/vol); to degrade the hemicellulose and lignin. The wood was then transferred back and forth between the two solutions to promote degradation. The combination of the two was hypothesized to increase the porosity and the rate of degradation. After some time with the acid at room temperature it was decided the acid treatment should be carried out at 90 ºC. This is the temperature of the alum treatment and will accelerate degradation. The sodium hydroxide treatment was always kept at room temperature. A routine was established after some time of six days in each solution and rinsing in several changes of tap water between treatment baths. A more prolonged rinse of 170 h was used at the end to remove the base following final base treatment in hot tap water (90 ºC) and the final rinse showed a pH of 7. Batch two finished on an acid treatment and there is a note that this could have an effect. Batch 1 spent a total of 4784 h in acid, 295 h of which was in hot acid. 1006 h were spent in a basic solution of sodium hydroxide. The pH of the rinsed wood was found to be between 6 and 7. This resulted in a 45% reduction in density with an average final density of (0.382±0.040) g/cm^3 after having been freeze-dried. A Labconco Free Zone Triad freeze drier (model

7400030) was used with the collector temperature at -80 °C. The chamber temperature was set to -14 °C.

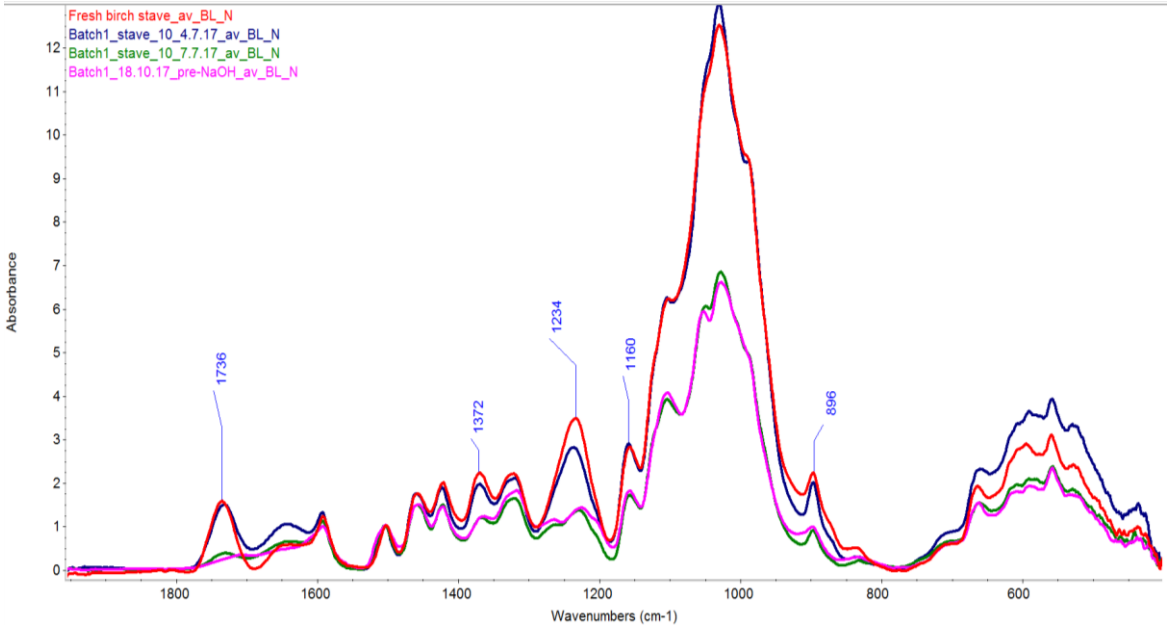

Figure 6-1: IR spectrum showing the effect of sulphuric and and heat for different soaking times on wod. The undegraded wood is shown in red. The blue curve shows 0 hours heating and 165 hours total time in acid solution. The green curve shows the wood spectrum after 23.5 hours of heating and 188.5 hours total in acid solution. The pink curve shows 49.5 hours of heating and 2661 total hours in acid solution. (Braovac, 2018)

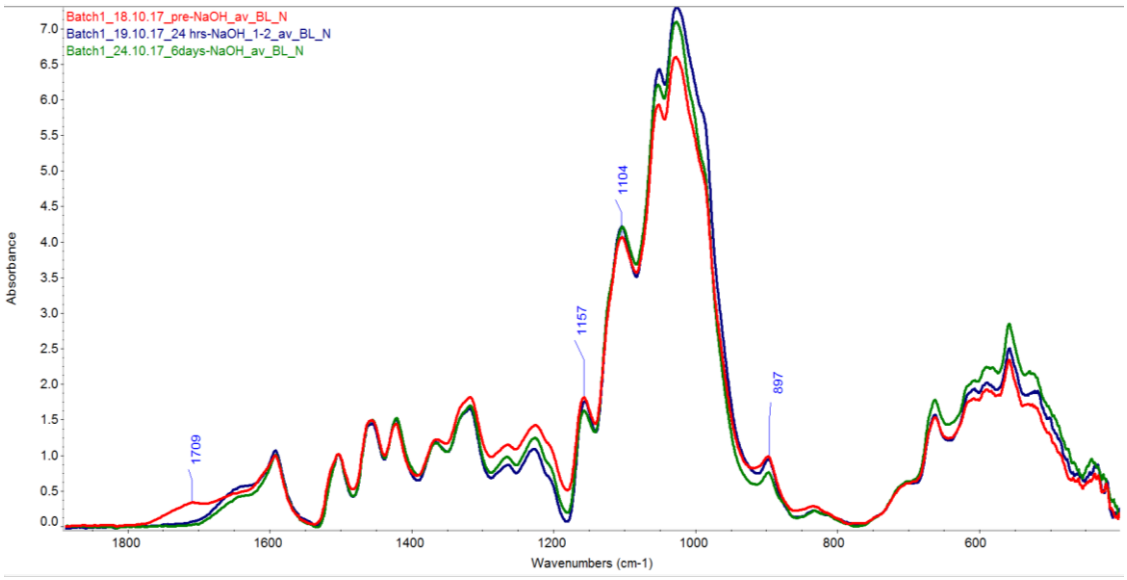

Figure 6-2: IR spectra of wood after acid treatment (2661 hours in acid (of which only 49.5 hours was held at 90°C)) followed 5% NaOH. Red line before NaOH treatment, blue line after 24h NaOH treatment and green line after 6 day treatment in 5% NaOH. The staves were rinsed with tap water before transferring from acid to base (Braovac, 2018).

The samples were placed in a conventional -20 ^{o}C freezer prior to being placed in the freeze drier. The wood was dried for seven days at 1.03 mbar. FTIR was carried out to monitor the degradation shown in Figure 6-1 and Figure 6-2 .Batch 2 was not ready at the start of this project, but showed 60% reduction in density having spent 558 h in acid with 455 h in 90 ^{o}C acid and 1760 h in base. This increased time in hot acid and in bases appears to have increased the degradation.

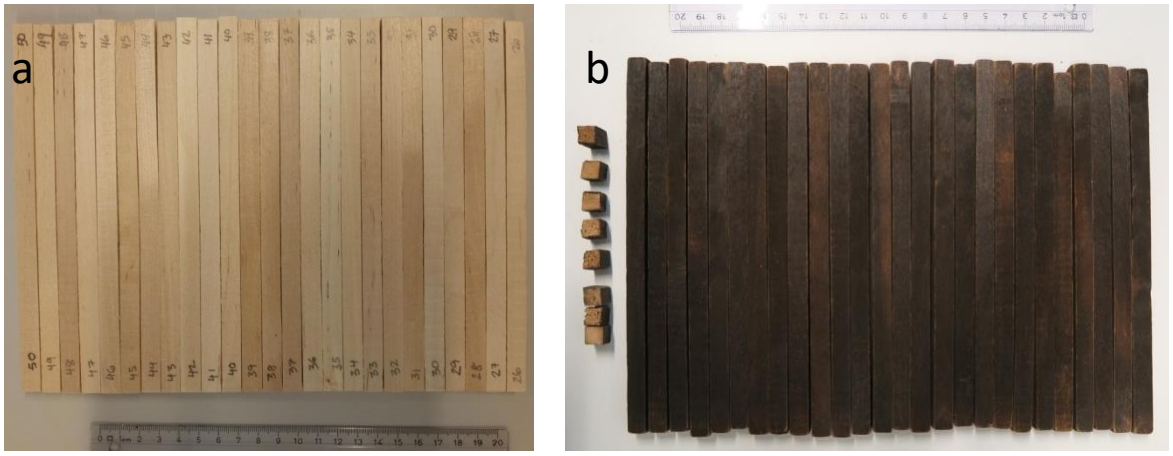

Figure 6-3: Photo of wood staves a) prior to treatment batch 3. b) Batch 2 after degradation. Only the outer wood is darked so greatly by treatment as apparaent when the wood was cut (Braovac, 2018).

Figure 6-1 shows marked degradation following the immersion in heated acid. Degradation can be seen at 1736, 1372, 1234 and 896 cm^{-1} peaks which, are assigned to holocellulose. Figure 6-2 shows degradation of hemicellulose from enhancement of absorbance bands at 1269 cm^{-1} and 1224 cm^{-1}, cellulose degradation from reduction of 987 cm^{-1}, holocellulose and lignin degradation from an increase in 1030 cm^{-1} and lignin degradation from a reduction in 835 cm^{-1} following basic treatment.

Heated acid caused darkening of the outside of the wood staves and darkening of the treatment solution (Figure 6-3). Freeze drying caused 7 staves from batch 1 to crack longitudinally.

Whilst preparing samples for this project, 1 cm or 2 cm pieces were cut from each stave allowing analysis into how density varied along the staves. (see Figure 6-4 and Table 6-1) It is clear, although there is some small variability within each stave densities are fairly consistent. There is greater variability between staves unfortunately. Due to the large number of treatments that were tested, it is not possible to use one stave for all variation; hence, it was decided to randomise the pieces to be used for each treatment.

The average density of batch 1 was (0.363 ± 0.028) g/cm^3, which is over three times higher than the archaeological wood in this investigation. These had a basic density of (0.144 ± 0.033) g/cm^3 and the Oseberg wood has a density of 0.1 g/ml. The variability in density of the artificially degraded wood is slightly lower than archaeological wood and the variability in degradation of cells is expected to be more consistent.

Table 6-1: Densities of pieces cut from staves from Batch Unless specified, pieces are 1 cm lengths and are numbered consistently from one end to the other. Not all parts of the stave were used. The values for the whole stave are courtesy of S.Braovac. The densities of samples are based on the weight at 30% RH but whole stave average density is based on the freeze-dried weight (Braovac, 2018).

Sample	Density (g/cm^3)	Sample	Density (g/cm^3)	Sample	Density (g/cm^3)
3.1	0.373	5.1	0.340	15.1	0.330
3.2	0.368	5.2	0.351	15.2	0.358
3.3	0.349	5.3	0.355	15.3	0.352
3.4	0.406	5.4	0.351	15.4	0.346
3.5	0.379	5.5	0.371	15.5	0.349
3.6	0.378	5.6	0.370	15.6	0.351
3.7	0.386	5.7 (2 cm)	0.362	15.7	0.346
3.8	0.382	5.8 (2 cm)	0.356	15.8 (2 cm)	0.351
3.9	0.378	5.9 (2 cm)	0.361	15.9 (2 cm)	0.361
3.10	0.377	5.10	0.363	15.10 (2 cm)	0.348
3.11	0.373	Average	0.358	Average	0.349
3.12	0.381	Stdv	0.009	Stdv	0.008
3.13	0.391	Whole Stave	0.363	Whole Stave	0.342
3.14	0.391				
3.15	0.370	9.1	0.352	16.1	0.323
Average	0.379	9.2	0.403	16.2	0.330
Stdv	0.013	9.3	0.388	16.3	0.333
Whole Stave	0.401	9.4	0.386	16.4	0.335
		9.5	0.372	16.5	0.327
4.1	0.353	9.6	0.372	16.6	0.306
4.2	0.341	9.7 (2 cm)	0.409	16.7 (2 cm)	0.332
4.3	0.341	9.8	Broken	16.8 (2 cm)	0.300
4.4	0.351	9.9 (2 cm)	0.381	16.9 (2 cm)	0.310
4.5	0.343	9.10 (2 cm)	0.379	16.10	0.314
4.6	0.358	9.11	0.372	16.11	0.320
4.7	0.388	9.12	0.379	16.12	0.329
4.8	0.383	9.13	0.379	16.13	0.330
4.9	0.389	9.14	0.359	16.14	0.314
4.10	0.384	Average	0.379	Average	0.322
4.11	0.377	Stdv	0.016	Stdv	0.011
4.12	0.342	Whole Stave	0.319	Whole Stave	0.267
4.13	0.388				
4.14	0.380	10.1	0.316	19.1	0.408
4.15	0.376	10.2	0.328	19.2	0.410
4.16	0.369	10.3	0.345	19.3	0.418
4.17	0.364	10.4	0.343	19.4	0.430
Average	0.366	10.5	0.343	19.5	0.431
Stdv	0.018	10.6	0.314	19.6	Damage
Whole Stave	0.397	10.7 (2 cm)	0.351	19.7 (2 cm)	0.403
		10.8 (2 cm)	0.368	19.8 (2 cm)	0.416
20.7(2 cm)	0.404	10.9 (2 cm)	0.354	19.1	0.417
20.8(2 cm)	0.376	Average	0.340	19.2	0.408
20.9(2 cm)	0.400	Stdv	0.018	Average	0.417
Average	0.393	Whole Stave	0.361	Stdv	0.011
Stdv	0.015			Whole Stave	0.353
Whole Stave	0.413				

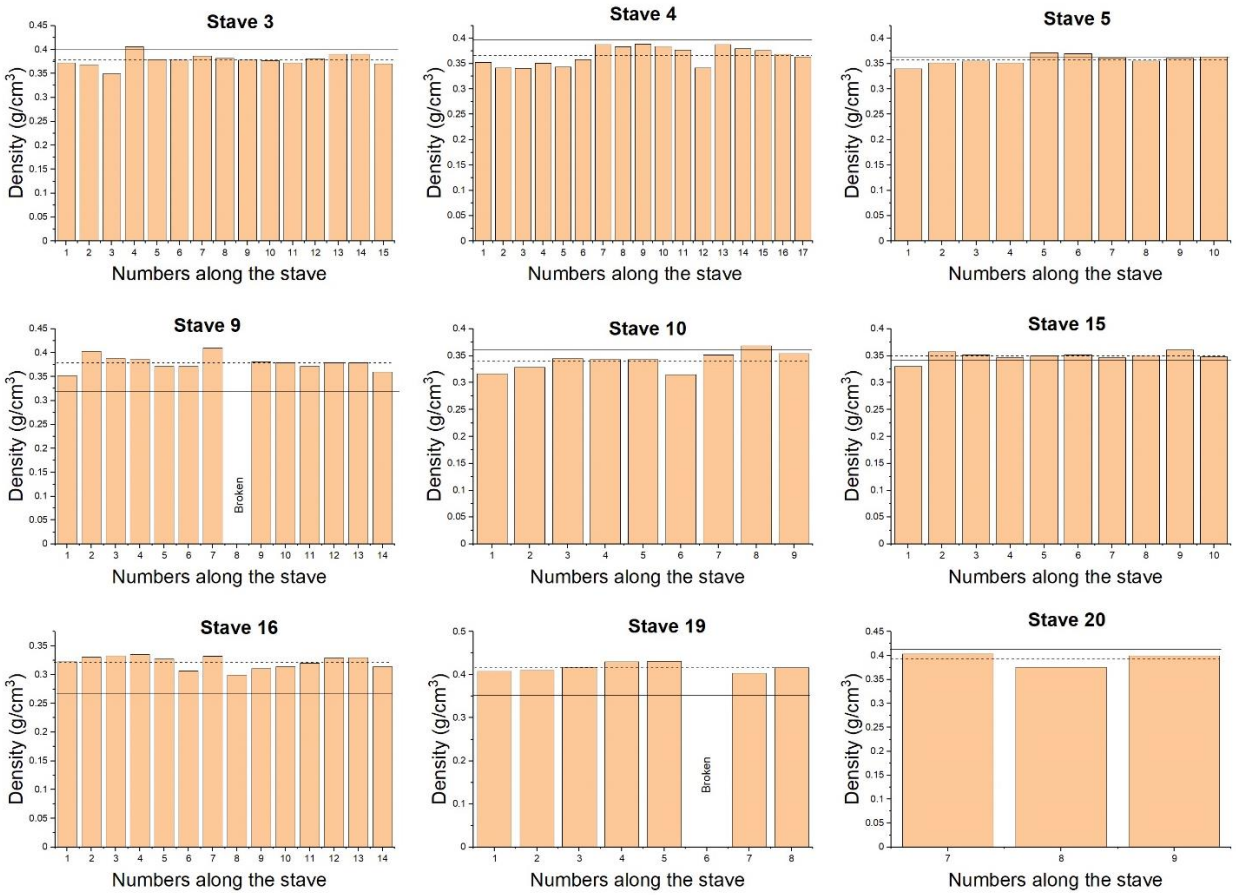

Figure 6-4: Bar grapghs of the densities of staves 3, 4, 5, 9, 10, 15, 16, 19 and 20. These were cut into 1 (or 2 cm) lengths based on weights and dimensions measured at ca. 30% RH. Dashed lines is the average density for each of the pieces. The plain line is the density of the whole staves before it was cut into pices. The density of the whole staves is courtesy of S.Braovac.

6.2.2 Wood treatment

1.1.1.1 Wood preparation-artificially degraded wood

Lengths of 1 cm and 2 cm pieces were cut with a hand saw from the 18 cm sticks of artificially degraded, sound birch. The 2 cm pieces were taken from the middle. A little notch was then put into each piece, so the measurements and photographs can be taken from the same side for correct comparison. The dimensions and weight of each piece were measured, and densities calculated of each piece. Each piece was also scanned on a photocopier and photographed. These will later be used for comparison of before and after treatment.

Table 6-2: Treatments, concentrations and size and number of artifically degraded wood treated.

Treatment	**Concentration**	**Sizes + number of pieces**
Chitosan in 0.01M acetic acid	5%	1 (2x1x1 cm)
Chitosan acetate	10%	2 (1x1x1 cm) 1 (2x1x1 cm)
AEA	2%	2 (1x1x1 cm)
HEA	4%	2 (1x1x1 cm) 1 (2x1x1 cm)
PEG	20%	2 (1x1x1 cm) 1 (2x1x1 cm)
PEG and AEA	20% PEG in 2% AEA	2 (1x1x1 cm)
PEG and Chitosan acetate	20% PEG and 5% Chitosan acetate	1 (2x1x1 cm)
Water		2 (1x1x1 cm)

The samples for aqueous experiments were saturated with water before treatment overnight and then placed in a vacuum immersion chamber for 2x10 min. Finally, the wood was placed in the treatment solution: 2x1 cm pieces in one vial and the 2 cm piece in another (see Table 6-2). They were then left in the solutions for 2 weeks. The surface was wiped off with cotton buds and the pieces of wood then freeze-dried with a labconco free zone triad freeze drier (model 7400030).

The weight and dimension measurements were taken at room temperature and ambient humidity before and after treatment, but RH was in a similar range: 35% RH before, 36% RH after treatment.

The concentrations chosen in Table 6-2 were based on the consistency of the treatment solutions: too thick and the treatment is unlikely to penetrate the wood, but the highest concentration is likely to produce the best consolidation results. Hence the chosen concentration for chitosan and aminocellulose were arbitrarily chosen based the highest concentration possible without the solution becoming incredibly viscous. The concentrations can be varied to obtain the best treatment if the treatment appears to be successful.

6.2.2.1 Wood preparation-archaeological degraded wood

The waterlogged archaeological oak pieces were obtained from storage at the museum (unknown origin) and were used as the highly degraded archaeological wood samples. The wood was stored in water at the museum and hence was still waterlogged. The wood was cut into 1.5x1.5x2 cm pieces and patted with paper to dry the surface; this was then placed in a pre-weight beaker of water and the weight difference measured on a 4 decimal place balance was used as the weight of the waterlogged wood. The samples were then measured with a caliper and photographed as described below. Then the samples were placed in treatment baths given in Table 6-3. They were then left in the solutions for 2 weeks. The surface was wiped off with cotton buds and and the pieces of wood then freeze dried with a labconco free zone triad freeze drier (model 7400030). The treatment concentrations were chosen based on viscosity. If the

viscosity is too high, it is unlikely the consolidant will seep into the wood. A concentration of 10% was chosen for Chitosan and HEA, but this appeared too viscous in the case of HEA, so the HEA was diluted to 5%. 3 concentrations of PEG were chosen as the required concentration is based on degree of degradation. Concentrations of 20% and 40% are often used so these were chosen. 10 percent was used as a lower concentration, the same concentration as chitosan and double that of HEA for easier comparison.

Table 6-3: Treatments and concentrations used for archaeological wood.

Treatment	**Concentration**
Chitosan in 0.01 M acetic acid	10%
Chitosan acetate	10%
AEA	2%
HEA	5%
PEG	10%
PEG	20%
PEG	40%
PEG and HEA	20% PEG and 5% HEA
PEG and Chitosan acetate	20% PEG and 5% Chitosan acetate
Water	

ASE and swelling measurements were carried out at ~32% RH.

They were calculated as follows:

$$\text{Swelling} = \frac{new\ volume - orginal\ volume}{original\ volume}\ x100 \qquad \textbf{5-1}$$

$$\text{ASE} = \frac{\Delta\ volume\ of\ treatment - \Delta\ volume\ of\ oven\ dried}{\Delta\ volume\ of\ oven\ dried} \qquad \textbf{5-2}$$

Where $\Delta\ volume = new\ volume - original\ volume$

6.2.3 Analysis and documentation after treatment

6.2.3.1 Weight and dimensions

The weights were measured on a four-decimal balance. Dimensions in millimetres were recorded with a two decimal place digital caliper. The dimensions and weight were used to calculate density. The density is an approximation as some samples are not perfectly square, but as the samples were measured before and after in the same manner, this was not considered a problem. The change in density, volume and weight from different treatments can then be compared. Each time the dimensions were measured in the same place the notch was made on one side, in order to distinguish which side faces upwards and the measurements were taken in the middle to try and ensure the same place was measured each time.

6.2.3.2 Photographs and scans

Each side of each piece of wood was scanned on a photocopier before and after treatment. This was less time consuming than photographing each side and the scans are to scale. However, photographs have depth and have better resolution. Together both can be used to document changes resulting from the treatment.

6.2.3.3 Spectrophotometer

A hand-held spectrophotometer from Konica Minolta, CM-700d, was used to measure samples before and after treatment using the 4 mm aperture and the spectral component excluded (SCE) mode. This measures three chromatic coordinates of the CIELAB

colour system. The total colour change ΔE is based on three chromatic coordinates of the CIELAB colour system a* (green-red axis), b* (blue-yellow axis) and L*(white-black axis, hence lightness). It is calculated from Eq. 5.3.

$$\Delta E^*_{2,1} = [(\Delta L^*)_2 + (\Delta a^*)_2 + (\Delta b^*)_2]^{1/2} \quad \textbf{5-3}$$

For artificially degraded wood, the measurements were taken before and after hence calculatation from eq 5.3 was used. For the archaeological wood results were compared to control hence Eq. 5.4 was used, spectrophotometers measure l, a and b. l the lightness and a and b chromaticity indices.

$$\Delta E = \sqrt{(l - lc)^2 + (a - ac)^2 + (b - bc)^2} \quad \textbf{5-4}$$

c for control lc, average ac, bc and l, a, b of untreated wood.

6.2.3.4 Sample preparation for IR and SEM

6.2.3.4.1 Fourier-transform Infrared spectroscopy (FTIR)

FTIR spectra in ATR mode were recorded on a Thermo Scientific Nicolet iS50 spectrometer, equipped with a diamond crystal and DTGS detector. Spectra were recorded with 32 scans at 4 cm^{-1} resolution, within the range 4000–400 cm^{-1}. Spectra of each treated sample were compared to that of the control sample and to that of the pure consolidant to determine the consolidant's presence in the wood. The surface and core of the wood samples were also compared to assess consolidants' distribution.

6.2.3.4.2 Scanning electron microscopy - energy dispersive X-ray spectroscopy (SEM-EDS)

Analyses were performed using a FEI Quanta 450 Scanning Electron Microscope coupled with an Oxford X-Max^N 50 mm^2 detector, using low vacuum mode at (70 Pa) and a voltage of 15 kV. The spot size, working distance (~10 mm) and pressure were modified depending on the sample.

SEM was used to see if the consolidants could be detected within the wood and to try and establish how they interact with the wood, i.e. whether cells are filled, lined or if only the vessels are filled or lined. SEM can also tell whether an attempt at consolidation may have damaged the cells in the process. The EDS can also be used to confirm penetration and how it fills the wood when elements other than carbon and oxygen are in the consolidant.

6.2.3.4.3 X-ray tomography

The tomographic microscopy and coherent radiology experiments (TOMCAT) were carried out at the Paul Scherrer Institute (PSI) in Switzerland to obtain tomographic microscopy images of the wood, Broavac carried out the analysis on my behalf. They were carried out on a TOMCAT-X02DAa; analysis was carried out at 12 keV, with an exposure time of 200 ms, at a 10 mm distance with both absorption and phase contrast mode, phase constrast delta 1x10-7 and phase contrast beta 1x10-9.

6.2.4 Strength/consolidation

6.2.4.1 Fruit Penetrometer – Hardness

Hardness is an important factor for conservation, the wood must be made stronger. To numerically establish if the treatments successfully consolidated the wood and added strength and to what extent, a fruit penetrometer was used to determine the hardness of the wood. This method has previously been used by Petrou and Pournou (2018) to evaluate the level of degradation of waterlogged archaeological wood. It was thought this method could possibly be applied to treated and untreated wood to establish consolidation. The fruit penetrometer handle was turned 200^{o} to 1.1mm depth into the wood and the force was recorded. This was carried out on the 4 outer sides on the wood, but not the cross section.

6.2.4.2 Tape test –consolidation of surface

Surface consolidation was evaluated using the 'tape test'. This sort of method has previously been used to investigate stone consolidation (Drdácký et al., 2012). It was recommended for this research by members of the Saving Oseberg group. They are working on standardising this method for wood. Double-sided tape was purchased from a local hardware store by a member of the saving Oseberg group, Clas Ohlson brand. 1 cm squares of tape were backed on to paper and the silicone release paper on the other side was removed. Each piece was weighed. It was then applied to the sample surface using as consistent pressure as possible, rubbing three times with one finger. The tape was then removed, weighed again and photographed. This was carried out

with all 6 sides of the wood to calculate the average and average standard deviation. If the wood was consolidated well, there would be little material removed from the sample. The extent of powder removed was evaluated on a scale of 1 to 5, where 1 had little removal, while 5 had most powder removed. Category assignment was performed, in instances when both powder and larger pieces are removed from the sample; the extent of removal of powder is prioritized over the extent of removal of larger pieces. For example, the removal of one large piece would be given a category 2, as little powder was removed, even though the total weight removed was high. This distinguishes samples with poor/no consolidation from those with good, but weak, consolidation.

6.2.4.3 3-point bend test

3-point bend test was performed on treated balsa wood (15x0.5x0.5 cm) to assess increase in strength from treatment variations of HEA and PEG. Treatments of 2% HEA, 4% HEA, 4% HEA+5% PEG, 2% HEA+10% PEG, 10% PEG and 5% PEG treated balsa wood were compared untreated and water controls. Two other treatments 5% chitosan in 0.1M acetic acid and 5% chitosan in 0.1M acetic acid followed by rinsing in water and immsersion in 10% vanillin in 10% ethanol were also investigated. The wood was immersed in water in a vacuum chamber until no more air bubbles were removed. The wood was then immersed in treeatment solution for 2 weeks and then freeze dried. The weight and measurements were recorded before and after treatment.

A stable micro system TA.HD.plus texture analyser was used determine the force at fracture point and the slope at the steepest point of force vs distance to calculate the

MOE and MOR. The cross head was lowered at 1 mm/s and the wood distance length for 3-point bend was 40 mm.

6.3 Results

6.3.1 Weight and volume change of artificially degraded wood

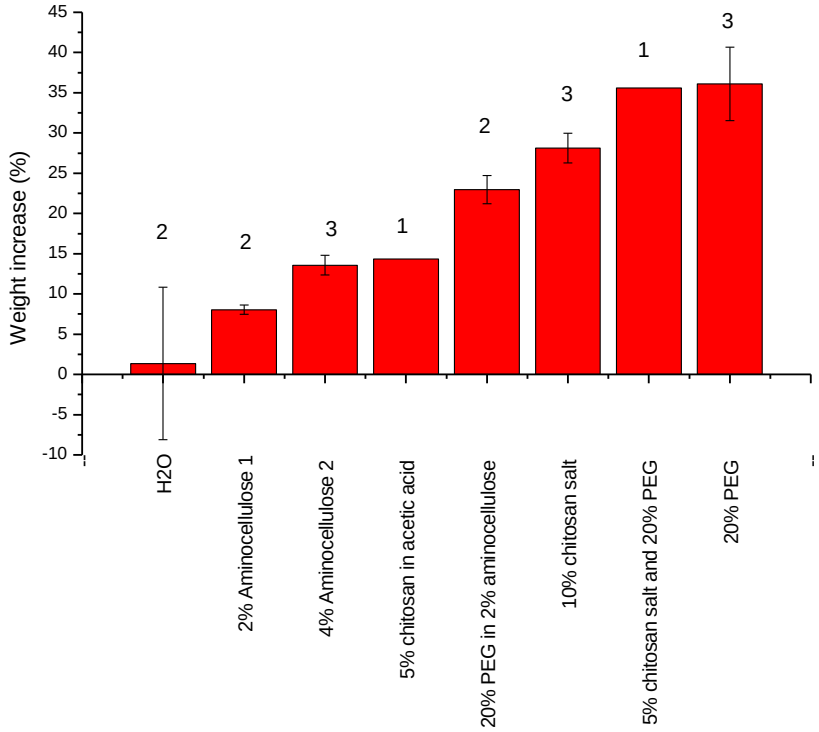

Figure 6-5: Percentage weight increase of different treatments on artificially degraded wood. Numbers above are the number of pieces of wood treated with each treatment.

Weight increase showed that the treatment material was taken up by the wood. Volume change is also important to assess, as a change in volume could cause cracking and deform designs on the artefacts.

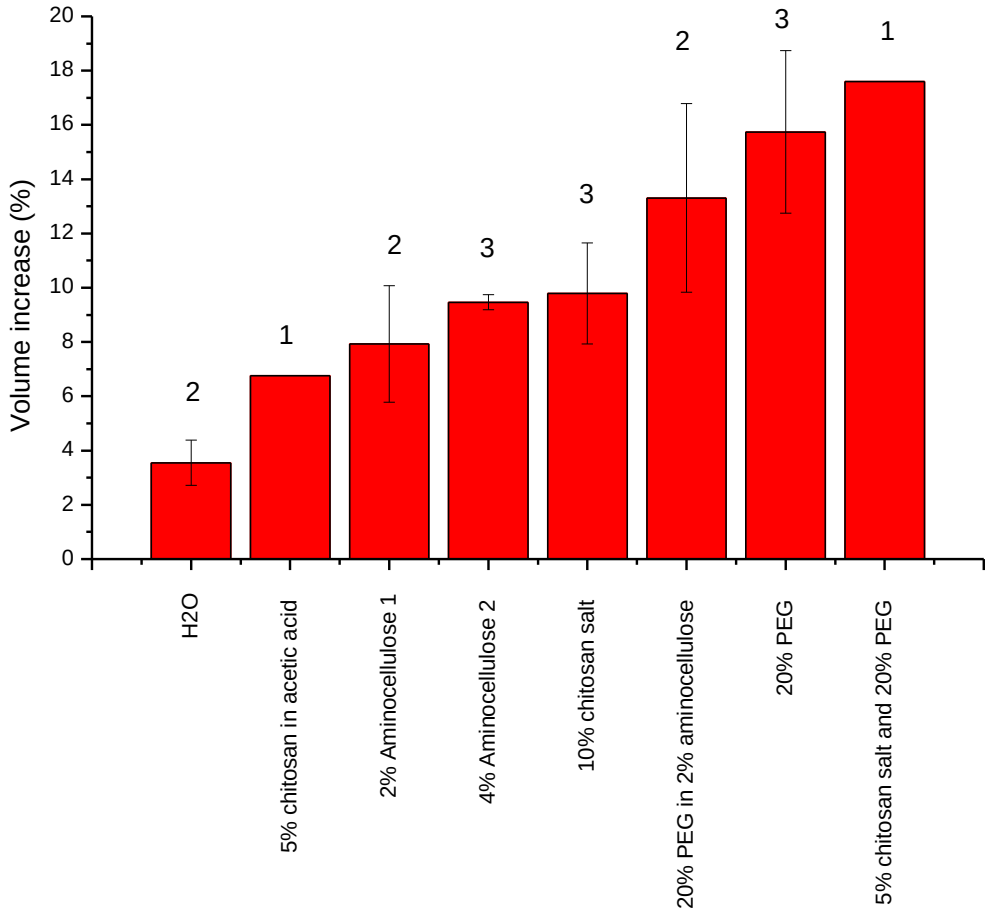

Figure 6-6: Percentage volume increase for different treatments on artificially degraded wood.

Figure 6-5 shows the percentage weight increase of the wood samples after treatment. Comparing the weight increase alone would be misleading as it is dependent on the size of the piece of wood: a larger piece of wood could take up more consolidant. According to Figure 6-5, water shows a large increase; however, the standard deviations reveals there is a larger error margin. Hence, some wood gained weight and some lost weight. Aminocellulose 1 and 2 (AEA and HEA) show the smallest weight change from treatments, which is expected, as they have the lowest concentration and therefore have a much lower percentage increase. For PEG however, the increase in weight is much higher, but the results more variable. Aminocellulose with PEG

showed a lower increase in weight compared to PEG alone, but less variable results than PEG alone. Chitosan in acetic acid has a lower weight increase compared to chitosan acetate salt, however, concentrations can account for this. Chitosan salt and PEG show similar weight gain to that of PEG alone.

Figure 6-6 shows percentage volume change vs. treatment methods. The standard treatment, PEG, showed a 15 % volume change. Almost all other treatments were lower than this. The chitosan in acetic acid showed the least volume change (Figure 6-6) and showed a smaller volume change than the chitosan salt. Combining PEG with chitosan salt increased the volume change. Combined with aminocellulose, the volume change was lowered. The aminocelluloses have a mid-range volume change, higher than that of the control, but more than a third less than PEG.

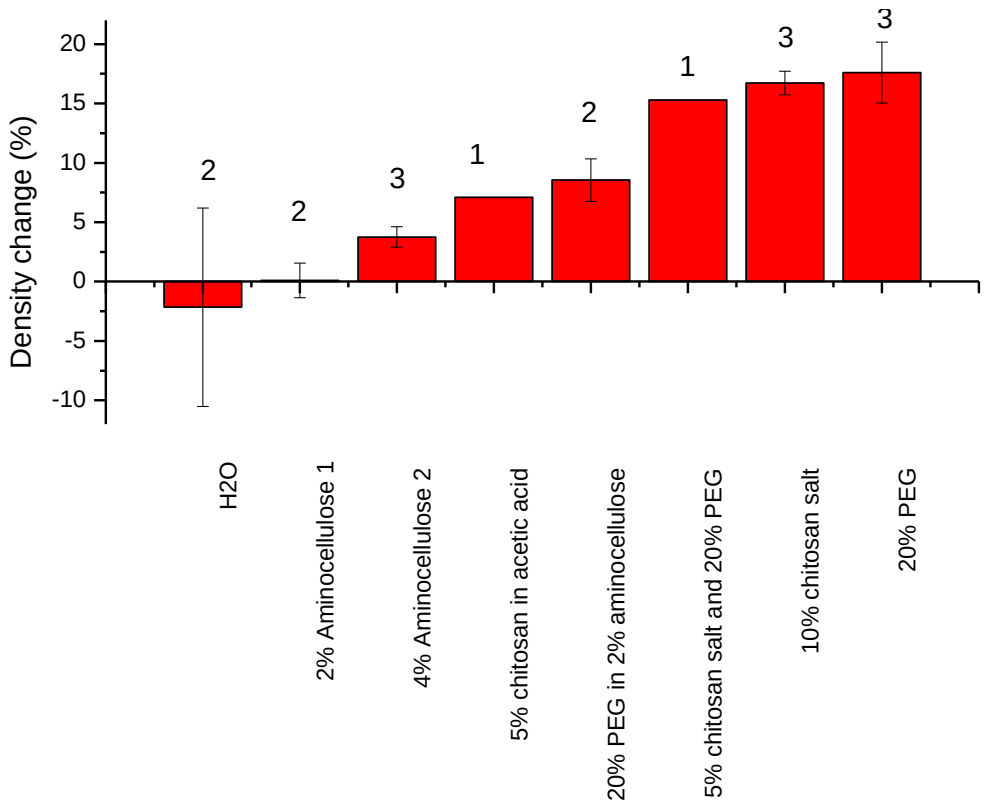

Figure 6-7: Density change for different aq. treatments on artificially degraded wood.

Figure 6-7 shows the density change, hence, increase in weight but takes into account the volume of the pieces of wood and the volume change. Aminocellulose 1 and 2 show the smallest density change. Chitosan salt has resulted in a density increase nearly as high as PEG. This is also the case with PEG and chitosan combined, but not with aminocellulose 2 and PEG.

6.3.2 ASE and density of treated archaeological wood

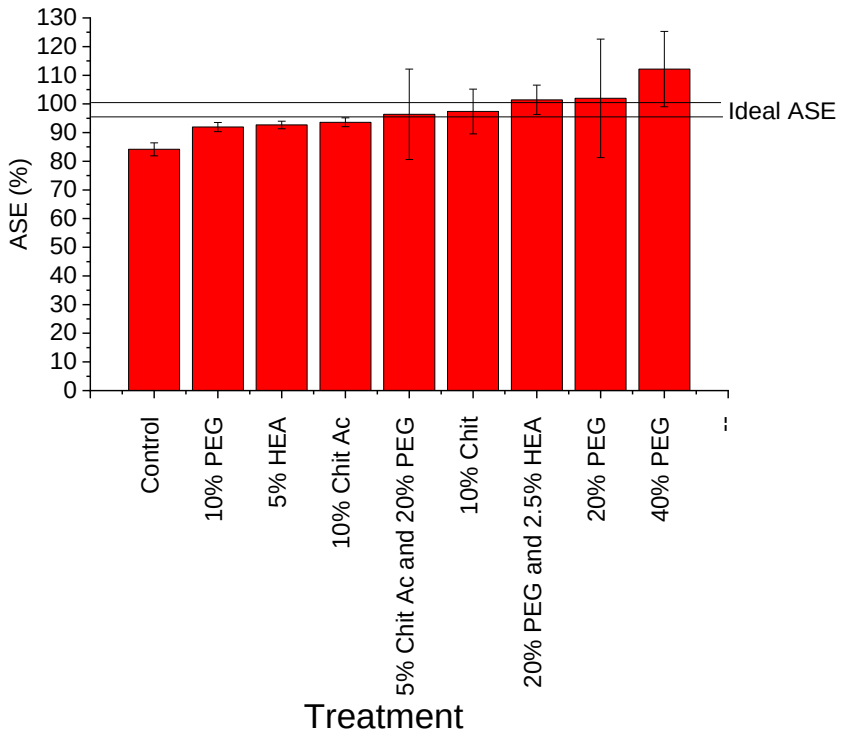

Figure 6-8: ASE for different aq. treatments on archaeological wood.

Anti-shrink efficiency (ASE) of different treatments (Figure 6-8 and Figure 6-9) shows that 20% PEG 2000, the most commonly used treatment in conservation, gave varied results but on average resulted in only a slight swelling. The variety of results can be seen in Figure 6-9. Chitosan acetate salt, by contrast, shows a much lower ASE, but had more consistent results, a small improvement over 10% PEG, but probably not statistically valid. Aminocellulose results are also varied, although not as much as

PEG. Aminocellulose showed improved ASE compared to 10% PEG, despite being half the concentration. The mixture of aminocellulose and PEG appears to strike a good balance, with more consistent results (see standard deviation in Figure 6-8 and raw data Figure 6-9) but still only very slight swelling on average (Figure 6-6). 40% PEG resulted in swelling (Figure 6-6). Figure 6-9 shows two samples swelling; one shrank though only slightly.

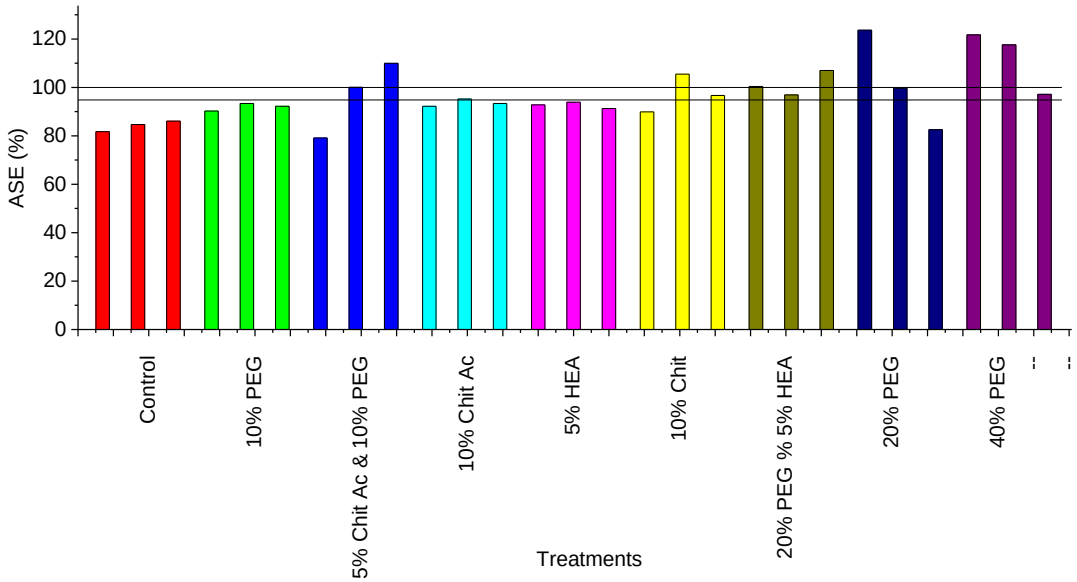

Figure 6-9: ASE each piece of archaeological wood showing treatment method.

A higher density would suggest greater uptake of the consolidant material. However, the variation in the archaeological wood means it is very difficult to separate the uptake of consolidants compared to variation in the wood. The control of just three pieces already shows great variation. There is however, an increase above the variation seen in the control, suggesting all consolidants were absorbed by the wood. Aminocellulose 2 and aminocellulose with PEG showed similar density to 20% PEG (Figure 6-10).

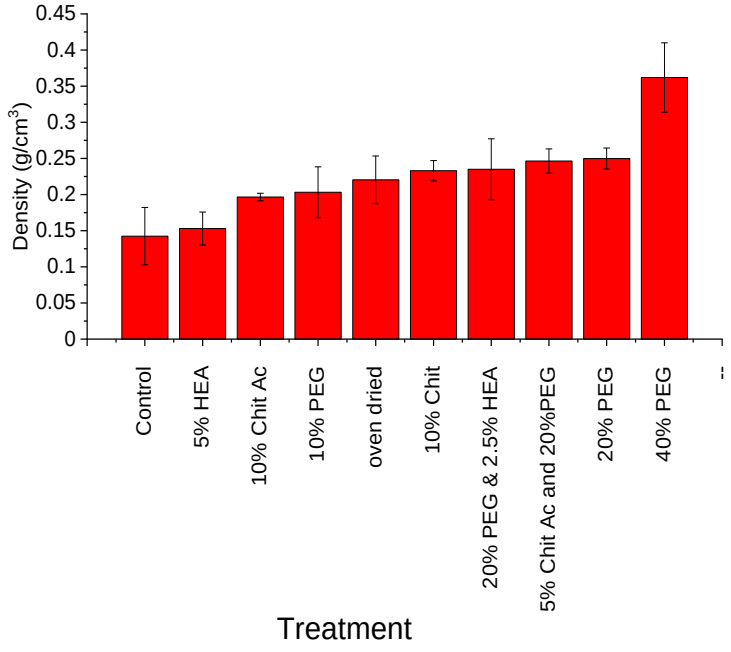

Figure 6-10: Density (g/cm^3) of treated archaeological wood.

6.3.3 Consolidation of untreated and treated archaeological wood

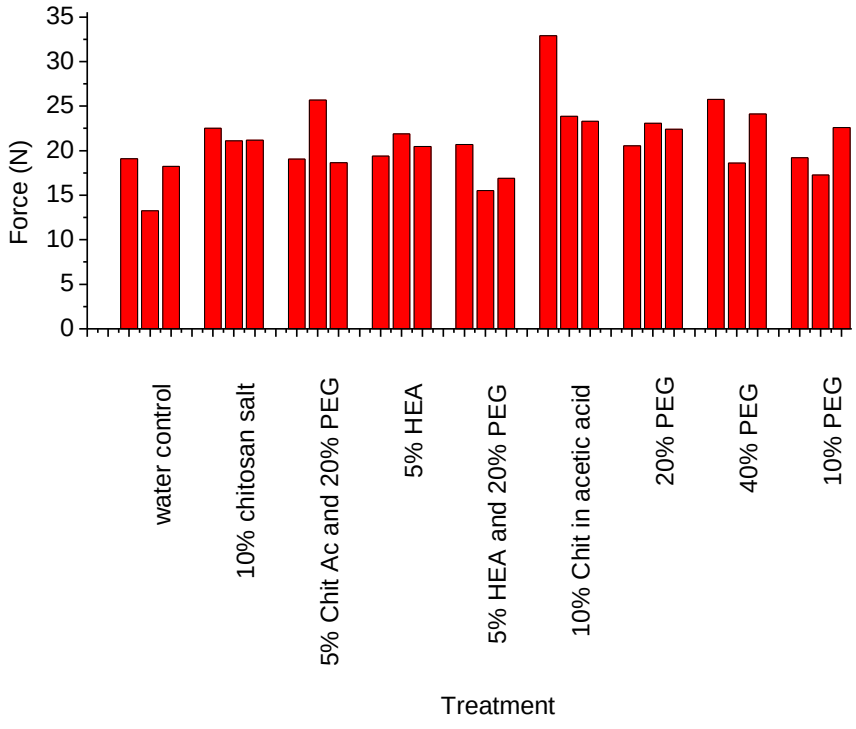

Figure 6-11: Force (N) vs treatments of aqueous treated archaeological wood.

In Figure 6-11, hardness alone is established by the force (N) taken to rotate 200^{O}, i.e. deform to a depth of 1.1 mm. This produced such variable results for the control that it was impossible to say with any certainty that hardness was due to the consolidant, rather than the variability in the wood. It was decided to combine this data with the density, to try to separate the effects of consolidants from the effects of variability in the wood. Figure 6-12 showed this did separate results, but still not enough to make definitive conclusions. However, 40% PEG does appear to have improved the properties of the wood.

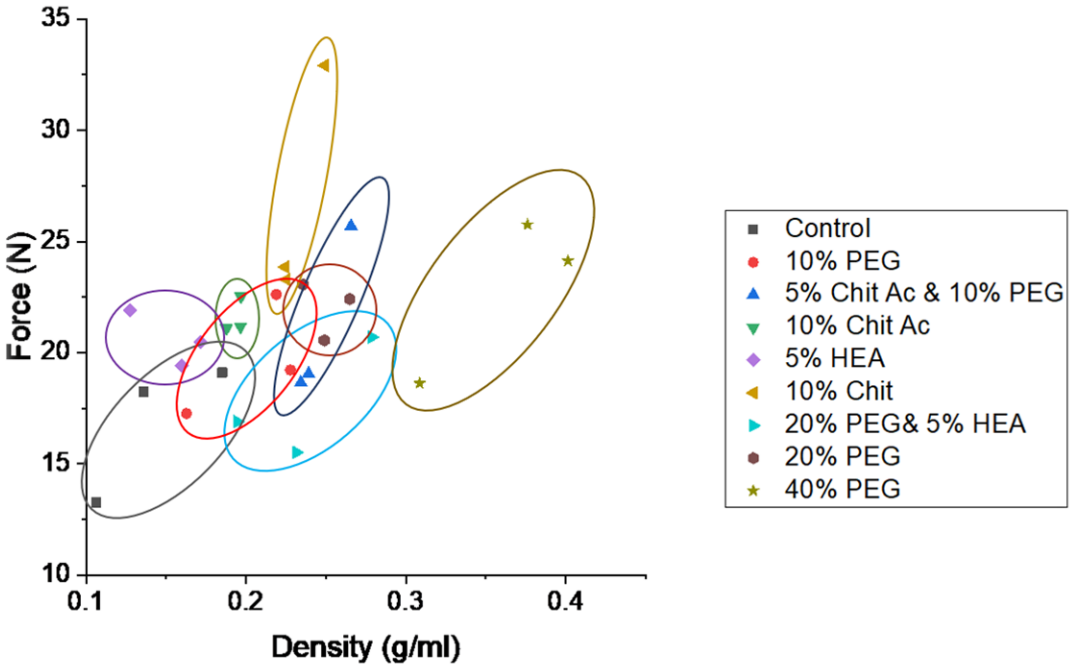

Figure 6-12: Density (g/cm^3) vs hardness/force (N) of aqueous treated archaeological wood.

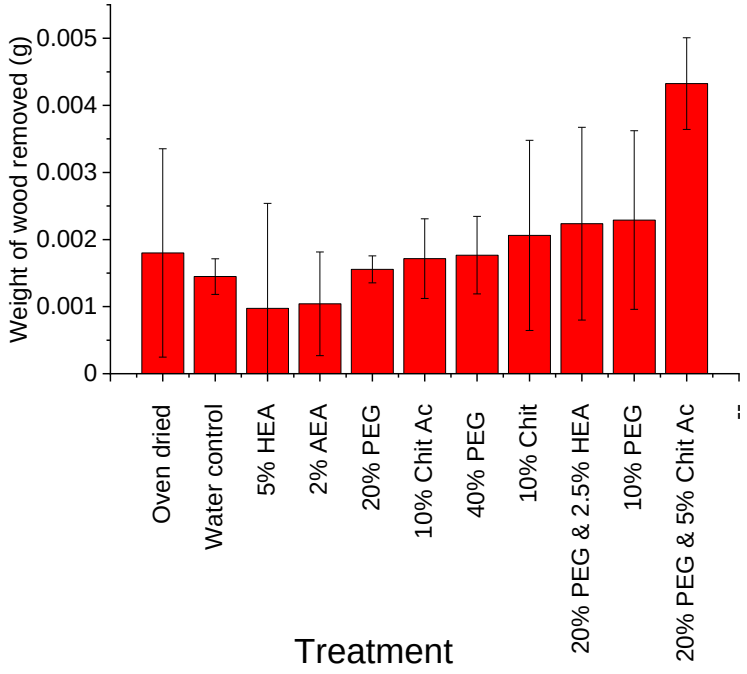

Figure 6-13: Surface consolidation of aqueous treated archaeological wood (weight of wood removed during tape test).

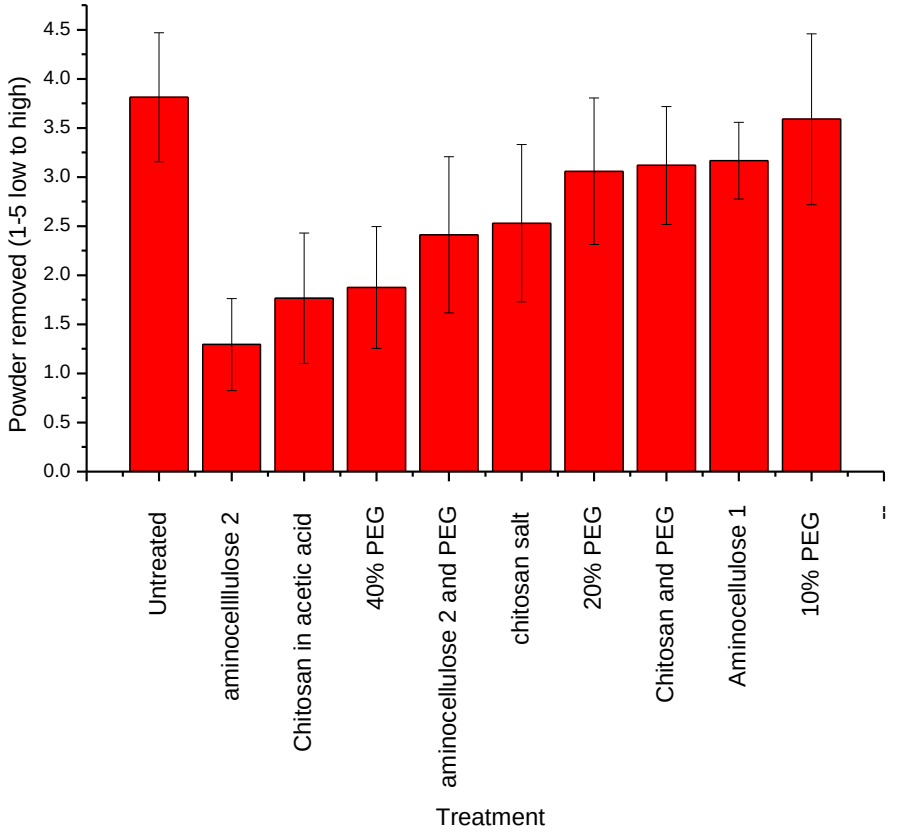

Figure 6-14: Extent of powder removed using the tape test (average with stdv of powder removed according to photos 1-5 low powder to high powder (fine)).

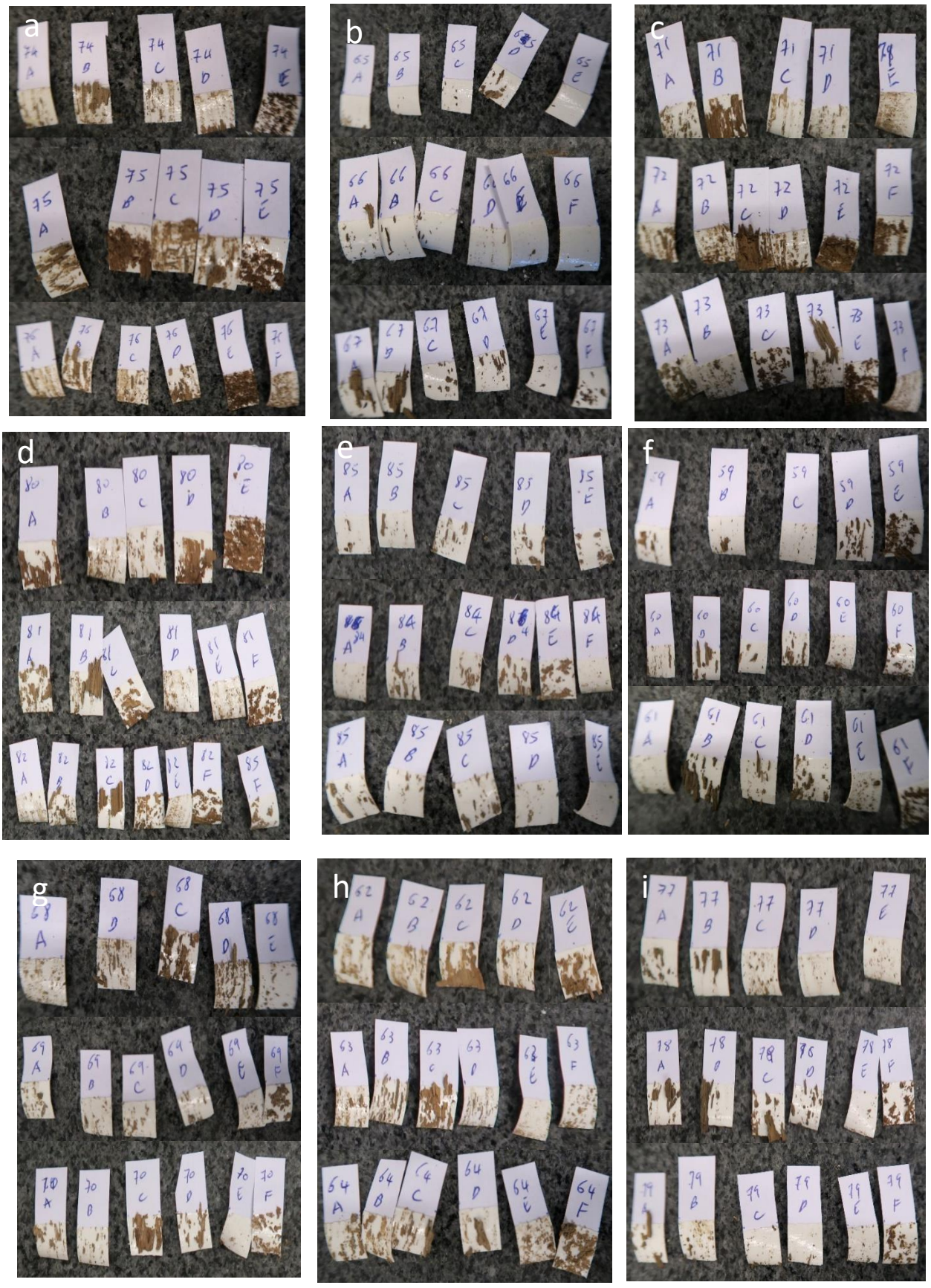

Figure 6-15: Photographs of tape results showing powder removed from treated and untreated archaeological wood. a) water control, b) aminocellulose 2, c) 10% PEG, d) 20% PEG, e) 40% PEG, f) chitosan salt, g) aminocellulose 2 and PEG, h) chitosan and PEG and i) chitosan in acetic acid.

Figure 6-16: Powder removed from 2% aminocelulose 1 (AEA) treated wood.

Figure 6-13 shows weight removed. The photographs (Figure 6-15 and Figure 6-16) show the powder removed from each sample by the tape test. Figure 6-14 summarises this using a scale from 1 (low amount of powder removed) to 5 (higher amounts of powder removed), showing a larger amount was removed from the control than the other samples. Aminocellulose clearly shows the least removed. The mixture of aminocellulose and PEG shows a larger quantity removed; however, what is removed is mainly large chunks, rather than fine powder, suggesting some consolidation. After aminocellulose, 40% PEG shows the least powder, 10% PEG is similar to the control, 20% PEG shows a lot removed as well, but some of it is larger chunks suggesting some consolidation. Chitosan in acetic acid is also very promising. The wood that is removed by the tape is in larger pieces, again suggesting consolidation. Chitosan acetate is less promising than chitosan, but again larger pieces are seen, rather than the fine powder seen in the control. Mixtures with chitosan acetate and PEG seem worse than chitosan acetate alone. Aminocellulose is less promising, but that would be due to the lower concentration used.

6.3.4 Consolidation – cutting the wood observations

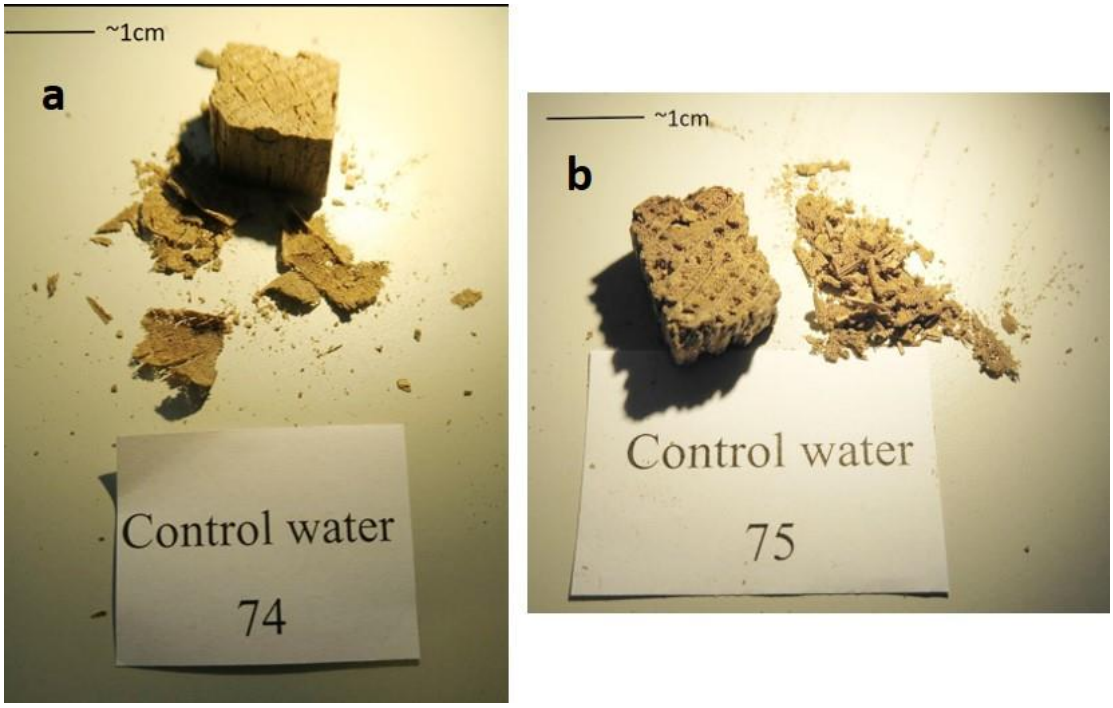

Figure 6-17: Photographs showing results of slicing a.) water control archaeological wood (74), b.) water control archaeological wood (75).

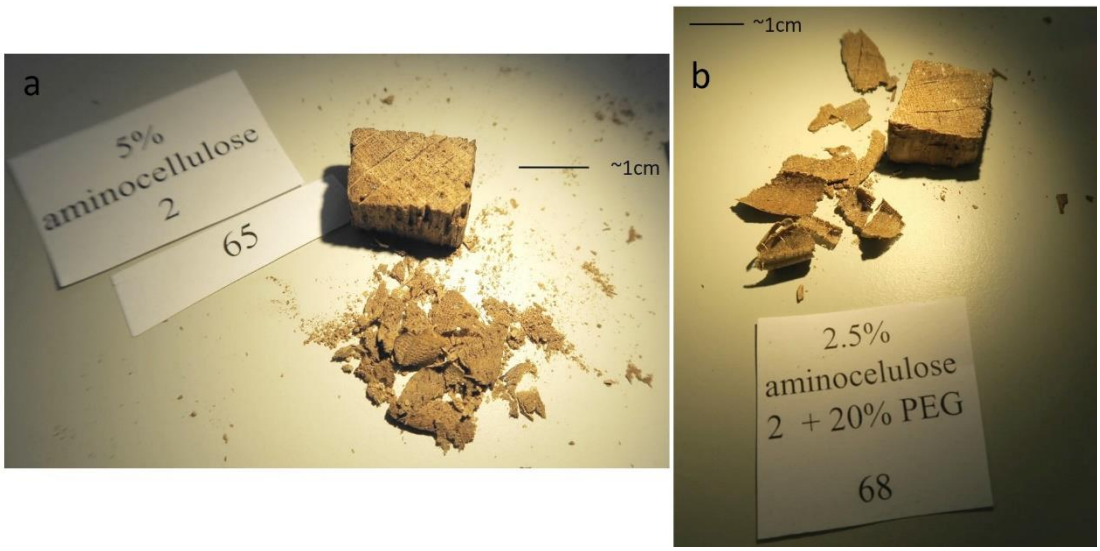

Figure 6-18: Photographs showing results of slicing a.) 5% aminocellulose-treated archaeological wood (65), b.) 2.5% aminocellulose and 20% PEG treated archaeological wood (68).

Figure 6-19: Photographs showing results of slicing a.) chitosan acetate treated archaeological wood (59),b.) 10% chitosan in acetic acid treated archaeological wood (77) c.) chitosan acetate and PEG-treated archaeological wood (62), d.) 10% PEG- treated archaeological wood (71).

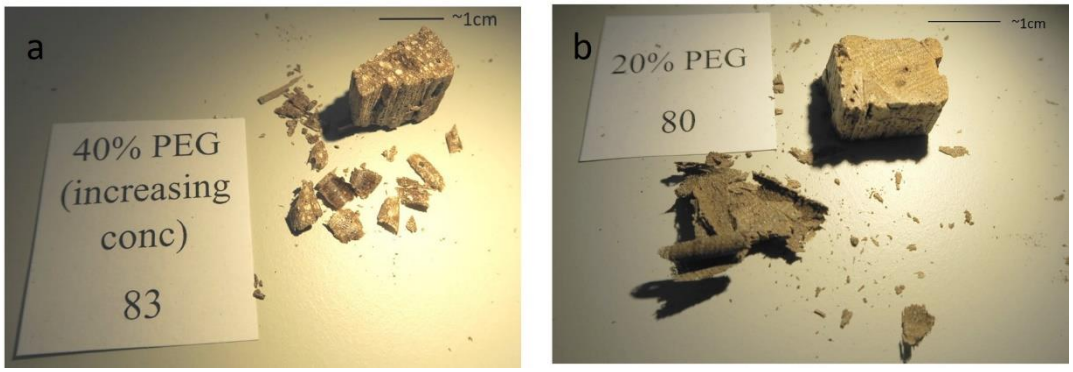

Figure 6-20: Photographs showing results of slicing a) 40% PEG treated archaeological wood by increasing concentration (83), b.) 20% PEG treated archaeological wood (80).

Photographs inside the centre of the wood show the consolidant in some cases and shows how brittle the wood is. When the centre of the wood was sliced with a razor blade to get a clean cut (a microtome was tried, but the surface was not smooth enough for SEM so a razor blade was used to slice it to get a smooth surface), it became clear which pieces of wood were more consolidated. The water controls also show the variation in the wood without treatment. Sample 74 (Figure 6-17 a) was in better condition and the wood could be removed in slices to some extent, whereas sample 75 (Figure 6-17 b) resulted completely in powder. Aminocellulose 2 (HEA) sample 65 (Figure 6-18 a) also produced slices indicative of consolidation. The mixture of aminocellulose and PEG sample 68 (Figure 6-18 b) showed very good consolidation. 10% chitosan acetate sample 59 (Figure 6-19 a) was also very powdery when sliced, as was the mixture of chitosan acetate with PEG sample 62 (Figure 6-19 c). 10% chitosan in acetic acid sample 77 (Figure 6-19 b) showed good consolidation, with the wood coming off in slices, rather than powder. This again suggests that, chitosan in acetic acid is a better consolidant than chitosan acetate. 10% PEG sample 71 showed some consolidation (Figure 6-19 d), 40% PEG sample 80 exhibited very good consolidation (Figure 6-20 a) and 20% PEG sample 83 (Figure 6-20 b) also revealed very good consolidation.

6.3.5 Colour change from treatments

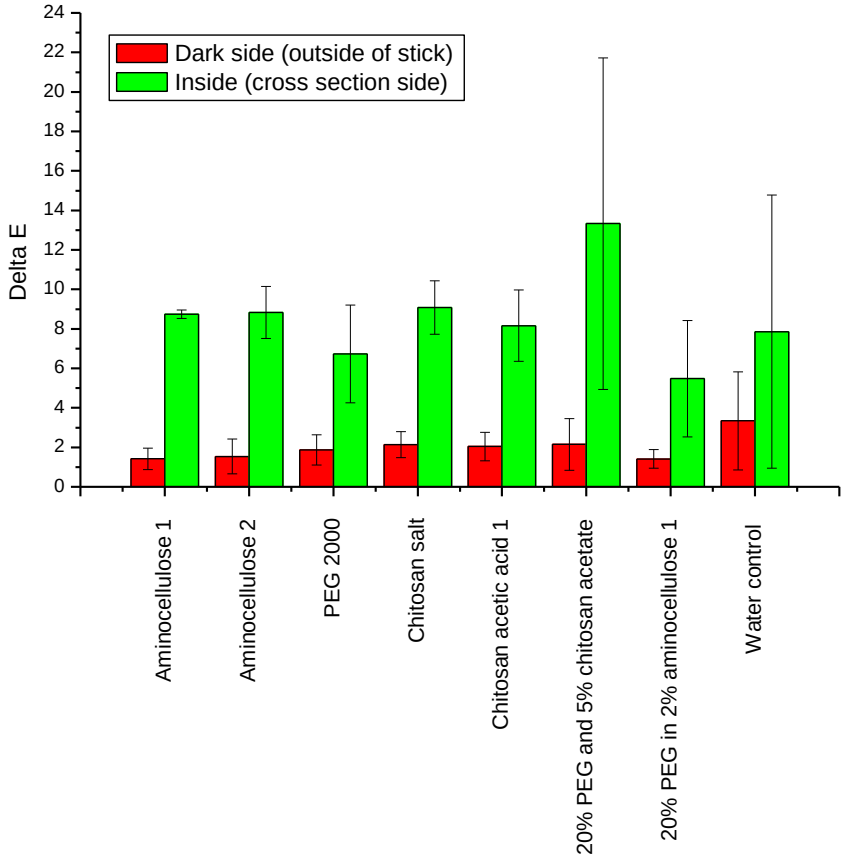

Figure 6-21: Colour change after treatment for artificially degraded wood compared to untreated artificially degraded wood.

ΔE values of 3 and above are visible to the naked eye ((Shiraishi and Hon 2001). Hence, the colour change of treatment on the dark side of the wood is not distinguishable. The ΔE of the light wood, i.e. the inside cross section of treated wood, is similar to that of the water control (Figure 6-21). The PEG and chitosan produced the biggest colour changes. Aminocellulose and PEG, and PEG alone produced the smallest colour changes.

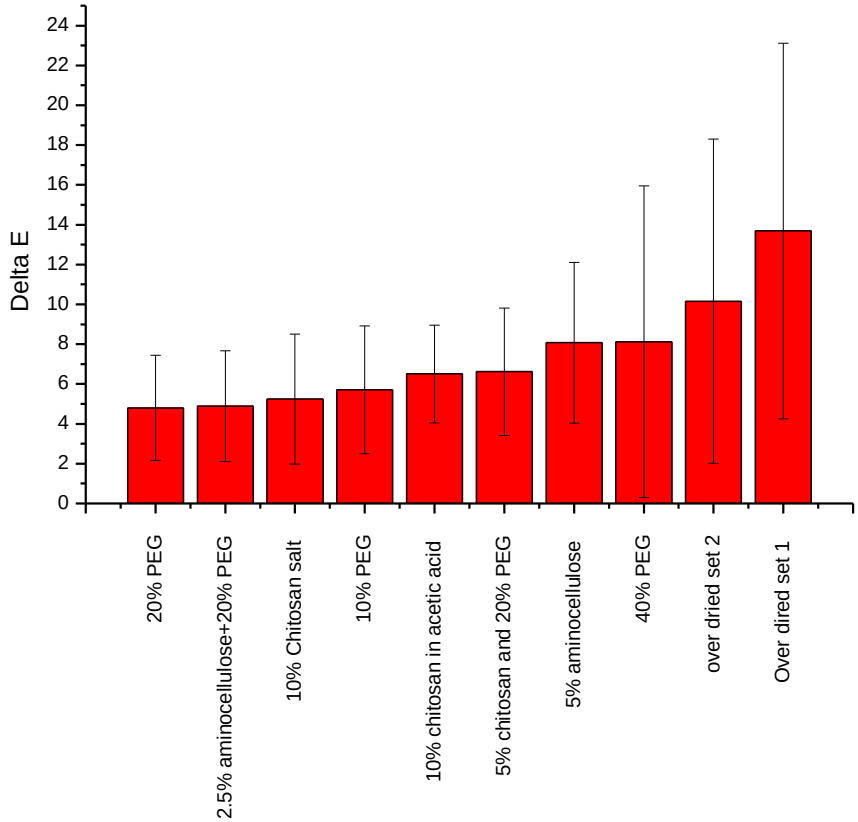

Figure 6-22: Colour change (ΔE) for treated archaeological wood samples compared to water control.

Figure 6-22 indicates colour change of treatment for archaeological wood compared to the water control. The oven dried samples produced the biggest colour change, greater than any of the other treatments. Hence, all treatments are better than air drying the wood. 20% PEG produces the least colour change, followed by aminocellulose and PEG. Aminocellulose does result in a larger colour change, where the wood was slightly darker than all the other treatments. However, this darkening although visible was not extreme. See Figure 6-23 to Figure 6-28

6.3.6 Before and after photograph of treated pieces

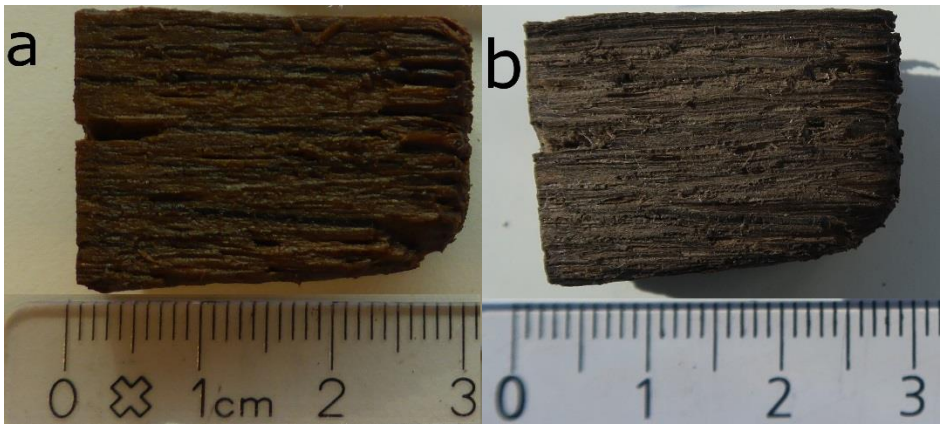

Figure 6-23: Photograph of archaeological waterloged wood pieces a) before treatment, b) after aminocellulose 2 treatment (wood piece number 65).

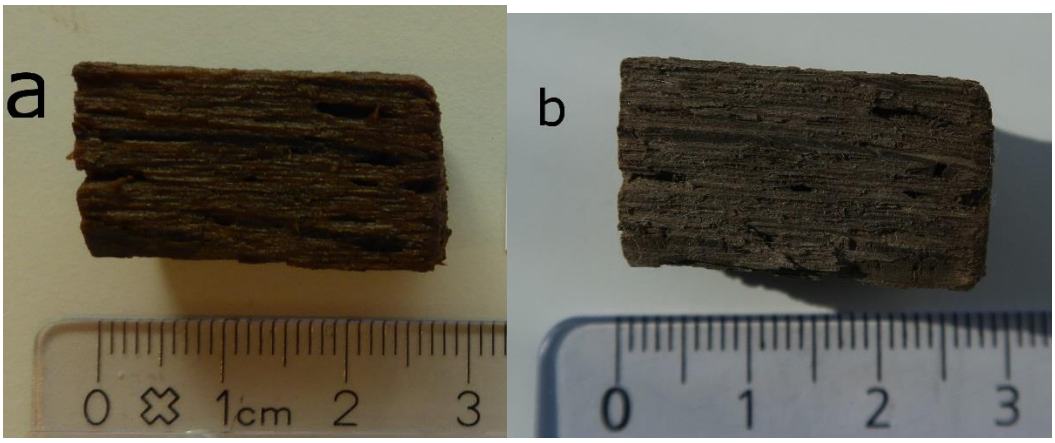

Figure 6-24: Photograph of archaeological waterloged wood pieces a) before treatment, b) after treatment with chitosan acetate (60).

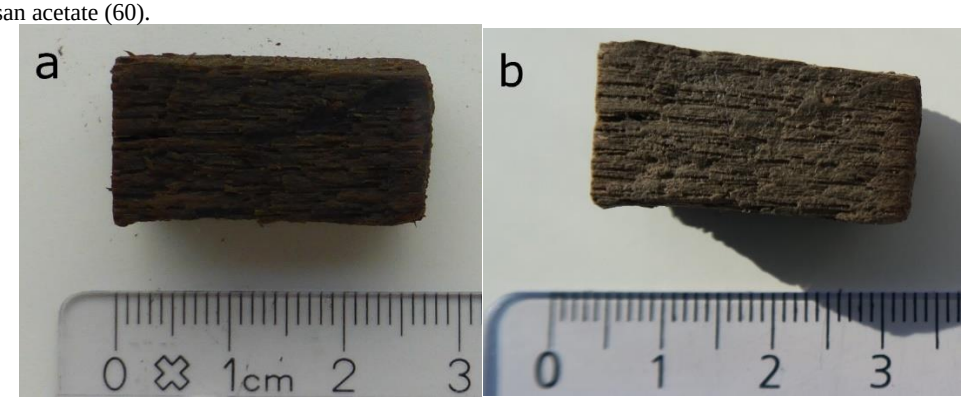

Figure 6-25: Photograph of archaeological waterloged wood pieces a) before treatment, b) after 20% PEG (82).

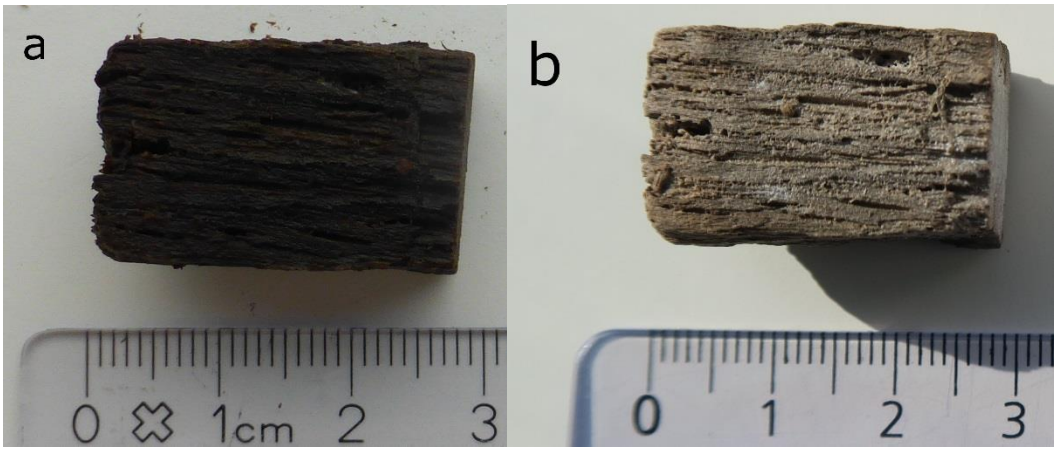

Figure 6-26: Photograph of archaeological waterloged wood pieces a) before, b) after 40% PEG (83).

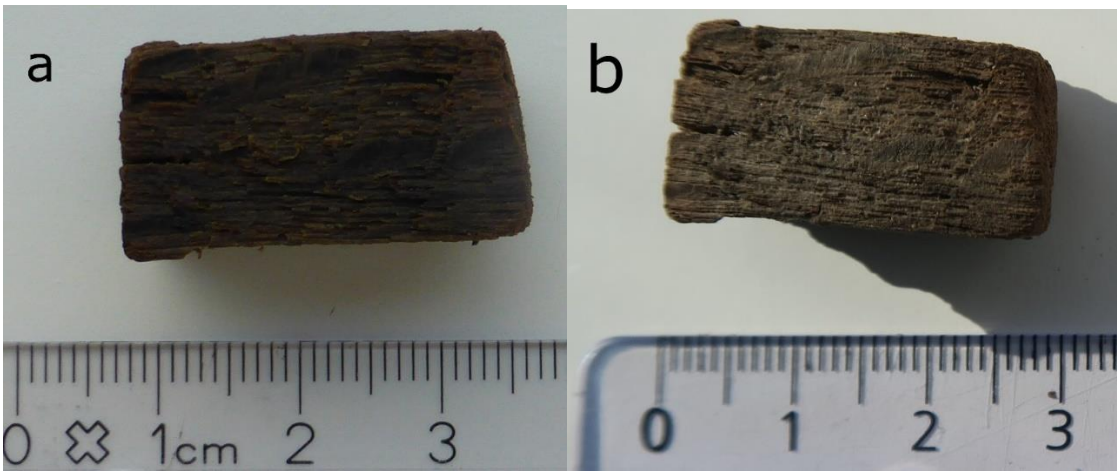

Figure 6-27: Photograph of archaeological waterloged wood pieces a) before, b) after treatment with chitosan in acetic acid (77).

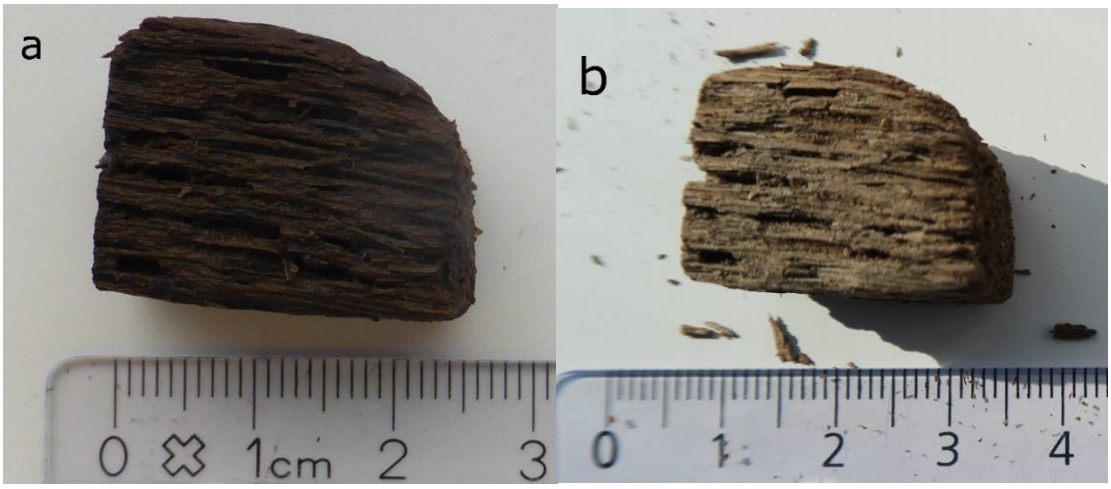

Figure 6-28: Photograph of archaeological waterloged wood pieces a) control before and b) after freeze drying.

Photographs are documented proof that very slight colour changes and changes in volume are barely visible and would not greatly impact interpretation of artefacts and do not greatly affect their aesthetic appearance. More photographs are included in the appendix on each piece of wood.

6.3.7 SEM, IR and X-ray tomography

6.3.7.1 Aminocellulose

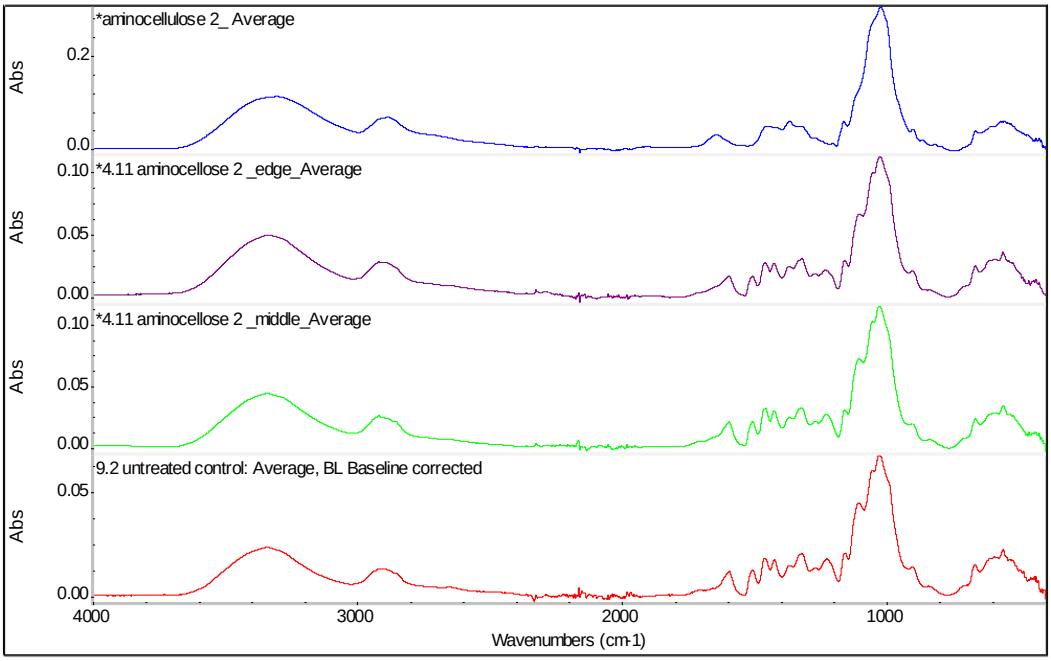

Figure 6-29: IR spectra in descending order of aminocellulose 2 (HEA), treated wood edge, middle and untreated laboratory degraded.

IR of aminocellulose 2 (HEA) (Figure 6-29), treated wood and untreated wood shows that aminocellulose is too similar to that of lab degraded wood. Hence, it is impossible to establish where the aminocellulose has managed to penetrate the lab degraded wood from the IR spectra Figure 6-29

The IR of PEG treated wood (Figure 6-30) clearly shows the presence of PEG at 2883 and 841 cm^{-1} in the middle of the wood.

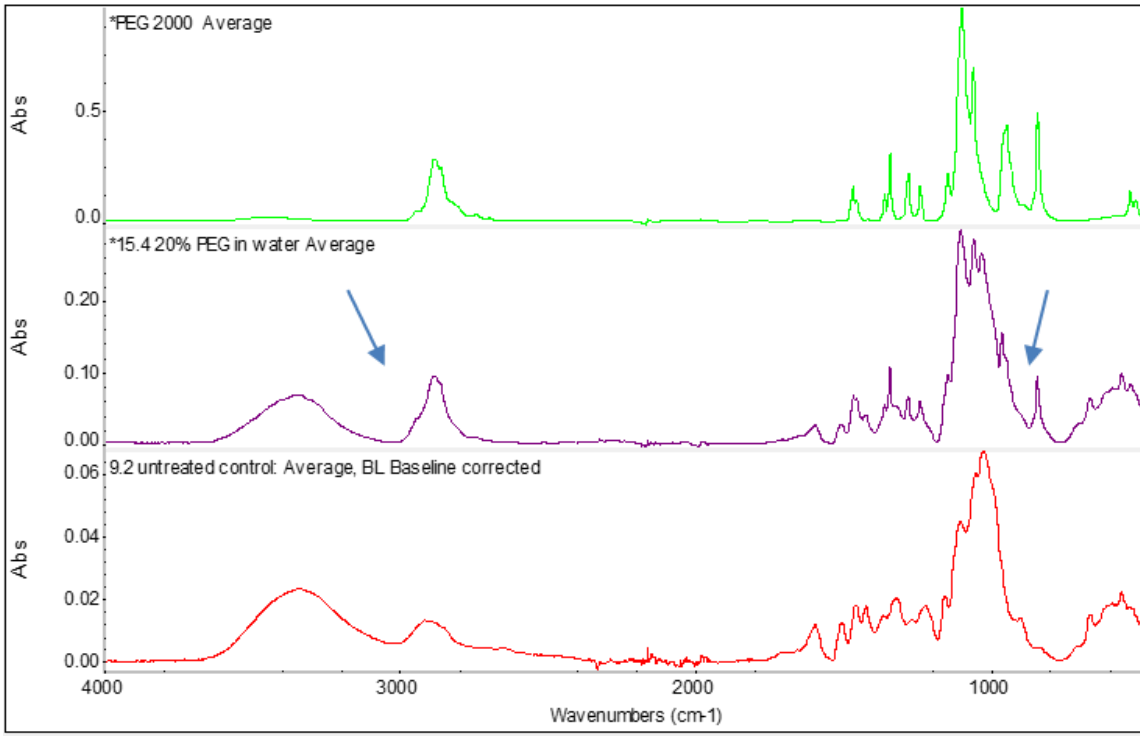

Figure 6-30: IR spectra of PEG treated wood. a) PEG, b) PEG treated wood and c) untreated laboratory degraded wood.

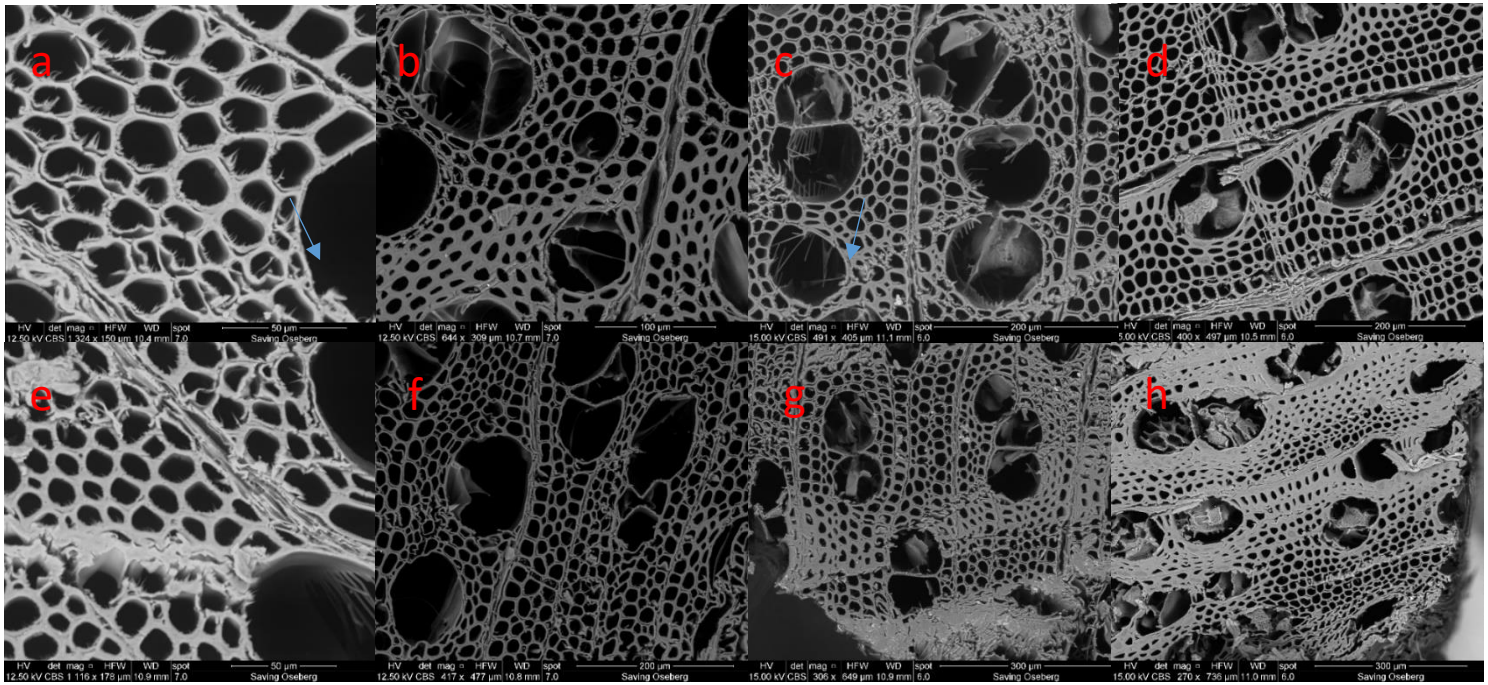

Figure 6-31: SEM image of the middle and edge of treated archaeological wood pieces a,e) untreated wood, b,f) aminocellulose treated, c,g) Aminocellulose and PEG treated and d,h) PEG treated.

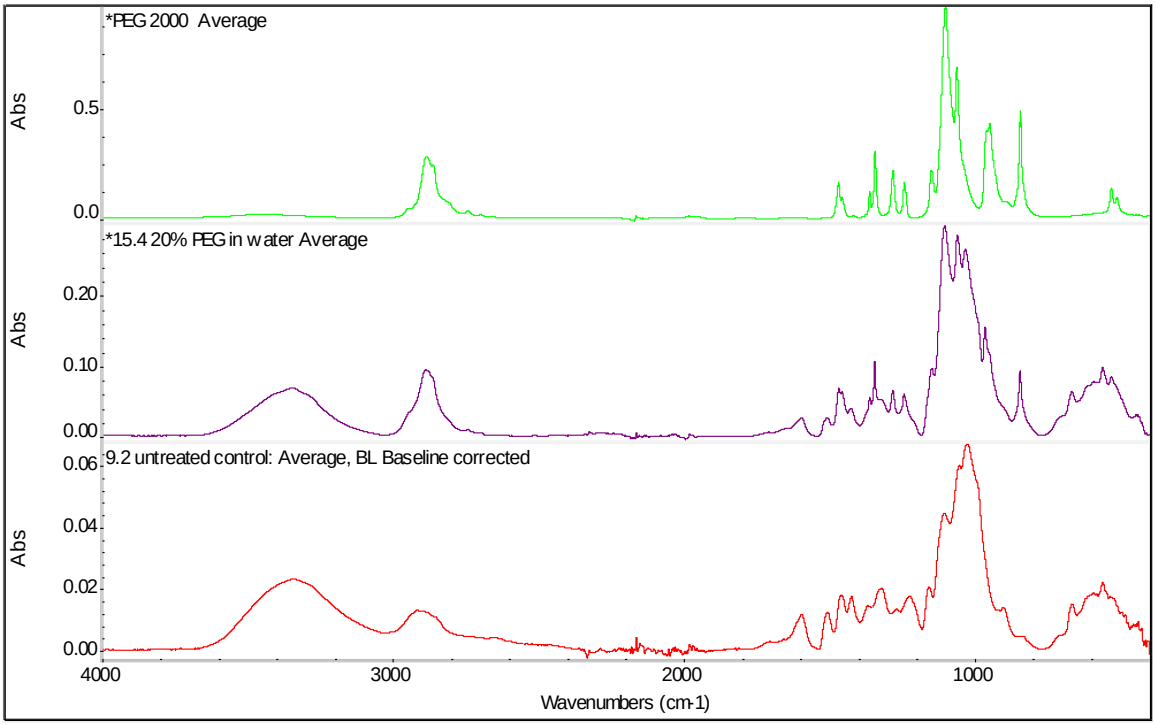

Figure 6-32: IR spectra of the PEG treated wood. Green line PEG 2000, purple 20% PEG treated artificially degraded wood (sample number 15.4) and the red line is untreated control (sample number 9.2).

Figure 6-31 shows SEM image of aminocellulose-treated lab degraded wood. Images indicated the wood had been cut smoothly, no collapse is seen in the aminocellulose-treated wood and an open structure is maintained. However, no collapse is seen in the untreated wood either, since the wood was freeze-dried in each case. Aminocellulose-treated samples have kept their structure well. However, no evidence of the aminocellulose is visible. PEG can be seen to block some cells, although that cannot be observed in the wood treated with aminocellulose 2 (HEA) and PEG. IR showed PEG reached the centre of the wood (Figure 6-32).

The EDS image (Figure 6-33) shows that aminocellulose HEA is present in the wood. Unfortunately, the nitrogen signal is too close to that of oxygen and carbon and therefore cannot be detected. However, the residual sulphur from tosyl and chlorine

from synthesis can be seen. To confirm that the signal seen was not from the wood, untreated wood was also investigated with EDS and the sulphur and chlorine were not visible.

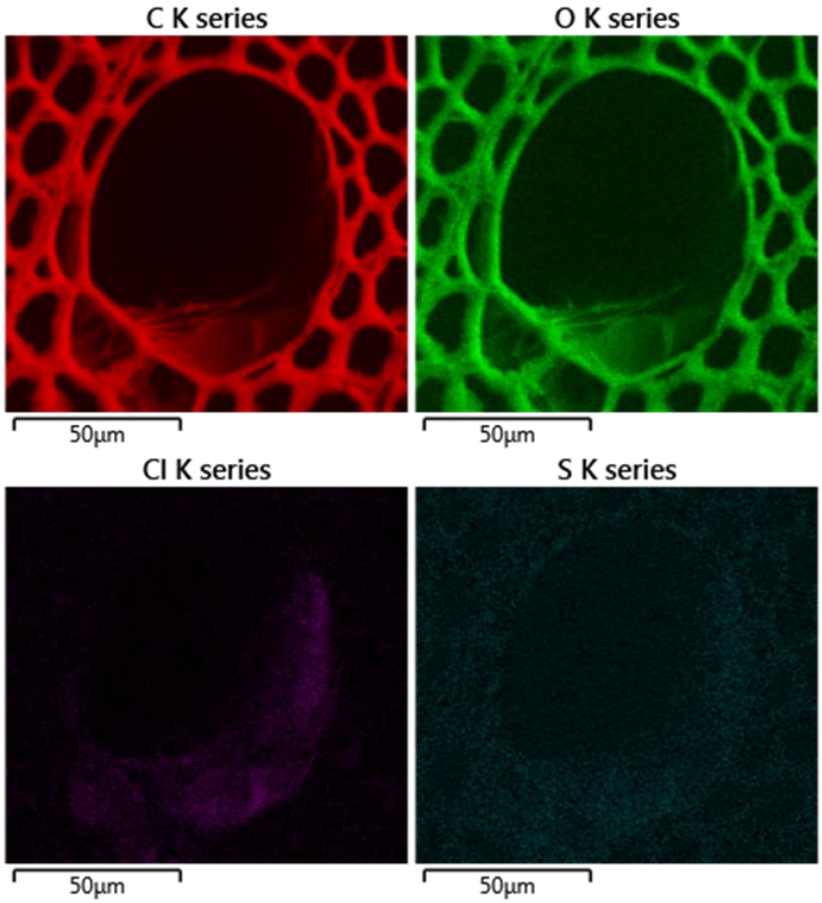

Figure 6-33: SEM-EDS images of different elements in aminocellulose HEA-treated laboratory degraded wood

The X-ray tomography images (Figure 6-34) show that the aminocellulose treatment maintains an open structure. The aminocellulose polymer cannot be seen in the image, hence, it is impossible to prove again that the aminocelulose has fully penetrated the wood. PEG cannot be seen either in the X-ray tomography of the wood.

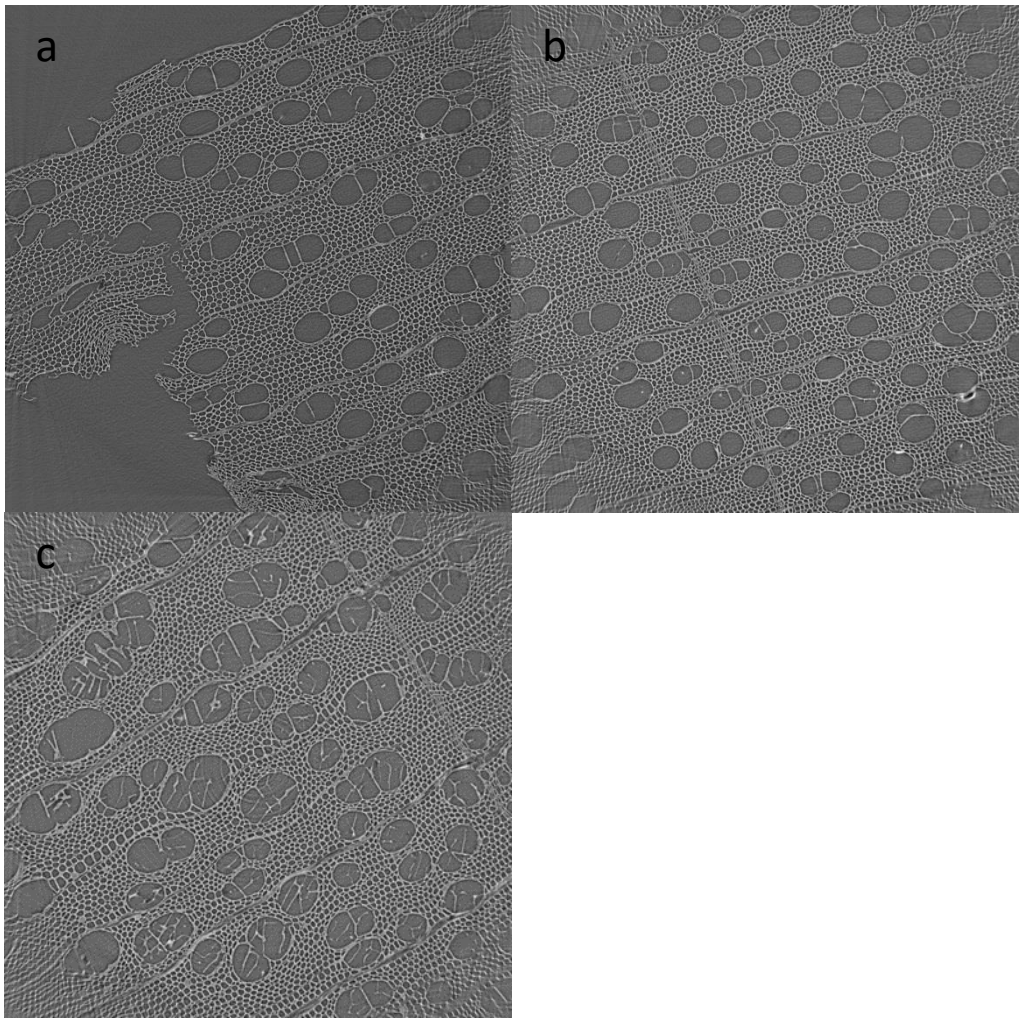

Figure 6-34: X-ray tomography images a) untreated wood lab degraded, b) aminocellulose 2 (HEA) and c) PEG. (acquired by Braovac)

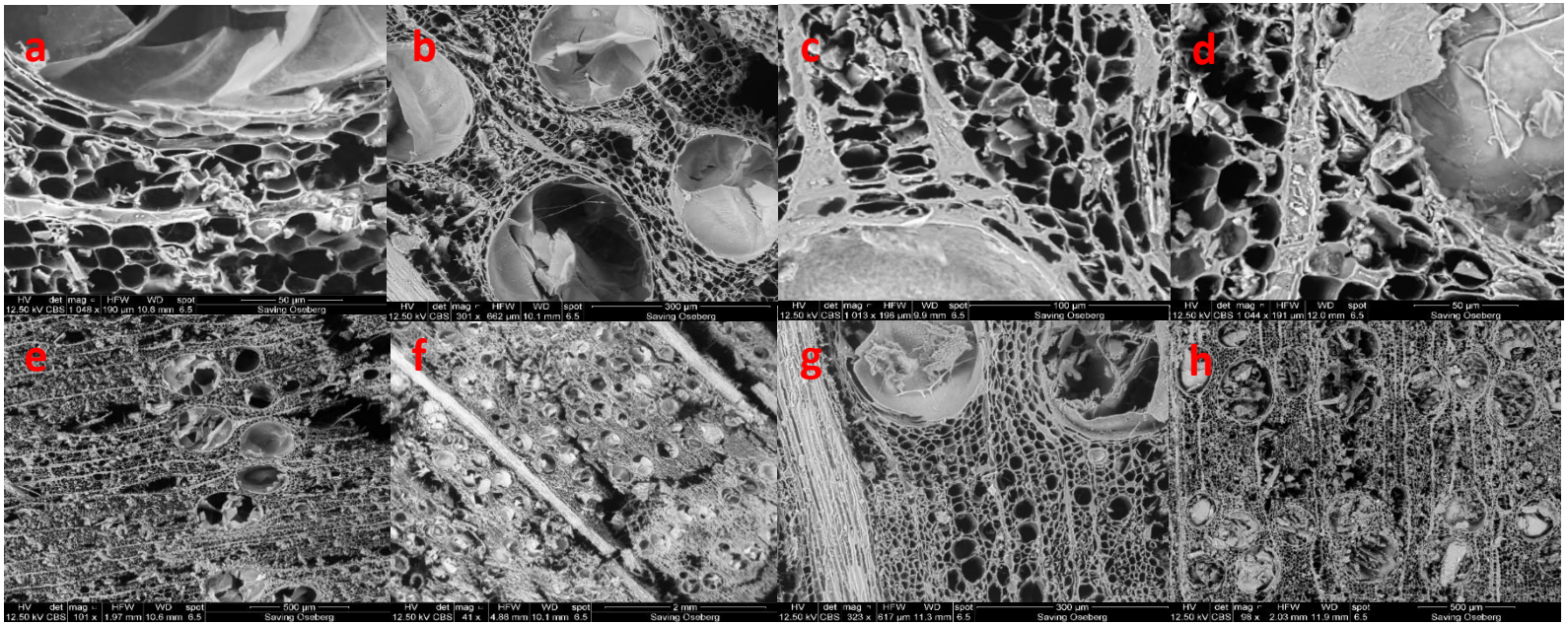

Figure 6-35: SEM images of archaeological wood. Images from centre of the wood a, e) untreated, b, f) aminocellulose 2(HEA), c, g) aminocellulose 2 and PEG, d, h) PEG.

The SEM of aminocellulose HEA-treated archaeological wood Figure 6-35 shows similar results to artificially treated wood. No collapse is seen from freeze-drying alone and this is also the case in all treated samples. The aminocellulose is not visible; the PEG is not particularly visible either. It was difficult cutting the wood completely smoothly due to the brittle nature of the archaeological wood, although treatment helped. Although the cuts appeared clean under a light microscope, under the SEM it is clear that fragments had broken off, and these are on the surface obscuring the image of the cells. It is still clear that cells are not being filled with aminocellulose and therefore, retreatment would be possible, which might also be the case for low concentrations of PEG, less than 20% and for mixtures.

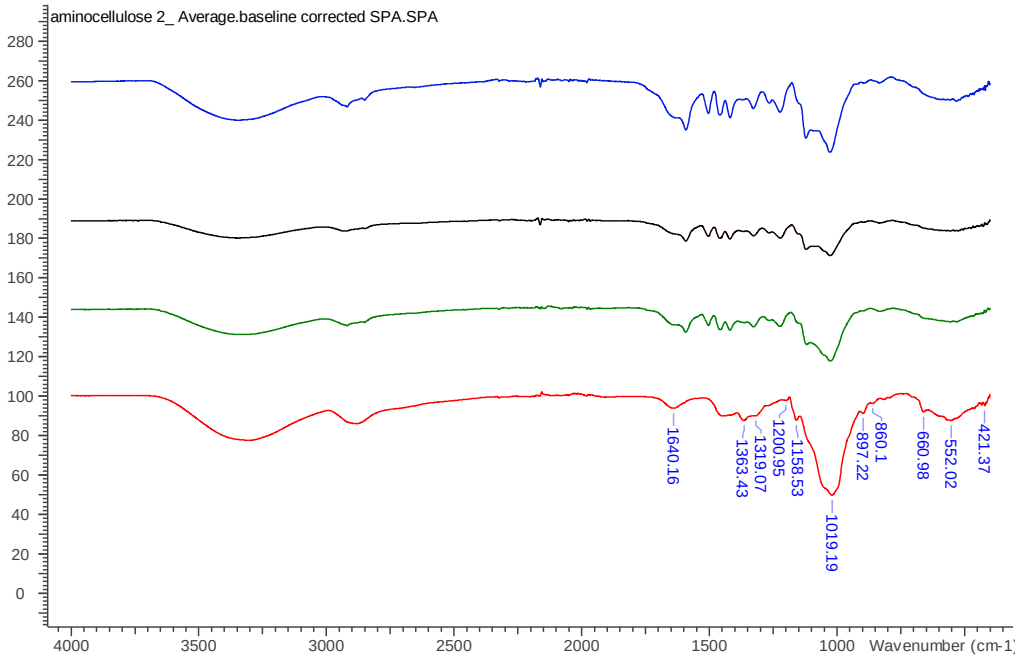

Figure 6-36: IR spectra of archaeological wood treated with aminocellulose HEA. Blue line is untreated wood, black is from the middle of the treated wood, green is from the outer section of the treated wood and red is from aminocellulose HEA alone.

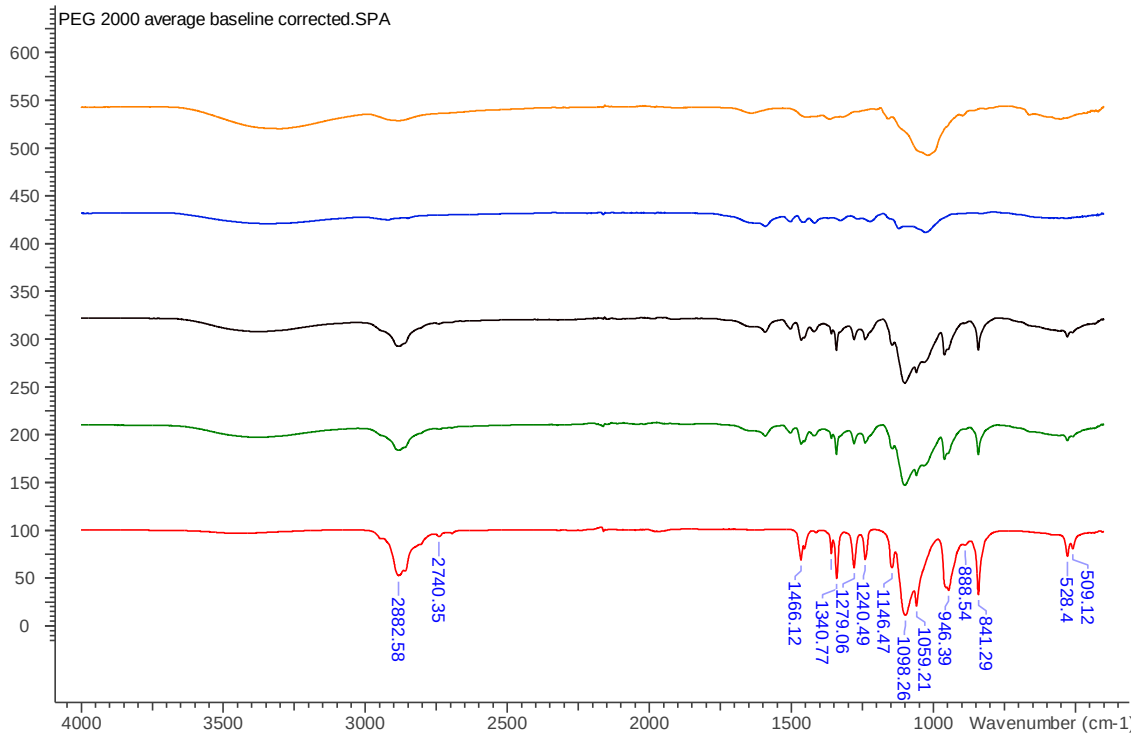

Figure 6-37: IR spectra of aminocellulose HEA and PEG treated wood. organge line is HEA, blue is untreated wood, black is middle of HEA and PEG treated wood, green is edge of HEA and PEG treated wood and the red line is PEG alone.

The IR of aminocellulose HEA-treated archaeological wood shows a very small broadening between the 1130 and 1020 wood peaks (Figure 6-36). Elemental analysis is required to confirm the presence of aminocellulose in the centre of the wood, as it is not clear from the IR.

The presence of PEG in the HEA and PEG treatment is clearly evident in archaeological treated wood (Figure 6-37) from peaks at 2882 and 841 cm^{-1} in the treated wood. However again the aminocellulose signal is too close to the wood signal to detected. Again, elemental analysis is required. There is a broad/peak at 1098, but that is predominately or entirely from the PEG.

6.3.7.2 Chitosan

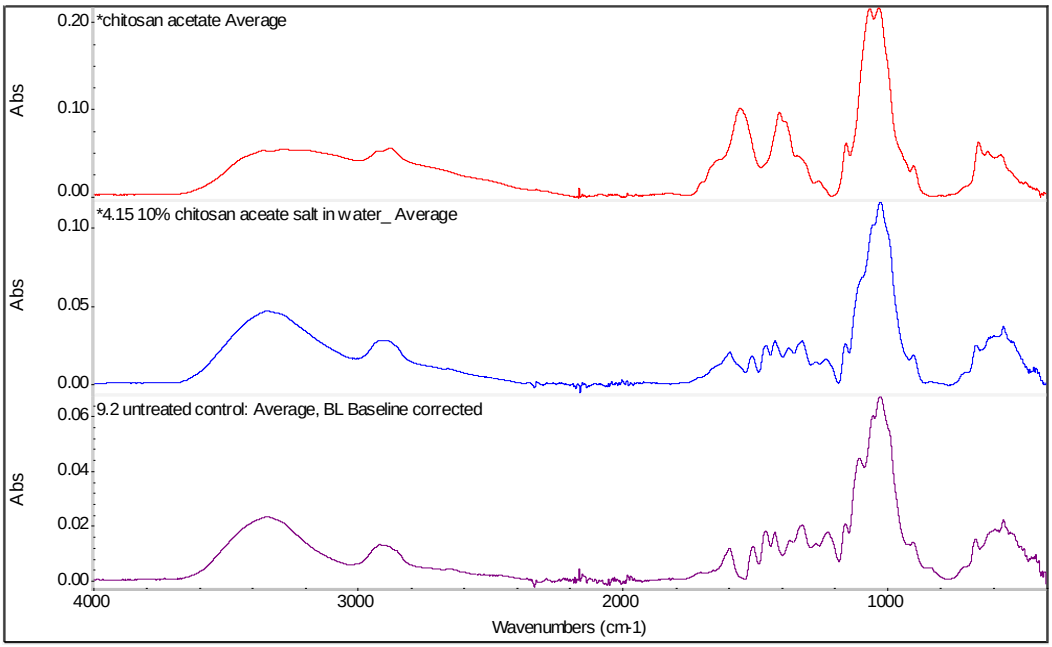

Figure 6-38: IR spectra in descending order of chitosan acetate, treated wood, untreated lab degraded wood.

IR spectrums of chitosan acetate-treated wood shown in Figure 6-38 indicate that again the peaks of chitosan overlap with that of the wood. What can be seen is one peak broadening in the treated wood, which could be due to the presence of chitosan acetate. However ideally, more than one peak would show a change, to confirm the polymer has fully penetrated the wood. IR spectrum of the chitosan-treated wood was not taken for the laboratory degraded wood, the sample being stored should it become desirable to test in the future. However, since the acetate is not visible, there is no reason to think the chitosan would be detectable.

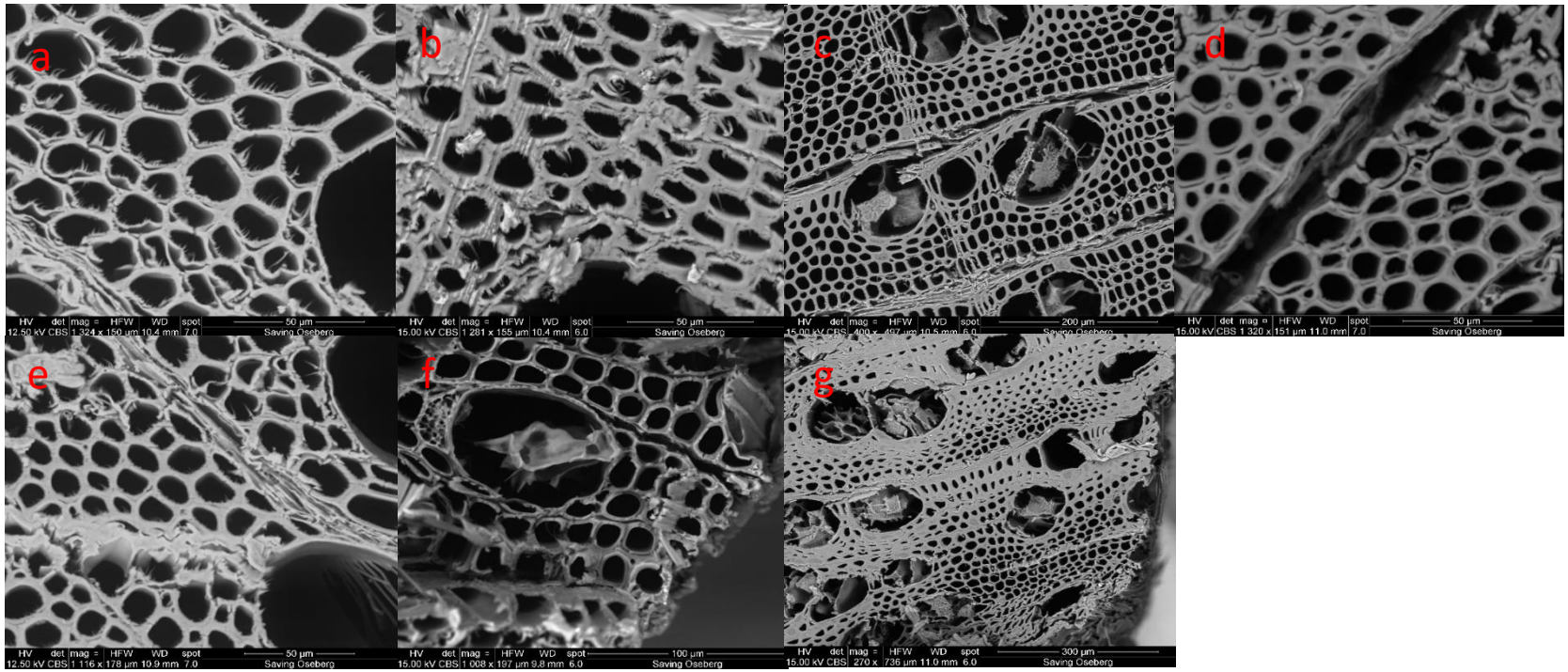

Figure 6-39: SEM images of treated artificially degraded wood chitosan and chitosan acetate showing middle and edge below a, e) water control, b,f) chitosan acetate c,h) PEG, d) chitosan in acetic acid.

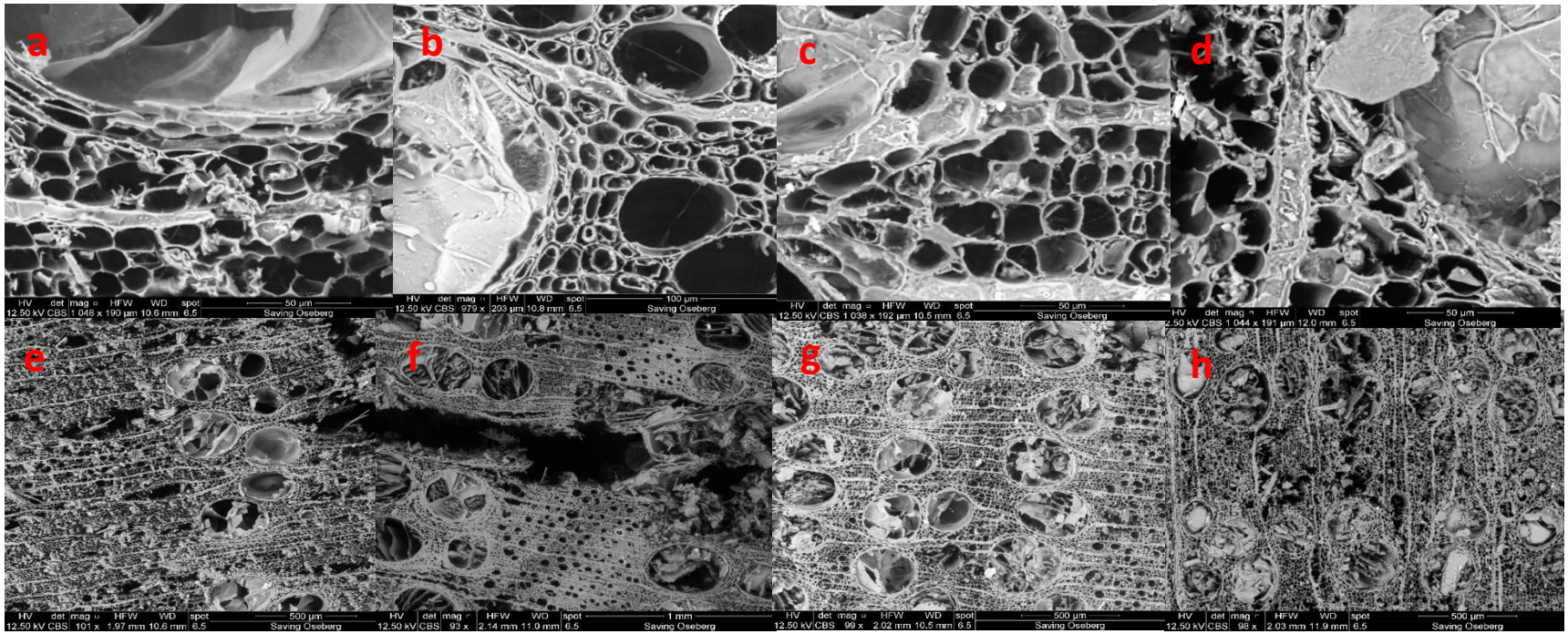

Figure 6-40: SEM images of archaeological wood treated showing middle zoomed in and out below a,e) untreated, b,f) chitosan acetate, c,g) chitosan acetate and PEG, d,h) PEG.

The SEM and X-ray tomography of artificially degraded wood showed cells did not collapse under any treatment (Figure 6-39 and Figure 6-42). Smoother cuts for PEG and chitosan in acetic acid suggest wood is stronger and easier to cut and is not ripping and powdering on cutting. Cells also appear to have thicker walls with all treatments, but there is a possibility this is due to the angle the wood is cut at or the angle at which the images are taken. PEG is seen to block some cells and thicken others, especially around the edges of the wood.

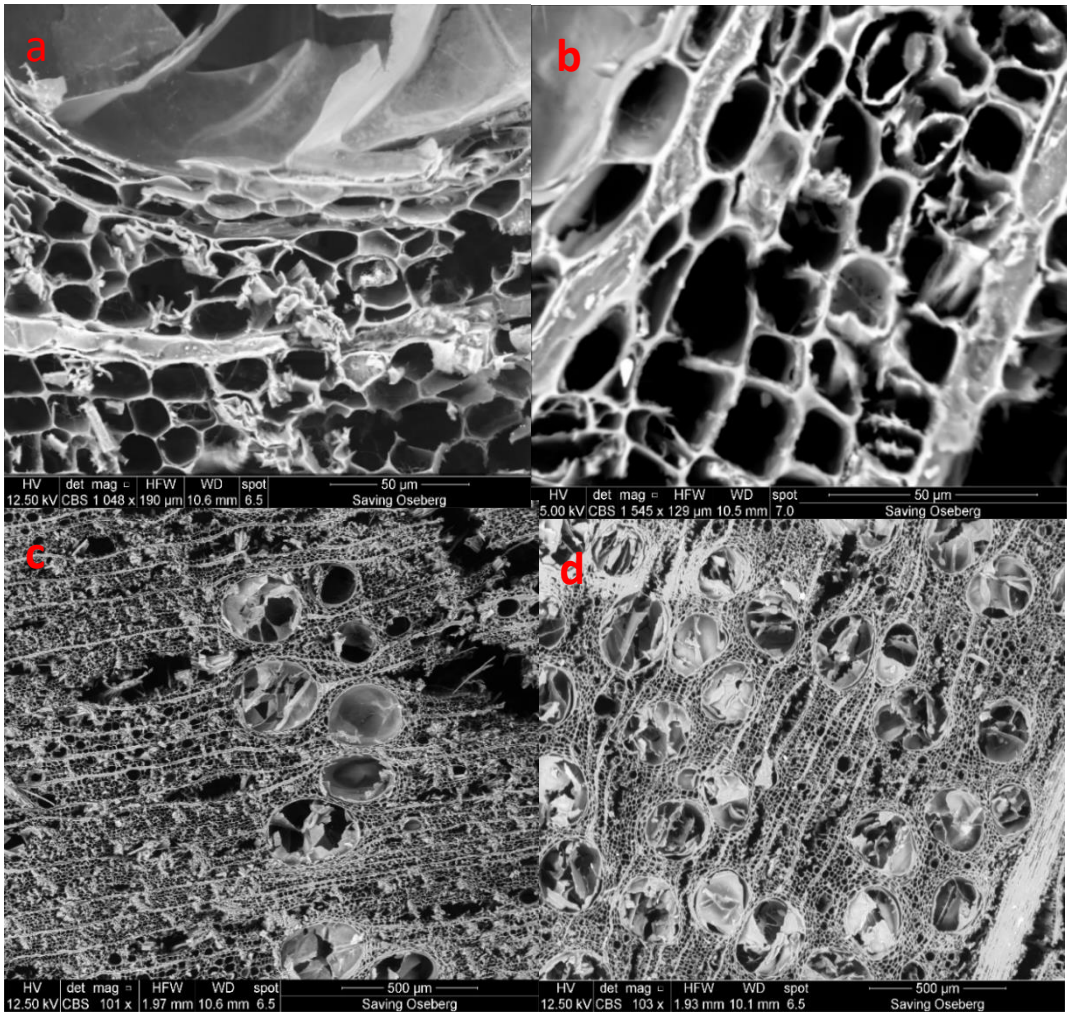

Figure 6-41:SEM images of archaeological wood treated smiddle showing zoomed in and out below a,c) untreated b,d) chitosan in acetic acid.

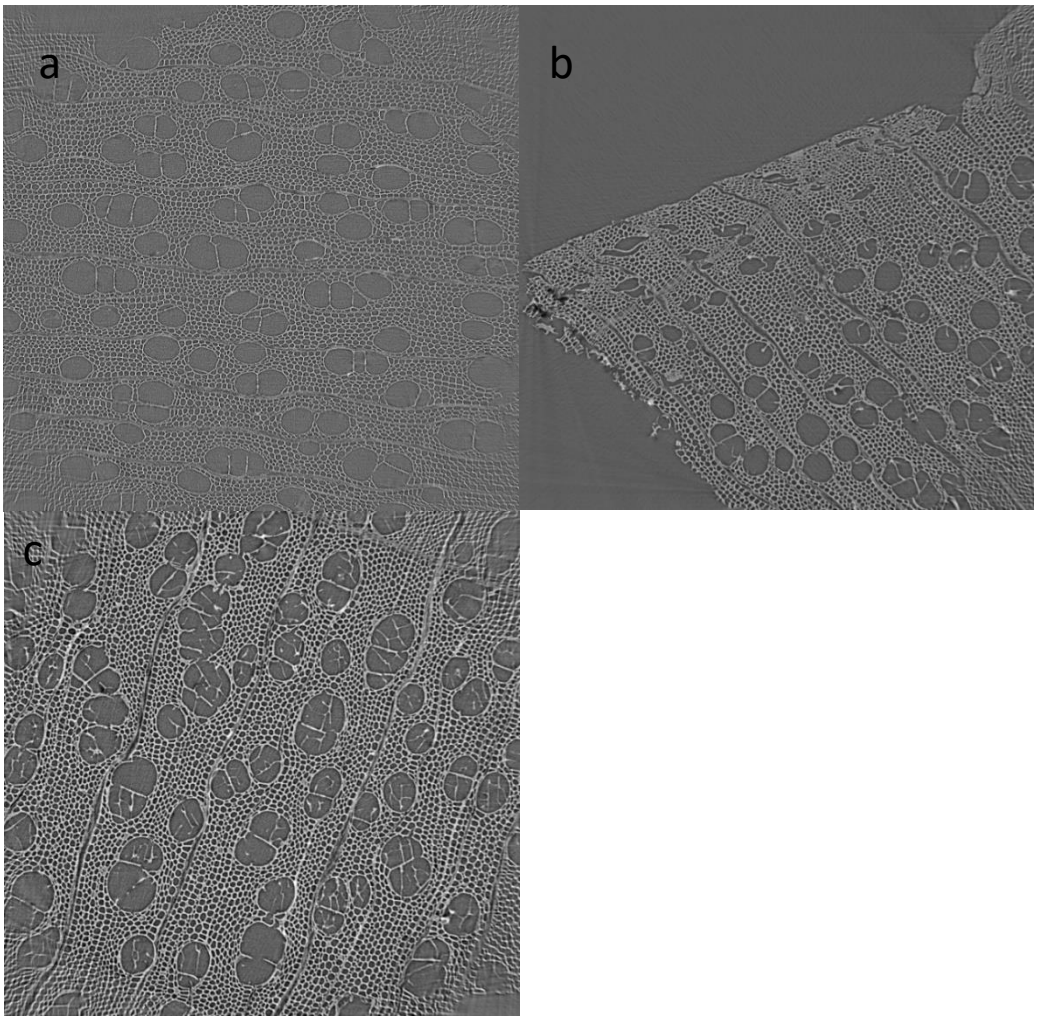

Figure 6-42: CT tomography images of treated artificially degraded wood. a) untreated, b) chitosan acetate, c) 20% PEG. (acquired by Braovac)

The SEM images of untreated archaeological wood (Figure 6-40), show it is in moderately good condition, not showing any cell collapse, but several broken fragments can be seen on the surface. When examining the samples impregnated with chitosan acetate, there is, again, no collapse seen. However, some of the cell wall seems to have become detached. This could be the chitosan acetate which lined the cell wall but as the wood dried it became detached from the cell wall. If this is the case, it could be the reason less consolidation ability is seen. Coating the walls would

provide strength, but if it detached it would not provide any strength as it does not fill the cell either. Chitosan acetate and PEG show the same detachment but in only one or two cells. Chitosan in acetic acid (Figure 6-41) does not show the same detachment from the cell wall. There is a lot of damage visible in the chitosan acetate treated wood and in the 20% PEG treated wood; however, it is not clear if this is due to treatment or wood degradation state before treatment. The latter seems more likely.

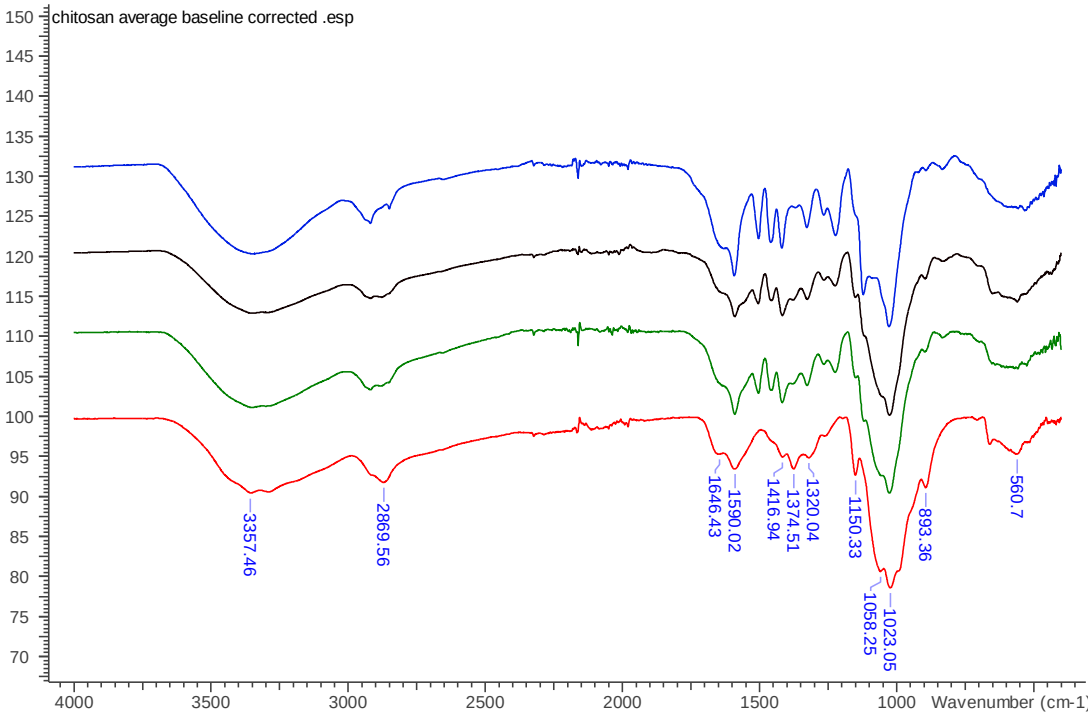

Figure 6-43: IR spectra of chitosan treated wood. Blue line is water control wood, black line is middle of the treated wood, green line is the edge of the treated wood, red line is chitosan alone.

The

The X-ray tomography scans of the laboratory degraded wood (Figure 6-42) treated with chitosan acetate again also show no collapse and clear open cells. This would make re-treatment easy should it become necessary.

The IR of chitosan-treated wood (Figure 6-43) does not clearly show the presence of chitosan. However, the pattern of peaks around 1374 is a little different, as is the pattern of peaks above 1023, which may indicate the presence of chitosan or variability in the wood. Elemental analysis is required for confirmation as IR alone is not sufficient.

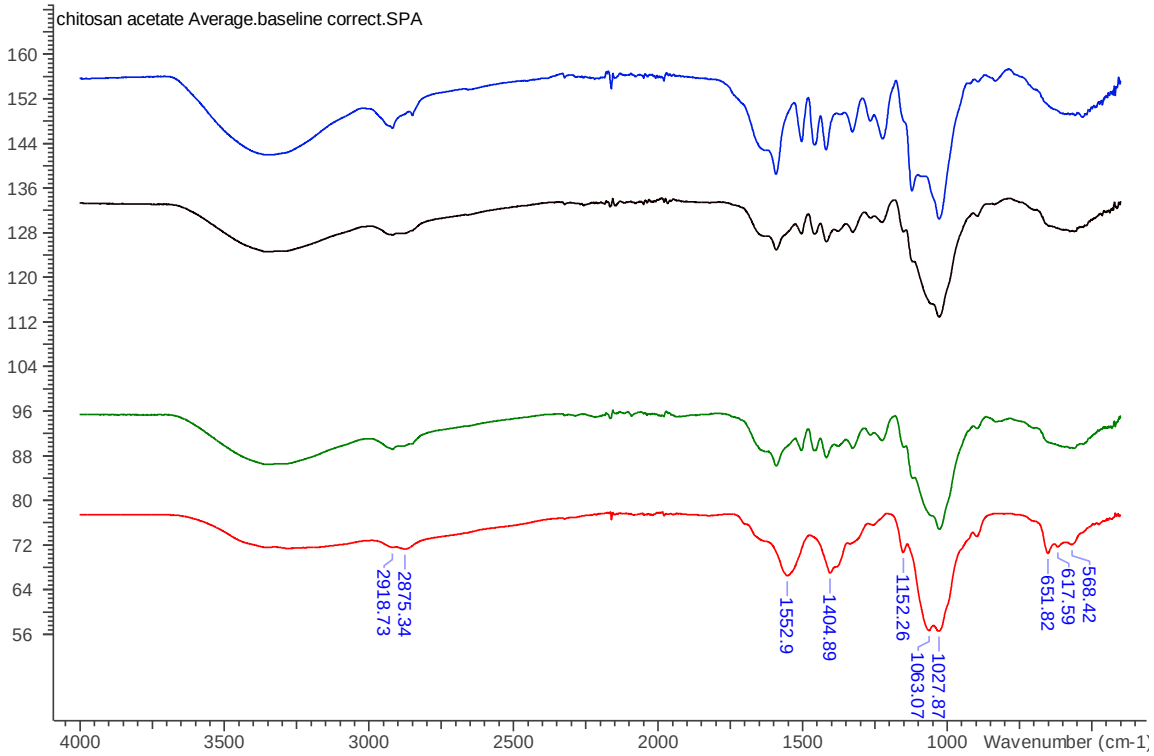

Figure 6-44: IR spectra of chitosan acetate treated archaeological wood. The blue line is the water control treated wood, the black is the middle of the wood, the green line is from the edge of the treated wood and the red line is the chitosan acetate alone.

The broadening of peaks around 1553, 1405 and 1063 could be due to the presence of chitosan acetate in the treated wood (Figure 6-44); elemental analysis is required to confirm this.

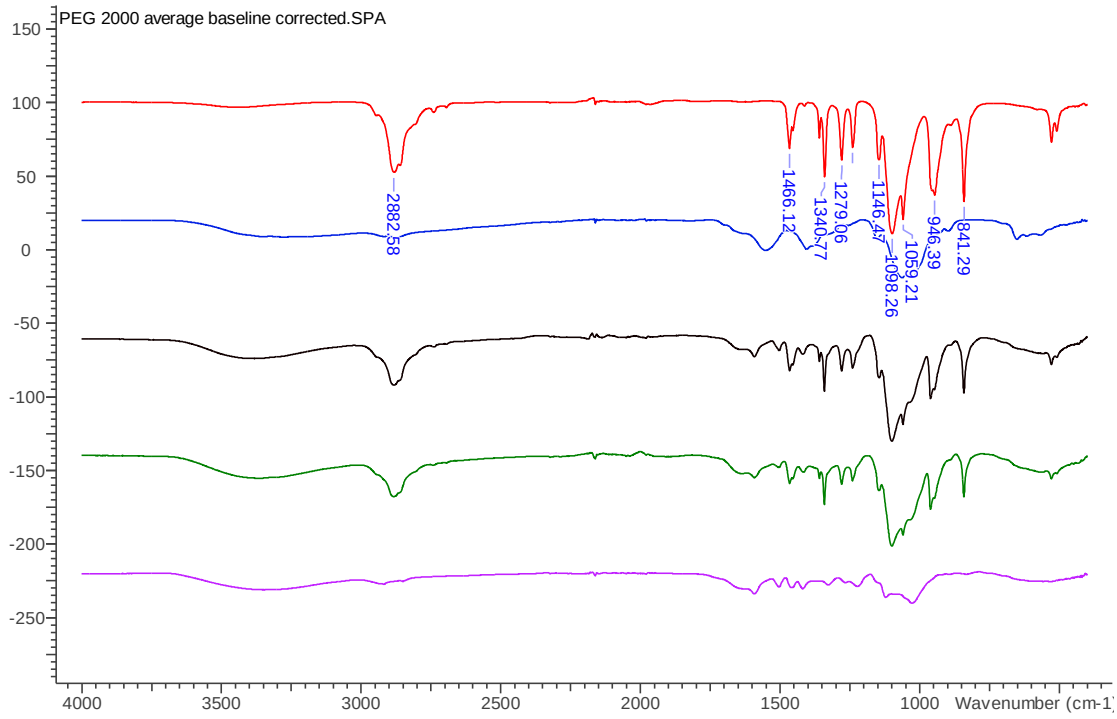

Figure 6-45: IR spectra of chitosan acetate and PEG treated wood. the red line is the PEG alone, the blue line is chitosan acetate alone, the black line is the middle of the treated wood and the green line is the edge of the treated wood and the pink line is the water control.

The IR for the chitosan and PEG treated archaeological wood (Figure 6-45) clearly shows PEG is present from the 2883, 1341, 1098, 946 and 841 cm^{-1} peaks. The presence of chitosan acetate cannot be confirmed.

The IR of PEG treated archaeological wood clearly shows the presence of PEG particularly from 2883, 956 and 841 cm^{-1} peaks and it is also clear these peaks are large with higher concentration of treatment (Figure 6-46).

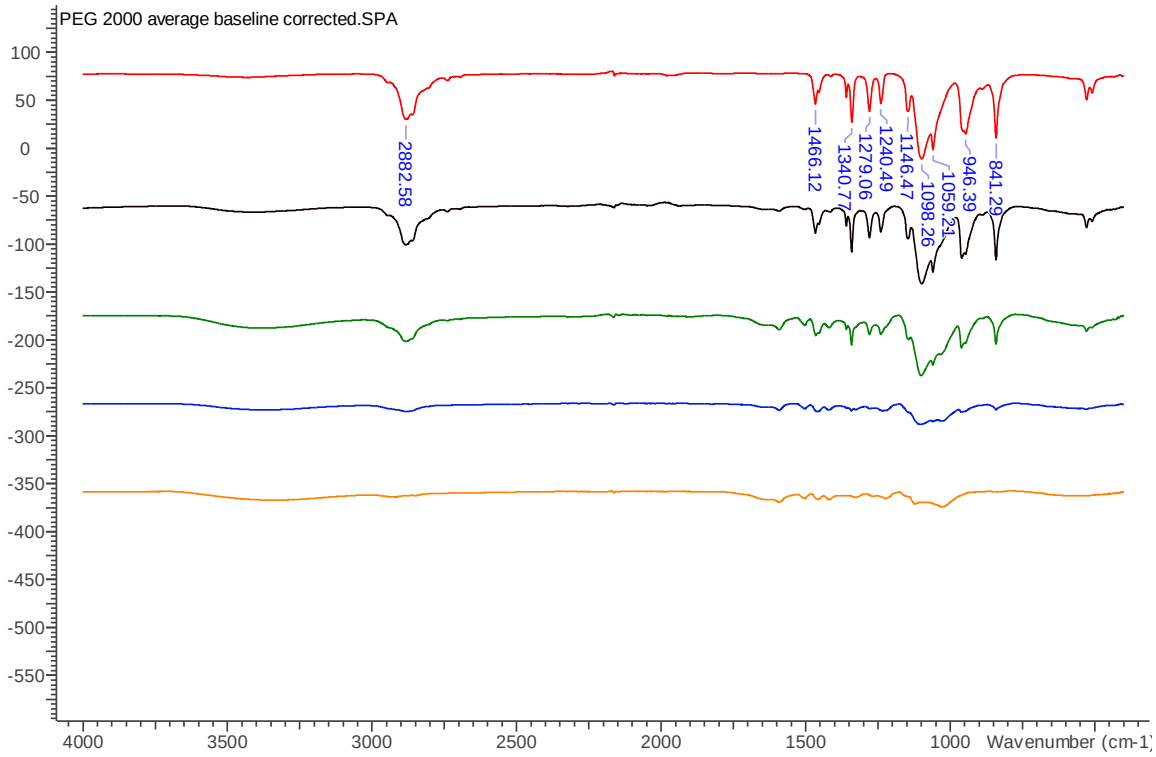

Figure 6-46: IR spectra of middle of PEG treated archaeological wood. Red line is PEG alone, black line in middle of 40% PEG treated archaeological wood, green is 20% PEG treated, blue is 10% PEG treated and the orange line is water control archaeological wood.

6.3.8 Cross sections showing the middle of the treated archaeological oak

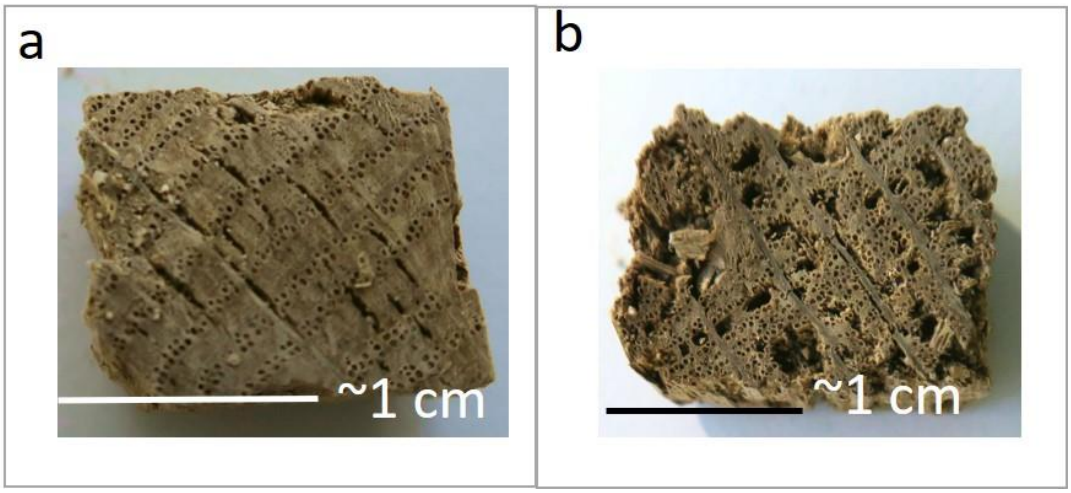

Figure 6-47: Photograph of the cross section from the middle of the water controls.a) sample 74 b) sample 75.

Figure 6-47 shows cross sections of the control, which demonstrate the variation in the wood condition. This must enter in consideration when looking at the treatments results (Figure 6-48). The aminocellulose shows an open structure but the aminocellulose might be seen as shiny flakes/layers within some of the vessels. The aminocellulose and PEG shows the PEG is filling the vessels. 20% PEG works by filling the vessels. The chitosan in acetic acid also appears to form layers in the vessels. The PEG and chitosan acetate treated wood shows the PEG forms inside the vessels but seems weaker, perhaps because it appears to form flakes rather than the solid PEG seen in other samples.

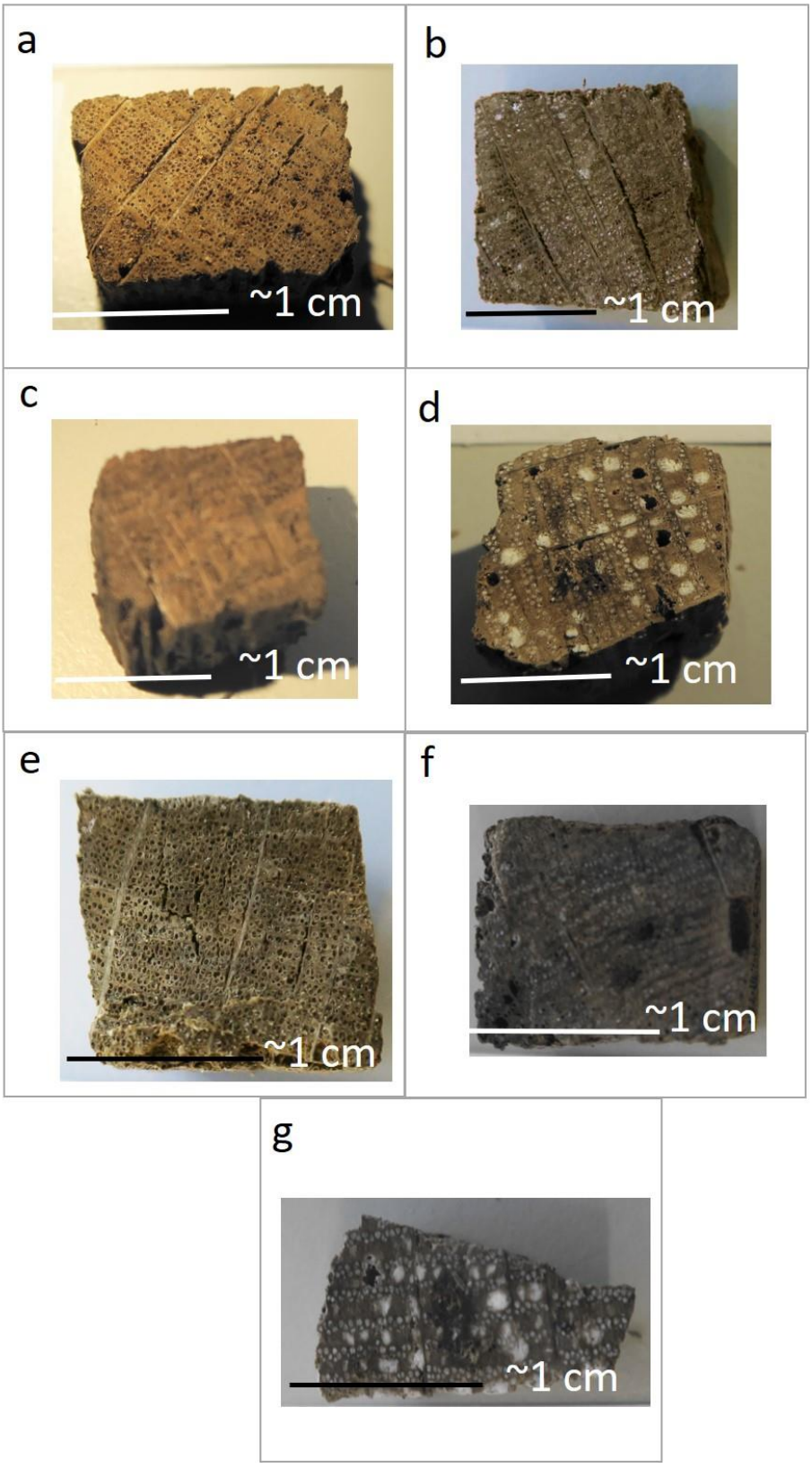

Figure 6-48: Photograph of the cross section showing the inside of treated pieces of archaeological wood to show how treatments filled or affected cells a) aminocellulose 2, b) aminocellulose 2 and PEG, c) chitosan acetate, d) Chitosan acetate and PEG, e) acetic acid, f 20% PEG and g 40%PEG.

6.3.9 3-point bend test on balsa wood

The 3-point bend test, as discussed in Chapter 5, assesses the modulus of elasticity (MOE) and can also be used to determine the modulus of rupture (MOR).

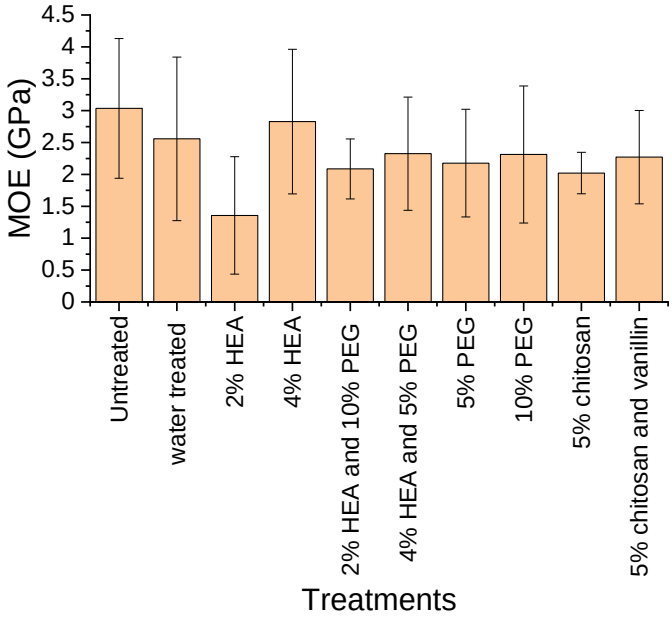

Figure 6-49: Plot of modulus of elasticity (MOE) of treated balsa wood and control showing lines of best fit.

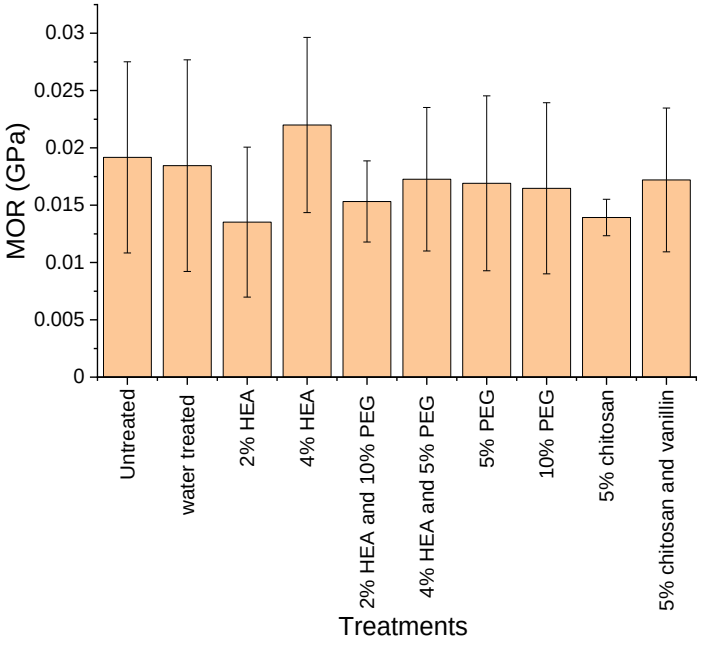

Figure 6-50: Plot of MOR of treated balsa wood

Individually, these revealed little information due to the variation in results (see Figure 6-49 and Figure 6-50). Variation in MOE was also observed during investigations into the Vasa, part of the problem was due the difference in PEG concentration, the other, was due to varying levels of degradation and natural variation in wood (Lechner et al., 2013). It is also well established there is also a strong correlation of MOE and density in wood, this was observed during the Vasa investigation and also in this investigation (Lechner et al., 2013). Balsa wood has also specially been investigated for the link between structure properties and density (Shishkina et al., 2014). It was observed that elastic moduli increased with increasing density, the same was observed in this investigation (see Figure 6-51, and Figure 6-52). From Figure 6-51 and Figure 6-52 it is apparent that the treatments appear to increase the MOE and hence flexibility.

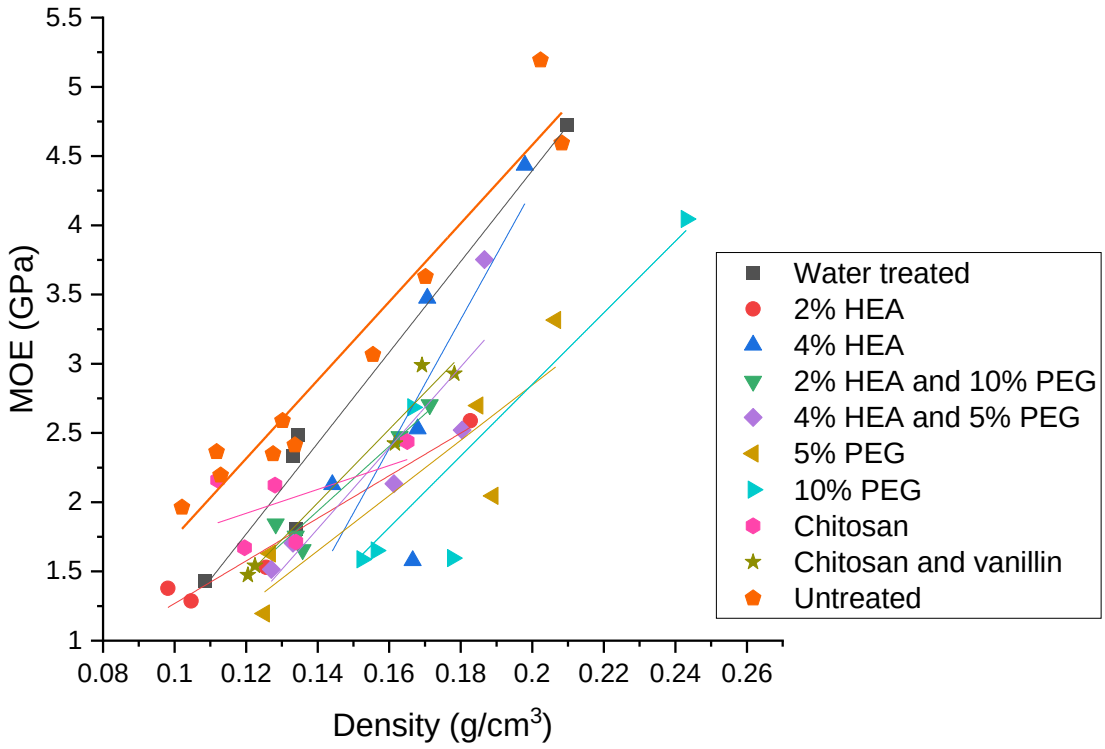

Figure 6-51: Plot of density vs MOE for different treatments. The density here is from after the treatment of balsa wood. Lines of best fit have been included with corresponding colours given in the legend.

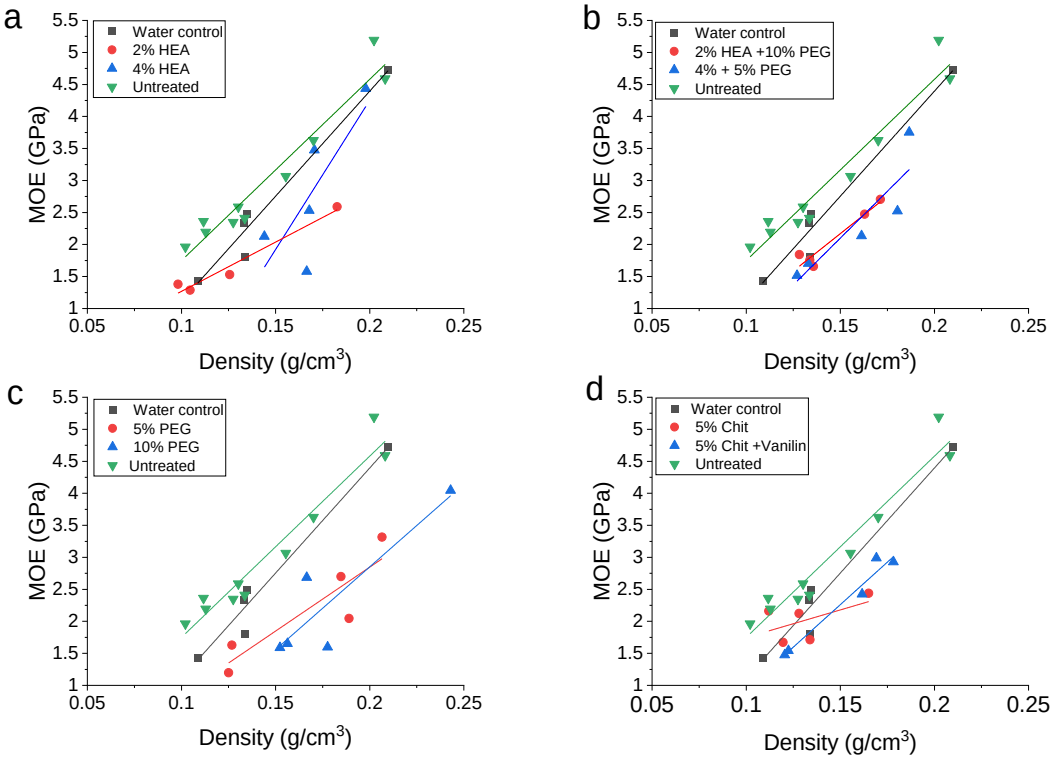

Figure 6-52: Plots of density vs MOE for different treatments. a) HEA and controls, b) HEA and PEG treatments vs controls, c) PEG treatments and controls and d) chitotsan (chit) and controls). The density here is from after the treatment of balsa wood. Lines of best fit have been included with corresponding colours given in the legend.

However, when plotted in combination, a clear trend is seen for the untreated wood. The correlation between MOE and MOR is well established (Endo et al., 2010; Green, 2005; Hein and Brancheriau, 2018). A shift in the position of the tend is noted by Endo et al. (2010). A shift in the tend is also seen with treatments in this investigation.

The water control shows a clear shift in position above that of the original line for untreated wood, suggesting the water-soaked wood, once dried, is more flexible and stronger than the untreated wood (Figure 6-53). To ensure this was real and not an artefact of the small sample size, the first five untreated wood samples were plotted along with the second set of five and the total. Although the equation for the line changes for the untreated wood and even if other points were selected as the five, it is still clear that the water control linear fit sits above the untreated wood, suggesting it is more elastic and stronger.

Interestingly, 10% PEG shows little change to the position of the line of best fit. 5% however, visibly shifts the line upward again suggesting, with the addition of 5% PEG, the wood is more flexible and can accept a higher load (Figure 6-54). This is to be expected for PEG, a flexible polymer; however, it is unclear why 10% should decrease the flexibility. It could be once the cells are saturated the pressure on the cells is greater making them less flexible and more likely to break. More samples and a greater variety of concentrations are required to properly assess this.

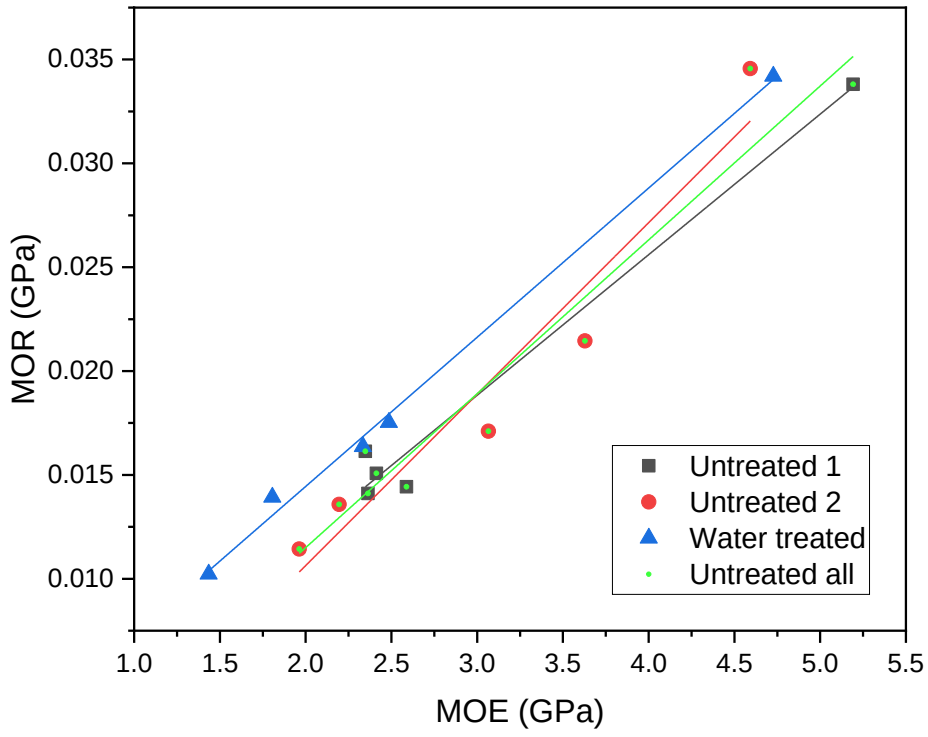

Figure 6-53: Plot of MOE vs MOR for untreated balsa wood and water treated control balsa wood

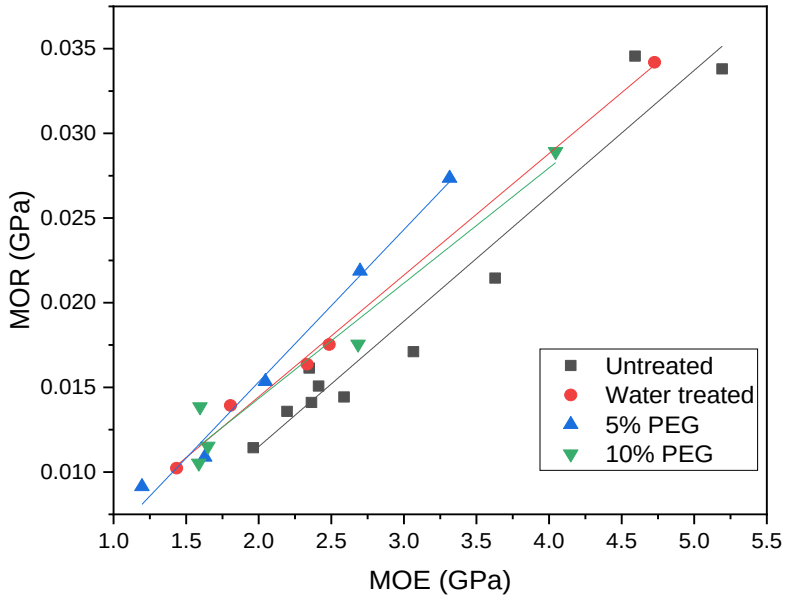

Figure 6-54: MOE vs MOR to assess strength and flexibility of wood untreated, water treated and treated with 5% and 10% of PEG

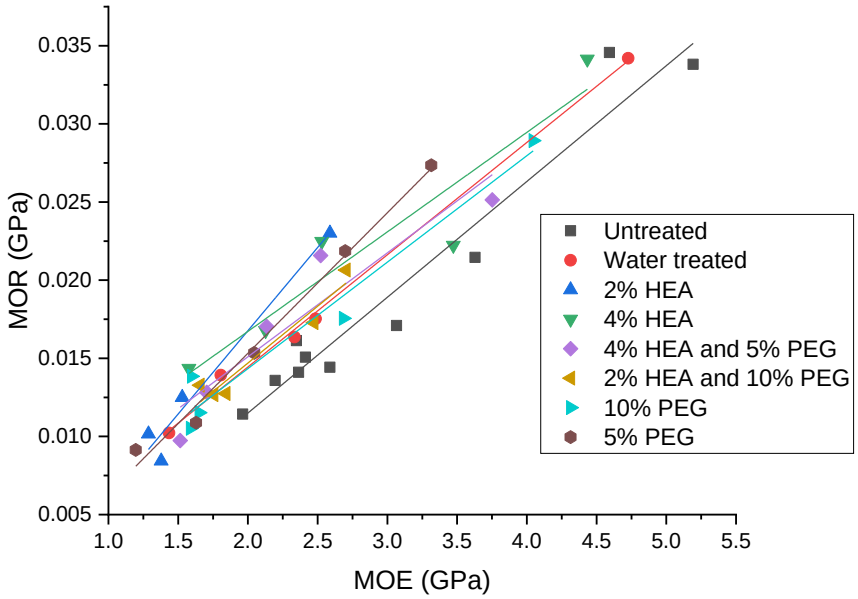

Figure 6-55: Plot of MOE vs MOR for HEA and PEG of various concentrations and combinations

Concentration of HEA appear to make the wood stronger and more flexible (see Figure 6-55). 5% PEG, as previously discussed, also improves the flexibility and strength.

However, 10% PEG has very little effect and if anything lowers flexibility and strength. The combination in both cases of concentration has very little affect on flexibility and strength. The biggest effect is from the treatment in water (water control), this in all likelihood, dissolves some component and causes hydrolysis, resulting in increased flexibility and strength due to the reduction in brittleness.

Waterlogged archaeological wood would fare differently with treatment; as the majority of the damage would been done already, hence a few weeks water would have very little affect on further degradation of the wood at that stage. However, the treatments, in all likelihood, would have a much bigger consolidation due to the very brittle and weak nature of waterlogged wood. However, as previously stated, archaeological wood must be used sparingly, and it would be a waste to use such material in these tests unless necessary. Future work could however include more highly degraded fresh wood in hope of having a closer comparison to the impact of a treatment of the archaeological wood. From these results it appears treatments such as HEA and PEG can improve flexibility and strength, but concentration must be carefully considered and chosen. The most appropriate concentration is likely to be based on level of degradation of the wood, as the extent of degradation of the wood will affect how the cells filled and how the consolidation interacts with the wood.

If the flexibility and strength of a consolidant are similar to that of the wood, it is unsurprising that the difference would not be noticeable. However, that does not mean it has not improved the consolidation, hence, these results need to be considered in line with the other results.

In terms of the chitosan as can be seen in Figure 6-56 the strength appears reduced compared to water alone. However, the addition of vanillin appears to increase the strength and flexibility, although the increase in weight could mean this improved strength is as a result of the vanillin crystals rather than crosslinking the chitosan.

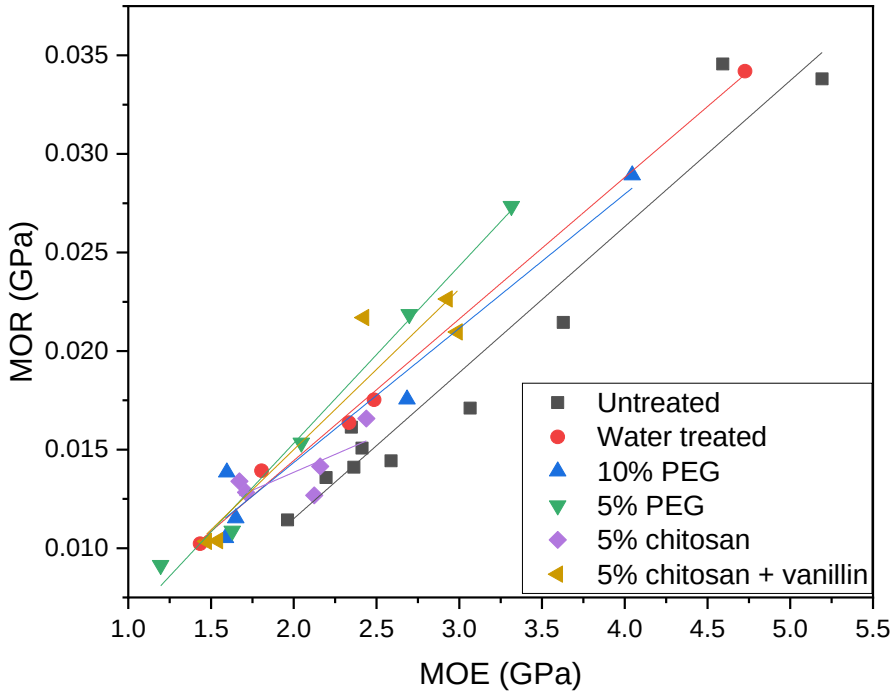

Figure 6-56: Plot of MOE vs MOR chitosan vs no treatment and PEG treatment

The weight increase after treatment of balsa wood (Figure 6-57) used for the 3-point bend test reveal the amount of consolidant that is in the wood, which may account for the the small changes in MOE and MOR. This also means densities after treatment denote both the original density of the wood and the treatment material that has been absorbed. The density of the original wood, is a proxy for the original condition/strength of the individual pieces of wood prior to treatment. The density is then compared to MOE, an indication of flexibility, after treatment and compared to a

untreated wood and a water control (Figure 6-58 shows all treatments and Figure 6-59 separate the treatment types to make it easier to evalulate).

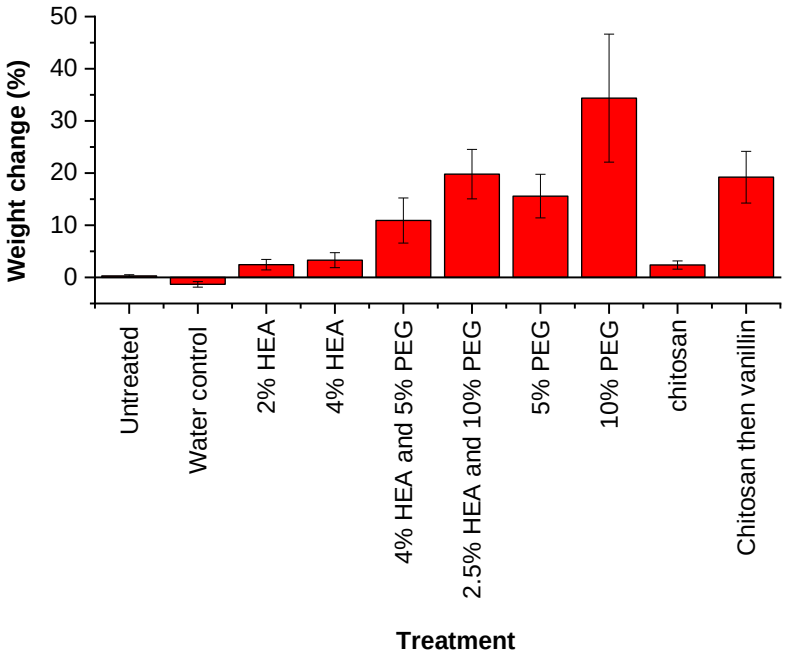

Figure 6-57: Average weight increase (%) of balsa wood after treatment for 3 point bend test. (same pieces as for 3 point bend test)

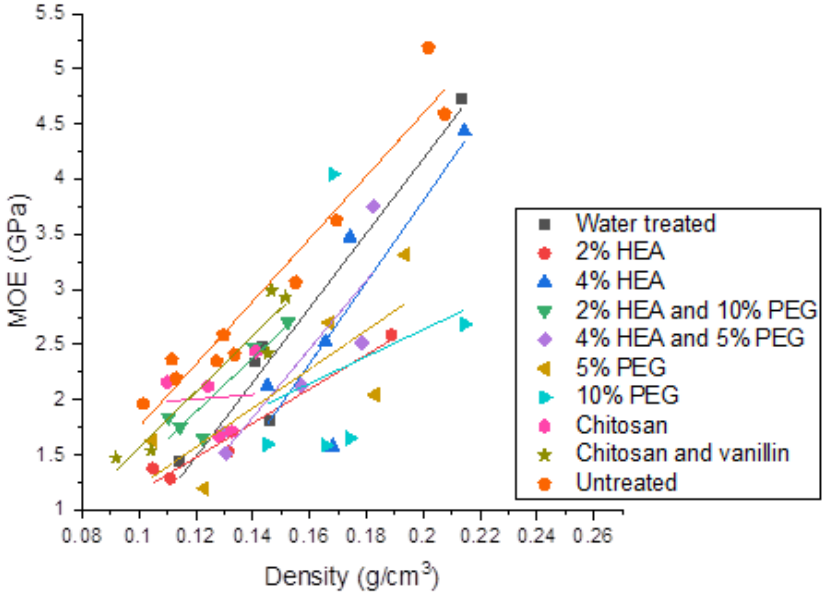

Figure 6-58: Plot of density vs MOE for different treatments. The density is from before the treatment of balsa wood. Lines of best fit have been included with corresponding colours given in the legend.

This shows water treatment alone increases flexibility; HEA, PEG and combination treatments appear to improve flexibility further. Although at low starting density 2% HEA and 10% PEG appears to reduce flexibility. 5% chitosan, however, reduces flexibility at low density and improves flexibility at higher density. Although, when chitosan is followed by immersion in vanillin, which is known to form a flexible gel with chitosan, the flexibility of the wood improves compared to chitosan alone.

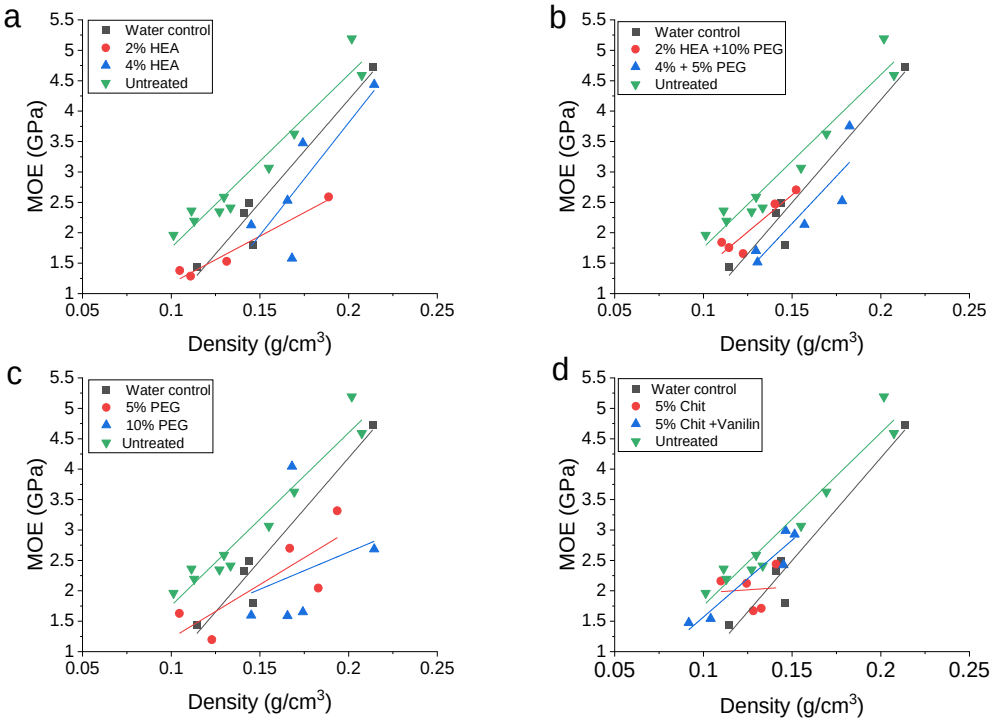

Figure 6-59: Plots of density vs MOE for different treatments. a) HEA and controls, b) HEA and PEG treatments vs controls, c) PEG treatments and controls and d) chitotsan (chit) and controls). The density here is from after the treatment of balsa wood. Lines of best have been included with corresponding colours given in the legend.

6.3.10 Additional concentrations tested

6.3.10.1 ASE and density

ASE using the original water air-dried control shrinkage gave different results to using the subsequent air-dried controls produced in parallel to this batch of samples (Table

6-4, Figure 6-60 and Figure 6-61). A new control was carried out to establish difference to original results. The new control group shrank more than the original control group. It is apparent that treatments improved ASE. However, from Figure 6-62 it is also apparent all treatments produced poorer results. A larger sample size is required for a comprehensive evaluation. PEG, however, did have similar results. 5% HEA +10% PEG and 6.5% HEA may have produced poorer results due to the their higher viscosity. Alternatively, the wood in the air-dried control showed that the original wood produced less shrinkage, so some of the variation in results could be due to the condition of the wood. However, the freeze-dried water control and PEG results suggest the difference may be due to treatment and greater sample sizes would clarify this. Chitosan treatments varied greatly (see Figure 6-63) and the vanillin hypothesised to improve the wood strength further through a Schiff base reaction with the lignin, did not greatly improve the ASE.

Table 6-4: Shows results of new set of concentrations freeze-dried and air-dried and showing ASE based on original water control and based on new control

Drying method	**Treatment**	**ASE (old water control)**	**Standard deviation**	**ASE (new water control)**	**Standard deviation**
Freeze-dried	water	83.33	4.45	84.50	4.14
	6.5% HEA	88.71	4.15	89.50	3.86
	20% PEG	101.48	2.58	101.38	2.40
	5% HEA + 10% PEG	92.55	3.56	93.07	3.31
	chitosan	83.92	3.10	85.04	2.89
	chitosan + vanillin	86.32	6.85	87.28	6.37
Air-dried	water	-7.52	6.11	0.00	5.68
	5% HEA	-4.05	23.57	3.22	21.92
	20% PEG	25.51	13.82	30.72	12.85

Air-dried wood treatments showed superior results with PEG than with HEA (Table 6-4, Figure 6-65 and Figure 6-64). A greater sample size is required, along with a

variation in concentrations. However, these preliminary results show PEG is superior as wood must be air-dried.

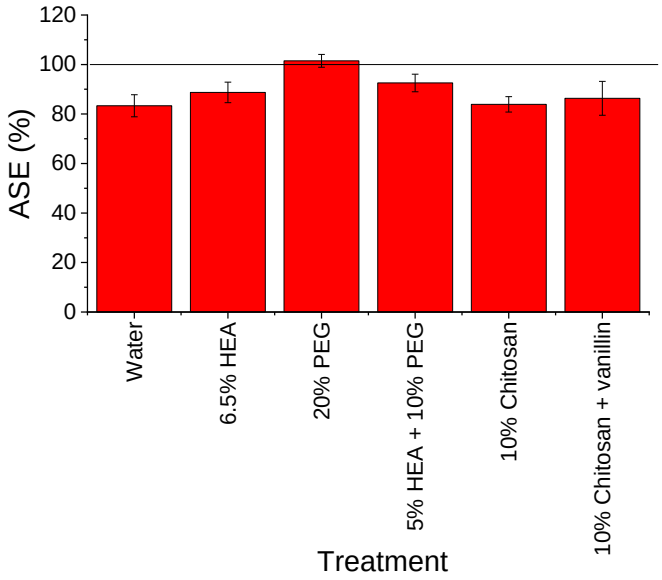

Figure 6-60: Bar chart showing ASE results of second set of concentrations based on the original shrinkage of oven dried sample

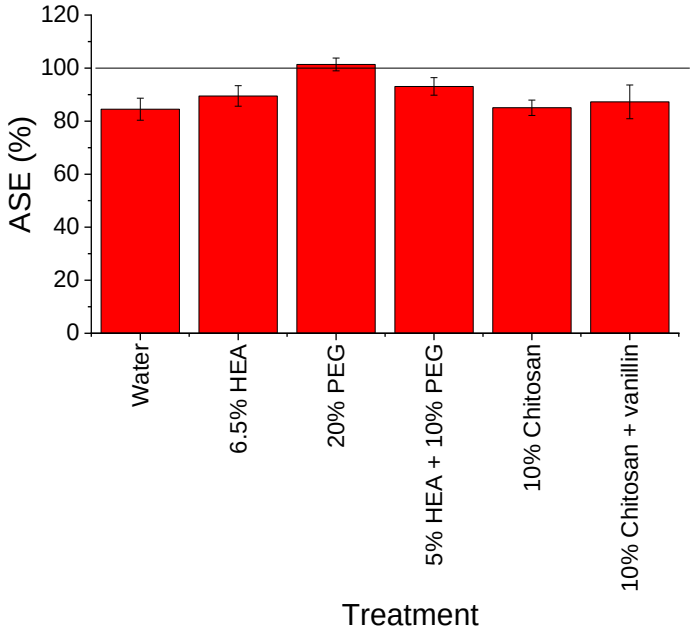

Figure 6-61: Bar chart showing ASE results of second set of concentrations based on the shrinkage of new water oven dried control

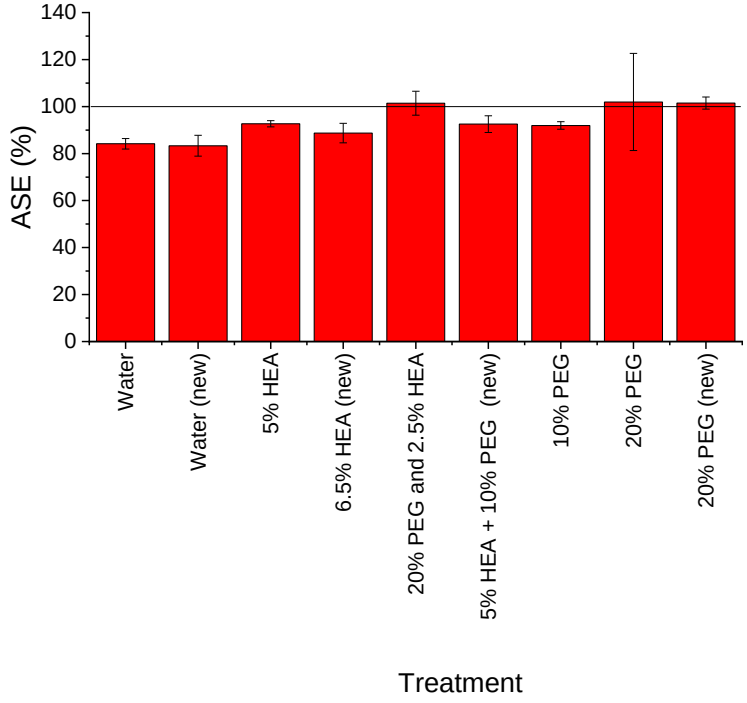

Figure 6-62: Bar chart showing ASE results of aminocellulose, aminocellulose and PEG, and PEG treatments new and old

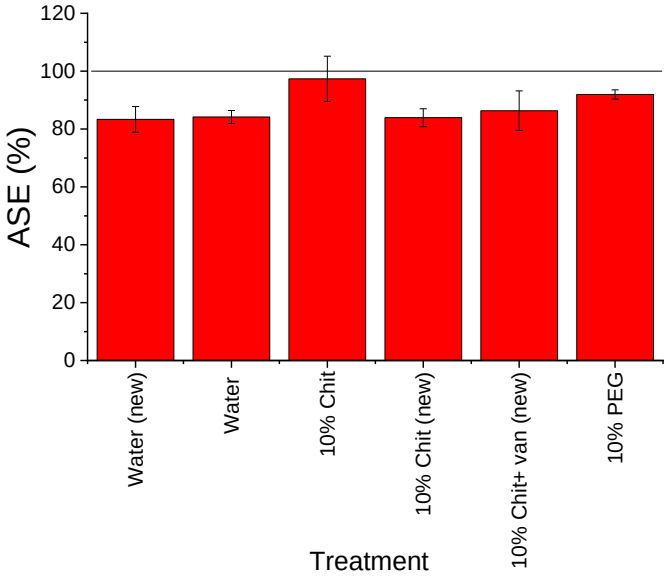

Figure 6-63: Bar chart showing ASE results of chitosan (chit), chitosan followed by vanillin (chit + van) treatment and PEG treatments new and old with original oven dried samples used for comparison.

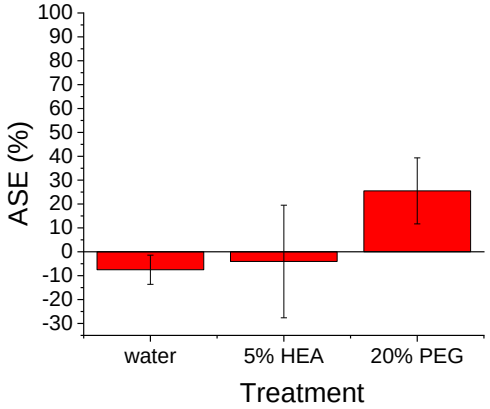

Figure 6-64: Bar chart showing ASE results of air-dried concentration based on the skrinkage of the original oven dried samples.

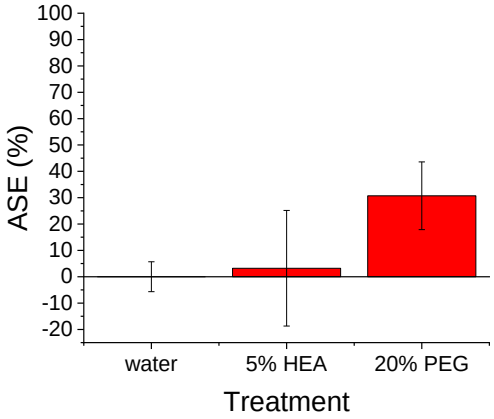

Figure 6-65: Bar chart showing ASE results of airdried concentration based on the skrinkage of the new water air-dried control

Density can be used as a proxy for consolidant uptake; although some consolidant appears to be taken up in almost all cases (Figure 6-66), it appears that compared to the first batch of treatments, less consolidant was taken up (Figure 6-67) despite higher

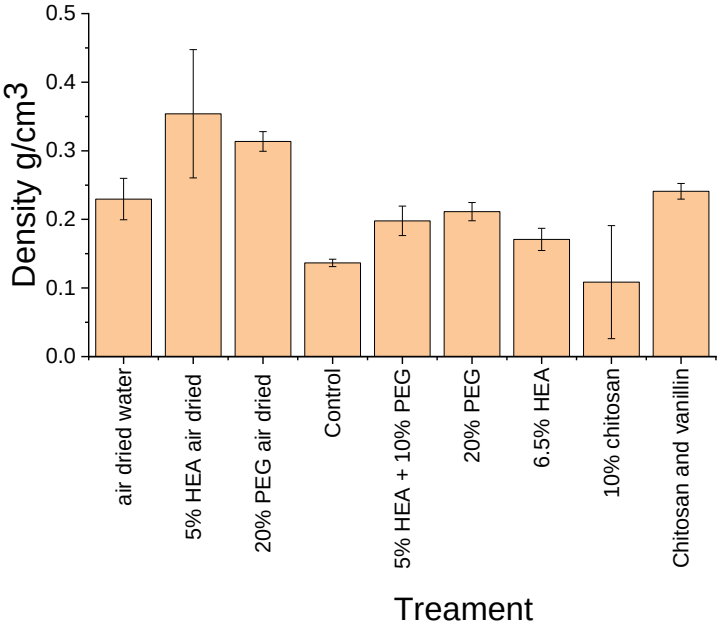

Figure 6-66: Bar chart of density of different treatments of new concentrations

concentration of HEA being used. This could explain the ASE results. The low uptake could be due to increased viscosity from the increase in concentration.

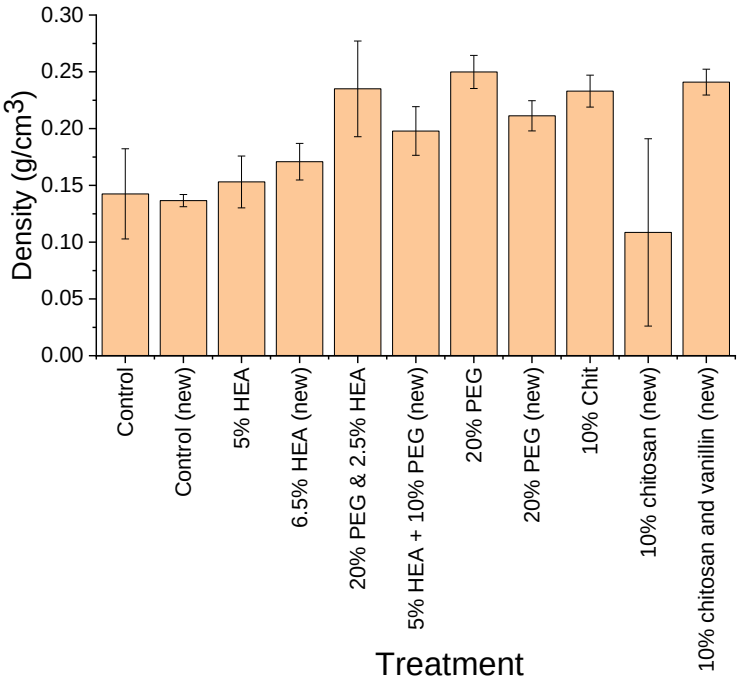

Figure 6-67: Density of different treatments. From original batch and new batch

6.3.10.2 Tape test

Freeze-dried control (water) shows a significant quantity of wood removed from the surface; 10% PEG and 2.5% HEA had little effect; 20% PEG freeze-dried wood showed only slightly reduced weight removal; 6.5% HEA did reduce weight removed (see Figure 6-68). Air-dried treatments showed improvement with PEG and further improvement with HEA (see Figure 6-68). The tape tests resemble results from the original experimental set (Figure 6-69). Both showed HEA improved surface consolidation.

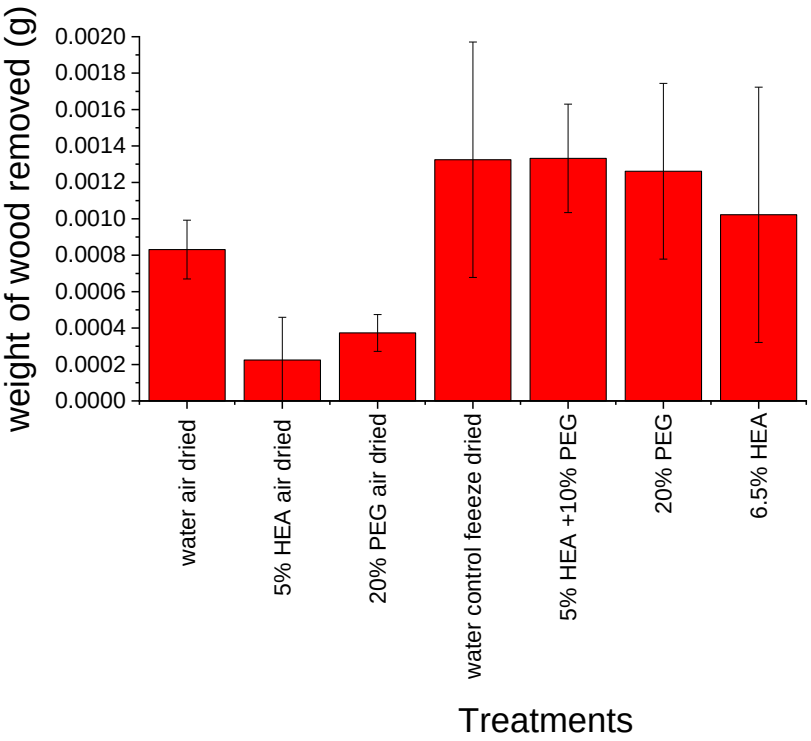

Figure 6-68: Bar chart showing tape test results weight of wood removed (g) for different wood treatments

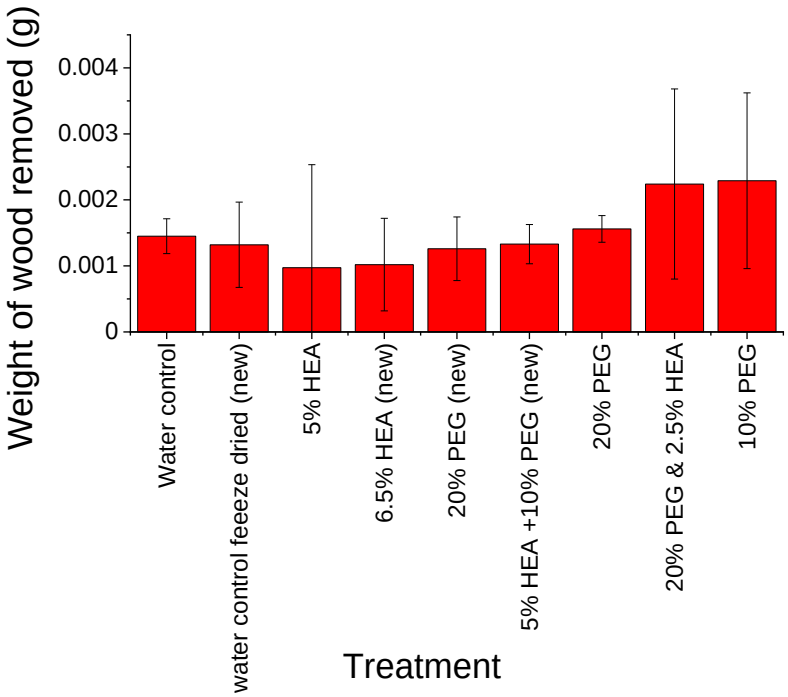

Figure 6-69: Bar chart showing tape test results weight of wood removed (g) comparison of new concenration and original concentrations.

6.4 Discussion

Evaluation of consolidation could be complicated by the alum and variation in condition of the Oseberg wood, hence, artificially degraded wood, which is relativity consistent, is used as the first point of investigation. This is compared with results with treated archaeological wood (oak), which can better establish consolidation. However, archaeological wood inherently contains more variability, hence, the combination of the two can better establish effects of treatments.

6.4.1 Weight, volume change and ASE

The artificially degraded wood was weighed and measured with a calliper to determine the volume. There were large margins of error (seen in weight changes Figure 6-5). The large margin of error and the mixture of weight gain and weight loss for water treatment could be due to the fluctuations in humidity in the air, as these pieces of wood were not conditioned at a set humidity before and after treatment. However, the ambient humidity was very similar and the start and end of treatment (went from 35 to 36% RH). The larger error in treatments could also be due to this. All treatments showed a weight gain, suggesting the polymers are being taken up by the wood, at least to some extent. IR and SEM help to establish if the treatments have fully penetrated the wood. PEG showed the highest uptake (36.09 ± 5.44%), however that is expected as a result of the higher concentrations used. For comparison, Broda (2018) found that with increasing concentration; 10-40% PEG 400, followed by 40% PEG 4000 in water, resulted in a (27.32 ± 4.16)% Weight percentage gain (WPG); 50% methyltrimethoxysilane (MTMS) in ethanol resulted in (33.19 ± 5.96)%. WPG (Broda,

2018). In our investigation, higher WPG was observed for PEG 2000. The state of degradation will have a large effect on WPG. The more degraded, the higher WPG is possible as the open pores will allow greater consolidant uptake. Chitosan acetate and PEG showed similar weight change, but the aminocellulose and PEG mixture results in a reduced weight increase compared to PEG alone. There are a number of possible reasons for this: the aminocellulose is known to self-associate (Chapter 3); larger molecular weight aminocellulose may be obstructing the surface and preventing PEG from entering; aminocellulose may be getting into the wood and hydrogen bonding to the cell wall, building up layers that block the PEG penetrating further or the reduced uptake could be due to the change in viscosity. Higher molecular aminocellulose has a higher viscosity which reduces uptake of consolidant as it struggles to flow into the wood.

With reference to the volume change, water shows the smallest change and PEG with chitosan the greatest. The difference between chitosan and chitosan acetate could be due to the fact one is in a salt form, or due to the concentration difference. PEG showed a large increase in volume, however, when combined with aminocellulose, the volume change was lowered, which could be because less PEG impregnated the wood (based on Figure 6-6). Both types of aminocelluloses show a small volume change which is encouraging. Visually the volume change was not noticeable. (See electronic appendix photos and scans of wood)

The artificially degraded wood was treated from the dry state, so while ASE could not be established, but weight and volume change could. The archaeological wood was

treated from the waterlogged state, so ASE could be established but weight increase could not. However final density can give an idea of which polymer was taken up best.

ASE values range between 84% - 112% ASE. A paper published by Gratten et al. (1980) mentions that a 75% ASE would be deemed acceptable. This was repeated by Parrent (1985) when establishing if sucrose could be used for conservation. However, today much higher ASE would be expected and wanted for conservation, especially of artefacts with precious carvings, where distortion could seriously damage the artefact and the aesthetics of the artefact (Grattan et al., 1980; Parrent, 1985). Freeze drying alone can be seen in these results to be above this threshold. The aim in this investigation was to obtain at least 90%; ideally an ASE of above 95% is really required to make a good recommendation for treatment. Some treatments produced relatively consistent results (stdev 1.3); others showed a great deal of variation (stdev 20.5). The variation in ASE results could be partly due to the level of degradation of the wood, hence; ideally more pieces should be treated to investigate this further. Based on these results, 40% PEG caused considerable swelling. The concentration of PEG used for conservation is dependent on the level of degradation and 20% gave good results; 10% however did not prevent shrinkage as expected. For the same concentration, chitosan produced slightly better results than PEG, but the results differences were marginal. Chitosan in acetic acid produced better ASE results within the 95% threshold. This suggests that the salt form may not be as efficient as the chitosan in acetic acid, which is unfortunate as chitosan cannot be used due to the requirement of acetic acid to aid dissolution. Aminocellulose, despite being half the concentration of 10% PEG, resulted in a better ASE on average and above the 95% threshold, although one wood sample was significantly lower. The 20% PEG produced

a good average ASE (just above 100%) as expected from Grattan et al's (1982) research, which would expect an ASE above 90% (Figure 6-70) (Grattan, 1982). However, in this research the 20% PEG results were surprisingly variable, although some difference would be expected due to the different wood being used and different molecular weight PEG, here PEG 2000 was used and Grattan used PEG 400. The combination of aminocellulose and PEG resulted in similar average ASE values, and improved the consistency of the results. Ideally, more wood samples would be tested to better establish if the results are purely from the effects of polymers or from variation of wood degradation. For comparative purposes ASE results have been compared to other investigations into consolidants (Table 6-5). Sucrose has produced ASE results of between 53-85%; according to Pearson (2014) aminocellulose had a higher ASE. Mannitol produced ASE of 96% compared to 87 % PEG (Pearson, 2014). However, the problem with some sugars is the hygroscopicity and microbial growth.

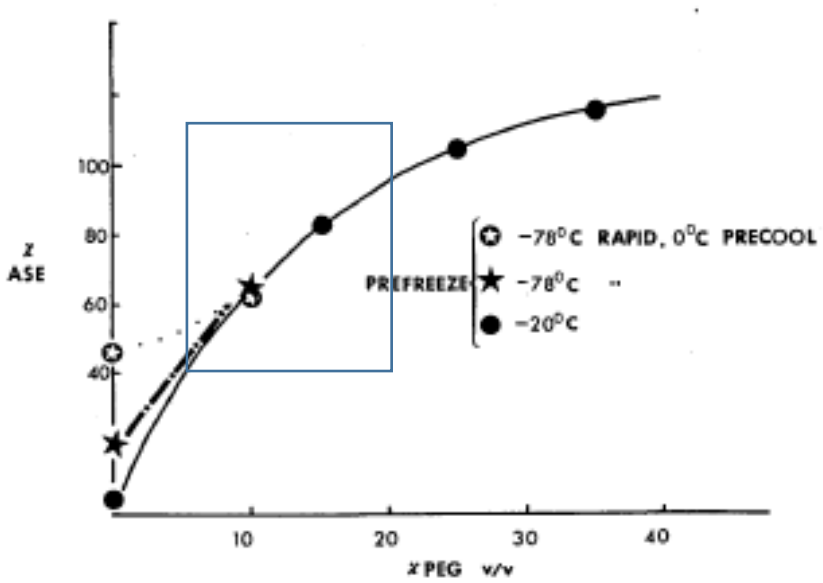

Figure 6-70: Plot of ASE of PEG 400 at different concentrations from Grattan et al. (1982).

Density can give an idea of the state of degradation of wood and an idea of the uptake of consolidants. The density of aminocellulose-treated archaeological wood is likely more related to the degradation state of the wood before it was treated than to the aminocellulose it contains. This conclusion is drawn from the fact that in artificially degraded wood, not as much aminocellulose as PEG was taken up and with a lower concentration a lower final density would be expected. The aminocellulose and PEG mixture, however, could be due to higher starting density, but it could be that the more porous archaeological wood allowed more aminocellulose and PEG to be taken up and the pores were not clogged up as easily by the self-associating aminocellulose. In comparison, chitosan and chitosan with PEG showed opposite results to those in the artificially degraded wood, where the density increase was similar to that of 20% PEG. This means chitosan did not prevent uptake of PEG.

Table 6-5: Dimensional changes with sugar treatment ((Pearson, 1987))

Worker	**Type of dimensional change of wood on air drying**	**% area of cross-section**	**% AEA**	**Type and concentration of sugar**	**%ASE PEG**	**Type and concentration of PEG**	**RH of dimensional measurements**
Barkman et al	Collapse and shrinkage	25	85	43% sucrose	52	43% PEG 1000	60%
Grosso	Collapse and shrinkage	11-70	84 80	40% sucrose	87 75	50% PEG 540 blend	?
Seamm	Tree shrinkage	8.8	53 69 83 96	Sucrose Invert sucrose Sucrose Invert sucrose	100 75 100 73	25% PEG 400 25% PEG 3350 25% PEG 400 25% PEG 3350	0 0 50% 50%
Grattan and cook	Collapse and shrinkage	29 39 (oak) 25 21.5 (oak) 73 18 (birch) 91 34 (birch) 58 7.5 (populus)	-13/1 19/18 30/25 96/96 57/22 38/32	20% sucrose 20% sucrose	44 82 87 104 75	20% PEG 200 and freeze dried	40%

Overall, in terms of ASE, the weight and volume change, aminocellulose HEA, HEA and PEG, chitosan and 20% PEG all appear promising. Although the volume change with 20% PEG on artificially degraded wood would suggest prioritising the use of HEA aminocellulose and chitosan, consolidation and colour change must also be considered.

6.4.2 Consolidation

6.4.2.1 Strength

Consolidation is hard to establish from a quantitative angle. Measuring hardness (force required to penetrate 1.1 mm into the wood.) was attempted, as was tape test, which measured the extent of powder on the surface of the wood, as well as qualitative assessment from handling the wood and cutting the wood. Photos were included as proof of consolidation (see appendix).

Due to the small size of the wood pieces, normal strength tests such as modulus of elasticity and stress at failure could not be done. The artificially degraded wood was 1 cm^3 in order to be able to observe whether or not penetration of the polymer occurred. Tongue depressors used by Tahina *et al.* (2016) would be too thin to establish if the polymers can penetrate the wood. The other consideration was the limited amount of consolidant available for research. For archaeological wood, the availability of the wood was part of the reason for the size of the pieces. The short length of the pieces of wood meant mechanical testing instruments such as Instron could not be used, as they require pieces of wood which are at least 20 cm long.

A fruit penetrometer has previously been used to establish the degradative condition of waterlogged wood (Petrou and Pournou, 2018). It was thought this could help to also establish effectiveness of a consolidant. All treatments appear to have improved at least regarding the density of samples, but the effect on the strength is less clear. When referring to hardness alone, PEG and chitosan in acetic acid appear to be the most promising. However, variability in results means other treatments should not be disregarded, as much larger sample sizes are required and other methods of establishing consolidation rather than hardness alone are required. Instruments designed for the food industry to establish properties might be more appropriate to the size of samples than instruments traditionally used to analyse wood. Hardness, flexibility (3-point bend tests) and cutting tests (it has often been commented that treated wood is easier to cut coherently, but this does not provide numerical proof as it is purely qualitative based on researchers observations (McHale et al., 2017)). Future work could combine this with the use of an acoustic recorder to record the sound of the wood cracking. The combination would permit a quantitative assessment of the same previously reported qualitative test. Fragile, brittle wood would be expected to produce more sound than flexible wood under pressure. These investigations could also be carried out in a controlled humidity and temperature environment to remove as many external factors as possible. Again, larger sample sizes of ideally 15 samples for each treatment, but at least 5 samples, should be investigated with at least 10 replicates for the control, to establish the variability in the untreated archaeological wood.

6.4.2.2 Surface cohesion (tape test)

Surface cohesion of the wood can be a clue to the condition of the wood. A good consolidant should secure the surface and prevent fragments of wood being detached. Therefore, to establish how powdery the surface is, a piece of tape was applied to the surface of the wood. The weight of the tape after removal from the wood can establish how much powder was pulled off the surface. What was found was that, even in cases where the surface appeared consolidated, some wood was ripped off. The adhesive tape stuck to the wood and if the consolidant was weak, chunks were ripped off due to strength of the tape, rather than because the surface was powdery. Hence, the weight must be considered alongside the images showing what was removed from the wood surface. Sets with some tape with very little powder and some with chunks suggest the surface was consolidated.

All treatments, except 10% PEG and the chitosan and PEG mixture, improved consolidation. Aminocellulose appears to be the most promising and 20% PEG the least promising out of the remaining archaeological wood samples. PEG is commonly used in conservation and it would have been expected to show better results. The reason for the results may be the softness of PEG, resulting in consolidation but still easy removal of surface on pressure applied to remove a layer of wood. Aminocellulose is very promising from these results. Aminocellulose with PEG appears less promising, though larger sample numbers are required to rule out the possibility of wood being in better condition prior to starting treatment. The fact that such a low concentration can produce such good results is very interesting in terms of costs and sustainability, as less material will be required and less wasted.

6.4.2.3 Qualitative assessment of consolidation (slicing the archaeological wood)

The pieces of wood were sliced in two with a small saw and a razor blade was used to try to get a clean cut for the SEM. Whilst cutting the wood for the SEM, it was observed some were very powdery and broke into pieces, whereas others were stronger and when sliced the layers stayed together. From this it appears that 20% PEG, 40% PEG and aminocellulose 2 with PEG produced the most consolidated wood. Chitosan in acetic acid also produced very good results.

This is in disagreement with the tape tests as they suggested aminocellulose consolidated better than aminocellulose and PEG. A larger sample size is needed for these tests to better establish which method is best.

6.4.3 Colour change

In terms of both the artificially degraded wood and archaeological wood, 20% PEG showed one of the smallest delta E values, hence, smallest colour change. Aminocellulose 1 (HEA) with PEG for the artificially degraded wood and aminocellulose 2 (AEA) with PEG for the archaeological wood showed the smallest and second smallest delta E value. For archaeological wood, 40% PEG and aminocellulose showed the biggest colour change for treated samples. Oven-dried wood showed the biggest colour change of all samples. Visibly, aminocellulose 2 darkened the wood slightly and 40% PEG lightened the wood slightly.

6.4.4 Penetration (IR, SEM and X ray tomographic microscopy)

IR shows PEG penetrated the wood fully. Aminocellulose, unfortunately, has a very similar IR to wood, therefore the peaks are probably hidden under the peaks of the wood. Chitosan acetate treated wood has a small shoulder on one of the peaks, which may be evidence of chitosan in the centre of the wood, but the shoulder is not enough for this to be conclusive.

From the increase in weight, it is known that some aminocellulose was taken up; however, the SEM images show an open structure is maintained which means re-treatment would be easy, should it become necessary in the future. Increased strength was observed when cutting the wood and from the tape tests, this consolidation ability may be due to the aminocellulose adhering to the cell walls, providing more strength whilst maintaining an open structure. Similarly, chitosan acetate may be behaving the same; however, on one image it looks as if some material may have detached from the cell wall. It is possible that the chitosan acetate also adheres to the cell wall as well to begin with but, as the wood fully dries, the chitosan acetate detaches from the wall leading to the reduced consolidation observed. Chitosan in acetic acid does not appear to show the detachment from the cell wall as seen with the chitosan acetate suggesting it is possibly adhering to the cell wall better; again, this could be the reason for the improved consolidation and strength.

Tomography for artificially degraded wood shows an open structure, but the polymers are not observed. This could be due to the polymers coating the cell.

6.4.5 Additional concentrations ASE and tape test

Additional wood treatments on archaeological wood were carried out to establish the effect of concentration of HEA and how different combinations of HEA and PEG affect ASE and density. The new set of air-dried control (water) shrank more than the original set of air-dried control (water). Density showed lower uptake of HEA due to the higher concentration, which probably caused higher viscosity. This lower uptake resulted in reduced ASE. However, greater sample sizes and a larger concentration range are definitely a prerequisite to determination of best consolidation. Tape test shows that 5% HEA produced better consolidation than 20% PEG and freeze-dried control in both the original set and the new set of treatments of different concentration.

6.5 Future work

Ideally the work should be repeated on a larger sample size as the variability in the wood is obvious and could have a direct effect on the results and interpretation. A humidity chamber should be used, if available, if this work is repeated on more samples. This applies to artificially degraded wood and archaeological wood but the effects are more pronounced in the latter. A greater number of control samples are also required to establish the variability among the controls to confirm that any differences observed are a direct result of treatment and not inherent variability. Although humidity is not thought to have had a large affect as measurements were taken at the same ambient humidity, it is worth acclimatising the samples to rule it out as a cause of error. In terms of mechanical testing, the polymers themselves should ideally be tested along with larger pieces of wood at least 20 cm long, so that standard wood

analysis can be carried out, as done by the timber industry. Alternatively, a new method must be sought, possibly from techniques used in the food industry and designed for much smaller items. Possibilities include: a three-way bend test for biscuits to establish flexibility or a hardness test, although such new methods would have to be adapted for analysing archaeological wood. Potential problems might include that the direction of each side of wood might have to be established first and much larger sample sizes are required as this will have the same problem as the fruit penetrometer; however, some error may be limited by electronic controls rather than manual controls. Finally, slicing has previously been reported and this was also observed to be easier with some treated samples. Hence, a slicing instrument may be able to evaluate this numerically. The force required for cutting could give an indication of hardness and the point of cracking; less force required towards the end could establish brittleness of a sample. An acoustic recorder used in conjunction with these measurements could give a better idea of how brittle a sample is. Finally, all mechanical analysis should be carried out in a controlled humidity and temperature chamber. The wood should also be acclimatised before and after analysis to avoid effects of humidity. The stability of the polymers aminocellulose and chitosan and the stability of treated wood need to be assessed. For the polymers, they can be subjected to acid degradation with sulphuric acid and GC-MS and viscosity used to assess stability. For the wood, artificial ageing, through high temperature and humidity could be used, along with separate studies on humidity cycling and UV artificial ageing to get a full well-rounded estimate of future degradation effects. The chelation properties of the degraded chitosan and aminocellulose could be assessed with a colorimeter using iron sulfate. The corrosion effect on a nail could also be compared in a petri-

dish, one set in just water for longer term study and one set with sodium chloride added to accelerate the corrosion. Hygroscopicity is another important factor, water absorption is one way to assess the effect of the polymer (Muhcu et al., 2017) this work would be useful to undertake as part of a full assessment of the consolidant.

Chitosan may not be applicable to the Oseberg artefacts due to the requirement of acetic acid for its dissolution but may be useable for other industries. For example, in the construction industry, where wood needs to be kept in good condition for long periods of time, but also in older buildings, which may be listed, where old wood must be preserved, e.g. treating an old window sill and repainting could be cheaper than a new window but also means that original features can be kept.

6.6 Conclusion

Chitosan acetate salt was not very effective for conservation as evident from tape tests and slicing treated wood. The hardness tests were not conclusive. Hence, this is not an option for conservation. It appears that the acetate component appears not to bind to the cell wall, which could be because the acetate component is preventing hydrogen bonding with the cell walls. Chitosan looks very promising in terms of consolidation; however, the acetic acid needed for dissolution means that it could put artefacts at risk in the long term to further acid degradation. Although, the strength of the acid is not as strong as the sulphuric acid already in the wood and the chitosan in acetic acid solution was measured as pH5 the same pH as fresh wood. PEG is an alternative, although it has other/similar issues in terms of acidic breakdown products and PEG's breakdown can be catalysed by acid or iron sample as other organic polymers.

Aminocellulose appears to be a promising alternative. In artificially degraded wood at only 4% concentration, there was a ~15% increase in weight, and in terms of ASE there was greater than 95% ASE. Colour change is a concern as the colour change was greater with aminocellulose; however, this colour change was not dramatic and if sufficient consolidation is gained and future stability is greater, this could be an area of compromise, considering the colour change is small. In terms of consolidation, the tape test and slicing did suggest good consolidation. Flexibility and strength of treated wood requires future investigation with larger pieces of wood and with larger sample numbers, to be able to differentiate between variation in initial condition and the effects of treatment.

Combining aminocellulose with PEG is also a possibility. This showed a greater than 20% increase in weight and, again, good ASE, although still causing swelling but no more than PEG and with more consistent results. Aminocellulose and PEG also showed less colour change than aminocellulose alone and comparable colour change to PEG. The consolidation appears to be weaker in terms of the tape test compared to aminocellulose alone, but better than 20% PEG. In terms of slicing the wood, aminocellulose and PEG showed better results than aminocellulose alone. It may be possible to optimise the ratio of aminocellulose to PEG to produce even better results. This is also worthy of further investigation. Aminocellulose, with or without PEG, could be of particular interest for artefacts that have anticipated future problems with PEG alone, due to iron or sulphur content. Aminocellulose alone would also make re-treatment easier, as the original aminocellulose treatment would not have to be removed prior to further treatment. PEG on the other hand fills the cells, meaning it may have to be removed in order to re-treat the wood. Aminocellulose has not yet been

investigated for reversibility, but may prove to be reversible or partially reversible in addition to the wood being re-treatable.

Chapter 7. Non-Aqueous treatment of wood

7.1 Introduction

This chapter discusses results from non-aqueous wood treatments. Small pieces of alum-treated wood of little archaeological importance from the Oseberg collection have been used as test pieces and those in very poor condition have disintegrated entirely in the water as alum was supporting the structure. In other pieces the re-treatment with polyethylene glycol (PEG) has significantly darkened the wood but other pieces of wood appear perfectly acceptable (Braovac and Sahlstedt, 2019). This is the reason that a non-aqueous treatment is sought. Butvar B98 and Paraloid B72 were selected as non-aqueous treatment comparisons, as they are currently used in conservation. PEG was also selected for laboratory-degraded wood treatment comparison in order to compare the work to aqueous and non-aqueous treatment. PEG was historically used with *tert*-butanol before it was used with water (Grattan, 1982; Jespersen, 1981; Unger et al., 2001). Solvents were carefully chosen as were the consolidants for comparison.

7.1.1 Solvent choice

Selecting potential solvents for wood conservation can be difficult as there are so many aspects to consider: solubility of lignin, chemical interaction with lignin, swelling of the wood, toxicity, waste disposal and sustainability. Solvents can be removed in one of two ways: controlled evaporation or freeze drying.

Polar solvents have been found to cause wood to swell; non-polar solvents have not. Aliphatic and aromatic fractions have low viscosity, which aids in penetration of the

wood. However, as the solvent evaporates, compounds can be pulled back out of the wood. Higher viscosity can result in more even distribution (Unger et al., 2001).

Solvents currently used in conservation include ethanol, acetone, ethyl acetate, isopropanol, toluene and white spirit. Ethanol and acetone, however, are not preferable due to their swelling factor and their fast evaporation rates, which are likely to crack the wood. Toluene is to be investigated but it is not the best in terms of sustainability and there is concern there may be new legislation limiting its use in the near future (Alder et al., 2016). However, it has been previously used in conservation making it more likely to be accepted by conservators and it did not cause significant swelling (see Table 7-1).

Dimethyl carbonate is relatively promising in terms of sustainability, but has been found to methylate lignin (Sen et al., 2015).

Swelling factor, evaporation rates, flammability and toxicity to humans and the environment are the most important factors, along with lack of reactivity or solubility of lignin. Other important factors include ease of penetration, any propensity of retention and migration behaviour and sustainability would be preferable (Unger et al., 2001).

Swelling factor has been measured against water for some solvents (see Table 7-1 and Table 7-2). Red denotes solvents that are unlikely to be good for conservation of wood. Solvents highlighted in green with stars display good properties for conservation.

Table 7-1: Swelling factor compared to water of various solvents Mantanis et al. 1994 referenced in Unger et al., 2001. Green with stars most favourable (less swelling than acetone), red with circles least favourable (more swelling than water).

Solvent	Swelling factor (water 100)
★ Octane	★ 8
★ Tetrachloromethane	★ 13
★ Toluene	★ 17
★ Chloroform	★ 30
★ Ethyl acetate	★ 37
★ 1-Propanol	★ 60
Acetone	69
Ethanol	76
1,4 Dioxane	83
Methanol	90
Acetic acid	102
○ Ethylene glycol	○ 109
○ Dimethylformamide	○ 138
○ DMSO	○ 157
○ 1-Butylamine	○ 191

Table 7-2: Maximum tangential swelling caused by solvent relative to that in water at 23°C (Mantanis et al., 1994).

Solvent	Sitka	Douglas fir 1	Douglas fir 2	Sugar maple	Quaking Aspen
Water	8.1±0.2	8.8±01	10.0±0.3	10.6±0.3	8.9±0.3
Ethanol	7.0±0.2	6.3±0.2	7.3±0.2	6.9±0.1	7.7±0.3
Propanol	4.9±0.1	5.1±0.2	6.6±0.1	5.3±0.2	6.0±0.2
Acetone	5.7±0.2	4.6±0.2	7.2±0.3	7.1±0.2	7.5±0.2
Ethyl acetate	2.6±0.3	2.7±0.3	2.6±0.1	3.7±0.1	5.5±0.1
Toluene	1.6±0.2	1.5±0.2	1.7±0.1	1.5±0.0	1.6±0.1

Wood swells significantly in water, hence solvents after 1-propanol in Table 7-2 become less and less preferable. However, cellulose is responsible for the majority of swelling and there is very little if any cellulose left in the Oseberg artefacts; this might mean swelling is less of a factor but is still worth avoiding. Hydrogen bonding with molecules in the wood reduces the mobility of polar solvents, another reason why non-polar solvents are preferable. Waterlogged wood, however, is an exception as water is already present.

Shrinkage after treatment is also important. Table 7-3 contains a list of solvents and the resulting shrinkage and surface tension. This must also be kept in mind.

Table 7-3:Wood shrinkage on treatment with solvent (Rosenquist, 1959).

Solvent	Shrinkage (vol. %)	Surface tension (dynes cm.)	Boiling point (ºC)
Water	85	72.75	100
Ethyl Alcohol	60	22.3	78.5
Chloroform	53	27.1	61.3
Acetone	52	23.7	56.5
Xylene	26	c 30	c 140
Ethyl ether	12	17.0	34.6

Evaporation rate (Table 7-4) is also a factor that must be balanced: too low and solutes may not be transported deeply; however, too high and solutes may penetrate fully then be transported back towards the surface as the solvent evaporates. The other concern is retention of solvents within wood, i.e. incomplete evaporation which can result in reduced glass transition temperature of a polymer and hence, reduced elasto-mechanical properties. Also, solutes could re-dissolve and re-solidify the polymer which could lead to cracking of the wood. Hence, medium evaporation rates such as with toluene are preferred. Viscosity is also involved in terms of penetration of solvent and material into the wood. Table 7-5 shows the viscosity of several solvents with low viscosity highlighted in green.

The process of treatment and drying is also very important. In particular, super critical CO_2 needs to be further investigated to see if it is an option. However, the focus in this investigation is the new consolidant itself.

The most preferable solvents are isopropanol, ethyl acetate and butyl acetate in terms of sustainability (Table 7-6), health and safety, swelling and viscosity. Toluene is not

preferable but is already used in conservation and does not cause too much swelling. 3,6-di-O-tert-butyldimethylsilyl (TBDMS)-chitosan had limited solvent choices, hence, 50:50 toluene/ethyl acetate was chosen. However, some research could be done in mixing solvents to find the best combination or limit the quantity of toluene used. The degree of substitution also appears to be a factor and if TBDMS appears promising, future work could try to modify the DS to allow for ethyl acetate alone as a solvent or isopropanol or butyl acetate.

Table 7-4: Solvent evaporation number and boiling point (Unger et al., 2001), red with circles least favourable, green with stars more favourable.

Solvent	**Boiling point**	**Evaporation number**
○ n-Hexane	○ 69	○ 1.4
○ Acetone	○ 56	○ 2.1
Chloroform	61	2.5
Ethyl acetate	78	2.9
Benzene	80	3.0
n-Heptane	98	3.3
Cyclohexane	81	3.5
Tetrachloromethane	76	4.0
Petroleum ether	50-115	4.5
★ Toluene	★ 111	★ 6.1
Methanol	65	6.3
Ethanol	78	8.3
2-Propanol	82	11.0
Xylene	144	13.5
1-Propanol	97	16.0
1-Butanol	117	33.0
○ Ethyl glycol	○ 135	○ 43.00
○ Water	○ 100	○ ~80
○ Turpentine	○ 150	○ ~170

Table 7-5: Viscosity of solvents from a chemical supplier (Sigma Aldrich, 2020). The preferable solvents are shown in green with stars.

Solvent	**Viscosity (cP) at 20 °C**
Acetone	0.32
★ Heptane	★ 0.42
★ Ethyl acetate	★ 0.46
★ THF	★ 0.55
★ Methanol	★ 0.55
★ Toluene	★ 0.59
Water	1.00
Isoproply alcohol	2.86

Table 7-6: Aspects of sustainability of various solvents (Alder et al., 2016).

Solvent	Type of solvent	Bp	Mp	Vap	Incineration	Recycling	Bioreactment	VOC Emissions	Aquatic impact	Air impact	Health	Exposure potential	Flammability	Reactiveity	Life cycle	Swelling factor of wood (water=100)	Comments
Methanol		65	-98		4	7	3	3	10	7	4	6	5	10	8	90	
Ethanol		78	-114		5	5	3	4	9	5	10	8	6	10		76	
Acetone		56	-95		5	6	2	2	10	6	10	6	4	9	7	69	
Dimethyl carbonate	Ester	91	-1		7	9	9	7	9	8	4	5	8	10			May methylate lignin (Sen et al., 2015) Methylation of softwood kraft lignin with dimethyl carbonate)
White spirt/petroleum spirt	Hydrocarbon	55	-73		8	9	4	2	5	5	1	6	2	10	7		Not very sustainable but already used in conservation
Toluene		110			10	7	6	7	7	2	7	6	5	10	7		
Isopropanol	Alcohol	82	-88		5	5	3	5	8	7	10	6	6	8	4	1-propanol =60	Used in conservation

Solvent	Type of solvent	Bp	Mp	Vap	Inci-nera-tion	Rec-ycli-ng	Bioreact-ment	VOC Emissions	Aquatic impact	Air impact	Heal-th	Expos-ure potent-ial	Flammab-ility	Reacti-veity	Life cycle	Swelling factor of wood (water=100)	Comments
2-Butanol	Alcohol	100	-115		4		6				8		7	9	6	37	Freeze dry or evaporate?
t-Butanol	Alcohol	82	25		5	5	3	5	9	5	4	7	6	10	8		Freeze dry or evaporate?
Ethyl acetate	Ester	77	-84		5	6	5	4	9	5	10	7	5	10	6		Approved in conservation
Isobutyl acetate	Ester	118	-99		7	9	8	6	9	6	10	6	8	10			
Anisole	Aromatic/ether	154	-38		8	8	8	8	7	6	7	8	7	9	5	Toluene =17	Instead of toluene (better in terms of sustainability)
p-Xylene	Aromatic	138	-13		10	9	6	7	5	2	7	7	5	10	7		Instead of toluene (better in terms of sustainability) Flammability might be an issue
Cyclohexane	Hydrocarbon	81	7		10	6	5	4	3	5	10	6	2	10	7		Evaporate or freeze dry?

Solvent	Type of solvent	Bp	Mp	Vap	Inci-nera-tion	Rec-ycli-ng	Bioreact-ment	VOC Emissions	Aquatic impact	Air impact	Heal-th	Expos-ure potent-ial	Flammab-ility	Reacti-veity	Life cycle	Swelling factor of wood (water=100)	Comments
2Me-THF	Ether	78	-137		6	5	3	4	7	4	4	3	4	6	4		Instead of THF (better in terms of sustainability). Toxcicity might be an issue
Di(ethylene glycol)	Ether	246	-10													(ethyl glycol=109)	Freeze dry? Swelling could be an issue

7.1.2 Consolidants investigated

A short introduction to each consolidant can be found in Chapter 1. More detail is given below.

7.1.2.1 B72

Paraloid B72 is known to have many positive properties for conservation; it is a flexible polymer that dries clear and is less glossy then polyvinylacetate (PVA). It has been found not to discolour even at high temperatures, hence, theoretically, ages well (Hamilton, 1999). Paraloid B72 is made from two polymers: ethyl methacrylate and methyl acrylate (70:30). It has a Tg of 40 ^{o}C and a refractive index of 1.49 (Chapman and Mason, 2003). It is used for its stability in many areas of conservation. It has been used in stained glass conservation for loose paint (Chapman and Mason, 2003), fossil conservation (Larkin and Makridou, 1999; López-Polín, 2012a; Rutzky et al., 2005), ceramic conservation (Constâncio et al., 2010; Koob, 1986), stone fossils (Favaro et al., 2006) and bone conservation (Johnson, 1994b). B72 is mostly used in art conservation but there has been some research and use in wood conservation (Tuduce Trăistaru et al., 2011). An added advantage is it is a reversible treatment, at least for small pieces (Appelbaum, 1987; Brajer, 2009). The concern with B72 involves the ester bonds in the structure which are acid sensitive. This is a concern for the alum-treated artefacts that are acidic. However, the acidic problem could possibly be improved by the use of nanoparticles prior to B72 treatment or by combining B72 and alkali nanoparticles in one treatment.

Investigations show that wood alone can also be treated with B72. Tuduce Trăistaru *et al.* (2011) treated sound poplar wood with B72 in different concentrations and solvents. It was found that 10% B72 in acetone and ethanol resulted in the highest weight percent gain (WPG) compared to 10% in toluene. However, the consolidant is still taken up in toluene; in addition, 10% concentration also showed improved weight gain compared to 5% in both instances (Tuduce Trăistaru et al., 2011). Scanning electron microscopy (SEM) for 10% B72 in acetone and ethanol showed B72 fills lumen of fibres and also fills pits of rays. The distribution observed was uneven, but better penetration was observed on the longitudinal direction via fibres and vessels (Tuduce Trăistaru et al., 2011). Although Tuduce Trăistaru *et al.* (2011) found better results with acetone and ethanol, they did not investigate swelling of the wood and toluene has been found to cause less swelling than both acetone and ethanol (see Table 7-2 data taken from (Mantanis et al., 1994)).

Although Tuduce Trăistaru et al. (2011) found uneven distribution with B72 investigated with SEM, similar research by Schniewind and Eastman (1994), who investigated degraded douglas fir, showed a drop in the percentage of cells with visible resin in the first 7mm, then a steady drop in concentration in the case of B72 in acetone. In the case of B72 in toluene, there was an initial drop then it stabilised, but the concentration was lower than that of B72 in acetone except at 21mm, where there is a slightly higher percentage of filled cells with toluene compared to acetone (Schniewind and Eastman, 1994).

Research into Fourier-transform infrared spectroscopy FTIR to determine concentration by Timar et al. (2014) found distribution was affected by concentration.

Research into B72 in sound poplar wood by Timar et al. (2014) showed that FTIR can semi-quantitatively determine concentration. The research also investigated concentration at different depths along the longitudinal direction, to determine if it was evenly distributed. It found that 5% B72 was evenly distributed, but at 10% the B72 concentration went deeper into the wood (Timar et al., 2014). This investigation was for sound wood, *hence*, heavily degraded wood could probably still take higher than 5% B72.

Muhcu et al. (2017) found a higher weight percentage gain (WPG) with 24h immersion rather than vacuum treatment. Other treatments have found vacuum immersion more effective (Mańkowski et al., 2015). This current piece of research will investigate TBDMS chitosan with different treatment lengths and vacuum vs immersion alone. Longer treatment lengths, as mentioned in the Chapter 6 on aqueous treatments, will be used to ensure maximum uptake.

An additional advantage of treatment with B72 is that it lowers water absorption (hygroscopicity) (Muhcu et al., 2017). Muhcu et al. also investigated anti-fungal effects of B72 treatment. B72 was only found to reduce weight loss with rot fungus *T.vesicolor* but not *F.Palustris,* except if nanoparticle CuO or B_2O were added. With the addition of nanoparticles, weight loss for white rot could be almost completely prevented (Muhcu et al., 2017). Nanoparticles to prevent weight loss for fungi are not required for wood conservation in museum-kept artefacts, as with good storage conditions fungal growth is not possible due to humidity and temperature controls (Yu et al., 2001).

B72 has previously been used as a dry treatment for wood and other artefacts. The problem is that alum-treated wood is acidic and B72 is acid sensitive due to the ester bonds in the polymer. However, although B72 will degrade slowly over time, B72 has been investigated as a pre-consolidant to be followed up by the removal of the alum and acid (Häggström and Sandström, 2013). It was shown that alum could successfully be removed after treatment with B72 at room temperature. At 40 ^{o}C, due to B72's low T_g, the B72 softened and salt removal caused artefacts to fall apart. Re-conservation with B72 showed no increase in cracking. B72 was also found to reduce surface flaking. The negative effect was that B72 resulted in a slightly shinier surface; however, this was deemed acceptable (Häggström and Sandström, 2013). Following pre-consolidation with B72 and alum removal, the wood can be left as it is or treated with PEG.

Therefore, B72 appears to be a possibility for the conservation of alum-treated wood and hence was used for comparison to determine if TBDMS chitosan is a plausible alternative option for treating alum-treated wood. With TBDMS chitosan, it may be possible to leave the alum in place to limit the risk to the artefacts.

7.1.2.2 B98

According to Eastmans (a supplier of B98), Butvar B98 is a polyvinyl butyl polymer which is formed from a reaction of aldehydes and alcohols. B98 is a polymer formed from a mixture of three monomers. The three monomer units are PV butyral, PV alcohol and PV acetate with a hydroxyl content of 18-20%, acetate 0-2.5% and butyral makes up 80%. B98 has a molecular weight of 40-70 kg/mol, 10% a viscosity of 75-

200 cP and a refractive index of 1.490. According to American Society for Testing and Materials ASTM D543-56T, it has excellent resistance to strong acids. This is highly relevant to its application to alum-treated wood which can be highly acidic. The modulus of elasticity (apparent) according to ASTM D638-58T 3.1-3.2105psi. B98, has a Tg value of 72-78 ^{o}C, hence, is more suitable for concentration in hot countries compared to B72 (Eastmans- supplier information). B98 has previously been used for wood conservation, commonly in an ethanol toluene mix between 5-20% B98. Schniewind and Eastman (1994) investigated whether 20% B98 is better in ethanol or in ethanol and toluene 40/60 mix for treating significantly degraded douglas fir foundation piles (70 years old). They found B98 in a 40/60 mix of ethanol/toluene on average had a higher number of tracheids with visible resin throughout the wood compared to B98 in ethanol alone. Gravimetrically, uptake of B98 in a 40/60 mix of ethanol/toluene was better than B98 in ethanol alone (Schniewind and Eastman, 1994). Wang and Schniewind (1985) also found greater consolidant retention when B98 was dissolved in toluene and ethanol, compared to ethanol alone. This could be due to the viscosity of 20% B98; the addition of toluene significantly lowers the viscosity. The modulus of elasticity (MOE) of wood treated with B98 was slightly increased at 20% B98 in 40/60 ethanol/ toluene. However, B72 at 20% in either toluene or acetone resulted in a higher MOE than for the control, or wood treated with 20% B98. The modulus of rupture (MOR) was higher than the control with 20% B98 and even higher with 20% B72 independent of the solvent (Wang and Schniewind, 1985). Wang and Schniewind (1985) reported the molecular weight of B98 as 30-34 kg/mol, MOE of polymer alone is 3.1-3.2 x10^{-5} psi and Tg 62-68 C (Wang and Schniewind, 1985). SEM analysis by Spirydowicz et al. (2001) showed that 10% B98 vacuum treatment

resulted in greater uptake compared to immersion. B98 fills vessels and cell lumina and coats some cell walls. A needle harness test with a load of 2.4 mm penetration showed significant improvement on treatment with 10% B98 (Spirydowicz et al., 2001b).

This suggests that B98 is a good option for alum-treated wood, either as a pre-consolidant, possibly as a consolidant, or as a consolidant combined with $Ca(OH)_2$ nanoparticles to increase the pH. B98 has been reported to have good acid stability. However, the ester groups suggest some susceptibility to acid, so this needs to be investigated further.

7.2 Methodology

7.2.1 Wood treatment

7.2.1.1 Wood preparation: artificially degraded wood (laboratory degraded wood)

Lengths of 1 cm and 2 cm pieces were cut with a hand saw from the 18 cm sticks of artificially degraded sound birch. The 2 cm pieces were taken from the middle. The preparation of this artificially degarded wood otherwise called laboratory degraded wood is described in methodology in Chapter 6.

A little notch was then put into each piece, so the measurements and photographs could be taken from the same side for correct comparison. The dimensions and weight of each piece were measured: this was used to calculate the density of each piece. Each

piece was also scanned on a photocopier and photographed. These will later be used for comparison of before and after treatment. The weight and dimension measurements were taken at room temperature and ambient humidity before and after treatment, but RH was in a similar range: 35% RH before, 36% RH after treatment.

7.2.1.2 Archaeological wood

The waterlogged archaeological oak pieces were obtained from storage at the museum (unknown origin), these were used for aqueous treatment, and were used as the highly degraded archaeological wood samples. The wood was stored in water at the museum and hence was still waterlogged. The wood was cut into 1.5 x 1.5 x 2 cm pieces and patted with a blue roll to dry the surface; this was then placed in a pre-weight beaker of water and the weight difference, measured on a 4 decimal place balance, was used as the weight of the waterlogged wood. The samples were then measured with a caliper and photographed as described below. The samples were then freeze dried and weighed. Then the samples were placed in treatment baths given in Table 6-3. They were left in the solutions for two weeks. The surface was wiped off with cotton buds and then air dried with pierced parafilm over the container for a few days and then the parafilm was removed.

7.2.1.3 Non-aqueous treatment

The non-aqueous samples were first placed in solvent and then placed in a vacuum immersion chamber for 2 x 10 min, and for an additional 10 min if the pieces still floated. Finally, the wood was placed in treatment solution: 2 x 1 cm pieces in one vial

and the 2 cm piece in another. They were then left in the solutions for two weeks; see Table 7-7, Table 7-8, Table 7-9 and Table 7-10. The treatment concentrations were made on a weight: weight basis.

Table 7-7: Injection treatments for artificially degraded wood.

Consolidant	**Concentration**	**Solvent**
TBDMS chitosan	5%	50:50 Toluene/ethyl acetate
	5%	Isopropanol
B72	10%	50:50 Toluene/ethyl acetate
B98	10%	40:60 Ethanol/toluene

Table 7-8: Artificially degraded wood immersion treatments.

Consolidant	**Concentration**	**Length**	**Solvent**	**Drying method**
TBDMS chitosan	10%	2 weeks	50:50 Toluene/ethyl acetate	Air dried
	10%	2 weeks	*Tert*-butanol	Air dried
	10%	2 weeks		Freeze dried
B72	10%	2 weeks	50:50 Toluene/ethyl acetate	
B98	10%	2 weeks	40:60 Ethanol/toluene	

Table 7-9: Archaeological wood injection treatments.

Consolidant	**Concentration**	**Solvent**
TBDMS chitosan	5%	50:50 Toluene/ethyl acetate
B72	10%	50:50 Toluene/ethyl acetate
50:50 TBDMS chitosan +B72	2.5%, 2.5%	50:50 Toluene/ethyl acetate
B98	10%	40:60 Ethanol/toluene

Table 7-10: Immersion treatments for archaeological wood.

Consolidant	**Concentration**	**Length**	**Solvent**
TBDMS chitosan	5%	2 Weeks	50:50 Toluene/ethyl acetate
	10%	3 Days, vacuum immersion	
		2 Weeks	
		2 Weeks	
		1 Month	
	20%	2 Weeks	
B72	10%	2 Weeks	50:50 Toluene/ethyl acetate
B98	10%	2 Weeks	40:60 Ethanol/toluene

7.2.2 Analysis/documentation

7.2.2.1 Weight/dimensions

The weights were measured on a four-decimal balance. Dimensions in millimetres were recorded with a two decimal place digital caliper. The dimensions and weight were used to calculate density. The density is an approximation as some pieces of wood were not perfectly square but as the samples were measured before and after in the same manner, this was not considered a problem. The change in density, volume and weight of different treatments could then be compared. Each time the dimensions were measured in the same place, the centre of each side. A notch was made on one side, in order to distinguish which side faces upwards, and the measurements were taken in the middle to try to ensure that the same place was measured each time.

7.2.2.2 Photographs and scans

Each side of each piece of wood was scanned before and after treatment. This was less time consuming than photographing each side, and the scans are to scale. However, photographs have depth and have better resolution. Together both can be used to document changes resulting from the treatment.

7.2.2.3 Spectrophotometer

A hand-held spectrophotometer from Konica Minolta, CM-700d, was used to measure samples before and after treatment using the 4 mm aperture and the spectral component excluded (SCE) mode. This measures three chromatic coordinates of the CIELAB colour system. The total colour change ΔE is based on three chromatic coordinates of the CIELAB colour system: a* (green-red axis), b* (blue-yellow axis) and L*(white-black axis hence lightness). It is calculated from ΔE*2,1 = [(ΔL*)2+ (Δa*)2 + (Δb*)2]1 (Eq. 7.1) For laboratory-degraded wood, the measurements were taken before and after. For the archaeological wood, spectrophotometers measure L, a and b. The L is the lightness and a and b chromaticity indices (See Chapter 5).

$$\Delta E=\sqrt{(l-lc)^2+(a-ac)^2+(b-bc)^2} \quad \textbf{7-1}$$

c for control lc, average ac, bc l, a, b of untreated wood.

7.2.3 Fourier-transform Infrared spectroscopy (FTIR)

FTIR spectras in ATR mode were recorded on a Thermo Scientific Nicolet iS50 spectrometer equipped with a diamond crystal and DTGS detector. Spectra were recorded with 32 scans at 4 cm^{-1} resolution, within the range 4000–400 cm^{-1}. Three scans were taken each time and averaged; these were then baseline corrected. For each treated sample the IR of the control was compared to the treated sample and the pure consolidant to determine its presence. The outside and inside of the wood were also compared to establish if the treatment method resulted in good penetration or if most of the consolidant was on the other part of the wood.

7.2.4 Scanning electron microscopy – energy - dispersive X-ray spectroscopy (SEM-EDS)

Analyses were performed using a FEI Quanta 450 Scanning Electron Microscope coupled with an Oxford X-Max^N 50 mm^2 detector, using low vacuum mode at (70 Pa). The other parameters (spot size 5 or 6, voltage (10-15 kve), pressure (70 Pa), and working distance (~10 mm)) were modified depending on the sample.

SEM was used to see if the consolidants could be observed within the wood and to try to establish how they interact with the wood. This is whether cells are filled or lined, or if only the vessels are filled or lined. SEM can also tell whether an attempt at consolidation may have damaged the cells in the process. The EDS can also be used to confirm penetration of the consolidant into the wood and how it fills the wood when elements other than carbon and oxygen are in the consolidant.

7.2.5 X-ray tomography

The same methology was used as for aqueous treatment see Chapter 6.2

7.3 Results of non-aqueous treatment

7.3.1 Artificially degraded wood results

7.3.1.1 Weight and density

7.3.1.1.1 Injection

Table 7-11: Percentage weight increase from injection treatments of artificially degraded wood.

Sample	**2.5% TBDMS chitosan**	**5% TBDMS chitosan**	**5% B72**	**5% B98**
Percentage weight increase	10.31	7.57	12.52	6.28
Percentage volume increase	2.74	2.92	2.24	5.90
Percentage density increase	7.35	4.52	10.03	0.41

The TBDMS chitosan dissolved, but then precipitated back out in the case of isopropanol as the solvent. Figure 7-1a and Table 7-11 also show that less material went into the wood and the wood swelled more; this solvent should be ruled out for this treatment. Ethyl acetate and toluene as a solvent gave more promising results: 2.5% TBDMS showed a larger increase in uptake and smaller swelling than 5% for injection. B72 showed a similar increase in weight to 2.5% TBDMS and showed less swelling and less variability than the others.

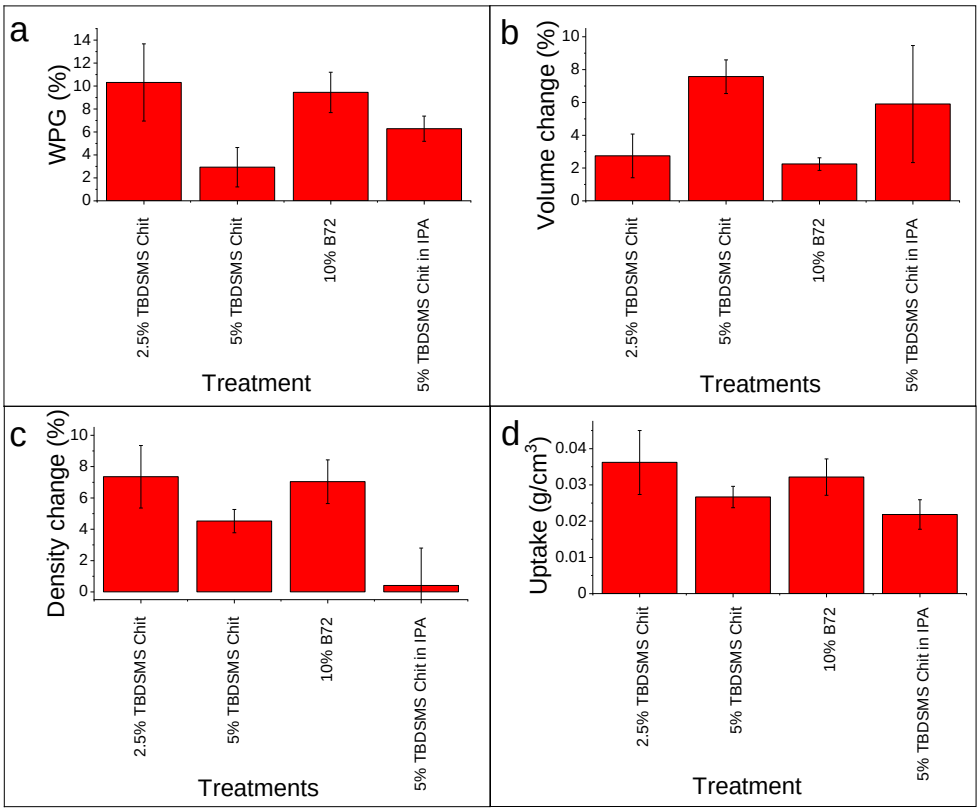

Figure 7-1: Results of treatment of artificially degraded wood via injection. a) weight percentage gain (WPG) of different treatments. b) volume change, c) density change, d) uptake of consolidant. IPA=isopropanol.

7.3.1.1.2 Immersion

Table 7-12: Percentage weight increase from immersion treatments of artificially degraded wood

Sample	**Control 50:50 toluene /ethyl acetate**	**10% TBDMS chitosan**	**10% B72**	**10% B98**	**10% TBDMS chitosan in t-butanol air-dried**	**10% TBDMS chitosan in t-butanol freeze-dried**	**10% PEG in t-butanol**	**t-butanol control**
Percentage weight increase	7.99	19.62	24.75	22.64	11.36	11.55	11.49	2.46
Percentage volume increase	2.05	3.79	3.27	4.20	2.99	1.61	2.07	-0.22
Percentage density increase	5.81	15.25	54.62	17.72	8.20	9.82	9.42	-2.62

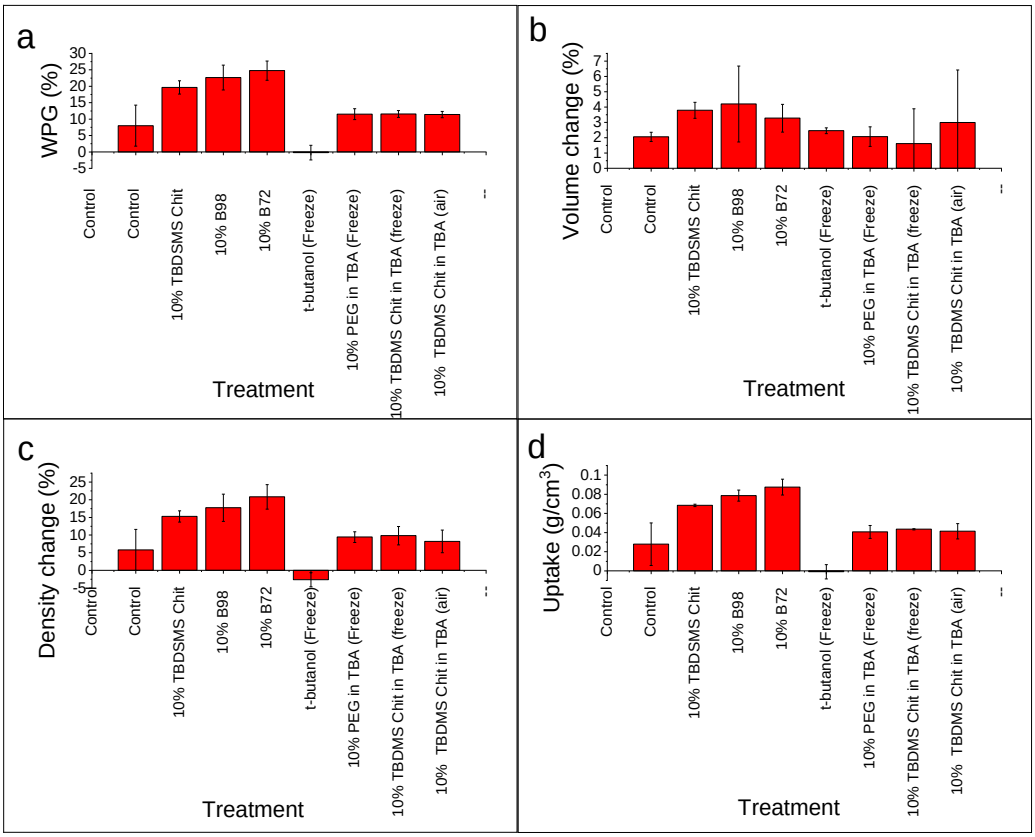

Figure 7-2: Results of treatment of artificially degraded wood via immersion. a) percentage weight gain (WPG) of different treatments. b) volume change, c) density change, d) uptake of consolidant. TBA=tert-butylethanol.

Immersion resulted in a higher weight increase than injection (Figure 7-1, Figure 7-2, Table 7-12:). T-butanol resulted in a lower weight increase. This is probably due to the solubility and viscosity of the materials. PEG actually needed a higher temperature to fully dissolve in t-butanol, which was not recognised at the start. The reason 40 ^{o}C was chosen is it kept the t-butanol liquid and all the t-butanol experiments were carried out at the same temperature. The T-butanol control had a smaller weight increase; this could be due to the difficulty in removing toluene and it is possible that the wood pieces needed longer to dry. They were dried until a constant weight was reached. However, it is possible all the ethyl acetate was removed but more time was needed for the toluene. T-butanol resulted in a similar volume change to ethyl acetate relative

to the control. However, with the addition of TBDMS chitosan the swelling was less but the variability in results was much greater. PEG in t-butanol with freeze-drying produced less swelling than B72 and B98; however, the weight increase was less. Between TBDMS chitosan, B72 and B98, B72 showed the greatest increase in weight followed by B98. In terms of swelling, B72 volume increase was most favourable, followed by TBDMS then B98; however, all produced more swelling than the control, although this was less than with aqueous treatment (See Chapter 6).

7.3.1.2 Spectrophotometer

7.3.1.2.1 Immersion

Table 7-13: Immersion results colour change

Sample	**ΔE Dark side (side 1,2,3,4)**	**ΔE light side (side 5,6)**
10% B72	2.71±0.69	5.65±3.38
10% B98	2.02±0.76	13.03±6.65
10% chitosan TBDMS	2.56±0.42	10.44±2.10
Control 50:50	1.88±0.36	7.91±7.61

7.3.1.3 SEM and IR

7.3.1.3.1 Injection

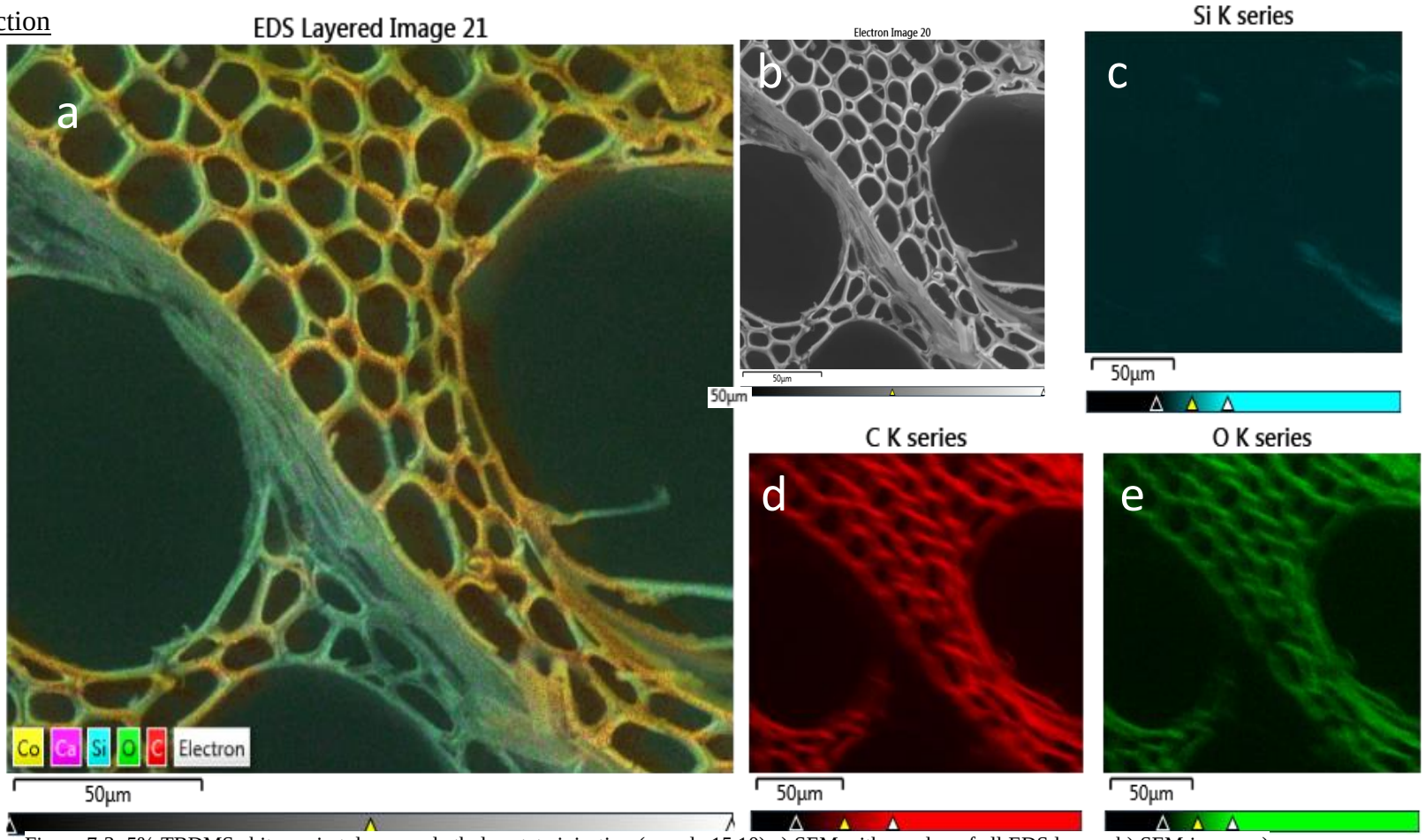

Figure 7-3: 5% TBDMS chitosan in toluene and ethyl acetate injection (sample 15.10) a) SEM with overlay of all EDS layers, b) SEM image, c) EDS-SEM of silicon content, d) EDS-SEM of carbon content and e) EDS-SEM of oxygen content.The same area was used for SEM and EDS all images have a 50 µm scale bar.

Injection of TBDMS chitosan did result in some consolidant successfully reaching the centre of the wood (Table 7-13, Figure 7-3, Figure 7-5). Using EDS with the SEM it is possible to see silicon in the wood and Figure 7-4 shows the water control does not contain silicon, proving that the silicon is from the treatment. The IR also confirms the presence of TBDMS chitosan. IR (Figure 7-5) adds a secondary confirmation that TBDMS chitosan reached the centre of the wood.

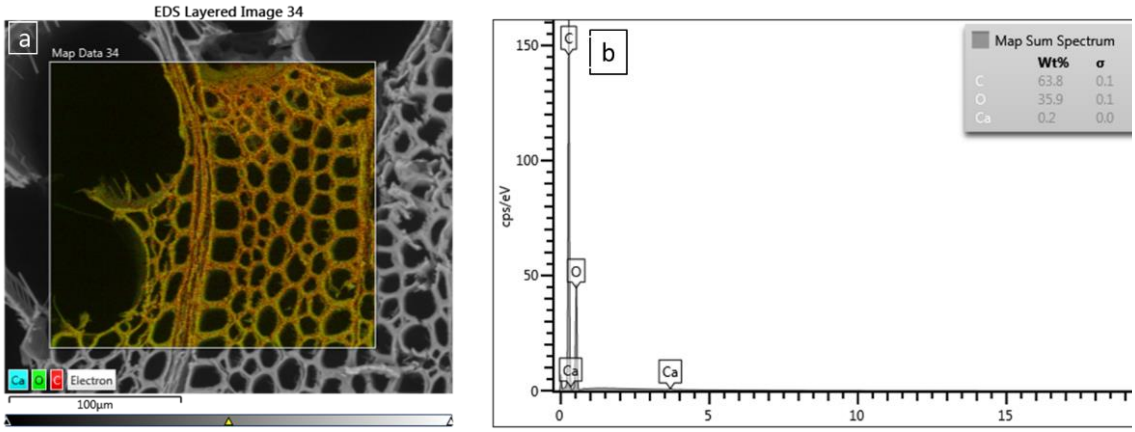

Figure 7-4: a) SEM image of water control in artificially degraded wood (4.9) and b) EDS element components for the water control.

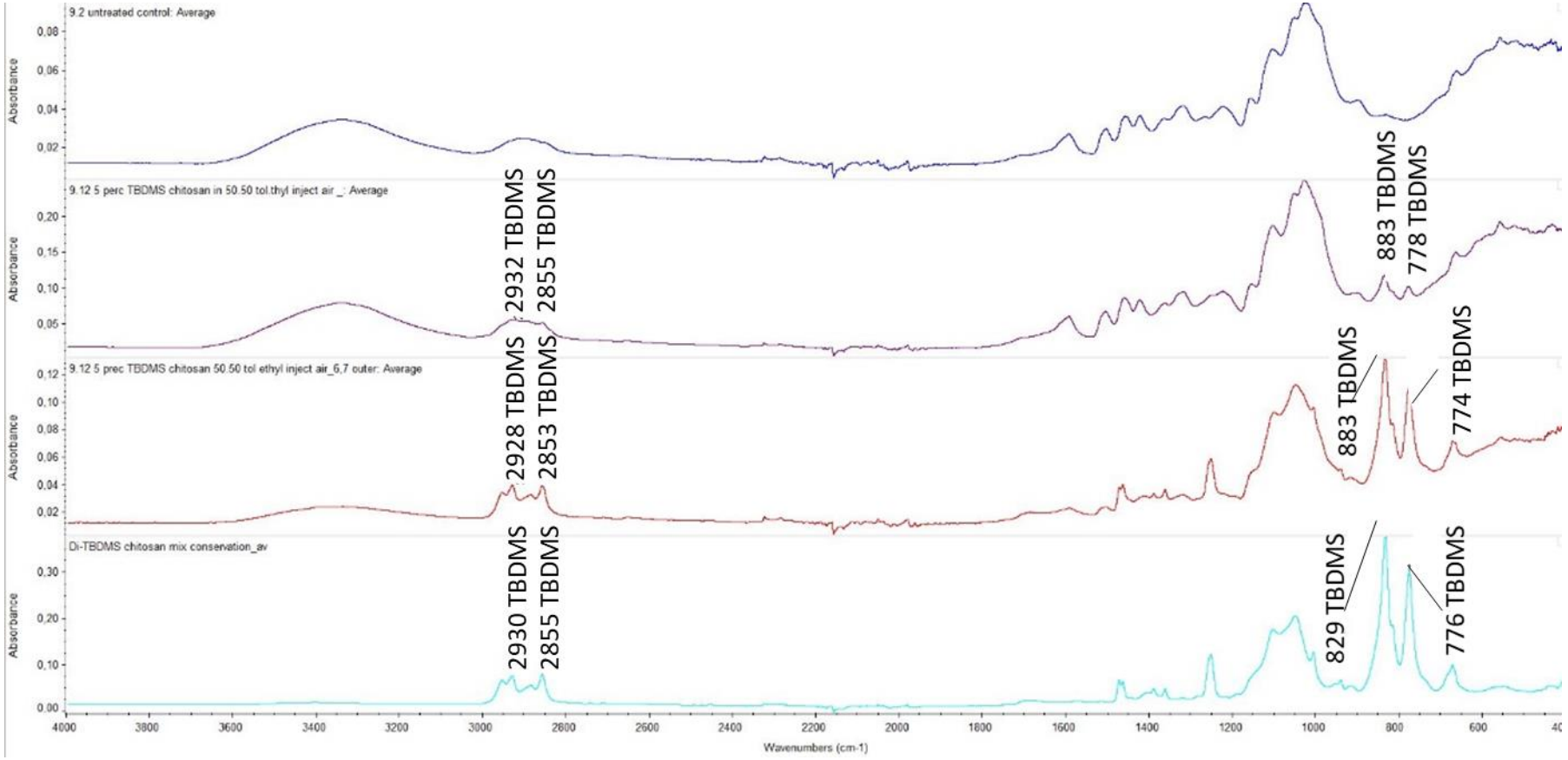

Figure 7-5: IR spectra of TBDMS chitosan in artificially degraded wood. Top to bottom graphs are; the of average of 9.2 untreated control, 9.12 inject TBDMS chitosan in 50:50 toluene/ethyl acetate from the middle of the wood , 9.12 inject TBDMS chitosan in 50:50 toluene/ethyl, acetate from the edge of the wood and TBDMS chitosan alone.

7.3.1.3.2 Immersion

7.3.1.3.3 EDS-SEM, IR and X-ray tomography

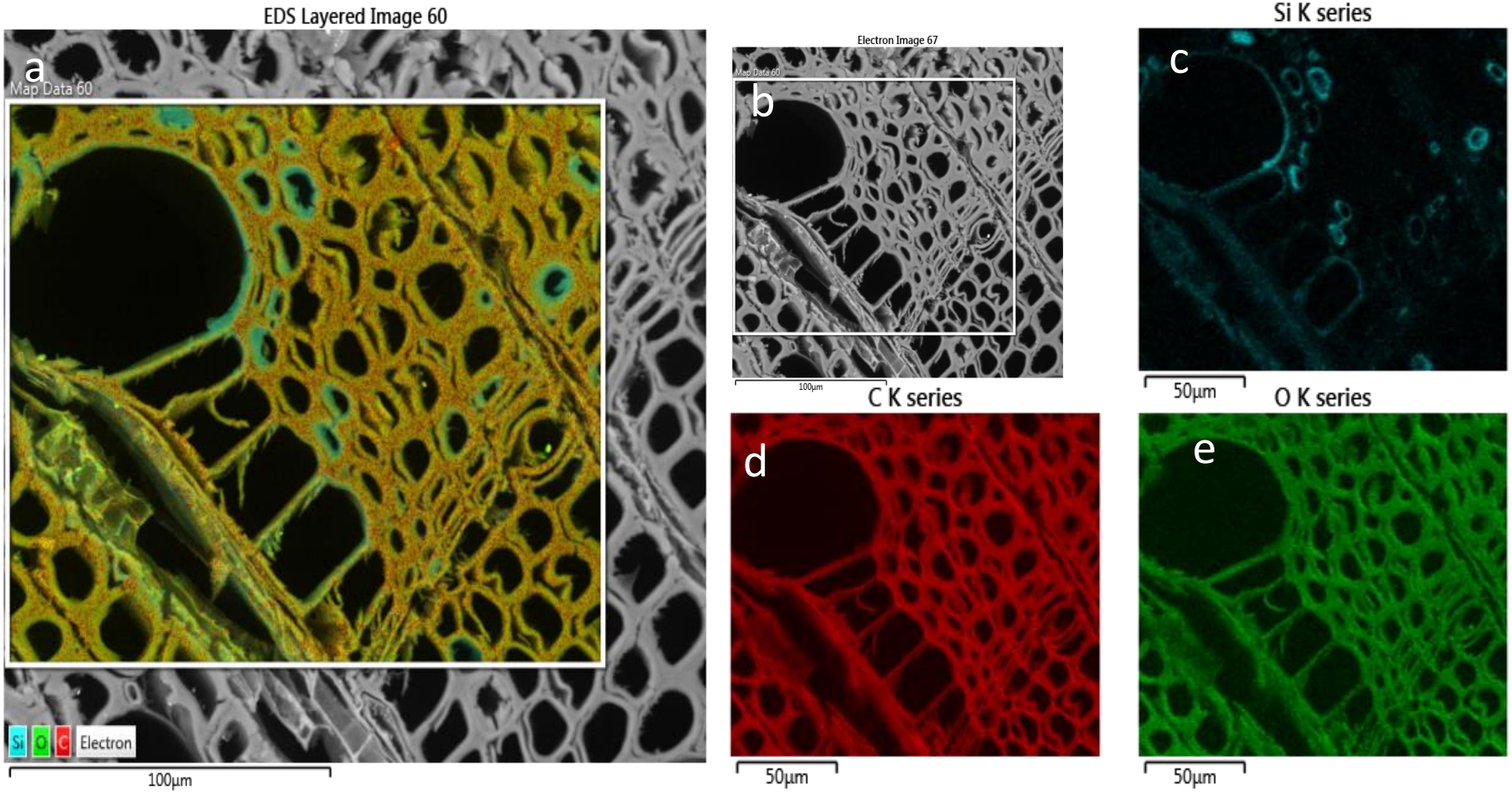

Figure 7-6: 4.10 10% TBDMS immersion in toluene and ethyl acetate a) SEM with overlay of all EDS layers, b) SEM image, c) EDS-SEM of silicon content, d) EDS-SEM of carbon content and e) EDS-SEM of oxygen content. The scale bar for the SEM is 100 µm and 50 µm for EDM images.

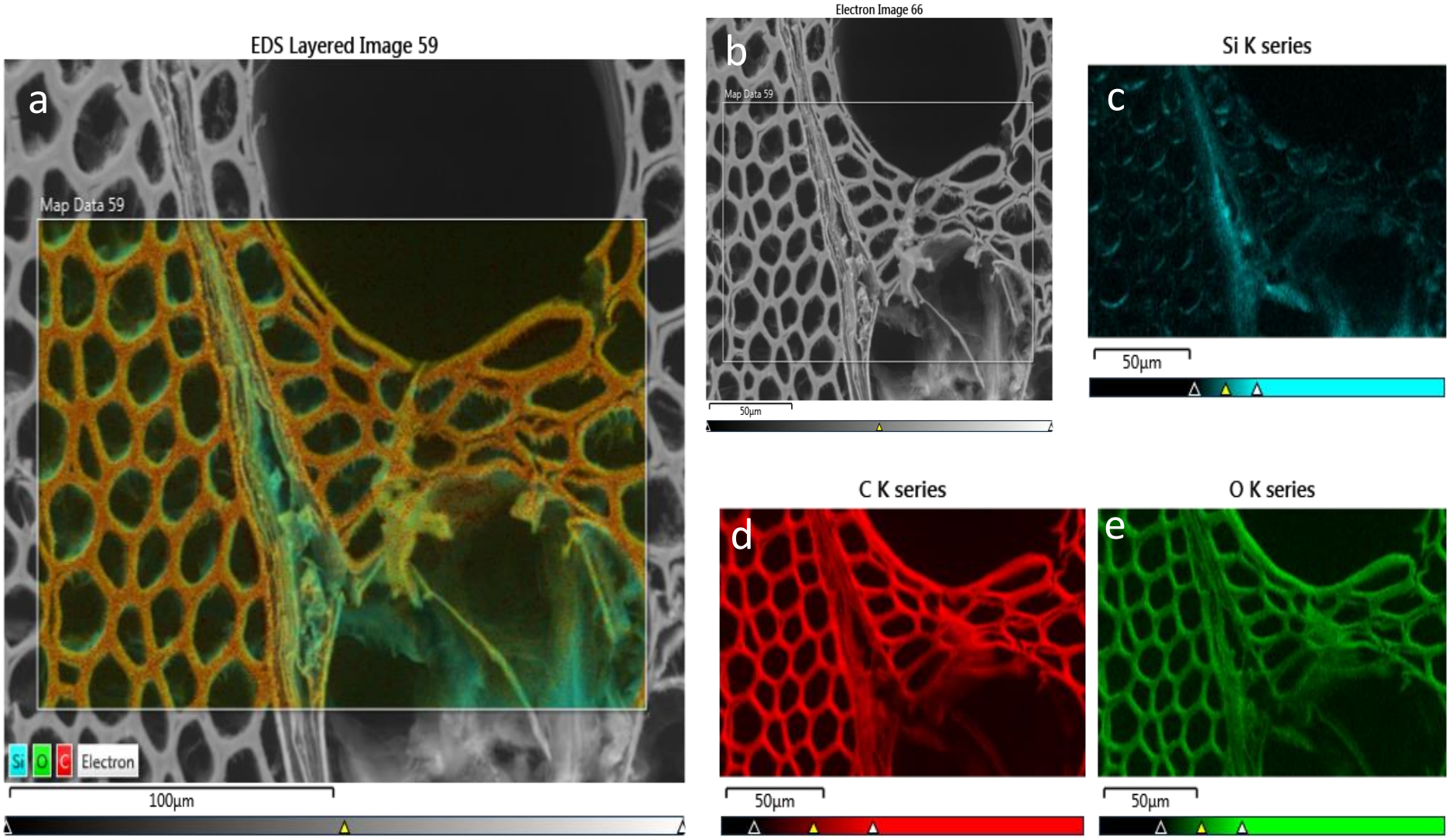

Figure 7-7: 15.5 TBDMS chitosan in t-butanol a) SEM with overlay of all EDS layers, b) SEM image, c EDS-SEM of silicon content, d EDS-SEM of carbon content and e EDS-SEM of oxygen content. The scale bar for the SEM with EDS overlay is 100 µm and 50 µm for all the others.

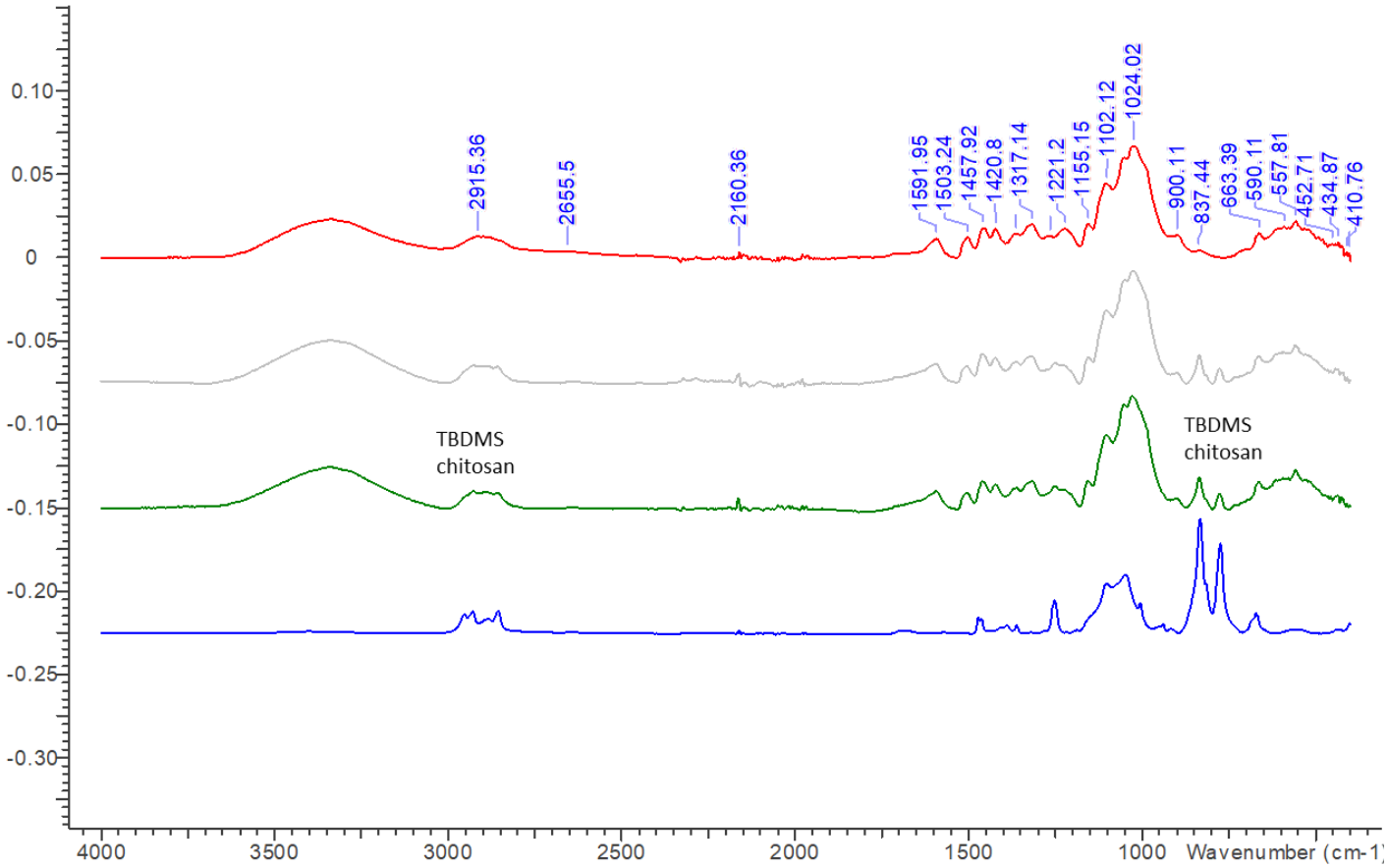

Figure 7-8: IR spectra of all laboratory degraded wood. Red line: untreated; grey line: edge of wood 10% TBDMS chitosan treated; green line centre of 10% TBDMS chitosan treated wood and blue line TBDMS chitosan.

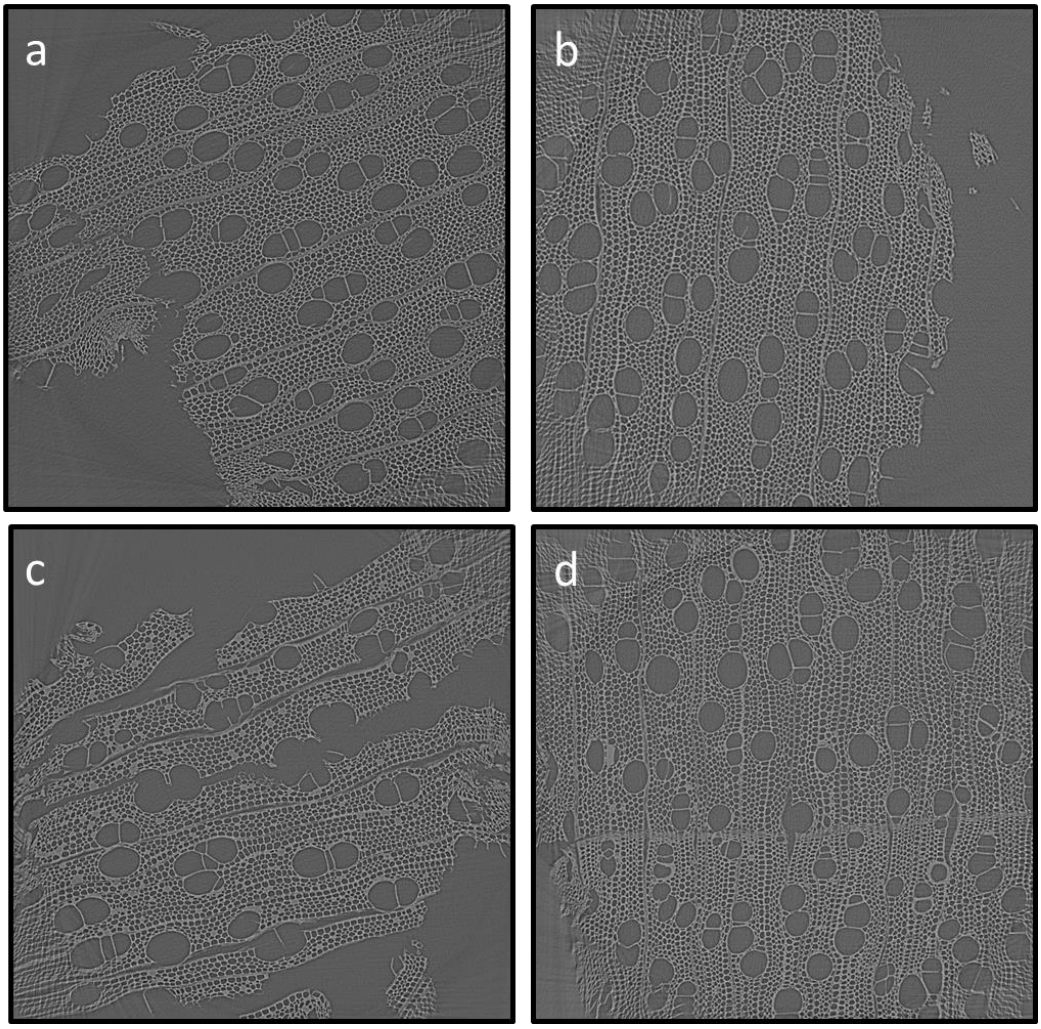

Figure 7-9: X-ray tomorgraphy images of laboratory degraded wood a) untreated, b) 10% B98, c) 10% B72: Note some of the cells are filled with the polymer and d) 10% TBDMS chitosan.

It is clear from EDS-SEM Figure 7-6 and Figure 7-7 that TBDMS chitosan did successfully penetrate into the wood cells when the wood is immersed for treatment. It also shows that TBDMS chitosan is more evenly distributed with t-butanol. IR (Figure 7-8) also shows TBDMS chitosan penetrated to the centre of the wood.

X-ray tomograph (Figure 7-9) shows that not all the cells were filled by B98, B72 or TBDMS chitosan hence retreatment would be possible.

7.3.2 Archaeological wood results

7.3.2.1 Weight and volume change

7.3.2.1.1 Injection

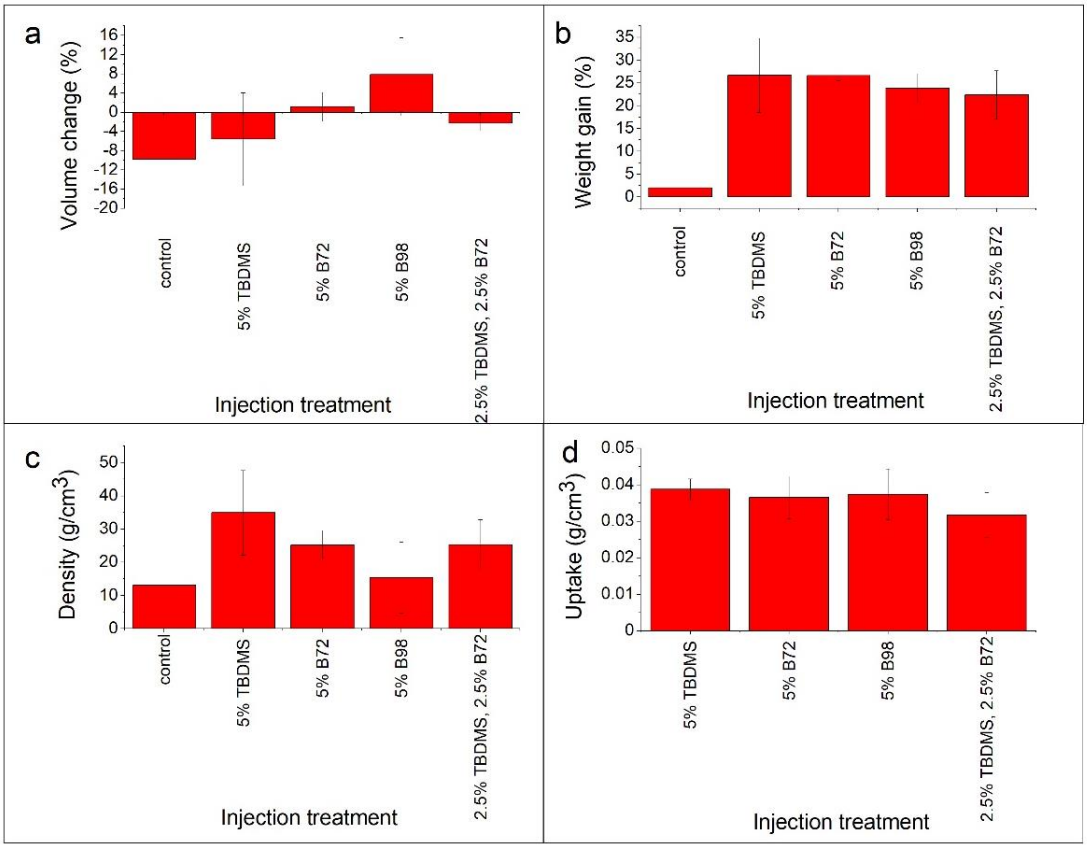

Figure 7-10: Results of treatment of archaeological wood via injection. a) weight percentage gain (WPG) of different treatments. b) volume change, c) density change and d) uptake of consolidant.

The archaeological wood (Figure 7-10) showed greater uptake of materials, as expected, with the lower density being found in untreated wood. Very good uptake was observed in all samples. Mixing 2.5% and 2.5% TBDMS chitosan and B72 leads to a smaller weight increase than 5% of either material. Some gelling was observed when these two were mixed which provides a reason for why this occurs. In terms of volume change, B72 was the most favourable; the control shrank with solvent

treatment. B72 prevented this. TBDMS did not prevent shrinkage. B98 also prevented shrinkage but resulted in more swelling than B72 and more variability than B72.

7.3.2.1.2 Immersion of different treatments -weight and volume change

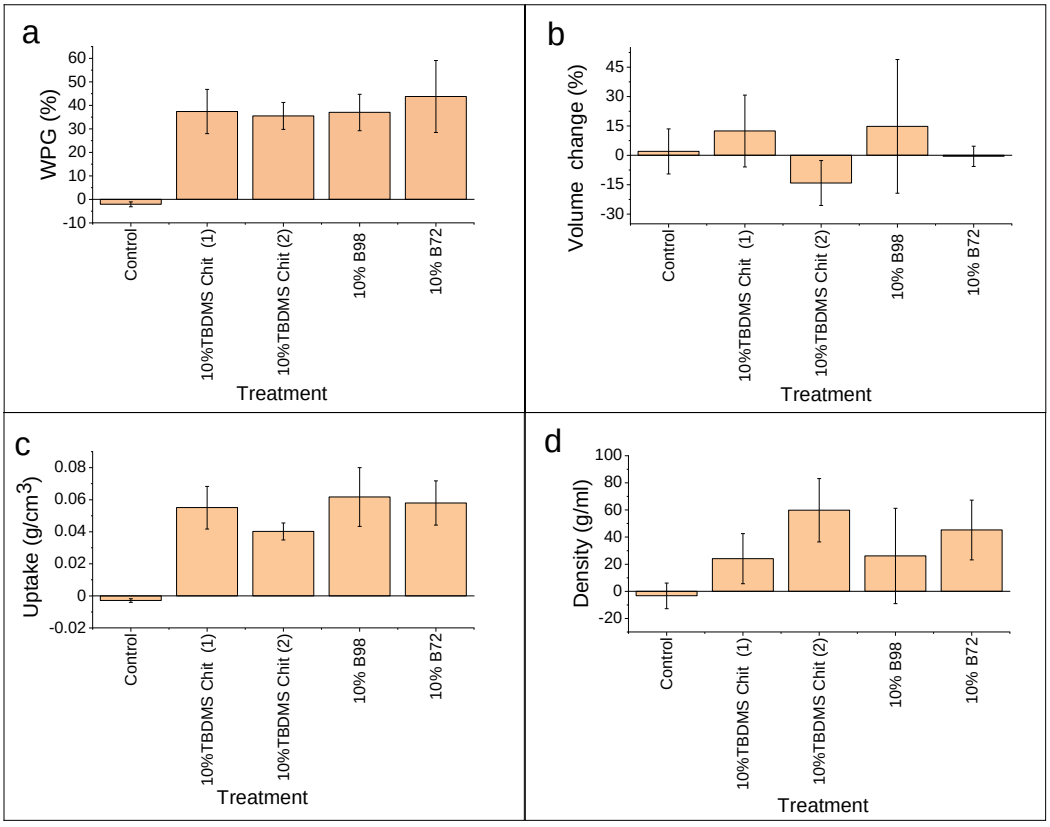

Figure 7-11: Results of treatment of archaeological wood via immersion. a) weight percentage gain (WPG) of different treatments. b) volume change, c) density change and d) uptake of consolidant.

Immersion of archaeological wood resulted in a larger percentage weight gain than laboratory degraded wood, again probably due to the density (Figure 7-11). Immersion also resulted in a slightly higher percentage weight increase compared to injection (Figure 7-10). B72 resulted in the highest percentage increase; however, the percentage increase in weight was similar for all treatments. The control lost weight and with the laboratory degraded wood there was a small increase in weight,

questioning whether all the toluene was removed. However, the archaeological wood is more porous, allowing the toluene to evaporate more easily.

B72 showed the smallest change in volume with the smallest variability in results. TBDMS chitosan had very different results between the two batches of treatments. Despite the TBDMS chitosan treatment being the same treatment i.e., same concentration and length, there was variability of results. The control also shows great variability which might be due to variability in the wood. B98 also shows great variability and also the largest swelling. The increase in swelling over other treatments is probably due to the use of ethanol in the solvent mixture, as that increases the polarity. Ethanol is already known to have an effect on the swelling of archaeological wood (Mantanis et al., 1994).

7.3.2.1.3 Immersion with different concentrations -weight and volume change

Increasing the concentration from 5% to 10% increased the percentage weight gain (Figure 7-12). However, the percentage weight gain did not increase between 10-20%; the weight gain even decreased a little. 10% TBDMS showed the greatest variation in terms of volume change. 5% showed the smallest variability but did cause some swelling. With 20% TBDMS, the wood shrank a little.

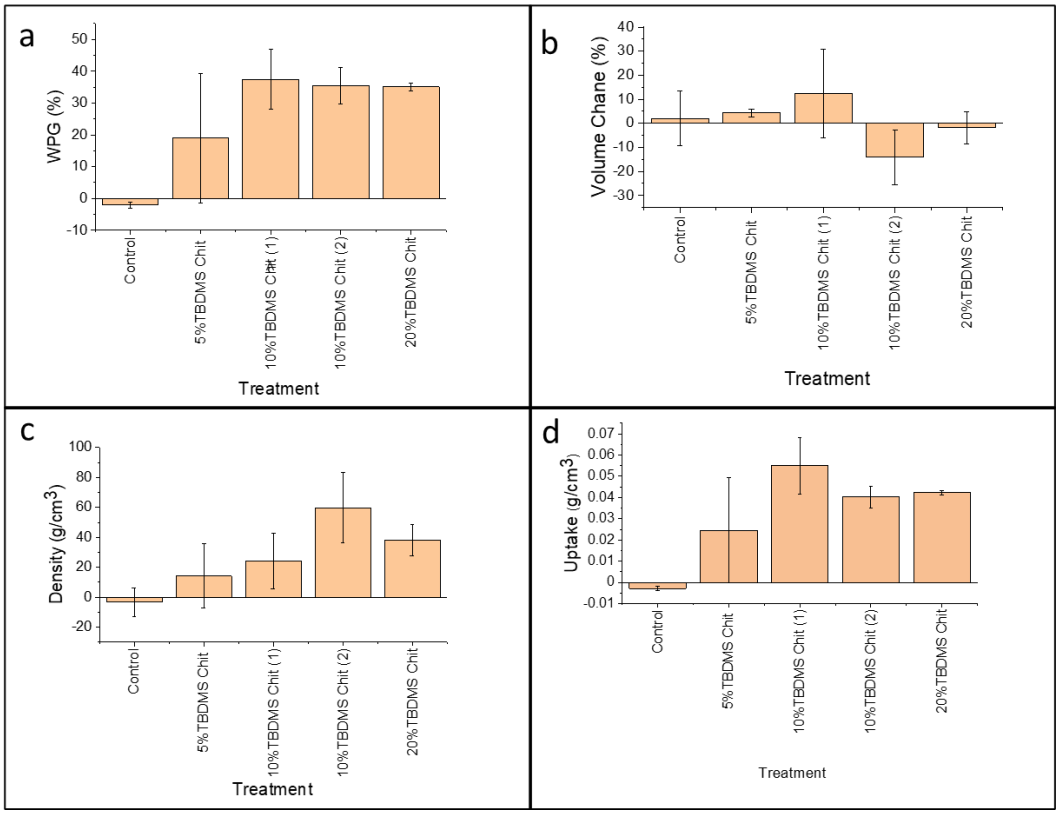

Figure 7-12: Results of treatment of archaeological wood with different concentrations. a) percentage weight gain (WPG) of different treatments. b) volume change, density change, uptake of consolidant.

7.3.2.1.4 Immersion- different treatment lengths -weight and volume change

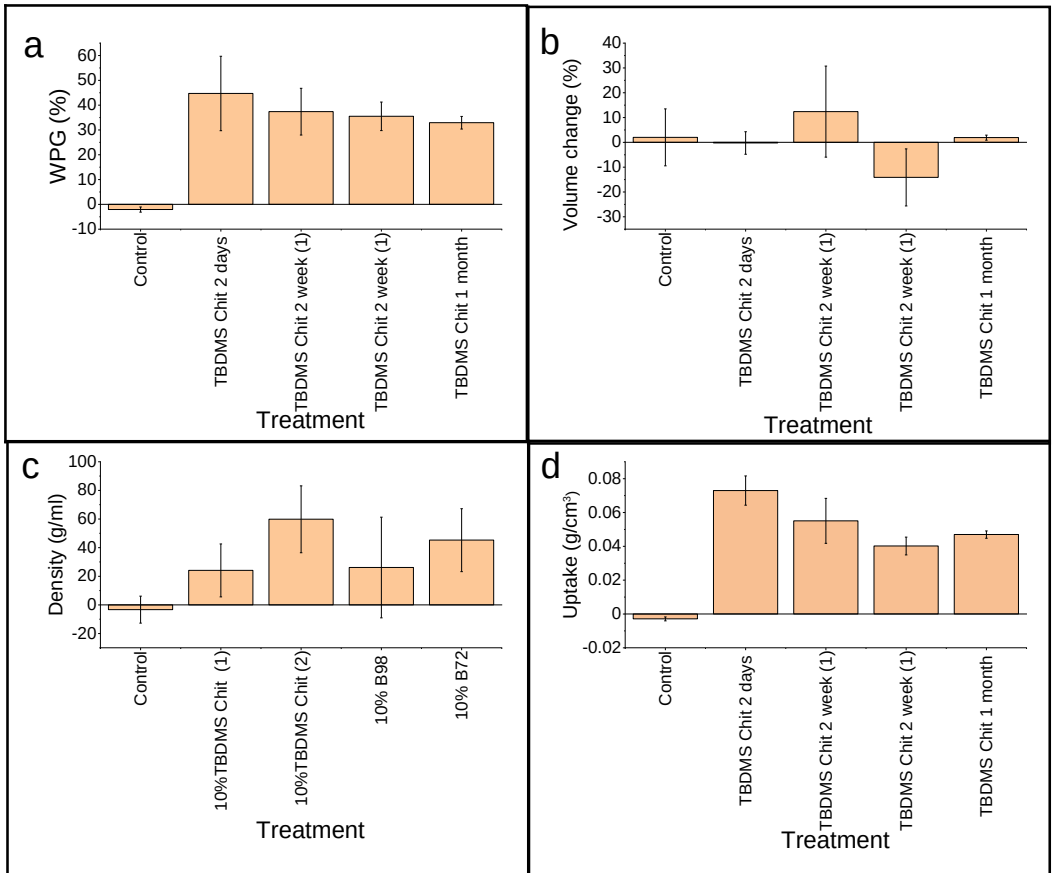

Figure 7-13: Results of treatment of archaeological wood with different treatment lengths a) percentage weight gain (WPG) of different treatments. b) volume change, density change, uptake of consolidant.

The same polymer (TBDMS chitosan) was used for all the treatments. Only the length of treatment was varied, except for the two days treatment where a vacuum was applied to lower the pressure at the start of treatment to draw treatment into the wood. According to Figure 7-13, the shorter the treatment, the larger the increase in weight gain. In terms of volume change, the control shows a large variation (Figure 7-13). The two-day treatment with vacuum immersion showed the smallest volume change, followed by the one-month treatment.

7.3.2.2 SEM, IR and X-ray tomography

7.3.2.2.1 Injection treatments

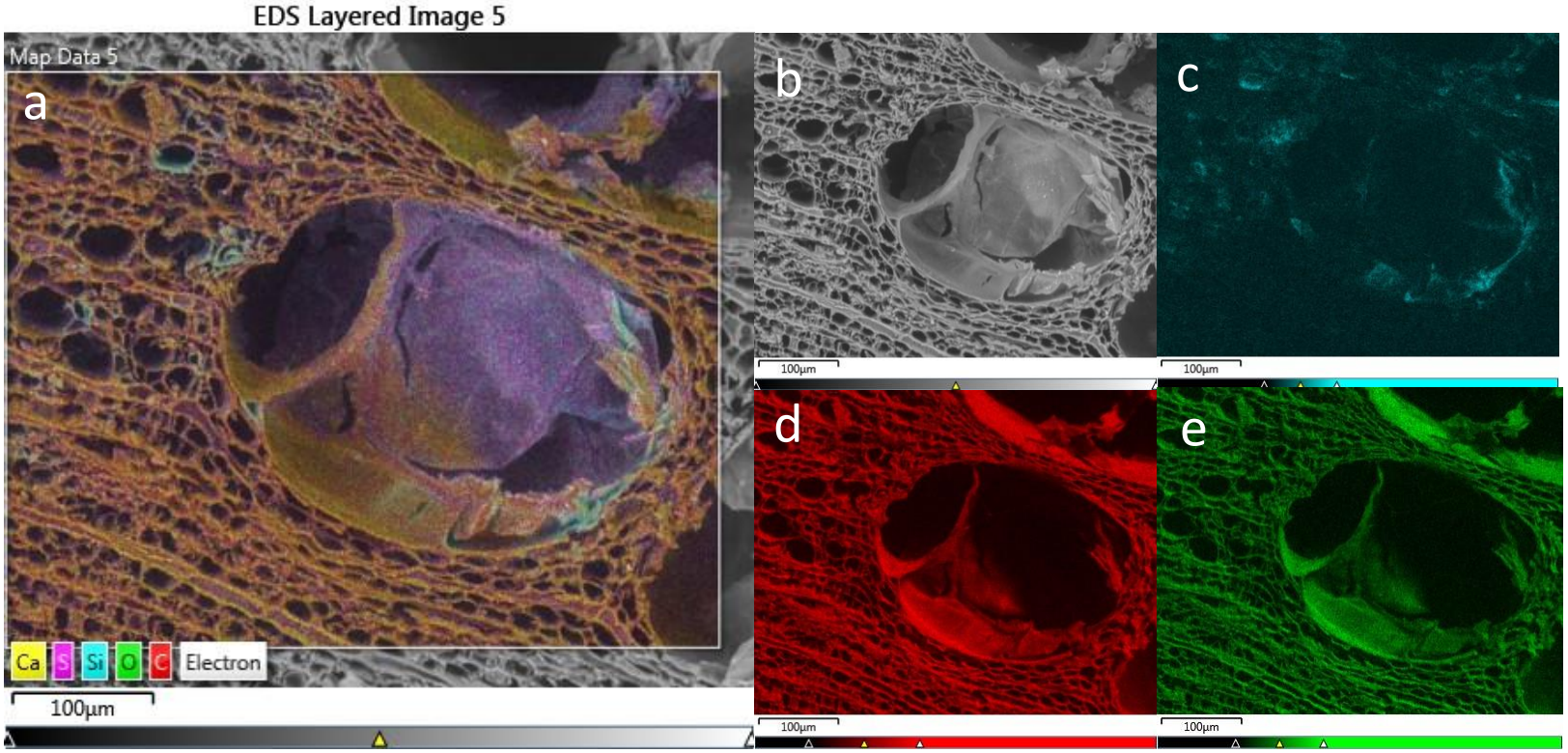

Figure 7-14: 5% TBDMS chitosan. The blue shows the silicon from the TBDMS chitosan in the wood. (wood centre). a) SEM with overlay of all EDS layers, b) SEM image, c) EDS-SEM of silicon content, d) EDS-SEM of carbon content and e) EDS-SEM of oxygen content. The scale bar on all the images is 100 µm.

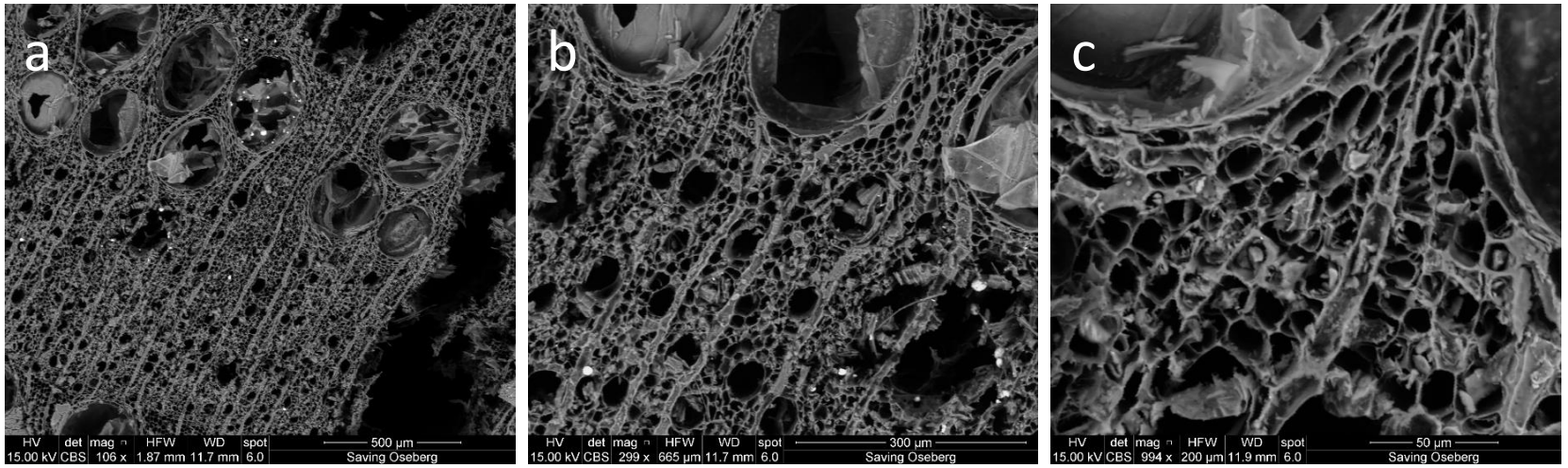

Figure 7-15: SEM images of centre of archaeological wood from 5% B72 injection middle (wood centre). a) with 500µm scale bar, spot size 6, HV 15.00 kV, working distance (WD) 11.7 mm, mag 106x. b) with 300 µm scale bar, spot size 6, HV 15.00 kV, WD 11.7 mm, mag 299x and c) zoomed in to 50 µm scale bar, spot size 6, HV 15.00 kV, WD 11.9 mm, mag 994x.

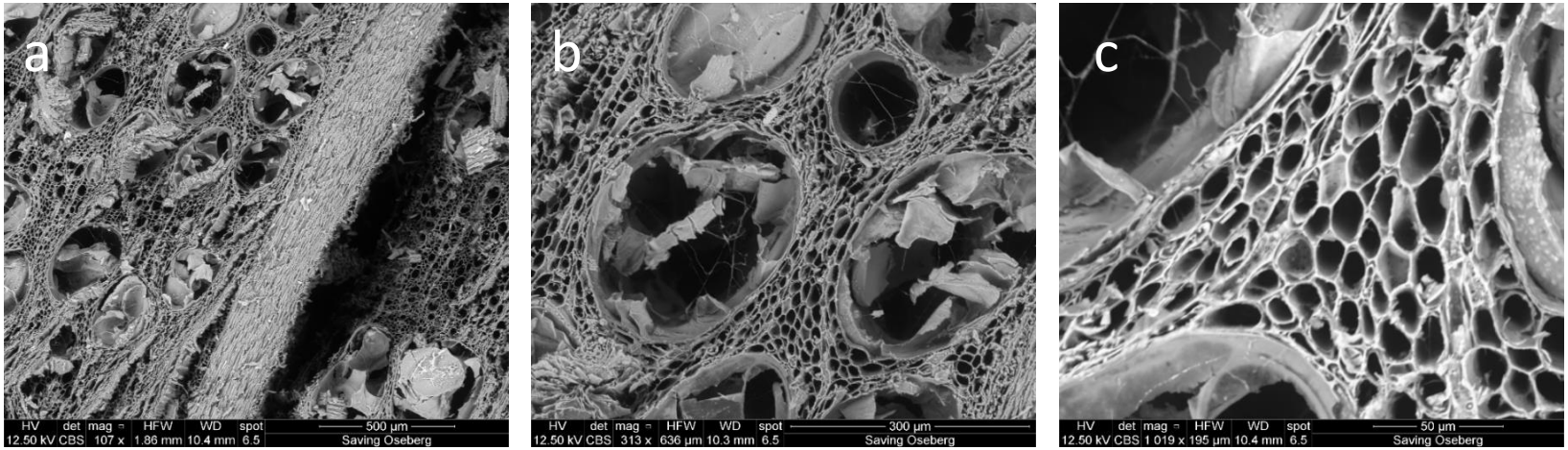

Figure 7-16: SEM images of centre of archaeological wood from B98 Injection (centre wood) a) with 500µm scale bar, spot size 6.5, HV 12.50 kV, WD 10.4 mm, mag 107x, b) with 300 µm scale bar, spot size 6.5, HV 12.50 kV, WD 10.3 mm, mag 313x and c) zoomed in to 50 µm scale bar, spot size 6.5, HV 12.50 kV, WD 10.4 mm, mag 1019x.

7.3.2.2.2 Immersion treatment

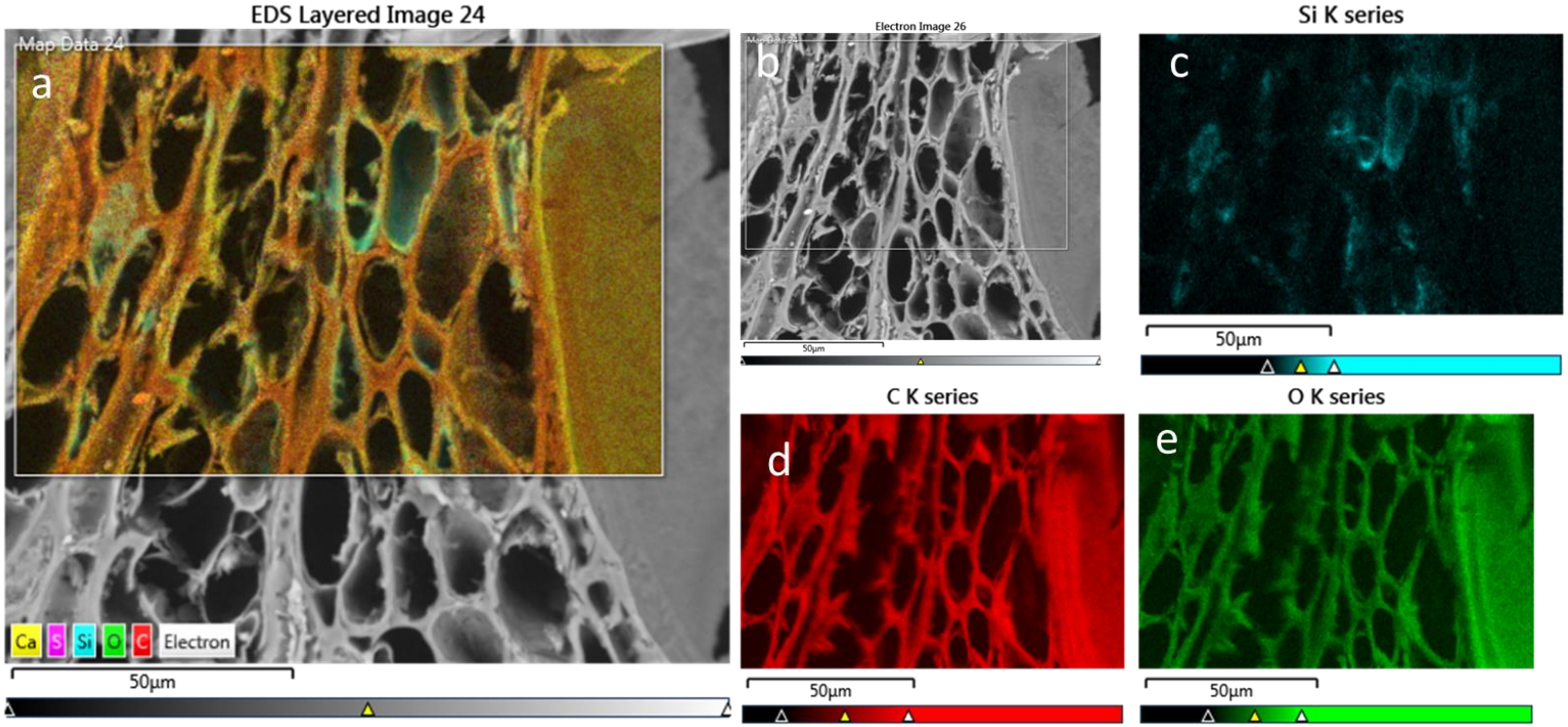

Figure 7-17: SEM-EDS images of centre of archaeological wood from 5% TBDMS, 2-week treatment a) SEM with overlay of all EDS layers, b) SEM image, c) EDS-SEM of silicon content, d) EDS-SEM of carbon content and e) EDS-SEM of oxygen content. The scale bar is 50 µm on all images.

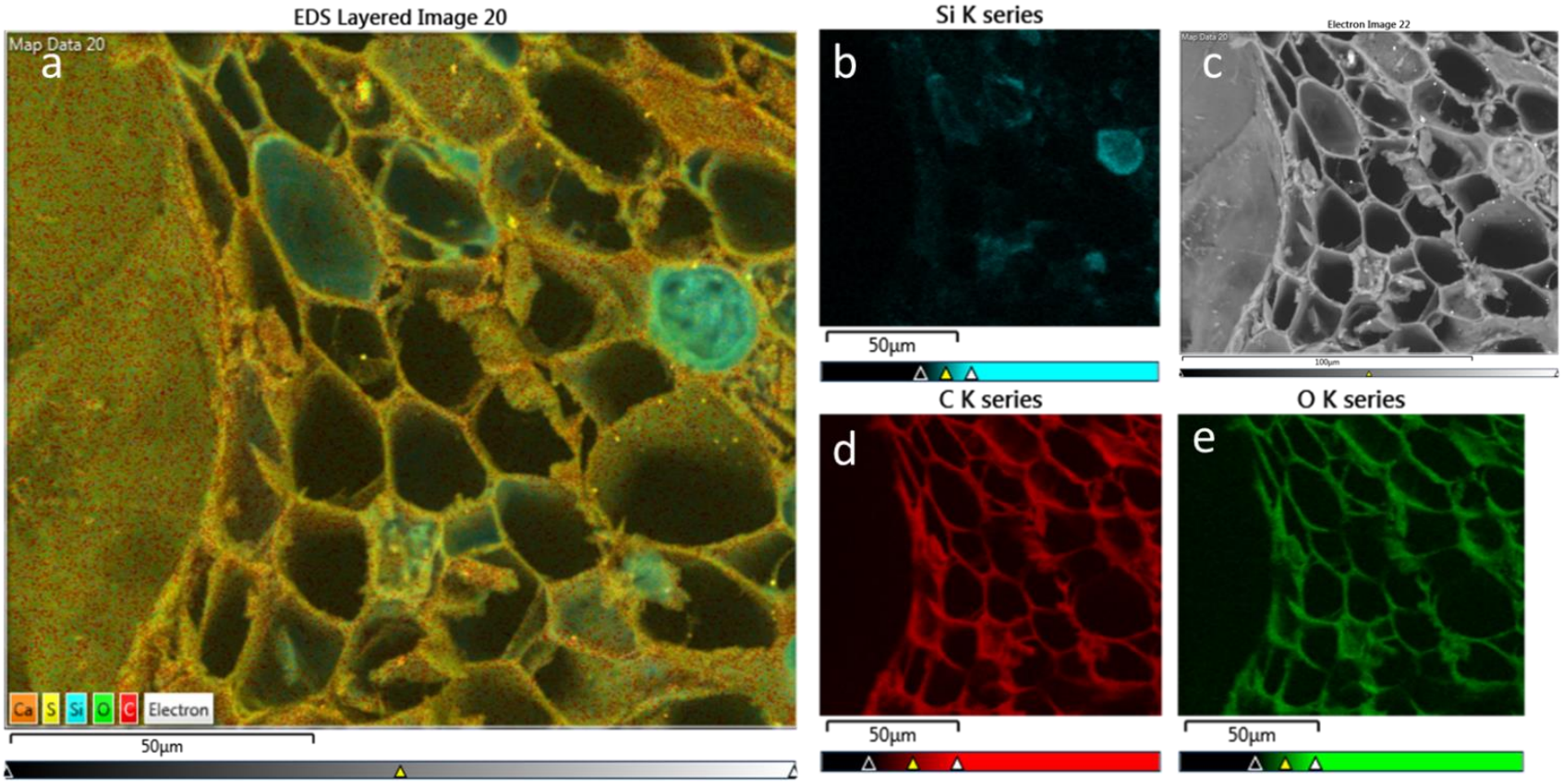

Figure 7-18: SEM-EDS images of centre of archaeological wood from 10% TBDMS chitosan two week treatment (wood centre). a) SEM with overlay of all EDS layers, b) SEM image, c) EDS-SEM of silicon content, d) EDS-SEM of carbon content and e) EDS-SEM of oxygen content. The scale bar is 50 µm on all images.

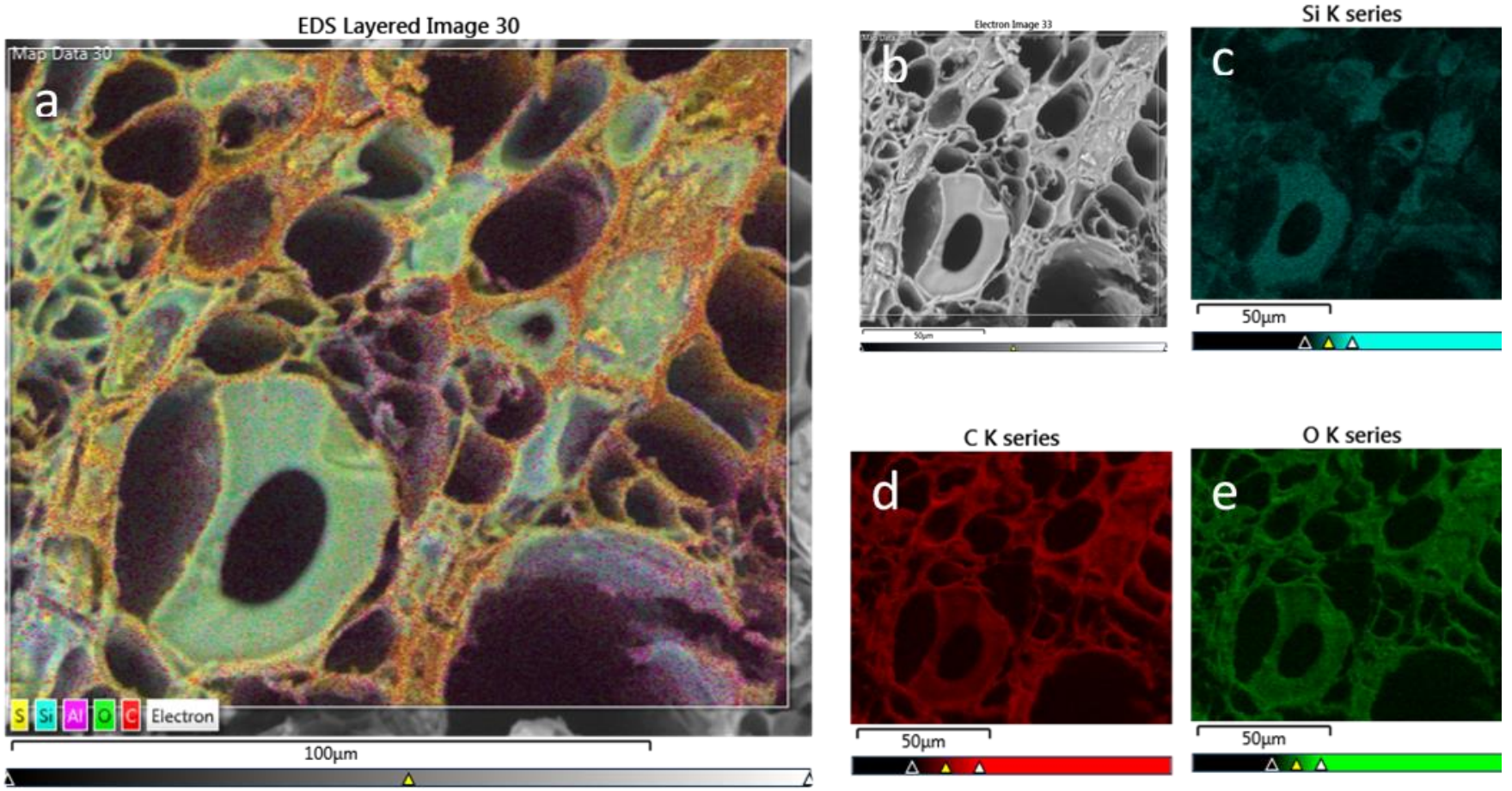

Figure 7-19: SEM-EDS images of centre of archaeological wood from 10% TBDMS chitosan batch 2 a) SEM with overlay of all EDS layers, b) SEM image, c) EDS-SEM of silicon content, d) EDS-SEM of carbon content and e) EDS-SEM of oxygen content. The scale bar for the SEM with EDS is 100 µm and all the others are 50 µm.

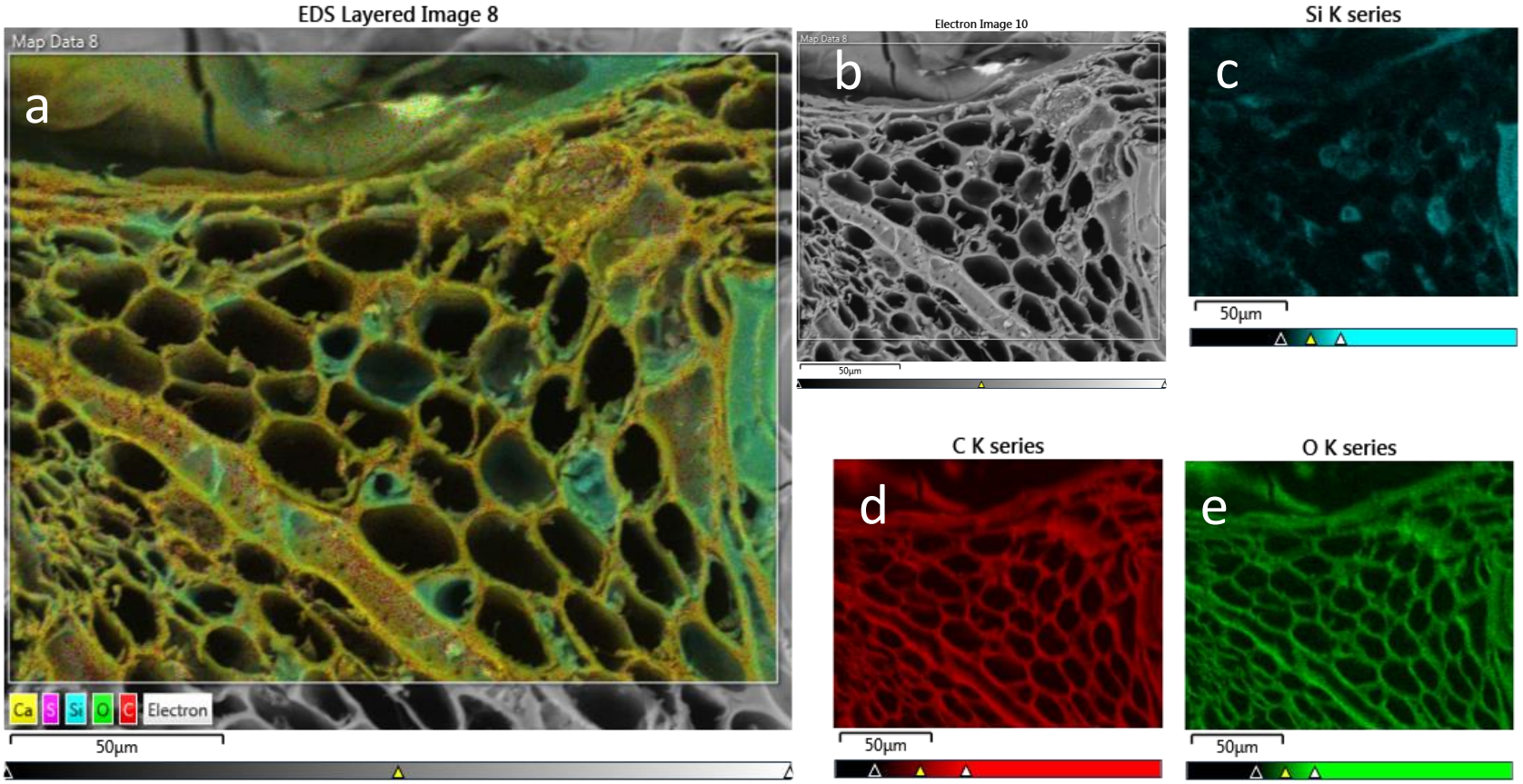

Figure 7-20: SEM-EDS images of centre of archaeological wood from 10 % TBDSMS chitosan 2 vac immersion wood centre) 2 a) SEM with overlay of all EDS layers, b) SEM image, c) EDS-SEM of silicon content, d) EDS-SEM of carbon content and e) EDS-SEM of oxygen content. The scale bar is 50 µm on all images.

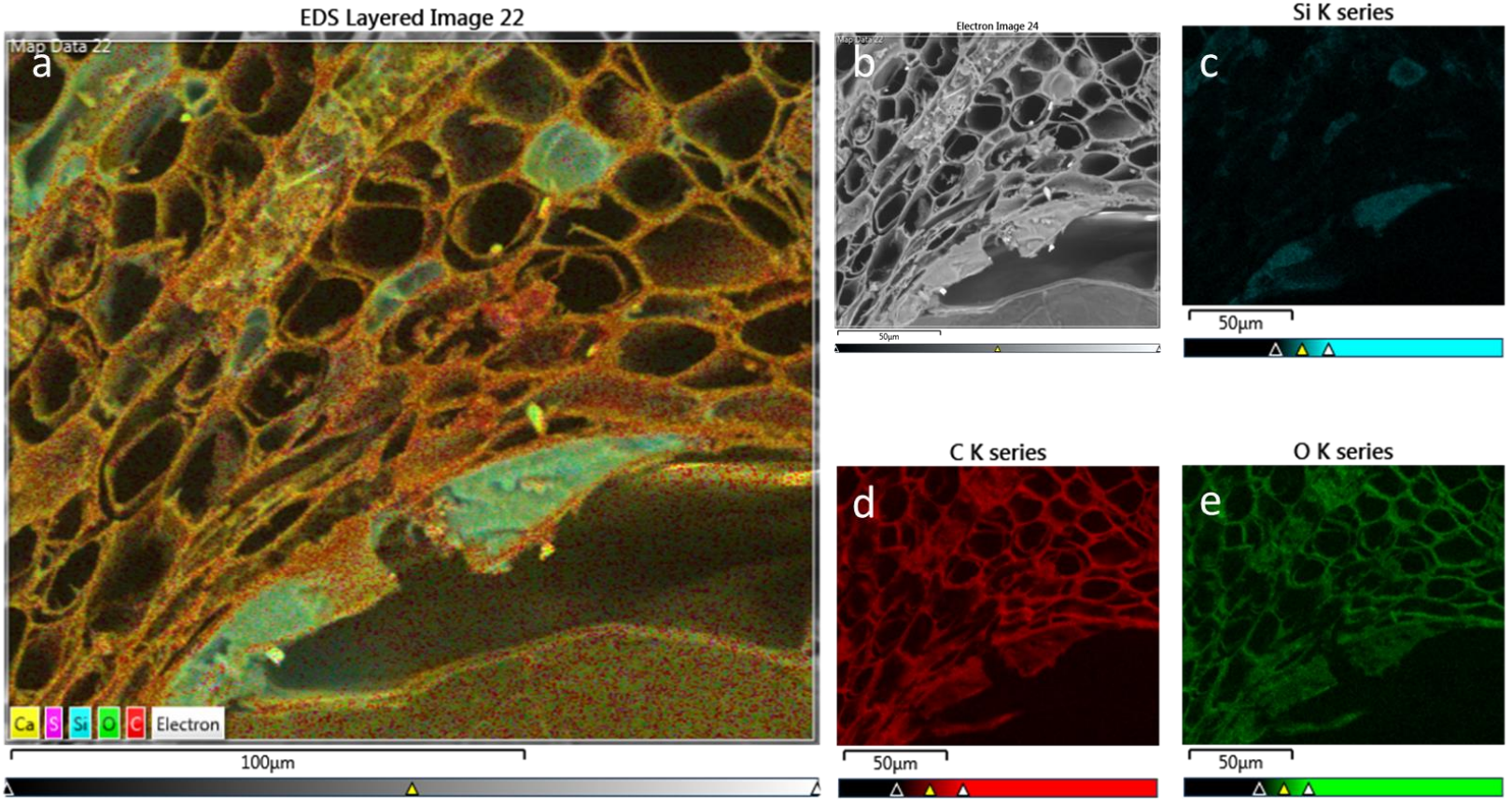

Figure 7-21: SEM-EDS images of centre of archaeological wood from 20% TBDMS chitosan arch 43 wood centre) 2 a) SEM with overlay of all EDS layers. The scale bar is 100 µm, b) SEM image, c) EDS-SEM of silicon content, d) EDS-SEM of carbon content and e) EDS-SEM of oxygen content. The scale bar is 50 µm images b, c, d and e.

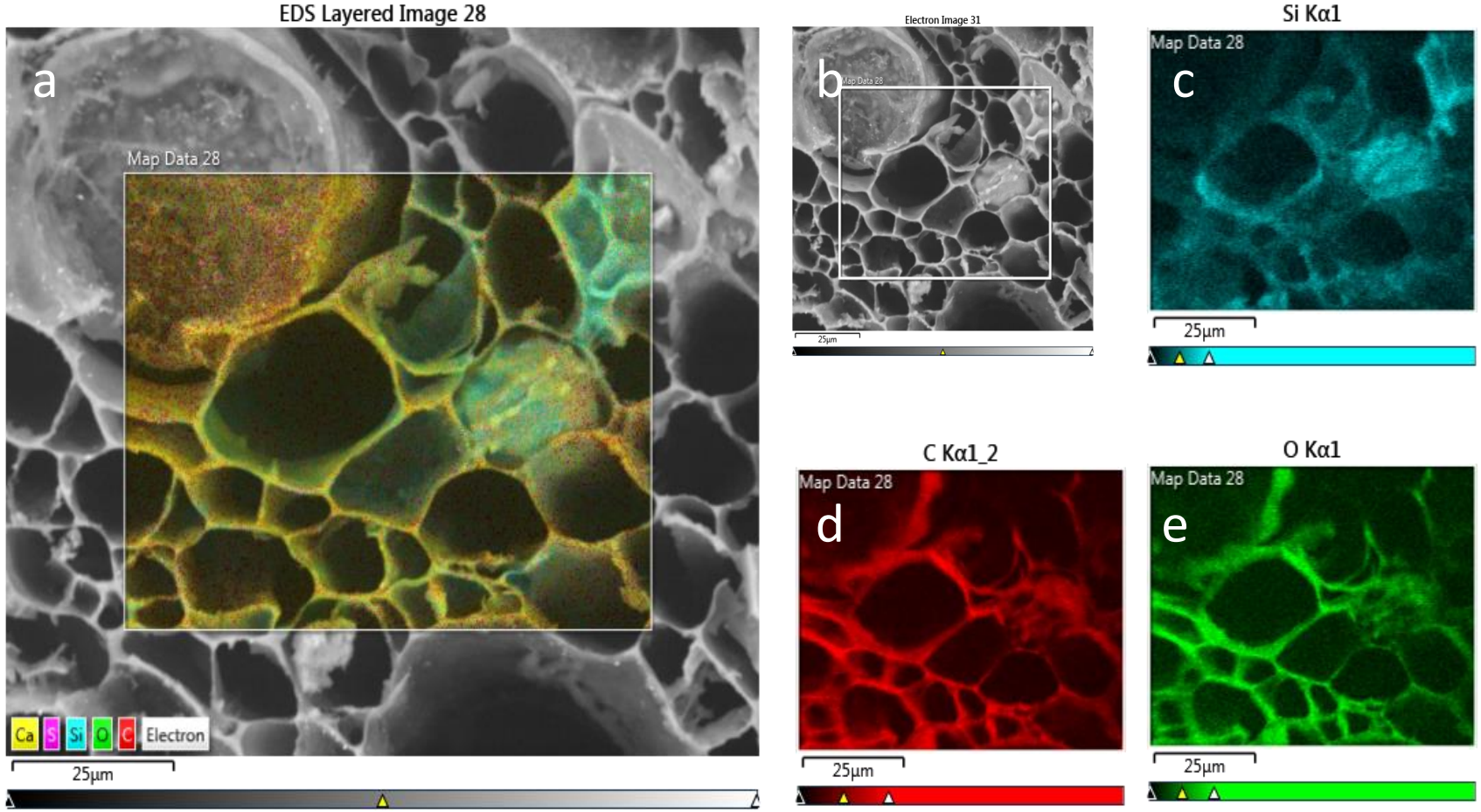

Figure 7-22: SEM-EDS images of centre of archaeological wood from 10% TBDMS chitosan one month arch 20 (wood centre) 2 a) SEM with overlay of all EDS layers, b) SEM image, c) EDS-SEM of silicon content, d) EDS-SEM of carbon content and e) EDS-SEM of oxygen content. The scale bar is 25 µm.

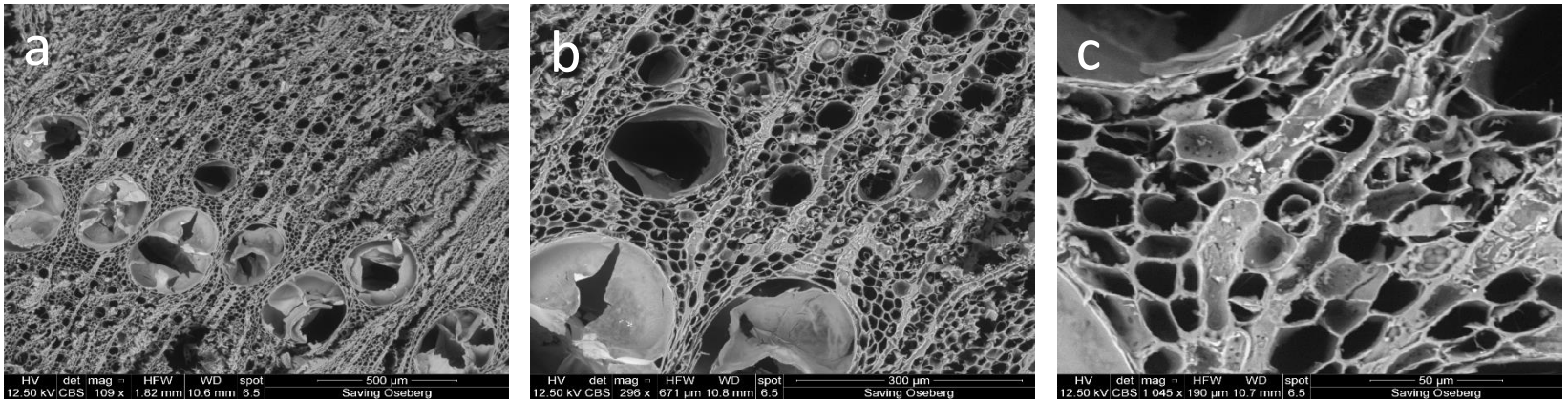

Figure 7-23: SEM images of 10% B72 immersion (wood centre) arch 37, spot size 6.5, HV 12.50 kV, WD 10.6 mm, mag 109x a) with 500 µm scale bar, spot size 6.5, HV 12.50 kV, WD 10.8 mm, mag 296x, b) with 300 µm scale bar and c) zoomed in to 50 µm scale bar, spot size 6.5, HV 12.50 kV, WD 10.7 mm, mag 1045x.

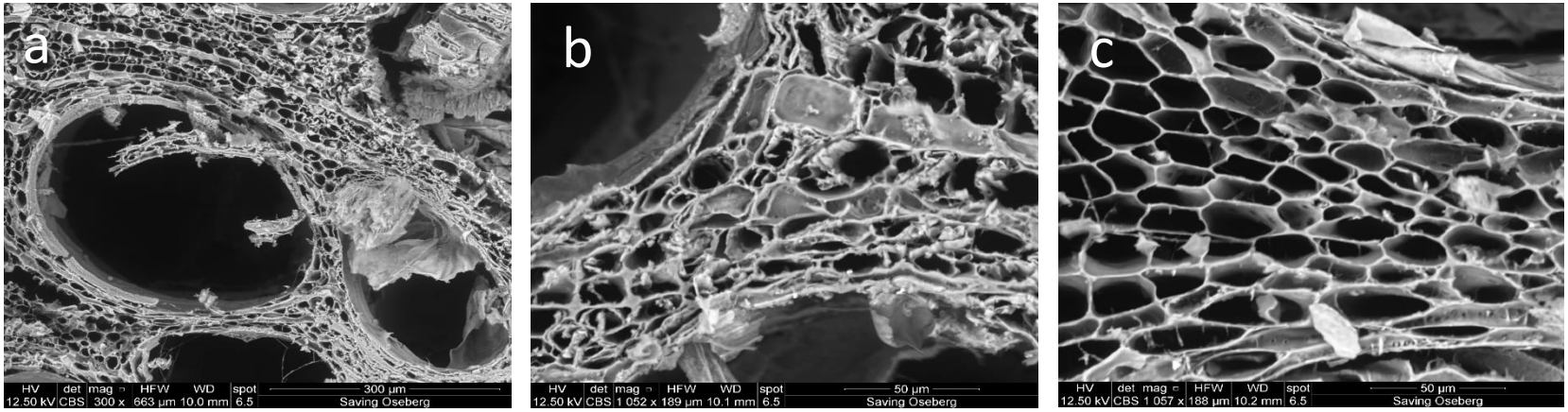

Figure 7-24: SEM images of 10% B98 immersion (wood centre) arch 51 a) with 500 µm scale bar, spot size 6.5, HV 12.50 kV, WD 10.0 mm, mag 300x, b) zoomed in to 50 µm scale bar, spot size 6.5, HV 12.50 kV, WD 10.1 mm, mag 1052x and c) zoomed in to 50 µm scale bar in a slightly different location spot size 6.5, HV 12.50 kV, WD 10.2 mm, mag 1057x.

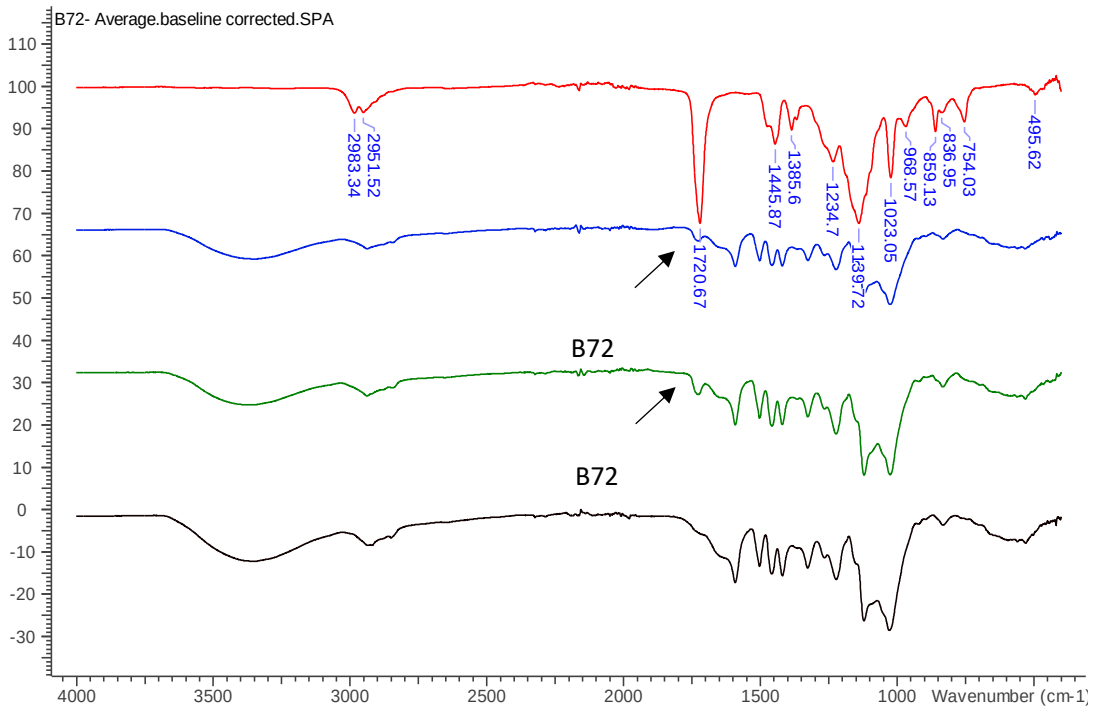

Figure 7-25: IR spectra of B72 treated archaeological wood; red B72 alone, blue edge 72 treated archaeological wood, green middle of archaeological treated wood, untreated archaeological wood.

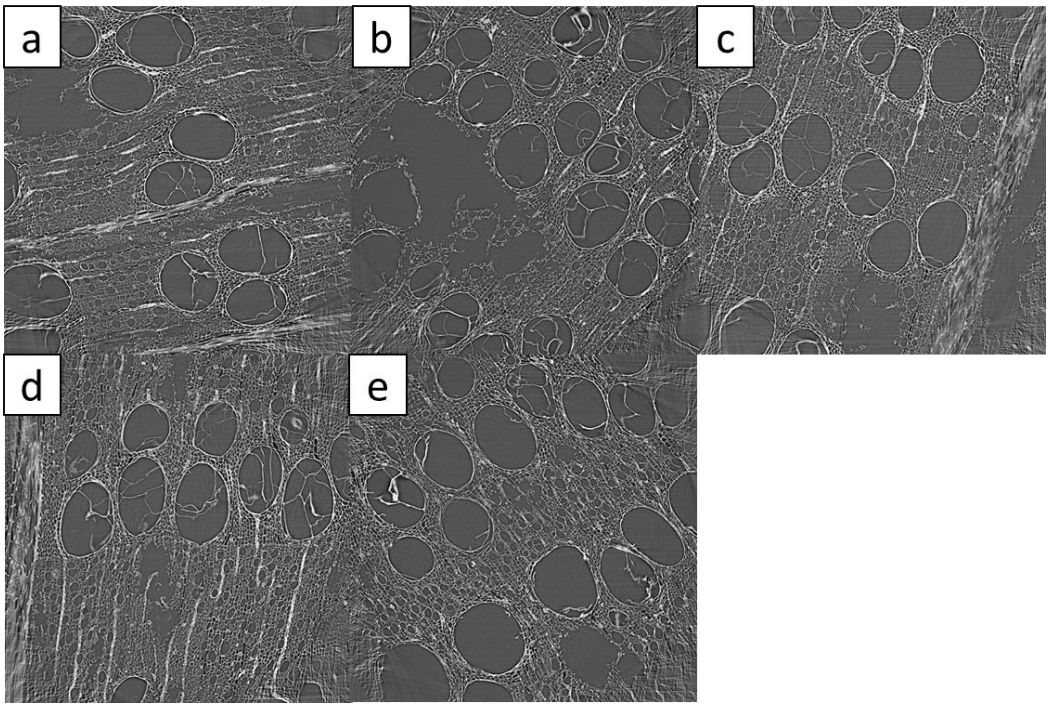

Figure 7-26: X-ray tomography images a) untreated, b) control 50:50 toluene and ethyl acetate, c)10% TBDMS chitosan, d) 10% B72 and e) 10% B98. All treatments were for two weeks. X-ray tomography results were obtained by Braovac.

The SEM-EDS results Figure 7-14 and Figure 7-17 to Figure 7-22 show that TBDMS chitosan penetrates into the centre of the wood as the silicon from the TBDMS group can be seen in the centre of the wood. The images show that TBDMS chitosan coats the cell walls and fills the cells. They also show that an open structure is retained which means re-treatment should be possible should it become necessary.

Treatment with B72 and B98 is similar to TBDMS chitosan as they appear to line the cells and then fill some cells (Figure 7-15, Figure 7-16, Figure 7-23 and Figure 7-24). However, without the silicon the polymers cannot be detected with the EDS. The SEM again shows an open structure.

The IR (Figure 7-25) shows that the B72 did successfully penetrate the wood.

The X-ray tomography showed that freeze drying prevented cell collapse in all samples prior to treatment. Treatments also did not show collapse and showed that a relatively open structure was maintained with all treatments (Figure 7-26 and Figure 7-27).

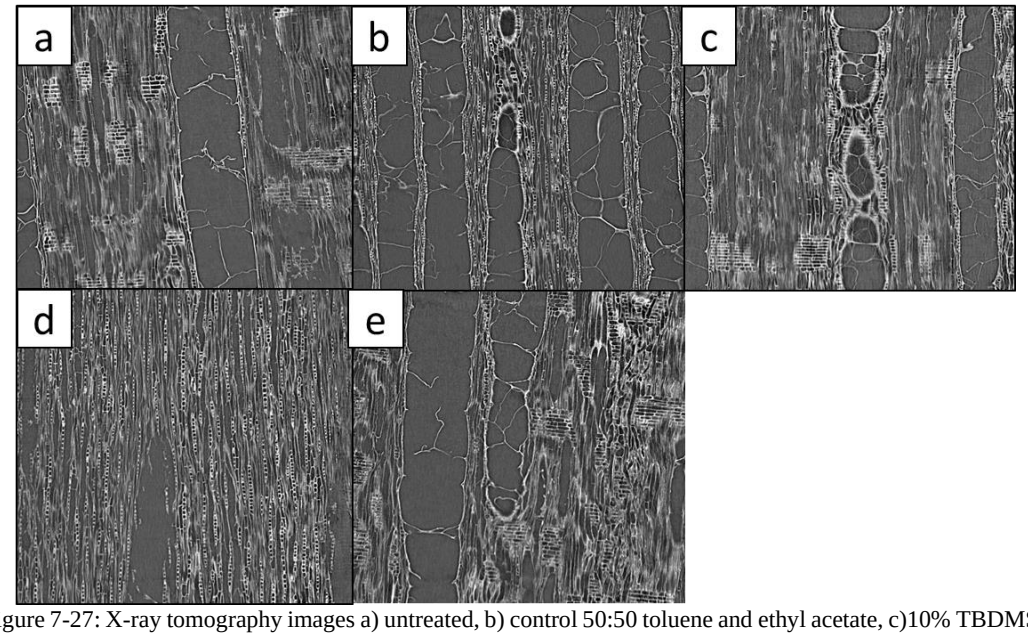

Figure 7-27: X-ray tomography images a) untreated, b) control 50:50 toluene and ethyl acetate, c)10% TBDMS chitosan, d) 10% B72 and e) 10% B98. All treatments were for 2 weeks.

7.3.2.3 Spectrophotometer

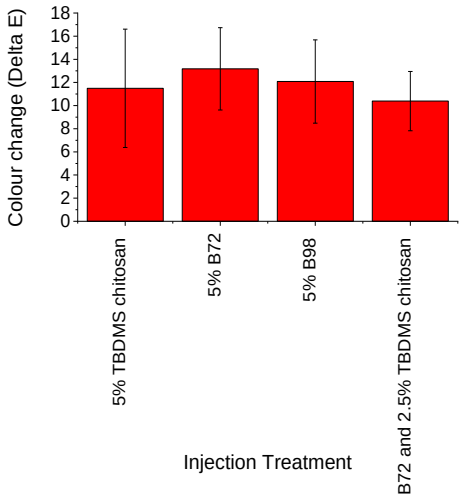

Figure 7-28: Colour change (Δ E) of different non-aqueous injection treatments on archaeological wood.

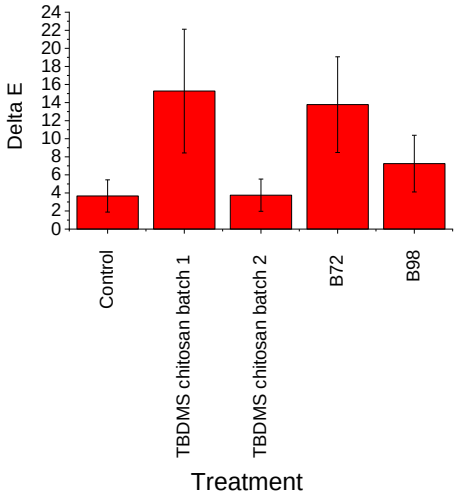

Figure 7-29: Colour change (Δ E) of different immersion treatments.

According to Figure 7-28 and Figure 7-29, solvent treatment alone does cause a small colour change. Figure 7-29 and Figure 7-30 showed 10% TBDMS has variable results: one batch showed very slight colour change but the other resulted in a greater colour change. B98 showed a smaller colour change than the B72 and one of the batches of TBDMS chitosan.

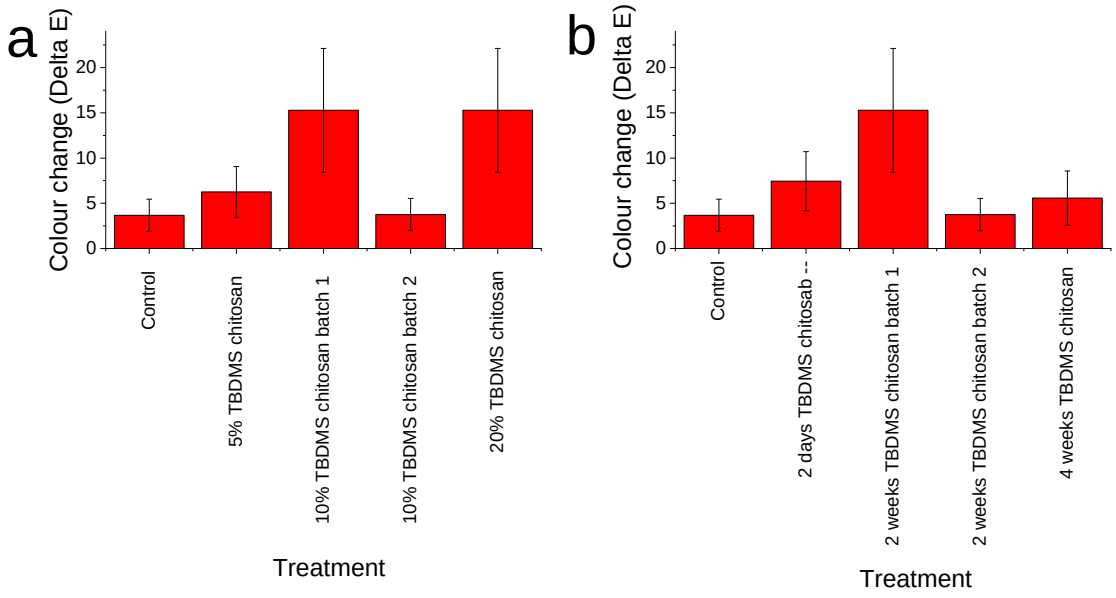

Figure 7-30: Colour change (Δ E) of different concentrations of immersion treatments.

7.3.2.4 Surface consolidation

7.3.2.4.1 Injection

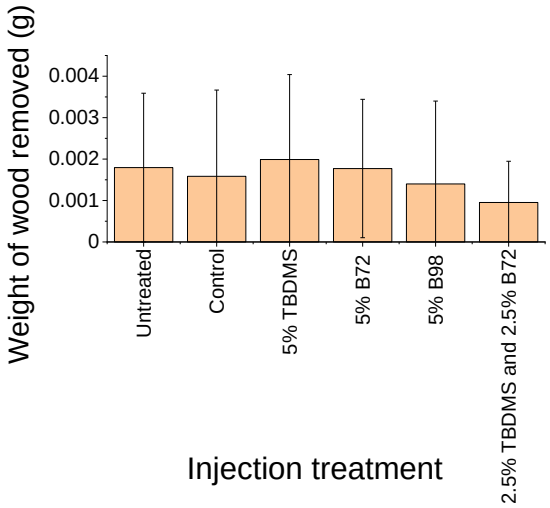

Figure 7-31: Surface consolidation expressed through tape test. Average powder removed in weight for different injection treatments. The error is the average of the standard deviation of each of the sides for each treatment.

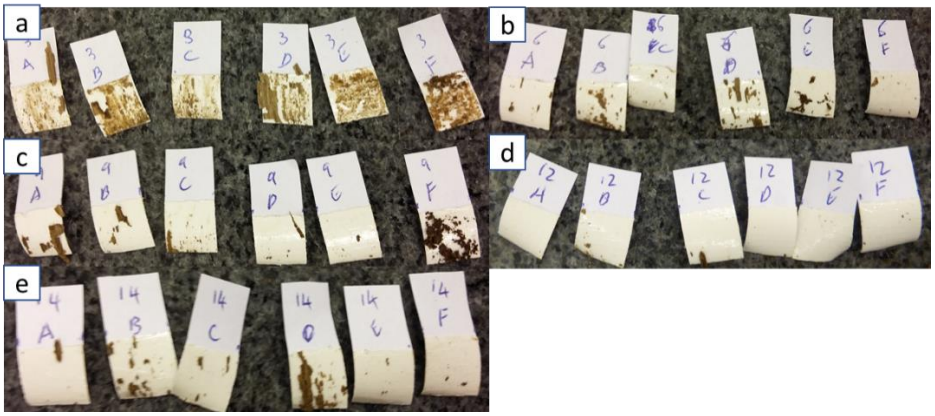

Figure 7-32: Photographs of tape test results. One example of each a) Untreated, b) TBDMS chitosan, c) B72, d B98 injection and e) B72 and TBDMS chitosan.

Figure 7-31 and Figure 7-32 shows that B98 had the smallest amount of powder removed from the surface according to weight; 2.5% TBDMS and B72 showed the second smallest amount of powder removed. The other treatments showed

similar weights of powder removed to that of the untreated samples and the control.

1.1.1.3 Immersion – different treatments, concentrations and lengths

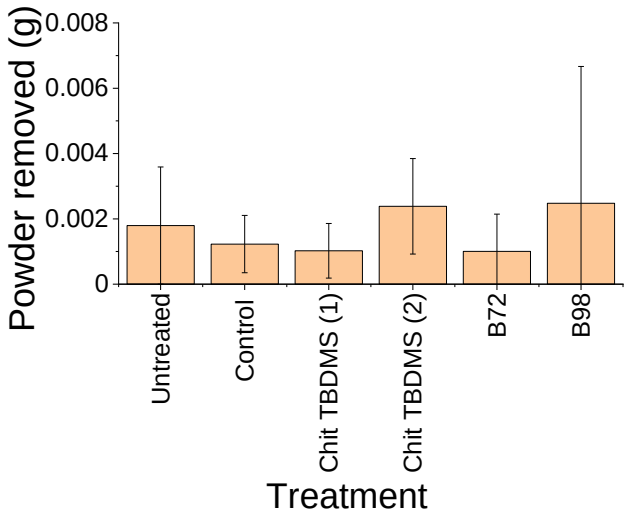

Figure 7-33: Tape test results. Powder removed from wood surface by weight (g) for different immersion treatments.

Figure 7-33 of immersion treatments showed B72 resulted in the smallest weight of powder removed from the surface, hence, the most consolidation. B98 showed a great deal of variability. TBDMS chitosan of different concentrations and lengths of treatments were brittle when cut open and generally show poor surface consolidation (Figure 7-34, Figure 7-35 and Figure 7-36). The first batch of 10% TBDMS chitosan two-week treatment showed reasonably good surface consolidation but when the wood was cut it was found to be brittle.

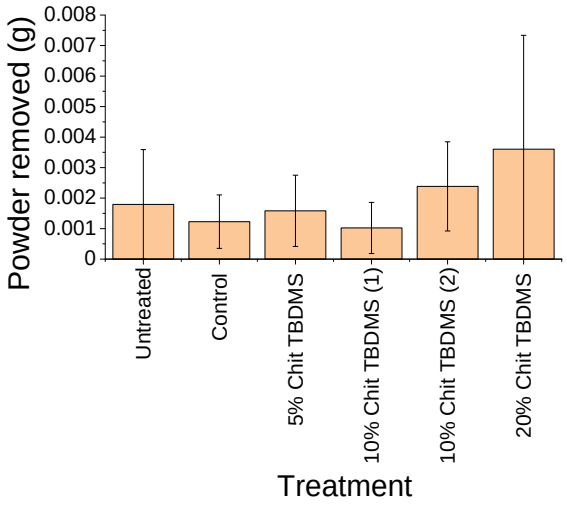

Figure 7-34: Tape tests results. Powder removed from wood surface by weight (g) for different concentrations of TBDMS chitosan.

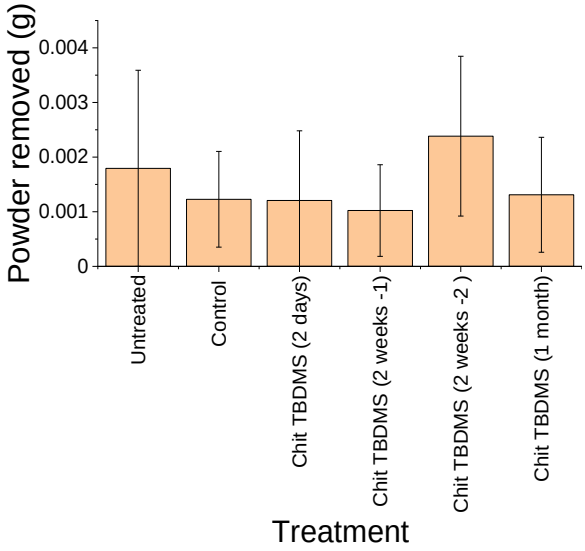

Figure 7-35: Tape tests results. Powder removed from wood surface by weight (g) for different treatment lengths of TBDMS chitosan.

7.3.2.5 Photographs pre- and post-treatment

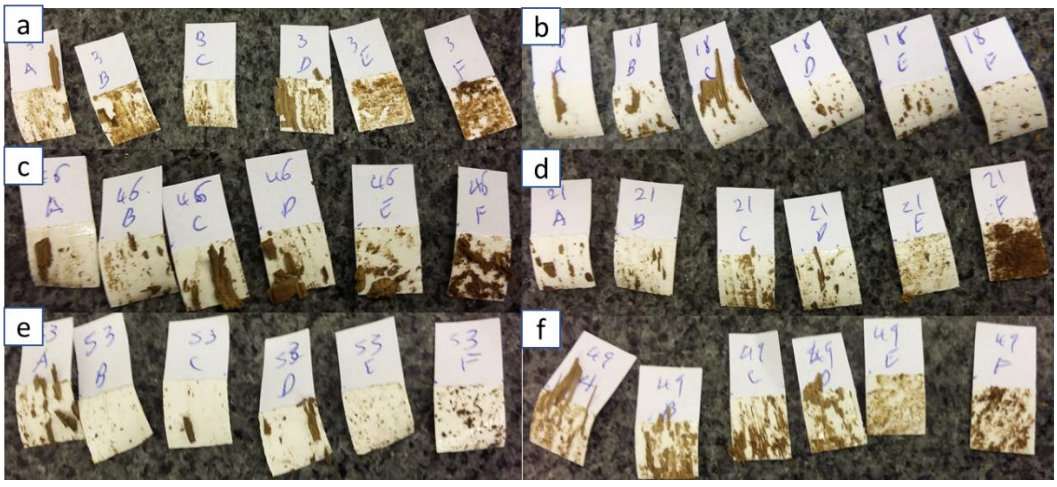

Figure 7-36: Photographs of tape test results a) untreated, b) TBDMS chitosan vacuum treatment, c) batch 2 TBDMS chitosan two weeks treatment, d) one month TBDMS chitosan treatment, e) B98 and f) control.

7.4 Discussion

7.4.1 Treatment material-immersion

7.4.1.1 Weight and volume changes

The weight and volume change are the simplest form of analysis but one of the most important, as they tells us how much consolidant is taken up and how much swelling occurs. If there is too much swelling, a polymer will be deemed to be unsuitable as a consolidant for archaeological conservation. T-butanol resulted in a lower volume change than the ethyl acetate and toluene mix. However, it was accompanied by a lower weight increase. Although a smaller volume change is preferable, there is a concern that there is insufficient consolidant uptake. However, the uptake of consolidant is low with t-butanol. The SEM shows improved distribution; this could be due to the increase in polarity resulting in increased interaction with the cell wall and hence, better coating. However, the low uptake is a concern, as is the toxicity of t-butanol. The low uptake of PEG in t-butanol could be due to the temperatures used; 40 ^{o}C was used to avoid the t-butanol solidifying. However, a higher temperature is required to dissolve the PEG. This was not known prior to starting the experiment. The PEG was well dispersed in the solution but had not dissolved.

The control (50:50 toluene/ethyl acetate treated wood) was found to have quite a high increase in weight, which might be due to residue toluene that did not completely evaporate. The weight was taken when the weight stopped dropping but it is possible it may have temporarily stabilised as the evaporation slowed. This must be taken into

consideration when looking at the weight increase for consolidants. There was a good uptake on each consolidant; the order was B72>B98>TBDMS chitosan. Tuduce Trăistaru et al. (2011) found a much smaller WPG; however, their investigation was in sound wood (0.5-5.5% WPG) (Tuduce Trăistaru et al., 2011). They found that the WPG increases with immersion time from 2h-24h. A duration of two weeks was used in these experiments to ensure the highest possible uptake and fullest penetration into the wood. Tuduce Trăistaru *et al.* (2011) found that ethanol with acetone resulted in higher WPG than toluene. It could be that the more polar solvents help with adhesion. Toluene with ethyl acetate was used so that the results could be compared, as toluene and ethyl acetate were used with TBDMS chitosan. Toluene, however, has been found to produce less swelling than polar solvents. The swelling order, from least to most, was the control<B72 <TBDMS chitosan<B98. B72 is therefore preferable as a consolidant in terms of the swelling of the wood. B98 might have had the most swelling as the solvent was more polar due to the addition of ethanol.

In terms of archaeological wood, the t-butanol version was not followed up on due to the low uptake of TBDMS chitosan. Weight increase/uptake was in the following order: B72>B98>TBDMS chitosan batch 1>TBDMS batch 2. The second batch of TBDMS chitosan was carried out by mistake; the second batch was supposed to be a one-week treatment. However, having two batches shows the variability with the same treatment. Volume change in particular showed variability as batch 1 resulted in swelling and batch 2 resulted in shrinkage. Archaeological B98 treated wood was similar to laboratory degraded treated wood and showed more swelling than TBDMS chitosan and B72. B72 had very good results with very little volume change.

It must be taken into consideration for conservation treatment that the swelling observed for non-aqueous treatments was in all cases significantly lower than those observed with aqueous treatments for artificially degraded wood. The non-aqueous consolidants would also allow for the alum to be left in, at least initially. This is important as, in the fragile wood, the alum is supporting the structure of the wood greatly and its removal could be destructive. Therefore, the low volume change seen here for B72 combined with the work of Sahlstedt in Häggström and Sandström (2013) on B72 as a pretreatment followed by successful desalination in cold water indicates B72 could be a successful pre-treatment or possibly a treatment if combined with alkali nanoparticles to increase the pH.

7.4.1.2 Distribution

The SEM with EDS also proves that the TBDMS chitosan got into the centre of the archaeological wood and the laboratory-degraded wood. Tomography of the laboratory-degraded wood showed that an open structure was maintained in the case of B72, B98 and TBDMS chitosan. B72 was observed filling some of the cells. Schniewind and Eastman (1994) found B72 filled cells but that there was a drop in the number of filled cells after 7 mm. Although some cells were filled, many remained open. Tuduce Trăistaru et al. (2011) investigated treatment of B72 on sound wood and were able to observe the B72 through SEM at 10% concentration. Despite the same concentration, the B72 was less visible in the SEM of archaeological wood. This is probably because the degraded cells have larger pores due to the degradation of the cell walls, hence, the cells are harder to fill. Therefore, the B72, although filling some cells did not fill others and instead lined some; hence it was less obvious. A higher

concentration of B72 and B98 could be used which might improve consolidation; however, more cells would be filled and this might prevent retreatment unless the B72 or B98 were removed first. The advantage of TBDMS chitosan is it appears to coat the cells rather than fill them.

7.4.1.3 Colour change

Colour change is also important as it is undesirable to have an extreme colour change which may affect how the public perceives the artefacts.

In the laboratory-degraded wood, the outside changed colour the most with treatment. B98 resulted in the least colour change. The colour change in the inside of the wood was least pronounced with B72, followed by the control, then 10% chitosan and lastly the B98.

In the archaeological wood the control showed some colour change. Similarly, with other results the two batches of TBDMS chitosan gave very different results, with batch 2 showing similar colour change to the control. B98 had the next lowest colour change followed by B72 and finally batch 1 of TBDMS chitosan. This makes B98 the best treatment in terms of colour change. A larger sample size of wood for all treatments is required to be sure the results are representative. The variation in the TBDMS chitosan results is a concern. B72 caused significant colour change. Nevertheless, visually, the colour change in all samples was not drastic. Small colour change would be acceptable if the treatment gave greater stability for the artefacts.

7.4.1.4 Surface consolidation

Surface consolidation (the tape test) of archaeological wood showed very little improvement compared to untreated wood and control; 50:50 toluene/ethyl acetate. The tape test measures the mass of wood removed from the surface of wood. Chitosan TBDMS showed variable results with two different batches of treatment. B72 showed the best results. B98 showed a large variation of results. This large variation could be because no wood was taken off in some cases and in others large pieces of wood ripped off the surface, resulting in a large weight on average; however, small quantity of powder was removed hence improved consolidation. It was observed in some cases that large chunks were ripped off and in other cases of high weight of powder was removed. Photos were taken but lost; had these been available it would have been possible to differentiate powder form pieces like in the Chapter 6 with aqueous treatments. However, as these photos have been lost and there were only a few photographs, the full effects of the tape test cannot be analysed like in the previous chapter. Due to this, B98 should not be ruled out. Photos of slicing would also have been useful in assessing consolidation but the importance of this was not realised until later and they were not taken for the non-aqueous treated wood. A recommendation would be to make sure photos of slicing and of tape tests after surface is removed should be kept. A larger sample size and corresponding photos are required to make a conclusion regarding the best consolidant.

7.4.2 Concentration of treatment

An investigation into the effect of concentration of the TBDMS chitosan treatment was carried out to find the ideal concentration to use for treatment. Increasing the concentration increases the weight percentage gain (WPG) from 5-10% but not from 10-20% TBDMS chitosan. Therefore, in terms of WPG, 10% is the most promising. Volume change must also be considered in finding the best treatment. The volume change varied with concentration but with no discernible pattern; 5% swelled slightly more than control but less than 10% and had the lowest variability, 20% shrank slightly, and 10% was very different between batch 1 and batch 2. On average, one batch shrank whereas one other swelled and both showed large variability. The shrinkage observed with 20% could be due to high viscosity preventing the consolidant from entering the wood. The uptake, however, was similar to the second 10% batch, although WPG was not significantly higher and much lower than the first 10% batch. It is therefore hard to conclude whether less consolidant got into the wood but it is clear that increasing concentration did not increase uptake, which is likely due to the viscosity. From the surface consolidation tape test, 20% TBDMS chitosan also does not seem favourable in terms of consolidation. Finally, 20% also had a higher colour change. 5% did not show improvement in terms of surface consolidation compared to 10% batch 1, but a small improvement over 10% batch 2. In terms of colour change, 10% batch 2 was favourable to 5% but 5% was favourable to 10% batch 1.

From SEM, all treatments reached the centre of the wood and had a relatively good quantity of TBDMS chitosan and distribution but the second batch of 10% appeared

to show the most TBDMS chitosan in the centre of the wood. Altogether, this suggests 10% TBDMS chitosan is most favourable.

7.4.3 Length of treatment

The two-day vacuum immersion resulted in the highest WPG and also the highest uptake i.e. when the volume of the original wood is taken into account. This seems to be the opposite of what Muhc*u* et al. (2017) discovered. They found the WPG for 10% B72 in acetone on treated laboratory degraded wood, degraded through fungi treatment, was 13.49% with vacuum and 17.83% after 24 h immersion (Muhcu et al., 2017). Spirydowicz et al. (2001) found similar results to this investigation; under SEM, 10% B72 showed more consolidant with vacuum immersion rather than at room pressure. They also found B98 showed improved consolidation at 10% with the pin test and further improvement was found with vacuum immersion (Spirydowicz et al., 2001b).

In this current piece of research two-day vacuum treatment also showed the smallest volume change of all samples including the control (two week immersion control). Muhcu et al. (2017) found 10 % B72 vacuum treatment resulted in 11.69 % volume swelling with 2 h treatment and 13.05% with 24 h treatment. They also found 6.40% swelling for 2h immersion and 11.27% for 2 h immersion (Muhcu et al., 2017). Therefore, they found vacuum treatment did not cause as big a volume change. This current piece of research found smaller volume changes than Muhcu et al. (2017). The one month treatment showed the smallest uptake and a small volume change; smaller than the two week immersion.

In this current research, two-day vacuum immersion showed a similar surface consolidation in terms of weight to the control and a slightly higher surface consolidation than the first batch of two-week treatment. The second batch of two-week treatment showed a much higher weight of wood removed from the surface. The one-month treatment showed a slightly reduced surface consolidation, i.e. a slightly higher weight of wood removed from the surface.

In terms of colour change, two-day vacuum treatment showed more colour change compared to the control and more colour change than the second batch for two-week treatment. The one-month treatment showed smaller colour changes than the two-day vacuum treatment and significantly lower than the first batch of two-week treatment.

From SEM it is clear that the two-day vacuum treatment led to good distribution right through to the centre of the wood. The one-month treatment also showed very good distribution in the centre, coating most cells. The two-week treatment varied greatly but both show TBDMS successfully reaching the centre of the wood, but more TBDMS chitosan could be seen in the second batch.

The two day 10% vacuum treatment is certainly favourable in terms of time and produces good WPG, small swelling and reasonable colour change compared to the two-week treatment. The two-week treatment would be the alternative if the wood could be vacuum treated due to its size. However, the B72 and B98 appear favourable compared to the TBDMS chitosan.

7.4.4 Injection vs immersion

Injection in laboratory degraded wood showed a higher weight percentage gain (WPG) (10.31) with 2.5% TBDMS chitosan compared to 5% TBDMS chitosan (7.57%). 10% immersion gave a higher WPG (19.62%). This shows immersion is favourable in terms of retaining the most consolidant. It was found that the volume increase was marginally lower with injection compared to immersion. Immersion is not always an option, hence, despite the lower WGP, injection should not immediately be dismissed.

Archaeological wood was investigated next; despite the higher WGP with 2.5% TBDMS chitosan, 5% was chosen due to the high level of degradation of the archaeological wood anticipated to allow for easier uptake. Treatment of archaeological wood resulted in a ~27% WPG compared to 19% with 5% TBDMS chitosan two week immersion; however, 10% immersion resulted in ~36% WPG over two weeks and 45% weight gain with vacuum immersion. This again shows immersion is favourable in terms of greater WPG. However, as stated, injection can be favourable under some circumstances. It is clear that some consolidants can be taken up this way and the EDS-SEM also showed that injection treatment of TBDMS chitosan can still reach the centre of a ~1.2 x 1.2 x 2.5 cm piece of wood. The surface consolidation did not seem favourable to the control in terms of wood weight removed. However, photos show that larger chunks were removed rather than fine powder suggesting surface consolidation. The injection also resulted in a harder surface which might make the artefacts easier to handle. However, TBDMS chitosan did appear to be brittle in the centre of the wood. The TBDMS chitosan treatment was also compared to existing

conservation treatments B98 and B72 to assess which would be favourable for injection.

For laboratory-degraded wood, B72 resulted in the most favourable WPG and volume change. This was also the case with the archaeological wood. Combining B72 and TBDMS chitosan resulted in a slighter lower WPG and a small shrinkage of the wood, but less than TBDMS chitosan alone and did not result in swelling like B72. B98 produced the least colour change in archaeological wood. B98 also resulted in the best surface consolidation. The mixture of B72 and TBDMS was second best. However, it must be noted that the weight removed does not always directly reflect consolidation, as the strength of the tape can rip wood off the surface that is consolidated.

7.4.5 B72 vs B98

The intention of this research was to investigate TBDMS chitosan as a consolidant. It also gives us an opportunity to compare B72 and B98 for injection vs immersion. Injection resulted in a WPG 27% vs B98 WPG 24%. Immersion resulted in 44% (B72) and 37% (B98) showing immersion is favourable in terms of WPG. Muchu et al. (2017) and Spirydowicz et al. (2001) report differing results on the effect of B72 and B98 vacuum immersion vs immersion alone. This needs to be investigated further to definitely determine whether vacuum immersion is beneficial. These results support Muchu et al.'s (2017) work; however, this would need to be repeated with B98 and B72.

Volume change also favours B72 immersion (0.5% shrinkage) over injection (1% swelling) and over B98. B98 injection (8% swelling) was more favourable than

immersion (15% swelling). However, in the case of B98, two pieces of wood produced a small shrinkage of 7% and 3%. However, one piece of wood broke during treatment but stuck together during drying resulting in a 54% swelling for that piece. Hence, a small amount of shrinkage for B98 should be assumed. In laboratory-degraded wood B72 produced less colour change. By contrast, in archaeological wood, B98 produces less colour change than B72. The difference was minimal with injection but more pronounced with immersion. The surface consolidation was also better with B98 than with B72 shown by weight of wood removed for injection, but the reverse was found for immersion. However, as previously stated, this work needs to be repeated with photographs to record the extent of fine powder or chunks rated 1-5. This can account for high weight due to the strength of the tape removing a chunk of wood that had been consolidated. Large consolidated chunks are different from a fine powder easily removed from the surface. From the SEM it can be seen that neither B72 or B98 fully filled the cells; rather they appears to coat the cell walls preferentially. This correlates with the mercury intrusion tests carried out by Crisci et al. (2010), which showed a very small reduction in porosity. Their findings also show that B72-treated wood showed very little colour change after exposure to solar radiation (Crisci et al., 2010).

Based on the structure of B98 and B72, B98 could be recommended as an injection treatment for the Oseberg wood over B72, from the surface consolidation tests and colour changes but also because of its structure: B98 contains ether bonds which are less acid sensitive than the ester bonds in B72. B98 has also been shown under standard conditions to form butyraldehyde rather than butyric acid as a major breakdown product, but also little breakdown is observed and more acid would not be introduced (Harrison, 2009). However acidic conditions should be investigated. Therefore, B72

would be recommended for immersion over B98 as a result of improved uptake and improved surface consolidation. However, in this case this would be as a pre-consolidant to be followed by washing out the alum. This could then be followed up by further consolidation with an aqueous treatment if it were deemed necessary. This recommendation is also based on Häggström and Sandström's (2013) findings that showed alum could be washed out following B72 treatment (Häggström and Sandström, 2013). Future research is required to identify cases where immersion is not an option. In the cases where immersion is not possible and injection is best, B98 might be the best option but research is needed to check that another option is not favourable. B98 is relativity stable but long-term acidic conditions require further investigation. B72 could also be mixed with nanoparticles to increase the pH but more research is required into combined use. Muhcu et al. (2017) investigated B72 with nanoparticles in order to improve resistance to fungal attack rather than increase pH, but their research shows it is possible to combine treatment (Muhcu et al., 2017). Carretti et al. (2013) also investigated B72 with $Ca(OH)_2$ nanoparticles looking at the combined mechanical properties for conservation of inorganic material. However, the research is informative for this project too; it appears the Tg value increases slightly but the hydrophobicity of the polymer is maintained, which would help reduce moisture and hence help prevent further degradation. Carretti et al. (2013) also performed the tape test and found that the combination improved the consolidation of stone (Carretti et al., 2013). Future research is required to see if the B72 can be used with Ca(OH) nanoparticles for wood treatment to improve consolidation with the B72 and protect the B72 and wood for acid degradation with alkali nanoparticles.

7.5 Conclusion

From the results for TBDMS chitosan treatment it appears that two-day vacuum immersion would be the best in terms of treatment time, but also in terms of weight percentage gain and volume change. TBDMS chitosan also gave comparable consolidation results to the control; however, some treatment concentration and lengths made it worse. However, TBDMS chitosan results indicated that it tended to give external strength but was very brittle when cut. This brittleness could be a problem; hence, the recommendation would be to use B72 as a pre-consolidant before removal of the alum and acid. Alternatively, if immersion of the artefact is not an option, then injection with B98 appears preferable to B72. B72 immersion could possibly be combined with nanoparticle treatment to increase pH and remove the need to remove the alum. Both B72 and B98 gave good results and warrant further investigation with alum-treated wood to see if they could be used in these very particular cases.

Chapter 8. Conclusion and future work

8.1 Oseberg artefacts past conservation and new approach

The Osbeberg collection is of striking importance in the history of the Vikings and of Europe. It is an assemblage of artefacts that are quite unique and therefore their preservation is of the utmost importance. The alum treatment carried out between 1905-1912 prevented the artefacts cracking and wrapping and allowed pieces to be put back together. However, this treatment produced sulfuric acid which has slowly degraded the cellulose and the lignin. Some of the artefacts also contain iron from original nails and from those used in the conservation process. The Vasa and Mary Rose found that the combination of PEG, iron and sulfuric acid could be detrimental. For this reason, an alternative is sought to PEG. Chitosan has previously been investigated for wood treatment, with promising results. It is sustainable, the amine group could help increase the pH and it is known to chelate metal ions. Aminocellulose is a similar polymer modified synthetically from cellulose. Again, the amine group could help increase the pH and aid in metal chelation as well as conservation.

Some artefacts are more robust than others and could cope with an aqueous treatment. Others would require a non-aqueous treatment. Modification of chitosan could aid its solubility in organic solvents.

8.2 Chitosan and aminocellulose

Christensen (2013) investigated chitosan and depolymerised chitosan for wood conservation for the Oseberg collection, he found that when the chitosan was depolymerised to 6.25 kDa (determined via GPC) a higher content of chitosan was found in the wood. The quantity of chitosan was determined via glucosamine content, the monomeric unit of chitosan. Chitosan previously investigated by Christensen (2013) was determined via AUC in this project to have a weight average molecular weight of (14.2±1.2) kDa. MultiSig analysis revealed a distribution of 5-37 kDa with components peaking between 10-17 kDa. It appears the distribution of molecular weight particularly at the high end, may have reduced uptake into the wood. These findings led to the decision to reduce the molecular weight to increase uptake. The chitosan was depolymerised with hydrogen peroxide and UV light leading to a $M_{w,app}$ of (4.9±0.7) kDa with a distribution of 0-12 kDa peaking around 5kDa. The tighter lower molecular weight distribution should allow higher uptake of polymer into the wood. The molecular weight of the combined batches; therefore, the chitosan used for the actual wood treatments had an slightly higher $M_{w,app}$ (6.2±0.3) kDa. Future work would be to create a F(M) vs M plot for depolymerised chitosan by converting the SV plot by carrying out SE analysis on different molecular weights or by combining SEC-MALLS data and AUC data.

Aminocellulose AEA and HEA were found from SV and SE to self-associate. HEA self-associated into species of higher molecular weight than AEA. AEA had a monomeric molecular weight of 4.5 kDa and HEA slightly higher at 5.5 kDa. This is comparable to the $M_{w,app}$ of the depolymerised chitosan. Hence, this helps make a fair

comparison. The speed of self-association could affect how easily the polymers penetrate the wood and would be worth further investigation.

8.3 Aqueous treatment

To evaluate the effectiveness of consolidants, the consolidants chitosan, aminocellulose and PEG were first tested on artificially degraded wood and then on archaeological wood. In the case of the artificially degraded wood, no treatment was gauged to be unsuccessful, hence, all treatments were continued with on archaeological wood. All showed an increase in weight according to the concentration used and the newly proposed consolidants produced less swelling than PEG 2000 which is already used in conservation. Aminocellulose and chitosan in acetic acid produced the least swelling.

With waterlogged archaeological wood treatment 10% chitosan produced a (97.4±7.8)% ASE for archaeological waterlogged wood, which led to a ~54% surface consolidation improvement (reduction in powder removed from the wood surface compared to the control) and the wood was easier to cut and appeared less brittle. Treatment of sound balsa wood showed increased strength and flexibility were obtained through chitosan treatment, proved through MOR and MOE.

Chitosan acetate salt did not aid in consolidation; ASE was low (93.6±1.5)% with only a 33% improvement in surface consolidation and the wood appeared weak on cutting.

Aminocellulose HEA produced good results for conservation, appearing suitable either alone (ASE (96.4±15.8)% and 66% improvement in surface consolidation and

MOR vs MOE showed an improvement in strength and flexibility of sound balsa wood) or in combination with PEG (ASE (101.4±5.1)% and 37% surface consolidation improvement). In conjunction with PEG, the MOR vs MOE showed little change to the water control so there was no clear addition of strength. HEA does appear to have some advantages to PEG and the prospect of increasing pH and chelation of metal ions make it of great interest. Future work needs to evalulate the acid stability and long-term stability to confirm its suitability as a new consolidant.

PEG in comparison showed lower ASE for the same concentration as chitosan and for double the concentration of AEA (10% PEG ASE (92.0±1.6)% and 6% surface consolidation improvement). However, at higher concentration PEG did give superior ASE results (20% PEG ASE (102.0±20.7)% and 20% surface consolidation improvement,) while combining PEG and HEA kept the high ASE results, it decreased the variability. This suggests combining PEG and HEA is particularly promising. PEG actually appeared to improve the surface consolidation less than HEA and chitosan or HEA and PEG. The mechanical testing on balsa wood found 5% PEG increased strength and flexibility but 10% PEG did not show an improvement on the water control.

Aminocellulose HEA alone or in combination with PEG, appears the most promising for consolidation of artefacts that are not too fragile and have high acid and iron content. If the iron content is not high, PEG could possibly still be used but more research is required. A greater number of samples should ideally be investigated with a range of different concentrations of HEA and also with some as blends with PEG,

again with different concentration combinations. This would hopefully identify the ultimate treatment.

8.4 Chemical modification

Chitosan was degraded to ~5-6 kDa and this appears to penetrate and has good uptake. However, elemental analysis is required to determine for absolute certainty that it has penetrated into the wood and reached the centre with an even distribution. It also gave good consolidation results. Some of the artefacts, however, could not support a water-based treatment, therefore an organic soluble treatment was sought. Chitosan appeared to be a promising starting point with functional groups that could be modified to improve solubility. Reductive amination and click chemistry were attempted, but reactions were unsuccessful or the product insoluble in the desired solvents.

Silylation was tried next; this was previously reported to be successful but with different molecular weight chitosan (Rúnarsson et al., 2008b). This proved also successful with 5-6 kDa chitosan in this research. In the first reaction, however, the product precipitated out and the reaction did not go to completion. However, the addition of toluene halfway through the reaction was anticipated to dissolve the product to allow the reaction to go to completion; this was successful, allowing for a higher degree of substitution, and hence improved solubility. Solubility in isopropanol, *tert*-butanol and ethyl acetate were of particular interest. This reaction was scaled up, and multiple batches made to produce enough to investigate wood treatment. However, when batches were mixed and solubility tested again, the product, although it initially

dissolved in isopropanol, would precipitate out. The same was true for ethyl acetate, although the addition of toluene allowed it to remain soluble.

The molecular weight was investigated through the intermediate as it was not possible to analyse the TBDMS chitosan directly due to lack of solubility in solvents suitable for AUC analysis, due to compatibility of solvents with AUC cell components and density of the solvents which must allow the polymer to sediment to be analysable. The molecular weight was calculated to be on average 9.7 kDa. The low molecular weight and the solubility in ethyl acetate/toluene mixture 50:50 allowed it to be tested on wood as a non-aqueous treatment option.

8.5 Non-aqueous treatment

Similarly, to the aqueous treatment wood investigation, the TBDMS chitosan was tested on artificially degraded wood and archaeological wood. The TBDMS chitosan treatment was also compared to three treatments used in conservation: parloid B72, butvar B98 and PEG. Artificially degraded wood treatment showed *tert*-butanol caused less swelling than 50:50 toluene and ethyl acetate but *tert*-butanol appeared to reduce uptake of TBDMS chitosan and PEG. Future work would ideally repeat treatment with PEG in *tert*-butanol at a higher temperature as, although PEG was well dispersed in *tert*-butanol, it had not dissolved which could have lowered uptake. This was not continued with in this project as uptake was low and time constraints meant following up on 50:50 toluene and ethyl acetate methods was more favourable. TBDMS chitosan in isopropanol was also briefly investigated but TBDMS chitosan precipitated out which reduced uptake. Lowering the degree of substitution just

slightly, to under a degree of substitution of 2, could increase solubility in isopropanol and ethyl acetate. Although the ideal solubility may have a very small range of suitable degree of substitution. The artificial wood testing showed uptake of all consolidants and showed TBDMS chitosan did successfully penetrate the wood, according to EDS_SEM results that show silicon from the silyl group in the centre of the wood.

Archaeological wood was subsequently treated. Length and concentration of TBDMS chitosan was investigated and 2 day vacuum immersion produced the best results. However, although TBDMS chitosan-treated wood showed strengthening and consolidated the wood, in some instances pieces were very brittle and hence TBDMS chitosan cannot be recommended for wood conservation. B72 and B98 appeared promising for wood conservation. B72 is not acid stable due to the ester bond, hence, B72 is more suitable as a pre-consolidant for consolidating the wood prior to washing out the alum. If required, PEG could be used after washing out the alum. Alternatively, B72 could be used in combination with calcium hydroxide nanoparticles to increase the pH. Calcium hydroxide nanoparticles are currently being investigated in the Saving Oseberg group. Future work combining B72 and nanoparticles would be advantageous. B72 gave good results as an immersion treatment. B98 gave better results than B72 as an injection method. B98 is predicted to be more acid stable than B72, although acid stability requires a full investigation. Wood treatment with a greater number of samples is ideally required and mechanical testing. Although these results and results from artefacts previously treated with B72 B98 confirm B72 and B98 as possiblities, these are both synthetic polymers hence sustainablility could be a future problem. Solvents recycling could be investigated to improve sustainability of treatment.

8.6 Future work

A number of further experiments that could be done have been highlighted through out this thesis. The most important to follow up on for the conservation of archaeological wood and particularly the Oseberg artefacts are described here.

In terms of aqueous treatment, the most promsing consolidant was aminocellulose (HEA), the most pressing work to be done next is a stability investigation. How stable is it in the long term and whether it is stable under mildly acid conditions (for an aqueous treatment the acid would be washed out) are important to assess. There was concern during the project of an amine smell, which could suggest the detachment of the amine group from the backbone, and this requires a full investigation. Viscosity decrease with time could be investigated along with GC-MS and LC-MS to determine degradation products, if any. Treatment solutions have been kept and these could be tested to investigate degradation along with a timed study under different conditions: time, temperature and pH. Volatiles from the treatment solution and final wood pieces could be collected and investigated using GC-MS. Toxicity must be assessed: although similar aminocelluloses have been found to be non-toxic, the aminocellulose used must also be assessed. Once the stability and toxicity have been assessed, and if stable, this treatment material becomes a very realistic possibility for treatment of artefacts, given the results in this study, either alone or in combination with PEG. To finalise the work and put it forward for recommendation, an investigation should also be carried out to determine the chelation properties. This could be done through colourimetry. The ability to prevent corrosion is also important; iron nails could be placed in treatment solutions, with and without salt, with water and a salt solution as a control to determine

if corrosion is inhibited. Many artefacts contain iron nails and a consolidant that also prevents iron corrosion rather than exacerbating the situation is desired; there is no universally agreed upon treatment that can both consolidate wood and preserve iron. Finally, treatment of large pieces of archaeological wood and artefacts must be tested. A range of other aminocelluloses could also be investigated to see if any have superior properties to HEA, but the investigations suggested and those already carried out for HEA would need repeating. The aminocellulose HEA appears incredibility promising currently, but the work above must also be performed to be able to put forward aminocellulose (HEA) as a suitable consolidant with full confidence.

Potential work that could be done on TBDMS chitosan is highlighted in the thesis. However, in terms of a non-aqueous treatment, unfortunately TBDMS chitosan does not appear successful due to its brittle nature, therefore no future work is recommended for wood conservation of museum objects, including the Oseberg artefacts. There may be some scope for its use as a water-resistant coating for artefacts kept outside (some boats, for example). However, the degree of substitution would require further investigatation to see if it is possible to control the degree of substitution to allow for it to be soluble in a less toxic solvent. A non-toxic, or less toxic, solvent will be required to treat outside artefacts that are too large for a fume hood; it may be possible to use a portal extractor hood to reduce exposure to fumes. The superhydrophic properties of the TBDMS may help to reduce penetration of water and hence help conserve artefacts, although a full investigation into its use for that purpose would need to be carried out, which was not the aim of this study. Returning to the Oseberg artefacts, the existing consolidants B72 and B98 did give good results, the only issue preventing their recommendation is their stability under acid conditions. Therefore,

future work should investigate their stability under acid conditions and also investigate if they can be used alongside alkali nanoparticles such as nanoparticles of sodium hydroxide (currently being investigated by the Saving Oseberg group). This could be done as a two-step treatment, or as a combined treatment potentially, but this needs investigating. Alternatively, if this proves unsuccessful and no alternative is found, B72 could be used as a pre-consolidant; the wood could be treated with B72 and the alum and acid subsequently washed out and, if necessary, further treated with PEG, however this poses more risk to the artefacts. Hence a combined treatment of B72 or B98 with nanoparticles would be preferable. B98 being more stable would be anticipated to be favourable in terms of a combined treatment.

8.7 Overall conclusion

Chitosan with a $M_{w,app}$ of 5-6 kDa appears to be of suitable molecular weight to penetrate into the wood. Despite the mass increase of the silylated version, TBDMS chitosan, with a similar length backbone to the original chitosan, was observed through EDS-SEM in the centre of the wood. The percentage weight increase observed on chitosan treatment, along with the TBSMS chitosan results, suggests chitosan in aqueous treatment also penetrated the wood. However, the choice of solvent may have resulted in variation in uptake. Elemental analysis is required to confirm chitosan is present in the centre of the wood as from the SEM it is not visible, probably due to hydrogen bonding to the cell wall making it indistinguishable from the cell wall on the SEM. Chitosan acetate gave very poor consolidation results. Self-associating aminocellulose HEA gave good consolidation results with very high ASE and good consolidation observed through a tape test on the surface of the wood. HEA and PEG

also gave very good results. Both HEA alone and HEA and PEG together appear promising as an alternative to PEG alone. However, long-term stability and acid stability need to be fully assessed before these can be applied to artefacts. A larger sample size of test wood and larger pieces would also ideally be tested prior to HEA use as a consolidant on artefacts. Results from this investigation are very promising, the only concern being long-term stability, as an amine smell was noticed when treating some of the wood.

Non-aqueous treatment experiments ruled out the use of TBDMS chitosan, unless combined with another polymer, as the TBDMS chitosan alone is brittle. B72 and B98 are promising alternatives, B72 as a pre-consolidant for immersion of artefacts to consolidate them prior to alum removal and, if required, further consolidation with an aqueous method. Alternatively, B72 and B98 could be researched in combination with nanoparticles to increase the pH. B98 appears to give good results as an injection treatment. More research is required to test a larger batch of samples with larger pieces prior to treatment of artefacts and long-term acid stability requires assessment. The Oseberg artefacts are in dire need of conservation and the large range of variability and stability of artefacts means multiple treatment options are required. At least one consolidant must be water-soluble and another must be non-aqueous treatment. HEA is a suitable aqueous method where PEG cannot be used; B98 and B72 are options for when the alum cannot be removed and a non-aqueous method is required.

References

Afifi, H., Hamed, S.A.E.-K.M., Mohamedy, S., and Dawod, M. (2019). A dating approach of a refundable wooden Egyptian coffin lid. Sci. Cult. *5*, 15–22.

Agresti, G., Bonifazi, G., Calienno, L., Capobianco, G., Lo Monaco, A., Pelosi, C., Picchio, R., and Serranti, S. (2013). Surface Investigation of Photo-Degraded Wood by Colour Monitoring, Infrared Spectroscopy, and Hyperspectral Imaging.

Aguilar, R., Torrealva, D., Moreira, S., Pando, M.A., and Ramos, L.F. (2018). Structural Analysis of Historical Constructions: An Interdisciplinary Approach (Springer).

Alder, C.M., Hayler, J.D., Henderson, R.K., Redman, A.M., Shukla, L., Shuster, L.E., and Sneddon, H.F. (2016). Updating and further expanding GSK's solvent sustainability guide. Green Chem. *18*, 3879–3890.

Almkvist, G., and Persson, I. (2008). Analysis of acids and degradation products related to iron and sulfur in the Swedish warship Vasa. Holzforschung *62*, 694–703.

Alonso, E., Sherman, A.M., Wallington, T.J., Everson, M.P., Field, F.R., Roth, R., and Kirchain, R.E. (2012). Evaluating Rare Earth Element Availability: A Case with Revolutionary Demand from Clean Technologies. Environ. Sci. Technol. *46*, 3406–3414.

Amberger, M.L. (2019). Archaeological finds - Museum of Cultural History.

Andriulo, F., Giorgi, R., Steindal, C.C., Kutzke, H., Braovac, S., and Baglioni, P. (2017). Hybrid nanocomposites made of diol-modified silanes and nanostructured calcium hydroxide. Applications to Alum-treated wood. Pure Appl. Chem. *89*, 29–39.

Andriulo, F., Giorgi, R., and Steindal, C.C. (2018). Nanotechnonologies for the restoration of alum-treated archaeological wood. In Proceedings of the 13th ICOM-CC Group on Wet Organic Archaeological Materials Conference, Florence 2016, (ICOM), p.

Appelbaum, B. (1987). Criteria for Treatment: Reversibility. J. Am. Inst. Conserv. *26*, 65–73.

Arslanoglu, J. (2003). Evaluation of the Use of Aquazol as an Adhesive in Paintings Conservation. WAAC Newsl. *25*, 12–18.

Arslanoglu, J. (2004). Aquazol as used in conservation practice. West. Assoc. Art Conserv. WAAC *26*.

Atkinson, J.K. (2014). Environmental conditions for the safeguarding of collections: A background to the current debate on the control of relative humidity and temperature. Stud. Conserv. *59*, 205–212.

Aufderheide, A.C. (2009). Reflections about bizarre mummification practices on mummies at Egypt's Dakhleh oasis: a review. Anthropol. Anz. Ber. Uber Biol.-Anthropol. Lit. *67*, 385–390.

Babiński, L. (2007). Influence of pre-treatment on shrinkage of freeze-dried archaeological pine-wood. Folia For. Pol. Ser. B *38*, 3–12.

Babiński, L. (2015). Dimensional changes of waterlogged archaeological hardwoods pre-treated with aqueous mixtures of lactitol/trehalose and mannitol/trehalose before freeze-drying. J. Cult. Herit. *16*, 876–882.

Baig, N.R.B., and Varma, R.S. (2013). Copper on chitosan : a recyclable heterogeneous catalyst for azide– alkyne cycloaddition reactions in water. Green Chem. *15*, 1839–1843.

Ball, P. (2007). The click concept. RSC Chem. World 46–51.

Barclay, L.R.C., Xi, F., and Norris, J.Q. (1997). Antioxidant Properties of Phenolic Lignin Model Compounds. J. Wood Chem. Technol. *17*, 73–90.

Barner-Kowollik, C., Du Prez, F.E., Espeel, P., Hawker, C.J., Junkers, T., Schlaad, H., and Van Camp, W. (2011). "Clicking" Polymers or Just Efficient Linking: What Is the Difference? Angew. Chem. Int. Ed. *50*, 60–62.

Barral, K., Moorhouse, A.D., and Moses, J.E. (2007). Efficient conversion of aromatic amines into azides: a one-pot synthesis of triazole linkages. Org. Lett. *9*, 1809–1811.

Bell, L.S. (2012). Forensic Microscopy for Skeletal Tissues: Methods and Protocols (Humana Press).

Bell, L.S. (2012). Forensic Microscopy for Skeletal Tissues: Methods and Protocols (Humana Press).

Berkowitz, S.A., and Philo, J.S. (2015). Chapter 9 - Characterizing Biopharmaceuticals using Analytical Ultracentrifugation. In Biophysical Characterization of Proteins in Developing Biopharmaceuticals. Ed., D.J. Houde, and S.A. Berkowitz, eds. (Amsterdam: Elsevier), pp. 211–260.

Bicchieri, M., and Mucci, B. (2009). Hydroxypropyl Cellulose and Polyvinyl Alcohol on Paper as Fixatives for Pigments and Dyes. Restaurator *17*, 238–251.

Björdal, C.G. (2012). Microbial degradation of waterlogged archaeological wood. J. Cult. Herit. *13*, S118–S122.

Björdal, C.G., Nilsson, T., and Daniel, G. (1999). Microbial decay of waterlogged archaeological wood found in Sweden Applicable to archaeology and conservation. Int. Biodeterior. Biodegrad. *43*, 63–73.

Blades, N., Oreszczyn, T., Cassar, M., and Bordass, W. (2000). Guidelines on Pollution Control in Museum Buildings. In In: Martin, D, (Ed.) UNSPECIFIED Museums Association: London. (2000), D. Martin, ed. (London: Museums Association), p.

Blaeuer, C., Verges-Belmin, V., and Franzen, C. (2013). Simple field tests in stone conservation. (New York), p.

Blanchette, R.A., Haight, J.E., Koestler, R.J., Hatchfield, P.B., and Arnold, D. (1994). Assessment of Deterioration in Archaeological Wood from Ancient Egypt. J. Am. Inst. Conserv. *33*, 55–70.

Boukraa, L., and Sulaiman, S.A. (2009). Rediscovering the Antibiotics of the Hive.

Bradley, S. (1984). Strength testing of adhesives and consolidants for conservation purposes. Stud. Conserv. *29*, 22–25.

Brajer, I. (2009). Taking the wrong path: learning from oversights, misconceptions, failures and mistakes in conservation. Examples from wall painting conservation in Denmark. CeROArt Conserv. Expo. Restaur. D'Objets D'Art.

Braovac, S. (2015). Alum-treated wood, material characterisation, a case study of the Oseberg finds. Thesis. The Royal Danish Academy of Fine Arts.

Braovac, S. (2018). Annual Report. Deliverable 3.7: Standard degraded wood samples (Oslo: University of Oslo, Museum of Cultural History.).

Braovac, S., and Dahl, M.I. (2015). Saving Oseberg 2013-2015.

Braovac, S., and Kutzke, H. (2012). The presence of sulfuric acid in alum-conserved wood – Origin and consequences. J. Cult. Herit. *13*, S203–S208.

Braovac, S., and Sahlstedt, M. (2019). Personal correspondance.

Braovac, S., McQueen, C.M.A., Sahlstedt, M., Kutzke, H., Łucejko, J.J., and Klokkernes, T. (2018a). Navigating conservation strategies: Linking material research on alum-treated wood from the Oseberg collection to conservation decisions. Herit. Sci. *6*.

Braovac, S., McQueen, C.M.A., Sahlstedt, M., Kutzke, H., Łucejko, J.J., and Klokkernes, T. (2018b). Navigating conservation strategies: linking material research on alum-treated wood from the Oseberg collection to conservation decisions. Herit. Sci. *6*, 77.

Brock, F., Dee, M., Hughes, A., Snoeck, C., Staff, R., and Ramsey, C.B. (2018). Testing the effectiveness of protocols for removal of common conservation treatments for radiocarbon dating. Radiocarbon *60*, 35–50.

Broda, M. (2018). Biological effectiveness of archaeological oak wood treated with methyltrimethoxysilane and PEG against Brown-rot fungi and moulds. Int. Biodeterior. Biodegrad. *134*, 110–116.

Broda, M., Majka, J., Olek, W., and Mazela, B. (2018). Dimensional stability and hygroscopic properties of waterlogged archaeological wood treated with alkoxysilanes. Int. Biodeterior. Biodegrad. *133*, 34–41.

Bronitsky, G. (1986). The Use of Materials Science Techniques in the Study of Pottery Construction and Use. Adv. Archaeol. Method Theory *9*, 209–276.

Brown, P.H., Balbo, A., Zhao, H., Ebel, C., and Schuck, P. (2011). Density Contrast Sedimentation Velocity for the Determination of Protein Partial-Specific Volumes. PLoS ONE *6*.

Buda, A.-M., and Sandu, I. (2015). Monitoring Of Pollutants In Museum Environment. Gruyter *9*, 173–180.

Bugani, S., Colombini, M.P., Giachi, G., Modugno, F., and Morselli, L. (2008). Evaluation of Conservation Treatments for Archaeological Waterlogged Wooden Artefacts. In 9th International Conference on NDT of Art, (Jerusalem Israel), p. 6.

Bugani, S., Modugno, F., Lucejko, J., Giachi, G., Cagno, S., Cloetens, P., Janssens, K., and Morselli, L. (2009). Study on the impregnation of archaeological waterlogged wood with consolidation treatments using synchrotron radiation microtomography. Anal. Bioanal. Chem. *395*, 1977–1985.

Bulwan, M., Wójcik, K., Zapotoczny, S., and Nowakowska, M. (2012). Chitosan-Based Ultrathin Films as Antifouling, Anticoagulant and Antibacterial Protective Coatings. J. Biomater. Sci. Polym. Ed. *23*, 1963–1980.

Burke, A., Yilmaz, E., Hasirci, N., and Yilmaz, O. (2002). Iron(III) ion removal from solution through adsorption on chitosan. J. Appl. Polym. Sci. *84*, 1185–1192.

Byrne, F.P., Jin, S., Paggiola, G., Petchey, T.H.M., Clark, J.H., Farmer, T.J., Hunt, A.J., McElroy, C.R., and Sherwood, J. (2016). Tools and techniques for solvent selection: green solvent selection guides. Sustain. Chem. Process. *4*, 7.

Calienno, L., Pelosi, C., Picchio, R., Agresti, G., Santamaria, U., Balletti, F., and Monaco, A.L. (2015). Light-induced color changes and chemical modification of treated and untreated chestnut wood surface. Stud. Conserv. *60*, 131–139.

Can, A., and Sivrikaya, H. (2016). Dimensional stabilization of wood treated with tall oil dissolved in different solvents. Maderas Cienc. Tecnol. *18*.

Cappitelli, F., and Sorlini, C. (2005). From Papyrus to Compact Disc: The Microbial Deterioration of Documentary Heritage. Crit. Rev. Microbiol. *31*, 1–10.

Cappitelli, F., and Sorlini, C. (2008). Microorganisms Attack Synthetic Polymers in Items Representing Our Cultural Heritage. Appl. Environ. Microbiol. *74*, 564–569.

Cappitelli, F., Zanardini, E., and Sorlini, C. (2004). The Biodeterioration of Synthetic Resins Used in Conservation. Macromol. Biosci. *4*, 399–406.

Carretti, E., Chelazzi, D., Rocchigiani, G., Baglioni, P., Poggi, G., and Dei, L. (2013). Interactions between Nanostructured Calcium Hydroxide and Acrylate Copolymers: Implications in Cultural Heritage Conservation. Langmuir *29*, 9881–9890.

Cassar, M. (2013). Environmental Management: Guidelines for Museums and Galleries (Routledge).

Cesar, T., Danevčič, T., Kavkler, K., and Stopar, D. (2017). Melamine polymerization in organic solutions and waterlogged archaeological wood studied by FTIR spectroscopy. J. Cult. Herit. *23*, 106–110.

Chafe, D.S.C. (1993). The effect of boiling on shrinkage, collapse and other wood-water properties in core segments of Eucalyptus regnans F. Muell. Wood Sci. Technol. *27*, 205–217.

Chapman, S., and Mason, D. (2003). Literature Review: The Use of Paraloid B-72 as a Surface Consolidant for Stained Glass. J. Am. Inst. Conserv. *42*, 381–392.

Christensen, M. (2013). Developing new consolidants for archaeological wood. Thesis. University of Oslo.

Christensen, M., Kutzke, H., and Hansen, F.K. (2012). New materials used for the consolidation of archaeological wood–past attempts, present struggles, and future requirements. J. Cult. Herit. *13*, S183–S190.

Christensen, M., Larnøy, E., Kutzke, H., and Hansen, F.K. (2015a). Treatment of waterlogged archaeological wood using chitosan- and modified chitosan solutions. Part 1: Chemical compatibility and microstructure. J. Am. Inst. Conserv. *54*, 3–13.

Christensen, M., Larnøy, E., Kutzke, H., and Hansen, F.K. (2015b). Treatment of Waterlogged Archaeological Wood Using Chitosan- and Modified Chitosan Solutions. Part 1: Chemical Compatibility and Microstructure. J. Am. Inst. Conserv. *54*, 3–13.

Chtchigrovsky, M., Primo, A., Gonzalez, P., Molvinger, K., Robitzer, M., Quignard, F., and Taran, F. (2009). Functionalized Chitosan as a Green, Recyclable, Biopolymer-Supported Catalyst for the [3+2] Huisgen Cycloaddition. Angew. Chem. *121*, 6030–6034.

Ciferri, O. (2002). The role of microorganisms in the degradation of cultural heritage. Stud. Conserv. *47*, 35–45.

Cipriani, G., Salvini, A., Baglioni, P., and Bucciarelli, E. (2010). Cellulose as a renewable resource for the synthesis of wood consolidants. J. Appl. Polym. Sci. *118*, 2939–2950.

Clausi, M., Crisci, G.M., La Russa, M.F., Malagodi, M., Palermo, A., and Ruffolo, S.A. (2011). Protective action against fungal growth of two consolidating products applied to wood. J. Cult. Herit. *12*, 28–33.

Cole, J.L., Lary, J.W., P Moody, T., and Laue, T.M. (2008). Analytical ultracentrifugation: sedimentation velocity and sedimentation equilibrium. Methods Cell Biol. *84*, 143–179.

Collis, S. (2015). Revisiting Conservation Treatment Methodologies for Waterlogged Archaeological Wood: An Australian Study. AICCM Bull. *36*, 88–96.

Constâncio, C., Franco, L., Russo, A., Anjinho, C., Pires, J., Vaz, M.F., and Carvalho, A.P. (2010). Studies on polymeric conservation treatments of ceramic tiles with Paraloid B-72 and two alkoxysilanes. J. Appl. Polym. Sci. *116*, 2833–2839.

Creeth, J.M., and Harding, S.H. (1982). Some observations on a new type of point average molecular weight. J. Biochem. Biophys. Methods *7*, 25–34.

Crisci, G.M., La Russa, M.F., Malagodi, M., and Ruffolo, S.A. (2010). Consolidating properties of Regalrez 1126 and Paraloid B72 applied to wood. J. Cult. Herit. *11*, 304–308.

Croisier, F., and Jérôme, C. (2013). Chitosan-based biomaterials for tissue engineering. Eur. Polym. J. *49*, 780–792.

Dam, J., and Schuck, P. (2004). Calculating Sedimentation Coefficient Distributions by Direct Modeling of Sedimentation Velocity Concentration Profiles. In Methods in Enzymology, (Academic Press), pp. 185–212.

Dardes, K., and Rothe, A. (1998). The Structural Conservation of Panel Paintings: Proceedings of a Symposium at the J. Paul Getty Museum, 24–28 April 1995 (Getty Publications).

David, A.R. (2001). Benefits and disadvantages of some conservation treatments for egyptian mummies. Chungara Rev. Antropol. Chil. *33*, 113–115.

David, R. (2008). Egyptian Mummies and Modern Science (Cambridge University Press).

Dodson, J.R., Hunt, A.J., Parker, H.L., Yang, Y., and Clark, J.H. (2012). Elemental sustainability: Towards the total recovery of scarce metals. Chem. Eng. Process. Process Intensif. *51*, 69–78.

Dodson, J.R., Parker, H.L., García, A.M., Hicken, A., Asemave, K., Farmer, T.J., He, H., Clark, J.H., and Hunt, A.J. (2015). Bio-derived materials as a green route for precious & critical metal recovery and re-use. Green Chem. *17*, 1951–1965.

Dong, J., Krasnova, L., Finn, M.G., and Sharpless, K.B. (2014a). Sulfur(VI) fluoride exchange (SuFEx): another good reaction for click chemistry. Angew. Chem. Int. Ed Engl. *53*, 9430–9448.

Dong, J., Krasnova, L., Finn, M.G., and Sharpless, K.B. (2014b). Sulfur(VI) fluoride exchange (SuFEx): another good reaction for click chemistry. Angew. Chem. Int. Ed Engl. *53*, 9430–9448.

Drdácký, M., and Slížková, Z. (2013). Enhanced affordable methods for assessing material characteristics and consolidation effects on stone and mortar. J. Geophys. Eng. *10*.

Drdácký, M., and Slížková, Z. (2015). In situ peeling tests for assessing the cohesion and consolidation characteristics of historic plaster and render surfaces. Stud. Conserv. *60*, 121–130.

Drdácký, M., Lesák, J., Rescic, S., Slížková, Z., Tiano, P., and Valach, J. (2012). Standardization of peeling tests for assessing the cohesion and consolidation characteristics of historic stone surfaces. Mater. Struct. *45*, 505–520.

Ebert, B., Singer, B., and Grimaldi, N. (2012). Aquazol as a consolidant for matte paint on Vietnamese paintings. J. Inst. Conserv. *35*, 62–76.

Eikenberry, E.F. (1982). Sedimentation theory: A more rigorous approach. In Centrifugation in Density Gradients. Ed. Price C.A., (New York: Academic Press), p. p 86.

Eikenes, M., Alfredsen, G., Christensen, B.E., Militz, H., and Solheim, H. (2005). Comparison of chitosans with different molecular weights as possible wood preservatives. J. Wood Sci. *51*, 387–394.

Ellanki, A.R., Islam, A., Rama, V.S., Pulipati, R.P., Rambabu, D., Rama Krishna, G., Malla Reddy, C., Mukkanti, K., Vanaja, G.R., Kalle, A.M., et al. (2012). Solvent effect on copper-catalyzed azide–alkyne cycloaddition (CuAAC): Synthesis of novel triazolyl substituted quinolines as potential anticancer agents. Bioorg. Med. Chem. Lett. *22*, 3455–3459.

Endo, R., Kamei, K., Iida, I., Yokoyama, M., and Kawahara, Y. (2010). Physical and mechanical properties of waterlogged wood treated with hydrolyzed feather keratin. J. Archaeol. Sci. *37*, 1311–1316.

Favaro, M., Mendichi, R., Ossola, F., Russo, U., Simon, S., Tomasin, P., and Vigato, P.A. (2006). Evaluation of polymers for conservation treatments of outdoor exposed stone monuments. Part I: Photo-oxidative weathering. Polym. Degrad. Stab. *91*, 3083–3096.

Feller, R.L., and Wilt, M. (1990). Evaluation of Cellulose Ethers for Conservation (Getty Conservation Institute).

Fellowes, D., and Hagan, P. (2003). Pyrite oxidation: the conservation of historic shipwrecks and geological and palaeontological specimens. Stud. Conserv. *48*, 26–38.

Fors, Y., and Richards, V. (2010). The Effects of the Ammonia Neutralizing Treatment on Marine Archaeological Vasa Wood. Stud. Conserv. *55*.

Fors, Y., and Sandström, M. (2006). Sulfur and iron in shipwrecks cause conservation concerns. Chem. Soc. Rev. *35*, 399–415.

Francesko, A., Fernandes, M.M., Ivanova, K., Amorim, S., Reis, R.L., Pashkuleva, I., Mendoza, E., Pfeifer, A., Heinze, T., and Tzanov, T. (2016). Bacteria-responsive multilayer coatings comprising polycationic nanospheres for bacteria biofilm prevention on urinary catheters. Acta Biomater. *33*, 203–212.

Fulcher, K. (2014). The diverse use of AJK dough in conservation. J. Inst. Conserv. *37*, 32–42.

Ganske, K., Wiegand, C., Hipler, U.-C., and Heinze, T. (2016). Synthesis of Novel Cellulose Carbamates Possessing Terminal Amino Groups and Their Bioactivity. Macromol. Biosci. *16*, 451–461.

Giachi, G., Capretti, C., Macchioni, N., Pizzo, B., and Donato, I.D. (2010). A methodological approach in the evaluation of the efficacy of treatments for the dimensional stabilisation of waterlogged archaeological wood. J. Cult. Herit. *11*, 91–101.

Giachi, G., Capretti, C., Donato, I.D., Macchioni, N., and Pizzo, B. (2011). New trials in the consolidation of waterlogged archaeological wood with different acetone-carried products. J. Archaeol. Sci. *38*, 2957–2967.

Gillis, R.B. (2014). Protein polysacchride complexes permanent/non-permanent interactions between polysacchrides and polypeptides. University of Nottingham.

Gillis, R.B., Adams, G.G., Heinze, T., Nikolajski, M., Harding, S.E., and Rowe, A.J. (2013a). MultiSig: a new high-precision approach to the analysis of complex biomolecular systems. Eur. Biophys. J. *42*, 777–786.

Gillis, R.B., Adams, G.G., Heinze, T., Nikolajski, M., Harding, S.E., and Rowe, A.J. (2013b). MultiSig: a new high-precision approach to the analysis of complex biomolecular systems. Eur. Biophys. J. *42*, 777–786.

Giorgi, R., Chelazzi, D., and Baglioni, P. (2005). Nanoparticles of Calcium Hydroxide for Wood Conservation. The Deacidification of the Vasa Warship. Langmuir *21*, 10743–10748.

Grattan, D.W. (1982). A Practical Comparative Study of Several Treatments for Waterlogged Wood. Stud. Conserv. *27*, 124–136.

Grattan, D.W., McCawley, J.C., and Cook, C. (1980). The Potential of the Canadian Winter Climate for the Freeze-Drying of Degraded Waterlogged Wood: Part II. Stud. Conserv. *25*, 118–136.

Green, D.W. (2005). Mechanical Grading of 6-inch-diameter Lodgepole Pine Logs for the Traveler's Rest and Rattlesnake Creek Bridges (U.S. Department of Agriculture, Forest Service, Forest Products Laboratory).

Gregory, D., Jensen, P., Matthiesen, H., and Strætkvern, K. (2007). The Correlation between Bulk Density and Shock Resistance of Waterlogged Archaeological Wood Using the Pilodyn. Stud. Conserv. *52*, 289–298.

Grzywacz, cecily M. (2006). Monitoring for Gaseous Pollutants in Museum Environments (Los Angeles, CA: Getty Conservation Institute).

Guibal, E. (2004). Interactions of metal ions with chitosan-based sorbents: a review. Sep. Purif. Technol. *38*, 43–74.

Guilminot, E., Dalard, F., and Degrigny, C. (2002). Mechanism of iron corrosion in water–polyethylene glycol (PEG 400) mixtures. Corros. Sci. *44*, 2199–2208.

Häggström, C., and Sandström, T. (2013). Alum-treated archaeological wood : characterization and re-conservation (Sweden: Riksantikvarieämbetet).

Hamed, S. a. M., Ali, M., and Hadidi, N.M.E. (2012). Using SEM in monitoring changes in archaeological wood: A review. Curr. Microsc. Contrib. Adv. Sci. Technol.

Hamilton, D. (1999). Methods for Conserving Archaeological Material from Underwater Sites (Conservation Files: ANTH 605, Conservation of Cultural Resources I. Nautical Archaeology Program, Texas A&M University).

Hamilton, D. (2010). Methods of Conserving Archaeological Material from Underwater Sites (Nautical Archaeology Program Department of Anthropology).

Hamilton, D.L. (1975). Overview of conservation in archaeology; basic archaeological conservation procedures - Conservation Manual - Conservation Research Laboratory - Center for Maritime Archaeology and Conservation - Texas A&M University.

Hammill, S. (2016). Technical: Kintsugi. J. Aust. Ceram. *55*, 70.

Harding, S.E. (2005a). Challenges for the modern analytical ultracentrifuge analysis of polysaccharides. Carbohydr. Res. *340*, 811–826.

Harding, S.E. (2005b). Analysis of Polysaccharides by Ultracentrifugation. Size, Conformation and Interactions in Solution. In Polysaccharides I, T. Heinze, ed. (Springer Berlin Heidelberg), pp. 211–254.

Harding, S.E. (2005c). Challenges for the modern analytical ultracentrifuge analysis of polysaccharides. Carbohydr. Res. *340*, 811–826.

Harding, S.E. (2012). Viscometry, analytical ultracentrifugation and light scattering probes for carbohydrate stability. In Stability of Complex Carbohydrate Structures: Biofuels, Foods, Vaccines and Shipwrecks, (Royal Society of Chemistry), pp. 80–98.

Harding, StephenE. (1994). Determination of Macromolecular Homogeneity, Shape, and Interactions Using Sedimentation Velocity Analytical Ultracentrifugation. In Microscopy, Optical Spectroscopy, and Macroscopic Techniques, C. Jones, B. Mulloy, and AdrianH. Thomas, eds. (Humana Press), pp. 61–73.

Harding, S.E., Schuck, P., Abdelhameed, A.S., Adams, G., Kök, M.S., and Morris, G.A. (2011a). Extended Fujita approach to the molecular weight distribution of polysaccharides and other polymeric systems. Methods San Diego Calif *54*, 136–144.

Harding, S.E., Schuck, P., Abdelhameed, A.S., Adams, G., Kök, M.S., and Morris, G.A. (2011b). Extended Fujita Approach to the Molecular Weight Distribution of Polysaccharides and other Polymeric Systems. Methods San Diego Calif *54*, 136–144.

Harding, S.E., Adams, G.G., Almutairi, F., Alzahrani, Q., Erten, T., Samil Kök, M., and Gillis, R.B. (2015). Chapter Eighteen - Ultracentrifuge Methods for the Analysis of Polysaccharides, Glycoconjugates, and Lignins. In Methods in Enzymology, J.L. Cole, ed. (Academic Press), pp. 391–439.

Harding, S.E., Gillis, R.B., and Adams, G.G. (2016). Assessing sedimentation equilibrium profiles in analytical ultracentrifugation experiments on macromolecules: from simple average molecular weight analysis to molecular weight distribution and interaction analysis. Biophys. Rev. *8*, 299–308.

Harrison, A. (2008). The Effects of Butvar B-98 on Bronze. In ANAGPIC Student Conference Papers, p.

Harrison, A.C. (2009). A Study of Butvar and its Effects on Bronze. WAAC Newsl. *31*, 4.

Haseneder, R., Fdez-Navamuel, B., and Härtel, G. (2007). Degradation of polyethylene glycol by Fenton reaction: a comparative study. Water Sci. Technol. J. Int. Assoc. Water Pollut. Res. *55*, 83–87.

Hatchfield, P.B. (2002). Pollutants in the Museum Environment: Practical Strategies for Problem Solving in Design, Exhibition and Storage (London: Archetype Publications Ltd).

Hearn, E.J. (1997). Chapter 1 - Simple stress and strain. In Mechanics of Materials 1 (Third Edition), E.J. Hearn, ed. (Oxford: Butterworth-Heinemann), pp. 1–26.

Hein, R.G., and Brancheriau, L. (2018). Comparison between three-point and four-point flexural tests to determine wood strength of eucalyptus specimens. Maderas Cienc. Tecnol. *20*, 333–342.

Hein, C.D., Liu, X.-M., and Wang, D. (2008). Click chemistry, a powerful tool for pharmaceutical sciences. Pharm. Res. *25*, 2216–2230.

Heinze, T. (2019). Personal correspondance.

Heinze, T., Pfeifer, A., and Petzold, K. (2007). Functionalization pattern of tert-butyldimethyl-silyl cellulose evaluated by NMR spectroscopy. BioResources *3*, 79–90.

Heinze, T., Nikolajski, M., Daus, S., Besong, T.M.D., Michaelis, N., Berlin, P., Morris, G.A., Rowe, A.J., and Harding, S.E. (2011). Protein-like Oligomerization of Carbohydrates. Angew. Chem. Int. Ed. *50*, 8602–8604.

Heinze, T., Siebert, M., Berlin, P., and Koschella, A. (2016). Biofunctional Materials Based on Amino Cellulose Derivatives--A Nanobiotechnological Concept. Macromol. Biosci. *16*, 10–42.

Hernández-Ledesma, B., and Herrero, M. (2013). Bioactive Compounds from Marine Foods: Plant and Animal Sources (John Wiley & Sons).

Heux, L., Brugnerotto, J., Desbrières, J., Versali, M.-F., and Rinaudo, M. (2000). Solid State NMR for Determination of Degree of Acetylation of Chitin and Chitosan. Biomacromolecules *1*, 746–751.

Hocker, E., Almkvist, G., and Sahlstedt, M. (2012). The Vasa experience with polyethylene glycol: A conservator's perspective. J. Cult. Herit. *13*, S175–S182.

Hoffmann, P., and Jones, M.A. (1989). Structure and Degradation Process for Waterlogged Archaeological Wood. In Archaeological Wood, (American Chemical Society), pp. 35–65.

Hollenberg, G.W., Terwilliger, G.R., and Gordon, R.S. (1971). Calculation of Stresses and Strains in Four-Point Bending Creep Tests. J. Am. Ceram. Soc. *54*, 196–199.

Holme, H.K., Davidsen, L., Kristiansen, A., and Smidsrød, O. (2008). Kinetics and mechanisms of depolymerization of alginate and chitosan in aqueous solution. Carbohydr. Polym. *73*, 656–664.

Huijbregts, Z., Martens, M., Conen, K., Nugent, I., Schijndel, I., and Schellen, H.S. (2012). Damage risk assessment of museum objects in historic buildings due to shifting climate zones in Europe. p.

Hvilsted, S., and Mortensen, M.N. (2010). Formic Acid as a Marker for Polyethylene Glycol Degradation in Conserved Archeological Wood - a Radiocarbon Study. In International Conference on Wet Organic Archaeological Materials ICOM-WOAM - East Carolina University, Greenville, North Caroline, USA, (East Carolina University, Greenville, North Caroline, USA), p.

Ifuku, S., Miwa, T., Morimoto, M., and Saimoto, H. (2011a). Preparation of highly chemoselective N-phthaloyl chitosan in aqueous media. Green Chem. *13*, 1499–1502.

Ifuku, S., Wada, M., Morimoto, M., and Saimoto, H. (2011b). Preparation of highly regioselective chitosan derivatives via “click chemistry.” Carbohydr. Polym. *85*, 653–657.

Imazu, S., Morgós, A., Ito, K., Ailawa, T., István, S., Editor: Williams, E., and Editor: Hocker, E. (2018). A post-treatment assessment of wood-iron composites from the remains of the mongol fleet from 1281. In Proceedings of the 13th ICOM-CC Group on Wet Organic Archaeological Materials Conference, (Florence 2016: ICOM), p.

Jatunov, S., Franconetti, M., Gómez-Guillén, M., and Cabrera-Escribano, F. (2012). Design of Aromatic Aldehyde Chitosan Derivatives for biological and Industrial Applications. In Conference Hall D. Polymer and Supramolecular Chemistry, p.

Jeong, Y., Lee, J., and Ryu, J.-S. (2016). Design, synthesis, and evaluation of hinge-binder tethered 1,2,3-triazolylsalicylamide derivatives as Aurora kinase inhibitors. Bioorg. Med. Chem. *24*, 2114–2124.

Jeremic, D., Cooper, P., and Brodersen, P. (2007). Penetration of poly(ethylene glycol) into wood cell walls of red pine. Holzforschung *61*, 272–278.

Jespersen, K. (1981). Conservation of waterlogged wood by use of tertiary butanol, peg and freeze-drying. In Conservation of Waterlogged Wood. International Symposium on the Conservation of Large Objects of Waterlogged Wood, Amsterdam, 24-28 Sept. 1979, (Amsterdam: International symposium on the conservation of large objects of waterlogged wood), pp. 69–76.

Johnson, J.S. (1994a). Consolidation of Archaeological Bone: A Conservation Perspective. J. Field Archaeol. *21*, 221–233.

Johnson, J.S. (1994b). Consolidation of Archaeological Bone: A Conservation Perspective. J. Field Archaeol. *21*, 221–233.

Johnston-Feller, R. (2002). Color science in the examination of museum objects: Nondestructive procedures. Color Res. Appl. *27*, 456–457.

Jones, D.M. (2010). Waterlogged Wood: Guidelines on the recording, sampling, conservation and curation of waterlogged wood. Engl. Herit. Publ.

Jung, A., and Berlin, P. (2005). New water-soluble and film-forming aminocellulose tosylates as enzyme support matrices with Cu2+-chelating properties. Cellulose *12*, 67–84.

Jung, A., Wolters, B., and Berlin, P. (2007). (Bio)functional surface structural design of substrate materials based on self-assembled monolayers from aminocellulose derivatives and amino(organo)polysiloxanes. Thin Solid Films *515*, 6867–6877.

Kaye, B. (1995). Conservation of Waterlogged Archaeological Wood. 35–43.

Keeble, B.R. (1988). The Brundtland report: 'Our common future.' Med. War *4*, 17–25.

Kennedy, A., and Pennington, E.R. (2014). Conservation of chemically degraded waterlogged wood with sugars. Stud. Conserv. *59*, 194–201.

Khan, A., Badshah, S., and Airoldi, C. (2014). Environmentally benign modified biodegradable chitosan for cation removal. Polym. Bull. *72*, 353–370.

Kim, S.-K. (2013). Chitin and Chitosan Derivatives: Advances in Drug Discovery and Developments (CRC Press).

Kim, S.-K., and Rajapakse, N. (2005). Enzymatic production and biological activities of chitosan oligosaccharides (COS): A review. Carbohydr. Polym. *62*, 357–368.

Kitamura, M., Kato, S., Yano, M., Tashiro, N., Shiratake, Y., Sando, M., and Okauchi, T. (2014). A reagent for safe and efficient diazo-transfer to primary amines: 2-azido-1,3-dimethylimidazolinium hexafluorophosphate. Org. Biomol. Chem. *12*, 4397–4406.

Kjøniksen, A.-L., Nyström, B., Iversen, C., Nakken, T., Palmgren, O., and Tande, T. (1997). Viscosity of Dilute Aqueous Solutions of Hydrophobically Modified Chitosan and Its Unmodified Analogue at Different Conditions of Salt and Surfactant Concentrations. Langmuir *13*, 4948–4952.

Klosowski, J.M., and Smith, C.W. (2003). Archaeological Conservation Using Polymers: Practical Applications for Organic Artifact Stabilization (College Station: Texas A & M University Press).

Kolb, H.C., and Sharpless, K.B. (2003). The growing impact of click chemistry on drug discovery. Drug Discov. Today *8*, 1128–1137.

Koob, S. (1998). Obsolete Fill Materials Found on Ceramics. J. Am. Inst. Conserv. *37*, 49–67.

Koob, S.P. (1986). The use of Paraloid B-72 as an adhesive: its application for archaeological ceramics and other materials. Stud. Conserv. *31*, 7–14.

Kratky, O., Leopold, H., and Stabinger, H. (1973). The determination of the partial specific volume of proteins by the mechanical oscillator technique. Methods Enzymol. *27*, 98–110.

Kučerová, I. (2012a). Methods to measure the penetration of consolidant solutions into 'dry' wood. J. Cult. Herit. *13*, S191–S195.

Kučerová, I. (2012b). Methods to measure the penetration of consolidant solutions into 'dry' wood. J. Cult. Herit. *13*, S191–S195.

Kulbokaite, R., Ciuta, G., Netopilik, M., and Makuska, R. (2009). N-PEG'ylation of chitosan via "click chemistry" reactions. React. Funct. Polym. *69*, 771–778.

Kumbar, S., Laurencin, C., and Deng, M. (2014). Natural and Synthetic Biomedical Polymers (Newnes).

Kurita, Y., and Isogai, A. (2010). Reductive N-alkylation of chitosan with acetone and levulinic acid in aqueous media. Int. J. Biol. Macromol. *47*, 184–189.

Kurita, K., Mori, S., Nishiyama, Y., and Harata, M. (2002). N-Alkylation of chitin and some characteristics of the novel derivatives. Polym. Bull. *48*, 159–166.

Kurita, K., Ikeda, H., Shimojoh, M., and Yang, J. (2007). N-Phthaloylated Chitosan as an Essential Precursor for Controlled Chemical Modifications of Chitosan: Synthesis and Evaluation. Polym. J. *39*, 945–952.

Kyushik, L., Jaeeun, Y., Hyeyoun, L., Inhee, G., Ikjoo, K., and Kungnip Munhwajae, Y. (2012). Conservation of wooden objects (National Research Institute of Cultural Heritage).

Larkin, N.R., and Makridou, E. (1999). Comparing gap-fillers used in conserving sub-fossil material. Geol. Curator *2*, 81–90.

Larnøy, E., Militz, H., and Eikenes, M. (2005). Uptake of chitosan based impregnation solutions with varying viscosities in four different European wood species. Holz Als Roh- Werkst. *63*, 456–462.

Larnøy, E., Eikenes, M., and Militz, H. (2006a). Evaluation of factors that have an influence on the fixation of chitosan in wood. Wood Mater. Sci. Eng. *1*, 138–145.

Larnøy, E., Dantz, S., Eikenes, M., and Holger, M. (2006b). Screening of properties of modified chitosan-treated wood. Wood Mater. Sci. Eng. *1*, 59–68.

Lechner, T., Bjurhager, I., and Kliger, R.I. (2013). Strategy for developing a future support system for the Vasa warship and evaluating its mechanical properties. Herit. Sci. *1*, 35.

Li, K., Xing, R., Liu, S., Qin, Y., Meng, X., and Li, P. (2012). Microwave-assisted degradation of chitosan for a possible use in inhibiting crop pathogenic fungi. Int. J. Biol. Macromol. *51*, 767–773.

Lionetto, F., and Frigione, M. (2012). Effect of novel consolidants on mechanical and absorption properties of deteriorated wood by insect attack. J. Cult. Herit. *13*, 195–203.

Ljaljević-Grbić, M., Stupar, M., Vukojević, J., Maričić, I., and Bungur, N. (2013). Molds in museum environments: Biodeterioration of art photographs and wooden sculptures. Arch. Biol. Sci. *65*, 955–962.

López-Polín, L. (2012a). Possible interferences of some conservation treatments with subsequent studies on fossil bones: A conservator's overview. Quat. Int. *275*, 120–127.

López-Polín, L. (2012b). Possible interferences of some conservation treatments with subsequent studies on fossil bones: A conservator's overview. Quat. Int. *275*, 120–127.

Lu, C., Zhou, Q., Yan, J., Du, Z., Huang, L., and Li, X. (2013). A novel series of tacrine-selegiline hybrids with cholinesterase and monoamine oxidase inhibition activities for the treatment of Alzheimer's disease. Eur. J. Med. Chem. *62*, 745–753.

Łucejko, J.J., La Nasa, J., McQueen, C.M.A., Braovac, S., Colombini, M.P., and Modugno, F. (2018). Protective effect of linseed oil varnish on archaeological wood treated with alum. Microchem. J. *139*, 50–61.

Macchioni, N., Pizzo, B., Capretti, C., and Giachi, G. (2012). How an integrated diagnostic approach can help in a correct evaluation of the state of preservation of waterlogged archaeological wooden artefacts. J. Archaeol. Sci. *39*, 3255–3263.

Madera-Santana, T.J., Herrera-Méndez, C.H., and Rodríguez-Núñez, J.R. (2018). An overview of the chemical modifications of chitosan and their advantages. Green Mater. *6*, 131–142.

Majka, J., Zborowska, M., Fejfer, M., Waliszewska, B., and Olek, W. (2018). Dimensional stability and hygroscopic properties of PEG treated irregularly degraded waterlogged Scots pine wood. J. Cult. Herit. *31*, 133–140.

Malik, J.M., Ozarska, B., and Santoso, A.P. (2018). Colour changes and morphological performance of impregnated jabon wood using polymerised merbau extractives. p.

Manchun, S., Dass, C.R., and Sriamornsak, P. (2012). Targeted therapy for cancer using pH-responsive nanocarrier systems. Life Sci. *90*, 381–387.

Mańkowski, P., Kozakiewicz, P., and Krzosek, S. (2015). Retention of polymer in lime wood impregnated with Paraloid B-72 solution in butyl acetate. Mater. Sci.

Mannhalter, C. (1993). Biocompatibility of artificial surfaces such as cellulose and related materials. Sens. Actuators B Chem. *11*, 273–279.

Mantanis, G.I., Young, R.A., and Rowell, R.M. (1994). Swelling of Wood. Part II. Swelling in Organic Liquids. Holzforschung *48*, 480–490.

Mao, S., Shuai, X., Unger, F., Simon, M., Bi, D., and Kissel, T. (2004). The depolymerization of chitosan: effects on physicochemical and biological properties. Int. J. Pharm. *281*, 45–54.

Matsuo, M., Yokoyama, M., Umemura, K., Sugiyama, J., Kawai, S., Gril, J., Kubodera, S., Mitsutani, T., Ozaki, H., Sakamoto, M., et al. (2011). Aging of wood: Analysis of color changes during natural aging and heat treatment. Holzforschung *65*.

McHale, E., Braovac, S., Steindal, C.C., Gillis, R.B., Adams, G.G., Harding, S.E., Benneche, T., and Kutzke, H. (2016a). Synthesis and characterisation of lignin-like oligomers as a bio-inspired consolidant for waterlogged archaeological wood. Pure Appl. Chem. *88*, 969–977.

McHale, E., Steindal, C.C., Braovac, S., Kutzke, H., Benneche, T., Harding, S.E., Gillis, R., and Adams, G. (2016b). Synthesis and characterisation of lignin-like oligomers as a bio-inspired consolidant for waterlogged archaeological wood. Pure Appl. Chem. *88*, 969–977.

McHale, E., Steindal, C.C., Kutzke, H., Benneche, T., and Harding, S.E. (2017). In situ polymerisation of isoeugenol as a green consolidation method for waterlogged archaeological wood. Sci. Rep. *7*, srep46481.

McQueen, C.M.A., Tamburini, D., Łucejko, J.J., Braovac, S., Gambineri, F., Modugno, F., Colombini, M.P., and Kutzke, H. (2017). New insights into the degradation processes and influence of the conservation treatment in alum-treated wood from the Oseberg collection. Microchem. J. *132*, 119–129.

McQueen, C.M.A., Tamburini, D., and Braovac, S. (2018). Identification of inorganic compounds in composite alum-treated wooden artefacts from the Oseberg collection. Sci. Rep. *8*.

McQueen, C.M.A., Braovac, S., Łucejko, J.J., and Modugno, F. (2019). Unexpected ammonium compounds in alum-treated wood from the Oseberg collection. In 14th

ICOM-CC Wet Organic Archaeological Materials (WOAM) Working Group Conference, (Portsmouth), p.

Meier, D. (2001). Mummies on display: conservation considerations. Chungará Arica *33*, 83–85.

Mirzaei, G., Mohebby, B., and Ebrahimi, G. (2017). Glulam beam made from hydrothermally treated poplar wood with reduced moisture induced stresses. Constr. Build. Mater. *135*, 386–393.

Mitchell, P. (2008). The Vasa and P.E.G. Submerged.

Mizoguchi, H., Watanabe, R., Minami, S., Oikawa, H., and Oguri, H. (2015). Synthesis of multiply substituted 1,6-dihydropyridines through Cu(I)-catalyzed 6-endo cyclization. Org. Biomol. Chem. *13*, 5955–5963.

Morris, G.A., Castile, J., Smith, A., Adams, G.G., and Harding, S.E. (2009a). Macromolecular conformation of chitosan in dilute solution: A new global hydrodynamic approach. Carbohydr. Polym. *76*, 616–621.

Morris, G.A., Castile, J., Smith, A., Adams, G.G., and Harding, S.E. (2009b). The kinetics of chitosan depolymerisation at different temperatures. Polym. Degrad. Stab. *94*, 1344–1348.

Morris, G.A., Adams, G.G., and Harding, S.E. (2014). On hydrodynamic methods for the analysis of the sizes and shapes of polysaccharides in dilute solution: A short review. Food Hydrocoll. *42*, 318–334.

Muhcu, D., Terzi, E., Kartal, S., and Yoshimura, T. (2017). Biological performance, water absorption, and swelling of wood treated with nano-particles combined with the application of Paraloid B72®. J. For. Res.

Munteanu, M., Sandu, I., Vasilache, V., and Sandu, I.C.A. (2016). Disadvantages of using some polymers in restoration of old icons on wooden panels. Int. J. Conserv. Sci. *7*, 9.

Nikmawahda, H.T., Sugita, P., and Arifin, B. (2015). Synthesis and characterization of N-alkylchitosan as well as its potency as a paper coating material. Adv. Appl. Sci. Res. *6*, 141–149.

Nikolajski, M., Adams, G.G., Gillis, R.B., Besong, D.T., Rowe, A.J., Heinze, T., and Harding, S.E. (2014). Protein–like fully reversible tetramerisation and super-association of an aminocellulose. Sci. Rep. *4*.

Nilsson, T., and Rowell, R. (2012). Historical wood – structure and properties. J. Cult. Herit. *13*, S5–S9.

No, H.K., Young Park, N., Ho Lee, S., and Meyers, S.P. (2002). Antibacterial activity of chitosans and chitosan oligomers with different molecular weights. Int. J. Food Microbiol. *74*, 65–72.

Oakley, S.H., Coles, M.P., and Hitchcock, P.B. (2004). Poly(guanidyl)silanes as a new class of chelating, N-based ligand. Dalton Trans. 1113–1114.

Odegaard, N., and Sadongei, A. (2005). Old Poisons, New Problems: A Museum Resource for Managing Contaminated Cultural Materials (Rowman Altamira).

Ohsugi, S., Nishide, K., Oono, K., Okuyama, K., Fudesaka, M., Kodama, S., and Node, M. (2003). New odorless method for the Corey–Kim and Swern oxidations utilizing dodecyl methyl sulfide (Dod-S-Me). Tetrahedron *59*, 8393–8398.

Onsosyen, E., and Skaugrud, O. (1990). Metal recovery using chitosan. J. Chem. Technol. Biotechnol. *49*, 395–404.

Pangallo, D., Šimonovičová, A., Chovanová, K., and Ferianc, P. (2007). Wooden art objects and the museum environment: identification and biodegradative characteristics of isolated microflora. Lett. Appl. Microbiol. *45*, 87–94.

Park, J.W., Choi, K., and Park, K.K. (1983). Acid-base equilibria and related properties of chitosan. Bull. Korean Chem. Soc. *4*, 68–72.

Parrent, J.M. (1985). The Conservation of Waterlogged Wood Using Sucrose. Stud. Conserv. *30*, 63–72.

Pearson, C. (1987). Conservation of Marine Archaeological Objects (Butterworth & Co. Ltd).

Pearson, C. (2014). Conservation of Marine Archaeological Objects (Elsevier).

Pelosi, C. (2011). A study of colour change due to accelerated sunlight exposure in consolidated wood samples. Wood Res. *56*, 511–524.

Petersen, N., and Gatenholm, P. (2011). Bacterial cellulose-based materials and medical devices: current state and perspectives. Appl. Microbiol. Biotechnol. *91*, 1277.

Petrou, M., and Pournou, A. (2018). testing the efficiency of a fruit penetrometer to acess the condition of small waterlogged wooden artifacts. In 13th ICOM_CC Group on Wet Organic Archaeological Material Conference, (Florence 2016), p.

Phillips, E.M., Mesganaw, T., Patel, A., Duttwyler, S., Mercado, B.Q., Houk, K.N., and Ellman, J.A. (2015). Synthesis of ent-Ketorfanol via a C–H Alkenylation/Torquoselective 6π Electrocyclization Cascade. Angew. Chem. Int. Ed. *54*, 12044–12048.

Ponting, M. (2004). The scanning electron microscope and the archaeologist. Phys. Educ. *39*, 166.

Powell, K.L., Pedley, S., Daniel, G., and Corfield, M. (2001). Ultrastructural observations of microbial succession and decay of wood buried at a Bronze Age archaeological site. Int. Biodeterior. Biodegrad. *47*, 165–173.

Preston, J., Smith, A.D., Schofield, E.J., Chadwick, A.V., Jones, M.A., and Watts, J.E.M. (2014). The Effects of Mary Rose Conservation Treatment on Iron Oxidation Processes and Microbial Communities Contributing to Acid Production in Marine Archaeological Timbers. PLoS ONE *9*, e84169.

Ravi Kumar, M.N.V. (2000). A review of chitin and chitosan applications. React. Funct. Polym. *46*, 1–27.

Reis, R.L., Neves, N.M., Mano, J.F., Gomes, M.E., Marques, A.P., and Azevedo, H.S. (2008). Natural-Based Polymers for Biomedical Applications (Boca Raton, Fla.: Woodhead Publishing).

Rinaudo, M. (2006). Chitin and chitosan: Properties and applications. Prog. Polym. Sci. *31*, 603–632.

Roberts, J.C., Merkle, A.C., Carneal, C.A., Voo, L.M., Johannes, M.S., Paulson, J.M., Tankard, S., and Uy, M. (2013). Development of a Human Cranial Bone Surrogate for Impact Studies. Front. Bioeng. Biotechnol. *1*.

Roemhild, K., Wiegand, C., Hipler, U.-C., and Heinze, T. (2013). Novel bioactive amino-functionalized cellulose nanofibers. Macromol. Rapid Commun. *34*, 1767–1771.

Rosenquist, A.M. (1969). The Oseberg Find, Its Conservation and Present State. In Proceedings (ICOMOS Symposium on the Weathering of Wood, (Ludwigsburg, Germany), pp. 77–78.

Rosenqvist, A.M. (1959). The Stabilizing of Wood Found in the Viking Ship of Oseberg: Part II. Stud. Conserv. *4*, 62–72.

Rostovtsev, V.V., Green, L.G., Fokin, V.V., and Sharpless, K.B. (2002). A Stepwise Huisgen Cycloaddition Process: Copper(I)-Catalyzed Regioselective "Ligation" of Azides and Terminal Alkynes. Angew. Chem. Int. Ed. *41*, 2596–2599.

Rúnarsson, Ö.V., Malainer, C., Holappa, J., Sigurdsson, S.Th., and Másson, M. (2008a). tert-Butyldimethylsilyl O-protected chitosan and chitooligosaccharides: useful precursors for N-modifications in common organic solvents. Carbohydr. Res. *343*, 2576–2582.

Rúnarsson, Ö.V., Malainer, C., Holappa, J., Sigurdsson, S.Th., and Másson, M. (2008b). tert-Butyldimethylsilyl O-protected chitosan and chitooligosaccharides: useful precursors for N-modifications in common organic solvents. Carbohydr. Res. *343*, 2576–2582.

Rutzky, I.S., Elvers, W.B., Maisey, J.G., and Kellner, A.W.A. (2005). Chemical preparation techniques. In Vertebrate Paleontological Techniques:, (Cambridge University Press), p.

Sadeghifar, H., Venditti, R., Jur, J., Gorga, R.E., and Pawlak, J.J. (2017). Cellulose-Lignin Biodegradable and Flexible UV Protection Film. ACS Sustain. Chem. Eng. *5*, 625–631.

Saito, H., Tabeta, R., and Ogawa, K. (1987). High-resolution solid-state carbon-13 NMR study of chitosan and its salts with acids: conformational characterization of polymorphs and helical structures as viewed from the conformation-dependent carbon-13 chemical shifts. Macromolecules *20*, 2424–2430.

Sandström, M., Jalilehvand, F., Persson, I., Fors, Y., Damian, E., Gelius, U., Hall-Roth, I., Dal, L., Vicki, R., and Ian, G. (2003). The sulfur threat to marine archaeological artefacts : acid and iron removal from the Vasa. In Conservation Science Edinburgh 22-24 May 2002, (Edinburgh: Archetype Publications), pp. 79–87.

Sandström, M., Jalilehvand, F., Damian, E., Fors, Y., Gelius, U., Jones, M., and Salomé, M. (2005). Sulfur accumulation in the timbers of King Henry VIII's warship Mary Rose: a pathway in the sulfur cycle of conservation concern. Proc. Natl. Acad. Sci. U. S. A. *102*, 14165–14170.

Sarwar, A., Katas, H., Samsudin, S.N., and Zin, N.M. (2015). Regioselective Sequential Modification of Chitosan via Azide-Alkyne Click Reaction: Synthesis, Characterization, and Antimicrobial Activity of Chitosan Derivatives and Nanoparticles. PLoS ONE *10*, e0123084.

Schindelholz, E., Blanchette, R.A., Cook, D., Drews, M., Hand, S., Held, S., Jungens, B., and Seifert, B. (2005). An Evaluation of Supercritical Drying and PEG/Freeze Drying of Waterlogged Archaeological Wood (The Mariners' Musuem).

Schniewind, A.P., and Eastman, P.Y. (1994). Consolidant Distribution in Deteriorated Wood Treated With Soluble Resins. J. Am. Inst. Conserv. *33*, 247–255.

Schuck, P. (2000). Size-Distribution Analysis of Macromolecules by Sedimentation Velocity Ultracentrifugation and Lamm Equation Modeling. Biophys. J. *78*, 1606–1619.

Schuck, P. (2003). On the analysis of protein self-association by sedimentation velocity analytical ultracentrifugation. Anal. Biochem. *320*, 104–124.

Schuck, P., Gillis, R.B., Besong, T.M.D., Almutairi, F., Adams, G.G., Rowe, A.J., and Harding, S.E. (2014a). SEDFIT-MSTAR: molecular weight and molecular weight distribution analysis of polymers by sedimentation equilibrium in the ultracentrifuge. The Analyst *139*, 79–92.

Schuck, P., Gillis, R.B., Besong, T.M.D., Almutairi, F., Adams, G.G., Rowe, A.J., and Harding, S.E. (2014b). SEDFIT-MSTAR: Molecular weight and molecular weight distribution analysis of polymers by sedimentation equilibrium in the ultracentrifuge. The Analyst *139*, 79–92.

Selwyn, L.S., Rennie-Bisaillion, D.A., and Binnie, N.E. (1993). Metal Corrosion Rates in Aqueous Treatments for Waterlogged Wood-Metal Composites. Stud. Conserv. *38*, 180–197.

Sen, S., Patil, S., and Argyropoulos, D.S. (2015). Methylation of softwood kraft lignin with dimethyl carbonate. Green Chem. *17*, 1077–1087.

Shafiee, S., and Topal, E. (2009). When will fossil fuel reserves be diminished? Energy Policy *37*, 181–189.

Shishkina, O., Lomov, S.V., Verpoest, I., and Gorbatikh, L. (2014). Structure–property relations for balsa wood as a function of density: modelling approach. Arch. Appl. Mech. *84*, 789–805.

Sigma Aldrich (2020). Physical Properties of Solvents.

Singh, A.P. (2012). A review of microbial decay types found in wooden objects of cultural heritage recovered from buried and waterlogged environments. J. Cult. Herit. *13*, S16–S20.

Smidsrød, O., Haug, A., and Larsen, B. (1966). The influence of pH on the rate of hydrolysis of acidic polysaccharides. Acta Chem. Scand. *20*, 1026–1034.

Smith, C.W. (2003). Archaeological Conservation Using Polymers: Practical Applications for Organic Artifact Stabilization (Texas A&M University Press).

Smith, C.W. (2010). Reports - Archaeological Preservation Research Laboratory.

Song, W., Gaware, V.S., Rúnarsson, Ö.V., Másson, M., and Mano, J.F. (2010). Functionalized superhydrophobic biomimetic chitosan-based films. Carbohydr. Polym. *81*, 140–144.

Spirydowicz, K.E., Simpson, E., Blanchette, R.A., Schniewind, A.P., Toutloff, M.K., and Murray, A. (2001a). Alvar and Butvar: The Use of Polyvinyl Acetal Resins for the Treatment of the Wooden Artifacts from Gordion, Turkey. J. Am. Inst. Conserv. *40*, 43–57.

Spirydowicz, K.E., Simpson, E., Blanchette, R.A., Schniewind, A.P., Toutloff, M.K., and Murray, A. (2001b). Alvar and Butvar: The Use of Polyvinyl Acetal Resins for the Treatment of the Wooden Artifacts from Gordion, Turkey. J. Am. Inst. Conserv. *40*, 43.

Stainforth (2006). The National Trust Manual of Housekeeping: The Care of Collections in Historic Houses Open to the Public (Elsevier).

Sterflinger, K. (2010). Fungi: Their role in deterioration of cultural heritage. Fungal Biol. Rev. *24*, 47–55.

Sterflinger, K., and Piñar, G. (2013). Microbial deterioration of cultural heritage and works of art — tilting at windmills? Appl. Microbiol. Biotechnol. *97*, 9637–9646.

Svedberg, T. (1926). The Svedberg, The Ultracentrifuge.The Nobel Prize in Chemistry 1926. In Chemistry 1922-1941, (Amsterdam: Nobel Lectures, Elsevier Publishing Company, (1966)), p.

Tahira, A., Howard, W., Pennington, E.R., and Kennedy, A. (2017). Mechanical strength studies on degraded waterlogged wood treated with sugars. Stud. Conserv. *62*, 223–228.

Tanford, C. (1961). Physical Chemistry of Macromolecules (New York: John Wiley & Sons Inc).

Tarkow, H., Feist, W.C., and Southerland, C.F. (1966). Interaction of wood with polymeric materials. Penetration versus molecular size. Prod J *16*, 61–65.

Tejedor, C.C. (2010). Re-conservation of Wood from the Seventeenth-Century Swedish Warship the Vasa with Alkoxysilanes: A Re-treatment Study Applying Thermosetting Elastomers. Thesis. Texas A&M University.

Tejedor, C.C. (2012). Summary of a Master's Thesis: Re-Conservation of Wood from the Seventeenth-Century Swedish Warship the Vasa with Alkoxysilanes. WOAM Newsl.

Tian, F., Liu, Y., Hu, K., and Zhao, B. (2003). The depolymerization mechanism of chitosan by hydrogen peroxide. J. Mater. Sci. *38*, 4709–4712.

Timar, M., TUDUCE TRĂISTARU, A.-A., Patachia, S., and Croitoru, C. (2011). An investigation of consolidants penetration in wood. Part 2: FTIR spectroscopy. LIGNO-Wwwprolignoro *Vol. 7*, 25–38.

Timar, M., Sandu, I., Beldean, E., and Sandu, I. (2014). FTIR Investigation of Paraloid B72 as Consolidant for Old Wooden Artefacts Principle and Methods. Mater. Plast. *51*, 382–387.

Tombs, M., and Harding, S. (1997). An Introduction to Polysaccharide Biotechnology (London ; Bristol, PA: Taylor & Francis).

Tuduce Trăistaru, A.A., Timar, M.C., and Campean, M. (2011). Studies upon penetration of Paraloid B72 into poplar wood by cold immersion treatments. Bull. Transilv. Univ. Braşov *4*.

Turk, J., Mauko Pranjić, A., Hursthouse, A., Turner, R., and Hughes, J.J. (2019). Decision support criteria and the development of a decision support tool for the selection of conservation materials for the built cultural heritage. J. Cult. Herit. *37*, 44–53.

Turkulin, H., Holzer, L., Richter, K., and Sell, J. (2007). Application of the ESEM Technique in Wood Research: Part I. Optimization of Imaging Parameters and Working Conditions. Wood Fiber Sci. *37*, 552–564.

Ulery, B.D., Nair, L.S., and Laurencin, C.T. (2011). Biomedical applications of biodegradable polymers. J. Polym. Sci. Part B Polym. Phys. *49*, 832–864.

Unger, A. (2012). Decontamination and "deconsolidation" of historical wood preservatives and wood consolidants in cultural heritage. J. Cult. Herit. *13*, S196–S202.

Unger, A., Schniewind, A., and Unger, W. (2001). Conservation of Wood Artifacts: A Handbook (Berlin ; New York: Springer).

Varma, A.J., Deshpande, S.V., and Kennedy, J.F. (2004). Metal complexation by chitosan and its derivatives: a review. Carbohydr. Polym. *55*, 77–93.

Victoria and Albert Museum, O.M. (2011). The Ethics of Conservation Practice: A Look From Within.

Vieira, A.P., Badshah, S., and Airoldi, C. (2013). Ibuprofen-loaded chitosan and chemically modified chitosans--release features from tablet and film forms. Int. J. Biol. Macromol. *52*, 107–115.

Vold, I.M.N., Vårum, K.M., Guibal, E., and Smidsrød, O. (2003). Binding of ions to chitosan—selectivity studies. Carbohydr. Polym. *54*, 471–477.

Wakefield, J.M.K., Gillis, R.B., Adams, G.G., McQueen, C.M.A., and Harding, S.E. (2018). Controlled depolymerisation assessed by analytical ultracentrifugation of low molecular weight chitosan for use in archaeological conservation. Eur. Biophys. J. EBJ *47*, 769–775.

Walsh, Z., Janeček, E.-R., Jones, M., and Scherman, O.A. (2014a). Natural polymers as alternative consolidants for the preservation of waterlogged archaeological wood. Stud. Conserv.

Walsh, Z., Janeček, E.-R., Hodgkinson, J.T., Sedlmair, J., Koutsioubas, A., Spring, D.R., Welch, M., Hirschmugl, C.J., Toprakcioglu, C., Nitschke, J.R., et al. (2014b). Multifunctional supramolecular polymer networks as next-generation consolidants for archaeological wood conservation. Proc. Natl. Acad. Sci. *111*, 17743–17748.

Walsh, Z., Janeček, E.-R., Hodgkinson, J.T., Sedlmair, J., Koutsioubas, A., Spring, D.R., Welch, M., Hirschmugl, C.J., Toprakcioglu, C., Nitschke, J.R., et al. (2014c). Multifunctional supramolecular polymer networks as next-generation consolidants for archaeological wood conservation. Proc. Natl. Acad. Sci. *111*, 17743–17748.

Walsh, Z., Janeček, E.-R., Jones, M., and Scherman, O.A. (2017). Natural polymers as alternative consolidants for the preservation of waterlogged archaeological wood. Stud. Conserv. *62*, 173–183.

Wang, Y., and Schniewind, A.P. (1985). Consolidation of Deteriorated Wood with Soluble Resins. J. Am. Inst. Conserv. *24*, 77–91.

Wang, S.-M., Huang, Q.-Z., and Wang, Q.-S. (2005). Study on the synergetic degradation of chitosan with ultraviolet light and hydrogen peroxide. Carbohydr. Res. *340*, 1143–1147.

Wang, Z., Winestrand, S., Gillgren, T., and Jönsson, L.J. (2018). Chemical and structural factors influencing enzymatic saccharification of wood from aspen, birch and spruce. Biomass Bioenergy *109*, 125–134.

Watkinson, D. (2018). Conserving cultural material: ethical challenges for the conservator.

Welton, T. (2015). Solvents and sustainable chemistry. Proc R Soc A *471*, 20150502.

Whitmore, P.M., and Bogaard, J. (1994). Determination of the Cellulose Scission Route in the Hydrolytic and Oxidative Degradation of Paper. Restaurator *15*, 26–45.

Younes, I., and Rinaudo, M. (2015). Chitin and chitosan preparation from marine sources. Structure, properties and applications. Mar. Drugs *13*, 1133–1174.

Yu, D., Klein, S.A., and Reindl, D.T. (2001). An Evaluation of Silica Gel for Humidity Control in Display Cases. p.

Zarth, C.S.P., Koschella, A., Pfeifer, A., Dorn, S., and Heinze, T. (2011). Synthesis and characterization of novel amino cellulose esters. Cellulose *18*, 1315–1325.

Zervos, S. (2010). Cellulose: Structure and Properties, Derivatives and Industrial Uses. Chapter 5 Natural and Accelerated Ageing of Cellulose and Paper: A Literature Review (Nova Publishing).

Zou, X., Gurnagul, N., Uesaka, T., and Bouchard, J. (1994). Accelerated aging of papers of pure cellulose: mechanism of cellulose degradation and paper embrittlement. Polym. Degrad. Stab. *43*, 393–402.

Appendix

An electronic appendix is attached to this thesis. Photographs and scans of each piece of wood on all sides and before and after treatment were taken. An example of each was included in the thesis. However, in case it is required to review this data in the future, all phototgraphs and scans are included in the appendix. Photographs show the top of the wood and the side. The scans allowed for all 6 sides to be documented.

Also included in this electronic appendix is other raw data that might be of use to others in the future, such as SEM images, see appendix content for more details.